International Journal of Engineering Works (IJEW)

OPEN ACCESS

ISSN E 2409-2770
ISSN P 2521-2419

IJEW

VOL. 7-2020
Printable Version Vol. 7 Issue 01-12, Page: 414-421

www.ijew.io/

https://www.ijew.io/rss/2020

Editorial Board

Table of Content

Vol. 7, Issue 10, PP. 326-332, October 2020

Design of CZTS-Perovskite thin-film Hetero-Junction Solar Cell
Vol. 7, Issue 10, PP. 318-325, October 2020

Novel Application of Whale-Optimization-Algorithm Integrated with Local Search Deterministic Techniques to Solve Economic-Load-Dispatch-Problem with Valve-Point-Loading-Effect and Gaseous Emission
Vol. 7, Issue 09, PP. 312-317, September 2020

Hindko Sign Language (HSL) Recognition Using Convolutional Neural Network
Vol. 7, Issue 09, PP. 305-311, September 2020

Economic Dispatch Solution for Generating Units through Optimization
Vol. 7, Issue 09, PP. 298-304, September 2020

Intrusion Detection System for SDN based IoT Devices using Deep Neural Network
Vol. 7, Issue 09, PP. 293-297, September 2020

Role of Women in Energy Management at Household level in Peshawar, Pakistan
Vol. 7, Issue 08, PP. 286-292, August 2020

Analysis of Conventional and Microwave Assisted Technique for the Extraction of Concentrated Oils from Citrus Peel
Vol. 7, Issue 08, PP. 282-285, August 2020

Reliability Improvement of Micro-Inverter through AC-Ripples Voltage Compensator
Vol. 7, Issue 08, PP. 274-281, August 2020

Comparasion of Different Configuration of Hybrid Electrical Power System â€“ A Case Study of a Site in Peshawar
Vol. 7, Issue 08, PP. 268-273, August 2020

Ceramic Membrane Coating with Graphene Oxide for Tannery Wastewater Treatment
Vol. 7, Issue 07, PP. 264-267, July 2020

Analysis of Green Technologies for Motorway Interchange
Vol. 7, Issue 07, PP. 259-263, July 2020

Policy Analysis of Thermal Power Generation in Pakistan
Vol. 7, Issue 07, PP. 255-258, July 2020

Design and Analysis of Dual Band Circular Slotted Patch Antenna at 2.45GHZ and 5.8GHZ for RFID Applications
Vol. 7, Issue 07, PP. 251-254, July 2020

A Fast and Efficient Absorbant BYW-01 and its Applications in Coking Plant Wastewater Treatment
Vol. 7, Issue 06, PP. 247-252, June 2020

Micro Grid Automation with Unique Features of Power Flow Control by using SCADA
Vol. 7, Issue 06, PP. 238-246, June 2020

Analysis of Energy Performance and Application of Wall Insulation on an Academic Building using EQUEST
Vol. 7, Issue 06, PP. 233-237, June 2020

Implementation of Mobility Model for V2V Communication on LTE using NS3 and SUMO
Vol. 7, Issue 05, PP. 228-232, May 2020

Causes of Delay in the Establishment of Public Sector University in Newly Merged District of KP, Pakistan Vol. 7, Issue 05, PP. 221-227, May 2020

Methodology of Material Selection for Evaporator Coil in Air Conditioning System Vol. 7, Issue 04, PP. 217-220, April 2020

Frequencies Dominations for Different Rating of Distribution Transformer under Transients Vol. 7, Issue 04, PP. 211-216, April 2020

Spatial Variation of Temperature and Rainfall Trends in Kabul River Basin Vol. 7, Issue 04, PP. 207-210, April 2020

A Revolution in Health Sector using Wireless Body Area Networks Vol. 7, Issue 04, PP. 203-206, April 2020

Simulation and Design of CIGS Thin Film Solar Cell using Distributed Bragg Reflector Vol. 7, Issue 04, PP. 197-202, April 2020

Multi-Robot Exploration in Unstructured and Dynamic Environments Vol. 7, Issue 03, PP. 189-196, March 2020

Adaptive Under-Frequency Load Shedding Scheme for Islanded Distribution Network based on Swing Equation Vol. 7, Issue 03, PP. 183-188, March 2020

Operation and Fault Monitoring of Electric Generator using IOT Vol. 7, Issue 03, PP. 178-182, March 2020

Published online Operation and Fault Monitoring of Electric Generator using IOT Significance of Power Quality in Power Systems Vol. 7, Issue 03, PP. 173-177, March 2020

Comparing the Properties of Virgin & Aged Bitumen by the addition of Rejuvenators Vol. 7, Issue 03, PP. 168-172, March 2020

Analyzing the Consumer`s Buying Behavior towards Green Products Vol. 7, Issue 03, PP. 161-167, March 2020

Design, Fabrication, Testing and Performance Evaluation of Double Axis Solar Tracker Vol. 7, Issue 02, PP. 154-160, February 2020

Performance Analysis of a Parabolic trough Concentrated Solar Power Technology in Pakistan Vol. 7, Issue 02, PP. 161-166, February 2020

Numerical Simulation for Enhancement of output Performance of WS2 based Thin Film Solar Cells Vol. 7, Issue 02, PP. 149-153, February 2020

Application-based forwarding in Delay-Tolerant Networks Vol. 7, Issue 02, PP. 143-148, February 2020

Design & Fabrication Of Novel Maximum Power Point Tracking (MPPT) Based Charge Controller For Enhanced Electrical Performance Vol. 7, Issue 02, PP. 138-142, February 2020

National Power Policies of Pakistan Concerning Global trend toward Sustainable Energy and its Prospects Vol. 7, Issue 02, PP. 129-137, February 2020

Role of Biomass in the Mitigation of Energy Crises in Pakistan

Vol. 7, Issue 02, PP. 116-128, February 2020

Optimization of Power Conversion Efficiency for Perovskite Solar Cell using GPVDM
Vol. 7, Issue 02, PP. 109-115, February 2020

Potential & Current Status of Solar Energy in Pakistan Policy, Planning & Strategy
Vol. 7, Issue 02, PP. 98-108, February 2020

Power Generation Through VAWT Implementation on Highways & Stabilization the Output Voltage by Controlled Buck-Boost Converter
Vol. 7, Issue 02, PP. 93-97, February 2020

Conversion of a Solar Geyser to Solar Cooker & Its Performance Evaluation
Vol. 7, Issue 02, PP. 84-92, February 2020

CFD Based Optimization of Kaplan Turbine Blade Profile
Vol. 7, Issue 02, PP. 80-83, February 2020

Designing, Fabrication, Testing and Evaluation of a Straight Bladed Darrius Type Vertical Axis Wind Turbine Vol. 7, Issue 01, PP. 74-79, January 2020

Implementation of Chiller Plant Management System to Optimize the Building Primary HVAC System Energy Consumption
Vol. 7, Issue 01, PP. 68-73, January 2020

Comparative Analysis of Different Storage Technologies for Energy Critical Application
Vol. 7, Issue 01, PP. 62-67, January 2020

Indirect Gross Calorific Value prediction using Random Forest
Vol. 7, Issue 01, PP. 58-61, January 2020

Comparative Analysis of Virtual Inertia Techniques in Wind Energy
Vol. 7, Issue 01, PP. 48-57, January 2020

Investigating Future Consumption of Electricity Estimates in Pakistan using Linear Regression Analysis Vol. 7, Issue 01, PP. 39-47, January 2020

Designing, Fabrication, Performance Evaluation and Implementation of Solar-Biomass Hybrid Tunnel Dryer for Commercial Scale Drying of Several Types of Agricultural Products
Vol. 7, Issue 01, PP. 31-38, January 2020

An charging Interface for Lithium ion Batteries Compatible with Current in-use UPS System
Vol. 7, Issue 01, PP. 27-30, January 2020

Speech Sources Separation Based on Models of Interaural Parameters and Spatial Properties of Room
Vol. 7, Issue 01, PP. 22-26, January 2020

Multiband Microstrip Patch Antenna for 5G Wireless Communication
Vol. 7, Issue 01, PP. 15-21, January 2020

Improving the Mechanical Properties of Fine Soil using Marble Waste
Vol. 7, Issue 01, PP. 10-14, January 2020

Application of Unified Power Quality Conditioner in Grid Integration of Solar PV System
Vol. 7, Issue 01, PP. 01-09, January 202

IJEW 国际工程期刊 International Journal of Engineering Works انجینئرنگ کاموں کا بین الاقوامی جرنل

International Journal of Engineering Works
ISSN-p: 2521-2419
ISSN-e: 2409-2770
Vol. 7, Issue 01, PP. 01-09, January 2020
https://www.ijew.io/
https://doi.org/10.34259/ijew.20.7010109

Application of Unified Power Quality Conditioner in Grid Integration of Solar PV System

Niaz Ali[1], Prof. Dr. Muhammad Naeem Arbab[2], Rizwan Kamal[3], Muhammad Bilal[4]
[1,2,3,4] US Pakistan Center for Advanced Studies in Energy, University of Engineering and Technology, Peshawar
engr.niazi91@yahoo.com[1], mnarbab@yahoo.com[2], rkrizwan891@gmail.com[3], engr.bilal92@gmail.com[4]
Received: 14 December, Revised: 20 December, Accepted: 27 December

***Abstract*—**Modern power electronics has developed a great interest in grid integration of solar photovoltaics. The penetration of renewable energy resources causes problems of power quality, due to their intermittent behavior. These problems include but are not limited to reactive power flow, voltage dip or sag, over-voltage, distortions in current and voltage waveforms. Similarly, non-linear loads have been consistently increased on the consumer side. These power electronics-based equipment bring harmonics into the power system and as result demand of reactive power rises. This research aims a Unified Power Quality Conditioner for grid integration of solar PV. In the proposed technique, a part of the PV power is used for the power quality management and the rest of the power is sent back into the grid. The major constituents of PV system are; DC-DC boost converter, PV array, whereas, P &O algorithm is adopted to ensure the maximum power point operation of the PV array. The analysis and testing of the proposed approach have been successfully accomplished in MATLAB/Simulink. The results of the simulation reveal that along with the active power injection to the grid, the conditioner is capable to; pay compensation for harmonics, corrects sags and swells in voltage and also regulates the load voltage at its nominal value.

***Keywords*—** Solar PV, Unified Power Quality Conditioner, Power Quality, Grid Integration.

I. INTRODUCTION

The demand for electric power in several developing countries, specifically in Pakistan, is growing gradually. Due to environmental and economic concerns, renewable energy resources have been emerging widely in order to meet this demand, among these resources, sunlight is the most abundant one. Useful electrical energy can be achieved from the luminous energy of the sun by making use of solar photovoltaic. The major advantages and characteristics of a solar photovoltaic system are: environment friendly energy without the emission of greenhouse gases, long-lasting operation, installation is effortless, operational cost is negligible, no moving or rotating components are entailed in generating power, and most importantly, the PV system is much cheaper than other renewable resources such as wind energy system and hydropower system. Middle class people cannot only recover some money as far as their electricity bills are concerned but can vend the excess power to the utility by supplying it back to the grid.

With the advances in modern power electronics, non-linear loads have been strongly grown on the distribution network. Moreover, the injection of a huge amount of harmonics in the electrical system can increase the system reactive power demand and hence, degrade the power quality. This low power quality can damage the equipment on the consumer side. This research gives energy consumers an opportunity to contribute in power generation and sell it. Thus, the system suggested in this work can contribute towards Pakistan's power sector by making use of solar energy for refining the power quality as well as active power injection to the grid.

This paper is structured as Section II provides an overview about the background of the research, Section III presents a general description of the proposed system, Section IV describes the system in detail, whereas, Section V analyzes the process of simulation and presents an overview of the results, and the last section i.e. Section VI portrays the conclusion of this research article.

II. BACKGROUND

Grid penetration of solar energy has been emerging since the development of modern power electronics [1]. However, integrating solar PV with grid is not a simple job because it may give rise to problems of power quality [2].

Power quality has become the principal concern for the realization of a smart grid [3]. Renewable energy resources such as wind and Solar PV behave intermittently. As far as weak distribution systems are concerned this behavior leads to power quality problems [4]. Few of the power quality issues, that may rise as a result of entrance of solar energy in the power network, are distortions in current and voltage waveforms, over-voltage (voltage swell) and voltage dip (sag), reactive power flow [3]-[9]. Such disturbances in voltage may also often initiate erroneous tripping and may damage the switching equipment. Capacitor banks heat up as a result of these disturbances [7], [10]. Likewise, non-linear loads are considerably growing on the consumer side. such a wide range

usage of power electronics-based, non-linear loads cause the problems of power quality. As a result, the quality of power is becoming a concern for the utilities and also for the consumers. Such type of loads give rise to harmonics in current, which is the main cause of power quality issues. The current harmonics give rise to harmonics in system voltage. These power quality issues badly disturb the operation of the equipment connected to the power grid and can even cause damage to them. Due to these disturbances, transmission and distribution losses may also increase [11].

Several methods have been used to resolve the issues concerning power quality. Some of the frequently adopted methods to refine the quality of power are power filters, passive or active or their mutual combination which is named as hybrid filters. Active Power Filters (APFs) have two basic configurations based on their connection i.e. shunt or series APF, Active power filters can be used together with passive filters and such combination is termed as Hybrid filters. Another possible combination is of series and shunt APFs which is known as Unified Power Quality Conditioner (UPQC), distribution static compensator and static Volt Ampere Reactive Compensator (VAR compensator).

In this work an effort is made to inspect a technique for the grid connection of solar PV that is also capable of mitigating the issues of power quality. UPQC has proven to be effective in removing both the current and voltage distortions [11]. In UPQC the voltage and current disturbances are handled by the series and shunt APFs, respectively. PV array is connected in between the two APFs (at the DC link) to deliver the power necessary for compensating the power quality problems and the extra power is supplied back to the distribution station. A recent research uses a UPQC for the same purpose. The UPQC proposed in [1] is fed by a solar PV array. However, the system is limited only to harmonics compensation and problems like voltage sag and swell are not tackled.

III. PROPOSED SYSTEM

The overall layout of the proposed UPQC is illustrated in Figure 1. This study uses a single-phase system. A simple and easy control strategy is employed to control the series APF. The phase angle of the voltage from the grid side is obtained by means of a Phase Locked Loop (PLL). While, the nominal value of RMS voltage of the grid is used in generating the load reference voltage. The controller effectively monitors the operation of the series APF to compensate for the issues linked with grid voltage.

A single-phase Synchronous Reference Frame (SRF) technique is used to design controller for the shunt APF. The controller effectively monitors the operation of shunt APF to remove harmonics in current and avoid their entrance back into the grid.

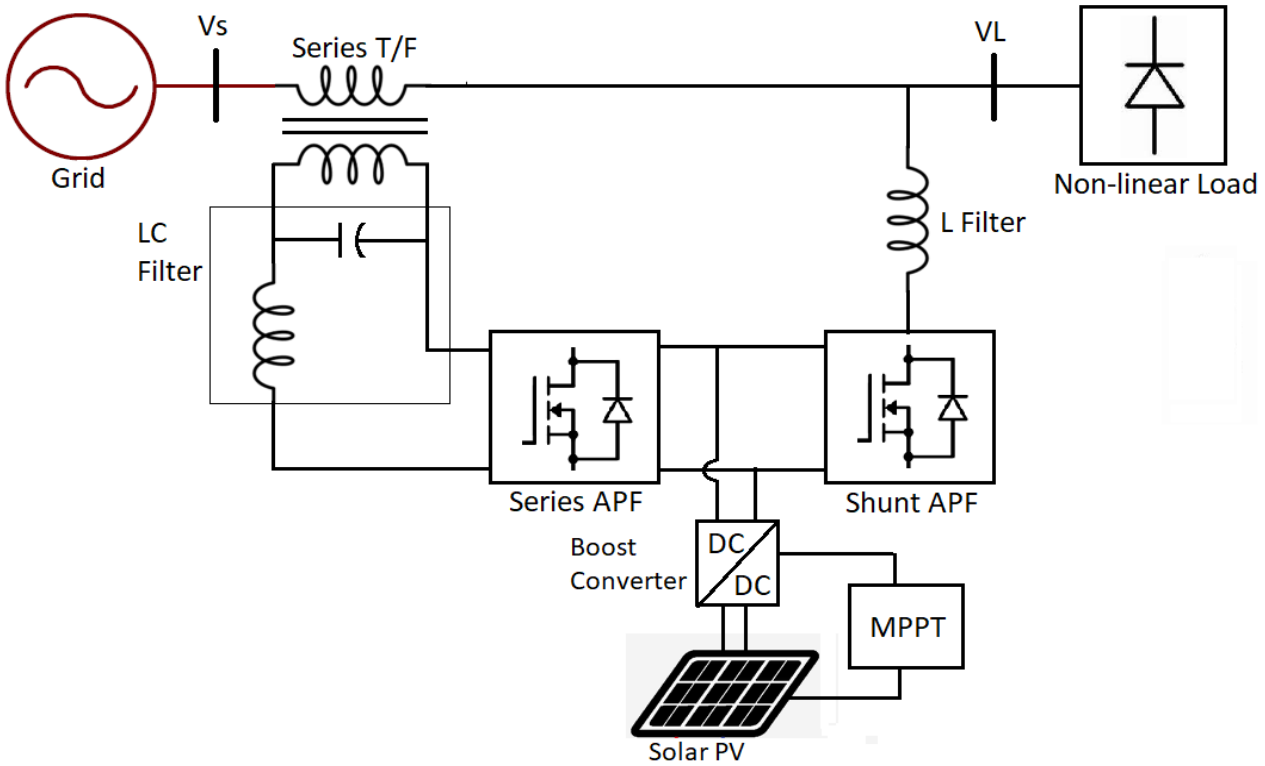

Figure 1. Layout of the Overall System

IV. SYSTEM DESCRIPTION

This section describes the significant parts of the system under study. Implementation and simulation of the system has been accomplished in Simulink/MATLAB. The process of simulation has been depicted in Figure 2. Each subsystem is described in the following subsections.

A. Solar PV Subsystem

The Simulink arrangement of the solar PV subsystem can be viewed in Figure 3. Each part of this subsystem is described below.

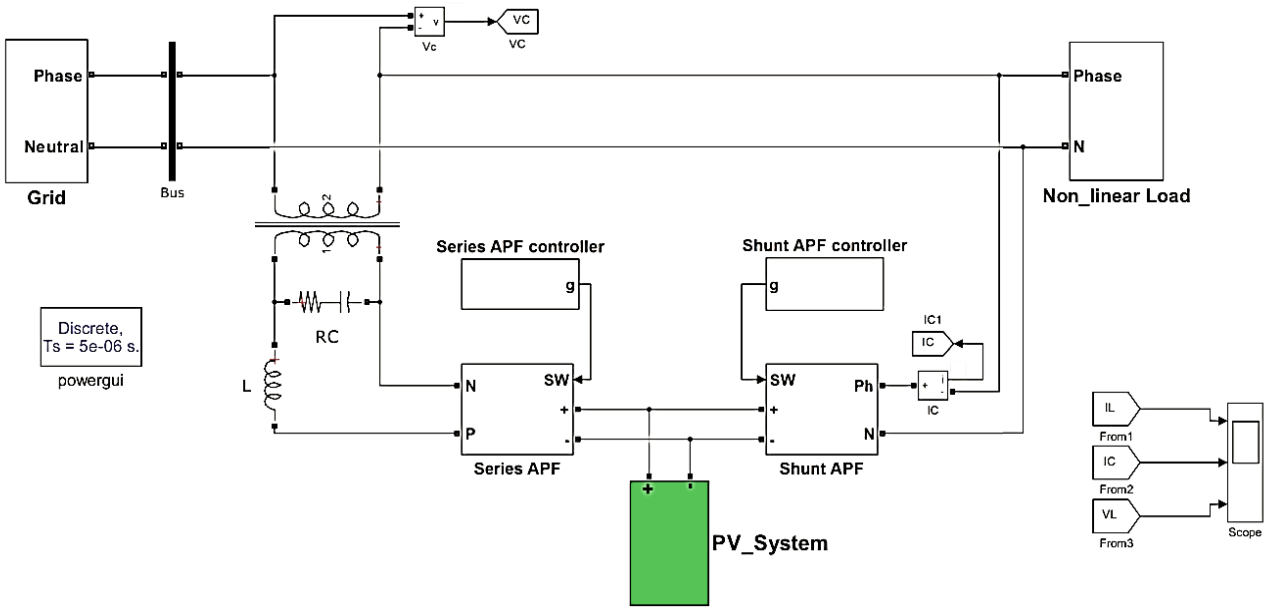

Figure 2. Simulink Diagram of the Proposed System

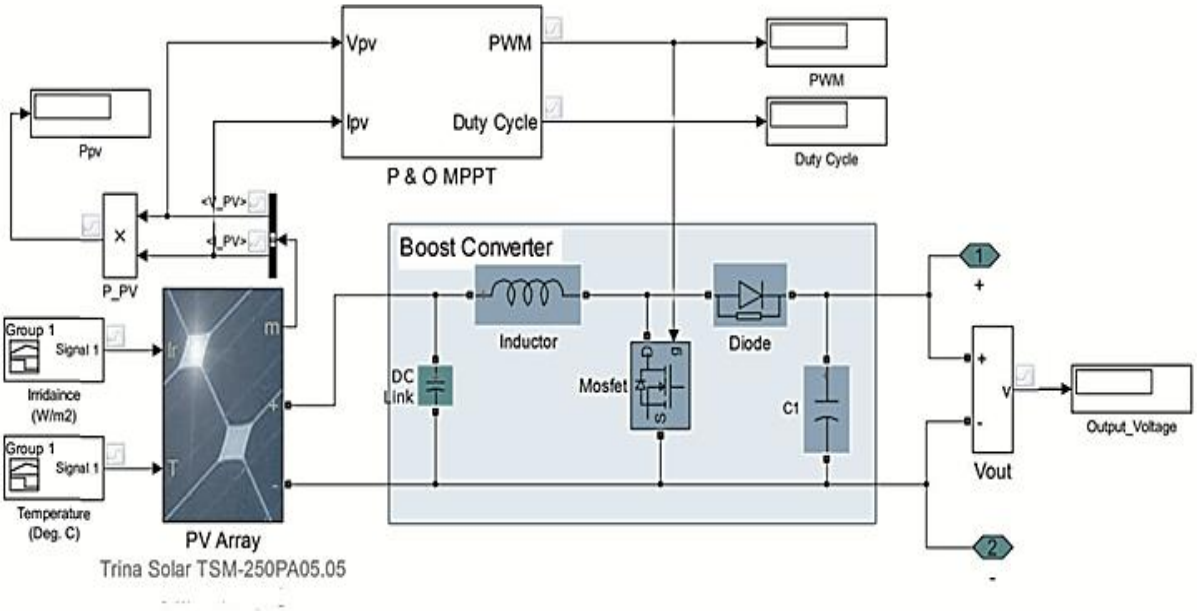

Figure 3. Simulink Diagram of the Solar PV Subsystem

1) Solar PV Array Block

A negligible amount of power is produced individually by each cell of the module. Therefore, for applications that require high power, PV cells are connected in series and parallel configurations to form module. Panels are made up of these modules. Similarly, to configure the PV array for the desired output power, a number of panels are connected together using series and parallel connections.

The PV array block of the proposed system contains 8 parallel strings each with 10 modules tied in series. The PV array has a maximum power of 20KW. The solar PV array of the system is based on mathematical equivalent model of a PV cell with single diode. Figure 4 shows a Thevenin-based equivalent circuit of a single diode cell.

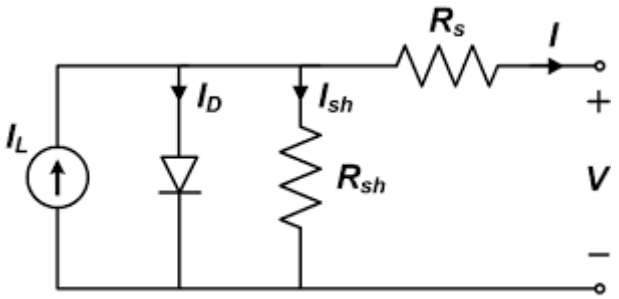

Figure 4. Thevenin-based Equivalent Circuit of PV Cell

The single diode model comprises of a diode connected across a photon current source (I_L), shunt resistance R_{sh}, and series resistance R_s. Trina Solar TSM-250PA05.05 (datasheet is given in Table I) has chosen for the proposed system. This block takes two input signals i.e. irradiance (W/m^2) and temperature (^{o}C).

TABLE I. SPECIFICATIONS OF THE PV MODULE

Quantity	Value
R_S (Series resistance)	0.2351Ω
R_{SH} (Parallel resistance)	286.8727Ω
I_{sc} (short circuit)	8.55A
V_{oc} (open circuit)	37.4V
P max	249.86W
V_{MPP} (MPP Voltage)	31V
I_{MPP} (MPP Current)	8.06A
Diode ideality factor (a)	0.96295
I photovoltaic	8.5728A
I leakage	9.6463x10^{-11}A

2) Boost Converter

The PV array is coupled with a supercapacitor that helps to minimize the variations in the PV output. The supercapacitor is then coupled with a step-up boost converter. This converter always has its output voltage more than its input voltage for all the values of the duty ratio. A Pulse Width Modulation (PWM) signal is produced that operates the Metal Oxide Semiconductor Field Effect Transistor (MOSFET) based Switch. The converter intends to increase the voltage and maintain the Maximum Power Point (MPP) operation of the PV array.

The MPP is tracked through a proper MPP Tracking (MPPT) algorithm by fine-tuning of the duty cycle of the switching signal. The optimal working of the converter requires the input resistance to be equal to the optimal resistance [12] i.e. to fulfill the condition for maximum power transfer [13].

Eq (1) and Eq (2) are used for estimating the parameters of the converter, inductor and capacitor respectively.

$$L_c = \frac{D(1-D)^2 R}{2f} \quad (1)$$

$$C_c = \frac{D}{R(\Delta V_o / V_o) f} \quad (2)$$

Estimated parameters of the boost converter can be viewed in Table II.

TABLE II. ESTIMATED PARAMETERS OF BOOST CONVERTER

Parameter	Value
Switching Frequency	10KHz
Inductor	30uH
Capacitor	10mF
Dc Link Capacitor	5000uF

3) Perturb and Observe MPPT Algorithm

Various blocks from the Simulink library are used to create P & O MPPT algorithm. The Simulink diagram is given in Figure 5. In P & O scheme, the duty ratio in the beginning is either steped up or down from its initial predefined value and the path of process is maintained if the power moves up, otherwise, the path of process is changed [14].

B. Shunt APF Control

Current compensation is provided through proper generation of the compensating current. There are several techniques that can be adopted for this purpose. Here, a Synchronous Reference Frame (SRF) based controller is employed to obtain the reference signal. The current or voltage fundamental components are converted from stationary reference frame (abc) into a rotating reference frame (dq-synchronous) that rotates at a synchronous speed. The Simulink diagram of the single phase SRF-based control algorithm is given in Figure 6. The load current I_L is chosen as actual fictitious component I_α and the component I_β is obtained through a phase delay of $\pi/2$ radians, see Equation 3.

$$\begin{bmatrix} I_\alpha \\ I_\beta \end{bmatrix} = \begin{bmatrix} I_L(\theta) \\ I_L(\theta - \pi/2) \end{bmatrix} \quad (3)$$

Once, the dual-phase rotating reference frame dq has been obtained from the dual-phase stationary reference frame, the direct component of current, Id is then obtained using

Equation 4. The line voltage angle is extracted by means of a PLL (Phase Locked Loop) and the DC component of current, Id_{DC} is extracted using a low pass filter (second-order). The shunt APF also regulates the DC bus voltage by making use a PI controller. Difference of the actual DC link voltage and a preset reference is obtained and is given to a PI controller to achieve I_{dc}. This control signal also signifies the over-all active power transmitted from the PV to the DC bus. This signal along with regulation of the DC link voltage also recompenses for the losses. Equation 5[15] is implemented to obtain the sinusoidal reference current for the shunt APF.

$$id = i_{\alpha}.\cos\theta + i_{\beta}.\sin\theta \tag{4}$$

$$i_s^* = \left(Id_{DC} + I_{dc}\right)\cos\theta \tag{5}$$

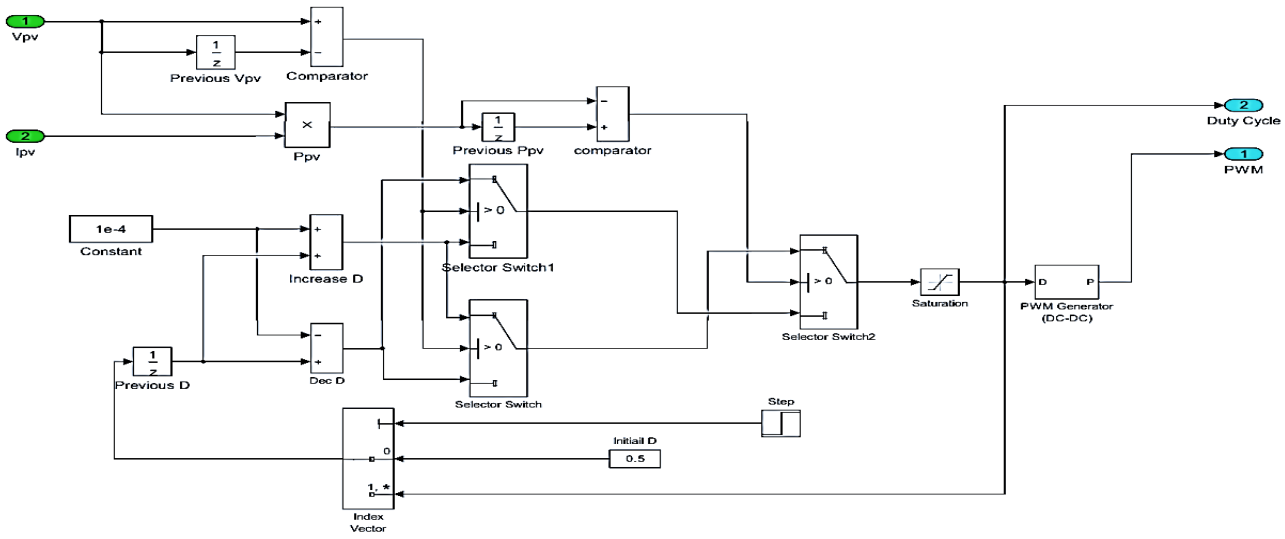

Figure 5. Simulink Diagram of P & O MPPT

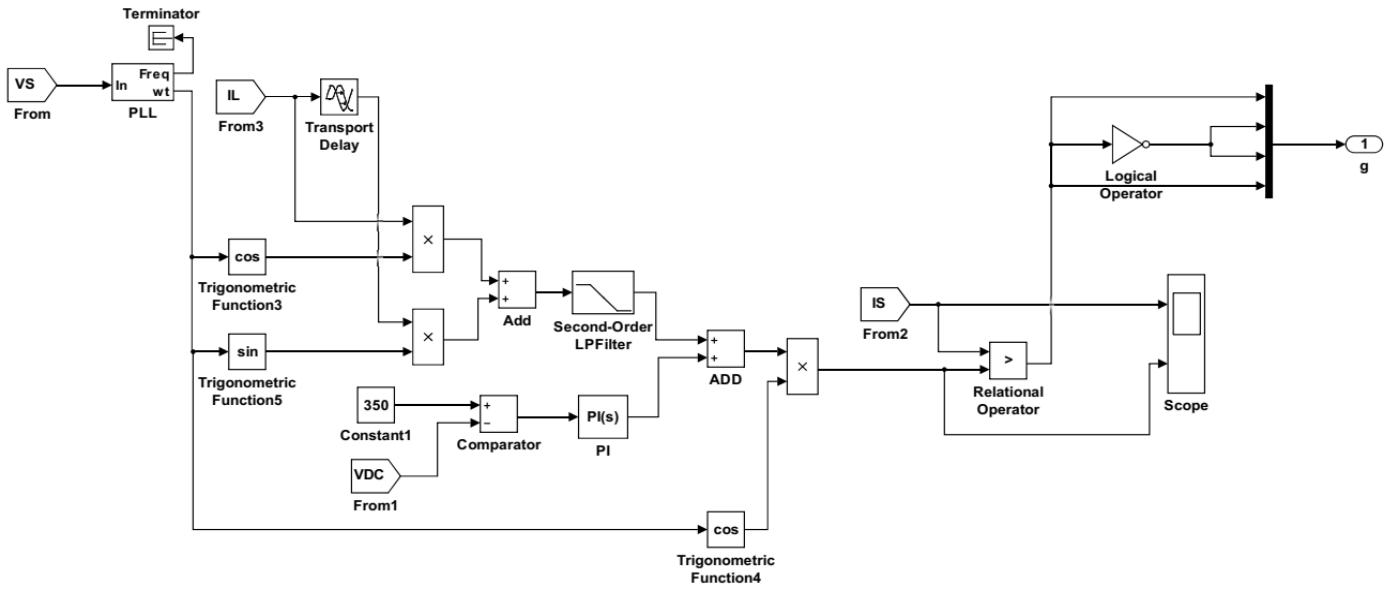

Figure 6. Simulink Diagram for the Control Signal Generation for Shunt APF

C. Series APF Control

This control strategy generates a reference load voltage and compares it to the actual load voltage to get rid of the line voltage distortions. Thus, there is no distortions in the load voltage. The Simulink model of this control strategy is given in Figure 7. The angle of the line voltage is determined by making use of a Phase-Locked Loop (PLL) is acquired to determine the angle of the line voltage and then by using sine function the quadrature unit vector *sin wt* is produced. Then the desired value of amplitude is multiplied with the sinusoidal waveform and in this way the reference load voltage signal is generated. Finally, the actual voltage across the load and the reference load voltage are compared. The output of the comparator is then fed to a hysteresis band controller to generates a switching signal that operates the inverter (Series APF) switches.

D. Utility Grid

This simulation uses a controlled voltage source as a grid to properly apply the voltage-related issues to the system. Harmonics in voltage waveform and voltage sag and swell can be produced through the grid model to check this system under these disturbances. The nominal grid voltage is taken as 230V (RMS) under normal operating conditions.

E. Non-Linear Load

Model of the non-linear load is made up of of a full bridge rectifier. The output of the bridge rectifier is coupled to a resistor. Simulink schematic of the non-linear load is given in Figure 8.

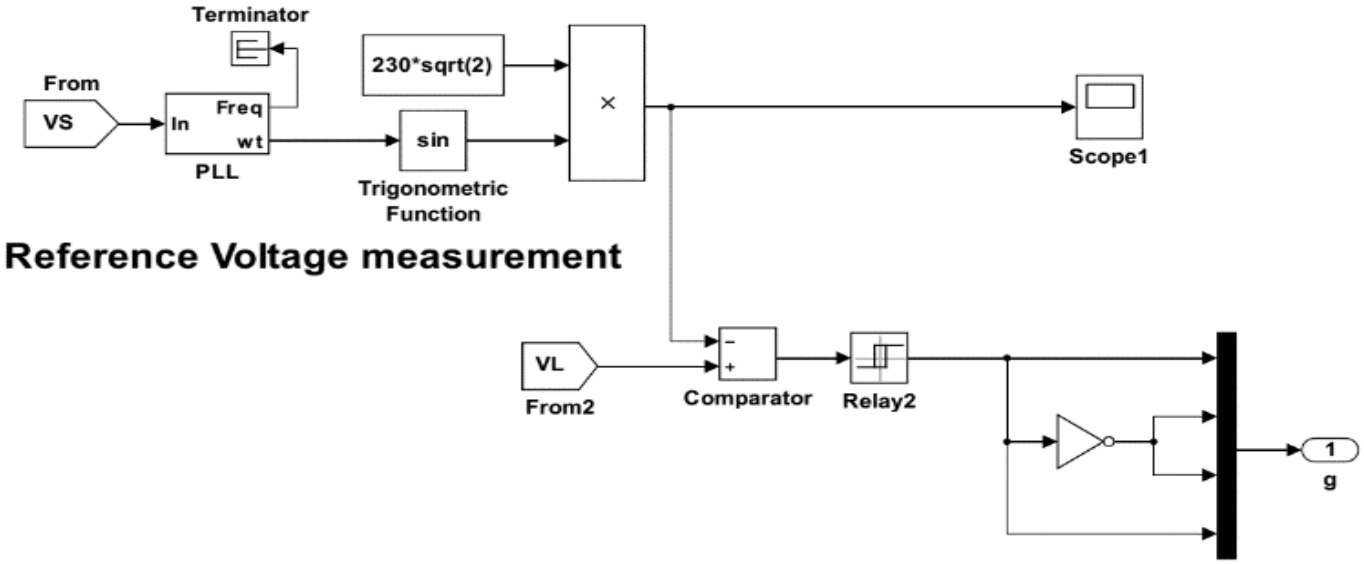

Figure 7. Control Diagram for Series APF

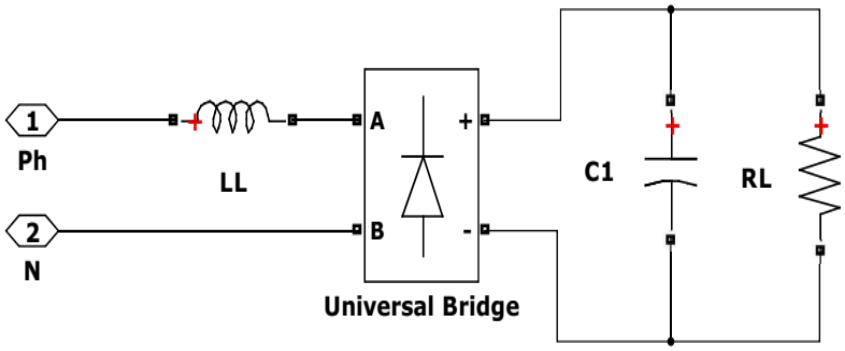

Figure 8. Simulink Diagram of non-linear load

V. SIMULATIONS & RESULTS

The model has been simulated by applying different power quality disturbances and the following cases have been considered.

A. The Load Current Harmonics

The performance of the aproach is analyzed under distorted load current. The waveforms of the distorted load current, shunt APF supplied current and the supply current are shown in Figure 9. THDs (Total Harmonic Distortions) for both the load and supply currents are presented in figures 10 and 11 respectively. Total Harmonic Distortion (THD) of the load current is 104.7%. Waveform and THD of the load current confirm that the load current is entirely distorted by the non-linear load. THD of the supply current is 2.57%. Waveform of the supply current and its THD confirm that the harmonics are successfully blocked from flowing back into the grid. Waveform of the current supplied by the Shunt APF verifies that the current generated by PV go back into the grid, along with the necessary compensation.

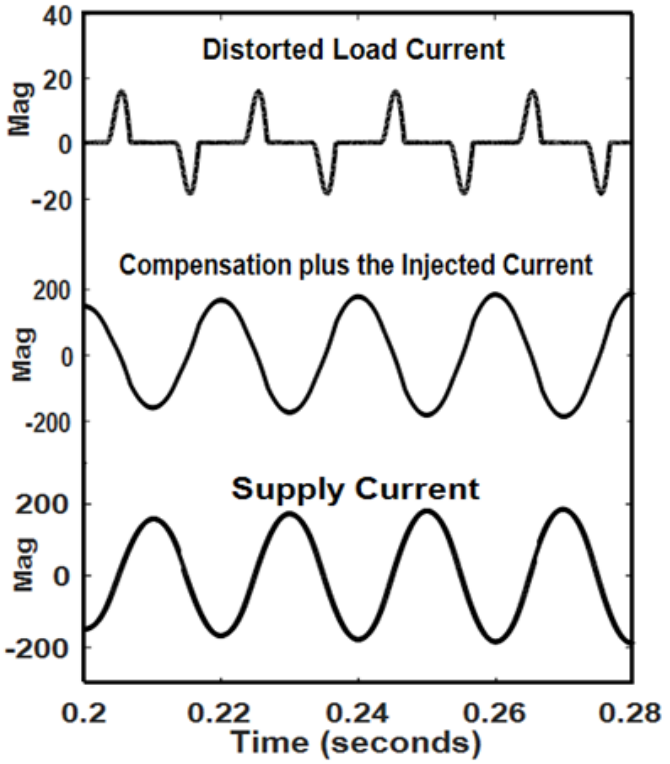

Figure 9. Current Harmonics

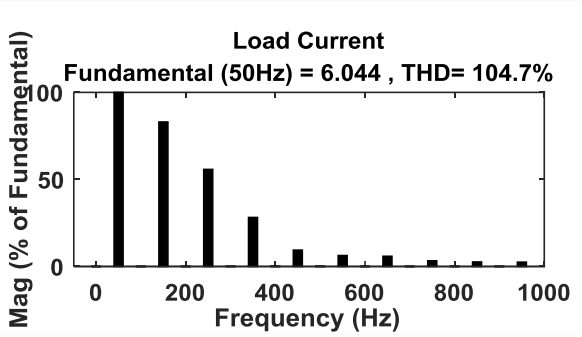

Figure 10. Total Harmonic Distortion

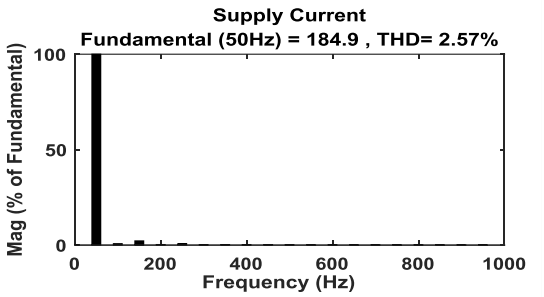

Figure 11. Supply Current THD

B. Voltage Swell

The system is analyzed under voltage swell fault at the supply side. Waveforms of the grid voltage, voltage provided by the series APF and load voltage can be seen in Figure 11. The diagram shows that the required compensation voltage is generated by the series APF and there is no voltage swell on the load side. Thus, the voltage across the load is maintained at the nominal RMS voltage of the grid voltage. Consequently, the sensitive loads are protected against the voltage swell.

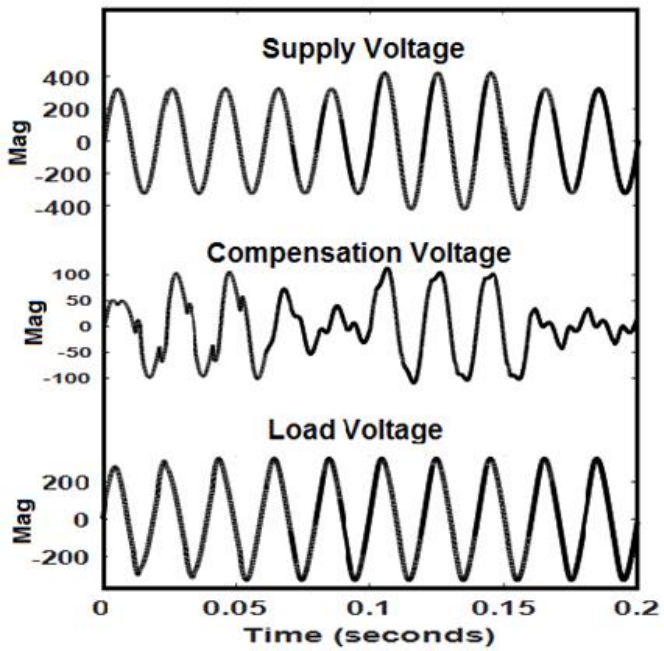

Figure 12. Voltage Swell

C. Voltage Sag

A voltage dip from the grid side is introduced into the system. The line voltage, load voltage and compensation voltage are shown in Figure 13. Waveform of the load voltage shows that there is no voltage sag on the load side. So, the series APF effectively created the necessary compensation to retain the load voltage at the estimated RMS value.

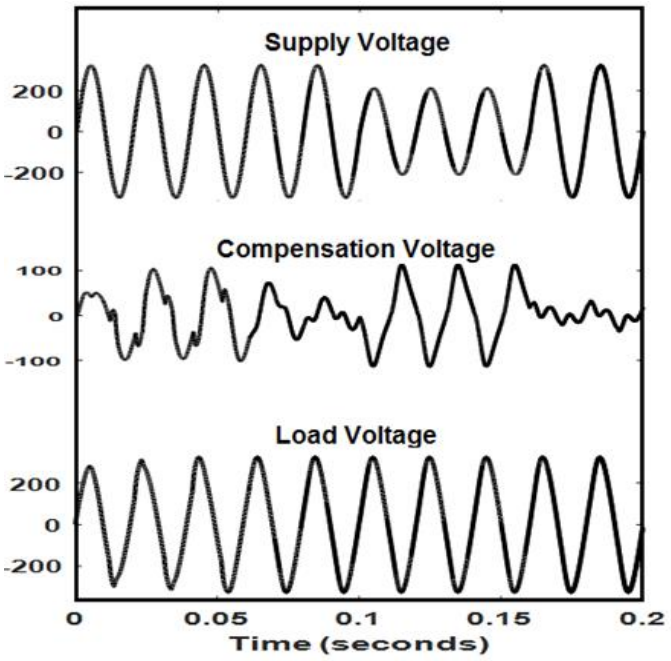

Figure 13. Voltage Sag

D. Supply Voltage Harmonics

The supply voltage is distorted by introducing third, fifth and seventh harmonics. waveforms for different voltages are given in figure 14.

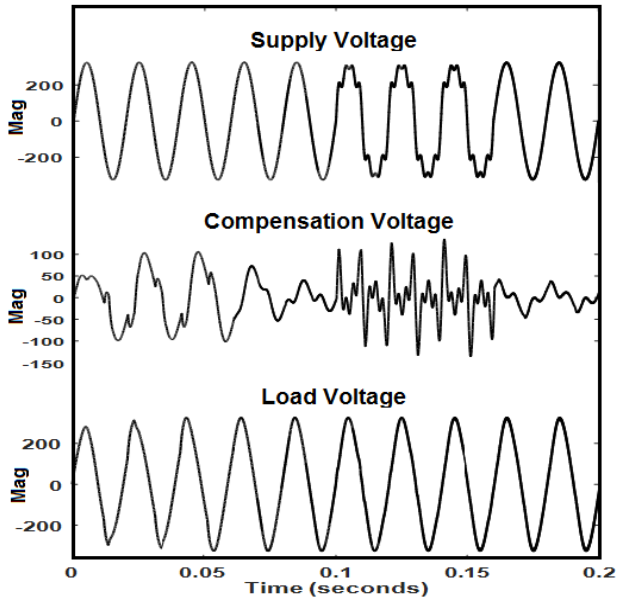

Figure 14. Voltage Harmonics

The grid and load voltage THDs are displayed in figures 15 and 16 respectively. The THD of the load voltage is 4.94% and that of the supply voltage is 21.32%. It is clear from the waveforms and THD values that the harmonics of the supply have been overcome and protection of sensitive load has been improved.

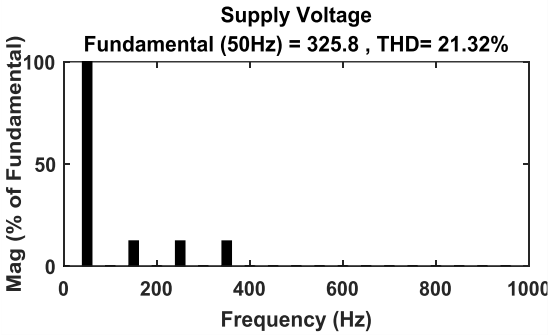

Figure 15. Supply Voltage THD

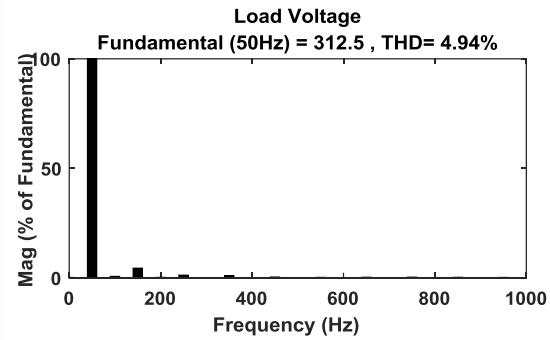

Figure 16. Load Voltage THD

CONCLUSION

A UPQC with PV array at its DC link was implemented and simulated in Simulink/MATLAB. The system was properly explained and the results were thoroughly analyzed. Proper control techniques for the Series and Shunt APFs were implemented to solve the voltage and current related distortions, respectively. An SRF control method was employed for the shunt APF. The compensation current provided by this APF of the system was proved to be successful in removing the current harmonics. This APF was also responsible to send the active power of the PV array to the grid and also maintain the voltage across the DC link at a predefined reference.

PV system with a boost converter was used in the DC link of the UPQC. The MPP operation was ensured using the Perturb and Observe MPPT method.

The system was observed under harmonics in load current and supply voltage. THDs of the voltage and current waveforms were obtained on both the load side and supply sides. The load current THD decreased from 104.7% to 2.57%. In other words, a 97.54% reduction in load current THD was attained. Similarly, THD of the supply voltage was decreased from 21.32% to 4.94% at the load side i.e. a reduction of 76.83% supply voltage THD was attained. Thus,

the THD values observed in simulation verify that the current harmonics were successfully blocked from entering back into the grid and voltage harmonics were blocked to keep the voltage sensitive loads safe. Supply voltage sag and swell faults were also corrected appropriately by the conditioner. In addition to the specified functionality, the PV array active power was successfully exported to the grid by the conditioner.

ACKNOWLEDGMENT

We are glad to show gratitude to our supervisor, Prof. Dr. Naeem Arbab, who is one of the most experienced Professors in the University of Engineering and Technology, for his supervision and directions. Moreover, we want to acknowledge the department of US-PCASE for financially supporting us throughout the course of this research. We are also extremely grateful to the officials of KP Directorate of Science & Technology for facilitating this research work.

REFERENCES

[1] Yahia Bouzelata, Erol Kurt, Rachid Chenni, Necmi Altın, Design and simulation of a unified power quality conditioner fed by solar energy, International Journal of Hydrogen Energy, Volume 40, Issue 44, 26 November 2015, Pages 15267-15277, ISSN 0360-3199.

[2] Akagi H, Watanabe EH and Aredes M. Instantaneous power theory and applications to power conditioning. Wiley-IEEE Press, April 2007, New Jersey, USA.

[3] Patel, Ashish, Hitesh Datt Mathur, and Surekha Bhanot. "A new SRF- based power angle control method for UPQC- DG to integrate solar PV into grid." International Transactions on Electrical Energy Systems 29.1 (2019): e2667.

[4] X. Liang, "Emerging Power Quality Challenges Due to Integration of Renewable Energy Sources," in *IEEE Transactions on Industry Applications*, vol. 53, no. 2, pp. 855-866, March-April 2017. doi: 10.1109/TIA.2016.2626253.

[5] Farhoodnea, Masoud, et al. "Power quality impact of grid-connected photovoltaic generation system in distribution networks." Research and Development (SCOReD), 2012 IEEE Student Conference on. IEEE, 2012.

[6] Renders, Bert, et al. "Profits of power-quality improvement by residential distributed generation." 2007 42nd International Universities Power Engineering Conference. IEEE, 2007.

[7] Devassy, Sachin, and Bhim Singh. "Design and performance analysis of three-phase solar PV integrated UPQC." IEEE Transactions on Industry Applications 54.1 (2017): 73-81.

[8] E. Yao, P. Samadi, V. W. S. Wong, and R. Schober, "Residential demand
side management under high penetration of rooftop photovoltaic units," IEEE Transactions on Smart Grid, vol. 7, no. 3, pp. 1597–1608, May 2016.

[9] A. Parchure, S. J. Tyler, M. A. Peskin, K. Rahimi, R. P. Broadwater, and M. Dilek, "Investigating pv generation induced voltage volatility for customers sharing a distribution service transformer," IEEE Trans. Ind. Appl., vol. 53, no. 1, pp. 71–79, Jan 2017.

[10] Singh, A. Chandra and K. A. Haddad, Power Quality: Problems and Mitigation Techniques. London: Wiley, 2015.

[11] Mahela, Om Prakash, and Abdul Gafoor Shaik. "Comprehensive overview of grid interfaced solar photovoltaic systems." Renewable and Sustainable Energy Reviews 68 (2017): 316-332.

[12] Kumar, Ajay, Nitin Gupta, and Vikas Gupta. "A Comprehensive Review on Grid-Tied Solar Photovoltaic System." Journal of Green Engineering 7.1 (2017): 213-254.

[13] Garg, Akash, R. Saida Nayak, and Susma Gupta. "Comparison of P & O and Fuzzy Logic Controller in MPPT for Photovoltaic (PV) Applications by Using MATLAB/Simulink." IOSR Journal of Electrical and Electronics Engineering (IOSR-JEEE) 4 (2015).

[14] M. A. G. de Brito, L. P. Sampaio, L. Galotto Jr., C. A. Canesin, "Evaluation of the Main MPPT Techniques for Photovoltaic Applications," IEEE Transactions on Industrial Electronics, vol. 60, no.3, pp. 1156-1167, March 2013.

[15] Da Silva, Sérgio A. Oliveira, et al. "Single-phase grid-connected photovoltaic system with active power line conditioning." Power Electronics Journal 20.1 (2015): 8-18.

Niaz Ali has received his B.Sc Electrical Engineering degree from the University of Engineering and Technology Peshawar, Pakistan in 2014. He is currently pursuing his M.Sc Electrical Energy System Engineering from US Pakistan Center for Advanced Studies in Energy, University of Engineering and Technology Peshawar, Pakistan. His major research interests include Solar PhotoVoltaic (PV), MPPT techniques for Solar Photovoltaic, DC-DC converters, Active Power Filters (APFs) and Unified Power Quality Conditioners (UPQCs). Picture is attached.

Professor Dr. Muhammad Naeem Arbab is a Professor in University of Engineering and Technology Peshawar in Electrical Department. He got his Ph.D. from UK and is an author of two engineering books i.e., High Voltage Engineering and Electrical Power Generation and published more than 25 research papers.

Rizwan Kamal has received B.Sc Electrical Engineering degree from department of Electrical Engineering University of Engineering and Technology Peshawar, Pakistan in 2014. He is currently pursuing M.Sc degree in Electrical Energy Systems Engineering from United States Pakistan Center for Advanced Studies in Energy (USPCAS-E) at University of Engineering and Technology Peshawar. He worked on first hybrid renewable energy system of Pakistana which is consist of solar PV, Micro-hydro and Biomass resources installed at Sakhakot, Malakand division KP, Pakistan.

Muhammad Bilal has received his Master's in Electrical Energy System Engineering from from United States Pakistan Center for Advanced Studies in Energy (USPCAS-E) at University of Engineering and Technology Peshawar in 2019. He worked as a research scholar at Power system Lab of Arizona State University U.S.A in 2016. Currently he is working as Assistant Manager in an R & D Department of public sector industry, Pakistan. He is also doing a project on Grid connected 5MW Solar project for that industry with increased efficiency. His major research is in snart micro-grid architecture, control and economic dispatch problems.

IJEW 国际工程期刊 International Journal of Engineering Works انجینئرنگ کاموں کا بین الاقوامی جرنل

International Journal of Engineering Works
ISSN-p: 2521-2419
ISSN-e: 2409-2770
Vol. 7, Issue 01, PP. 10-14, January 2020
https://www.ijew.io/
https://doi.org/10.34259/ijew.20.7011014

Improving the Mechanical Properties of Fine Soil using Marble Waste

Abid Ali[1], Nauman Izhar[2], Qaiser Iqbal[3], Tahir Ahmad[4], Rooh Ullah[5]
[1,4,5] Department of Civil Engineering, University of Engineering & Technology Peshawar, Pakistan
[2,3] Department of Civil Engineering, Sarhad University of Science & Information Technology, Landi Akhun Ahmad, Hayatabad Link. Ring Road, Peshawar, Pakistan
abid.ali@uetpeshawar.edu.pk[1], engrnaumanizhar@gmail.com[2] , qi.civil@suit.edu.pk[3], tahirahmad667@gmail.com[4], roohi.civil@gmail.com[5]
Received: 02 December[2019], Revised: 12 December, Accepted: 05 January

***Abstract*—**In past many researchers used industrial waste to improve soil stabilization as low cost material and to save environment. Keeping this in mind, an attempt is made to evaluate the use of Marble Waste Powder (MWP) to stabilize the spacious clay. Marble industry is producing substantial amount of slurry with fairly good engineering characteristics. In this study, the marble waste slurry has been added to the soil to reduce the permeability of the dam cores. MWP was mixed with the soil with different varying proportions. Laboratory experiment include atterberg limits, liquid limit, hydrometer test, falling head permeability test, moisture density relation test, sieve analysis were performed on the treated and untreated soils. The result revealed that addition of 10-15% of MWP to the soil significantly improve in the density and strength and at the same time reduction in the permeability and plasticity of the stabilized soil with respect to varying moisture conditions is also very much improved..

***Keywords*—** Marble waste powder, stabilization, expansion soil, properties, dam core

I. Introduction

Construction of any structure requires stable ground for its foundation to rest on it and with least possible movement to enhance the life span and utility of the structure. Expansive soil is also called black cotton soil, because of its color and suitability for cotton crops. Expansive clay is the type of soil with most movement compared to sand and gravel because it undergoes heave when it absorbs water and undergoes hogging when it loses water. So that to improve the engineering properties, the expansive soil should be enhanced with soil stabilization method.[1]

Construction on expansive soils has always been a problem for geotechnical engineers so as construction on the weaker soils that inhibit excessive seepage thus making the structures even weaker and less durable. On the other hand the industrial waste disposal has become a major problem all across the globe. The sustainable solution for which is the reuse of the industrial waste rather than disposing it off as it creates more and more health hazards as a result. On the other hand if the disposed material improves the engineering properties of the soils it is an extra edge for the soils.

II. Background

Soil Stabilization is in practice for centuries now, it is required when the soil available for construction is not suitable for the intended purpose. It is used to reduce the permeability and compressibility of the soil mass in the earth embankment and to increase its shear strength [2]. Cohesive soils are most commonly used in dam cores due to their low permeability characteristics but these soil show a quite high degree of loss of strength on wetting. Due to their low strength flat slopes angles are usually required to resist the geostatic stresses. This cause an increase in the size of the core and hence the cost. If the soil is stabilized to increase the strength with a reduction in permeability economical dam cores can be designed. The marble powder classified as Dolomite is a natural agglomerate of Calcium magnesium carbonate, white in colour has a rock forming material that contains extraordinary affinity for water absorption and dispersion.

III. Litrature Review

Marble industry is producing huge quantity of powdered marble waste as increasing in demand for marble product in the construction industry rises the generation of MWP. During the process of cutting marble rocks, the dust of the marble and water mixes together and become waste marble mud where around 25% marble is resulted in dust. The waste produced during the cutting and grinding of marble is very fine but non-plastic (rock flour) and almost well graded.[4]-[7] The particle size of the powdered waste depends on the strength of marble, type of the cutter or grinders and the pressure applied during cutting and grinding. Hard marble and low cutting produces finer particles and vice-versa.[8] The marble powder although non plastic

contains an appreciable colloidal fraction that forms a gel which significantly reduces the permeability and allows deformation without cracking which is desirable for dam cores.[9]

This paper aims to study the use of MWP in different proportion with soil in order to enhance the engineering properties like strength, permeability and plasticity. The current world is facing the shortage of naturally suitable materials for construction, the flip side of this problem is the excessive environmental pollution as a result of this industrialization, the by products are so gigantic in size that they are required to be utilized or quickly being properly disposed. One of the biggest source of pollution is Carbon dioxide, which is causing the depletion of the ozone layer, cement industry alone is generating 10 percent of the total Carbon dioxide produced globally.[10] Researchers focus mainly now on decreasing the pollution sources, by changing fuels, so is the case for construction industry, there are efforts made to utilize the by products like Polyethene, rice husk, baggase ash and marble dust to improve the properties of soil and concrete and the results are fruitful so far. The industrial by products are used as a partial replacement with the conventional material, so they can be called as admixtures, so that the natural resources are sustained for long now.[11] The marble waste can be used in other industries like ceramics, white cement, bricks, infiltration plants and tiles. Other areas of utilization are clinker production and filler materials along with usage in bitumen made pavements.

Okagbue and Onyebi replaced a portion of soil with Marble dust and found a considerable increase in the engineering properties of the soil, after the tests the plasticity of the soil was reduced by 20 percent to about 33 percent and the CBR increased by 27 percent to 55 percent.

Cai et al. investigated the use of lime with soil through Scanning Electron Microscope and found that there was a reaction between lime and the soil, which changed the soil fabric permanently causing an improvement in strength properties of the soil.Al-Mukhtar et al. proved the phenomenon and termed the reaction between the soil and lime as Pozzolanic reaction, that occur micro structural level, not visible with naked eyes. Marble dust decreased the swelling potential of the soil and increased the Unconfined Compressive strength of the soil. In extreme conditions lime was helpful against the freeze and thaw action.

Wishwanthan et al. found that lime and fly ash class F can be used as good stabilizers for sandy and silty bases for highways.

Abdullah Demirbas and Ismail Zorluer found that addition of the lime and fly ash showed an increase in strength after 28 days of curing, because the reactions are slower in the start, an estimated of 3.5 times in strength occurred later on.

Hassini concluded that the impermeable layers cycled much at landfills by performing experiments about freezing and thawing to quantify shear strength and permeability, it was found that 10-15% of grain loss did not had any effect on the strength of the soil.

Zorluer mixed marble dust in variable proportions with soil and then compacted it according to Standard Proctor Compaction test, he also checked for swelling potential in consolidation test, and found that marble dust improved the soil quality against swelling, also the mixing of marble dust with the soil showed an increase in unconfined compressive strength.

Altug SAYGILI found that after mixing clayey soils with different marble dust proportions the engineering properties of soils are substantially improved, the samples were classified into two classes as a result of their plasticity, it was found that high plasticity samples showed better performance in direct shear test and swelling test while the low plasticity test showed better performance in unconfined compressive strength test.

IV. Problem Statement

Marble industry is producing tons of waste each day which is of no use and causes a lot of health hazards and environmental issues it should be used properly to improve soil properties.

V. Objectives

The objective of the study is soil improvement for increasing the strength and control the seepage under dams, with the aim to cope with abundant production of marble waste to use in improving the soil properties and improve environment.

SCOPE: The results are applicable to cohesive fine grained soils with medium plasticity and the waste comprised of the fine marble powder type.

VI. Experimental Proframme

SOIL SAMPLE COLLECTION:

The soil samples were collected from the site of Jalozai small dam, 25km from main GT road on Pabbi-Cheratroad. Samples were collected from 2.5m depth pit-hole. Soil was stiff clay and dark brown in colour as shown in Figure 1.

Figure 1: The Expansive Soilat the Borrow Area

MARBLE WASTE POWDER:

Marble waste was obtained from factories at Warsak Road Pirbala at about 30km from Peshawar. Then the marble stone were crushed into powder as shown in Figure 2.

Figure 2: The Marble Sample as Sold and Powder

PREPARATION AND TESTING

A laboratory testing program was conducted on soil mixed with MWP. Laboratory experiments included atterberg limits (liquid and plastic limit), permeability test, hydrometer test, falling head permeability test, moisture density relation test, sieve analysis. Classification and gradation curves for soil marble powder are shown in the Figure 3.

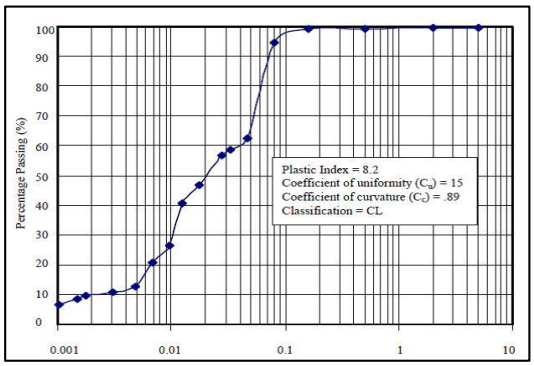

Soil (Marble Powder-0%)

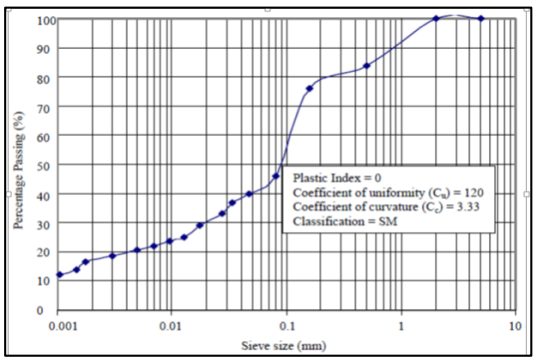

Marble powder

Figure 3: Gradation curve for Soil and marble powder

Marble slurry (white marble) was mixed with the soil and the gradation curves for the different mix ratios (5, 10 and 20%) were drawn and shown in the Figure 4. The Coefficient of uniformity (Cu) and the coefficient of curvature (Cc) were calculated for each gradation curve. The values were then plotted with respect to varying percentages of the marble slurry and are shown in the Figure 5.

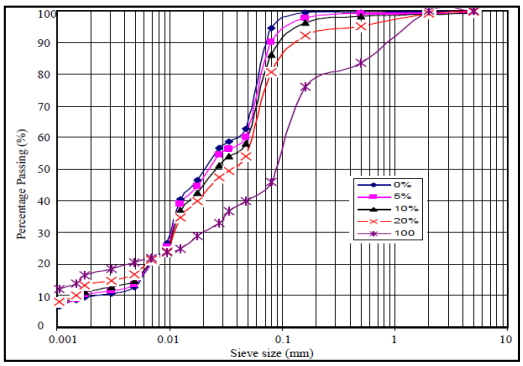

Figure 4: Gradation curve of soil mixed with varying percentage of marble powder

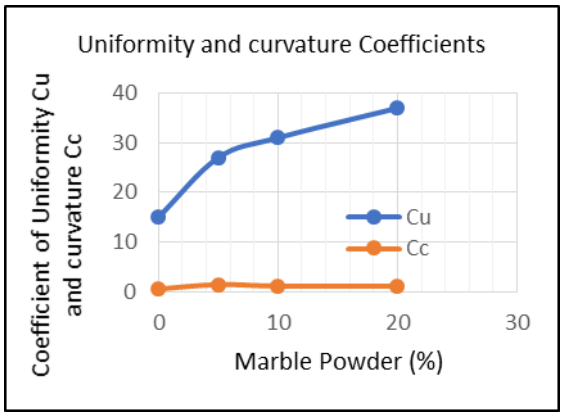

Figure 5: Variation of Cu and Cc of soil mixed with varying percentage of marble powder

The moisture density relationship of the soil- marble powder mixtures, standard proctor compaction test (using 2.5 kg rammer) was performed. The curves were plotted as shown in the Figure 6. The maximum dry density and the optimum moisture content for different mixes were determined.

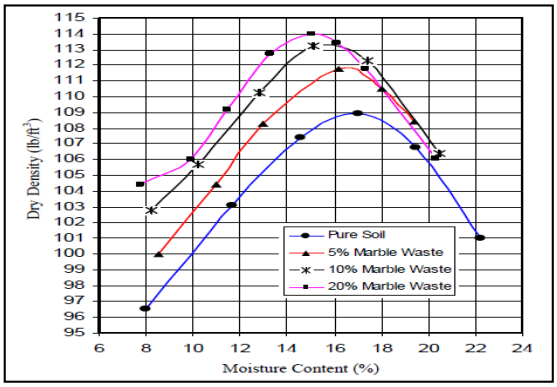

Figure 6: Moisture density curve of soil mixed with varying percentage of marble powder

In order to study the effect of marble slurry percentage on the maximum dry density and the optimum moisture content, curves were plotted and shown in the Figure 7 and Figure 8.

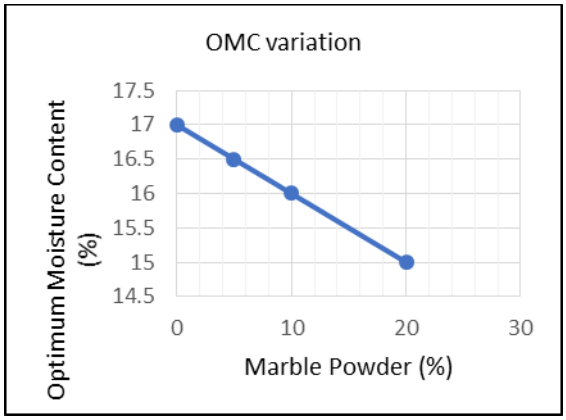

Figure 7: Variation in Optimum Moisture Content with varying Percentage of Marble powder

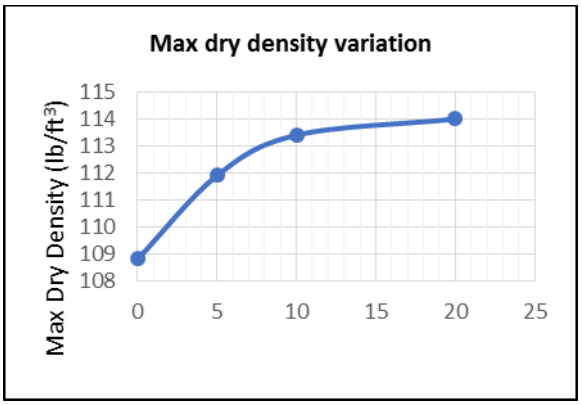

Figure 8: Variation in max dry density mixed with varying Percentage of Marble powder

Different soils-marble powder mixtures were compacted in the permeability test moulds, in three layers using static compaction. The compaction was made at optimum moisture content achieving the maximum dry density as determined in the compaction tests. The permeability value for each mix ratio was determined. The curve of permeability values versus marble powder is plotted and shown in the Figure 9

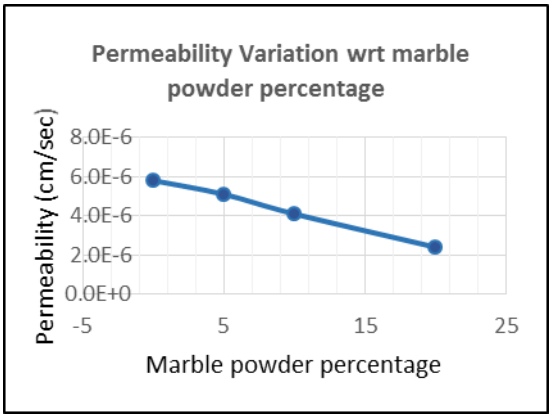

Figure 9: Variation in Permeability of Soil mixed with varying percentage of marble powder

VII. Results and Discussion

Based on size distribution and atterberg limits the soil was classified as poorly graded lean clay of medium plasticity as per USCS standards, it was designated by CL. On the other hand, the marble powder was classified as well graded with non-plastic properties with particle size comparable to that of silt and sand with approximately 13% of particles smaller than 0.001mm (gradation curve shown in Figure 3) according to USCS, classified as SM. Results showed that the addition of marble powder improved the gradation of the soil from poorly graded to nearly well grade with the maximum dry density increased with the increase in the percentage of the marble slurry. The optimal economical dose of marble powder was about 10%. For compaction, the optimum moisture content (OMC) decreased with the increasing percentage of marble powder. Being classified as uniformly graded, it helped in improving structure of the soil having more voids initially to comparatively lesser voids later on, the coefficient of permeability decreased with increasing percentage of the marble slurry.

Conclusion and Recommendations

Overall the study met its desired results of confirming the addition of marble waste to the soil as a 10-15% replacement of soil is feasible for improving the mechanical properties of the soil, by being able to utilize a waste material which is hazardous for health of the near living community mostly causing the breathing problems. Based on the experimental results obtained from this study, finding new utilization areas for waste marble powder will decrease environmental pollution and by the utilizing these wastes material in problematic soils have great contribution to the economy and conservation of resources. Marble powder waste is an excellent material for mechanical stabilization of plastic/ cohesive soils. The soil stabilized with marble powder will give more stable and economical dam cores.

The limit of the marble powder for the maximum improvement in properties ranges from 10-15% however the type of soil and the marble powder will affect the upper limit in other cases.

Depending on the requirement of stabilization, the mix may require to be designed for each project. The results are

representative of the white marble slurry and may not be applied to all types of the marble wastes.

ACKNOWLEDGEMENTS

The authors would like to thank every person/department who helped thorough out the research work, particularly EE department, ORIC and Engr. Dr Munir Ahmed. The careful review and constructive suggestions by the anonymous reviewers are gratefully acknowledged.

CONFLICT OF INTEREST

All the authors declares that there is no conflict of interest.

REFERENCES

[1] Viswanath S.M, What are the difference between clay and black cotton soil?, Durham University 2014

[2] Zumrawi M.M.E, Award M, Effect of Bitumen and Fly Ash on Expansive Soil Properties, Journal of Scientific and Engineering Research, : 228-237,2017

[3] Arora D.K.R, Soil Mechanics and Foundation Engineering 6th Edition, 170S-B, Nai Sarak, Delhi 110006, 903p, 2003

[4] Saygili A, Use of Marble Dust for Stabilization of Clayey soil, J. Mater. Sci, 21(4) 2016.

[5] British standard (BS-1377-part-2). (1990) Method of test for Solid for civil engineering purposes. British Standard Institution. London.

[6] Zumrawi M.M.E, Eltayab K.A Laboratory Investigation of Expansive soil stabilized with calcium chloride. Int. J. Envirom. Chem. Ecol. (2), (2016)

[7] Arora D.K.R, Soil Mechanics and Foundation Engineering, 6th edition, 170S-B, Nai Sarak, Delhi-llOOO6, 903 p, 200

[8] Pappu, A., Saxena, M., Asolekar, S.R. Solid Wastes Generation in India and Their Recycling Potential in Building Materials Building and Environment 42 2007: pp. 2311 – 2320

[9] Saboya, F., Xavier, G.C., Alexandre, J. The Use of the Powder Marble By-Product to Enhance the Properties of Brick Ceramic Construction and Building Materials 21 2007: pp. 1950 – 1960.

[10] Zorluer, I., Usta, M. Stabilization of Soils by Waste Marble Dust Proceeding of the fourth national marble symposium, Afyonkarahisar, Turkey 2003: pp. 297 – 305

[11] Bhavsar S.N, Patel A.J, Analysis of Clayey Soil using Waste Material. Int. J Innov. Res. Sci. Technol. 1(6):125–130, 2014

[12] Zumrawi M.M.E, Awad M, Effect of Bitumen and Fly Ash on Expansive Soil Properties, Journal of Scientific and Engineering Research, 4(9): 228-237, 2017.

[13] Eskioglou, Panagiotis Ch. (1996). Influence of soil type on stabilization with marble dust for forest road construction. Department of Forestry and Natural Environment,Thessaloniki.

[14] Sabat, Akshaya Kumar and Nanda, Radhikesh P. (2005).

[15] Effect of marble dust on strength and durability of rice husk ash stabilized expansive soil. Internat. J. Civil & Structural Engg., 1(4): 939- 94

[16] NA Joulani, Effect of Stone Powder and Lime on Strength, Compaction and CBR Properties of Fine Soils, Jordan Journal of Civil Engineering, 2012, 6(1), 1-16

[17] Saygili, A. (2015). Use of waste marble dust for stabilization of clayey soil. Materials Science, 21(4), 601-606.

[18] Ali, R., Khan, H., & Shah, A. A. (2014). Expansive soil stabilization using marble dust and bagasse ash. Int. J. Sci. Res, 3(06), 2812-2816.

[19] Zorluer, I., & Demirbas, A. (2013). Use of marble dust and fly ash in stabilization of base material. Science and Engineering of Composite Materials, 20(1), 47-55.

[20] Bhavsar, S. N., Joshi, H. B., Shrof, P. K., & Ankit, P. J. (2014). Impact of marble powder on engineering properties of black cotton soil. Int. J. Develop. Res, 3, 158-163.

[21] Fırat, S., Yılmaz, G., Cömert, A. T., & Sümer, M. (2012). Utilization of marble dust, fly ash and waste sand (Silt-Quartz) in road subbase filling materials. KSCE Journal of Civil Engineering, 16(7), 1143-1151.

IJEW 国际工程期刊 International Journal of Engineering Works انجینئرنگ کاموں کا بین الاقوامی جرنل

International Journal of Engineering Works
ISSN-p: 2521-2419
ISSN-e: 2409-2770
Vol. 7, Issue 01, PP. 15-21, January 2020
https://www.ijew.io/
https://doi.org/10.34259/ijew. 20.7011521

Multiband Microstrip Patch Antenna for 5G Wireless Communication

Waqar Hussain[1], M.irfan Khattak[2], Mushtaq A.K.Khattak[3], Muhammad Anab[4]
[1,2,3,4]UET Peshawar, Pakistan
w.hussain@uetpeshawar.edu.pk[1]
Received: 05 August[2019], Revised: 20 October[2019], Accepted: 06 January

Abstract— In current time's an immense proliferation occurred in the user's density of wireless communication, not so far but in near past one channel was enough for the necessities of a single mobile user. Now even 4G technology is inadequate to deliver its clienteles a wider bandwidth, gain and fast communication. For need of high hasten communication technology alteration is under way and is switching from 4G to 5G. For multi-channel communication necessity, communicating gadgets are integrated with multiple bands having peculiarity to work on disparate frequency channels in a single device. In this projected work microstrip patch antenna is used as communicating tool and analyzed for one band and dual band communication at higher frequencies (mm-waves). Microstrip patch antenna is selected because of its simple design, low price, compactness and compatibility with circuit elements. A dual band U-shaped slotted Microstrip patch antenna with 28GHz and 38GHz operating bands is presented in this paper. The total area of antenna is$8.5 \times 8 \times 0.254mm^3$, the substrate used in designing is Rogers RT 5880 having a dielectric constant 2.2. The antenna resulted in return loss of -32dB at 28GHz and -40dB at 38GHz. The simulated gain of proposed dual band is 6.7dB at 28GHz and 7.92dB at 38GHz.

Keywords— MPA, Microstrip antenna array, 5G, mm-waves, Return Loss.

I. INTRODUCTION

. The user density is increasing day by day there is a big difference between the current density of users now and a few years ago after each year a large number of new users get access to the channel, therefore there is a prominent development in the arena of wireless technology, As the user density is aggregate similarly higher data rates and wide bandwidth increase the importance to accommodate that massive user density, it is indispensable to provide them multiple channels so that they can get uninterrupted service, in current era the field of 5G is emerging, now communication will takes place on higher frequencies (mm-band), therefore to allot the users high data rates various techniques are used linked with antenna to meet the requirements of higher number of users, for this purpose multiband antennas are usually used with diverse optimization approaches like using of array , slot or MIMO approach in recent era MIMO approach plays an gigantic role in providing higher emitted efficiency of the emitted EM waves both in near and far field regions and the data rate is quite high, both in 4G and now in 5G.when you have to provide access to multiusers at a time you will need a vast quantity of broad casting devices on both side via transmitter or receiver [1], by proper enactment of Slot, MIMO or Array approach, there is an extreme development in data rate, user allotting and handling aptitude. The mm frequency bands at the present time are under consideration around the globe because it is the probable sturdy entrant for meeting the congested user density [2]. Research is proceeding on the mm bands that come under the umbrella of 5G, these mm frequencies ensembles are comprised of 28GHZ, 38GHZ, 60GhHZ some even work on more than 70 GHz. In broadcasting devices antenna act as imperative player in wireless system. The radiated waves usually in mm bands agonize after atmospheric fascination, it include the issue of path loss also. Therefore the manufacturing and outline of an antenna has two main concerns, first a high gain and second a covenant size which is nothing more than a challenge. Bandwidth amplification and dimensions detraction are appropriate prevailing design politeness for the pragmatic consumption of MPA [4], it is indispensable for an antenna element to have a low profile dimension, low budget, to have the peculiarity to work on distinct mm bands. Enormous research considerations have been adopted with multiband antenna devices that utilize the mm bands [5]. A profound number of designs employed on mm bands are addressed in today era and are appropriate for 5G [5], the architecture of a circular geometrical alignment of MPA is illustrated in [6] with a slot acquainted in patch operating at 28GHz, one MIMO outline which is investigated in [7] works on three dissimilar bands. This design is composed of 2D antenna having an introduced slot designed for 28GHz band. In [8] an MPA antenna has been depicted with multiband peculiarity and used slot technique for 2x4MIMO attaining of multiband characteristics, the projected design is set up above the dielectric material made of FR4 having **k**=4.2 & 1.6mm thickness, it resonates at 7.4 GHz possess a 308 MHz bandwidth along with 9.68 GHz, 12.04 GHz & 12.86 GHz under the stag frequency range of 4.8 GHz. The antenna has return loss of -21.45 dB, -33.51 dB, -16.48 dB and - 10.78 dB at operating frequencies. For gain enhancement researches are

focusing on antenna arrays like one illustrated in [9] in which MPA (parasitic) comprised of 42-elements is capable of working on mm-wave frequencies, antenna provides 6.3% FBW and 1.96 VSWR for frequencies varying from 26.83-28.56GHz. Antennas intended for 5G technology is projected to be minor in size with elevated gain as compared to others that are utilized for both 3G, 4G networks. 5G antennas require extra
innovative steering and scanning approaches with the aim to act adequately. It offers the likelihood possession of extended channel frequency extent conceivably varying from 1 to 2 GHz, a 4 element double band printed antenna array with slots formation for 5G is depicted that offers an adequate impedance matching at 28/38 which are sought bands in mm waves, |S11| is lower than -10 dB, having 10.58 dB gain at 28 GHz and 12.15 dB at 38 GHz [10]. Numerous configurations are delineated in [11] and [12] for bandwidth augmentation, for instance enlarging the thickness of dielectric material (substrate), usage of a small truncated substrate, the adoption of miscellaneous tactics for impedance equivalency and patch invigorating, the adoption of diversified resonators [13], use of aperture coupling fed technique in [14], the utilization of slot antenna for gain melioration [15] or acquainting of thickened parasitic patch substrate [16].

A dual band U-shaped slotted Microstrip patch antenna is designed for 5G technology with 28GHz and 38GHz as operating bands. In first phase of designing a single band Microstrip patch antenna with Rogers RT 5880 substrate and 2.2 dielectric constant was designed and analyzed for 28GHz band, substrate has $8 \times 8.5 mm^2$ dimeniosn with 0.254mm hight.The single band is fed by inset fed line approach, the projected single band antenna has a return loss of -48dB at 28GHz and VSWR less than 2. For attaining the multiband features two U-shaped slots were introduced in patch design, two distinct bands of 28GHz and 38G were attained with the help of these inserted slots, the proposed dual band slotted microstrip patch antenna has gain of 6.7dB at 28GHz and 7.92dB at 38GHz respectively. The dual band has a return loss of -32dB at 28GHz and -40dB at 38GHz band.

II. DESIGN OF SINGLE BAND MICROSTRIP PATCH ANTENNA

The substrate used in design of single band MPA antenna is Rogers RT 5880 having $\varepsilon_r = 2.2$ and $8 \times 8.5 \times 0.254\ mm^3$dimensions, total area of radiating patch is $3.27 \times 4.09 \times 0.035\ mm^3$. For excitation of patch inset feed approach is used. The designed single band antenna is analyzed at 28GHz frequency. The parameters used for designing of said antenna is projected in table 1.

TABLE I DESIGNING PARAMETERS OF SINGLE BAND MPA

Description	Values	Parameter
Substrate length	8 *mm*	L_s
Substrate width	8.5 *mm*	W_s
Substrate height	0.254 *mm*	h_s
Patch length	3.27 *mm*	L_p
Patch width	4.09 *mm*	W_p
Feedline length	3.12 *mm*	L_f
Feedline width	0.782 *mm*	W_f

The width of inset feedline cut is $0.411mm$.The listed mathematical equations were used in calculating the dimensions of designed single band MPA like equation (1) for width calculation, equation (2) for calculation of effective length, equation (3) for factual length, and (4) for determination of feedline width

$$w = \frac{c}{2f_r\sqrt{\frac{er+1}{2}}} \ldots\ldots\ldots\ldots\ldots(1)$$

$$L_{eff} = \frac{c}{2f_r\sqrt{\varepsilon_{reff}}} \ldots\ldots\ldots\ldots(2)$$

$$L = L_{eff} - 2\Delta L \ldots\ldots\ldots\ldots (3)$$

$$w_f = \left(\frac{377}{Z_o\sqrt{\varepsilon_r}}\right) h \ldots\ldots\ldots\ldots\ldots (4)$$

The front and perspective view of designed Microstrip patch antenna is delineated in figure 1

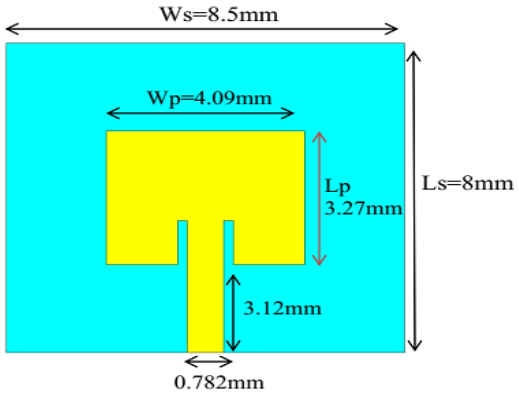

(a)Front view

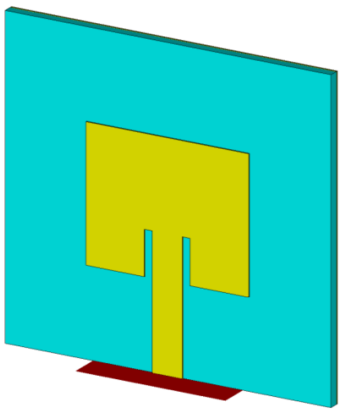

(b)Perspective View

Figure 1: Front and perspective view of designed single band MPA is delineated

After simulation at 28GHz operating frequency the designed single band MPA resulted with return loss of -48dB and voltage standing wave ratio in between 1 and 2. The simulated results for both S11 and VSWR are delineated in figure 2 and 3 respectively

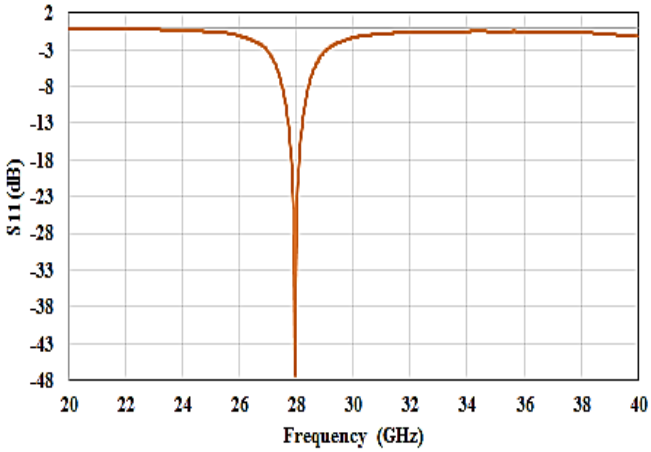

Figure 2: S11 of single band MPA at 28GHz frequency

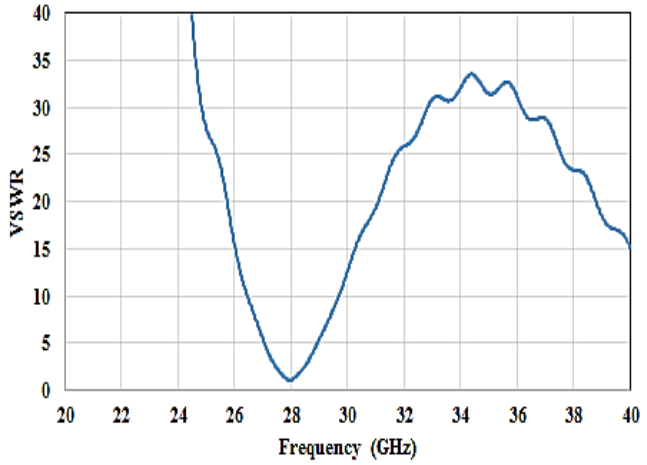

Figure 3: VSWR of single band MPA at 28GHz frequency

III. INSERTION OF U-SHAPED SLOTS IN PATCH

Owing to addition of two U-shaped slots in patch of prior designed single band MPA, an additional 38GHz band was attained. Due to the insertion of slots the proposed antenna got multiband characteristics. The substrate used in designing of proposed dual band antenna is of Rogers RT 5880 with epsilon 2.2. Total area of the proposed antenna is $8 \times 8.5 \times 0.254 mm^3$ .An inset feedline of 50Ω is provided to patch. Designing parameters of substrate, patch, feedline and slots along with description are delineated in table 2.

TABLE II DESIGNING PARAMETERS OF PROPOSED DUAL BAND SLOTTED MPA

Parameters	Values	Description
L_s	8 *mm*	Length of substrate
W_s	8.5 *mm*	Width of substrate
L_p	3.27 *mm*	Length of patch
W_p	4.09 *mm*	Width of patch
L_f	3.12 *mm*	Length of feedline
W_f	0.782 *mm*	Width of feedline
H	0.254 *mm*	Height of substrate
Mt	0.035 *mm*	Thickness of patch
Wc	0.411 *mm*	Width of inset feed cut
W1	1.6 *mm*	Slot width
L1	1.20 *mm*	Slot length
Mx	0.2 *mm*	Space between two slots
D1	0.245 *mm*	Distance between patch and slot length
D2	0.37 *mm*	Distance between patch and slot width
T1	0.2 *mm*	Slot thickness

The front and perspective view of proposed dual band MPA antenna is depicted in figure 4 (a and b).

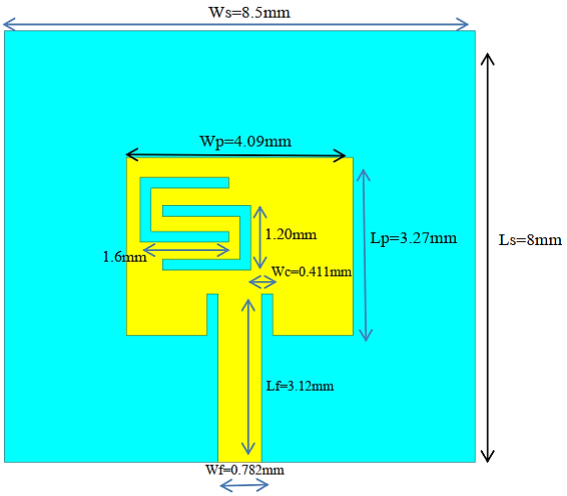

(a)Front view

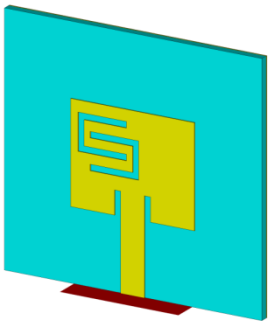

(b) perspective View

Figure 4: Front and perspective view of proposed dual band MPA antenna

The labeled structure of slots introduced in patch is delineated in figure 5

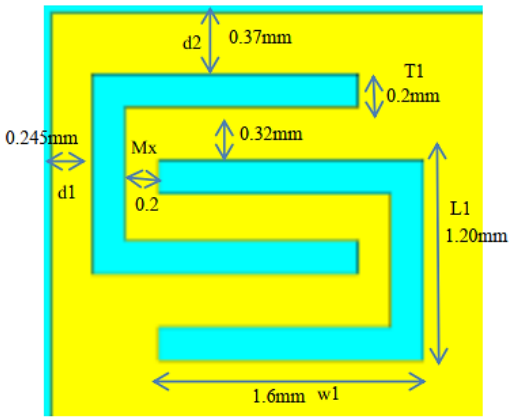

Figure 5: U-shaped slots introduced in patch for dual band peculiarity

Simulations performed on proposed dual band antenna resulted in adequate results in term of return loss, VSWR, gain and directivity both at 28GHz and 38GHz.

IV. Results and Simulations

(A) Return Loss

For an adequate wireless communication S11 should be less than -10dB. The proposed dual band gives a return loss of -32dB at 28GHz and -40dB at 38GHz respectively. S11 of dual band is depicted in figure 6

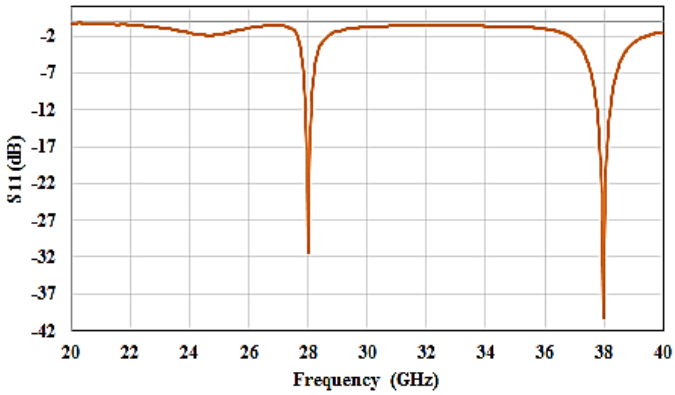

Figure 6: S11 of proposed dual band antenna

(B) Voltage Standing Wave Ratio

For an ample wireless communication VSWR must be less than 2. The proposed dual band antenna resulted in VSWR in between 1 and 2 at both bands which is quite an acceptable result at higher frequencies. The VSWR of the proposed dual band antenna is projected in figure 7.

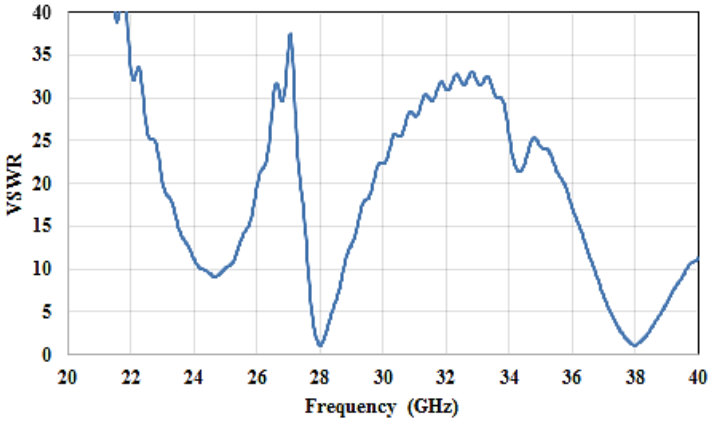

Figure 7: VSWR of proposed dual band antenna

(C) 3-D gain of proposed dual band Antenna

The proposed dual band slotted MPA resulted in a gain of 6.7dB at 28GHz and 7.92dB at 38GHz. The 3D gain at both bands is delineated in figure 8.

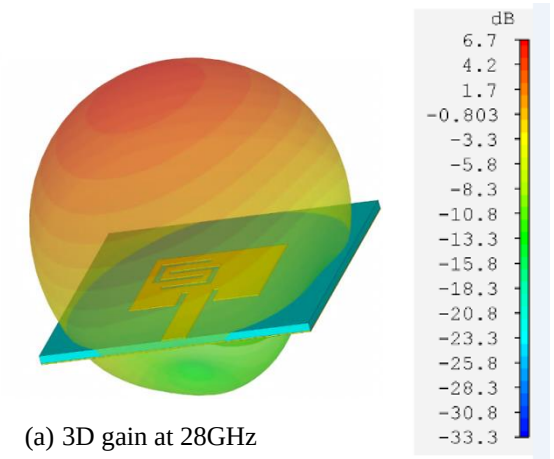

(a) 3D gain at 28GHz

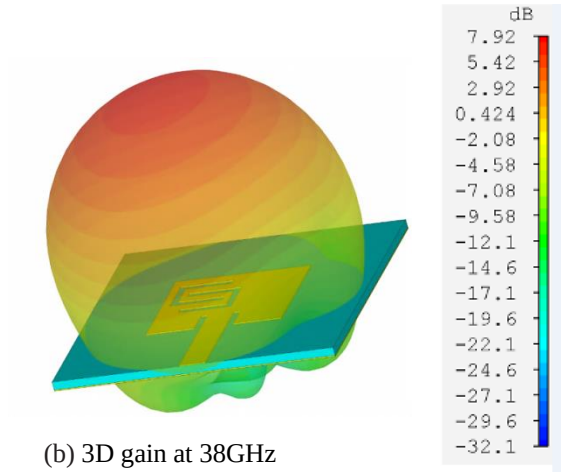

(b) 3D gain at 38GHz

Figure 8: 3-D gain at 28GHz and 38GHz is delineated in this figure.

The gain at both bands in graphical form is depicted in figure 8.

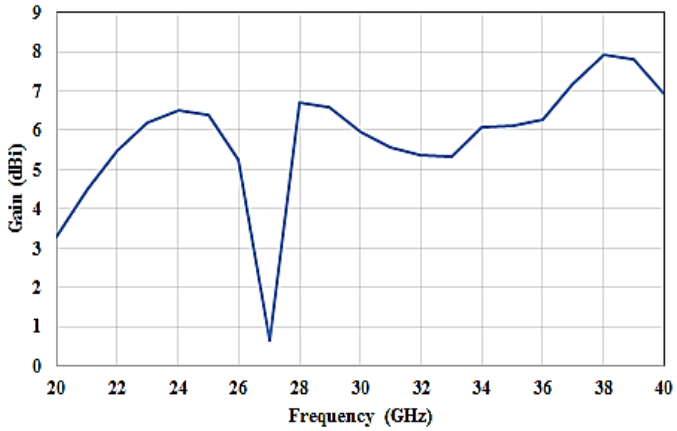

Figure 9: Simulated gain at both bands of proposed dual band antenna

(D) E and H plane of proposed dual band Antenna

The simulated results for E and H planes in polar form at both bands are depicted in figure 9.

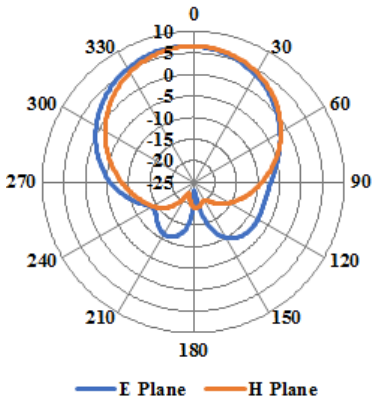

(a) E and H plane at 28GHz

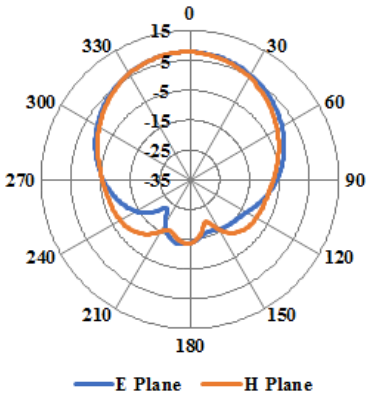

(b) E and H plane at 38GHz

Figure 10: E-plane and H-plane at 28GHz and 38GHz is depicted in this figure

The results of proposed dual band slotted MPA is delineated in table 3.

TABLE III RESULTS OF PROPOSED DUAL BAND SLOTTED ANTENNA

Operating Frequencies	**S11**	**VSWR**	**Gain**
28GHz	-32dB	1-2	6.7 dB
38GHz	-40dB	1-2	7.92dB

V. V. PARAMETRIC ANALYSIS OF PROPOSED DUAL BAND ANTENNA

A parametric study carried out on three different antenna parameters to check their impact on performance characteristics of antenna. The first parameter that was altered from its proposed value was patch length (L_p). Patch length was changed from its proposed value 3.27mm to 3.17mm and 3.37mm. At 3.27mm the antenna gives S11 of -32dB at 28GHz and -40dB at 38GHz, when changed to 3.17mm from its proposed value, antenna resulted in a return loss of -22dB at 28GHz and -27dB at 38GHz. At 3.37mm patch length antenna resulted in S11 of -22dB and -24dB.

The second parameter that was carried out for parameter study is width of patch element (W_p). The patch width is altered from its 4.09mm proposed value to 3.99mm and 4.19mm respectively. At 4.09mm proposed patch width antenna gives S11 of -32dB at 28GHz and -40dB at 38GHz whereas at 3.99mm patch width antenna gives S11 of -32dB at 28GHz and -22dB at 38GHz and at 4.19mm antenna gives a return loss of -32dB at 28GHz and -25dB at 38GHz. The third parameter which was investigated for parametric analysis is the distance between slots (Mx), the slots distance was altered from its proposed 0.2mm value to 0.1mm and 0.3 mm. At 0.2mm proposed distance antenna gives -32dB S11 at 28GHz and -40dB S11 at 38GHz, when the distance was changed to 0.1mm, return loss got changed and at 28GHz antenna has given an S11 of -31dB and -25dB at 38GHz similarly at 0.3mm distance S11 are -40dB at 28GHz and -21dB at 38GHz respectively. The parametric analysis of patch length, patch width and distance between slots for S11 is delineated in graphical form in figure 11, 12 and 13.

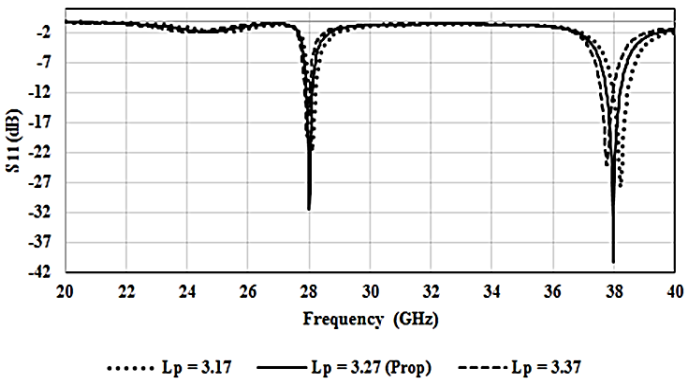

Figure 11: S11 owing to parametric analysis of length of patch element.

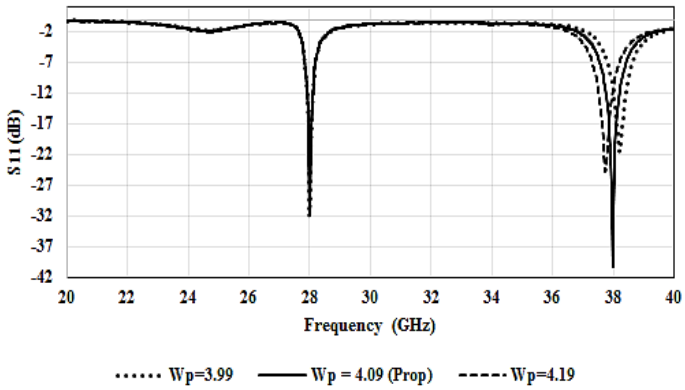

Figure 12: S11 owing to parametric analysis of width of patch element

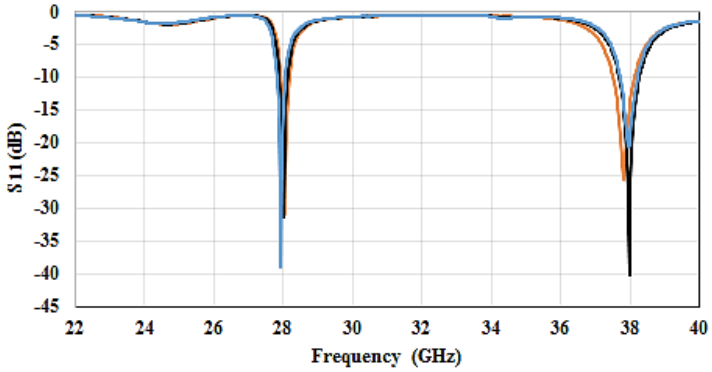

Figure 13: S11 owing to parametric analysis of slots distance

Return loss resulted due to parametric analysis of L_p, $W_p$and $M_x$are depicted in table IV.

TABLE IV TABLE COMPRISED S11 RESULTED FROM PARAMETRIC STUDY CONDUCTED ON Lp,Wp AND Mx.

Parameters	Values	S_{11}(dB)	
		28GHz	38GHz
L_p	3.27 *mm* (proposed)	-32	-40
	3.17 *mm*	-22	-27
	3.37 *mm*	-22	-24
W_P	4.09 *mm* (proposed)	-32	-40
	3.99 *mm*	-32	-22
	4.19 *mm*	-32	-25
M_x	0.2 *mm* (proposed)	-32	-40
	0.1 *mm*	-31	-25
	0.3 *mm*	-40	-21

CONCLUSION

A dual band U-shaped slotted Microstrip patch antenna with the peculiarity to operate at two distinct frequency bands i.e. 28GHz and 38GHz is delineated in this paper. The design comprised of two stages, in first phase a single band MPA was designed for 28GHZ band using Rogers RT 5880 substrate, later that antenna was further enhanced to multiband antenna by addition of two U-shaped slots, owing to insertion of slots communication was enabled on two different bands which are 28GHz and 38GHz. For single band, antenna resulted in S11 of -48dB at 28GHz whereas for dual band, antenna resulted in S11 of -32dB at 28GHz and -40dB at 38GHz. The VSWR for dual band is in acceptable range. The dual band resulted in an acceptable gain of 6.7dB at 28GHz and 7.92dB at 38GHz.

ACKNOWLEDGEMENT

This research is been carried out in Electrical Engineering Department,UetPeshawar.The author is very thankful to Dr.Irfan khattak for his supervision and unstinting help, the author is also grateful and oblige to antenna research team for their valuable support and guidance.

REFERENCES

[1] Babu, K. V. and B. Anuradha, "Design of multi-band minkowski MIMO antenna to reduce the mutual coupling," Journal of King Saud University-Engineering Sciences, 2018.

[2] Ashraf, N., O. M. Haraz, M. M. M. Ali, M. A. Ashraf, and S. A. S. Alshebili, "Optimized broadband and dual-band printed slot antennas for future millimeter wave mobile communication," AEUInternational Journal of Electronics and Communications, Vol. 70, 257–264, 2016.

[3] Sulyman, A. I., A. T. Nassar, M. K. Samimi, G. R. MacCartney, T. S. Rappaport, and A. Alsanie,"Radio propagation path loss models for 5G cellular networks in the 28 GHz and 38 GHz millimeterwave bands," IEEE Communications Magazine, Vol. 52, 78–86, 2014.

[4] Islam, M. T., M. N. Shakib, and N. Misran, "Broadband EH shaped microstrip patch antenna for wireless systems," Progress In Electromagnetics Research, Vol. 98, 163–173, 2009.

[5] Hong, W., Z. H. Jiang, C. Yu, J. Zhou, P. Chen, Z. Yu, et al., "Multibeam antenna technologies for 5G wireless communications," IEEE Transactions on Antennas and Propagation, Vol. 65, 6231–6249, 2017.

[6] Khattak, M. I., A. Sohail, U. Khan, Z. Barki, and G. Witjaksono, "Elliptical slot circular patch antenna array with dual band behaviour for future 5G mobile communication networks," Progress In Electromagnetics Research C, Vol. 89, 133–147, 2019.

[7] Kumar, A., A. Q. Ansari, B. K. Kanaujia, J. Kishor, and N. Tewari, "Design of triple-band MIMO antenna with one band-notched characteristic," Progress In Electromagnetics Research C, Vol. 86,41–53, 2018.

[8] Razin Ahmed,Md.Fokhrul Islam, "Slotted Microstrip patch antenna for multiband application." International Electrical Engineering Journal (IEEJ), Vol. 5 (2014) No.3, pp. 1293-1299,ISSN 2078-2365.

[9] Philip Ayiku Dzagbletey, Young-Bae Jung, "Stacked Microstrip Linear Array for Millimeter-Wave 5G Baseband Communication." DOI 10.1109/LAWP.2018.2816258, IEEE Antennas and Wireless Propagation Letters.

[10] Haraz, O., Ali, M.M.M., Elboushi, A. and Sebak, A.R. (2015) Four-Element Dual-Band Printed Slot Antenna Array for the Future 5G Mobile Communication Networks. 2015 IEEE International Symposium on Antennas and Propagation & USNC/URSI National Radio Science Meeting, Vancouver, 19-24 July 2015, 1-2.https://doi.org/10.1109/APS.2015.7304386

[11] Choi, S. H., J. K. Park, S. K. Kim, and J. Y. Park, "A new ultrawideband antenna for UWB applications," Microwave and Optical Technology Letters, Vol. 40, No. 5, March 5, 2004.

[12] Deshmukh, A. A. and G. Kumar, "Formulation of resonance frequency for compact microstrip antennas," IEEE Antennas and Propagation Society International Symposium, 2006.

[13] Kumar. G. and K. C. Gupta, "Broad-band microstrip antennas using additional resonators gap-coupled to the radiating edges," IEEE, Trans. Antennas and Propagate. Vol. 32, 1375-1379, 1994.

[14] D. M. Pozar, "Microstrip Antenna Aperture Coupled to a Microstrip line," Electronics Lett., Vol. 2, pp. 49-50, 1985.

[15] B. Suryakanth and S. N. Mulgi, "Slot loaded rectangular microstrip antennas for multiband operation," World Journal of Science and Technology Vol. 2, No. 10, pp 98-101, 2013

[16] Nishiayama, E. and M. Aikawa, "Wide-band and high gain microstrip antenna with thick parasitic patch substrate," IEEE, Trans. Antennas and Propagate, pp. 273-276, 2004.

Waqar Hussain: The author belong to district Nowshera,khyberpakhtunkwa pakistan.He did his BS in BEE department from comsats Abbottabad campus and now completed his MS degree in Electrical (communication) Engineering from Uet peshawar.

.

IJEW 国际工程期刊 International Journal of Engineering Works انجینئرنگ کاموں کا بین الاقوامی جرنل

International Journal of Engineering Works
ISSN-p: 2521-2419
ISSN-e: 2409-2770
Vol. 7, Issue 01, PP. 22-26, January 2020
https://www.ijew.io/
https://doi.org/10.34259/ijew.20.7012226

Speech Sources Separation Based on Models of Interaural Parameters and Spatial Properties of Room

Muhammad Israr[1], Muhammad Salman Khan[2], Khushal Khan[3]
[1,2,3] Department of Electrical Engineering, University of Engineering and Technology, Peshawar, Pakistan
muhammad.israr@uetpeshawar.edu.pk[1]
Received: 07 January, Revised: 16 January, Accepted: 18 January

***Abstract*—** This paper presents the extended evaluation in different reverberant scenarios for different mixtures of speech having interfere at one of the six angles {15^0, 30^0, 45^0, 60^0, 75^0, 90^0 } of the model which implementing spatial covariance with interaural parameter for improving the performance of MESSL. The binaural spatial parameters, such as interaural phase difference IPD and interaural level difference ILD and spatial covariance are modeled in the short-time Fourier transform. The parameters of the model are updated with the expectation-maximization algorithm. The performance of the model is checked in term of Signal-to-distortion ratio (SDR) and the perceptual evaluation of speech quality (PESQ), and the results confirmed that the performance of this proposed model is improved in highly reverberant rooms.

***Keywords*—** MESSL, Spatial covariance, SDR, PESQ, MESSL+SC

I. INTRODUCTION

Humans are mostly interested to focus theiraattention only on the speech of a single speaker, while other speakers and back ground noise is exist [1]. This ability is greatly reduced when someone is listening with one ear, especially in reverberant environment. For example in automatic speech recognition the machine focus on a speaker of interest and separate speaker from background noise[2][3]. The process of automated separation of sources from measured mixtures without any prior information is known as blind source separation (BSS)[4]. In blind sources separation the sound sources are separated from the mixtures in which both the numbers of mixtures and sources are unknown and only mixtures signals are available. In some situations we want to recover all individual sources from the mixture signal, or at least a specific source[5]. In laboratory conditions most of the algorithms perform fine where number of sources present in mixtures, mixing methodology and acoustic condition are already known before the separation of sources from mixtures. But in real life scenario this problem is much more complex.

The solution for source separation problem is proposed by researchers belongs to different communities[6][7][8][9]. Examples included convolution in frequencyadomain, blindasource separation (BSS), beamforming and computational auditory scene analysis (CASA). Underdetermined problem in sound sources separation, where the numberaofasources is more than the number of sensors can be handle through TF approach[10]. In timeafrequency (TF) masking for source separation, by exploiting these cues, the mask for each source can be obtained and hoped that only a single sourceaisaactive at each TF unit. CASA is a "machine listening" system that separate mixtures of sound sources in the same way that human listeners do. It uses cues like pitch, onset/offsetatime, interauralaleveladifference (ILD) and interauralatime difference (ITD) to separate the sources[11].

In this thesis speech sources are separated by using a CASA approach which perform sources segregation on the base of interaural parameters such as interauralaleveladifference (ILD), interauralaphaseadifference (IPD) and spatial properties of the room. The modelaparameters are determined by using the EMaAlgorithm.

The observation and initial values of the parameters are used for estimation of probabilities in E-step. These parameters for the model are updatedabased on the measurementsaand the posterior probabilitiesafrom theaE-step. Theaproposed model produces probabilistic TFamasks for single sourcesathat are used for theirareconstruction.

II. MOTIVATION AND OBJECTIVE OF THE WORK

The main motivation in Blind Source Separation (BSS) is the cocktail party problem. Imagine someone is in a loud party, he is trying to convey his voice message to his friend. During this conversation the sounds received at the listener's ear is mixture of the voice of different musical instruments, people and so on. The signal arrived to the ear is in single wave form containing all sounds, and still listener is able to understand talk from this mixture[2][1].

For music students the sound source separation is an important tool by which he can separate a single instrument if many instruments are active simultiously. Similarlrly, the ability to remove an instrument from recording is also useful, as it would allow a student to play a different instrument in the orignal track in place of the removed instrument[12][13].

III. OVERVIEW OF PROPOSED ALGORITHM

Some statisticalaproperties of the sourcesaprovide a base for separation of sound sources[14]. The common statistical assumption made in our model are that the sources are

statisticallyaindependent, statisticallyaaorthogonala and nonstationarya[7][5][15].

The reverberant mixtures at left and right microphones are represented as $l(t) = \sum_{i=1}^{I} s_t\ (t) * h_{li}(t)$, and $r(t) = \sum_{i=1}^{I} s_t\ (t) * h_{ri}(t)$. In this expression s_i show sources, h_{li} represent the Roomaimpulsearesponse RIRafrom the source s_i to the left microphone, h_{ri} represent the Roomaimpulsearesponse RIRafrom the source s_i to the right sensor, and "*" show theaconvolution.

A. The ILD, IPD and spatial covariance models

The interauralaspectrogram, the ratio of leftaandaright mixture at every TF point is given by equation $\frac{L(t,\omega)}{R(t,\omega)} = 10^{\frac{\alpha(t,\omega)}{20}} e^{j\varphi(t,\omega)}$ where $\alpha(t,\omega)$ is the ILD measured in dB while $\varphi(t,\omega)$ isaIPD at frequencyaω and "t" is time. TheaIPD must exist in the range of $[-\pi,\pi)$ [16]. For ILD and IPD each source are frequency-dependent and is given as $\tau(\omega)$, and $\alpha(\omega)$ [15]. The model requires that Fourier transform window used, 1024 points (64ms) must be larger than maximum ITD of ≈0.75ms. We use a top down approach where ITD is measured in term of IPD. The phase residual error, which is defined as difference between IPD observed and IPD predicted is given by equation $\varphi(\omega,t,\tau) = \frac{L(t,\omega)}{R(t,\omega)} e^{-j\omega\tau}$. The phase residual error is modeled with a normaladistribution with frequency-dependentamean $\xi(\omega)$ andavariance $\sigma 2\ (\omega)$[17],

$$p\big(\varphi(\omega,t)\big|\tau\ (\omega),\sigma(\omega)\big) = N\ (\hat{\varphi}(\omega,t;\ \tau\ )|\xi(\omega),\sigma^{2}(\omega)).$$

The ILD is also modeled with a normal distribution with mean $\mu(\omega)$ and variance

$$\eta^{2}\ (\omega), p(\alpha(\omega,t)|\mu(\omega),\eta^{2}\ (\omega)) = N\ (\alpha(\omega,t)|\mu(\omega),\eta^{2}\ (\omega)).$$

Signal $x(\omega,t)$, is mixture signal consisting spatial images of I sources mixed with each other in present each channel. This can be easily modeled as a zero-mean Gaussian distribution with the covariance matrix [16].

$$R_x(\omega,t) = \sum_{i=1}^{I} v_i(\omega,t) R_i(\omega)$$

In above equation $v_i(\omega,t)$ show scalar variance while $R_i(\omega)$ is the covariance matrix containing the spatial properties of the source i. [18][19] The probability distribution of the proposed method is given by [16].

$$P(x(\omega,t)|\{vi(\omega,t), Ri(\omega), \forall\ i\}) = \frac{1}{det(\pi Rx(\omega,t))} exp(-x\ H(\omega,t) R^{-1}\ x\ (\omega,t) x(\omega,t))$$

Where $(\cdot)^{H}$ is the Hermitian transpose.

B. Expectation maximization and source separation

Theainterauralatimeadifference (ILD), interauralaphase difference (IPD) discussed in MESSL model [1] and the spatial covariance models, are combined [6] in this paper and new model has been formed which is combination of MESSL and Spatial covariance model. For determining the parameters of the models the expectationamaximization algorithm is used foraitsasolution. Their corresponding parametersaas

$$p(\alpha(\omega,t),\varphi(\omega,t),x(\omega,t)|\Theta) = N\ (\alpha(\omega,t)|\mu(\omega),\eta^{2}\ (\omega)) \cdot N\ (\hat{\varphi}(\omega,t)|\xi(\omega),\sigma^{2}\ (\omega)) \cdot N\ (x(\omega,t)|0,R_x(\omega,t))$$

All the model's parameter is given in a vector represented by Θ and its equation is given as

$$\Theta\ = \{\mu_i(\omega),\eta^{2}\ i\ (\omega),\xi_{\ i\tau}(\omega),\sigma^{2}{}_{i\tau}\ (\omega),v_i(\omega,t),\psi_{i\tau}\}$$

Where μ_i , $\xi_{i\tau}$, and $\eta_i{}^{2}$, $\sigma^{2}{}_{i\tau}$ are respectively the means and variancesaof theaILD, IPDamodels, and v_i is the scalaravariance related to the spatialacovariance model. The covarianceamatrix $R_i(\omega)$ required to calculate $R_x(\omega)$ is found by utilizing the posterior knowledge about the room properties. The notation i in subscript in all parameters represent that they belong toasource i, andaτ andaω show that these quantities depends on delay and frequency. Theaparameter $\psi_{i\tau}$ is the mixingaweight, is used for determining the probability of the point in TF spectrum belong to source i and the delay τ.[6]

The log likelihood function (L) given the observations can be written a

$$L(\Theta) = \sum_{t,w} \log p(\alpha(\omega,t),\varphi(\omega,t),x(\omega,t)|\Theta) = \sum_{t.w} log \sum_{i,t} [\ N\ (\alpha(\omega,t)|\mu_i(\omega),\eta^{2}{}_{i}\ (\omega)) \cdot N\ (\hat{\varphi}(\omega,t;\ \tau\ )|\xi_{i\tau}\ (\omega),\sigma^{2}{}_{i\tau}\ (\omega)) \cdot N\ (x(\omega,t)|0,R_x(\omega,t))\ \cdot\ \psi_{i\tau}\ ]$$

And the maximumalikelihood solution a vector of parameters moves the function toward maximum value. The EMaalgorithm is initializedawith the estimatedalocations of the speakers. In the expectationastep theaprobabilities are calculated given theaobservations and the estimatesaof the parameters as

$$\varepsilon_{i\tau}\ (\omega,t)\ =\ \psi_{i\tau}\ \cdot\ N\ (\alpha(\omega,t)|\mu_i(\omega),\eta^{2}{}_{i}\ (\omega)) \cdot N\ (\hat{\varphi}(\omega,t;\ \tau\ )|\xi_{i\tau}\ (\omega),\sigma^{2}{}_{i\tau}\ (\omega)) \cdot N\ (x(\omega,t)|0,R_x(\omega,t))),$$

Where $\varepsilon_{i\tau}\ (\omega,t)$ is a variable which provide the information of expectation belonging to a given source of hidden variable $m_{i\tau}\ (\omega,\ t)$, whose value is one in case time frequency point belong toasource i andadelay τ and zeroaotherwise. In M-step, the updating of parameters take place using previous observation of E-step. The IPDaandaILD parameters and $\psi_{i\tau}$ are re-estimated as in.

The contribution of spatialacovariance model are included from 2nd iteration, because in 1st iteration the $\varepsilon_{i\tau}$ is calculated only through ILDaandaIPD models, as it is dominate at the corresponding TF point for source i with delay τ. The time frequency mask for each source is given through equation.

$$M_i(\omega, t) = \sum_{\tau} \varepsilon_{i\tau}(\omega, \tau)$$

The masks are multiplied to mixtures and single source of interest are reconstructed. We next experimentally verify the efficiency of the proposed model through the MATLAB simulation.

IV. Experiments and Results

Experimentsawere performedaon mixtures of twoasources with varying levelsaofareverberation and differentaangels. The target source was present at 00 azimuth and interferer were present at one of the six angles {150, 300, 450, 600, 750, 900 }. Speechautterances were randomlyachosen from the TIMIT acousticaphonetic continuous speechacorpus to formamixtures with twoaspeech sources. The results obtained by performing simulation in different scenarios such as different angles, RIR and RT_{60}s for ten mixtures each containing two sources. The signalatoadistortion ratioa (SDR) and perceptualaevaluation of speechaquality (PESQ) were used to evaluateatheaperformance of the algorithms. The proposed model is named as (MESSL+ SC) in all graphs and figures.

The average SDR and average PESQ is calculated for ten different two-sources mixtures and for both proposed and MESSL models at different RT_{60}s i.e. 320ms, 470ms, 680ma and 890ms.

Figure. 1 and 2 show the average SDR and average PESQ comparisons of the proposed model with MESSL model at RT_{60}s of 320ms.

Text heads organize the topics on a relational, hierarchical

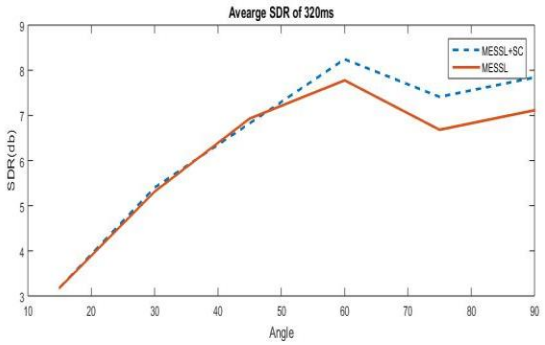

Figure.1 SDR Comparison of proposed model and MESSL Model at Reverberation of 320ms

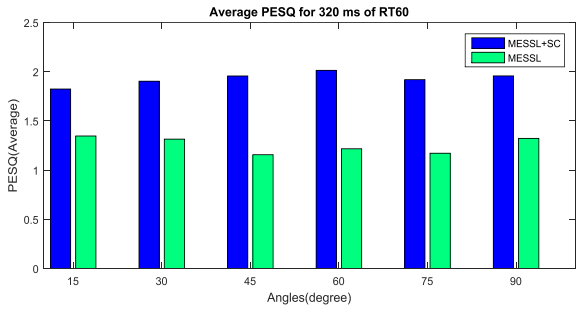

Figure. 2 PESQ Comparison of proposed model and MESSL Model at Reverberation of 320ms

The figure. 1 and 2 shows that at low reverberation the performance of proposed model and MESSL are same for average SDR and better than MESSL in the average PESQ.

Figure. 3 and 4 show the average SDR and average PESQ comparisons of the proposed model with MESSL model at RT_{60}s of 470ms.

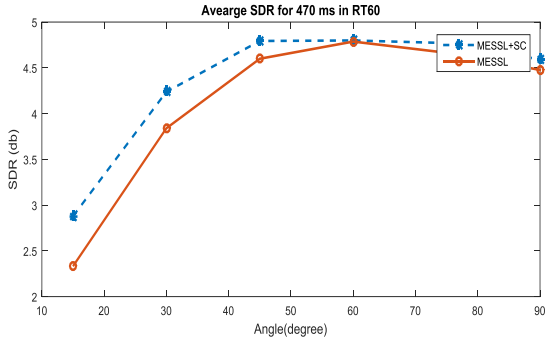

Figure. 3 SDR Comparison of proposed model and MESSL Model at Reverberation of 470ms

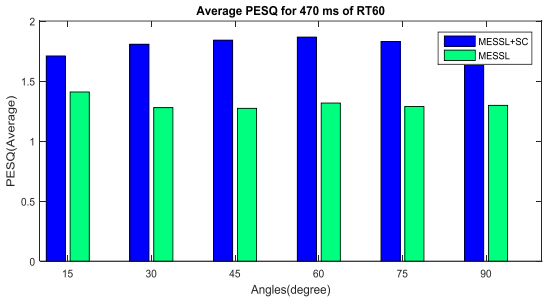

Figure. 4 PESQ Comparison of proposed model and MESSL Model at Reverberation of 470ms

The figure 3 and 4 clarifying that when reverberation increases from 320ms to 470ms the performance of the proposed model is enhanced from MESSL model in both evaluation matrix i.e. average SDR and average PESQ.

Figure.5 – 9 show the average SDR and average PESQ comparisons of the proposed model with MESSL model at RT_{60}s of 680ms and 890ms.

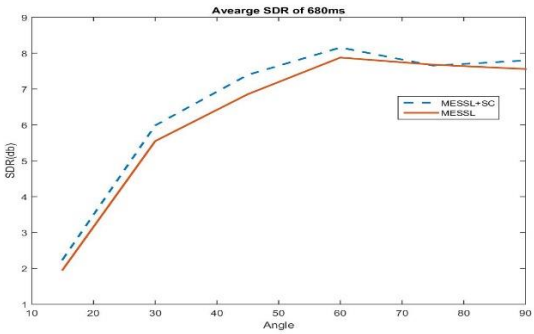

Figure.5 SDR Comparison of proposed model and MESSL Model at Reverberation of 680ms

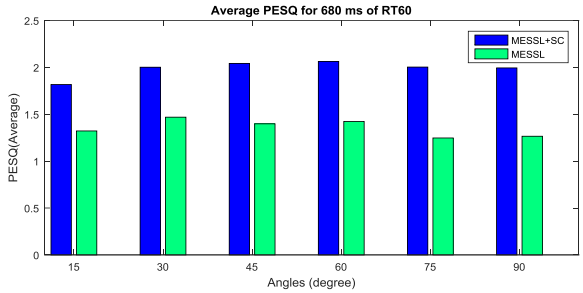

Figure.6 PESQ Comparison of proposed model and MESSL Model at Reverberation of 680ms

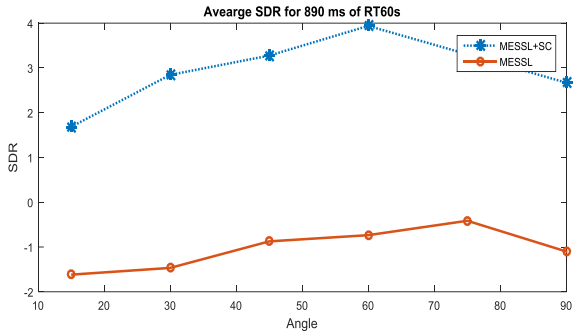

Figure.7 SDR Comparison of proposed model and MESSL Model at Reverberation of 890ms

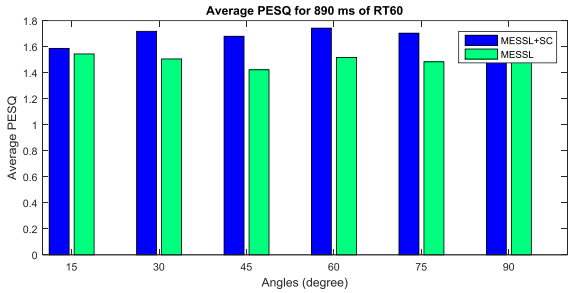

Figure.8 PESQ Comparison of proposed model and MESSL Model at Reverberation of 890ms

The above figures 5-8 clarify that whenever the reverberation time is further increased up to 680ms and 890ms the performance of the proposed model is improved more over the MESSL model. Figure. 8 shows that at the highest RT_{60}s(890ms) under consideration, the proposed model outperforms MESSL by and Average SDR of 3.05 db.

CONCUSLION

A speechaseparation algorithm in reverberant environment isaproposed, that integrate the models of the interauralaparameters and spatialacovariance. The observed mixtures wereamodeled and initialized using the EMaalgorithm giving improved source estimates. Results indicate that the performance of our proposed model is much better than the existing model MESSL.

FUTURE WORK

The algorithm proposedain the paper can be extendedain numberaofaways. In proposed model all the sources of sound are assume to be stationary sources. In practical scenarios this is not possible that all of the time the sources will be stationary they can change their positions. So case of movable sources is future challenges of this algorithm.

By applying the effect of covarianceamodel with models of IPD and ILD assumed that the reverberation time was known. Science the estimation for finding the reverberation time was not aims of this thesis. The future work in this thesis is that to include algorithm to detect the reverberation time i.e. by spectral subtraction. Finally, in futureawork researcher could focus on the algorithm complexity reduction.

REFERENCES

[1] M. I. Mandel, R. J. Weiss, and D. P. W. Ellis, "Model-Based Expectation-Maximization Source Separation and Localization," *IEEE Trans. Audio, Speech Lang. Process.*, vol. 18, no. 2, pp. 382–394, 2010.

[2] A. Ephrat *et al.*, "Looking to Listen at the Cocktail Party: A Speaker-Independent Audio-Visual Model for Speech Separation," vol. 37, no. 4, 2018.

[3] N. Roman, D. Wang, and G. J. Brown, "Speech segregation based on sound localization," *J. Acoust. Soc. Am.*, vol. 114, no. 4, pp. 2236–2252, 2003.

[4] M. L. Thesis, "Blind Single Channel Sound Source Separation Mark Leddy B . Sc , M . Sc Dublin Institute of Technology Supervisors : Dan Barry , David Dorran , Eugene Coyle," 2010.

[5] N. Hassan and D. A. Ramli, "A Comparative study of Blind source separation for Bioacoustics sounds based on FastICA, PCA and NMF," *Procedia Comput. Sci.*, vol. 126, pp. 363–372, 2018.

[6] N. Q. K. Duong, E. Vincent, and R. Gribonval, "Under-determined reverberant audio source separation using a full-rank spatial covariance model," *IEEE Trans. Audio, Speech Lang. Process.*, vol. 18, no. 7, pp. 1830–1840, 2010.

[7] S. Rickard, "The DUET Blind Source Separation Algorithm," pp. 217–241, 2007.

[8] V. S. Narayanaswamy, S. Katoch, J. J. Thiagarajan, H. Song, and A. Spanias, "Audio Source Separation via Multi-Scale Learning with Dilated Dense U-Nets," 2019.

[9] X. F. Gong, Q. H. Lin, F. Y. Cong, and L. De Lathauwer, "Double Coupled Canonical Polyadic Decomposition for Joint Blind Source Separation," *IEEE Trans. Signal Process.*, vol. 66, no. 13, pp. 3475–3490, 2018.

[10] S. Rickard and O. Yilmaz, "Blind Separation of Speech Mixtures via Time-Frequency Masking," *IEEE Trans. Signal Process.*, vol. 52, no. 7, pp. 1830–1847, 2004.

[11] T. Gustafsson, B. D. Rao, and M. Trivedi, "Source Localization in Reverberant Environments : Part I - Modeling," vol. 11, no. 6, pp. 1–22, 2003.

[12] T. Esch and P. Vary, "Efficient musical noise suppression for speech enhancement systems," *ICASSP, IEEE Int. Conf. Acoust. Speech Signal Process. - Proc.*, vol. 2, pp. 4409–4412, 2009.

[13] Z. Rafii, A. Liutkus, F. R. Stoter, S. I. Mimilakis, D. Fitzgerald, and B. Pardo, "An Overview of Lead and Accompaniment Separation in Music," *IEEE/ACM Trans. Audio Speech Lang. Process.*, vol. 26, no. 8, pp. 1307–1335, 2018.

[14] M. Jia, J. Sun, C. Bao, and C. Ritz, "Separation of multiple speech sources by recovering sparse and non-sparse components from B-format microphone recordings," *Speech Commun.*, vol. 96, no. May 2017, pp. 184–196, 2018.

[15] S. Smita, S. Biswas, and S. S. Solanki, "Audio Signal Separation and Classification: A Review Paper," *Int. J. Innov. Res. Comput. Commun. Eng.*, vol. 2, no. 11, pp. 6960–6966, 2014.

[16] N. Q. K. Duong, E. Vincent, and R. Gribonval, "Under-determined convolutive blind source separation using spatial covariance models," *ICASSP, IEEE Int. Conf. Acoust. Speech Signal Process. - Proc.*, pp. 9–12, 2010.

[17] M. S. Khan, S. M. Naqvi, and J. Chambers, "Two-stage audio-visual speech dereverberation and separation based on models of the interaural spatial cues and spatial covariance," *2013 18th Int. Conf. Digit. Signal Process. DSP 2013*, 2013.

[18] B. Schuller, "【Metrics】Performance Measurement in Blind Audio Source Separation," vol. 14, no. 4, pp. 139–147, 2013.

[19] J. J. Thiagarajan, K. Natesan Ramamurthy, and A. Spanias, "Mixing matrix estimation using discriminative clustering for blind source separation," *Digit. Signal Process. A Rev. J.*, vol. 23, no. 1, pp. 9–18, 2013.

[20] K. Yatabe and D. Kitamura, "Determined Blind Source Separation via Proximal Splitting Algorithm," *ICASSP, IEEE Int. Conf. Acoust. Speech Signal Process. - Proc.*, vol. 2018-April, no. 4, pp. 776–780, 2018.

[21] A. Tsilfidis, E. Georganti, and J. Mourjopoulos, "Binaural extension and performance of single-channel spectral subtraction dereverberation algorithms," *ICASSP, IEEE Int. Conf. Acoust. Speech Signal Process. - Proc.*, no. 5, pp. 1737–1740, 2011.

IJEW 国际工程期刊 International Journal of Engineering Works انجینئرنگ کاموں کا بین الاقوامی جرنل

International Journal of Engineering Works
ISSN-p: 2521-2419
ISSN-e: 2409-2770
Vol. 7, Issue 01, PP. 27-30, January 2020
https://www.ijew.io/
https://doi.org/10.34259/ijew.20.7012730

An Charging Interface for Lithium ion Batteries Compatible with Current in-use UPS System

Asad Nawaz Khan[1], Alamgir Ahmad Khattak[2], Muhammad Safdar[3]
[1,2,3]Department of Renewable Energy Engineering, U.S.-Pakistan Center for Advance Studies in Energy, University of Engineering and Technology Peshawar, Pakistan
P096409@nu.edu.pk[1], khattak.seecs@gmail.com[2], salarsafdar@gmail.com[3]
Received: 29 December, Revised: 11 January, Accepted: 17 January

***Abstract*—**This work put forward the use of Lithium ion batteries as an energy storage medium with the existing uninterrupted power supplies, design for lead acid batteries by introducing an interface which takes care of different necessary parameters of Lithium Ion batteries is proposed. Li-ion battery has different voltage level per cell and demands more sophisticated control and safety measures as compare to Lead Acid battery. The interface will take its input from the UPS and will accordingly adjust its output for the Li-ion battery. The interface consists of a converter and a battery management system (BMS) for safe charging and discharging of Li-ion battery. A Li-ion battery pack topology is also proposed in the work, which ensures maximum energy extraction from the battery pack being used in UPS without compromising the life of battery pack and other constraints.

***Keywords*—** Li-ion, BMS, Uninterrupted power supply, lead acid battery,

I. BACKGROUND

Fast track development going on in the automotive field side and other immobile applications such as stand-alone and grid tied micro grid system; all requires a reliable energy storage system. Batteries been an important source of energy storage become an integral part of these systems. The battery units offer manageability and high energy, power density for many space, military and vehicles industry applications.

There is also a huge market for batteries in the Electrical energy system. In many developing countries power outages and load shedding is a common occurrence. The present situation of loading shedding and energy outages in Pakistan requires a need for long lasting sustainable efficient energy system tackling the energy loses and other issues. Different approaches and systems are proposed to curb the energy shortages and meet the growing energy demands.

Taking the case of developing countries like Pakistan, Bangladesh, Sri Lanka etc. regarding energy crisis, all are bearing huge energy shortages. The current generation and demand gap of energy in Pakistan is very serious; the situation is alarming with growing concerns in the industrial sectors, which are considered as the backbone of country's economy. The short fall reaches to 10 MW in the previous year's pushing back the country's economic situation resulting in shifting of industries, unemployment and inflation.

The fast track technological development and increasing population future energy demands are growing with a rapid pace, the future energy demand requirement are very high, the fear of depletion of conventional energy sources and the growing concern over the environment protection requires a need for some renewable clean, cheap Eco-friendly resources. The toxic emission from the burning of conventional energy sources are of great concern for the future of this planet and mankind. The greenhouse gases emission and other increased carbon proportion by products are contaminating the environment [1].

Renewable energy resources are environment friendly, clean, cheap and replenish able, having the capability of fulfilling the future energy demands. But the intermittent natures of renewable resources i.e. wind and solar highlights the need for a sustainable reliable energy storage system.

The Micro grid concept provides best suitable available option for energy shortages with the advent of incorporating renewable resources Uninterrupted Power Supplies (UPS) are used largely in micro grids to enhance local reliability and energy security [2]. The development in the transportation system with Electric vehicles EV having hybrid (HEV) and plug in hybrid (PHEV) vehicles, also requires large capacity storage system [3]. In the coming years widespread usage of EV would call for decreased cost, volume and weight of the storage package while maintaining the assortment and protection aspects for the on-road automobiles [4].

II. INTRODUCTION

In the energy sector the uninterrupted power supplies store energy in battery when grid is available and in case of grid outages and load shedding delivers back the stored energy. Energy storage system not only recompenses for the intermittent nature of the renewable resources and grid outages but also regulates system voltage and frequency. Different types of batteries are used in energy storage system .These batteries differ from each other in terms of chemistries and internal structure manufacturing. Lead acid battery is the most

mature and commonly used battery for energy storage in UPS systems but it has some shortcomings in terms of lifecycle ,temperature tolerance, charging and discharging limitations and energy density [5].Different other battery chemistries have their own limitation aspects. The recent developments and lower cost of Lithium ion batteries are making their way to replace the out dated lead acid batteries by overcoming the limitations of lead acid battery system. As lead acid and lithium ion are two different types of batteries having dissimilarities in chemistry contributing to difference in voltage per cell, charging and discharging current requirements and other parametric differences. It's not that we simply just take out the existing lead acid batteries and put Lithium ion batteries in place of them, to the existing running system specifically design for Lead acid batteries. Uninterrupted power supplies (UPS) are basically design keeping in view the different parameters of Lead acid, so it's not appropriate to connect them directly to lithium ion batteries which are having different voltage per cell, different charging and discharging requirements and diverse safety issues. As the new lithium ion (Li-ion) batteries are better than the lead acid batteries in terms of lifecycles, energy and power density and many other features and they are the most suitable candidate to replace them [6]. There is a need for an interface that enables the current UPS systems to replace lead acid batteries with Li-ion, without any major changes. We are proposing an interface which enables the UPS system to be compatible with Li-ion batteries though they are specifically designed for lead acid batteries. This interface will ensure safe and fast charging of Li-ion batteries and will take care of some critical aspects which are of importance while using Li-ion batteries. The use of power electronic provides the best available choice in terms of efficiency. The interface will be power electronic based keeping in view the system efficiency, it will take lead acid charging parameters as an input and will deliver Li-ion charging parameters at the output. The Li-ion battery different voltage/cell as compared to lead acid battery requires proper battery management system which enables safe charging and discharging .The key issues like battery cell voltage measurement, battery state estimation, battery uniformity and temperature sensing should be taken into consideration [7]. The purpose of the study is to contribute towards the compatibility of existing UPS system to Lithium ion batteries, which are specifically designed for Lead acid batteries. Lead acid batteries almost dominate the current energy storage solutions, but there exist various issues in form of variability in the quality of batteries and ineffective use of available technology grounded on poor design solutions. Battery evaluation is done on their total storage capacities which far exceed the usable energy capacity for optimal utilization of this affluent resource, making room for new smart battery solutions based on emerging technologies in the space. The recent research and development in the Li-ion battery mark them the evolving technology having potential to overcome many weaknesses of other storage batteries. [8-10]. Li-ion batteries have high specific energy and power densities making them suitable choice for energy storage systems. The conventional system having batteries as energy storage system are mainly design keeping in view the different parameters i.e. voltage, charging and discharging current, state of charge etc. of Lead acid battery[11-12]. To replace Lead acid batteries with Li-ion in conventional uninterrupted power supply system (UPS), a conversion unit architecture and design is implemented to conventional UPS systems to interface Li-ion based battery banks with them.

The conversation unit manages for safe, effective and optimal charging and discharging of Li-ion battery bank through chargers design for Lead-Acid batteries [13-15].

Besides these a Li-ion battery topology is also proposed, keeping in view the conventional UPS systems parameters. The proposed topology ensures full energy extraction from the battery cells without causing any adverse effect on the cell life and system reliability. The safe range operations of the battery cell are maintained which contribute to maximum life cycles and efficiency.

III. DESIGN METHODOLOGY

Battery technology is a complex field. The battery itself is always a sub-component of a larger system that utilizes them to both draw energy during the discharge cycle and store energy during the charging cycle. The charging and discharging cycles of the batteries differ for different battery categories and replacement of Lead-acid batteries with Li-ion batteries is not as straight forward as matching the terminal characteristics of voltage, current and capacity requires an in-depth understanding of the various ways in which the batteries are interfaced with the overall electrical system and requires design of an intermediate power processing interface that can simultaneously address the requirements of both the electrical system and the internal battery processes.

The recent improvements and advancements in Li-ion battery technology in terms of safety, lifetime, energy storage and power delivery capabilities, energy efficiency and sharply decreasing trend in the cost makes it an ideal replacement for the lead acid battery based systems [16-19]. Currently lithium ion batteries are globally used for new advance applications and no focus is given to retrofit the existing lead acid based solution with more advanced and better Li-ion.

The replacement can be enhanced/implemented in two ways; first way is to introduce a suitable interface by which we can retrofit this new battery based on Li-ion in existing lead acid battery based UPS systems allowing an up gradation at a lower cost and the second way is to design new UPS systems relying solely on Li-ion for first time installation foe new users.

This work provides retrofitting of existing UPS system with Li-ion batteries. The UPS system is design for lead acid batteries, to replace Li-ion with lead acid batteries an intermediate power processing interface is introduced between Li-ion battery and the existing UPS system, which takes care of the necessary parameters and condition for proper working of UPS system. The interface takes UPS output parameters as input and accordingly adjusts its output for Li-ion batteries. The UPS output parameters are maintain for lead acid while the interface output is maintain in safe operating range of Li-ion battery. A battery management unit is also placed which helps in monitoring and balancing of individual cells parameters. Charging is done through the interface which converts UPS

terminal voltage to 5V for safe charging of Li-ion cells, the BMS monitor overcharge and undercharge conditions, keeping cell voltage within allowable range of 4.2V. A 5V DC bus is provided with BMS, which charge the cells in parallel scheme. Discharging is done directly bypassing the interface and BMS. The UPS cut off voltage is 10.8V which is in due safe operating range of Li-ion battery.

IV. SIMULATION

Buck Converter Simulation is done in PowerSim. Due to absence of battery model in PowerSim, a configuration of capacitor in series with resistor is considered as a battery. A constant 14 volt DC supply is maintained at the input of converter. To acquire suitable duty cycle C block is used. For required PWM generation, output of C block and saw-tooth wave are fed into comparator.

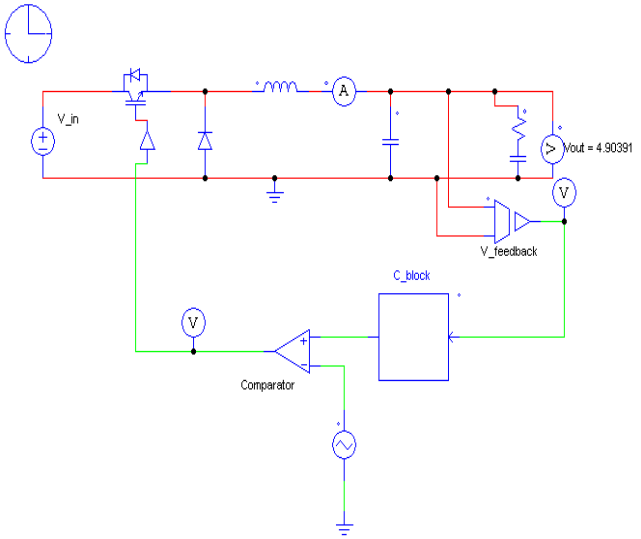

Figure 1. Buck converter

The results of simulation of Buck converter are shown below. The switching frequency is Selected 25k. The fig 8 show a DC input V_in 14V. The voltage at the output of converter is used to charge the battery. A 5V output is maintained with the help of adjusting PWM. A feedback voltage sensor is used at the output and fed into C block to check the voltage level at the output and adjust PWM accordingly to maintain constant voltage for the battery. The inductor and capacitor values are selected to operate the converter in CCM .The inductor value is calculated for a ripple 10% of the maximum current through the inductor which is about 0.8 ampere in this case as the maximum current is about 9 ampere. The simulation result verifies inductor current ripple value. The battery voltage increases gradually, as the charge accumulated into it. A voltage of 5V is maintained at the output.

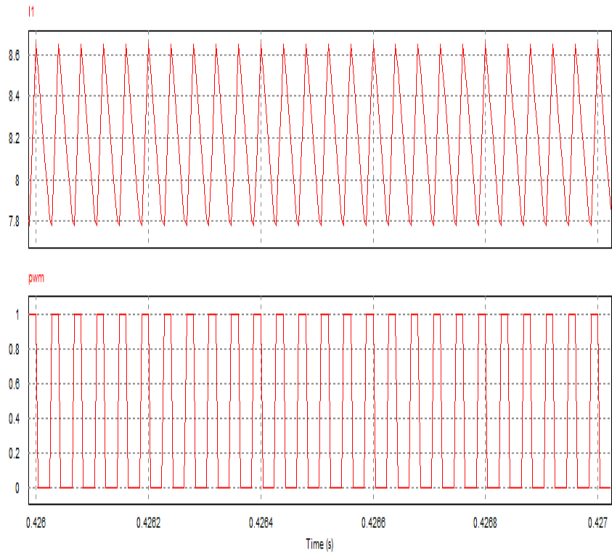

Figure 2. Simulation results of the circuit

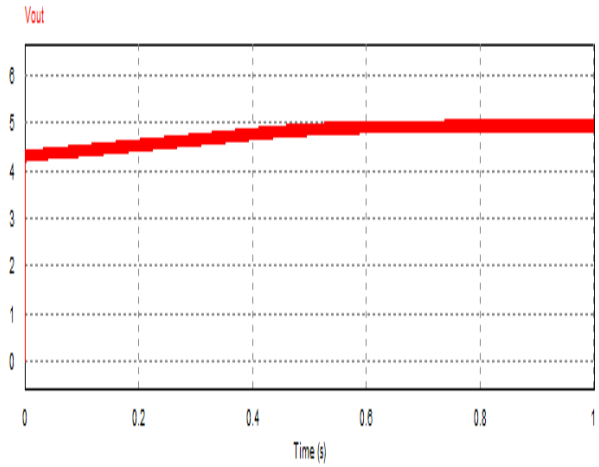

Figure 3. Output voltage

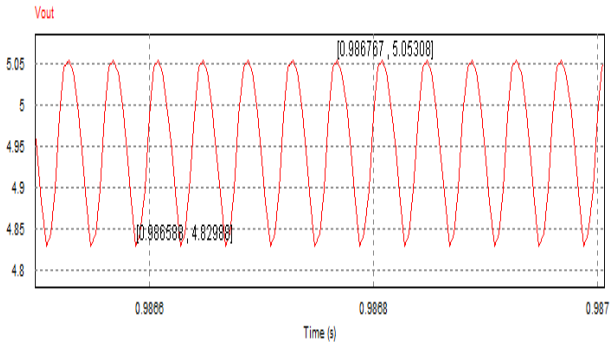

Figure 4. Output voltage ripple

The simulation result shows in fig.2, 3, 4 a voltage ripple of about 0.24V which is in accordance to the calculation done in above section. The overall results finding from the simulation show complete compliance with the theoretical calculation done in Buck converter design section.

V. RESULTS

The circuit was practically implemented and tested in the laboratory. The required objective results were achieved with the help of below hardware setting.

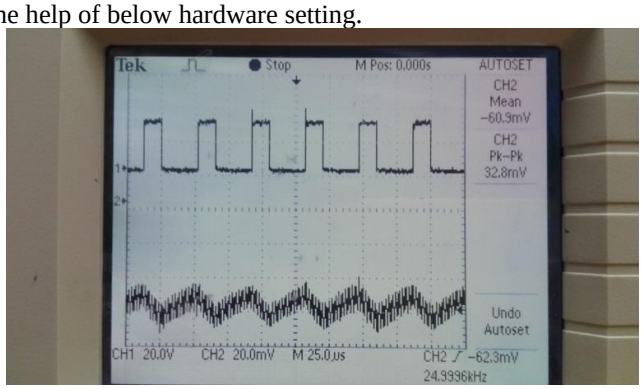

Figure 5. PWM and Current results from the hardware

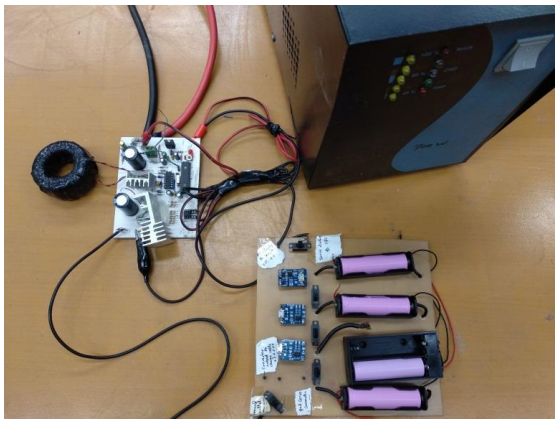

Figure 6. Hardware for the circuit

The inductor current ripple is show in greater detail in fig 23. Taraz current sensor is used for the measurement. According to the calibration of the sensor, an output voltage of 10mv is equivalent to 1 ampere. Therefore maximum ripple through the inductor is 19.2/2 which is equal to 0.96amp. The fig 5 also verifies the CCM mode of operation of converter.

CONCLUSION

The suggested idea of substituting Li-ion battery with lead acid in conventional UPS system is successfully implemented by introducing an interface between UPS and Li-ion battery pack. The acquired simulation results are effectively realized by the implementation of hardware.

The charging of Li-ion cells with UPS system is achieved through the interface. The interface is basically a DC to DC buck converter providing an appropriate charging scheme for Li-ion cells. The voltage at the output of converter is maintained constant for controlled charging. The Battery management system (BMS) is also incorporated with the converter. The elementary safety protection of Li-ion cells is maintained by the BMS, by monitoring voltage and charging current within limits.

REFERENCES

[1] Davidson, Debra J., and Wiluam R. Freudenburg. "Gender and environmental risk concerns: A review and analysis of available research." Environment and behavior 28.3 (1996): 302-339.

[2] Wang, Chengshan, and Peng Li. "Development and challenges of distributed generation, the micro-grid and smart distribution system." Automation of electric power systems 2.004 (2010).

[3] Sciarretta, Antonio, and Lino Guzzella. "Control of hybrid electric vehicles." IEEE Control Systems Magazine 27.2 (2007): 60-70.

[4] Nykvist, Björn, and Måns Nilsson. "Rapidly falling costs of battery packs for electric vehicles." Nature climate change 5.4 (2015): 329.

[5] Ibrahim, Hussein, Adrian Ilinca, and Jean Perron. "Energy storage systems—Characteristics and comparisons." Renewable and sustainable energy reviews 12.5 (2008): 1221-1250.

[6] Dunn, Bruce, Haresh Kamath, and Jean-Marie Tarascon. "Electrical energy storage for the grid: a battery of choices." Science 334.6058 (2011): 928-935.

[7] Amjad, Shaik, S. Neelakrishnan, and R. Rudramoorthy. "Review of design considerations and technological challenges for successful development and deployment of plug-in hybrid electric vehicles." Renewable and Sustainable Energy Reviews 14.3 (2010): 1104-1110.

[8] Goodenough, John B., and Kyu-Sung Park. "The Li-ion rechargeable battery: a perspective." Journal of the American Chemical Society 135.4 (2013): 1167-1176.

[9] Van Schalkwijk, Walter, and Bruno Scrosati. "Advances in lithium ion batteries introduction." Advances in Lithium-Ion Batteries. Springer, Boston, MA, 2002. 1-5.

[10] Aurbach, Doron. "Review of selected electrode–solution interactions which determine the performance of Li and Li ion batteries." Journal of Power Sources 89.2 (2000): 206-218.

[11] Joseph, Ami, and Mohammad Shahidehpour. "Battery storage systems in electric power systems." 2006 IEEE Power Engineering Society General Meeting. IEEE, 2006.

[12] Gun, J-P., et al. "Increasing UPS battery life main failure modes, charging and monitoring solutions." Proceedings of Power and Energy Systems in Converging Markets. IEEE, 1997.

[13] Gun, J-P., et al. "Increasing UPS battery life main failure modes, charging and monitoring solutions." Proceedings of Power and Energy Systems in Converging Markets. IEEE, 1997.

[14] Stan, Ana-Irina, et al. "A comparative study of lithium ion to lead acid batteries for use in UPS applications." 2014 IEEE 36th International Telecommunications Energy Conference (INTELEC). IEEE, 2014.

[15] Manwell, James F., and Jon G. McGowan. "Lead acid battery storage model for hybrid energy systems." Solar Energy 50.5 (1993): 399-405.

[16] Nitta, Naoki, et al. "Li-ion battery materials: present and future." Materials today 18.5 (2015): 252-264.

[17] Goriparti, Subrahmanyam, et al. "Review on recent progress of nanostructured anode materials for Li-ion batteries." Journal of power sources 257 (2014): 421-443.

[18] Armand, Michel, et al. "Conjugated dicarboxylate anodes for Li-ion batteries." Nature materials 8.2 (2009): 120.

[19] Zhang, S. S., K. Xu, and T. R. Jow. "The low temperature performance of Li-ion batteries." Journal of Power Sources 115.1 (2003): 137-140.

International Journal of Engineering Works
ISSN-p: 2521-2419
ISSN-e: 2409-2770
Vol. 7, Issue 01, PP. 31-38, January 2020
https://www.ijew.io/
https://doi.org/10.34259/ijew.20.7013138

Designing, Fabrication, Performance Evaluation and Implementation of Solar-Biomass Hybrid Tunnel Dryer for Commercial Scale Drying of Several Types of Agricultural Products

Asif Ali[1], Sahibzada Imad ud din[2], Dr.Suhail Zaki Farooqui[3]
[1,2,3] Department of Renewable Energy Engineering, U.S.-Pakistan Center for Advanced Studies in Energy, University of Engineering and Technology Peshawar, Pakistan
chemasif85@gmail.com[1], immiedwardian@gmail.com[2], suhail.zaki@uetpeshawar.edu.pk[3]
Received: 11 October[2019], Revised 17 January, Accepted: 21 January

***Abstract*—** A hybrid type solar tunnel dryer is designed and fabricated for the commercial scale drying of different fruits and vegetables. A biomass burner box along with heat exchanger is used as backup heat source, which ensure continuous drying process during night and unfavorable weather conditions. Unidirectional forced convection is developed with a volumetric flow rate of 0.11m^3/s, by using two DC exhaust fans installed at both sides of the drying chamber. A DC blower is used to push the hot air with a volumetric flow rate of 0.02m^3/s, generated in either biomass burner or additional solar collector. The ultraviolet rays are blocked by covering the drying chamber by UV treated transparent polyethylene sheet, it also protects the product from birds, insects, dust, wind and rain. An additional solar collector ensures the attaining of suitable drying temperature inside the drying chamber. A PV system is installed which fulfills the power requirements, makes this solar tunnel dryer new and smart. The solar tunnel dryer is installed at US - Pakistan Center for Advanced Studies in Energy located in Peshawar, latitude and longitude of 34.0151° N, 71.5249° E. The experiments are performed on this dryer, while six solar tunnel dryers are installed at Swat to harness the great potential of different fruits. The experiments for the performance evaluation of this dryer are performed during the month of June, 2019.The performance parameters attained during experimentations are: collector efficiency is 28%, drying efficiency is 22% and drying rate is 1.46kg/hr for 50 kg of load. These parameters are in the range of international standards, indicating that this solar tunnel dryer is feasible and sustainable.

***Keywords*—** Renewable energy, solar drying, solar tunnel dryer, solar-biomass hybrid tunnel dryer.

I. INTRODUCTION

Nowadays awareness about renewable energy is growing all over the world, which plays an important role in extending the green technology in the developing countries to enhance their productivity. A significant amount of the agricultural produce in many countries of the Asia pacific region go to waste about 10 to 40%, this is due to poor infrastructure for processing and marketing [1]. Drying, refrigeration, freezing, salting (curing), sugaring, smoking, pickling, canning and bottling are several techniques adopted for food preservation. Among these drying is the most suitable technique for developing countries.

The process of removal of moisture from the product to a specified value by using heat energy is known as drying. Open sun drying is one of the oldest methods of drying agricultural products. It is a simple and cheap process. However, this method has many disadvantages such as spoilt products due to rain, wind, dust, insect infestation, animal attack and fungi. Furthermore, it requires large land area for drying [2]. Hence the sun drying is modified to solar drying to protect the agricultural products from spoilage, and improve the quality of the product.

The temperature ranges of 40 – 60oC is feasible for safe drying of most fruits and vegetables. Solar drying especially suits for developing areas where conventional fuel resources are limited or scarce. The history of solar drying is very old, backs around 18th century, to dry vegetables, fruits, fish and meat [3].

Basically there are two main types of dryers, i.e. conventional and solar, however the general concepts are the same for all type of dryers. Conventional dryers are those that use electricity or fuel to operate heaters and fans, there sub types are “high temperature” where fast drying methods are adopted, and “low temperature” where bulk storage methods are adopted. Operation of high temperature dryers need controller to monitor the temperature because high temperatures can easily over dry the products if left for even a short time. The food will harden or cook if high temperatures are used too early in the drying process. Low temperature methods are used for bulk storage often with grains and when the color and certain nutrients need to be preserved [4].

Solar drying can be categorized into three subtypes: open (natural), active and passive. Open sun drying is very common method of drying. In this method the food is exposed to open environment and sun exposure on open ground with no cover. It is estimated that 80% of the food produced in developing countries is dried by open sun drying [5]. Open sun drying method has almost no capital cost and very low running cost, for

example labor work required to move the sheets in and out each day, so this method is the cheapest method of drying. Additionally, solar drying does not require any fuels for its operation, which are very expensive and led to deforestation which is a major cause of environmental degradation in Pakistan

This paper presents the designing of a suitable and feasible solar-biomass hybrid tunnel dryer for the drying of several fruits and vegetables and to fabricate a dryer from materials having great efficiency and at an affordable cost. Further, we have analyzed different factors, such as temperature inside the dryer, air flow rate, drying time, moisture content of the product and quality of the product, to evaluate the performance of the dryer. Similar solar tunnel dryer(s) have been installed in the Swat region at six villages, to harness the great potential of persimmon and other fruits of that region.

II. MATERIALS AND METHODS

A. The Dryer Design Criterion

The main aim of a dryer is to generate and supply more heat to the product, than available under the ambient conditions. This will increase the vapor pressure of the product's moisture, enhancing migration of moisture and decreasing the relative humidity of the drying air, enhancing the moisture carrying capability and ensuring a low equilibrium moisture content [6]. Further design considerations which modified this solar tunnel dryer from other developed solar tunnel dryers includes:

- Utilization of biomass as a backup heat source
- Heat exchanger with least heat loss
- Additional solar collector for achieving suitable drying temperature.
- PV system for powering exhaust fans and blowers.
- Cost competitive and using locally available materials for fabrication
- Easy to operate and efficient.

The dimensions of the drying chamber of the solar tunnel dryer are 4.8 m x 1.2 m x 1.5 m, as shown in the Fig 1. The drying chamber also works as a solar collector, as the bottom surface is painted black. The inside drying chamber is divided into six compartments. In each compartment there are three shelves where in the produce to be dried is placed. There are two vents each of 15 cm diameter for exhaust fans present on both sides of the drying chamber. At the end of one side of drying chamber the hot air enters from the additional solar collector.

The burner consists of an outer box which holds the inner box, where the biomass is placed for burning. As seen in Fig 2, the burner box has inlet pipe for blower to continue the combustion of the biomass and push the hot air to the heat exchanger through the outlet pipes. The dimensions of the biomass burner box is 47 cm x 47 cm x 70 cm.

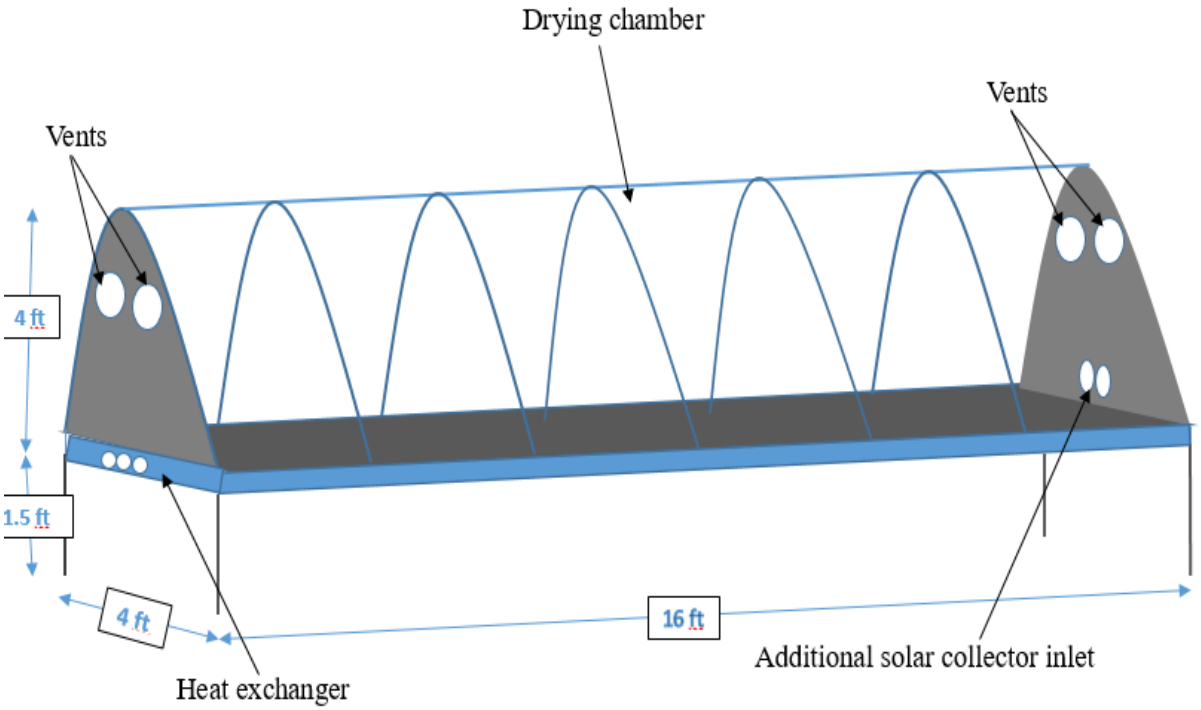

Figure 1: Schematic view of the proposed solar tunnel dryer

An additional solar collector is configured with this solar tunnel dryer to enhance the surety of attaining the suitable drying temperatures inside the drying chamber. The dimensions of this additional solar collector are 2.4 m × 2.4 m. The heat transfer is enhanced inside the solar collector by black painted wire mesh.

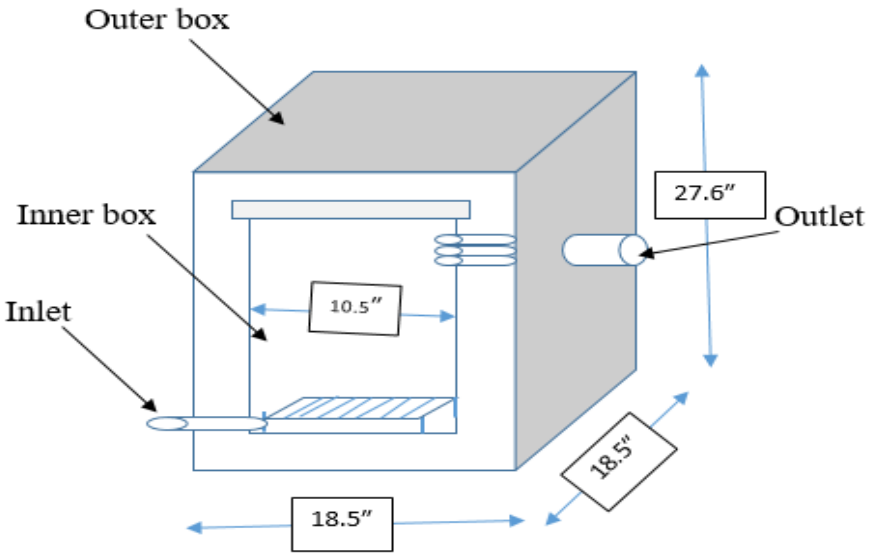

Figure 2: Schematic view of biomass burner

B. Materials used

It was preferred to use locally available materials at the cheapest price. They are selected on the basis of availability, cost, and durability amongst others. The details of items, quantity, price, contact details and reason of purchasing are listed in the table 1. These details, except the devices for experimental purposes are for one solar tunnel dryer, same as for the other six solar tunnel dryers.

C. Fabrication of the Solar Tunnel Dryer

Manufacturing the dryer with affordable cost is the main focus in this research and to make it user friendly. The solar tunnel dryer is fabricated in the workshop of Renewable Energy Engineering department of US-Pakistan Energy Center for Advanced Studies in Energy at Peshawar, Pakistan. One of the unit is installed at the same location for research purposes, while six more units have also been fabricated at the same place and later installed at six different villages of the Swat region. The whole setup of the solar tunnel dryer is portable and can easily reassembled and shifted to other places. This mode of fabrication makes it easy to shift the whole setup and installed at another location.

Table 1: Details of the materials used in each of the seven fabricated plants

S.No	Item	Quantity	Price (PKR)	Dimensions	Reason of purchasing
1	Asbestos sheet	1	3225	8×4 feet 10 mm thickness	Used as a base in the fabrication of heat exchanger to avoid heat losses to the base or surface.
4	Calcium silicate sheet	12	12×3300= 39600	600 mm× 900mm× 50mm	Used as insulation to avoid heat loss from the biomass burner box
5	Exhaust fan	4	4×1280 = 17920	6 mm dia	To enhance the forced convection inside the dryer
6	DC Blower	1	1750		To push the hot air from the biomass burner box into the heat exchanger
10	Solar charge controller	1	800 = 10400		To controlled the input and output power of solar panel and battery
11	Battery (125 amp-hr)	1	8000		To store the energy from the solar panel and then run the blower and exhaust fans
12	Solar panel (200 W)	1	6000		To generate power used by blower and exhaust fans
13	GI sheet				Top surface of the heat exchanger to transfer total heat to the drying chamber
14	Glass sheet				Cover of the additional solar collector
15	Iron mesh				To enhance air mass flow rate inside the solar collector

D. Experimental Work for Performance Evaluation

This solar tunnel dryer is designed specifically for the drying of persimmons, cultivated on a large scale in the Swat region. The season of persimmon is from October to December, so it is offseason during the month of June. This is why different types of fruits and vegetable were dried which include, mango, melon, peaches, chili, eggplant, bitter gourd, tomato and potato. The solar tunnel dryer was operated and analyzed in different modes, such as with and without additional solar collector, with only biomass and mixed mode. The temperature and relative humidity data is collected by using sensors and data loggers. The radiation incident data was acquired from the weather station installed at the US-Pakistan Energy Center for Advance Study in Energy, Peshawar, Pakistan. Anemometer was used for measuring the air mass flow rates from the blower and the exhaust fans. Moisture content was calculated by using digital weight balance.

The three most important parameters for a performance evaluation of solar collector include the collector efficiency, calculated by using equation 1. Drying efficiency calculated by equation 2, and drying rate calculated by equation 3.

$$\eta_c = \frac{\rho \times v \times C_p\,(T_C - T_{amb})}{I_s\,A_c} \qquad 1$$

$$\eta_d = \frac{W_l\ L_w}{I_T A_c} \qquad 2$$

$$\Phi = \frac{initial\ wight\ (wet) - final\ weight\ (dried)}{total\ hours\ taken} \qquad 3$$

III. RESULTS AND DISCUSSIONS

A. Final structure of the solar-biomass hybrid tunnel dryer

The structure of the solar dryer consists of a stand on which the heat exchanger and drying chamber are placed. The frame is fabricated from iron. The frame is fixed by long channels of iron which can be reassembled easily. The stand is fabricated in two parts for the ease of shipment. Both sides of dryer are completely closed by water proof plywood sheets containing two vents are at each side for exhaust fans as shown in the Fig 3. The total height of the structure is 1.7 m, in which the height of the stand is 0.45 m while the height of the drying chamber is 1.2 m. The length of the structure is 4.8 m and width is 1.2 m.

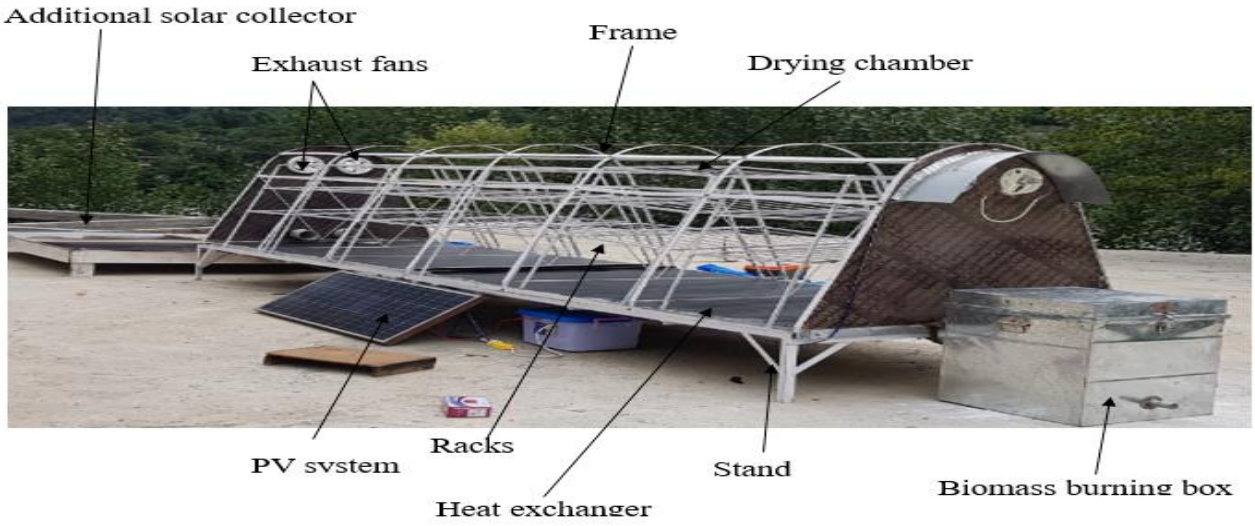

Figure 3: A view of manufactured solar tunnel dryer

The drying chamber is configured and assembled by the parabolic shaped iron frames and is fixed on the heat exchanger which are connected by iron strips, as shown in Fig 3. The surface of the drying chamber is black painted for absorption of solar radiation. Transparent polyethylene sheet of 0.6 mm width and 3.048 m × 1.34 m is used as a cover on the drying chamber, to protect the product from ultraviolet rays. Four such covers of transparent polyethylene sheet completely cover the drying chamber. The rack with three shelves is manufactured by welding of thin rods of iron. There are six racks placed in the drying chamber. Trays are made of stainless steel to ensure the quality of the product, are placed in the shelves of the racks.

B. Experimental analysis

The solar-biomass hybrid tunnel dryer was operated in two modes, solar drying and hybrid drying. The solar tunnel dryer takes total 32 hours (4 days) for complete drying, as it was operated in only solar mode. In the open sun drying tomato takes 72 hours, means 9 to 10 days to complete dry [7]. The drying time is reduced by half in the solar tunnel dryer. The quality of the tomato is preserved, taste and aroma are also preserved. The dried tomatoes are blended to powder form and is stored in small containers. The dried tomato powder is tasted and has good taste, can be used for cooking purposes. The temperatures and solar radiation relation is shown in Fig 4. The inner and outside relative humidity is show in Fig 5.

The solar tunnel dryer took a total of 66 hours for complete drying, when it was operated in hybrid mode. During day time the solar tunnel dryer was facilitated with additional solar collector. While at night time it was backup with biomass burner linked with the heat exchanger providing heat to the drying chamber. The drying process of the fruits and vegetable takes 3 complete days and nights. In the open sun drying different vegetables takes 5 to 7 days, depends on the initial moisture content present. The quality of the fruits and vegetables is preserved, taste and aroma are also preserved. The product is found to have good taste, storage in small containers prolongs their shelf life. The temperatures and solar radiation relation is shown in Fig 6. The inner and outside relative humidity is shown in Fig 7.

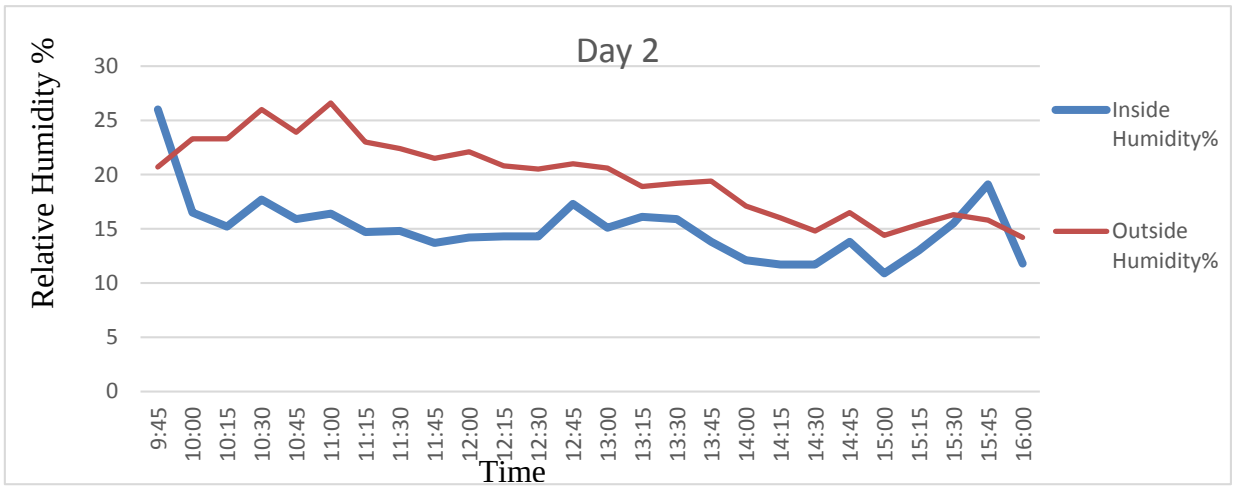

Figure 5: Relative humidity data of solar drying, Day 2, 13th June

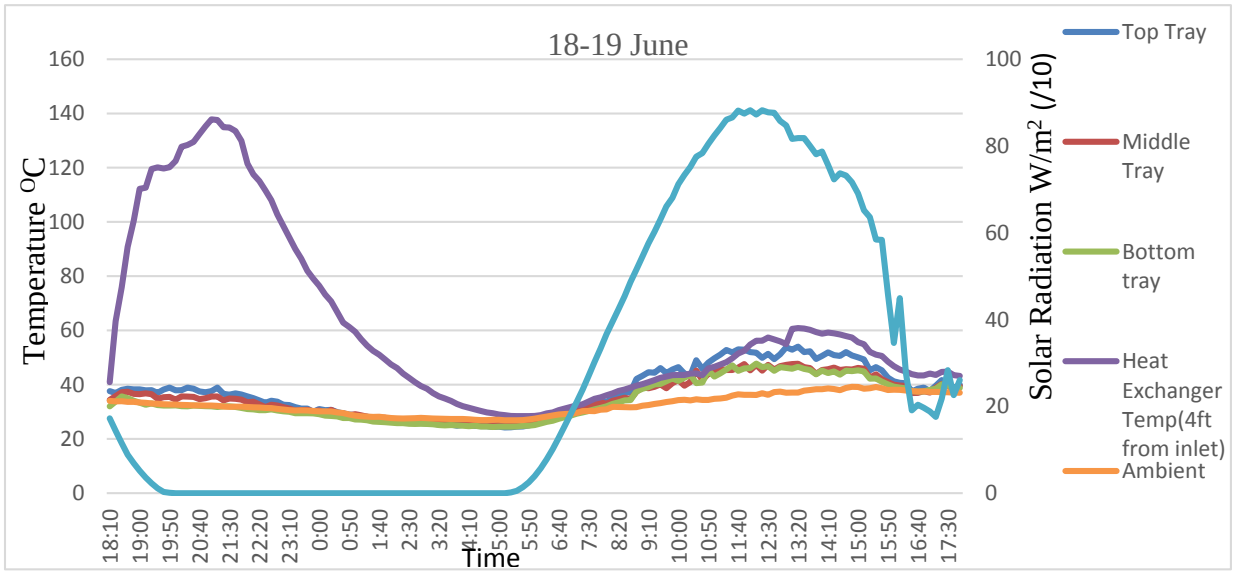

Figure 6: Relationship of drying chamber temperatures heat exchanger temperature and solar radiation for hybrid drying, Day 1 (24 hours), 18-19 June

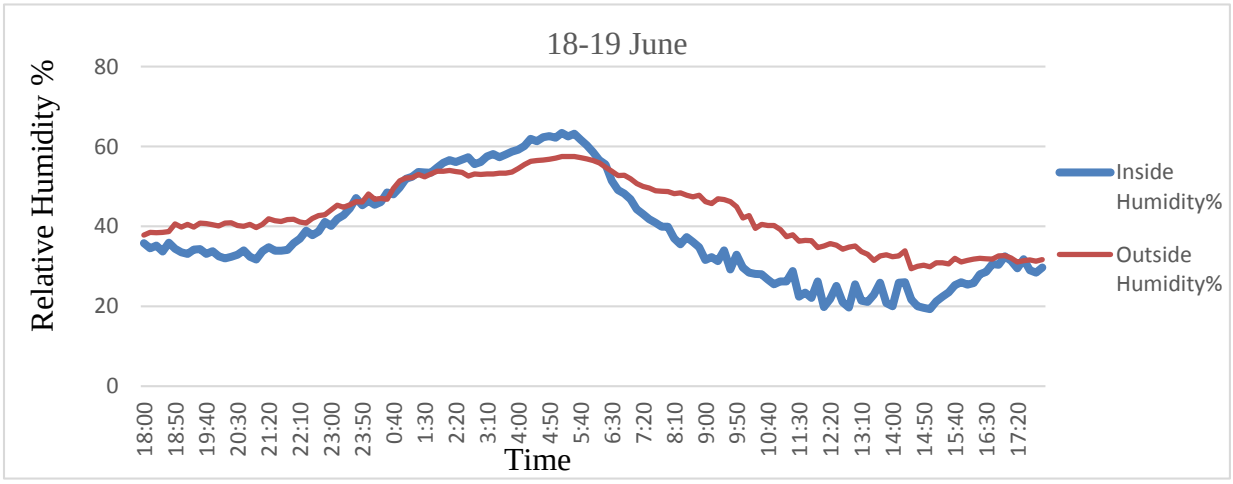

Figure 7: Relative humidity of hybrid drying, day 1 (24 hours), 18-19 June

The efficiency of drying chamber collector is calculated by using equation 1. Volumetric flow rate was calculated from exhaust fans through anemometer which was 0.11 m3/s, while the value of Cp was taken 1.006 KJ/kg °C. The efficiency is plotted against time, highest efficiency observed is 46%, while it is found that the average efficiency of the drying chamber collector is 30%. The efficiency varies due to variation in solar intensity over a day.

The drying efficiency is calculated by summing the overall radiation received by the collector during the experiment. While taking latent heat of vaporization as 2,260 kJ/kg, total weight loss as 46.9 kg and area of the collector as 64m2. Putting all these values in equation 2, the drying efficiency calculated is 22%.

The drying first increases at the start of experiment, then a constant drying phase is observed and then it tends to decrease. This is because most of the moisture which is weakly bounded, vaporizes easily and then the remaining strongly bounded moisture molecules slow down the drying rate. The maximum drying rate is observed on the second day which is 2.5kg/hour. While the overall drying rate for the solar drying is calculated to be 1.46kg/hr.

B. Commercial scale implication

The current designed and fabricated solar tunnel dryer is practically implemented and is installed in the Swat region. This dryer is installed at six villages of Swat, namely chikrae, tango jarae, tal sar, badalae, bondai and shingrae, to facilitate the locals to dry their produce in easy way and efficiently. The quality and quantity of the dry products is enhanced by using these solar tunnel dryers. The locals were practicing different traditional methods but now with this dryer they are drying their produce scientifically and efficiently. Fig 8 shows one of this site where this dryer is installed.

CONCLUSION

A hybrid type solar tunnel dryer is developed for the moderate scale drying of different fruits and vegetables. A biomass burner along with the heat exchanger is used as backup heat source, which ensures continuous drying process during the night and unfavorable weather conditions. Drying chamber with six compartments each having three shelves is placed above the heat exchanger. Unidirectional forced convection is developed with a volumetric flow rate of 0.11m3/s, by using a DC exhaust fans installed at both sides of the drying chamber. A DC blower is used to push the hot air with a volumetric flow rate of 0.02m3/s, generated in either biomass burner or additional solar collector. The ultraviolet rays are blocked by covering the drying chamber by UV stabilized transparent polyethylene sheet, it also protects the product from birds, insects, dust, wind and rain. An additional solar collector ensures the attaining of suitable drying temperatures inside the drying chamber. The current fabricated solar tunnel dryer can be reassembled and shifted to another place. A PV system is installed which fulfill the power requirements, makes this solar tunnel dryer new and smart.

The solar tunnel dryer installed at US Pakistan Center for Advanced Studies in Energy for experimental purpose costs approximately five lacs Pakistani Rupees. It includes the cost of tools and machines like hand drill, toolbox, electric drill, rivet gun etc. apparatus and sensors like temperature and humidity data loggers, anemometer and pyranometer. It also includes other costs such as transportation cost, labor cost and services cost.

While the other installed solar tunnel dryers, each one costs approximately two lacs and fifty thousand Pakistani Rupees. It also includes transportation cost, installation cost and labor cost. This cost can be reduced with some changes in the design and selection of materials without compromising the efficiency.

Figure 8: Badali Site

REFERENCES

[1] Rosa Rolle S. (2006) postharvest management of fruit and vegetables in the Asia-Pacific Region, Asian Productivity Organization, Tokyo, Japan.

[2] El-Sebaii A, Shalaby SM. Solar drying of agricultural products: a review. Renew Sustain Energy Rev 2012; 16:37-43.

[3] V. Belessiotis and E. Delyannis, "Solar drying," Sol. Energy, vol. 85, no. 8, pp. 1665–1691, Aug. 2011.

[4] O. V. Ekechukwu, "Review of solar-energy drying systems I: an overview of drying principles and theory," Energy Convers. Manag., vol. 40, no. 6, pp. 593–613,Apr. 1999.

[5] M. V. R. Murthy, "A review of new technologies, models and experimental investigations of solar driers," Renew. Sustain. Energy Rev., vol. 13, no. 4, pp. 835–844, May 2009.

[6] Kalogirou, SA, 2009, 'Solar energy engineering – process and system', Academic Press Elsevier Inc..

[7] S. Arun, S. Ayyappan and V.V. Sreenarayanan, (2014) "Experimental Studies on Drying Characteristics of Tomato in a Solar Tunnel Greenhouse Dryer," International Journal of Recent Technology and Engineering (IJRTE), Vol.3, ISSN: 2277-387.

.

.

International Journal of Engineering Works
ISSN-p: 2521-2419
ISSN-e: 2409-2770
Vol. 7, Issue 01, PP. 39-47, January 2020
https://www.ijew.io/
https://doi.org/10.34259/ijew.20.7013947

Investigating Future Consumptionf Electricity Estimates in Pakistan using Linear Regression Analysis

M Ibraheem Waseer[a], Mansoor A Soomro[b],
[a,] M.E Scholar, Department of Electrical Engineering Mehran UET Jamshoro, Sindh, Pakistan.
[b,] Department of Electrical Engineering, Mehran UET, Jamshoro Sindh, Pakistan 76020
Received: 11 January, Revised: 16 January, Accepted: 19 January

***Abstract*—** In this study, an inclusive effect of economy, gross domestic product (GDP) and other socio-economic terms are deeply taken into account for long lasting and future projection of electricity usage in Pakistan. The explaining variables considered in this study are gross domestic product GDP, per capita GDP, electricity consumption price/kwh and population, to develop the different regression models. The historical data considered for time period of past 47 years from 1970-2016. This paper is divided into two parts, in first part estimation of income, price and GDP elasticities are evaluated for residential, non-residential and total electricity consumption models. These elasticities showed that long-run and short-run price elasticities for domestic model are -0.30 and -0.32, for non-domestic model 0.42 and 0.64 where-as for total electricity consumption model price elasticities are 0.50 and o.93. In addition GDP/per capita and GDP resulted higher values. In second part, different statistical models are presented by using linear regression, which are based on the stationary or co-integrated time series data. Moreover for checking the validity of proposed models different statistical tests are conducted. A comparison with available national forecasts, which are proposed through different econometric models, like support-vector model or Pakistan's long range-energy alternative plaining (LEAP) model was exmined, resulting that proposed regression model has compatibility with national projections, with deviation of ±2% to ±12% for the best and worst case, these deviations are acceptable in the time span taken into account.

***Keywords*—** Forecasting, Electricity consumption Estimates, Multiple linear regression.

I. INTRODUCTION

Energy has major contribution in the development and better economic growth of any country. Growing demand for energy needs to be accurately estimated, to maintain the socioeconomic development and hence required to construct quick-witted forecasting models and algorithm. Prediction of energy consumption pattern based on non-economic and economic index may be accomplished by non-linear or linear statistical methods or by simulation models. Worldwide energy consumption is increasing fast (2.2% reported in the year 2017)[1] due to continuously changing living standards, increase in human population, focus on large scale industrialization and increasing rate of urbanization in the developing countries[2]. Pakistan is also a developing country and has registered a growth rate of 6.1% in its energy consumption in the year 2017 [1].There are six main sectors of electricity consumption, as illustrated in fig 1 percentage-wise sectorial electricity consumption of Pakistan([3][4]

Modeling and forecasting of electricity consumption is an important planning activity which needs to be conducted on regular basis to incorporate the dynamics of socioeconomic variables and policies that directly impact the electricity consumption profile of the country.

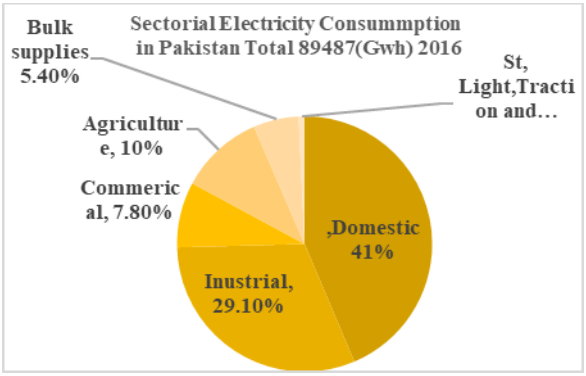

Fig1 Percentage-wise sectorial Electricity consumption of Pakistan (NTDC)[4]

Currently energy modeling is an interesting subject among the engineers and scientists concerned with the problem of energy supply and demand. Energy modeling in every sector assemble significant contribution in policy formation and planning, regarding to this energy management and planning can't possible without the information of past, present trend and future projection of energy demand. Future forecasting of energy demand helps to long-term policy makers in developing countries [5]. Lower estimation of consumption would lead to create shortfall between supply and demand, which may cause of deviation in economic growth rate, whereas higher estimation may cause of wasted financial resources due to unnecessary investment. Therefore it is desirable to propose energy consumption model with better accuracy for the best use of resources. Also it would be desirable that proposed model must handle the non-linear data of indicating variables [6]. It is important to understand the impact of co-related variables which are effecting electricity consumption. Some authors have

studded the behavior of electricity consumption drivers which are essential for forecasting. Review of published studies by national and international authors are discussed here. Tabasi, et al, [7] studied the behavior of indicating parameters and performed forecasting up-to 2022, by evaluating historical data from (2003-13), for Germany in the year of (2016) using linear regression analysis. Salari and Javid, (2016)[8] investigated the indicator of energy consumption and presents the alternative scenarios for reducing the residential energy demand of United States by using both static and dynamic estimation models. Mohamed and Bodger,[9] performed an critical analysis over correlation between the electricity usage and its demographical variables, and estimated the future energy consumption by using multiple linear regression analysis for New Zealand. S. Saravanan et al, [10] studied the influence of economical deviations on energy usage and investigated the future estimates of electricity consumption up-to (2021) in India with the help of Artificial neural network (ANN) and linear regression. M. Kankal and M. Ihsan, [5] considered gross domestic product (GDP), population import and export as explaining variables for electricity usage to analyze the correlation and investigate the future consumption in Turkey, they developed linear regression and (ANN) models. Bianco et al., (2009)[2] proposed linear regression model to analyze the impact of growing population , GDP, and electricity price per kwh over electricity consumption in Italy, and they performed forecasting up-to 2030 on the basis of 37 years historical data. The study caried out by same authers of refference [10], (2010) [11] they developed the linear regression and Grey prediction models based on the data from (1975-2007) for Romania, where they examined the income and price elasticities, also forecasted the future growth of electricity consumption. Erkan et al, (2009) [12] measured short-run and long-run price and income elasticities and estimated the future demand of energy, through co-integration tests and Auto Regressive Integrated Moving Average (ARIMA) model. They used time series data from (1984-2007) and considered different independent variables in the case of Turkey.

Literature regarding electricity consumption and its elasticities estimations in Pakistan will be discussed in well manner. N. Hussain et al, (2018)[13] developed Pakistan's Long-range Energy Alternative Paining (LEAP) model, and considered data from (1991-2015) they analyzed the electricity usage and predicted future consumption up-to (2050). In some studies of (2014) and (2017) [14]15] ARIMA and Holt Winter methods are focused for examining the relationship between dependent and independent variables and for future projections of electricity consumption. Mostly LEAP model was used in different recent studies [16] [17] [18] for energy consumption forecasting in Pakistan. Mamodia (2015) [19] developed multiple linear regression technique to determine the impact of economic changes on electricity usage for India. Rallapalli and Ghosh (2017)[20] used ARIMA and Time Trend method in India to make forecasts and investigate the influence of economic factors which are gross domestic product, population, price of electricity import and export considered as demographical variables. Literature review of national authors comprising on estimation of income and price elasticities of electricity consumption briefly analyzed. Akbar Ullah et al, (2019)[21] presented Auto Regressive Distributed lag (ARDL) and Econometric decomposition models to calculate the price and income elasticities. They considered modeling data for the period of (1972-2012) of explanatory variables which are electricity price and income. The concluded survey of estimations [22][23][24] presents the Econometric and log linear function over correlated variables such as income, price and no of customers. (Faisal Mehmood et al,) (2019)[25] developed ARDL and modified IPAT models to measure the casual relationship between electricity consumption and indicating parameters (i-e price and income) They accounted the data for the period of (1976-2013).

Pakistan is blessed with many optimum resources like hydro, coal, thermal, solar and wind energy, but unfraternally unable to meet its own demand only because of few reasons such as Government's poor future policy formation, planning and management and political interference, because every political party only think about its tenure. According to the best knowledge of authors' literature concerned with Pakistan is facing the problem of scientific analysis of demand drivers and estimation of price and income elasticities for non-domestic and domestic consumption. Different national authors mostly used different models other than statistical method named as multiple linear regression analysis which has an application of quick-weighted with better accuracy and easy to implement. The beauty of this study is to investigate the behavior of co-related variables and to provide the future prediction of electricity consumption in Pakistan for long-term policy formation using different econometric models, based on historical stationary data and its cointegration tests. In the first part of paper it is targeted to estimate price and income elasticities of electricity consumption. Where-as in second part the target is to propose forecasting models, with better accuracy. By using multiple linear regression, GDP, population and electricity price/kwh are selected as explaining variables to forecasts Pakistan's electricity consumption up-to 2040 is presented. For simplification of proposed regression models only income [ratio between GDP and population (GDP per capita)] is also selected as explaining variable.

The results of proposed models compared with the Pakistan's official National Transmission and Dispatch company(NTDC) forecasts, and with public private research organization's results which are concerned with the field of energy management. It is illustrated that there is best understanding among the different predictions .

II. METHODOLOGY

A. Data Sets

Time series data for forecasting is considered for the period of 1970-2016, on the annual electricity consumption of past 47 years, according to usage (domestic and non domestic), data is collected from National Transmission and Dispatch Company Limited (NTDCL) report[4], NTDCL is a public-private company provides services throughout the coutry except Karachi region, acts as Transmission Network system operator; also deal with cross-border electricity trade.

Time series data of electricity consumption are reported in fig.2 and the demographic variables (i.e.population, GDP, GDP per capita and price of electricity per kwh) are presented in fig.3.

It can be noted that growth trend of consumption remained substantial linear. but from 2000-2010 a marked declines in electricity usage was noticed due to energy shortage of that period [26]

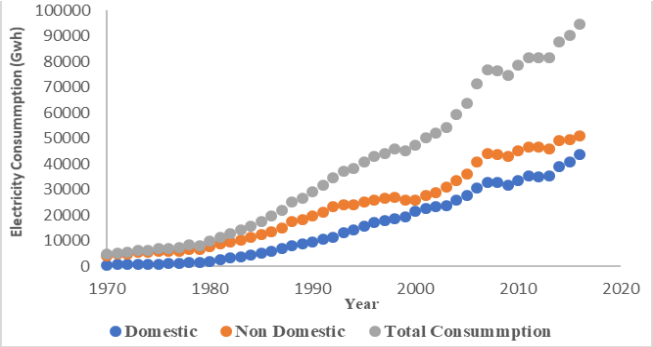

Fig.2.Represent historical data for electricity consumption

The historical data of GDP and GDP per capita is taken from the NTDCL report [4] if one compares the profile of Electricity consumption with GDP and population trend a percantage reduces in GDP and in response to that there is decrease in both domestic and non domestic consumption, so it can be observed that there is strong relation between GDP in fig.3.a, electricity consumption in fig.2. and population trend in fig.3.b. Around 2008 Electricity consumption grows faster because of three root causes, rapidly increasing GDP per capita, faster population growth rate and electricity intensity, which is the cause of summer air conditioning load, of mainly domestic and commercial costomers.

The time series data of population for same period is reported in fig.3.b.and it has linear trend through out the considered period with average growth rate of 2.965% and average death rate is 0.698% , the population data is collected from Pakistan Bureau of Statistics (PBS)[27], is the Government's offical institute which is concerned with country statistical record of population, labour force, empolyment,products, import and export etc. The data of electricity price reported in fig.3.d.it is distributed in three categories for the sake of understanding; domestic, non-domestic and total electricity price as shown in fig; data is collected from the NTDC[4] has interesting behavior slightly increasing up-to 1993 then increasing rapidly from1994-2016 because of different economic cycles, .and higher increments was detected in non-domestic tariff, in 2016 it reaches at peak value, the variations in oil and gas prices were the main causes of these sudden changes. Pakistan is a developing country in which mostly generation of electricity is dependent on imported oil and gas resources.[28]

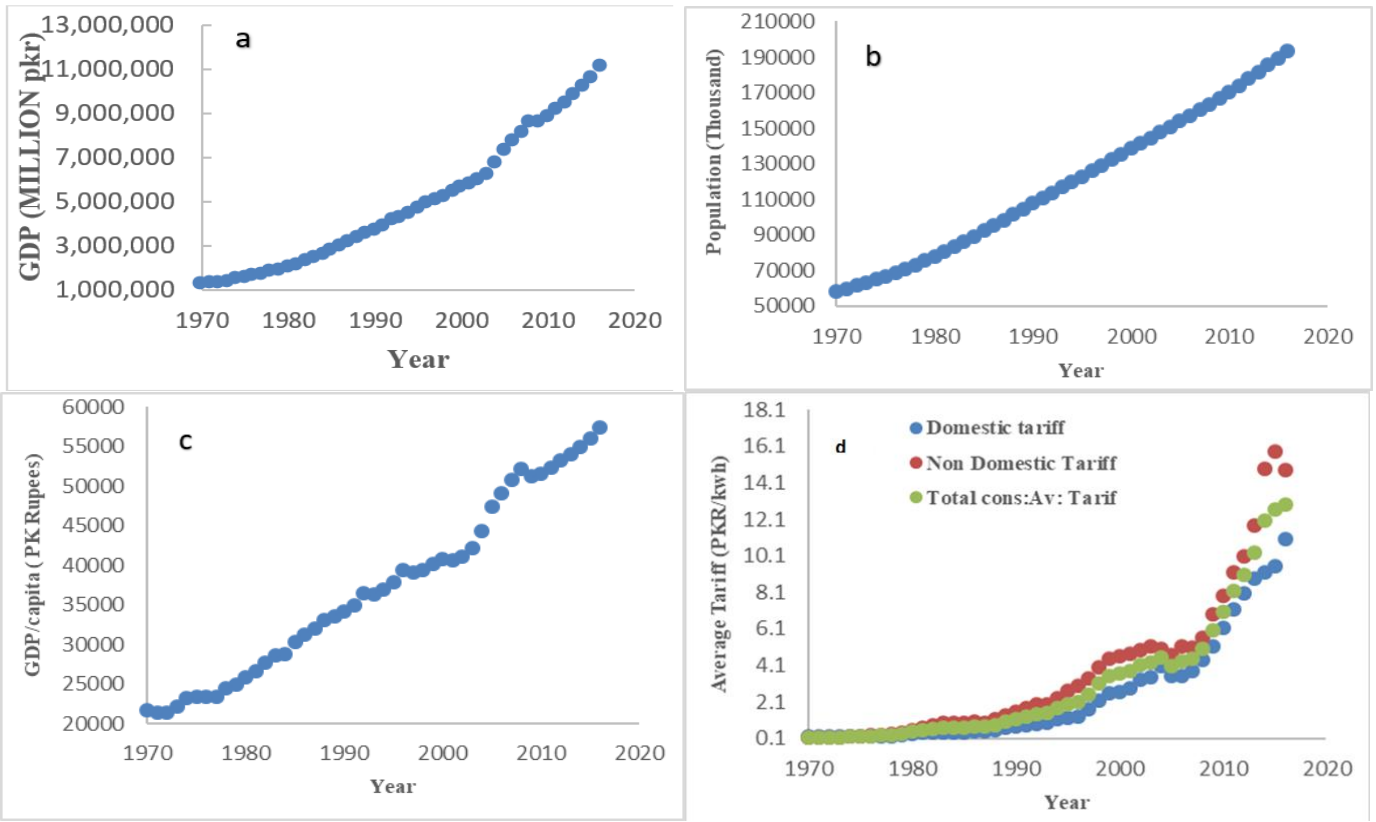

Fig.3.Represents historical data for selected explaining variables (i.e GDP, GDP per capita, population and price)

B. Estimation Of Elasticities

In this part three single equation consumption models are proposed, first one for domestic second for non-domestic and third for total electricity consumption. These models expressed in linear logarithmic form in which annual domestic electricity consumption is linking to annual values of domestic average tariff and GDP per capita for first model,

in second model non-domestic consumption links to non-domestic average tariff and GDP, where as in third model total electricity consumption links to total electricity average tariff, GDP and time trend which is proxy for technical progress[12][11][10]

Model 1

$$\text{Log}(E_{dom.t}) = \alpha_o + \alpha_1 \log(X_{1,t}) + \alpha_2 \log(P_t) + \alpha_3 \log(E_{dom,t-1}) \quad (1)$$

Where (Edom, t) is the domestic consumption. X1,t is the per capita GDP. Pt is the price for domestic customers , α0, α1, α2, α3 are coefficients of linear regression and t-i as subscript for the indication of lag term (i.e. t-1 defines lag1.

Model 2

$$\text{Log}\,(E_{ndom.t}) = \beta_0 + \beta_1 \log(x_{2.t}) + \beta_2 \log(PR_{.t}) + \beta_3 \log(PRN_{.t-1}) + \beta_4 \log(E_{ndom,t-1}) \quad (2)$$

Where (Endon, t) is the non-domestic consumption. X2,t is the GDP. PR, t is electricity price for non- domestic customer PRN t is a time trend β0 B1 β2 β3 β4 are regression coefficients.

Model 3

$$\text{Log}\,(E_{total.t}) = \gamma_0 + \gamma_1 \log((X_{3.t}) + \gamma_2 \log(PRT_{.t}) + \gamma_3 \log(PRTN_{,t-1}) + \gamma_4 \log(E_{total.t-1}) \quad (3)$$

Where (E total, t) is the total electricity consumption. X3, t is the GDP. PRT, t is the total electricity average price PRRTNt-3 is a time trend and γ0, γ1, γ2, γ3, γ4 are the regression coefficients.

From equation (1) coefficients α1 α2 represent the price and income elasticities in short-run for domestic electricity usage, and regression coefficients β1 β2 in equation (2) represent the short run price and GDP elasticities for non-domestic electricity usage, whereas from equation (3) regression coefficients γ1 γ2 represent short run GDP and total electricity price for total consumption[12]

From equation (1), (2) and(3) it is expected that short run GDP and GDP per capita (α1, β1, γ1) coefficients should be greater than zero for the reason of economic intensity and to increase the sale of electrical services and goods, where-as short run price elasticities coefficient (α2, β2, γ2)must be less than zero for usual cause economy[2]. Now the elasticities for long-run can be determined by dividing short run elasticities by (1-α3), (1- β4) and (1- γ4) for all above proposed models respectively as mentioned in[12]

$$Lm_1 = \alpha_1/(1-\alpha_3)$$
$$Lm_2 = \alpha_2/(1-\alpha_3)$$

$$Lmn_1 = \beta_1/(1-\beta_4)$$
$$Lmn_2 = \beta_2/(1-\beta_4)$$

$$Lsmc_1 = \gamma_1/(1-\gamma_4)$$

$$Lsmc_2 = \gamma_2/(1-\gamma_4)$$

Lm1 and Lm2 are the long run income and price elasticities for model.1, Lmn1 and Lmn2 are the long run GDP and price elasticities for non-domestic model.2 finally Lsmc1 and Lsmc2 are the long run GDP and total electricity price elasticities for model.3.

The results of estimated co-efficient are presented in Table I, for electricity consumption. Test for serial correlation Breusch-Godfrey serial correlation LM test is applied which notify that residuals are free from serial correlation. Moreover to investigate the presence of unit root and to determine integration order of the selected independent variables Augmented Dickey- Fuller (ADF) test is applied on the natural logarithmic form of variables for three models. (ADF) test statistics presented in Table II, the unit root for null hypothesis could not be rejected at the significance level of 10% only for series PR,t Stationarity is detected at first difference. Again (ADF) at first difference of variable defines that the series PR,t is integrated of order 1, 1(1).Whereas for all other series unit root for null hypothesis cannot be accepted at significance level of 10%, which concludes that they are integrated with order of 0, 1(0) in nature.

TABLE I Statistics summary of elasticities estimations and regression coefficients over the period of 1970-2016 for model 1, model 2 and model 3.

Domestic Model		**Non Domestic Model**		**Total Consumption Model**	
α_0	-20.6844	β_0	-0.27875	γ_0	-1.40868
α_1	5.48389	β_1	0.89937	γ_1	1.18662
α_2	-0.30116	β_2	0.42202	γ_2	0.50639
α_3	0.07019	β_3	-0.48206	γ_3	-0.708
Lm_1	5.89786	β_4	0.34088	γ_4	0.45802
Lm_2	-0.32389	Lmn_1	1.3645	Lmc_1	2.18943
R^2 adjusted	0.968	Lmn_2	0.64028	Lmc_2	0.93435
F	363.689	R^2 adjusted	0.98	R adjusted	0.9929
		F	1120.5	F	1126.24

TABLE II Summary of unit root test "Augmented Dickey-Fuller ADF" on the logarithm of selected variables. The level of confidence at which hypothesis can be rejected that the series contains unit root is illustrated in parenthesis

Variable	**ADF test statistics**	**Test equation**
$\mathbf{E_{dom,\,t}}$	0.031927 (99.55%)	Constant +Trend
$\mathbf{E_{ndon,\,t}}$	-0.490537 (98.06%)	Constant +Trend
$\mathbf{E_{\,total,\,t}}$	-0.084871 (99.37%)	Constant +Trend
$\mathbf{X_{1,t}}$	-0.216986 (92.88%)	Constant
$\mathbf{X_{2,t}}$	-0.502680 (97.99%)	Constant +Trend

P_t	1.117882 (99.71%)	Constant
PR, t	-1.298541 (87.59%)	Constant +Trend
PRT t	0.297423 (91.72%)	Constant

C. Multiple Linear Regression Models

For the visual analysis of annual electricity consumption up-to 2040, a multiple linear regression model is used, in which we focused annual population and GDP time series. Due to low elasticity impact of price is eliminated from model, as same technique is utilizes in [2]

Constructed models are illustrated as below.

$$E_{dom,t} = \alpha + \beta_1 X_{1,t} + \beta_2 X_{2,t} + \beta_3 E_{dom,t-1} + e \quad (4a)$$

$$E_{ndom,t} = \alpha + \beta_1 X_{1,t} + \beta_2 X_{2,t} + \beta_3 X_{2,t-1} + \beta_4 X_{1,t-1} + \beta_5 E_{ndom,t-1} + e \quad (4b)$$

$$E_{total,t} = \alpha + \beta_1 X_{1,t} + \beta_2 X_{2,t} + \beta_3 X_{1,t-1} + \beta_4 E_{total,t-1} + e \quad (4c)$$

Where Edom, t, Endom, t, Etotal, t are the domestic , non-domestic and total, annual electricity consumption in GWh, X1,t denotes annual GDP in million Pak: rupees, X2,t represents the population in thousands and α, β1, β2, β3, β4, and β5 are the regression coefficients and e is the random error.

The independent variable GDP (X1,t) and Population (X2,t) are forecasted by simple linear regression equations shown below for the time t.

$$X_{1,t} = d_1 + p_1 t \quad (5)$$

$$X_{2,t} = d_2 + p_2 t \quad (6)$$

d_1, d_2, p_1, p_2, are the regression coefficients.

However it is desirable to note that time t is equal to 1970. Equation 5 and 6 are introduced to forecast GDP and Population in order to forecast annual electricity consumption.

For the simplification of first model here another model is proposed on the basis of GDP per capita means ratio between GDP and population as independent variable which is illustrated as a simple linear regression in following equations.

$$E_{dom,t} = \alpha + \beta_1 X_{3,t} + \beta_2 E_{dom,t-1} + e \quad (7a)$$

$$E_{ndom,t} = \alpha + \beta_1 X_{3,t} + \beta_2 E_{ndom,t-1} + e \quad (7b)$$

$$E_{total,t} = \alpha + \beta_1 X_{3,t} + \beta_2 E_{total,t-1} + e \quad (7c)$$

E, t is the electricity consumption in GWh, X3,t is the annual GDP/capita or (income) in Pak: rupees and α, β1 β2 are the regression coefficient and e is the random error. Independent variable GDP per capita X2, t is generated by simple regression as in equation (5), (6)

$$X_{3,t} = d_1 + p_3 t \quad (8)$$

d_3 and p_3 are the coefficients.

Table III describes the matrix of correlation for all selected variables in Eqs (4a)-(4c) data for the period of 1970-2016, there is high degree of correlation between all the dependent and independent variables.

The Breusch-Godfrey Serial Correlation LM test is used to investigate the correlation between dependent and explanatory variables for Eqs (4a)-(4c) and Eqs (7a)-(7c) which shows that there is no serial correlation. For the unit root problem (ADF) test is applied to determine either the data is stationary or not on time series data for the period of 1970-2016 of considered variables (Edom,t, Endom,t, Etotal,t,, X1,t, X2,t, X3,t) and a unit root problem was detected means that the data is non-stationary. For making data stationary differentiated once and ADF test was applied again on the first difference so the variables becomes stationary meaning that there is no any unit root problem detected after first difference as explained in Table IV. Therefore it is decided that they are integrated with order of 1, 1(1)

TABLE III: Matrix of correlation for considered variables of Eq, (4a-4c)

	$E_{dom,t}$	$E_{ndom\ t}$	$E_{total,t}$	$X_{1,t}$	$X_{2,t}$
$E_{dom,t}$	1			0.9956	0.988
$E_{ndom\ t}$		1		0.9928	0.99
$E_{total,t}$			1	0.9962	0.9912
$X_{1,t}$				1	0.98786
$X_{2,t}$					1

TABLE IV: Augmented Dickey- Fuller (ADF) test results of considered variables on the first difference. The series contain a unit root can be rejected at high confidence level reported in parenthesis.

Variables	ADF test statistic		Test equations
$E_{dom,t}$	-4.1062	(>95%)	Constant
$E_{ndon,t}$	-4.6889	(>95%)	Constant
$E_{total,t}$	-4.5649	(>95%)	Constant
$X_{1,t}$	-2.5112	(>95%)	Constant
$X_{2,t}$	-3.1743	(>95%)	Constant
$X_{3,t}$	-4.6344	(>95%)	Constant

According to Engle and Granger if the selected variables are 1,1(1) as given in [12] then Eq.(4)-(7) can be calculated by ordinary least square (OLS) and resulting residuals are stationary, 1(0) then the (Edom,t, Endom,t, Etotal,t, X1,t, X2,t, X3,t) selected variables are said to be co-integrate. Hence the estimation equations are fine in equilibrium relation for long-term estimations.

Augmented Engle and Granger co-integration test is applied on residuals [29][30] of Eq. (4)-(7) conformed that the residuals of all equations are 1(0) and the hypothetical guess of unit root is unacceptable at high confidence level greater than (95%) as defined in Table V. Hence the equations which are estimated to forecast electricity consumption are valid and selected variables are co-integrated. All the regression coefficients are represented in Table VI. Fig:4 shows the residuals of Eq.(4a-4c)-(7a-7c) are all fit inside the average

range of (±3%) and there is no revealing a particular behavior, conformed that there is no serial correlation.

TABLE V: Summary of Augmented Engle Granger test

Residuals	ADF test statistic	ADF 95% critical value
Eq. (4a)	-5.1156	-2.9282
Eq.(4b)	-4.5262	-2.9435
Eq.(4c)	-4.7457	-2.9282
Eq.(7a)	-5.2249	-2.9282
Eq.(7b)	-5.1555	-2.9381
Eq.(7c)	-5.4729	-2.9281

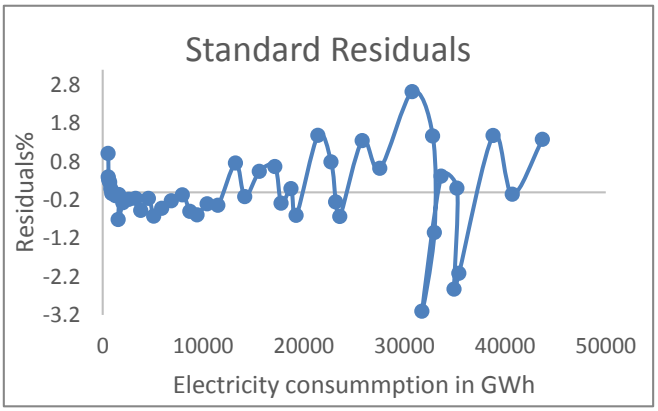

fig: 4 Residual plots of Eq, (4a)

D. Models On Percentage Difference Data Of Year To Year

In this sub section an alternative method is developed in which it is necessary to make the data stationary thereby obtaining the desired forecasting equations. There is a technique to differentiate the data for stationary data series as seen in pervious sub section. First derivative of variables will be involved in the resulting regression equations. On the other hand in a simple way equations will be difficult to handle with derivatives. The technique developed here is to create percentage difference on year to year of variables, as resulting equations can be utilized to measure the percentile deviations with respect to previous year which may be used to perform forecasting. The proposed technique explained in following form.

To determine the correlation in data series the Breusch-Godfey Serial Correlation LM test is applied on Eq. (9a)-(9c) and (10a)-(10c) which shows the residuals are free from serial correlation. The coefficients of Eq. (9) and (10) are presented in Table VIII. The hypothesis of all first differenced variables cannot be accepted at high confidence level more than (99%) except $\Delta X_{2,t}$ whose null hypothesis may be rejected at (95%) as shown in Table VII.

$$\Delta E_{dom,t} = \alpha + \beta_1 \Delta X_{1,t} + \beta_2 \Delta X_{2,t} + \beta_3 \Delta E_{dom,t-1} e \quad (9a)$$

$$\Delta E_{ndom,t} = \alpha + \beta_1 \Delta X_{1,t} + \beta_2 \Delta X_{2,t} + \beta_3 \Delta X_{2,t-1} + \beta_4 \Delta X_{1,t-1} + \beta_5 \Delta E_{ndom,t-1} + e \quad (9b)$$

$$\Delta E_{total,t} = \alpha + \beta_1 \Delta X_{1,t} + \beta_2 \Delta X_{2,t} + \beta_3 \Delta X_{1,t-1} + \beta_4 \Delta E_{total,t-1} + e \quad (9c)$$

Where Δ is the operator of percentage change (i.e. $\Delta E_{dom,t} = (\Delta E_{dom,t} - \Delta E_{dom,t-1}) / \Delta E_{dom,t}$) while the variables are same as defined in Eq. (4) and (7). The same variables also considered when the GDP per capita plays role in in electricity consumption leading to:

$$\Delta E_{dom,t} = \alpha + \beta_1 \Delta X_{3,t} + \beta_2 \Delta E_{dom,t-1} + e \quad (10a)$$

$$\Delta E_{ndom,t} = \alpha + \beta_1 \Delta X_{3,t} + \beta_2 \Delta E_{ndom,t-1} + e \quad (10b)$$

$$\Delta E_{total,t} = \alpha + \beta_1 \Delta X_{3,t} + \beta_2 \Delta E_{total,t-1} + e \quad (10c)$$

Whereas $\Delta X_{1,t}$, ΔX_{1t-1} and $\Delta X_{3,t}$ can be calculated be same equations (5), (6) and (8).

TABLE VI: Regression Coefficients summary of Eq. (4a)-(4c)-(7a)-(7c)

Model	α	β_1	β_2	β_3	β_4	β_5	D	p
Eq.(4a)	-2936.5396	0.866893	0.0284628	0.7496265				
Eq.(4b)	-2043.7572	5.3187987	-0.0087681	0.0520273	-5.3134733	0.8631775		
Eq.(4c)	-7824.1547	2.0572025	0.1701899	-0.064503	0.6531664			
Eq.(5)							-212.71698	211.07351
Eq.(6)							47067.588	2989.187
Eq.(7a)	-3781.9854	0.171353	0.8894045					
Eq.(7b)	-12057.1	0.6328497	0.541173					
Eq.(7c)	-14609.013	0.7101226	0.7400402					
Eq.(8)							17749.171	806.05336

TABLE VII: Unit root test Augmented Dickey-Fuller (ADF) on the considered variables in Eq. (9a-9c) and Eq. (10a-10c) the hypothesis that the series contain unit root can be rejected at confidence level reported in parenthesis.

Variables	ADF test statistic		Test equations
$\Delta E_{dom,\,t}$	-4.3518	(>99%)	Constant
$\Delta E_{ndon,\,t}$	-5.9565	(>99%)	Constant
$\Delta E_{\,total,\,t}$	-5.7819	(>99%)	Constant
$\Delta X_{1,t}$	-5.8652	(>99%)	Constant
$\Delta X_{2,t}$	-3.6144	(>95%)	Constant + Trend
$\Delta X_{3,t}$	-5.4092	(>99%)	Constant

E. Root Mean Square Error (RMSE) Analysis

For visual error analysis, based on root mean square error (RMSE), is a mathematical expression which is provided in order check the model reliability and performance. The standard error can be calculated by following equation.

$$S_{XE}=\sqrt{\frac{\sum_{i=1}^{N}(E-Eest)^2}{N}} \qquad (11)$$

Where E is the actual value and E, $_{est.}$ is the is the value of estimation from proposed models.

The model reported by Eq.(4a)-(4c) is within average standard residual of ±3.0% regarding actual time series data, where as the standard residuals for the Eq. (7a)-(7c) ranges between the ±2.0% to ±2.5%. also the similar behavior is detected for Eq. (10a)-(10c).Now for checking the validity of all proposed models in this paper electricity consumption is estimated for 5 years assuming the base year is 2011 so that as in[2]. Moreover for justification the modeling efforts, results are compared with Naïve forecast (i.e. simple regression over the time). As the Table IX, shows all the results of estimated equations with deviations which are somehow greater than acceptable range, but if we compare with Naïve forecasting (i.e. fit line) resulted deviations are close to similar or within acceptable ranges, even simple regression has a good accuracy. Also the validation results for non-domestic and total consumption are detected similar, which are omitted for simplification. It can be noted that equations to forecast electricity consumption with acceptable deviation ranges having good accuracy to the actual data, one can notice that the deviations for the year 2014-2016 are greater due to the average increasing rate of consumption is lower than the average increasing rate. Accordingly it is necessary to consider annual the time series data available (i.e. 1970-2016) to develop the equation for future projection, now we can say that proposed equations in this study are valid models for forecasting Pakistan's electricity consumption

III. RESULTS AND DISCUSSION

A. Price And GDP Elasticities

Price and income elasticity are estimated from Eqs. (1), (2) and (3) showed that the higher income elasticity and low price elasticity to the consumption. Short run elasticities are lower than the long-run elasticities as expected. For domestic model short-run and long-run price and income elasticity are calculated by using Eq. (1) short-run and long-run price elasticities are -0.30116 and -0.32389 respectively quit low which does not affect electricity consumption or in other word consumption cannot regulated by varying the electricity price in Pakistan, where-as income elasticities for short-run and long-run are 5.48389 and 5.89786 respectively has higher value which describes that electricity consumption is closely attached to income of domestic costumer but price policies cannot regulate domestic consumption. For example if income doubles, the consumption of electricity increase by nearly 589%. Such that between the period 1980-1992 if domestic customer's income increases nearly 102% as the corresponding increase in domestic consumption was 570% which reacts an similar increase to the estimated elasticity. An estimations for two other non-domestic and total consumption models short-run and long-run price GDP elasticity are reported in table I.

Where-as domestic consumption represents higher value of price elasticity which can be explained with their major flexibility in the use of electricity. Users may react to save energy in case of expensive bills. For instance turning off all unnecessary appliances or make their use for less time (i.e. air conditioning in summer season and electric heater in winter season). As in [31] other passible ways seems quite limited for Pakistan's domestic customers, it is considerable fact that most of the cooking and heating system are dependent on natural gas or LPG (Liquid Petroleum Gas). An-other possibility is the installation of photovoltaic plants which is the alternative of electricity generation for domestic customers, but the initial costs with government contribution are still high.

There are many limitations to save electricity for non-domestic customer, but some of the passible options are more difficult. For example the replacement of old electrical machinery and other appliances with new which require extra cost, may result to decrease profit over investment ratio which may difficult for any businessmen.

Increasing price elasticity by lunching new tariffs with different categories between working days and weekend, also between working hours and late night [32] may be fruitful for non-domestic users, if a businessmen could change his working plan for production and store of goods. Eventually extra salary problem must be in consideration, due to weekends and non-working hours in the trade-off between electricity savings. Smart metering information system also helps non-domestic consumers to reduce price of electricity.

TABLE VIII: Regression co-efficient summary of Eq. (9a-9c) and (10a-10c)

Model	α		β_1		β_2		β_3		β_4		β_5	
Eq.(9a)	-0.0038	-0.59%	-0.088	-1.46%	0.44573	-1.60%	0.97033	-45.06%				
Eq.(9b)	-0.0755	-2.18%	1.452055	3.90%	5.62541	2.94%	-3.13493	-1.93%	0.1043	0.27%	-0.1927	-1.30%
Eq.(9c)	-0.1012	-3.14%	1.329419	3.97%	6.38951	3.65%	-2.13944	-1.45%	0.2181	0.62%	-0.3012	-2.07%
Eq.(10a)	0.04124	2.57%	0.884258	1.78%	0.3341	2.45%						
Eq.(10b)	0.02833	2.54%	1.267065	3.27%	-0.0582	-0.41%						
Eq.(10c)	0.03835	3.28%	1.200596	3.18%	-0.0224	-0.16%						

Table IX: Presented equations are validated only on domestic electricity consumption model,(the percentage changes with respect to historical data are reported in parenthesis) and compared with a naïve forecasting. The values are in GWh.

Year	Eq(4a)		Eq(7a)		Eq(9a)		Eq(10a)		Naïve forecast	
2012	36745.6	(-4.94%)	36672	(-4.75%)	34715.58	(-0.61%)	34716.67	(-(0.61%)	35229	(-0.85%)
2013	36931	(-4.11%)	36542.9	(-3.09%)	35964.59	(-1.53%)	35981.08	(-1.58%)	34928.6	(-1.38%)
2014	37747.5	(-2.82%)	37149.1	(-4.47%)	42188.38	(-8.00%)	42260.56	(-8.15%)	35412	(-9.6%)
2015	40765.5	(-0.092%)	40358.1	(-0.91%)	42657.5	(-4.52%)	42708.93	(-4.63%)	38813	(-4.93%)
2016	42725.1	(-2.32%)	42295.8	(-3.36%)	46672.89	(-6.32%)	46749.86	(-6.48%)	40728	(-7.34%)

B Forecasts Of Electricity Consumption

Electricity consumption forecasts determined on the basis of linear regression equations compared with the NTDC forecasts results [4] and with an-other National forecasts presented by [14]The forecasts presented by National Transmission and Dispatch Company (NTDC) represents, the official statistical report of Pakistan's Ministry of energy. Their resultant co-efferent are on the basis of microeconomic model which considers the historical data of major sectorial GDP, Population, yearly customer class and selling price/kwh as independent variables for long term planning up to 2037

NTDC provides major contribution in power sector of Pakistan also in cross-border interconnections of Pakistan with south Asia regional countries. They provided national forecasts on the basis of multiple linear regressions

Total electricity consumption forecasts presented in fig; 5(a). All proposed equations declares good agreement with the historical data given in [4] where-as smaller deviations accruing between forecasting equations.

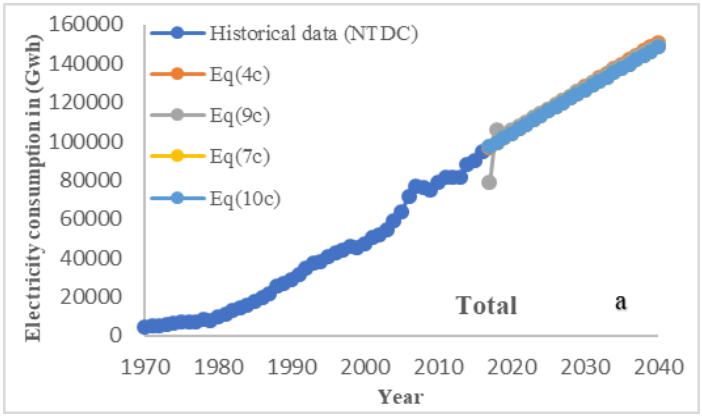

Figure 5 (a)

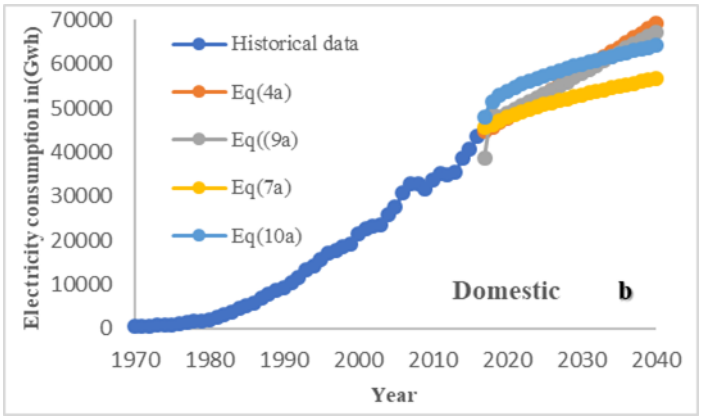

Figure 5 (b)

Fig. 5(b) represents the domestic electricity consumption forecasts, clearly demonstrate that Eq.(4a) and Eq.(9a) seem to in good agreement with data [27][4] where-as Eq.(7a) and Eq.(10a) lead to underestimate nearly 18% and 7% in 2040 respectivelyIt is necessary to mention here in Eq(7a) and Eq.(10a) the explanatory variable is GDP/capita only, where-as in Eq.(4c) and (9c) the considered explaining variables are GDP and population.

Non-domestic electricity consumption forecasts reported in fig; 5(c) nearly same deviations identified where Eq. (7b) and Eq.(10b) results underestimation about 7% and 13% in 2040. While Eq.(4b) and Eq.(9b) leads to perfectly fits the data given in [4].

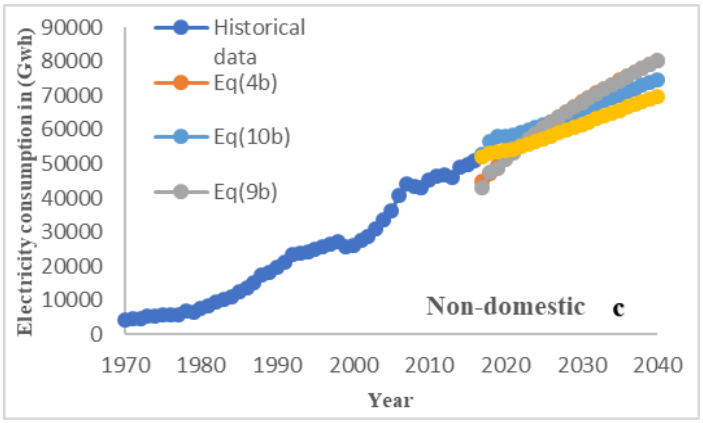

Figure 5 (c)

Fig; 5 (a), (b), (c) forecasts of electricity consumption

The meaning full result achieved from the comparison is that there is good similarities among the available forecasts of Pakistan[14] and proposed equations in this study, also difference between proposed models presents considerable deviations. In this study forecasting time period about 23 years is considered on the behalf of previous 45 years historical data. Prepared equations also has an-other important feature is that they are simple statistical models because there is only fundamental data of explaining variable is needed as input, permits to remove the cast linked to data searching which is basic need for econometric model[2]

Finally it is our personal opinion that the accuracy of proposed models could be increased by better forecasts of explaining variables such as accurate data of population projection available from Pakistan Bureau of Statistics [27] Moreover the accurate future forecasts of GDP could be avail from the State bank of Pakistan, ministry of finance or from merchant banks.

CONCLUSION

In the first part of study, analysis of price elasticities of non-residential and total electricity usage are quit limited, and price elasticities of domestic model results positive value which is greater than other two models. This analysis conclude two main ideas, Electricity price may not be considered as independent variable in forecasting models, for future projection of electricity consumption in Pakistan. And there is no any importance of pricing policies of national electric power regulatory authority (NEPRA) to make optimum usage of electricity in Pakistan. The

response of GDP and GDP per capita growth rate leading main role in electricity consumption, changing growth rate of GDP has proportionality to consumption, this relationship was detected from the estimation of elasticities. Therefore there is need to consider these variables as explaining variable for electricity consumption forecasts in Pakistan. In the second part of this paper different regression models were proposed for long-tern future projection of electricity in Pakistan. An increment in total electricity consumption will be result of both domestic and non-domestic consumption in the next years, would be expected with an average growth rate of about 2% per year in Pakistan. According to the data we can easily conclude that the eq.(4c) for total electricity consumption model, and Eq.(9a) and Eq.(4b) for other two models are valid with good accuracy for future projection of domestic and non-domestic consumption respectively, because these equations fit the data accurately. It is noticed that the analysis of elasticities, forecasts and our ideas presented in this study will be fruit full for policy makers and energy planers to build future scenario of electricity consumption in Pakistan.

REFERENCES

[1] "World energy review 2018."

[2] V. Bianco *et al.*, "Electricity consumption forecasting in Italy using linear regression models," *Appl. Energy*, vol. 34, no. 4, pp. 429–432, 2009.

[3] I. Zahid, "Enhancement of wind power generation in pakistan," no. February, 2017.

[4] P. Plan *et al.*, "Electricity Demand Forecast Report," *book*, 2014.

[5] M. Kankal and M. Ihsan, "Modeling and forecasting of Turkey ' s energy consumption using socio-economic and demographic variables," vol. 88, pp. 1927–1939, 2011.

[6] K. Kavaklioglu, H. Ceylan, H. K. Ozturk, and O. E. Canyurt, "Modeling and prediction of Turkey's electricity consumption using Artificial Neural Networks," *Energy Convers. Manag.*, vol. 50, no. 11, pp. 2719–2727, 2009.

[7] S. Tabasi, A. Aslani, and H. Forotan, "Prediction of Energy Consumption by Using Regression Model," vol. 02, no. March, pp. 110–115, 2016.

[8] M. Salari and R. J. Javid, "Residential energy demand in the United States : Analysis using static and dynamic approaches," *Energy Policy*, vol. 98, pp. 637–649, 2016.

[9] Z. Mohamed and P. Bodger, "Forecasting electricity consumption in New Zealand using economic and demographic variables," vol. 30, pp. 1833–1843, 2005.

[10] S. Saravanan, S. Kannan, and C. Thangaraj, "INDIA ' S ELECTRICITY DEMAND FORECAST USING REGRESSION ANALYSIS AND ARTIFICIAL NEURAL NETWORKS BASED ON PRINCIPAL COMPONENTS," vol. 6956, no. July, pp. 365–370, 2012.

[11] V. Bianco, O. Manca, S. Nardini, and A. A. Minea, "Analysis and forecasting of nonresidential electricity consumption in Romania," *Appl. Energy*, vol. 87, no. 11, pp. 3584–3590, 2010.

[12] E. Demand and A. Using, "Electricity Demand Analysis Using Cointegration and ARIMA Modelling: A case study of Turkey Erkan," *Energy*, no. 19099, 2009.

[13] N. Hussain, M. Aslam, and K. Harijan, "Long-Term Electricity Demand Forecast and Supply Side Scenarios for Pakistan (2015-2050): A LEAP Model Application for Policy Analysis Long-term electricity demand forecast and supply side scenarios for Pakistan (2015 e 2050): A LEAP model application for policy analysis," *Energy*, vol. 165, no. October, pp. 512–526, 2018.

[14] A. Hussain, M. Rahman, and J. Alam, "Forecasting electricity consumption in Pakistan : the way forward," vol. 90, pp. 73–80, 2016.

[15] S. Aziz, U. Rehman, R. Fazal, G. Valasai, and N. H. Mirjat, "An Integrated Modeling Approach for Forecasting," no. November, 2017.

[16] U. Perwez, A. Sohail, S. F. Hassan, and U. Zia, "The long-term forecast of Pakistan ' s electricity supply and demand : An application of long range energy alternatives planning," *Energy*, vol. 93, pp. 2423–2435, 2015.

[17] M. Syed, M. Farooq, and A. Qamar, "MODELING AND FORECASTING OF ENERGY SCENARIO IN PAKISTAN WITH Journal of Faculty of Engineering & Technology," no. October 2017, 2014.

[18] H. Ishaque and H. Ishaque, "Revisiting income and price elasticities of electricity demand in Pakistan Revisiting income and price elasticities of electricity demand in Pakistan," *Econ. Res. Istraživanja*, vol. 31, no. 1, pp. 1–15, 2018.

[19] T. Mamodia, "FORECASTING ELECTRICITY," no. August, 2015.

[20] S. R. Rallapalli and S. Ghosh, "Forecasting monthly peak demand of electricity in India-A critique," no. October, 2017.

[21] A. Ullah, Z. Neelum, and S. Jabeen, "Factors behind electricity intensity and efficiency : An econometric analysis for Pakistan," *Energy Strateg. Rev.*, vol. 26, no. August 2018, p. 100371, 2019.

[22] M. Zaman, F. Shaheen, A. Haider, and S. Qamar, "Examining Relationship between Electricity Consumption and its Major Determinants in Pakistan," vol. 5, no. 4, pp. 998–1009, 2015.

[23] M. Idrees, K. Raza, and B. Aziz, "An Econometric Analysis of Electricity Demand for the Residential Sector of Pakistan," vol. 9, pp. 1–18, 2013.

[24] M. Arshad and F. Abbas, "The dynamics of electricity demand in Pakistan : A panel cointegration analysis," *Renew. Sustain. Energy Rev.*, vol. 65, pp. 1159–1178, 2016.

[25] F. Mehmood, N. Fatima, and K. Ullah, "Impact of China-Pakistan economic corridor on Pakistan ' s future energy consumption and energy saving potential : Evidence from sectoral time series analysis," *Energy Strateg. Rev.*, vol. 25, no. March, pp. 34–46, 2019.

[26] I. N. Kessides, "Chaos in power: Pakistan's electricity crisis," *Energy Policy*, vol. 55, pp. 271–285, Apr. 2013.

[27] Y. Book, *PAKISTAN STATISTICAL YEAR BOOK*. 2016.

[28] O. Rauf, S. Wang, P. Yuan, and J. Tan, "An overview of energy status and development in Pakistan," *Renew. Sustain. Energy Rev.*, vol. 48, pp. 892–931, 2015.

[29] F. Egelioglu, "Economic variables and electricity consumption in Northern Cyprus," vol. 26, pp. 355–362, 2001.

[30] H. A. Amarawickrama and L. C. Hunt, "Electricity demand for Sri Lanka : A time series analysis," vol. 33, pp. 724–739, 2008.

[31] F. Jamil and E. Ahmad, "The relationship between electricity consumption , electricity prices and GDP in Pakistan," *Energy Policy*, vol. 38, no. 10, pp. 6016–6025, 2010.

[32] S. Bruno, M. De Benedictis, M. La, and I. Wangensteen, "Demand elasticity increase for reducing social welfare losses due to transfer capacity restriction : A test case on Italian cross-border imports," vol. 76, pp. 557–566, 2006.

International Journal of Engineering Works
ISSN-p: 2521-2419
ISSN-e: 2409-2770
Vol. 7, Issue 01, PP. 48-57, January 2020
https://www.ijew.io/
https://doi.org/10.34259/ijew.20.7014857

Comparative Analysis of Virtual Inertia Techniques in Wind Energy

Adnan Ismail[1], Saddam Ali[1], Abdul Basit[1]
[1]United States Pakistan Center for Advanced Studies in Energy UET Peshawar, Pakistan
Received: 09 January, Revised: 16 January, Accepted: 24 January

***Abstract*—** Recent decades have seen an incline in integration of wind energy in to power systems across the world. This invariably leads to lower share of conventional power plant which subsequently reduces the grid's inertia as a consequence of the decoupling rotational mass of the variable speed turbines and grid through power electronic converters. Accordingly, the overall system inertia is lowered leading to more frequent and intense frequency variations concomitant with the variation in the load. This research focuses on alleviating the rotational mass and inertia related problems caused by increasing wind power integration by adding an inertial loop to compensate the impact of frequency deviations due to abnormal transient conditions. The virtual inertia, thus added, reduces maximum rotational speed deviation while at the same time making the system slower and more oscillatory. The simulation consists of addition of synchronous generator capable of adapting its power output to the fluctuations in grid loads. A load step has been added for analyzing the performance improvement of the system as a result of the virtual inertia addition. The simulation has been modeled in Simulink MATLAB. The addition of the inertial power results in the improving the frequency drop from 58.42 to 59.31 Hz. This stabilization of 0.9 Hz carries a lot of significance for improving grid stability. In addition the angular speed of the turbine has also been enhanced as a result of the virtual inertia. These findings will prove extremely helpful in offsetting the drawbacks of greater wind energy addition to grid. The analysis needs to be further replicated with other transient conditions before being implemented in the grid.

***Keywords*—** Virtual Inertia, Renewable Energy, Wind Turbine

I. INTRODUCTION

Energy being the necessity for driving human life its secure and accessible supply is critical for progressing of modern developing societies. Increase in population and evolution of societies has increased the demand for energy. Constant use of fossils fuels for energy generation, transportation, industries and other works of modern-day life will lead the world towards multiples challenges like depletion of natural reserves, global warming, climatic changes and geopolitical concerns. Exponential increase in global energy consumption needs to be met without implicating environment damage shows existing energy sources will not be sufficient for the future requirements and we should look for unorthodox ways to harness energy and not endanger the life of current and future generation [1].

Global energy demand according to International Energy Agency will increase 35% by 2035 where 60% of increase would be contributed by China, India and Middle East. The push of incorporating renewables in power system is due to the global concern about the negative impacts of global warming, motivating the countries around the world to produce clean and cheaper electricity [2].The shift from producing electrical energy from fossil fuels to producing energy from more environment friendly cheaper and readily available sources impact of carbon emissions due to burning oil or coal and environmental effects due to nuclear and hydroelectrical power plants can be reduced [3].

Intergovernmental Panel on Climate Change (IPCC) predicts vital changes in energy supply should be done in near future to prevent more than 2 degrees Celsius climate change which is boundary line above which human civilization and natural world will be at risk of disastrous changes. Genesis of half the global warming pollution is due to burning of fossil fuels for electricity production. Industries in general accounts 78% green house gases accumulating in atmosphere and trapping heat. In the last four decades human population amassed half of global pollution which is in the air we breathe severely affecting health and climate change [3].

Alternative energy sources solar, wind, biomass and geothermal energy are inexhaustible and widely available and have potential to meet world energy needs. To bring diversity in energy markets, sustainability in energy supplies, reduction in environmental effects, development and utilization of renewable energy sources are very critical. Solar and wind energy systems have grown exponentially in the last decade which have resulted in comparatively less initial investment, cost of electricity and more refined functioning of these systems. Amount of energy production from different available resources all over the world for year 2016 is show in Fig.1 [1].

Competition among countries have erupted that who will be the first country to utilize only renewable energy for 100% of the demand occurring. China has by far largest installed capacity of wind of all the countries. During first half of 2018 Germany produced enough renewable energy to power every household in country for a whole one year. Denmark, Portugal, Spain, Ireland and Germany have static electricity production of 39%,18%, 16%, 14% and 9% respectively from wind energy [4].

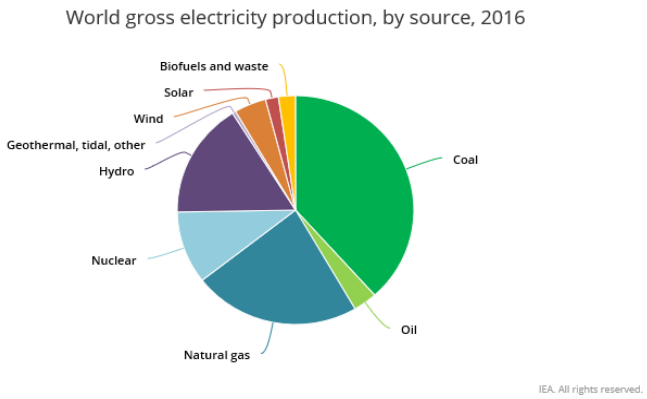

Figure.1 World Gross Electricity Production by Source, 2016

Conventional power plants are designed with large central controlled systems which are stable and more reliable compared to renewable power generation whom are distributed and independently controlled and their integration in power system confronts various challenges, uninterrupted power supply and impact of stability. Power quality issues arise from grid connected renewable generation as level of penetration increases, high fluctuations due to unstable nature of renewable sources can confront serious quality concerns. Unstable nature of these sources is because of varying weather conditions which also have an impact on the voltage and frequency fluctuation at interconnected power grid and transmission systems [5].

Power generated from sources solar photovoltaic (PV) system and wind turbine needs sunlight and wind to operate. Uncontrollable varying of the sunlight and wind gives inconsistent generation. Compared to solar power wind is less variable and changes occurs over hours not in seconds as in case of solar due to cloud cover. This fluctuating generation in turn needs instantaneous additional energy to balance out the supply and demand of power grid and frequency regulation and voltage support on transmission side. Improved weather forecasting can help predict the varying nature and help generate energy from solar and wind more accurately [5].

One of the major challenges with renewable power system is having less amount of rotational mass compared to conventional power systems which leads us to the minimum amount of inertia to maintain the proper operation and sustain any sudden changes in load and power generation. Wind power Systems must have greater flexibility to house the variation in supply side the generation limits and loads should be in synch. Sometimes with increase in load generation increases, but when wind generation increases, and load levels suddenly falls system needs to take additional control actions to balance gap between generation and demand. Adequate fast acting reserves needed to sustain up or down ramps of wind generation to keep system in equilibrium [6].

Charles Brush in 1888 was first to attempt generating electricity using wind turbine in United States. Turbine generated by brush had a diameter of 17meters and 144 rotor blades with generating capacity of 12kw power. Wind power like other renewable sources has gained importance in recent years. Generating energy from wind is increasing rapidly and large investments are done in increasing installed capacity. Marcellus Jacobs developed one of the first practical fault tolerant wind turbine system which had airfoil shaped blades and wane to keep the turbine in face of the wind. Types of wind turbines are differentiated from each other by orientation of their rotational axis. Horizontal axis wind turbines (HAWTs) are the most commonly used wind turbine which have evolved during the 20th century resulted in bigger, durable and advanced turbines. Vertical axis wind turbines (VAWTs) though having potential fell victim to the poor energy market or lack of interest and financial support kept away from public association. Vertical axis wind turbines are more suitable for tidal current power conversion [7].

Renewable energy technologies like solar and wind energy plants has little to zero inertia constant compared to power plants generating power from traditional sources. Wide adoption of these technologies and increase in share of global power generation is decreasing the rotating mass of synchronous generators, which has a significant effect on the stability and potential of power system in maintaining the frequency in desired limit during sharp changes in generation and load [8].These sudden load changes in conventional power plants are compensated through the kinetic inertia stored in rotor of the generator but in wind power plants virtual inertia method is implemented which imitates synchronous generator kinetic inertia to improve the dynamic response of the system [8].

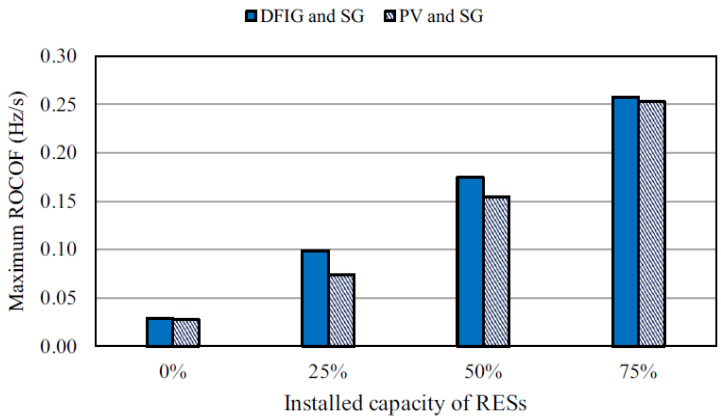

Figure 2: Increase in the rate of change of frequency in relation to different levels of RES integration

the integration of renewable energy system in a country's power system, in addition to increased reliability and improved voltage profile of the grid, also decrease the use of fossil fuel thus proving a net positive for the adopters [16-19]. The increasing penetration of the RESs however has been hampered by the concomitant challenges, such as frequency and inertia [20]. The challenges are manifesting in many forms. To start with the renewable energy systems are

generally regarded as low or nonexistent inertial response systems [21]. This is in part due to the fact that the wind turbines, being variable speed, are connected with the power network via power electronic converters, leading to practical decoupling of the wind turbine and the associated inertia from the system transient behavior. This ultimately leads to the overall reduction of power system inertial with increase in the RES integration_ a fact supported by the example of simulation on UK's energy system where researchers forecasted a decrease of inertia constant of the system by 70% between 2013/14 and 2033/34 as a direct outcome of increased renewable energy systems [22,23]. Consequently, the ROCOF (Rate of Change of Frequency) factor will be high enough to warrant power disconnection even in small imbalance situations. Figure 2 shows the ROCOF variation relative to the increased penetration of the renewable energy scenarios in a power grid covering 3.8 MW demand [24]. It is obvious that higher proportion of renewable energy systems in the grid leads to higher ROCOFs.

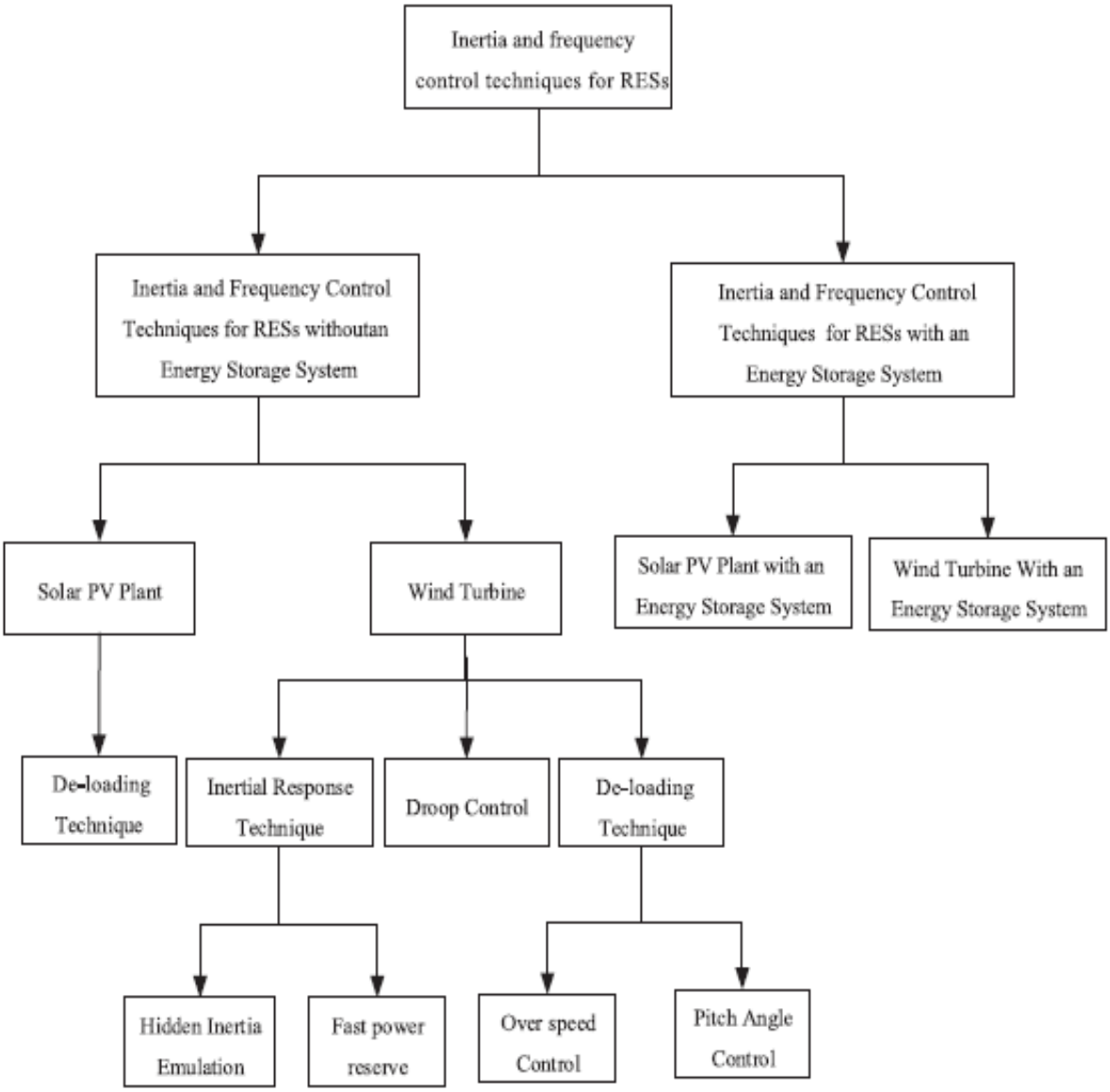

Figure 3 Renewable energy systems frequency and inertia control systems

Inertial control in wind power plants enables the release of the kinetic energy within 10 seconds of the frequency deviation in contrast to the reserve control system where pitch angle, and speed control or the combination of both results in balancing power output of the power plants. The general overview of the inertia response controls in RESs is shown in the figure 3.

The generator in the conventional power plants automatically releases the stored energy as per requirements, hence achieving stable operation. The wind power turbine, however, do not have the luxury hence necessitating a power controller. The inertia response is usually dealt with in two manners: Inertial emulation and fast power reserve. The former utilizes control loops for extracting kinetic energy stored in the blades upon requirements. The additional energy thus released compensates for the frequency disturbances. The later technique releases a predetermined constant power for a designated time to deal with the fluctuating frequency.

II. METHODOLOGY

Wind turbine used in this study is Doubly-fed Induction generator DFIG which is implemented for varying wind speeds. Wind turbine increasing penetration in power grid doesn't have effect on the frequency up and down. Responsibility of frequency regulation and automatic generational control lies on conventional generator to keep it in specified limit. Hence wind turbines do not increase or decrease their energy production when the frequency rise or falls, ultimately contributing nothing to the system inertia. DFIG turbines however has ability to deliver power and instantly reduce speed to release the stored kinetic energy to Block Diagram of proposed Wind Turbine System with Inertial Support help support conventional generator in restoring frequency to stable limits [50].

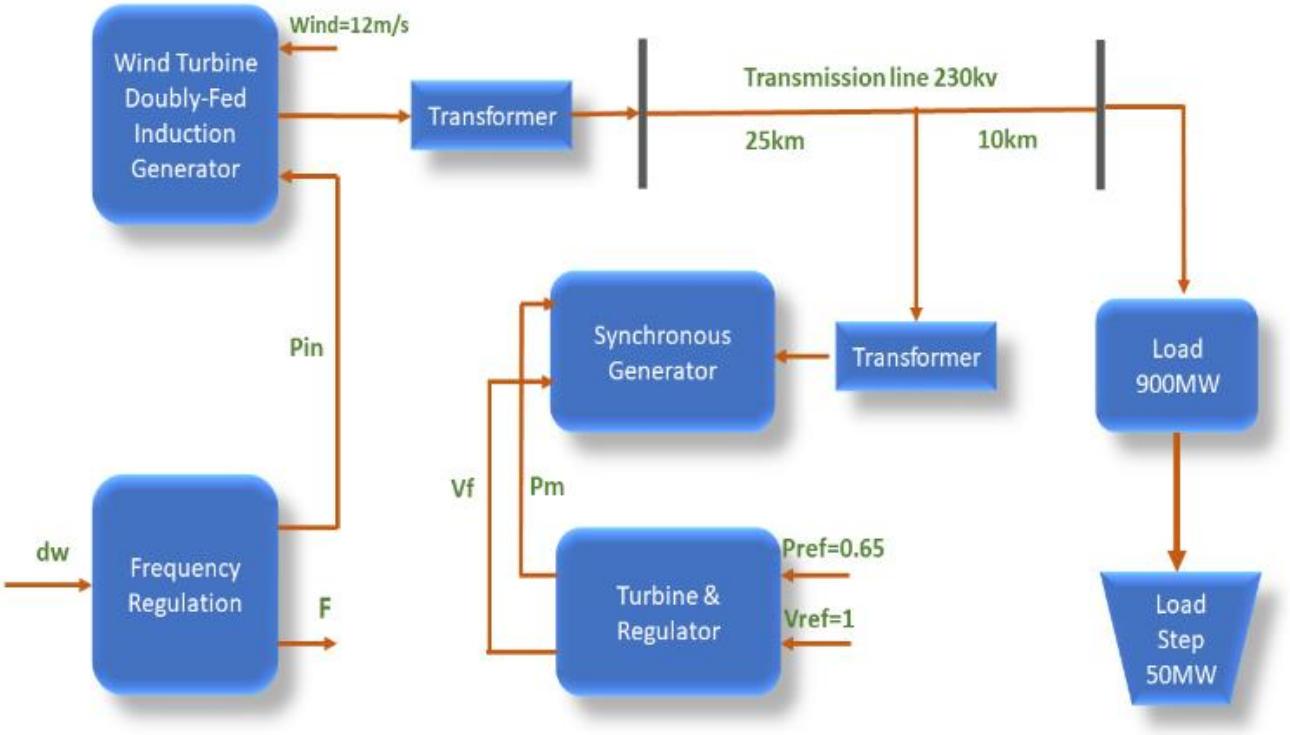

Figure.4 Block Diagram of proposed Wind Turbine System with Inertial Support

Wind turbine selected has the capacity of 225MW and wind set at 12m/s with 45 degree maximum pitch angle. Frequency for all the equipment is set at 60hz. A synchronous generator of capacity 900MVA connected with grid through the transmission line to provide the needed power in case of any unprecedent load changes or total fall. Synchronous Generator is not operating at its full capacity but at Pref =0.65 meaning the generator is operating at 585MW. A load of 930MW is also connected with grid and a load step of 50MW is introduced in the system at 100sec in the operation of the whole 150sec simulation.

All over the world it's a common practice of modern power system operator to reduce the rotational mass and replacing them with more efficient modern ways of producing power. Increasing use of power electronic converters due to the increasing penetration of renewable has led to the changing dynamic behavior of the power system. Renewable generating units, rotational mass from the grid are disassociated because they are connected via power electronic converter. Which lead the system operators to challenges; large power swings and frequency deviations [51].

Synthetic inertia is first line of defense to resist decreasing alternating current AC frequency which usually occurs due to tripping of large power plant which leaves the grid undersupplied consequently leaving the AC frequency to crash. Conventional power plants or synchronous generators have the capability to abruptly responds to the dips in frequency because of spinning turbines momentum whom are synched with the grid and resist any deceleration. Turbines momentum resist decrease in frequency, giving the power system precious secs to runup power reserves and fill the resulting supply gap [52].

Some studies show that negative grid stability can be upto an extent compensated by the renewable energy generators fast frequency response or by providing virtual inertia, but delay in response to the frequency change and the technology still in development compels the system operators to have some amount of synchronous generation for stability. Therefore synchronous generators are used in high renewable penetration power systems for inertial support [53]. Main advantage of synchronous generator is its physical inertia which can withstand changes in the grid parameters. Grid frequency can be measured from the generator speed of any generator connected on the synchronous grid. For any large shock like failure of power plant or transmission line the faster the rate of change of frequency, therefore grid needs inertia for stability [53]. In this study we have connected a synchronous generator with the DFIG wind turbine to analyze the effect of transients on the system with and without the inertial support.

For the synchronous generator to produce electricity and maintain constant voltage is supplied to the rotor of generator to produce magnetic flux that is essential for production of electricity. Current supplied to the synchronous generator excitation system is in alternating current AC fed from the generator output itself, in order to convert it to direct current DC it is passed through a thyristor-based rectifier and is then smoothen by passing through a filter. The level of DC can adjusted by firing signal of thyristor. The firing circuit of thyristor is controlled by voltage regulators which controls the excitation system of the generator. Current is directly fed to the generators rotor by way of slip rings which eliminates the problem of having another rotating machine [54]. A load step is added in the system to study transient condition and how the DFIG wind turbine react to any sudden increase in load.

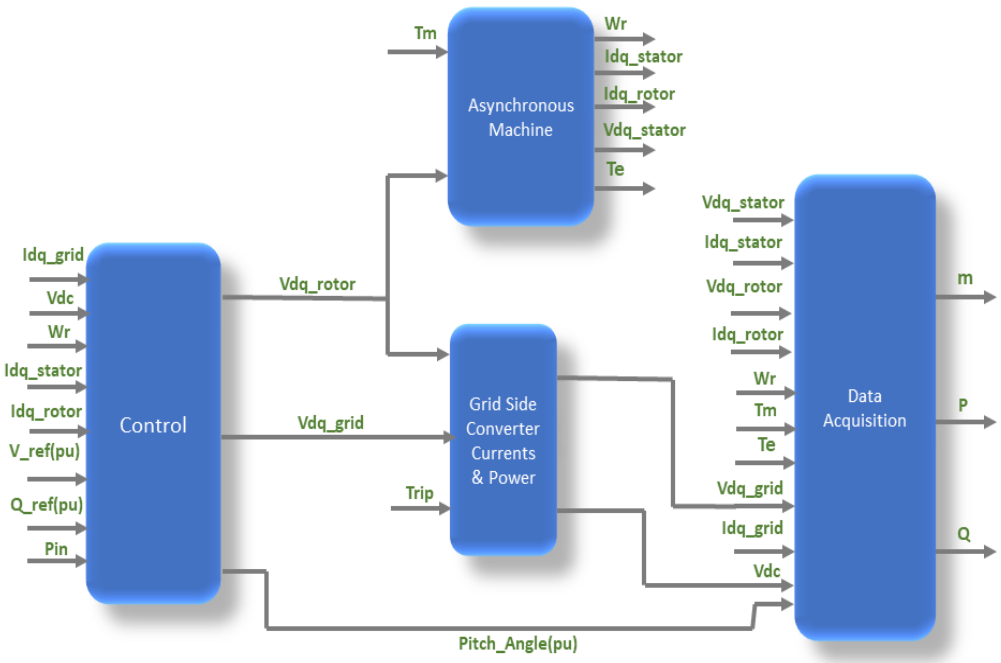

Figure.5 DFIG Wind Turbine Block Diagram

Electrical power system with multiple generators having low inertia would have to work efficiently and in coordinated way to keep the frequency steady. Present wind turbine technology with power electronic converter have inertia equal to zero connected to the grid are very like to behave unpredictably unstable and cause blackouts. Asynchronously generated energy for wind turbines mostly inject no inertia in power system because they are electronically decoupled from the grid [52].

Wind turbines can in principle emulate inertial behavior of conventional power plants and respond to the grid shocks by providing extra power through collaboration of power stored in flywheel of turbine and the solid-state power electronics. Kinetic energy accumulated in the rotational mass of wind turbines, extracted when system faces frequency deviation caused by the imbalance on power system, between load and generation [55].

Kinetic energy extracted to bring frequency back to optimal limit will reduce wind turbine rotor speed. Now accelerating the turbine to normal speed will absorb wind power which could be exported to the grid, reduction of 60% have been seen in ENERCON data. This post inertia recovery of wind turbine rotor speed could cause double dip in the system frequency, leading to triggering of protective relays and causing blackouts. To minimize frequency double dip risk system operators are re-evaluating synthetic inertia and plans 20% power reduction limit of turbine capacity during recovery of frequency [55].

Wind turbines are mostly implemented in rural and urban areas utilizing wind energy to generate electric power. When low wind speed then the voltage output from wind turbine after going through rectification is less, as this voltage is less compared to rated charging required voltage. This problem of less voltage is quite common in domestic regions cause wind speed is in range of 0 to 4m/s ultimately reducing efficiency to 20%. Therefore, buck boost converter is connected at the output terminal of wind turbines which boost the voltage produced at lower wind speeds to the required level of voltage. Buck boost converter is a cascaded DC DC converter connected in series with each other. When wind speed is low boost converter is activated and at higher speeds buck converter is activated to keep the voltage constant and keeping the system protected [56].

Voltage from wind turbine before being connected to grid is rectified then passed through a buck-boast converter to stabilize the voltage. Voltage on buck side is first converted to the direct current voltage and then through converter action buck or boosted to required voltage and is converted back to alternating current [56].

Optimizing the power output of wind turbine different control methods are used, generator speed control, pitch angle control and yaw control. Blade angle of turbine can be changed by using pitch control to attain certain rotor speeds by adjustment furl and stall. In stalling angle of attack is increased meaning flat side of the blade is further in the wind, furling angle of attack is deceased and flat side of the blade is perpendicular to the wind . It is most effective and proven way of limiting output power by varying the force applied on the blade aerodynamically at higher speeds of wind. On the other hand, Yaw control the horizontal axis rotation of turbine, making sure that turbine is constantly facing into the wind, because wind speed can vary very quickly misalign the turbine from facing into wind and costing losses in output power. The final type of control is done through electrical subsystems in which dynamic control of turbine is achieved by electronic converters which are connected at the terminal of generator [57]. All the different parameter of the system is taken to data acquisition for measuring and analysis purpose.

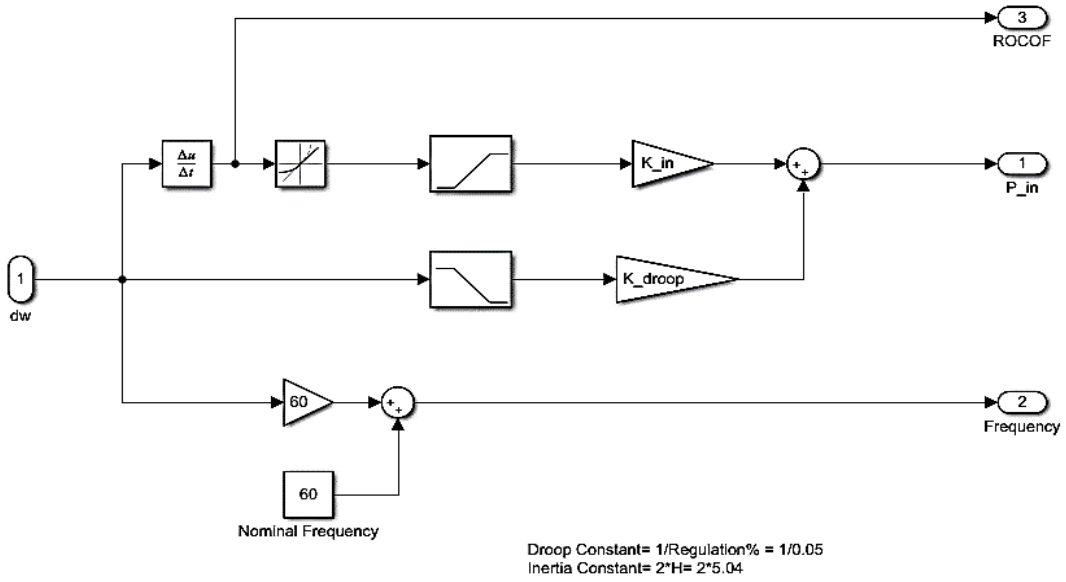

Figure 6: Inertial Loop

Virtual inertia is a feature used in renewable power systems with zero or low physical inertia, physical means having rotational inertia which in present power system is reducing rapidly as increase in renewable energy generation is integrated into the system. On one side integration of renewable is quite beneficial for the environment and long-term planning of power systems but on the other side it brings along some complications: varying power generation, weather constraints and having less or equal to zero inertial mass. Virtual inertia is control technique aiming to control the DFIG wind turbine to regulate its output power when frequency deviation occurs due transient conditions. Rate of change of frequency ROCOF elucidates a reference signal to provide extra power, added with the normal reference provided by the maximum power tracking controller MPPT [58].

Inertial loop is an extra added loop in the power reference block which provide active power reference signal to the rotor

side of the converter. 2H(df/dt) is term introduced by auxiliary signal, H is inertial constant expressed in seconds representing the time active power is provided by the wind turbine when rotor of turbine is decelerated to from nominal speeds to zero to extract the kinetic energy accumulated in the rotating mass.

$$P_{auxref} = K_{droop}(f - f_o)$$

Fo is nominal frequency 60Hz , Droop parameter for large conventional generator is in the range between 3 - 5%, depending on the type of generating unit [58].

This method is based on primary frequency controlled provided by the conventional generators. Droop controller are implemented on the wind farm level in place of applying to every single wind turbine. This shows that the signal generated from the controller is divided among the turbines in wind farms. Droop control loop reduces the torque accelerating rotor of the generator during the frequency dip. Combination of both droop controller and inertial controller is optimum for working of the DFIG wind turbines.

III. RESULTS AND DISCUSSIONS

1) Frequency Comparison

In figure 7, we are comparing the effect of virtual inertia compensation on the system frequency. There are two plot lines one is when inertial power required to bring frequency to stability . When inertial power is added the first harmonic of frequency drops to 59.31Hz while in the other condition frequency drops to 58.42Hz. Frequency in the latter condition recovers faster and with less harmonics. There is difference of 0.9Hz between the two. 0.9hz difference is large and if through this system frequency can improved then the system will quickly become stable and any unpredictable conditions can avoided.

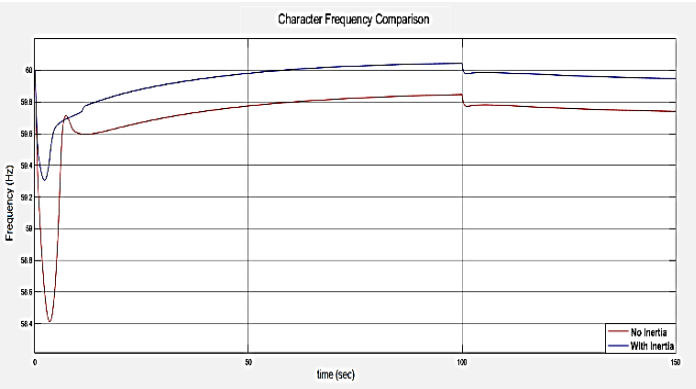

Figure 7: Frequency Comparison

2) Active Power of Wind Turbine

Active power of wind turbine is more when virtual inertia is added in the system. Virtual inertia addition makes the system slower and oscillatory due to which oscillation can be seen at the start of the operation. Additional active power during fault condition is drawn from the rotating masses. After the triggering of load step at 100sec mark active power has slightly increased again. The extra power produced by the wind turbine slightly reduces the ROCOF giving more time to active governors to kick in and respond. Active Power comparison figure 8.

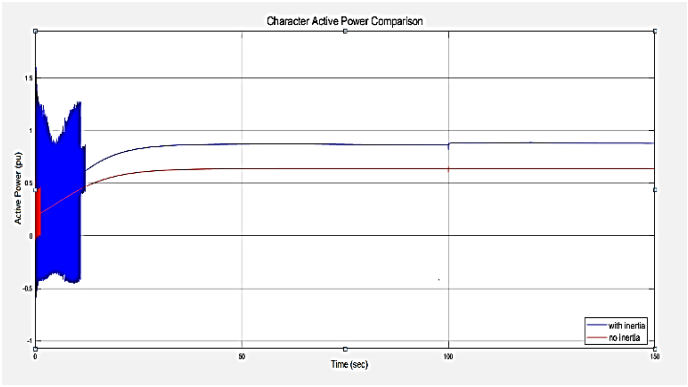

Figure 8: Active Power Comparison of Wind Turbine

3) Reactive Power of Wind Turbine

Generator utilization and generation of reactive power allows network operator to maintain the voltage stable throughout the power system. Reactive power plays crucial role in the stability of power system and flow of active power throughout the transmission system. For wind turbine to maintain the power factor equal to 1 reactive power supply in wind turbines is kept constant that is why reactive power management is essential. The fluctuation in the start of the plot is due to extraction of kinetic energy for addition of inertial power from the rotor of synchronous generator.

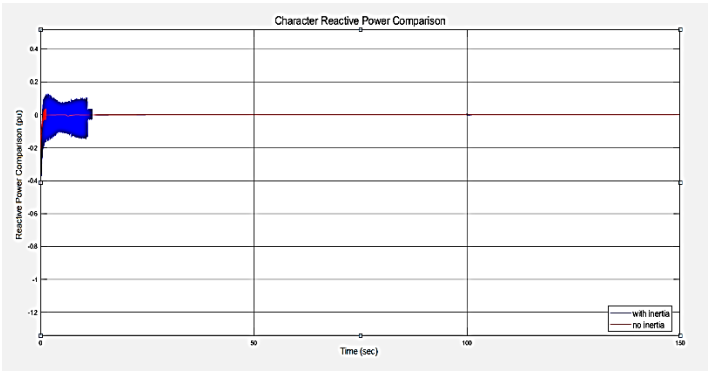

Figure 9: Reactive Power Comparison of Wind Turbine

4) Active Power of Generator

Generator power reference Pref was set at 0.65pu . In figure 10 the blue plot after getting stabilized reaches the desired reference point earlier compared to red plot which was the system behavior when generator was not providing the extra inertial power for bringing the deviation to normal limits.

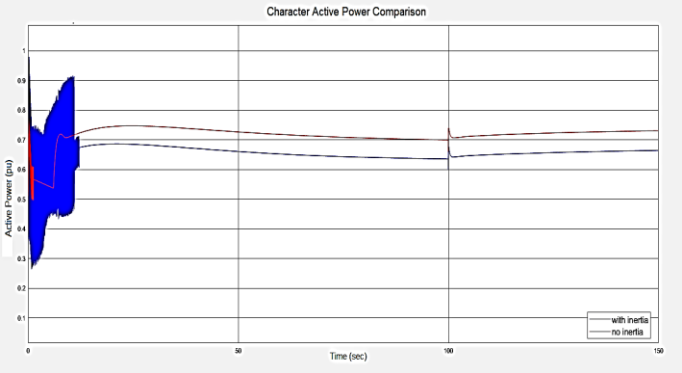

Figure 10: Active Power Comparison of Generator

5) Reactive Power of Generator

Loads connected to the system and load step at 100sec are purely resistive. We know that resistive load has no effect on the generator reactive power .That why in both the cases when load step is added they both react in the same way . Fluctuation in the start is due to generator startup which later on goes away when generator is stabilized.

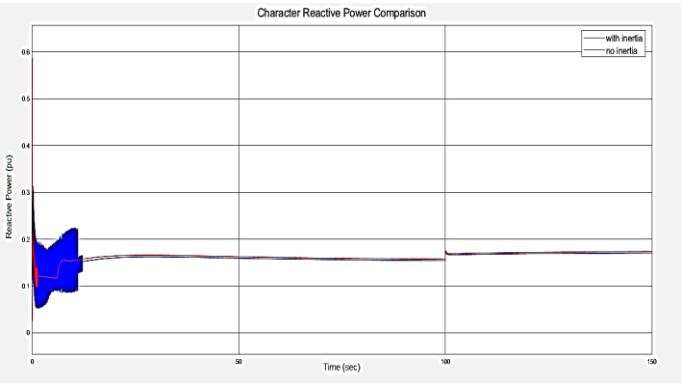

Figure 11: Reactive Power Comparison of Synchronous Generator

CONFLICT OF INTEREST

The author declares no conflict of interest.

CONCUSLION

This research focuses on alleviating the rotational mass and inertia related problems caused by increasing wind power integration by adding an inertial loop to compensate the impact of frequency deviations due to abnormal transient conditions. Reduced rotational inertia leads to faster frequency deviations and transient power exchanges over tielines in case of power fault. This may cause unexpected tripping of tielines due to automatic protection devices making the situation even critical. In this Study we found 0.9hz of frequency drop improvement from 58.42Hz to 59.31Hz with the addition of inertial loop in the system, which is quite a significant improvement for grid stability. Active power produced by wind turbine also increases reducing the Rate of change of frequency giving enough time to the rotating masses to respond to the transient situation. Active power or inertial power provided in this system is from a synchronous generator connected with grid. Reactive power of wind turbine is kept constant to keep the power factor unity. These findings will prove extremely helpful in offsetting the drawbacks of greater wind energy addition to grid. The analysis needs to be further replicated with reduction in load and other transient conditions before being implemented in the grid.

REFERENCES

[1] M. Asif, T. Muneer, “Energy supply, its demand and security issues for developed and emerging economies, Renewable and Sustainable Energy Reviews", Volume 11, Issue 7, 2007, Pages 1388-1413, ISSN 1364-0321.

[2] E. Bompard, G. Fulli, M. Ardelean, and M. Masera, “It’s a Bird, It’s a Plane, It’s a...Supergrid!: Evolution, Opportunities, and Critical Issues for Pan-European Transmission”, IEEE Power and Energy Magazine, vol. 12, no. 2, pp. 40–50, Mar. 2014.

[3] How to Solve Global Warming: It's the Energy Supply. Available Online At (https://www.scientificamerican.com/article/how-to-solve-global-warming-its-the-energy-supply/) [accessed 02-07-19]

[4] 11 countries leading the charge on renewable energy (https://www.climatecouncil.org.au/11-countries-leading-the-charge-on-renewable-energy/) [accessed 02-07-19]

[5] X. Liang, "Emerging Power Quality Challenges Due to Integration of Renewable Energy Sources," in IEEE Transactions on Industry Applications, vol. 53, no. 2, pp. 855-866, March-April 2017. Doi:10.1109/TIA.2016.2626253

[6] Bird, L., Milligan, M., and Lew, D. Integrating Variable Renewable Energy: Challenges and Solutions. United States: N. p., 2013. Web. doi:10.2172/1097911.

[7] Sandra Eriksson, Hans Bernhoff, Mats Leijon, Evaluation of different turbine concepts for wind power, Renewable and Sustainable Energy Reviews, Volume 12, Issue 5, 2008, Pages 1419-1434, ISSN 1364-0321 https://doi.org/10.1016/j.rser.2006.05.017.

[8] M. F. M. Arani and E. F. El-Saadany, "Implementing Virtual Inertia in DFIG-Based Wind Power Generation," in IEEE Transactions on Power Systems, vol. 28, no. 2, pp. 1373-1384, May 2013. Doi: 10.1109/TPWRS.2012.2207972

[9] Why wind energy? Available online at: (http://www.pmd.gov.pk/wind/Wind_Project_files/Page767.html) [Accessed 01-09-19]

[10] Dong J, Xue G, Dong M, Xu X. Energy-saving power generation dispatching in China: regulations, pilot projects and policy recommendations—a review. Renew Sustain Energy Rev 2015;43:1285–300.

[11] Saidur R, Rahim N, Islam M, Solangi K. Environmental impact of wind energy. Renew Sustain Energy Rev 2011;15:2423–30.

[12] Kyoto Protocol to the United Nations framework convention on climate change. Available online at: ⟨http://unfccc.int/resource/docs/convkp/kpeng.pdf⟩; 1997 [accessed 01.10.19]

[13] Cleaner and Cheaper: Using the clean air act to sharply reduce carbon pollution from existing power plants, delivering health, environmental, and economic benefits. Available online at: ⟨https://www.nrdc.org/file/3410/download? token=6c64p-xd⟩; 2014 [accessed 18.03.19]

[14] Renewable EnergyTarget Scheme. Available online at: ⟨http://www.aph.gov.au/ DocumentStore.ashx?id=17008e4b-e2f3-4ea3-9d53-fb3fb0cd4d85 & subId=351098⟩; 2014 [accessed 17.11.19]

[15] Renewables Global Status Report, REN21.Available online at: ⟨http://www.ren21. net/Portals/0/documents/Resources/GSR2012_low%20res_FINAL.pdf⟩; 2012 [accessed 01.05.19].

[16] Mahzarnia M, Sheikholeslami A, Adabi J. A voltage stabilizer for a microgrid system with two types of distributed generation resources. IIUM Eng J 2013:14.

[17] Chun Su. Line Effects of distribution system operations on voltage profiles in distribution grids connected wind power generation. Proc IEEE Power Syst Technol 2006:1–7.

[18] Ausavanop O, Chaitusaney S. Coordination of dispatchable distributed generation and voltage control devices for improving voltage profile by Tabu Search. In: Proc IEEE Elec Eng/Elect, Comp, Telecommun and Inform Technol Conf (ECTI-CON); 2011. p. 869–72.

[19] Sekhar ASR, Vamsi Krishna K. Improvement of voltage profile of the hybrid power system connected to the grid. Int J Eng Res Appl 2012;2:87–93.

[20] Bevrani H, Ghosh A, Ledwich G. Renewable energy sources and frequency regulation: survey and new perspectives. Renew Power Generation, IET 2010; 4: p. 438–57.

[21] Dehghanpour K, Afsharnia S. Electrical demand side contribution to frequency control in power systems: a review on technical aspects. Renew Sustain Energy Rev 2015;41:1267–76.

[22] Electricity Ten Year Statement (ETYS). Available online at ⟨http://www2. nationalgrid.com/UK/Industry-information/Future-of-Energy/Electricity-ten-year statement /⟩; 2014 [accessed 11.05.19]

[23] UK Future Energy Scenarios.Available online at ⟨http://www2.nationalgrid.com/ WorkArea/DownloadAsset.aspx?Id=10451⟩; 2013 [accessed 11.05.19]

[24] Jayawardena A., Meegahapola L., Perera S., Robinson D. Dynamic characteristics of a hybrid microgrid with inverter and non-inverter interfaced renewable energy sources: a case study. In: Proceedings of IEEE Power Syst Techno (POWERCON); 2012. p. 1–6.

[25] Ulbig A, Borsche TS, Andersson G. Impact of low rotational inertia on power system stability and operation. arXiv preprint arXiv:1312.6435; 2013.

[26] Thresher R, Robinson M, Veers P. To capture the wind. IEEE Power Energy Mag 2007;5:34–46.

[27] Mauricio JM, Marano A, Gómez-Expósito A, Martinez Ramos JL. Frequency regulation contribution through variable-speed wind energy conversion systems. IEEE Trans Power Syst 2009;24:173–80.

[28] Revel G, Leon AE, Alonso DM, Moiola JL. Dynamics and stability analysis of a power system with a PMSG-based wind farm performing ancillary services. IEEE Trans Circuits Syst I 2014;61(7):2182–93.

[29] Bianchi FD, De Battista H, Mantz RJ. Wind turbine control systems: principles, modelling and gain scheduling design. Springer Science & Business Media; 2006, ISBN: 978-1-84628-492-2.

[30] Singh B, Sharmay S. Stand-alone wind energy conversion system with an asynchronous generator. J Power Electr 2010;10:538–47.

[31] Lamchich MT, Lachguer N. Matlab simulink as simulation tool for wind generation systems based on doubly fed induction machines. INTECH Open Access Publisher; 2012.

[32] Knudsen H, Nielsen JN. Introduction to the modelling of wind turbines. Wind Power in Power Systems, Second Edition:767-97; 2005.

[33] Sun Y-z, Zhang Z-s, Li G-j, Lin J. Review on frequency control of power systems with wind power penetration. In: Proceedings of IEEE Power Syst Technol Conference (POWERCON), 2010. p. 1-8.

[34] Ekanayake J, Jenkins N. Comparison of the response of doubly fed and fixed-speed induction generator wind turbines to changes in network frequency. IEEE Trans Power Syst Energy Convers 2004;19:800–2.

[35] Gonzalez-Longatt F., Chikuni E., Rashayi E. Effects of the synthetic inertia from wind power on the total system inertia after a frequency disturbance. In: Proceedings of IEEE Ind Technol Conference (ICIT); 2013. p. 826–32.

[36] Morren J, Pierik J, De Haan SW. Inertial response of variable speed wind turbines. Electr Power Syst Res 2006;76:980–7.

[37] Wu L, Infield DG. Towards an assessment of power system frequency support from wind plant—modeling aggregate inertial response. IEEE Trans Power Syst 2013;28:2283–91.

[38] Morren J, De Haan SW, Kling WL, Ferreira J. Wind turbines emulating inertia and supporting primary frequency control. IEEE Trans Power Syst 2006;21:433–4.

[39] Zhang Z., Wang Y., Li H., Su X. Comparison of inertia control methods for DFIGbased wind turbines. in: Proceedings of IEEE ECCE Asia Downunder (ECCE Asia); 2013. p. 960–4.

[40] Wachtel S, Beekmann A. Contribution of wind energy converters with inertia emulation to frequency control and frequency stability in power systems.In: Proceedings of the 8th international workshop on large scale integration of wind power into power systems as well as on offshore wind farms, Bremen, Germany; 2009.

[41] Ullah NR, Thiringer T, Karlsson D. Temporary primary frequency control support by variable speed wind turbines—potential and applications. IEEE Trans Power Syst 2008;23:601–12.

[42] Hansen AD, Altin M, Margaris ID, Iov F, Tarnowski GC. Analysis of the short-term overproduction capability of variable speed wind turbines. Renew Energy 2014;68:326–36.

[43] El Itani S., Annakkage U.D., Joos G. Short-term frequency support utilizing inertial response of DFIG wind turbines. In: Proceedings of IEEE power and energy soc general meeting; 2011. p. 1–8.

[44] Keung P-K, Li P, Banakar H, Ooi BT. Kinetic energy of wind-turbine generators for system frequency support. IEEE Power Syst 2009;24:279–87.

[45] Mishra S., Zarina P., Sekhar P. A novel controller for frequency regulation in a hybrid system with high PV penetration. In: Proceedings of IEEE Power and Energy Soc General Meeting (PES); 2013. p. 1–5.

[46] Josephine R, Suja S. Estimating PMSG wind turbines by inertia and droop control schemes with intelligent fuzzy controller in Indian. Dev J Elect Eng Technol 2014;9:1196–201.

[47] Yao W., Lee K.Y. A control configuration of wind farm for load-following and frequency support by considering the inertia issue. In: Proceedings of IEEE Power and Energy Soc General Meeting; 2011. p. 1–6.

[48] Eid BM, Rahim NA, Selvaraj J, El Khateb AH. Control methods and objectives for electronically coupled distributed energy resources in microgrids:a review. IEEE Syst J 2014:1–13.

[49] Castro LM, Fuerte-Esquivel CR, Tovar-Hernández JH. Solution of power flow with automatic load-frequency control devices including wind farms. IEEE Trans Power Syst 2012;27:2186–95

[50] Mansour Jalali (2011). DFIG Based Wind Turbine Contribution to System Frequency Control. UWSpace. http://hdl.handle.net/10012/5730

[51] F. Blaabjerg, Z. Chen, R. Teodorescu and F. Iov, "Power Electronics in Wind Turbine Systems," 2006 CES/IEEE 5th International Power Electronics and Motion Control Conference, Shanghai, 2006, pp. 1-11.doi: 10.1109/IPEMC.2006.4777946

[52] Johan Morren, Jan Pierik, Sjoerd W.H. de Haan, Inertial response of variable speed wind turbines, Electric Power Systems Research, Volume 76, Issue 11, 2006, Pages 980-987, ISSN 0378-7796, https://doi.org/10.1016/j.epsr.2005.12.002.

[53] M. F. M. Arani and E. F. El-Saadany, "Implementing Virtual Inertia in DFIG-Based Wind Power Generation," in IEEE Transactions on Power Systems, vol. 28, no. 2, pp. 1373-1384, May 2013.doi: 10.1109/TPWRS.2012.2207972

[54] A. Kutsyk, M. Semeniuk, V. Tutka and T. Galiantyi, "A Pulse-Width Regulation of a Compound Excitation System for a Synchronous Generator," 2018 IEEE 3rd International Conference on Intelligent Energy and Power Systems (IEPS), Kharkiv, 2018, pp. 97-100. doi: 10.1109/IEPS.2018.8559510

[55] Can Synthetic Inertia from Wind Power Stabilize Grids? Available online at:(https://spectrum.ieee.org/energywise/energy/renewables/can-synthetic-inertia-stabilize-power-grids);2016 [accessed 18.09.19]

[56] Chandan, Shweta & Chayapathy, Venkataraman. (2014). Buck Boost Converter for Small Wind Turbine. IJLTEMAS. 3. 102-105.

[57] Eduardo José Novaes Menezes, Alex Maurício Araújo, Nadège Sophie Bouchonneau da Silva, A review on wind turbine control and its associated methods, Journal of Cleaner Production, Volume 174, 2018, Pages 945-953, ISSN 0959-6526, https://doi.org/10.1016/j.jclepro.2017.10.297.

[58] Margaris, Ioannis, et al. "Operation and Control of Wind Farms in Non-Interconnected Power Systems." Wind Farm-Impact in Power System and Alternatives to Improve the Integration. InTech, 2011, Doi: 10.5772/16532.

First A. Author Adnan Ismail is a postgraduate researcher at United States Pakistan Center for Advanced Studies in Energy at University of Engineering and Technology Peshawar, Pakistan. He is studying Electrical Energy System Engineering at MS level after doing his undergraduate degree in Electrical Engineering. His research interest include finding ways to integrate renewable energy in national grid and enchancing efficiency and stability of wind energy generation by utilizing virtual inertia techniques.This paper is a part of his Masters degree research studies.

IJEW 国际工程期刊 International Journal of Engineering Works انجینئرنگ کاموں کا بین الاقوامی جرنل

International Journal of Engineering Works
ISSN-p: 2521-2419
ISSN-e: 2409-2770
Vol. 7, Issue 01, PP. 58-61, January 2020
https://www.ijew.io/
https://doi.org/10.34259/ijew.20.7015861

Indirect Gross Calorific Value Prediction using Random Forest

Waqas Ahmed[1], Khan Muhammad[2]
[1]Msc Mining Enginnering Student at UET Peshawar Pakistan
[2]Assistant Professor Department of Mining Engineering UET Peshawar
waqas.Ahmed@uetpeshawar.edu.pk[1], khan.m@uetpeshawar.edu.pk[2]
Received: 14 January, Revised: 21 January, Accepted: 25 January

***Abstract*—**During operation of coal-based power plants, frequent calorific Value measurement is necessary. Previously, Artificial Intelligence based models have been developed for instant calorific value calculation based on proximate analyses or ultimate analyses or combination of both. In this paper, random forest was used for comparison of all the three methods and computing relative analyses parameters importance. This study uses well known USGS coal qual dataset. In this work, 10-fold validation strategy and R-squared was used as validation strategy and performance metric respectively. Ultimate analyses (R-squared = 0.9984) performed slightly better than proximate analyses (R-squared = 0.9861) or combination of both (R-squared = 0.9982). Lastly, carbon was found to be the most important feature in all models.

***Keywords*—** Gross Calorific Value, Random Forest, Proximate Analyses, Ultimate Analyses, Neural Networks.

I. Introduction

Energy demand of world is increasing and at the present time, whole world energy demand is mostly met by fossil-based fuels [1], [2]. The demand for coal which is most common among fossil-based fuels due to its huge abundance and greater life cycle has increased [3], [4]. Coal which supplies about 40-45% of the planet's energy needs [4], [5] is expected to remain the dominant energy source for the near future due to its financial advantages [5], [6]. During operation of coal based power plants, frequent calorific Value (the heat capacity of a unit weight of coal after burning completely [7], [8]) measurement is necessary because it decides the quality of coal [7]. Usually bomb calorimeter test method is used to measure calorific value however, such method is expensive, destructive, and needs an advanced technician. For that purpose, various researchers have tried to predict calorific value indirectly from proximate analysis [2], [6], [9]–[11] or ultimate analysis [5] or combination of both [12]–[16]. However, task of comparing all the three methods, computing relevant importance of analyses parameters in each method was not carried out previously. Such work is important to get better insight into various indirect calorific value prediction methods. In this study, Random Forest (RF) is used for this task. This paper uses samples derived from coal database (coalqual version 3.0) which was derived from U.S. Geological Survey (USGS) of Energy Resource Program in such a way that validation rating of data was not "Incomplete" or "Suspect" for both proximate and ultimate analyses parameters. The data is available at ncrdspublic.er.usgs.gov/coalqual/. For comparison of all the three methods, validation method and performance metric used was popular "10-fold cross validation" [17] and "R-squared". Analysis parameters importance was computed based on their homogeneity values while splitting inside random forest.

In the next section a background of Random Forest is presented followed by Coalqual dataset description. Next, methodology is detailed. Lastly, results are discussed followed by conclusion section.

II. Random Forest

The random forest (developed by Breiman in 2001 [18]) is very popular machine learning algorithm. Machine learning is branch of Artificial Intelligence consisting of supervised learning, unsupervised learning, semi-supervised learning, and reinforced learning [19]–[21]. Task at hand is "regression" which comes under category of supervised learning. Regression is estimating/learning relationship between dependent variable (calorific value in this case) and independent variables (Analysis parameters in this case). For regression, various algorithms are available such as neural networks, support vector machines, nearest neighbours, decision trees, and random forest etc [19]–[21].

All regression algorithms try to find mapping between independent and dependent variables and the main task of machine learning engineer is to find best mapping/validation accuracy [19]–[21]. Best validation accuracy is achieved by tuning hyper-parameters of respective regression algorithm. Hyper-parameters are initial parameters which are set before training process of algorithm starts [19]–[21]. Out of all regression algorithms, Random Forest (RF) is categorized as ensembling method which combines decision trees and use their mean value as final predicted value [18]–[21]. In RF, multiple decision trees are fitted on different training datasets generated using bootstrapping (A resampling technique to generate multiple random realizations) of original dataset [18]–

[21]. To understand RF, explanation of decision trees is presented.

Decision tree is well known method in which upside-down tree is constructed by dividing training dataset into subsets using best independent variables sequentially one after the other [18]–[21]. Best independent variable is one which gives greater homogeneity and is calculated using various algorithms such as Iterative Dichotomiser 3 (ID3) or Classification and Regression Trees (CART). In ID3, best independent variable computation is done in three steps:

A. Standard deviation of output variable calculation for complete dataset

$$S = \sqrt{\frac{\sum (x - \bar{x})^2}{n}}$$

Where x is dependent variable, $\bar{x}$ is mean of output variable, n is total number of samples, and S is Standard deviation of dependent variable for complete dataset.

B. Subsets from dataset are formed such that each subset contains single independent/input variable (analysis parameters) and dependent variable. For each subset, standard deviation is computed.

$$S(T, X) = \sum_{c \in X} P(c) S(c)$$

Where T is dependent variable, X is independent variable, c is different classes of that independent variable, P(c) is probability of class c in that independent variable, S(c) is standard deviation of dependent variable associated with class c of the independent variable.

C. For each subset, standard deviation reduction (SDR) value is computed by subtracting respective standard deviation from whole dataset standard deviation.

$$SDR(T, X) = S(T) - S(T, X)$$

Finally, best independent variable is the one whose subset gives maximum SDR value.

Best independent attribute computed for complete dataset is placed as root node followed by intermediate nodes which represent best independent attributes computed for subset of data created sequentially one after other using values of best independent attributes. Dividing data into subset of data continues till all data is processed. However, in such cases validation accuracies reduce. For that reason, hyper-parameters within decision trees such as Max_depth, Min_samples_split, Max_features, Min_samples_leaf are used to improve validation accuracy of decision tree. Main task of machine learning engineer is to find best values for these hyper parameters. Usually this task is done by trying out all combinations of ranges of hyper parameter values (Grid search).

As explained, mean of decision trees output gives RF prediction value. Depending on homogeneity of each independent variable, random forest also gives measure of variables importance.

III. Dataset Generation

Dataset used in this study was derived from coal database (coalqual version 3.0) which was derived from U.S. Geological Survey (USGS) of Energy Resource Program. Coalqual database contains proximate (Ash, Fixed Carbon, Volatile Matter, Moisture), and ultimate analyses (Hydrogen, Carbon, Nitrogen, Sulphur, and Oxygen) along with Gross Calorific Value results obtained from various ranks of coal including anthracite, bituminous, sub-bituminous, and lignite. All analyses carried out were in accordance to ASTM standards. This study includes samples which do not have "Incomplete" or "Suspect" validation rating for their respective analyses parameters. Summary statistics of data used is presented in Table I.

TABLE I. Summary Statistics of coalqual data

Category	**Variable Name**	**Summary Statistics**			
		mean	Std	min	max
Output	GCV (BTU)	11551	2314	3790	15193
Proximate Analysis	Moisture	8.233	10.05	0.4	52.5
	FC	47.93	11.31	4.1	87
	Ash	11.74	7.29	0.9	54.7
	VM	32.1	6.498	3	55.7
Ultimate Analysis	Hydrogen	4.331	0.799	0.21	9.12
	Carbon	65	12.5	22.5	88.2
	Nitrogen	1.282	0.343	0.2	5.6
	Oxygen	7.463	3.099	-0.9	18.96
	Sulphur	1.952	1.805	0.09	20.9

IV. Methodology

In this study, three different random forest models having 1) proximate analyses, 2) ultimate analyses, and 3) combination of both as input were developed in three steps. First, hyper-parameters were searched; second, models were developed and results were reported using 10-fold validation; third, feature importance was carried out for each model.

For each model, data was first split into 80:20 for training and testing/hyper-parameters tuning respectively. After splitting, hyper-parameter search was done in grid manner where each RF model was built for all combination of search ranges as shown in Table II. For each RF model, best hyper-parameter values were those which gave best accuracy on 20% test data.

TABLE II. HYPER-PARAMETERS RANGES TO BE SEARCHED

Hyper parameters	Range
Min_samples_leaf	(1 to 50)
Max_depth	(4 to 10) or Complete
Min_samples_split	(2 to 500)

Min_samples_leaf searched from 1 to 50 with increment of 3, Max_depth searched from 4 to 10 with increment of 2, Min_samples_split searched from 2 to 500 with increment of 10.

In second step, complete data was split into ten equal subsets where each model was trained on 9 parts and tested on remaining 10^{th} part. This process was repeated 10 times where each time 10^{th} part used for validation was different. In this way, all data was used for training as well as testing. Final value of performance metric was average of 10 values. Finally, feature importance of each input variable in all the three models was found using their respective homogeneity values.

V. RESULTS AND DISCUSSION

Main task in RF based models was finding optimum hyper-parameters values. It was found that increasing Max_depth value and decreasing Min_samples_leaf, Min_samples_split values were responsible for poor validation accuracy and vice versa. Optimum hyper-parameters values found for all models were same and is presented in Table III.

TABLE III. OPTIMUM HYPER-PARAMETERS FOUND

Hyper parameters	Range
Min_samples_leaf	10
Max_depth	Complete
Min_samples_split	22

RF model results using 10-fold validation are presented in Table IV and suggest that ultimate analyses performed slightly better than proximate analyses.

TABLE IV. 10-FOLD VALIDATION RESULTS

Model	R-squared
RF (Proximate)	0.9861
RF (Ultimate)	0.9984
RF (Proximate + Ultimate)	0.9982

As shown in Fig I, II, and III, carbon was most important feature for each model having ultimate or proximate or combination of both as inputs respectively.

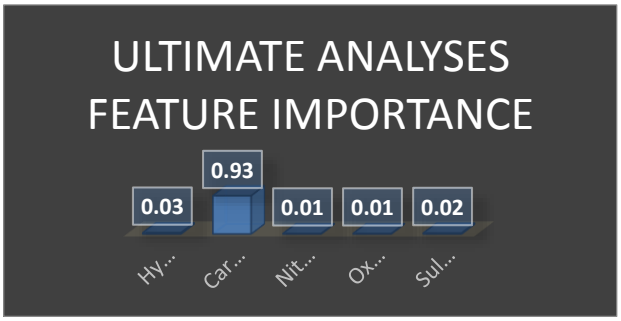

Figure I Ultimate Analyses Feature Importance

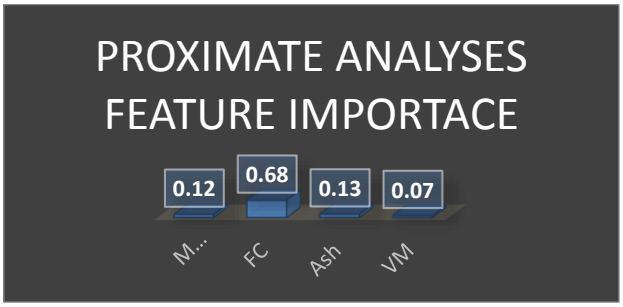

Figure II Proximate Analyses Feature Importance

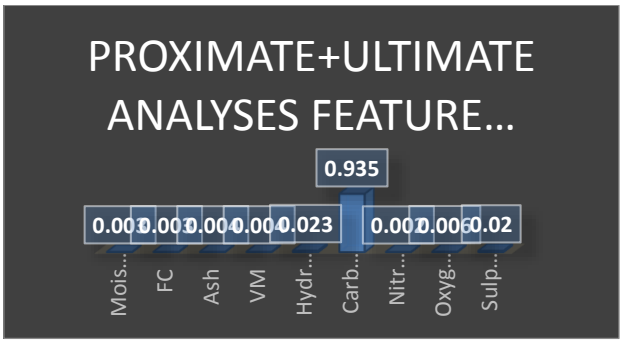

Figure III Proximate + Ultimate Analyses Feature Importance

CONCLUSION

This paper predicts calorific value using 1) proximate analyses parameters, 2) ultimate analyses parameters, and 3) proximate + ultimate analyses parameters. Results suggested that ultimate analyses performed slightly better than proximate analyses. Carbon was computed to be the most important feature in indirect determination of calorific value.

REFERENCES

[1] [M. Leahy, J. L. Barden, B. T. Murphy, N. Slater-thompson, and D. Peterson, "International energy outlook 2013," United States of America, 2013.

[2] A. V. Akkaya, "Proximate analysis based multiple regression models for higher heating value estimation of low rank coals," Fuel Process. Technol., vol. 90, no. 2, pp. 165–170, 2009.

[3] K. F. De Souza, C. H. Sampaio, and J. A. T. Kussler, "Washability curves for the lower coal seams in Candiota Mine - Brazil," Fuel Process. Technol., vol. 96, pp. 140–149, 2012.

[4] O. Sivrikaya, "Cleaning study of a low-rank lignite with DMS, Reichert spiral and flotation," Fuel, vol. 119, pp. 252–258, 2014.

[5] I. Yilmaz, N. Y. Erik, and O. Kaynar, "Different types of learning algorithms of artificial neural network (ANN) models for prediction of

gross calorific value (GCV) of coals," Sci. Res. Essays, vol. 5, no. 16, pp. 2242–2249, 2010.

[6] P. Tan, C. Zhang, J. Xia, Q. Y. Fang, and G. Chen, "Estimation of higher heating value of coal based on proximate analysis using support vector regression," Fuel Process. Technol., vol. 138, pp. 298–304, 2015.

[7] S. U. Patel et al., "Estimation of gross calorific value of coals using artificial neural networks," Fuel, vol. 86, no. 3, pp. 334–344, 2007.

[8] M. J. F. Llorente and J. E. C. García, "Suitability of thermo-chemical corrections for determining gross calorific value in biomass," Thermochim. Acta, vol. 468, no. 1–2, pp. 101–107, 2008.

[9] Q. Feng, J. Zhang, X. Zhang, and S. Wen, "Proximate analysis based prediction of gross calorific value of coals: A comparison of support vector machine, alternating conditional expectation and artificial neural network," Fuel Process. Technol., vol. 129, pp. 120–129, 2015.

[10] J. Akhtar, N. Sheikh, and S. Munir, "Linear regression-based correlations for estimation of high heating values of Pakistani lignite coals," Energy Sources, Part A Recover. Util. Environ. Eff., vol. 39, no. 10, pp. 1063–1070, 2017.

[11] M. Açıkkar and O. Sivrikaya, "Artificial neural networks for estimation of the gross calorific value of Turkish lignite coals," no. Imsec, pp. 1075–1079, 2018.

[12] S. Mesroghli, E. Jorjani, and S. Chehreh Chelgani, "Estimation of gross calorific value based on coal analysis using regression and artificial neural networks," Int. J. Coal Geol., vol. 79, no. 1–2, pp. 49–54, 2009.

[13] S. C. Chelgani, S. Mesroghli, and J. C. Hower, "Simultaneous prediction of coal rank parameters based on ultimate analysis using regression and artificial neural network," Int. J. Coal Geol., vol. 83, no. 1, pp. 31–34, 2010.

[14] N. Y. Erik and I. Yilmaz, "On the use of conventional and soft computing models for prediction of gross calorific value (GCV) of coal," Int. J. Coal Prep. Util., vol. 31, no. 1, pp. 32–59, 2011.

[15] S. S. Matin and S. C. Chelgani, "Estimation of coal gross calorific value based on various analyses by random forest method," Fuel, vol. 177, pp. 274–278, 2016.

[16] X. Wen, S. Jian, and J. Wang, "Prediction models of calorific value of coal based on wavelet neural networks," Fuel, vol. 199, pp. 512–522, 2017.

[17] S. Yadav and S. Shukla, "Analysis of k-Fold Cross-Validation over Hold-Out Validation on Colossal Datasets for Quality Classification," Proc. - 6th Int. Adv. Comput. Conf. IACC 2016, no. Cv, pp. 78–83, 2016.

[18] L. Breiman, "Random Forest Draft," pp. 1–33, 2001.

[19] S. J. Russell et al., Prentice Hall - Artificial Intelligence A Modern Approach. 2001.

[20] E. Sugawara and H. Nikaido, pattern recognition and machine learning, vol. 58, no. 12. 2014.

[21] A. Peña Yañez, "Elements of statistical learning," Rev. Esp. Enferm. Apar. Dig., vol. 26, no. 4, pp. 505–516, 1967.

IJEW 国际工程期刊 International Journal of Engineering Works انجینئرنگ کاموں کا بین الاقوامی جرنل

International Journal of Engineering Works
ISSN-p: 2521-2419
ISSN-e: 2409-2770
Vol. 7, Issue 01, PP. 62-67, January 2020
https://www.ijew.io/
https://doi.org/10.34259/ijew.20.7016267

Comparative Analysis of Different Storage Technologies for Energy Critical Application

Alamgir Ahmad Khattak[1], Muhammad Safdar[2], Asad Nawaz Khan[3], Adil Nawaz Khan[4]
[1,2,3] Department of Electrical Energy Systems Engineering, US Pakistan Centre for Advanced Studies in Energy, University of Engineering and technology Peshawar, Pakistan
[4]CECOS University of IT and Emerging Sciences Peshawar, Pakistan
khattak.seecs@gmail.com[1], salarsafdar@gmail.com[2], p096409@nu.edu.pk[3], isfmardan@gmail.com[4]
Received: 17 January, Revised: 21 January, Accepted: 27 January

***Abstract*—** The scope of this research work is the analysis and study of the rechargeable batteries. During this research, battery testbeds are developed for all under study battery technologies. A few hundreds of charging, discharging experimentation has been performed under a variety of charging profiles and discharging load patterns. These observations have been critically analyzed to capture the behavior of the batteries comprehensively. These behavioral profiles of these batteries have been utilized for developing an accurate battery model. The proposed model is a hybrid model composed of Diffusion model and combined electric circuit-based model, which accounts for nonlinearities of rate capacity effect, recovery effect, capacity fading, storage runtime and open circuit voltage, current-, temperature-, dependency to transient response. This proposed model would be a great help for energy aware circuit designing, because it's an equivalent circuit model that could be co-simulated in circuit simulation environment, like Matlab Simulink. A quantitative figure of merit for the selection of battery system for a specific microgrid application has been devised on the bases of important battery parameters.

***Keywords*—** Battery storage system, Micro-grid, Battery Model, Three stage battery charger, and constant current electronic load.

I. INTRODUCTION

The Conventional electrical power grid is undergoing a disruptive change as the development of smart grid is motivated by the energy crisis of the time throughout the globe [1]. The limited amount of fossil fuels availability and more precisely the fear of climate change caused by the greenhouse emissions are the agents of this development [2, 3]. It is prioritized that more Renewable Energy Sources (RES's) must be incorporated into system. Micro-grid is a critical infra-structure to integrate Distributed Energy Sources (DES's) for the deployment of smart gird [4, 5]. This development is around the corner and increasing of amount of research has been undergone in the last decade.

The smart grid is an electric grid integrated with Information and Communication Technologies (ICT) to embody a high-fidelity power-flow control having the ability heal if self, self-healing ability, ensuring a reliable and secure provision of energy [5]. Smart Grid refers to the set of technologies and infrastructure which would put intelligence in the present dump grid to transform it into a digital system which talks, listens, understand and adapt accordingly. Smart grids is demand responsive electricity system that balance out energy consumption and supply, and has the capability to integrate new Renewable Energy Sources (RES), while enabling the integration of energy storage systems and the use of electric vehicles (EV).

A Micro-grid is the local version electric grid implement in a small region and enables the integration of distributed energy resources (DER) having connected with local flexible loads. The micro-grids could be operated both in grid tied and in isolated islanded mode to ensure a required level of high reliability and resilience against disturbances in grid [4]. The micro-grid is a miniature of a smart gird operating into a small premise and having integrated RES's. ESS is an integral part of micro-grid infrastructure which enables it to improve the systems resiliency, stability and reliability. The objectives of the development of a Micro-grid are to provide clean electric energy with increased reliability and sustainability with economic considerations. Energy storage is an integral part of the Micro-grid which enables it to integrate intermittent RES's and to operate in stand-alone mode without compromising on the reliability. Though, the core functionality of a Micro-grid is considered to be the backup for power systems, however, it provides on-site real time control of both supply and demand and manage the available storage capacity and also enables the interaction with the grid to improve resiliency.

Micro-girds are evolving as a vital feature of future power systems that has been developed by different smart-grid initiatives, that can provide substantial environmental benefits by integrating and utilizing energy efficient Distributed Generation (DG) [6, 7]. Micro-grids are considered to provide a promising solution by improving the power system resiliency by integrating local sustainable resources and compensating the intermittent nature of these sources with incorporation of Electrical Energy Storage (EES) with in the systems [4, 8]. Solar PV systems, Wind Power Plants, Micro Hydro Power Plants and Fuel cell are the commonly exploited renewable energy resources and micro-grid incorporates one of them as their main source of energy supply. PV plants and Wind power depends on weather and they also

have a peak time with it produce maximum [9]. The fuel cells and micro hydro plants have a limited capacity and can't respond quickly to relatively large changes on load side. To make Micro-grids responsive to load changes and to provide the extra power when the source is short of the demand, an EES is employed [8].

EES serves the purpose of storing electrical energy from the electrical grid at times when it is generated in larger amount then that of the demand and supplies that stored energy at times when there is a shortage of energy on the grid. EES is used to incorporate renewable sources as they are of intermittent nature and thus needs a buffer to compensate this lag. EES improves the reliability and stability of the system with continuous supply of electrical energy. Battery Storage the EES stores energy in off peak hours and supplies back that energy in peak hours. Different EES technologies has been exploited for energy storage and all of them have their own pros and cons. Different Storage Technologies are given here

1) Mechanical Storage System

a) Pumped Hydro Electric Storage (PHES)

b) Compressed Air Energy Storage (CAES)

c) Flywheel System

2) Electrical Storage System

a) Capacitor and Super capacitor

b) Superconducting Magnetic Energy Storage

3) Battery storage Systems (Electrochemical Storage Systems)

4) Thermochemical Battery Storage

5) Chemical Energy Storage

6) Thermal Energy Storage

The listed energy storage systems store energy in one of the forms (potential, kinetic, electrical, chemical or thermal energy) with a certain efficiency and provides it back during discharge. Each of them is utilized in certain systems on the basis of compatibility, advantages and limitations. According the criteria battery storage systems are utilized in micro grid topologies as the most viable option. The scope of this research is limited to analysis of different battery technologies and their viability with a certain micro grid topology.

II. Literature Review

A. Electrochamical Storage System

Electrochemical batteries are storage systems which stores electrical energy as chemical energy that could be utilized later by converting back to electrical energy. A Battery is a combination of one or more electrochemical cells, which are connected electrically in series or parallel combination to achieve the desired voltage or current levels, though the stacking is also done for increasing energy storage capacity [10]. An electrochemical cell is composed in a compartment consists of an electrolyte, an anode (positive electrode) and cathode (negative electrode), and a separator (porous insulating material). The composition of these two electrodes are different, and both of them react with each other chemically in the presence electrolyte. The chemical reaction is bidirectional one, which occurs spontaneously during charging and is forced in reverse direction during charging.

These electrochemical cells are classified based on characteristics and state of electrolyte like flooded (wet) or dry (sealed) batteries. The flooded batteries are most widely used due to their low cost, while sealed batteries have been used where maintenance and safety is critical. They are also classificed based on depth of discharge and rate of transmission, and the two categories are of shallow and deep cycle batteries. Deep cycle batteries have thick plates to store charge, with a structure which facilitate high current provision instantaneously and a stable chemistry to with stand the high stress

B. Maintaining the Integrity of the Specifications

A number of battery technologies are under evaluation for such large-scale energy storage applications, a summarized review of these batteries will be providing in this section. The secondary batteries discussed here are listed here [11, 12, 13].

a) Lead Acid Battery

i) Flooded Lead Acid Battery

ii) Sealed Batteries

(1) Absorbent Glass Mat (AGM) Battery

(2) GEL (VRLA) Battery

b) Nickel-Cadmium (Ni-Cd) Battery

c) Nickel Metal Hydride (NiMH) Battery

d) Lithium- ion (Li-ion) Battery

e) Lithium Polymer (LiPo) Battery

f) Sodium- ion (Na-ion) Battery

1) Lead Acid Batteries

Lead Acid (LA) batteries is the oldest and most established rechargeable batteries, composed of spongy metallic anode, a cathode of lead di oxide and 37% solution of sulfuric acid as electrolyte. Lead Acid (LA) batteries were first developed in 1859, being the first of rechargeable kind of batteries. Since, there invention LA batteries prevails the market due to numerous advantages of, simple manufacturing process, low cost, rapid load response due to quick chemical reaction and good life cycle incase controlled conditions and proper maintenance is provided. The nominal LA cell voltage is 2.05, and the SOC Vs Voltage relations is relatively linear, which makes it desirable electrical energy storage application [13, 14]. The technology LA battery is an old and much mature one owing to its extensive use over the last hundred years [15].

Lead Acid (LA) Batteries are categorized in two distinct verities of flooded or Ventilated Lead Acid (VLA) batteries and Sealed/ Valve Regulate Lead Acid (SLA/ VRLA) Batteries. There are differentiated on the bases of their negative and positive plate structures, the two most commonly used plates flat pasted plates and tubular plates (Iron clad type), while the third type, which is extinct for long Planté plates.

During discharge both positive and negative active material reacts with sulfuric acid (Fig.1) and produce a layer of lead sulfate on the respective electrodes.

The overall discharge reaction is:

$$\mathbf{Pb}O_2 + \mathbf{Pb} + 2H_2SO_4 \rightarrow 2\mathbf{Pb}\,SO_4 + 2H_2\mathbf{O}$$

Anode:

$$\mathbf{Pb} + SO_4^{2-} \rightarrow 2\mathbf{Pb}\,SO_4 + 2e^-$$

Cathode:

$$\mathbf{Pb}O_2 + SO_4^{2-} + 4H^+ + 2e^- + \rightarrow 2\mathbf{Pb}\,SO_4 + 2H_2\mathbf{O}$$

When connected to charger, the reaction reverses its direction and thus the layers of lead sulfate on the electrodes starts to convert back into lead and lead dioxide. The overall reversible cell reaction looks like this;

$$\mathbf{Pb}O_2 + \mathbf{Pb} + 2H_2SO_4 \rightleftharpoons 2\mathbf{Pb}\,SO_4 + 2H_2\mathbf{O}$$

2) Nickel-Cadmium (Ni-Cd) Battery

The Nickel-Cadmium (Ni-Cd/ NiCad) battery is invented in 1899 by Waldemar Jungner, offering many advantages over the only available lead acid rechargeable batteries [16]. In the mid of twentieth century NiCad batteries came as the first and only choice for portable electronic devices and power storage critical low power applications until 1990's when Nickel Metal Hydride (NiMH) and Lithium ion (Li-ion) cells took over [17].

NiCad battery is a type of secondary batteries having a positive electrode (cathode) composed Nickel hydroxide (Ni(OH)2), a negative plate composed of Cadmium hydroxide (Cd(OH)2), Potassium hydroxide (KOH) as electrolyte and a separator of nylon or polypropylene (Fig.4). NiCad batteries have nominal voltage of 1.2V, which is maintained quite steady until full discharge in contrast to other batteries. This enables NiCad cells to deliver full high power until total discharge [16, 17]. The low internal resistance of NiCad batteries also enables them to deliver such high discharge power.

The basic chemical reaction and active materials of all types of NiCad are same, weather sealed or safety vented valve type. During charging, the active material of negative electrode, Cadmium hydroxide (Cd(OH)2) transform into metallic Cadmium (Cd) and release hydroxyl ions (OH-), while the active material of positive electrode transforms from nickel hydroxide (Ni(OH)2) into nickel oxy-hydroxide (NiOOH) by receiving the hydroxyl ions (OH-) [17, 18]. During discharge the reaction moves in reverse direction, the chemical reaction that occur in NiCad cells are;

The reaction on the negative electrode:

$$Cd(OH)_2 + 2e^- \longrightarrow Cd + 2OH^-$$

The reaction on the positive electrode

$$Ni(OH)_2 + 2OH^- \longrightarrow NiOOH + H_2O + e^-$$

The discharge and charge reversible reaction NiCad cells:

$$Cd + NiOOH + H_2O \rightleftharpoons Cd(OH)_2 + Ni(OH)_2$$

3) Nickel Metal Hydride (NiMH) Battery

There was a continuous effort to improve battery performance, energy density and power density, in the later-half of 20th century Nickel Metal Hydride (NiMH) is developed to cope some of the problems of NiCad [19, 20]. The research work on NiMH batteries had started at the Battelle-Geneva Research Center in 1967. In early years, the process was halted due the instabilities of metal-hydride and led to the development of the nickel-hydrogen (NiH) instead. With discovery of new hydrides in the 1980's, the stability is eventually achieved and NiMH battery has been developed with a double specific energy than that of NiCad.

The operating characteristic of NiMH mostly resembles to those of NiCad because it's technically an extension NiCad, with replacing Cadmium with hydrogen-absorbing metal alloy for the negative electrode. This substitution brings about improved energy density, provides the ability to increase storage capacity, it doesn't have the effect issues, and would easily construct in sealed packages (Fig.5) because the released O2 and H2 gases would be effectively consumed [18]. NiMH is considered environment friendly because it doesn't have that toxic cadmium. However, it lacks the capability high discharge power rates of the nickel-cadmium battery and it's less tolerant to overcharge and fast charging thus, charging would have to be managed. NiMH also have a very high self-discharge rate and relatively short cycle life compared to NiCad.

The electrical characteristic of NiMH is more and less same as those of NiCad, it has the same nominal voltage of 1.2V, during discharge the voltage curve as flat as that of NiCad but the internal resistance is relatively low [19]. However, NiMH is more sensitive to discharge condition as compared to its predecessor, because a low discharging and overcharging results in loss of cycle life. It also shows negative effects for trickling charge and thus a very small trickle charge is preferred.

The chemical reaction during charging that occurs on the cathode of NiMH is same as one occurs in NiCad:

$$Ni(OH)_2 + 2OH^- \longrightarrow NiOOH + H_2O + e^-$$

The reaction on anode of NiMH during charging is:

$$M + H_2O + 2e^- \longrightarrow MH + 2OH^-$$

During discharging both of these reactions revert their direction backwards. The overall reversible chemical reaction that occurs in NiMH battery is:

$$MH + Ni(OH)_2 \rightleftharpoons M + NiOOH$$

This overall chemical reaction shows the transfer of single H atom between metal alloy (M) and Ni(OH)2, depending that a charging or discharging operation of the cell.

4) Lithium- ion (Li-ion) Battery

The research on Lithium for battery application begun in 1912 under G.N. Lewis and it was Armand in 1970, who developed the first non-rechargeable lithium battery prototype that were made available for commercial use. Lithium being the lightest of elements has the greatest potential to be provide highest energy density batteries, this propels the research work and it was 1991 when Sony commercialized Lithium-ion (li-ion) rechargeable batteries with a (LiCoO2) as the active positive material [21, 22].

The synthesis of electrode materials for negative electrode was complex achievement as compared to that of positive electrode [34]. Research works has shown that graphite and some other carbonaceous materials can be blended with lithium ions, though this process of intercalation of solvent molecules of carbonaceous materials is complicated due to solvent reduction and Disruption of the carbon structure. Later, a stable battery chemistry was achieved, with a lithium ion cell having graphite anode (e.g. mesocarbon, microbeads, MCMB), and a cathode composed of lithium metal oxide (LiMO2, e.g. LiCoO2) while the lithium salt (e.g. LiPF6) is used as an electrolyte. The electrolyte of lithium salt is a mixture of organic solvent (e.g. ethylene carbonate–dimethyl carbonate, EC–DMC) which implanted on the propylene made separator [23, 24].

The basic structure of li-ion secondary cell is same, it's composed of two electrodes (anode and cathode), electrolyte and a separator, though the technology realization is quite complex (Fig.6). While, the basic internal operational methodology is the transfer lithium ion from one electrode to another depending charging or discharging operation. During discharging state, lithium ion flows from anode, through the electrolyte to the cathode, while in charging operation lithium ion moves backward [16]. The cathode of the li-ion batteries is of significant importance, and effects the battery characteristics greatly. The cathode of li-ion battery is composed of lithium metal oxides, the ones used commonly are lithium cobalt oxide (LiCoO2), Lithium iron phosphate (LiFePO4), lithium manganese oxide (LiMn2O4), Lithium manganese nickel oxide (Li2Mn3NiO8), lithium nickel cobalt aluminum oxide (LiNi0.8Co0.15Al0.05O2), and lithium nickel manganese cobalt oxide (LiNi0.33Mn0.33Co0.33O2) [22, 23]. These low conductivity and diffusion constant of these materials is improved by blending it with a conductive corban material. The commercially available li-ion batteries are named on their respective lithium-ion donating material as being the determinant of cell characteristics, such as nominal voltage etc [35, 36, 37, 38]. The commonly used anode material is graphite though some manufacturers uses lithium titanate (Li4Ti5O12). The mixture of lithium salts and organic solvents are used as electrolyte. The commonly used salt is lithium hexafluorophospate (LiPF6), lithium perchloride (LiClO4) and hexafluorosenate (LiAsF6). The most common separator is made of propylene and polyethylene. The lithium-ion batteries are available in different shapes (cylindrical and flat stacks), sizes and capacities.

The discharge reactions of lithium-ion cell with lithium cobalt oxide (LiCoO2) based cathode and graphite anode (C6) are;

The half reaction t positive electrode (cathode) during discharge:

$$\boldsymbol{CoO_2 + Li^+ + e^- \rightleftharpoons LiCoO_2}$$

The half reaction of the positive electrode (anode) during discharge:

$$\boldsymbol{LiC_6 \rightleftharpoons C_6 + Li^+ + e^-}$$

The overall li-ion cell reaction during discharge and charge operation is:

$$\boldsymbol{CoO_2 + LiC_6 \rightleftharpoons C_6 + LiCoO_2}$$

The over-discharge of the cell leads to the production of lithium oxide (Li2O), while overcharge produces cobalt oxide (CoO2) through irreversible reactions which causes loss capacity and release large amount of heat.

5) Lithium Polymer (Li-Po) Battery

Lithium Polymer (Li-Po) batteries are and advancement of lithium-ion (li-ion) batteries and thus have almost the same operational characteristics predecessors. The nominal voltage is 3.7V, same li-ion cell, while the specific energy is increased further. In Li-Po batteries a polymer electrolyte is used instead of liquid electrolyte [25, 26]. This polymer has ion transport properties comparable to those of commonly used liquid ionic solutions. The Li-Po batteries have many advantages due its polymer electrolytes compared to the conventional li-ion batteries, as they have no risk of internal shorting, no chance of electrolyte leakage and the reactant products are non-combustible[25]. The second variation is the use of metallic lithium for electrode which makes the design further lighter and increases energy density of the cell.

The commonly used polymer gel electrolyte is Poly ethylene oxide, Poly acrylonitrile, Poly methyl methacrylate, Poly vinyl chloride, Poly vinylidene fluoride, and Poly vinylidene fluoride-hexa-fluoro propylene. A Li-Po battery is designed by sandwiching the polymer electrolyte between the metallic lithium anode and a composite cathode. The electrochemistry is quite the same as that of Li-ion cells.

The discharge reactions of lithium-ion cell with lithium cobalt oxide (LiCoO2) based cathode and graphite anode (Li) are;

The half reaction on the positive electrode (cathode) during discharge:

$$\boldsymbol{CoO_2 + Li^+ + e^- \rightleftharpoons LiCoO_2}$$

The half reaction of the positive electrode (anode) during discharge:

$$\boldsymbol{Li \rightleftharpoons Li^+ + e^-}$$

The overall li-ion cell reaction during discharge and charge operation is:

$$\boldsymbol{CoO_2 + Li \rightleftharpoons LiCoO_2}$$

Here we don't have that heavy graphite anode, which made it possible for the manufacturer to build slick and thin batteries, in whatever design they like and secondly the packaging becomes quite simple and easy such as the pouch type batteries.

2.7 Sodium- ion (Na-ion) Battery

Due to numerous advantages over its comparative technologies' lithium-ion batteries got wide recognition and a large share of battery market. With this boom li-ion prices hiked and availability of lithium is felt unsustainable to the rising demand, which draws great interest from researcher to find a cheaper alternative such as Sodium (Na) ion based batteries. For many years Sodium-ion (Na-ion) batteries (NIBs) has been under researched, mainly focused on sodium intercalating materials. However, after 1970's and 1980's the attention of the researcher shifted towards lithium intercalation materials, until fairly recently, when a more stable and economical replacement of Li-

ion is felt crucial, attention shifted back towards NIBs [27]. The researchers have been intensively working for a decade, on the development of stable and potentially competitive Sodium-ion (Na-ion) based batteries to replace Lithium-ion batteries, at least for application where energy density is not that critical [28].

Sodium is one of the abundantly available elements, and battery grade sodium salts are also cheap, the main challenges is development high-performance and stable electrode materials [29]. The development of stable and competitive sodium batteries is infant stage and requires intensive research and development.

III. Research Methodology

In this study lead acid batteries, NiCad, NiMH, and Lithium-ion cells were charged and discharged and the patterns has been observed. An efficient, recognized and smart charger capable of data logging abilities and smart programmable loads to discharge these batteries at different schemes and to keep log of these discharge patterns for later analysis and comparison were must for this research.

A. Experimental Setup

The chargers needed for these experiments, has to be capable of measuring the amount of charge stored in a battery or cell and also have to log the charging current and voltage data during the charging for later analysis. For charging purpose, an "IMAX B6AC" professional balance charger was used, which is capable of charging Li-ion, Li-Po, Li-Fe, NiCad and NiMH single/multiple cells. While for lead acid batteries, a three-stage buck based charger with data logging capabilities is designed.

For observing the discharge patterns of the cells and batteries under study, the loads have to be capable of logging discharging current, voltages and amount of charge that is retrieved during discharging experiments, for later analysis and comparison. We have a "BK PRECISION 8510" programmable DC electronic load, that was used for battery discharge profiling of all the cells and batteries including NiCad, NiMH, Li-ion and Lead Acid batteries. This load has a discharge limitation of 120 watts, so, its unable to discharge lead acid batteries at a current greater than 10 Amperes, that's why we have to design a boost based constant current load for a current greater than 10 Amperes having data logging abilities.

B. Analytical Creterion

To evaluate these batteries for their energy efficiency, their charge and discharge operations eed to be observed. Having accounted for the temperature effects, capacity rate effect (Peukert's law) and recovery effect, batteries are discharged at low currents (C/10) for a specific time (to discharge a 10% of SOC), and then left the battery idle or at a very low discharge current (C/100) for a period of 30 minutes to enable recovery effect and avoid high temperature. This procedure is good for observing short term and long-term transients and in 30 minutes period of low current discharge give us an idea of the recovery effect. For capacity rate effect observation, batteries have been discharged at different C-rate from full charge level to full discharge.

The efficiency of each and every cycle was calculated and a pattern of decrease in efficiency during the later cycle life and capacity degradation is observed. On the basis of this data, the useful life of a battery is verified. While keeping in account the initial cost, cycle life and the energy efficiency, the cost per KWH was calculated. The other important aspects, such as specific energy, energy density, and specific power have been measured and compared against authentic literature,

The formula for energy efficiency is;

$$Energy\ Efficiency\ \eta = \frac{E_{out}(KWH)}{E_{in}(KWH)}$$

IV. Analytical Comperision

The energy efficiencies can be measured with a tolerance of 5% because it's dependent on a variety of the variables namely temperature, charging or discharging profiles, and DOD. The scope of this research has been limited to the Lead Acid, NiCad, NiMH, and Li-ion batteries . A summary of the important observations of the batteries under observation are presented in the table.

TABLE I. Important Parameters of Different Batteries

Battery System	Specific Energy (Wh/kg)	Energy Density (Wh/L)	Energy Efficiency (%)	Specific Power (W/kg)	Cycle Life
Lead Acid (Flooded)	**30**	**80**	**70-80**	**200**	**500 @ 50% DoD**
Lead Acid (Sealed)	**50**	**100**	**75-85**	**250**	**1200 @ 50% DoD**
NiCad	**70**	**200**	**70-80**	**300**	**1500 @ 60% DoD**
NiMH	**100**	**200**	**70-80**	**300**	**1500 @ 60% DoD**
Li-ion	**200**	**300**	**85-95**	**500-1000**	**3000 @ 80% DoD**

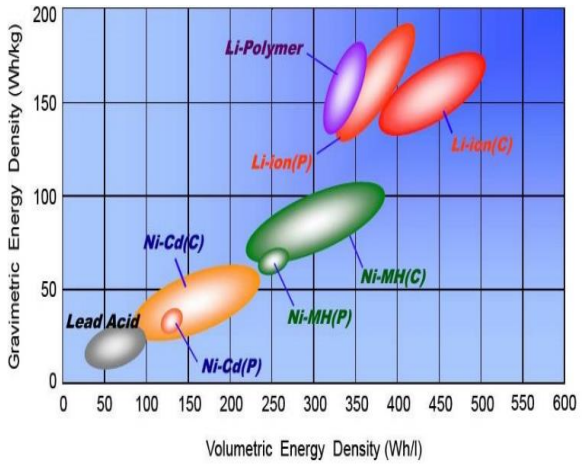

Figure 1. Volumetric Energy Density Vs Gravimetric Energy Density.

The cost of per KWH stored energy is most crucial for selection of a battery, which is directly attached to the estimated durability of the system. The useful life of the battery is normally defined on the basis of two aspects, battery capacity reduction and decrease in efficiency. The most reasonable limit for end of

useful life is a reduction of 70% battery capacity, or when the efficiency decreases below 50%. These two limitations don't have a coherence, when batteries are discharged deeply the capacity reduction is faster, while in case of high temperature and unmanageable charging the efficiency limit is reached earlier, but whatever limit is reached the has to be disposed then.

The cost calculation of per KWH stored energy is a complex and tricky concept, which has tackled in several ways by researcher. My observation and studies show that investment in a battery system has to be made weighing the durability (Cycle Life), storage capacity, and efficiency of the that specific technology. The cost of electrical and electronic infrastructure that needs to be installed for that specific battery technology is kept out of this calculation, because it's a one-time cost but batteries should be replaced after end of life. The formula based on this research for cost calculation of per KWH of stored energy, which would beneficial for making a smart and economical selection of a battery is given here;

$$\boldsymbol{Storage\ Cost} = \frac{\boldsymbol{Cost\ (KWH) * Cap * EC + Capital + MC}}{\boldsymbol{\eta * Cap * EsC}}$$

Where:

Storage Cost = Cost per Unit (KWH) energy storage

Cost (KWH) = Cost of Unit (KWH) energy

Cap = Storage Capacity of Battery

sC = Estimated Life Cycle (at an average DoD)

Capital = Initial Capital Investment

CoM = Cost of Maintenance

CONCUSLION

This research work results into development of an quantized creteria of camparision and selection of a specific battery system for a specific application. This analysis has been done for LA, NiCad, NiMH, and Li-ion batteries, and provides an accurate depiction of these technologies. A simple empirical formulas for the calculation of the energy efficiency of the batteries and per KWH cost of the stored energy in a specific storage system has been that could be used for battery selection. The research provides an understanding of how could we asses performance of a battery and estimate useful cycle life of a battery.

REFERENCES

[1] Disruptive forces on the electricity industry: A changing landscape for utilities Dev Tayal

[2] Getting Smart? Climate Change and the Electric Grid Jennie C. Stephens 1,*, Elizabeth J. Wilson 2 , Tarla R. Peterson 3 and James Meadowcroft 4

[3] Our electric automotive future: CO2 savings through a disruptive technology Jack Barkenbus

[4] Hybrid Energy Storage Systems for Renewable Energy Sources Integration in Microgrids: A Review A. Etxeberria

[5] Power Control in AC Isolated Microgrids With Renewable Energy Sources and Energy Storage Systems José G. de Matos B.Vineel, Dr.D.Vijaykumar, K.S.Goutham, J Vijaychandra as "Enhancing Power

[6] Quality to Sensitive Loads with Microgrid Using Fuzzy Logic Controller" in International Journal of Innovative Research in Science, Engineering and Technology (IJIRSET) Vol. 5, Issue 10, October 2016.

[7] Lidula, N. W. A., and A. D. Rajapakse. "Microgrids research: A review of experimental microgrids and test systems." Renewable and Sustainable Energy Reviews 15.1 (2011): 186-202.

[8] A Control Architecture to Coordinate Renewable Energy Sources and Energy Storage Systems in Islanded Microgrids Dan Wu, Fen Tang, Tomislav Dragicevic

[9] ReviewProgress in electrical energy storage system: A critical review Haisheng Chen a,b, Thang Ngoc Cong

[10] Daniel Claus, Besenhard Jurgen O, editors. Handbook of battery materialsSecond ed.. New Jersey: Wiley-VCH Verlag GmbH & Co. KGaA capacitors; 2011

[11] Molina MG, Dynamic modelling and control design of advanced energy storage for power system applications,

[12] Introduction: Batteries and Fuel Cells by M. Stanley Whittingham, Robert F. Savinell

[13] Handbook of batteries and fuel cells by Linden, D.

[14] Lead batteries for utility energy storage; A review by Geoffery J. May

[15] Electrical Energy Storage Technologies for Off-Grid or Partially Off-Grid Homes by Jessica Hanek

[16] Flooded (Vla), Sealed (Vrla), Gel, Agm Type, Flat Plate, Tubular Plate: The When, Where, And Why. How Does The End User Decide On The Best Solution? By W Rusch, K Vassallo, G Hart

[17] [Comparison of Characteristics - Lead Acid, Nickel Based, Lead Crystal and Lithium Based Batteries by Syed Murtaza Ali Shah Bukhari, Junaid Maqsood, Mirza Qutab Baig

[18] SUBAT: An assessment of sustainable battery technology byPeter Van den Bossche, Fr´ed´eric Vergels, Joeri Van Mierlo, Julien Matheys, Wout Van Autenboer

[19] Nickel-metal hydride batteries. The preferred batteries of the future? By Paul Ruetschi, Felix Meli, Johann Desilvestro

[20] Nickel-based rechargeable batteries by A.K. Shuklaa, S. Venugopalanb, B. Hariprakasha

[21] Rechargeable Batteries and Their Management: Part 30 in a series of tutorials on instrumentation and measurement by Nihal Kularatna

[22] Comparison of Lead Acid to Lithium-ion in Stationary Storage Applications Published by AllCell Technologies LLC

[23] The Development and Future of Lithium Ion Batteries by George E. Blomgren

[24] Characterization of commercially available lithium-ion batteries by Bradley A. Johnson, Ralph E. White]

[25] Review on gel polymer electrolytes for lithium batteries by A. Manuel Stephan

[26] Li Q, Itoh T, Imanishi N, Hirano A, Takeda Y, Yamamoto O. All solid lithium polymer batteries with novel composite polymer electrolytes. Solid State Ionics 2003;159:97.

[27] The re-emergence of sodium ion batteries: testing, processing, and manufacturability ny Roberts S

[28] Recent progress on sodium ion batteries: potential high-performance anodes Li Li,abc Yang Zheng,

[29] Sodium-ion batteries: present and future by Jang-Yeon Hwang

Alamgir Ahmad Khattak

The author belongs to District Mardan of Khyber Pukhtun khwa and have done BE Electrical Engineering From NUST SEECS Islamabad in 2013 and MS Electrical Energy Systems Engineering, USPCAS-E Universityy of Engineering and Technology, Peshawar, Pakistan. 2019.

IJEW 国际工程期刊 International Journal of Engineering Works انجینئرنگ کاموں کا بین الاقوامی جرنل

International Journal of Engineering Works
ISSN-p: 2521-2419
ISSN-e: 2409-2770
Vol. 7, Issue 01, PP. 68-73, January 2020
https://www.ijew.io/
https://doi.org/10.34259/ijew.20.7016873

Implementation of Chiller Plant Management System to Optimize the Building Primary HVAC System Energy Consumption

Muhammad Waseem Khan[1], Umar Ibrahim [2]
[1,2] Department of Mechanical Engineering, University of Engineering and Technology, Peshawar, Pakistan
waseem.pwmec@gmail.com[1], umar.marwat@gmail.com[2]
Received: 22 January, Revised: 29 January, Accepted: 30 January

***Abstract*—** The heating, ventilation and Air conditioning (HVAC) system in Pakistan consumes more than 50% of total energy utilized by the building sector. Due to current energy crises in Pakistan there is a need renewed focus on energy optimization in building sector. The aim of this research paper is to reduce building HVAC system energy consumption by implementing chiller plant management system to control on electrical energy consumption in existing primary HVAC system (Chillers, Pumps, Boilers and Cooling towers). The Johnsons control international building automation protocol has been implemented with weather load profile of Pakistan (Islamabad). The chiller plant management system has improved plant performance and decreased annual energy consumption. The results of implemented modern chiller plant management system shows at least 12.57% of energy saving. It is also observed that the chiller plant management system closely follow outdoor dynamic weather profile and indoor load profile.

***Keywords*—** HVAC, BMS, CPM, Building Automation, PID

I. INTRODUCTION

The chiller plant management system (CPM) is the automatic control, operation and monitoring of chillers, pumps, cooling tower and air handling unit etc. It not only automate the primary HVAC system but also enhance indoor human comport level and increase system efficiency, reduced maintenance and operational cost. The chiller plant management eliminates unnecessary operation of system it only operates those HVAC system equipments which are needed as per internal/external dynamic heating/cooling load. Therefore, reducing unnecessary operation increase building HVAC system energy efficiency and better control over all the system [1]. According to (ASHRAE) studies the chiller plant management system or building management system (BMS) reduces energy consumption up to 20% compare to building without building HVAC automation system [2]. Therefore, the implementation of building management system not only automate various building services but also increase sustainability, efficient operation of building systems, improved human comfort level in conditioned space, reduced energy consumption and operational costs and improved equipment expected life [3]. In past decades, various control strategies has been developed to ensure this [4]. In current research work, our focus is to optimize the energy consumption of a chiller plant for a portion of a centralized HVAC system taken (Chiller plant consist of chillers, boilers, Pumps and cooling tower) by implementing chiller plant management system considering the weather profile of Islamabad.

II. THE HVAC SYSTEM MODEL DESCRIPTION

The capacity of plant is 6000TR located in Islamabad region serve main passenger terminal building. The package chiller and boiler Plant include the following major equipments.

TABLE I. DESCRIPTION OF PRIMARY HVAC SYSTEM

H	Equipment	Qauntity	Capacity
1	Chiller's	6	1200 TR (740 KW)
2	Cooling Tower	6	1560 RT, P = (5.5x8) KW Each
3	Space hot water boiler	3	1410KW
4	Secoundry chilled water pump	7	185KW,367Amp,Flow242L/s,Head 62m
5	Primery chilled water pump	6	45KW,83.5Amp,Flow 218 L/s
6	Condenser water pump	6	90KW,168Amp,Flow 262 L/s,Head 26m
7	Primary hot water pump	3	15KW,51.1Amp,Flow 68L/s
8	Non chemical water treatment system motor	6	4KW,15.1 Amp
9	Boiler recirculation pump	6	Flow 22 L/s, H = 17 m, P = 7.0 KW Each
10	Booster pump	2	21 Kw,30Amp,Flow 26.2 L/s
11	Cooling tower expansion Tank	2	7 m3
12	Chilled water expansion tank	9	16.7 m3(sys-1) ,8.9m3(sys-2)
13	Cooling tower Expansion tank Pumps	2	Q = 426.2 L/s, H = 26 m, P = 2.5 KW Each

The return chilled water from the air handling units at main terminal building is pumped by constant speed primary chilled water pumps to centrifugal chillers and cooled to the designed chilled water temperature. Heat is rejected by the condenser water which is pumped by the condenser water pumps through the cooling towers. The supply chilled water is pumped to the passenger terminal building by variable speed secondary chilled water pumps via two secondary loop distribution-piping networks that is connected to constant speed primary chilled water loop across the de-coupler. Each chiller is equipped with a microprocessor control panel. The CPM is communicate with the chiller panels through a hardwire connection using software interface (Johnson Control). Other equipment such as pumps, cooling towers etc is the hardwire connected with the CPM for monitoring and control.

III. CONTROL PHILOSOPHY

The chiller plant is controlled as per the total cooling load requirement as evidenced by the change in return chilled water temperature. The total cooling load requirement is calculated based on the feedback from the supply chilled water header flow transmitter and the temperature differential between the supply and return primary chilled water heaters. Chillers is added or subtracted based on the feedback received from the bypass de-coupler flow transmitter and its flow direction & secondary temperature below the set-point. Chillers are being added based on the supply chilled water temperature feedback received from the secondary chilled water header once the set-point exceeds. The individual chillers are loaded / unloaded by the local chiller microprocessor panel based on the chiller leaving chilled water temperature set point. Similarly, whenever a chiller is started, cooling tower (CT) fan variable frequency drives (VFD) is enable and getting started. The temperature of cooling tower supply water to condenser is controlled at minimum limit of 33°C for stable operation of the chiller. This is accomplished by measuring the temperature of the cooling tower water returning to condenser and using this as input to a feedback-control algorithm The VFD also ramp up/down the fan speed of CT cells as per feedback command receive from condenser water supply temperature sensor. The CPM minimizes the potential for multiple boilers operating at reduced loads, thereby reducing boiler efficiency. It will also improve plant reliability, increase equipment life expectancy and reduce maintenance costs.

IV. CHILLER PLANT MANAGEMENT SYSTEM MODEL

The chiller plant management (CPM) is designed and implemented to minimize the combined electrical energy consumption of the operating chiller(s), chilled and condenser water pump(s), and cooling tower fan(s) as constrained by meeting the building chilled water load and temperature requirements. The CPM also minimize the potential for multiple chillers operating at reduced loads, thereby reducing any peak demand charges caused by unnecessary cycling. It also improves plant reliability, increase equipment life expectancy and reduce maintenance costs. The schematic diagram of implemented building management system sensors and control wiring between the chiller plant components is shown in figure 3. In the Chiller Plant Management System all the equipment interface is through ethernet TCP/IP to the others chiller plant control system server located at the Chiller Plant room. The interface method is BACnet protocols. The Field Equipment Controller (FEC) is a programmable digital controller that communicates via BACnet Master-Slave/Token Passing (MS/TP) protocol is connecting to each individual HVAC system equipment as shown in figure 1 [5].The digital and analog input signals like humidity, temperature ,equipment start/stop status is transfer to the chiller plant management system (CPM) through BACnet communications protocol .Digital/ Analog outputs from respective controller to connected equipment such as motorized valves, pumps, cooling towers and fans command their settings accordingly or to switch devices on and off. The field equipment controller is combined with the Input/ Output Module (IOM) shown in figure 2 which is BACnet Advanced Application Controllers (B-AACs) with integral RS-485 MS/TP communications. Typically, input output module (IOM) are install in two position (1) when installed on actuator or sensors bus of a field equipment controller (FEC) the IOMs expand the point count of these controllers (2) when installed on the Field Controller (FC) bus as point multiplexors, IOMs allow a Network Automation Engine (NAE) or Network Control Engine (NCE) to monitor and control supervisory points directly. The field equipment controller arrangement in series are shown in figure 5 and serial port connection in figure 5.

Figure 1. Field Equipment Controller (FEC)

Figure 2. Input/ Output Module (IOM)

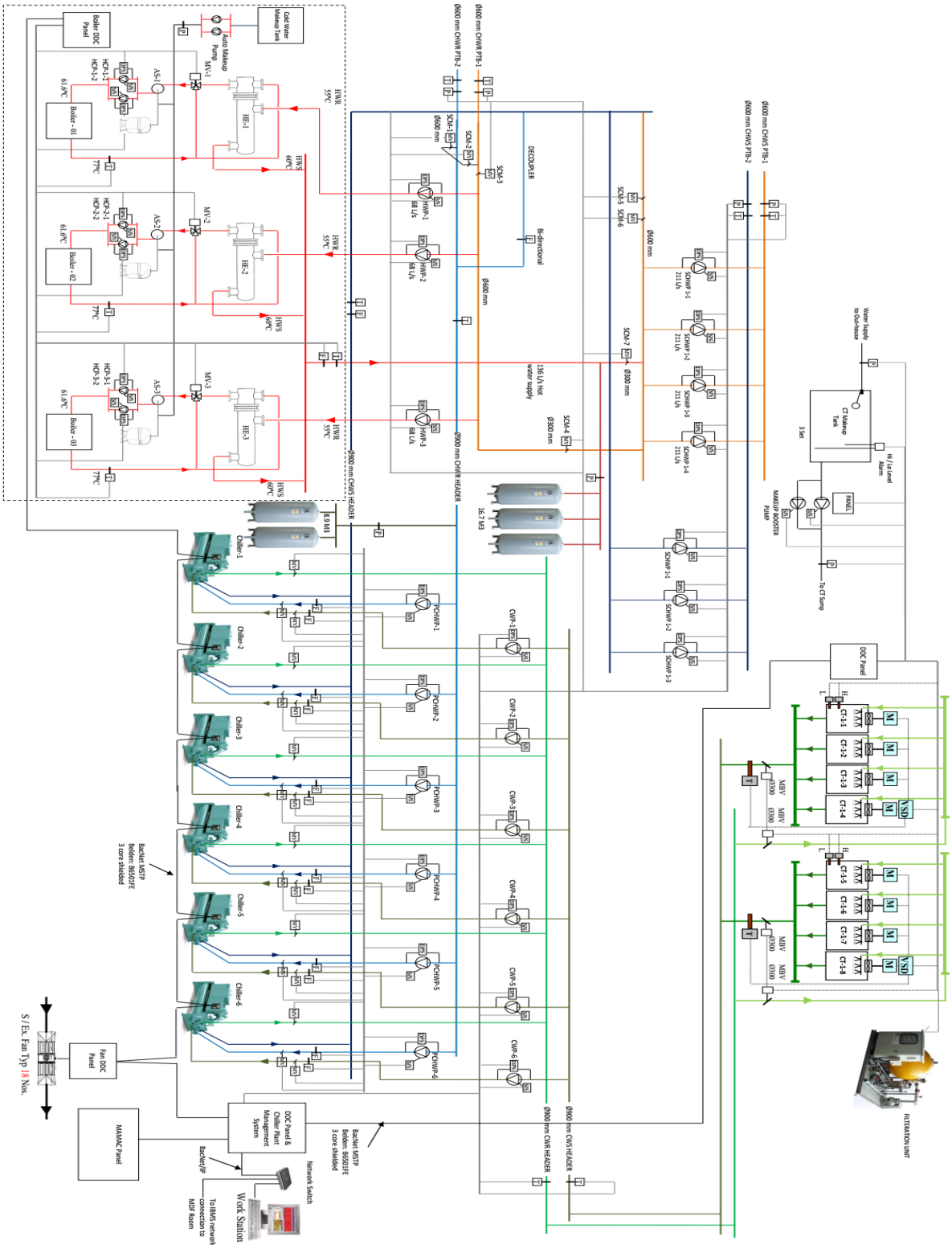

Figure 3. Schematic Diagram of Implemented chiller plant management system (CPM)

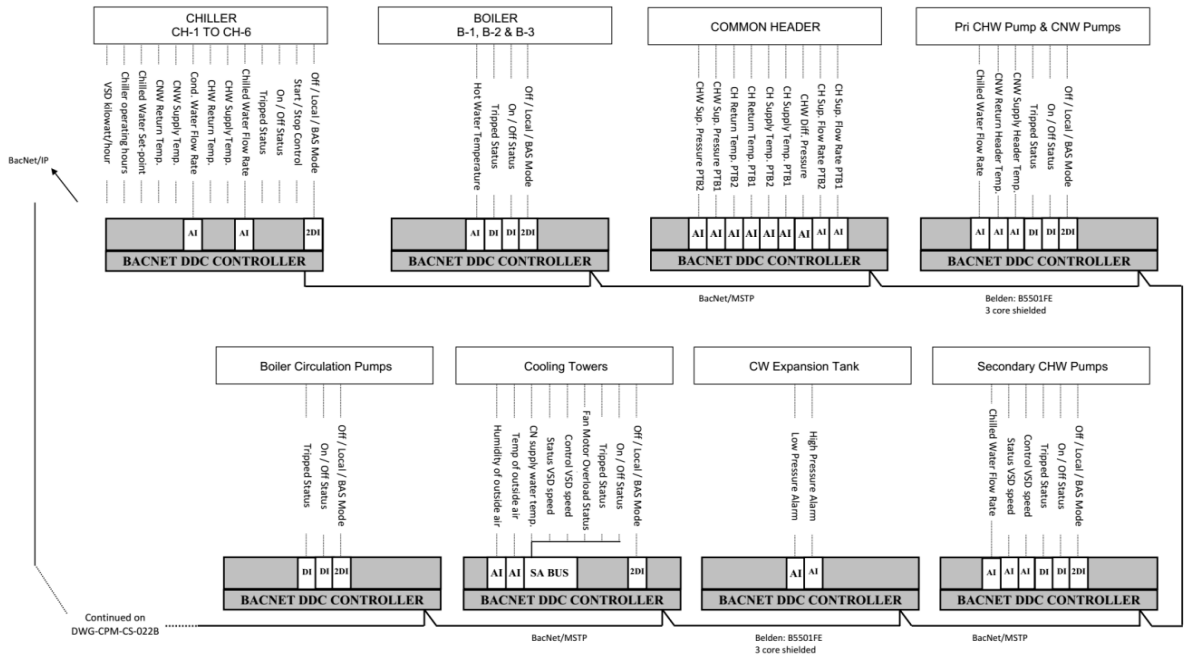

Figure 4. Control Logic of Chiller plant management system (CPM)

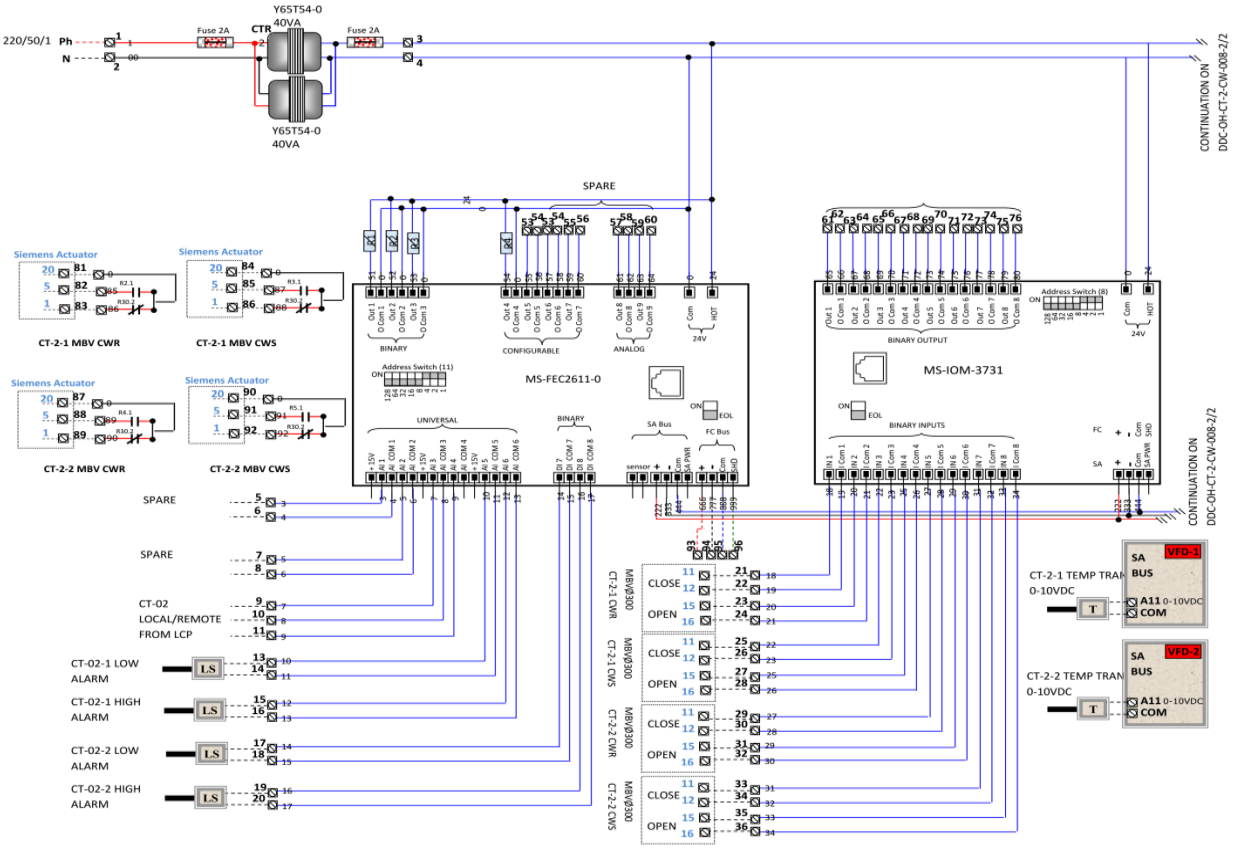

Figure 5. Field Equipment Controller connection detail

Figure 6. Real time data logging of implemented CPM system

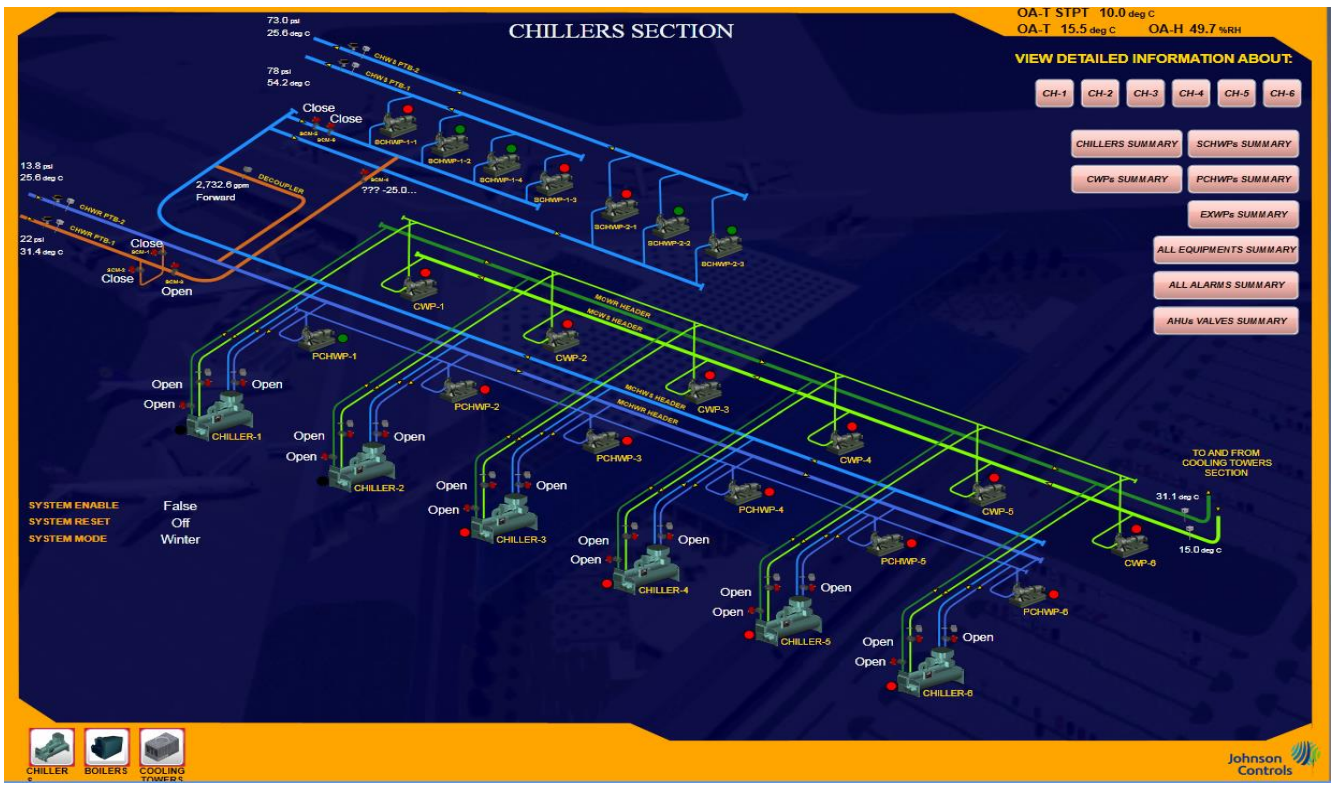

Figure 7. Graphic interface of CPM in METASYS Softwar

V. RESULTS AND DISCUSSION

Summary of real time data for the energy consumption by existing chiller plant from Dec 9, 2018 to Dec 14, 2018 without chiller plant management system and from Dec 9, 2019 to Dec 14, 2019 are presented in figure 8. Real time data present the operation of chiller plant in winter season where heating load at the highest while minimum cooling load available due to computer server rooms baggage handling system and ELV riser. It can be observed that the chiller plant energy consumption in case of without CPM control is the highest for the reference time. By comparing CPM control of HVAC system present the energy reduction up to 101845.5 KWh (12.57%) then without CPM control of chiller plant. Similarly, the energy consumption of the pump(s) also reduces, from 141112.8 KWh to 89856.8 KWh (36.32%). In the graph it can be observed that energy saving in pumps is the greatest and it is due to VFD drive secondary chilled water pumps pumping chilled water to Air handling Units. The monitoring facilities of a CPM system also monitor environmental conditions, plant operational status, and energy consumption. The current CPM system assist operator to log real time data of the building chiller plant operation process and to generate customized reports of alarms, trends, messages, and to log key cooling/heating plant performance indices as shown in figure 6 and 7.

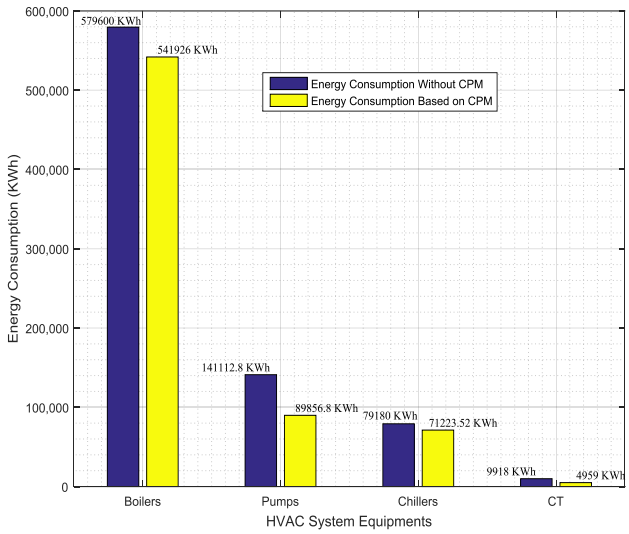

Figure 8. Energy consumption with and without CPM system

CONCLUSION

This paper has presented practical implementation of chiller plant management system (CPM) for automation of chiller plant. Due to the implementation of CPM system Significant improvement were achieved as the total energy saving by the Chiller plant for the reference days with CPM control is 101845.5 KWh (12.57%).The CPM system gives real time data that are beneficial for buildings owner facilitation management department providing information such as preventive maintenance requirement, the energy usage, and the generated alarm. The real time data is also crucial for accurate calculation of budget and allow the building's owner and managers to take decision of right time.

REFERENCES

[1] Foresti, G.L., Remagnino, O., 2005. Ambient intelligence: a new multidisciplinary paradigm. IEEE Transactions on Systems, Man, and Cybernetics – Part A: Systems and Humans, pp. 1–6.

[2] ASHRAE, 2015. ASHRAE Guideline 13-2015, Specifying Building Automation Systems. American Society of Heating, Refrigerating and Air-Conditioning Engineers (ASHRAE)., Atlanta-USA.

[3] SAYED, K., GABBAR, H.A., 2018. Energy Conservation in Residential, Commercial, and Industrial Facilities, First Edition. ed. The Institute of Electrical and Electronics Engineers, Inc. Published 2018 by John Wiley & Sons, Inc, Canada.

[4] Kwon, B., Lee, S., 2014. Joint energy management system of electric supply and demand in houses and buildings. IEEE Transactions on Power Systems, pp. 2804–2812.

[5] Johnson Controls, 2010. Field Equipment Controller (FEC) Series. USA.

IJEW 国际工程期刊 International Journal of Engineering Works انجینئرنگ کاموں کا بین الاقوامی جرنل

International Journal of Engineering Works
ISSN-p: 2521-2419
ISSN-e: 2409-2770
Vol. 7, Issue 01, PP. 74-79, January 2020
https://www.ijew.io/
https://doi.org/10.34259/ijew.20.7017479

Designing, Fabrication, Testing and Performance Evaluation of a Straight Bladed Darrius Type Vertical Axis Wind Turbine

Bilal Anwar
Department of Renewable Energy Engineering, U.S.-Pakistan Center for Advanced Studies in Energy, University of Engineering and Technology Peshawar, Pakistan
bilalktkiiui@gmail.com

Received: 17 January, Revised: 27 January, Accepted: 03 February

***Abstract*—**Designing, fabrication, testing and evaluation of vertical axis straight bladed Darrius type wind turbine are done. Calculations are carried out for a specified load, then Darrius type wind turbine, having the capacity to drive that load is designed. The airfoils of turbine are symmetrical with good lift to drag ratio. Initially turbine with fixed blade is designed, fabricated and its performance evaluated in lab with real wind. Efficiency has been calculated by testing the turbine with and without load

***Keywords*—**Darrius, VAWT, HAWT , design

I. INTRODUCTION

Wind power considered to be giant sustainable power resource is becoming progress progressively more critical in worldwide strength regulations in response to speedy weather adjustments. Therefore, the wind electricity plants are enhancing and developing countries arranging funds for harnessing a huge amount of wind electricity. Wind electricity considered to be the cleanest assets of energy and has been used for electricity for numerous hundreds of years. Wind is really a derivative of sun power. According to researchers, approximately 1% of solar's power obtained at earth floor is changed to wind electricity [1].Stress zones are created in atmosphere through choppy heating and cooling of the surface of earth. This glides air from excessive stress zones to zones of low stress. Air get high kinetic energy which may be converted to mechanical or electrical energy. Studies reveals that the total wind power that can be harnessed is 61 TW [2]. To obtain this power a massive wide variety of industrial wind turbines had been designed within the global. So, developing market for wind power exists and unique forms of wind turbine generators, have been made inclusive of vertical axis wind turbine (VAWT), horizontal axis wind turbine (HAWT), Darrius kind wind turbine, Savonus type turbine. Each of the turbines have a few upsides and downsides. HAWT are greater costly to supply than VAWT, due to high-priced substances and comparatively complex designs [3]. The next downside is that HAWT are used best in the regions of non-stop wind. One of the main drawbacks is that unequal gravitational force is acting at all airfoils of HAWT. On the opposite hand, benefits related to VAWT are numerous for instance:

- VAWTs can function in regions wherein HAWT **aren't** very useful. This is because the axis of rotation of blades is independent of wind current.
- VAWT does not yaw in direction of wind.
- VAWT has sturdy design and is capable of withstanding extraordinarily wind velocities.
- Price of VAWT is low as compared to HAWT due to straight-blade design.
- They can function even in turbulent wind flow.
- VAWT has easy Maintenance due to the fact they're at very low height from the surface of earth.

On the opposite hand, HAWT has higher efficiencies than VAWT [4]. Therefore, VAWTs are much less common and are not extensively commercially to be had. The efficiency of VAWT can be improved with certain modifications in design. The more particular intention for the paper is designing, constructing and testing a vertical axis wind turbine of Darrius type for a selected electrical load.

II. APPROACH AND METHODOLOGY

Darrieus type vertical axis wind turbine consisting of three blades is chosen. The turbine includes base, central shaft, generator, circular assisting plates, springs and different add-ons. The airfoils are kept at an angle of one hundred twenty degrees. The airfoils are placed on the edges of assisting plates. The assisting plates are constructed from acrylic sheet and its job is to support the airfoils. The turbine's shaft is made of steel and its function is to rotate assisting plates and airfoils. First of all, wind transfers its energy to the blades which in turn transfer it into assisting plates. Energy from the plates is transferred to the shaft. From the shaft it is transferred into generator via pulley and generator finally change it into useful electrical energy.

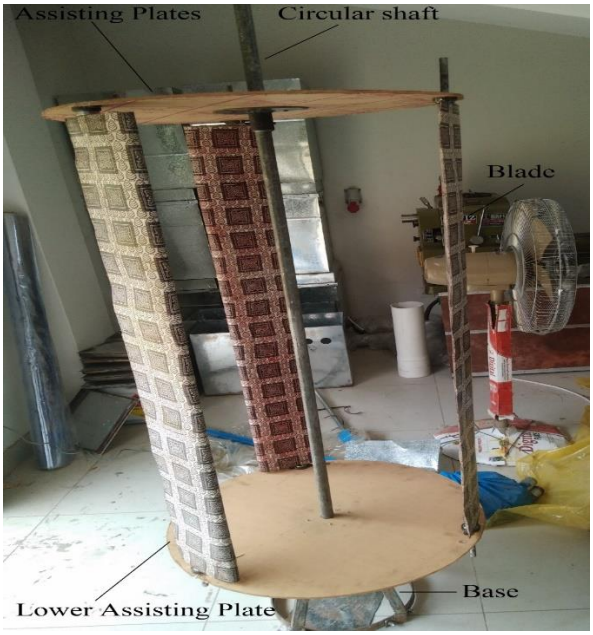

Figure 1. Figure 1 Turbine at rest

Turbine Airfoils

The airfoil selected for the paper is NACA 0018. The geometry of airfoil is symmetrical which provide extra lift to the blade. This geometry is too simple to be fabricated at any simple workshop.

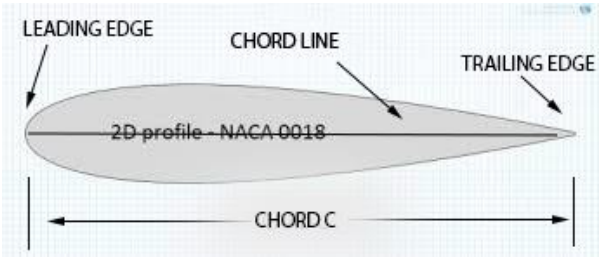

Figure 2. Figure 2 NACA 0018 Airfoil

Mathematical calculations of Aerodynamic evaluation of the NACA 0018

Table 1 indicates the performance of the blade on aerodynamics basis for 360°. Table shows that when the wind angle attacking the blade is 0°, simply the pressure existing is drag. Lift force increases with increase in relative angle of attacking wind. Lift is maximum at 45° angle and lowers with further increase in angle. The most lift force on the airfoil at an angle of 90° to the wind [5].

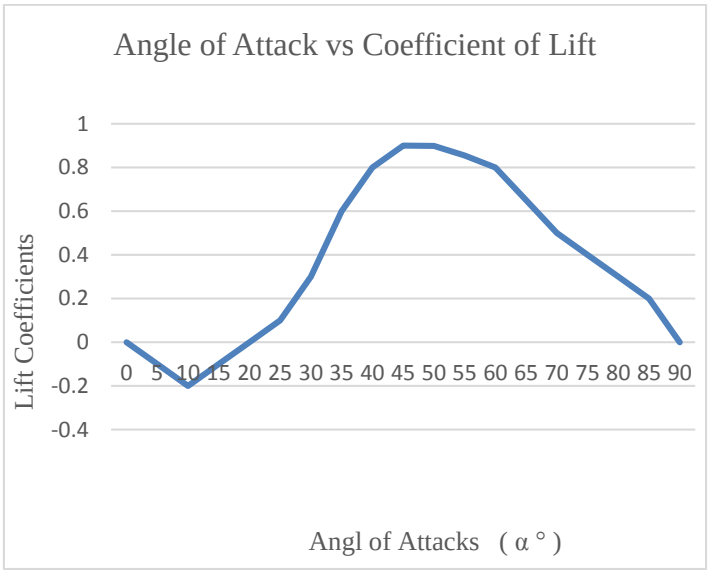

Figure 3. Coefficient of lift vs angle of attack

Phenomena occurring in blades of Darrieus turbines are:

a) Change in angle of attack

The pace of the wind at upstream and downstream of wind turbine isn't always identical [6]. So, the angle at which wind attacks the blades varies constantly. Fig. 4 demonstrates complete process. [7]

TABLE I. LIFT AND DRAG COEFFICIENTS OF NACA 0018

(α°) Angle of Attack	**(C_L) Lift Coefficient**	**(C_D) Drag coefficient**
0	0	.0385
1	-.0045	.0387
2	-.0154	.0391
3	-.0233	.0399
4	-.0368	.0410
5	-.0577	.0425
6	-.0839	.0443
7	-.1182	.0463
8	-.1501	.0489
9	-.1584	.0489
10	-.1423	.0574
11	-.1125	.0800
12	-.0767	.1230
14	.0085	.1580
16	.1051	.1960
18	.2070	.2380
20	.3111	.2820
22	.4172	.3290
25	.5775	.4050
30	.8550	.5700
35	.9800	.7450
40	1.0350	.920
45	1.0500	1.07550
50	1.0200	1.2150
55	.9550	1.3450
60	.8750	1.4700

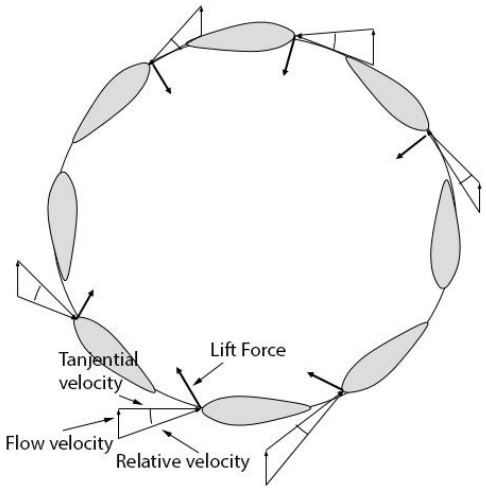

Figure 4. Turbine airfoils during rotation

Flow velocity: Velocity of wind received by turbine.

Relative velocity: Vector sum of tangential and flow velocities.

Tangential velocity: Velocity that is tangent to the airfoil.

Figure 5. illustrates that the angle of attacking wind is not uniform but varying thoroughly as it passes through the turbine. Therefore, both the lift and drag forces varies. These forces stronger at one point and weaker at others and are further explained in this figure [8]. The upwind and downwind shown in figure 6.

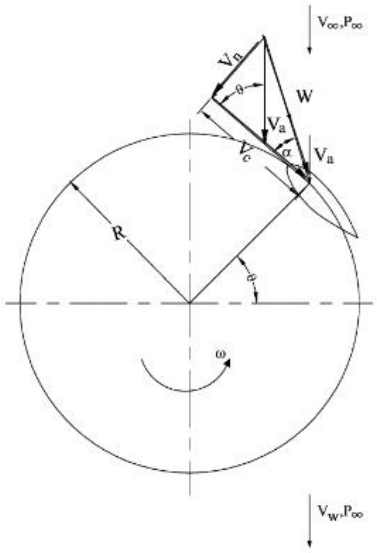

Figure 5. Lift and drag Forces

$\boldsymbol{V_\infty}$ Is in axial direction and has two components.

$\boldsymbol{V_c}$ = Chordial component of velocity

$\boldsymbol{V_n}$ = Normal component of velocity

Derivation

Both of the above components can be derived in the following way.

$V_c = v_a cos\theta + r\omega$---------- **(1)**

$V_n = v_a sin\theta$---------- **(2)**

$$v_a = \frac{V_\infty + V_W}{2}$$

$\boldsymbol{V_\infty}$= wind speed at turbine inlet

$\boldsymbol{v_a}$ = Wind axial flow velocity inducing through turbine

$\boldsymbol{v_W}$ = **Wind Velocity of wake** = velocity at turbine outlet.

$\boldsymbol{V_W}$ *is equall to* $\boldsymbol{v_\infty}$ - $\mathbf{v_a}$

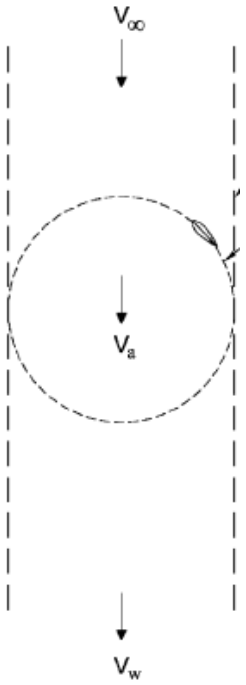

Figure 6. upwind and downwind

$\boldsymbol{\omega}$ = turbine angular velocity

$\boldsymbol{R}$ = **Turbine** radii

$\boldsymbol{\theta}$ = Angle of azimuth

Formula for attacking angle of wind can be calculated as

$$\alpha = \tan^{-1}\left({}^{v_n}/_{v_c}\right) \text{---------- (3)}$$

Putting values

$$\alpha = \tan^{-1} \times \left[\frac{\text{Sin}\theta}{\left(\frac{\frac{R\omega}{v_\infty}}{\frac{v_a}{v_\infty}}\right) + \cos\theta}\right] \text{---------- (4)}$$

Change in Relative Flow Velocities

As relative velocities of flow are given by [9]

$$W = \sqrt{{v_c}^2 + {v_n}^2} \text{---------- (5)}$$

Inserting values

$$\frac{w}{v_\infty} = \left({}^{W}/_{v_a}\right) \times \left({}^{v_a}/_{v_\infty}\right) =$$

$$\left({}^{v_a}/_{v_\infty}\right) \sqrt{\left[\left(\frac{\frac{R\omega}{V_\infty}}{\frac{V_a}{V_\infty}} + Cos\theta\right)\right]^2 + Sin^2\theta} \text{..... (6)}$$

Change in Tangential and Normal Components of Forces

Both components of forces i.e. Varies during 360° rotation of the blades. Normal and tangential sections of drag and lift forces on the airfoil are provided in figure 7.

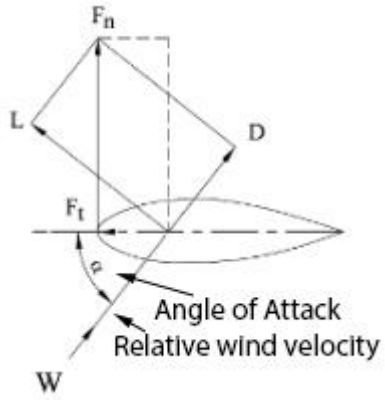

Figure 7. Angle of Attack of wind

$\boldsymbol{C_t}$ Shows the difference of tangential components of lift and drag force.

$\boldsymbol{C_n}$ Shows the difference between components of lift and drag forces that are normal.

Mathematical Calculations

$$C_T = C_1\text{Sin}\alpha - \text{C}_\text{D}Cos\alpha \text{---------- (7)}$$

$$C_n = C_1\text{Cos}\alpha - \text{C}_\text{D}Sin\alpha \text{---------- (8)}$$

$\mathbf{F_t}$ Show **the** sum of tangential forces and is equal to

$$F_t = C_t \times \frac{1}{2}\rho \times \text{C} \times \text{H} \times \text{W}^2 \text{..... (9)}$$

$\boldsymbol{F_n}$ Shows net normal forces.

$$F_n = C_n \times \frac{1}{2} \times \rho \times \text{C} \times \text{H} \times \text{W}^2 \text{---------- (10)}$$

ρ is density of air

C is chord′s lenght of airfoil

H is turbine′s height

W shows relative flow velocities

Mathematical calculations

Design calculations for a single blade are given below in figure. 8 (a) and 9 (b).

Figure 8. A single blade (a)

For calculating V_c we fine RPS
As

$\text{Rev/mint} = 166$
Hence
$\text{Rev/second} = {}^{166}/_{60}$
$\text{Rev/mint} = 2.8$
$\text{Turbine Diameter} = 0.60\ \text{m}$
$\text{Circumference of turbine} = \pi\ \text{D}$

Circumference of turbine $= 3.140 \times 0.60$ m $= S$
Circumference of turbine $= 1.93$ m
Speed of turbine $= 2.80 \times 1.90$ m/s
Speed of turbine $= V_c = 5.320$ m/s
$V_c = chordial\ component = 5.32$ m/s
$v_n = normal\ component = 4\ m/s$
Tip Speed Ratio $= {}^{5.32}/_{4}$
Tip Speed Ratio $= 1.4$

Figure 9. A single blade (b)

As
$tan\alpha = \dfrac{Perpindicular}{Base}$
Putting value
$\alpha = \tan^{-1}\left(\dfrac{4}{5.32}\right)$
$\boldsymbol{\alpha} = 36.94°$
It is the angle of attacking wind to the blade.

Design of the Project

Calculations for 50 watts of a turbine and wind of 7 m/s speed were done by using the formula

$power = \frac{1}{2} C_P\, \rho A v^3$ ..... (A)

$C_P = .300$

Air density at temperature $30℃ = 1.22\ kg/m^3$
$V = velocity\ of\ wind = 7\ m/s$

The following dimensions were calculated after putting all of the values in the power formula.

III. RESULTS

Wind turbine of these dimensions was fabricated and was tested in the wind of $4\ m/s$ speed in the laboratory. The following results were obtained.

Results for Unloaded Turbine

Initially results of turbine for no load were obtained in Table II and results for loaded turbine in Table III.

TABLE II. RESULTS FOR UNLOAD TURBINE

Rev/mint	Open Circuit Voltage(volts)
164	185
168	187
171	191
172	192
169	186
161	181
REV/MINT (Average) unloaded = 167	**VOLT(Average) unloaded = 187**

Results for loaded turbine

TABLE III. RESULTS FOR LOADED TURBINE

Height of Turbine (meter)	Diameter of Turbine (meter)	Chord's length of Blades (meter)	Area of Turbine (meter^2)
1.250	.620	.1240	.76880

A light bulb of power 5 watts was connected to the turbine. Current, voltage and RPM were measured.

Now calculating power
As we know that
$Power = Voltage \times Current$
$P = V \times I$
$P = 90 \times .0226$
$P = 2.34\ Watts$

The below table IV as shown below.

TABLE IV.

REV/MINT	Closed Circuit Generator Voltage (volt)	Current (Amp)
121	89	.025
122	92	.026
122	92	.028
125	94	.03
131	95	.035
123	93	.03
121	89	.029
120	89	.029
119	88	.028
Rev/Mint (Average) Loaded = 122	**VOLT(Average) Loaded = 91**	**CURRENT(Average) = 0.026**

Efficiency of the Turbine

As turbine was designed for a power of 5 watts and it is generating 2.34 watts so its efficiency is

$\text{Efficiency} = \dfrac{2.34}{5} \times 100$
$\text{Efficiency} = 46.8$

The figures 10 and 11are shown the tubine base and Led light energized by turbine respectively.

Figure 10. Turbine Base

Figure 11. Led light energized by turbine

CONCLUSION

Non-directional nature, high lift and easy maintenance enable vertical axis Darrius type vertical axis wind turbine to be used in area of high wind speed for power production. VAWT, Due to simple mathematical and aerodynamics calculations and easier manufacturing processes can be easily made at any local workshop.

REFERENCES

[1] A. P. dannemand, "Review of historical and modern utilization of wind power," Rose National Laboratory, 1998.

[2] S. Emies, Wind Energy Meteorology, Switzerland: Springer International Publications, 2017/2018.

[3] H. B. S. Eriksson, "Evaluation of different turbine concepts for wind power," Renewable and Sustainable Energy Reviews, vol. 12, pp. 2-5, 2008.

[4] I. G. K.Pope, "Energy and exergy efficiency comparison of horizontal and vertical axis wind turbines," Renewable Energy,, vol. 35, pp. 6-9, 2010.

[5] H. B. a. Y. Yao, "Effect of Camber Airfoil on Self Starting of Vertical Axis Wind Turbine .," Journal of Environmental Science and Technology, vol. 4, pp. 302-312, 2011.

[6] A. R. R. Ahmed M. El Baz, "Computational Modelling of H-type Darrius Vertical Axis Wind Turbine with," in Eleventh International Conference of Fluid Dynamics, Egypt, 2013

[7] W. Y. j. W. Ji Yao, "Numerical simulation of aerodynamic performance for two dimensional wind turbine airfoils," in International Conference on Advances in Computational Modeling and Simulation, Kunming , 2012

[8] D. S.-K. T. A. F. M. u. Islam, "Aerodynamic models for Darrieus-type straight-bladed vertical axis wind turbines," Renewable and Sustainable Energy Reviews, vol. 12, pp. 1087-1109, 2008

[9] D. S.-k. T. A. F. Muzahiril Islam, "Aerodynamic Model for Darrieus-type Streight-bladed Vertical Axis Wind Turbine," Renewable and Sustainable Energy Review, vol. 12, no. 4, pp. 8-12, 2018.

IJEW 国际工程期刊 International Journal of Engineering Works انجینئرنگ کاموں کا بین الاقوامی جرنل

International Journal of Engineering Works
ISSN-p: 2521-2419
ISSN-e: 2409-2770
Vol. 7, Issue 03, PP. 161-167, March 2020
https://www.ijew.io/
https://doi.org/10.34259/ijew.20.703161167

Analyzing the Consumer`s Buying Behavior towards Green Products

Kanwal Bai, Muhammad Saad Memon, Sonia Irshad Mari
Department of Industrial Engineering and Management, Mehran University of Engineering and Technology, Jamshoro, Pakistan

Received: 22 February, Revised: 28 February, Accepted: 01 March

***Abstract*—**Environment is basic and most important thing we have in our life if it is being ruined then it is our responsibility to prevent it. Since the leftover (wrappers, bottles and plastic packaging etc.) of non-green products cannot be disposed after the products are consumed; in that case they are buried, burnt and thrown into the sea; in all the cases, they pollute the environment, harm earth or poison our water. These three things (water, earth and air) are necessary for healthy life on earth. In order to prevent this the consumers are needed to buy the products which can be easily disposed with any harm. In this regard, this study has been conducted to analyze the buying behavior of consumers towards the green products. Data was collected by the help of questionnaire adopted from the literature. Data was collected online (by sending the link of Google form in email), at superstores, marts, supermarkets and shopping malls of Hyderabad Pakistan. The number of valid responses collected from the respondents was 200. Data analysis was conducted in the statistical package for social sciences (SPSS) version 22. Internal consistency of data was check by using the cronbach`s alpha test. Frequency distribution of demographic characteristics of the respondents was taken out along with descriptive statistics (mean, standard deviation, skewness and kurtosis). Skewness and kurtosis were calculated to indicate the normality and when it was revealed that the data was normal, the developed hypothesis were tested by Analysis of variance (ANOVA) test. Furthermore, the Pearson correlation of demographic characteristics (age, income and qualification) was calculated with Consumer`s interest, will and buying behavior towards the green products. On the same time Pearson correlation between the various constructs was also calculated. In last regression analysis was conducted on the various constructs. It was concluded that demographics were not in any association with the consumer`s interest, will and buying behavior but consumers` will, interest and buying behavior towards green products were weakly correlated with one another..**

***Keywords*—** Green products, consumer, purchasing.

I. INTRODUCTION AND LITERATURE

The increase in the population of earth after 1950s has threatened its health in terms of climate change, ozone depletion, depletion of forest cover, pollution in the atmosphere extensive loss of biodiversity [1]. With the increase in the consumption of consumer goods, there has been quick growth in the economy. On the huge demand of consumers non-green products are supplied which ruin the environment [2]. 44.7 million metric tons (4500 Eiffel towers) of e-waste was produced around the world. From that much e-waste, 0.7 million Mt were produced form oceans; 2.2 million Mt were produced from African countries; total of 11.2 and 12.3 million metric tons were produced from American and European countries respectively. Moreover, in 2017, Asian countries hold first position among all the continents [3]. While shopping, the consumer don`t think very much about the environment [4]. As per the researchers, politics and government are on the center to understand, analyze and shape the sustainability transformations [5]. It has become necessary to protect the environment by the help of green innovation [3]. The behavior of consumers towards the environment can be determined through the awareness about the environmental problems [2]. The more the individuals have knowledge about the environmental issues, their behavior can be favorable towards environment. Problems of environment and its deterioration have been the point of debate for researchers and practitioners and the solution they suggest is green products [3]. Businessman and consumer together confront the biggest challenge of protecting the resources and the environment of this planet [6]. On the same time the concept of eco innovation refers to the products` and processes` development through environmentally sustainable practices at the every point of production [7]. Similarly, it is the responsibility of the consumers to buy those products which are environment friendly or easily disposable. Some consumers are willing to pay more for the green products and on the same time some of the consumers don`t take this point of sustainability into consideration while purchasing. Purchasing decision is may be dependent on the background and experience of the consumers [7]. The greater number of companies has designed such process and products to save the environment because of understanding the impact of green consumption on the consumption behavior and the environment [8]. The companies have become conscious about the natural environment because they have realized that their production and consumption have direct impact on the natural environment [6]. With the increase in the environmental knowledge, consumers are willing to pay more for their safety, personal care the products having the

characteristics of environmental benefits [9]. Those consumers who considers the environmental deterioration because of their consumption pattern and tend to change their buying behavior are known as the green consumers [10]. Transformation towards sustainability has been at the central position in the research regarding global sustainability and the policy making in these years [5].

Green marketing is the phenomenon by which the products and services (having the features i.e. quality, comfort) are produced which are available at the reasonable price and don`t harm the natural environment [8]. It has become an important strategy of the business after the increased environmental awareness. The concept of global warming and climate change has boosted this concept among the public and the purchasing of green products as well [11]. Green purchase behavior is termed as the consumption of (environment friendly, recyclable and conservable) products [12]. Purchasing intention is defined as the willingness of consumer towards buying a product or service. The purchasing intention can be transformed into the green purchasing behavior buy consuming the green products on order to save the environment [9]. Green purchasing behavior is the kind of pro-environmental behavior. The nature if this behavior differs from the general buying behavior. The discussion of environmental issues and the green purchasing behavior has been the point of discussion [4]. The present research has been conducted with the objective of analyzing the consumer`s interest, will and buying behavior towards the green products.

Author	Environmental awareness	Consumer`s Interest to buy green products	Consumer`s will to buy Green Products	Consumer`s Green Purchasing Behavior	Customer Satisfaction	Consumer Choice	Price	Quality	Packaging	Durability
[2]	X		X	X	X					
[3]		X				X	X	X		
[12]				X			X	X	X	X
[6]	X			X			X	X		
[1]	X			X						
[5]	X		X	X						
[10]	X			X						
[13]	X			X						
[8]	X			X			X	X	X	
[11]				X				X		
[9]				X				X		
[7]				X						
[4]	X			X					X	

II. Research Gap

In order highlight the research gap, literature was reviewed, in relevance with the topic of present research. Tremendous literature is available on the consumer`s buying behavior but a little is about the consumer`s interest and will towards the green products. In the gravity of consideration to the results of above table, consumer`s interest, will have been investigated in very much research papers; thus these both factors are required to be investigated. Therefore, the present study, focus on the consumer`s interest to buy green products, consumer`s will to buy green products and consumer`s buying behavior towards green products.

III. Research Methodology

A. Data Collection

This cross-sectional and quantitative study was conducted in Hyderabad. Questionnaire was used as the research instrument. Data was collected from respondents at supermarkets, super stores and general stores: some of the samples were collected via email (by sending the link of Google form in email). 250 samples were distributed among the respondents; 230 were collected back and 30 questionnaires were incompletely filled thus excluded from the research.

B. Questionnaire and Measurement Scale

Questionnaire is consisted on four sections i.e. demographic characteristics, consumer`s interest towards the green products, consumer`s will to buy the green products and consumer`s buying behavior towards the green products. The first section is consisted on five characteristics i.e. gender, age, qualification, income and marital status. Second section is consisted on four items adopted from [14] and modified by the researcher. Third section is consisted of 5 items adopted form [15] and modified by the researcher. Fourth section was consisted on seven item which have been adopted from [16] and modified by the researcher. 7-point likert scale “Strongly Disagree = 1” to “Strongly Agree = 7” was used for the measurement of variables. Likert scales are designed to contain the options in fixed format for the measurement of attitudes and opinions [17].

C. Data Analysis

Data was analyzed in the statistical package for social sciences (SPSS) version 22. Reliability analysis was conducted by using cronbach`s alpha test (see table 1) from which the values of alpha was calculated to be 0.679 which indicated that the data was reliable. Alpha is calculated in order to reveal the internal consistency of data and the acceptable values are suggested ranging from 0.70 to 0.95 [18]. Descriptive Statistics (mean, standard deviation, skewness and kurtosis) of the variables was calculated. Normality (Skewness and kurtosis) of variables were only calculated to meet the assumptions of Analysis of variance (ANOVA) [19][20], Pearson correlation and multi-liner regression [21][22]; since, skewness and kurtosis are used to indicate the data as normal as suggested [23].

TABLE I. TABLE 1. RELIABILITY ANALYSIS OF THE DATA

N of Items	*Cronbach's Alpha*	*Remarks*
21	.70	Reliable

D. Developed Hypothesis

Fifteen hypothesis were developed in order to demonstrate the difference in the consumer`s interest, will and buying behavior towards the green products: the statements of null hypothesis are given as under.

1. There is no significant difference in the consumers` level of interest for green products across both genders.
2. There is no significant difference in the consumer`s will to buy green products across both genders.
3. There is no significant difference in the consumer`s buying behavior towards green products across both genders.
4. There is no significant difference in the consumers` level of interest for green products across all the age groups.
5. There is no significant difference in the consumer`s will to buy green products across all the age groups.
6. There is no significant difference in the consumer`s buying behavior towards green products across all the age groups.
7. There is no significant difference in the consumers` level of interest for green products across the different qualifications groups.
8. There is no significant difference in the consumer`s will to buy green products across the different qualifications groups.
9. There is no significant difference in the consumer`s buying behavior towards green products across the different qualifications groups.
10. There is no significant difference in the consumers` level of interest for green products across the different income groups.
11. There is no significant difference in the consumer`s will to buy green products across the different income groups.
12. There is no significant difference in the consumer`s buying behavior towards green products across the different income groups.
13. There is no significant difference in the consumers` level of interest for green products across the marital status.
14. There is no significant difference in the consumer`s will to buy green products across the marital status.
15. There is no significant difference in the consumer`s buying behavior towards green products across the marital status.

IV. RESULTS

The result is divided into four section: in first section, frequency distribution of respondents was conducted; in second section, descriptive statistics (mean, standard deviation, skewness and kurtosis) was conducted; in third section, correlation analysis was conducted and last section is contained of the regression analysis.

A. Frequency Distribution of Demographic Characteristics

The table of frequency distribution shows the different categories and the number of observations for each category [24]. The present research included only five demographic characteristics i.e. gender, age, monthly income, marital status and qualification. Among the total 200 respondents 100 were males and 100 were females. Age distribution of the respondents (table 2) shows that 100 (50%) patients belonged to the 18-26 years age group; the age group of 26-35 years was consisted of 61 (30.5%) respondents: 27 (13.5%) respondents belonged to the age group of 35-40 years: the last age group i.e. 40 years to onwards was consisted of 12 (6%) respondents.

TABLE II. FREQUENCY DISTRIBUTION OF DEMOGRAPHIC CHARACTERISTICS

Characteristic		*Frequency*	*Percent*
Gender	Male	100	50.0%
	Female	100	50.0%
Age	18-25	100	50.0%
	26-35	61	30.5%
	35-40	27	13.5%
	40 to onward	12	6.0%
Qualification	Intermediate	61	30.5%
	Bachelors	48	24.0%
	Masters	29	14.5%
	PhD	62	31.0%
Marital Status	Single	115	57.5%
	Married	71	35.5%
	Divorced	14	7.0%
Income	20000-50000	89	44.5%
	50000-80000	33	16.5%
	80000-110000	17	8.5%
	110000-above	61	30.5%

Qualification distribution of the respondents showed that 61 (30.50%) respondents were intermediate; 48 (24%) were graduates; 29 (14.5%) had the master degree and remaining 62 (31%) respondents had the PhD degree. From the distribution of marital status it was shown that 115 (57.5%) respondents were single; 71 (35.5%) respondents were married and remaining 14 (7%) respondents were divorced. Income distribution of the respondents indicated that 89 (44.5%) respondents had the income of 20000-50000; 33 (16.5%) respondents had the income of 50000-80000; 17 (8.5%) respondents had the income of 80000-110000 and remaining 61 (30.5%) respondents had the income greater than 110000.

B. Descriptive Statistics

The central tendencies i.e. mean and standard deviation, skewness and kurtosis were calculated in descriptive statistics. Skewness and kurtosis were calculated in order to check the assumption of normality.

TABLE III. DESCRIPTIVE STATISTICS OF THE VARIABLES

Variables	*Mean*	*Std. Dev.*	*Skewness*	*Kurtosis*
I cares about choosing green product	3.51	.880	-1.000	1.410

I Perceive variation in type of product.	2.98	1.309	-.266	-1.302
I understand the importance of right choice between green and non-green products.	3.51	1.288	-.536	-.873
I am willing to go out of my way to obtain green products.	3.78	1.208	-.848	-.291
I intend to go out for purchasing green products.	3.81	1.123	-.910	.120
My personal goal is to consume as much green products as possible.	3.84	1.172	-.922	.027
I will make every effort to purchase green products	3.85	1.257	-.763	-.643
I have seriously thought of buying more green products	3.75	1.147	-.817	-.190
I have a firm intention to buy green products in the future	3.73	1.207	-.738	-.558
I often buy green products.	3.4800	1.27188	-.547	-.809
I often buy products that are labeled as environmentally safe	3.6850	1.27826	-.820	-.415
I often buy products that are against animal-testing.	3.8050	1.12842	-.965	.141
I often buy products that are harmless.	3.7800	1.16118	-.768	-.268
When I consider buying a product, I will look for a certified environmentally-safe or organic stamp.	3.7600	1.13527	-.890	.111
I often buy products that support fair community trades	3.6700	1.32661	-.718	-.629
I often buy products that use recycled/ recyclable packaging	3.7650	1.15605	-.929	.174

Since, the normal values of skewness and kurtosis lie between +1 [23]; and a look at table 3 indicate that all the values of skewness and kurtosis lie in the normal range which mean the data is normally distributed.

C. Hypothesis Testing

After the data was indicated to be normally distributed the hypothesis can be tested by ANOVA. The confidence interval for ANOVA was set to be 95%. If the result of ANOVA test ($p < \alpha$), where α is called the significance level (0.05), then the null hypothesis will be rejected with probability > $(1-\alpha).100\%$ probability [20].

TABLE IV. HYPOTHESIS TEST RESULTS BY ANOVA

Type	***Hypothesis Statement***	***Sig.(two-tailed)***	***Remarks***
H_0	There is no significant difference in the consumers` level of interest for green products across both genders.	0.136	Failed to reject
H_0	There is no significant difference in the consumer`s will to buy green products across both genders.	0.794	Failed to reject
H_0	There is no significant difference in the consumer`s buying behavior towards green products across both genders.	0.806	Failed to reject
H_0	There is no significant difference in the consumers` level of interest for green products across all the age groups.	0.974	Failed to reject
H_0	There is no significant difference in the consumer`s will to buy green products across all the age groups.	0.947	Failed to reject
H_0	There is no significant difference in the consumer`s buying behavior towards green products across all the age groups.	0.568	Failed to reject
H_0	There is no significant difference in the consumers` level of interest for green products across the different qualifications groups.	0.373	Failed to reject
H_0	There is no significant difference in the consumer`s will to buy green products across the different qualifications groups.	0.411	Failed to reject
H_0	There is no significant difference in the consumer`s buying behavior towards green products across the different qualifications groups.	0.837	Failed to reject
H_0	There is no significant difference in the consumers` level of interest for green products across the different income groups.	0.769	Failed to reject
H_0	There is no significant difference in the consumer`s will to buy green products across the different income groups.	0.287	Failed to reject
H_0	There is no significant difference in the consumer`s buying behavior towards green products across the different income groups.	0.855	Failed to reject
H_0	There is no significant difference in the consumers` level of interest for green products across the marital status.	0.346	Failed to reject
H_0	There is no significant difference in the consumer`s will to buy green products across the marital status.	0.968	Failed to reject
H_0	There is no significant difference in the consumer`s buying behavior towards green products across the marital status.	0.270	Failed to reject

A look at the table 4 indicate that all the hypothesis were accepted/failed to reject because the p-value of ANOVA for all the enlisted hypothesis was > 0.05. All the hypothesis were developed in the consideration demographic characteristics (i.e. age, gender, qualification, income and marital status) and their rejection indicates that there is no difference in the consumer`s interest, will and buying behavior towards the green products. It can also be concluded from the results of ANOVA test that there is no impact of demographic characteristics on the consumer`s interest, will and the buying behavior towards the green products.

The demographic characteristics i.e. age, qualification and income were correlated with the consumer`s interest and the buying behavior towards the green products as shown in the table 5. During the analysis, confidence interval was set to be 95%. The value of coefficient of correlation (r) always lies between –1 and +1. The closer the value of r to +1 the stronger the direct relationship between variables; if value of coefficient of correlation is closer to -1 inidctes the stronger negative relationship of variables. Value of r closer to 0 demonstrates no linear relationship, there could be a nonlinear relationship between the variables though [21]. In table 5 none of the values of r is significant (<0.05) which clearly indicates no significant relationship between demographic characteristics and the

consumer`s interest, will and the buying behavior towards the green products.

TABLE V. RESULTS OF CORRELATION ANALYSIS AMONG CONSTRUCTS AND DEMOGRAPHIC CHARACTERISTICS

Demographic Variable	*Description of Values*	*Consumers` Level of Interest For Green Products*	*Consumer`s Will To Buy Green Products*	*Consumer`s Buying Behavior towards Green Products*
Age	Pearson Correlation	.078	.047	.064
	Sig. (2-tailed)	.274	.510	.366
Qualification	Pearson Correlation	.049	.018	.089
	Sig. (2-tailed)	.489	.797	.213
Income	Pearson Correlation	.009	.025	.088
	Sig. (2-tailed)	.896	.725	.216

Correlation analysis was also conducted among the consumer`s interest, will and buying behavior towards the green products in table 6. In contrast to the table 5, all the relationships in the table 6 are significant since, the significance values of all the relationship is < 0.05.

TABLE VI. RESULTS OF CORRELATION ANALYSIS OF VARIOUS CONSTRUCTS WITH ONE ANOTHER

Construct	*Description of Values*	*CLIFGP*	*CWTBGP*	*CBBTGP*
Consumers` Level of Interest For Green Products	Pearson Correlation	1		
	Sig. (2-tailed)			
Consumer`s Will To Buy Green Products	Pearson Correlation	.146*	1	
	Sig. (2-tailed)	.038		
Consumer`s Buying Behavior towards Green Products	Pearson Correlation	.145*	.339**	1
	Sig. (2-tailed)	.040	.000	

The results of analysis indicates the weak significant and positive relationship among the consumer`s interest and will (r = 0.146) towards the green products with the statistical significance of the 0.038. The coefficient of correlation was calculated to be 0.145 (sig. 0.040) for consumers` level of interest towards the green products and consumers` buying behavior towards the green products. The value of r for the relationship of consumers` will toward buying the green products and consumers` buying behavior towards the green products was calculated to be 0.339 with the statistical significance of 0.000.

D. Regression Analysis

Multi-liner regression analysis was conducted with two independent variables (i.e. Consumers` level of interest towards the green products and consumers` will for buying the green products) and one dependent variable (i.e. Consumers` buying behavior towards the green products). The coefficient of Regression 'R' = .353 or 35.3% which indicates that relationship between dependent and independent variables is positive. The coefficient of determination 'R2' = .124 indicates that independent variables explain 12.4% of the variation in dependent variable (see table 7).

TABLE VII. MODEL SUMMARY OF THE REGRESSION ANALYSIS

Model	*R*	*R Square*	*Adjusted R Square*	*Std. Error of the Estimate*
1	.353[a]	.124	.116	.68851

The value of F-test 14.001 is counted as significant because the significance level is = .000 (< 0.05). The significant values indicates the regression model as valid and relationship between dependent and independent variable is statistically significant (see table 8).

TABLE VIII. RESULTS OF ANOVA TEST FROM REGRESSION ANALYSIS

Model		*Sum of Squares*	*df*	*Mean Square*	*F*	*Sig.*
1	Regression	13.274	2	6.637	14.001	.000[b]
	Residual	93.387	197	.474		
	Total	106.661	199			

The coefficients are also counted as significant (see table 9) because the level of significance for them is <0.05 which can be seen in the table 9.

TABLE IX. COEFFICIENTS FROM THE REGRESSION ANALYSIS

Model		*Unstandardized Coefficients*		*Standardized Coefficients*	*t*	*Sig.*
		B	*Std. Error*	*Beta*		
1	(Constant)	1.879	.368		5.103	.000
	Consumers` Level of Interest For Green Products	.106	.073	.427	4.446	.000
	Consumer`s Will To Buy Green Products	.386	.080	.325	4.823	.000

V. DISCUSSION

In Pakistan, many factors have been report to have an impact on the consumers` buying behavior i.e. place, discounts, and cash rebates [3]. Another researcher indicated no relationship of demographic factors purchasing behavior of consumers towards green products [2]. Correlation analysis of the present research also indicates the same results that the demographic characteristics (age, qualification and income) have no statistically significant relationship with the consumers` level of interest, will and buying behavior towards the green product. One of the researcher reported that consumers` level of satisfaction towards the products affects the consumers` buying behavior [2]. While purchasing, the consumers` buying behavior have notable influence on the consumers` purchasing decision towards the green products [12][6]. Similarly in the present research, consumers` will to

buy the green products have a significant positive correlation (r = 0.339 with sig. 0.000) with the consumers` buying behavior towards the green products. It has been reported that the consumers between the age of 18-45 years who were postgraduates had the green attitude towards the environment [6]. The results of present study contradict with the reported results because the across all the age groups no difference was found in consumers` level of interest, consumers` will and consumers` behavior towards the green products. One of researchers reported that due to a little or no awareness regarding the green products and their benefits, consumers don`t know that they should buy the green products in order to save the environment; thus the companies should organize the seminars and workshop to provide the awareness to the consumers [4]. It has also been reported that one`s knowledge about the problem affects his/her decision making process [13]. The green products are not being consumed at the greater level because of higher prices as compared to non-green products [7]. In this regard government should decrease the tax and subsidies especially for green business so that the investors can be encouraged to invest in the ecological products; this is an effective way to promote the green marking the large scale to protect the natural environment [7]. In order to encourage the companies for green production, the government can also start training and organize workshops for them [3].

CONCLUSION AND SUGGESTIONS

It was indicated that consumers` buying behavior towards the green products was found to be the same across age, qualification and income; which indicates that there is little or no awareness among the consumers regarding the green products. Positive association between the consumer`s level of interest, consumers` will and the consumers` buying behavior towards the green products was found. Which explains that if the consumers are provided the knowledge about the green products, their benefits to humans and the environment; their level of interest can be attracted and if the interest is attracted then they can be influenced by their interest towards the purchasing of green products. This can be a good suggestion for the green marketers to provide the awareness regarding the green attitude, green products (about their features i.e. energy saving) and green purchasing so that the planet can be save with mutual efforts and benefits [13].

LIMITAIONS AND FUTURE WORK

The major and first limitation of this research is its sample size (i.e. 200) and it was only conducted Hyderabad. Few factors were included in this research; the boundaries of this research can be widened by considering factors i.e. price, durability, environmental awareness etc. The contribution of this research cannot be ignored since it has highlighted the relationship among the consumers` level of interest, consumers` will and consumers buying behavior towards the green products.

CONFLICT OF INTEREST

There is no conflict of interests among the authors of this research work.

REFERENCES

[1] H. R. da S. Tamashiro, J. A. G. da Silveira, E. M. Merlo, and C. R. Acevedo, "Structural Equation Modeling Applied to a Study on the Background of Green Buying Behaviors," PARIPEX - Indian J. Res., vol. 3, no. September, pp. 1–8, 2014.

[2] U. Makhdoomi and U. Nazir, "Consumers Purchase Behavior towards Green Products," in Marketing in Emerging Economies, Manakin Press Pvt Ltd, 2016.

[3] M. Danish, S. Ali, M. A. Ahmad, and H. Zahid, "The influencing factors on choice behavior regarding green electronic products: Based on the green perceived value model," Economies, vol. 7, no. 4, 2019, doi: 10.3390/economies7040099.

[4] R. Risqiani, "Antecedents of Consumer Buying Behavior Towards on Environmentally Friendly Products," Bus. Entrep. Rev., vol. 17, no. 2, pp. 145–164, 2017, doi: 10.25105/ber.v17i1.5196.

[5] J. Hojnik, M. Ruzzier, and M. K. Ruzzier, "Transition towards sustainability: Adoption of eco-products among consumers," Sustain., vol. 11, no. 16, 2019, doi: 10.3390/su11164308.

[6] C. Gan, H. Y. Wee, L. Ozanne, and T.-H. Kao, "Consumers ' purchasing behavior towards green products in New Zealand," Innov. Mark., vol. 4, no. 1, pp. 93–102, 2008.

[7] W. Atthirawong and W. Panprung, "A STUDY ON THE CONSUMERS â€TM BUYING BEHAVIOR TOWARDS," no. September, pp. 8–13, 2017.

[8] Arora and H. S. Chahal, "Exploring factors affecting consumer's behaviour towards green products and green marketing - A study of Punjab," J. Agroecol. Nat. Resour. Manag., vol. 4, no. 4, pp. 356–366, 2017.

[9] Y. C. Yang, "Consumer Behavior towards Green Products," J. Econ. Bus. Manag., vol. 5, no. 4, pp. 160–167, 2017, doi: 10.18178/joebm.2017.5.4.505.

[10] M. N. Mohd Noor, M. S. Masuod, A. M. Abu Said, I. F. Kamaruzaman, and M. A. Mustafa, "Understanding consumers and green product purchase decision in Malaysia: A structural equation modeling - partial least square (SEM-PLS) approach," Asian Soc. Sci., vol. 12, no. 9, pp. 51–64, 2016, doi: 10.5539/ass.v12n9p51.

[11] M. K. Durgamani and K. Abirami, "A study on consumers ' buying behaviour towards selected green products in kumbakonam .," vol. 119, no. 18, pp. 3177–3193, 2018.

[12] M. A. Collins, "Consumer Behavior towards Green Products: An Exploratory Study," Int. J. Manag. Bus. Strateg., vol. 3, no. 1, pp. 160–167, 2014, doi: 10.18178/joebm.2017.5.4.505.

[13] Y. Hassan, "Understanding Consumer Decision Making Towards Green Electronic Products," South East Asia J. Contemp. Business, Econ. Law, vol. 2, no. 1, pp. 27–33, 2013.

[14] Beharrell and T. J. Denison, "Involvement in a routine food shopping context," Br. Food J., vol. 97, no. 4, pp. 24–29, 1995.

[15] F. Liñán and Y. Chen, "Development and Cross-Cultural Application of a Specific Instrument to Measure Entrepreneurial Intentions," Entrep. theory Pract., vol. 33, no. 3, pp. 593–617, 2009.

[16] K. Lee, "Gender differences in Hong Kong adolescent consumers' green purchasing behavior," J. Consum. Mark., vol. 26, no. 2, pp. 87–96, 2009.

[17] L. Rensis, "A technique for the measurement of attitudes," Arch. Psychol., vol. 22, no. 140, p. 55, 1932.

[18] M. Tavakol and R. Dennick, "Making sense of Cronbach ' s alpha," Int. J. Med. Educ. 2011, vol. 2, pp. 53–55, 2011, doi: 10.5116/ijme.4dfb.8dfd.

[19] M. J. Blanca, R. Alarcón, J. Arnau, R. Bono, and R. Bendayan, "Non-normal data : Is ANOVA still a valid option ?," Psicothema, vol. 29, no. 4, pp. 552–557, 2017, doi: 10.7334/psicothema2016.383.

[20] E. Ostertagova and O. Ostertag, "Methodology and Application of One-way ANOVA," Am. J. Mech. Eng., vol. 1, no. 7, pp. 256–261, 2013, doi: 10.12691/ajme-1-7-21.

[21] V. Bewick, L. Cheek, and J. Ball, "Statistics review 7 : Correlation and regression," Citical Care 7, 2003. .

[22] R. J. Casson and L. Dm, "Review Understanding and checking the assumptions of linear regression : a primer for medical researchers," Clin.

Experiment. Ophthalmol., vol. 42, no. 6, pp. 590–596, 2014, doi: 10.1111/ceo.12358.

[23] H. Kim, "Statistical notes for clinical researchers : assessing normal distribution (2) using skewness and kurtosis," 2013.

[24] S. ManiKandan, "Frequency distribution," J. Pharmacol. Pharmacother., vol. 2, no. 1, pp. 54–56, 2011.

IJEW 国际工程期刊 International Journal of Engineering Works انجینئرنگ کاموں کا بین الاقوامی جرنل

International Journal of Engineering Works
ISSN-p: 2521-2419
ISSN-e: 2409-2770
Vol. 7, Issue 03, PP. 168-172, March 2020
https://www.ijew.io/
https://doi.org/10.34259/ijew.20.703168172

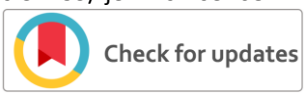

Comparing the Properties of Virgin & Aged Bitumen by the addition of Rejuvenators

Sameer Ahmed Mufti[1], Qaiser Iqbal[2], Fazli Kareem[3], Muhammad Babar Ali Rabbani[4], Muhammad Alam[5]
[1234]Department of Civil Engineering, Sarhad University of Science & Information Technology, Peshawar, Pakistan
[5]Department of Civil Engineering, Abasyn University Peshawar Campus
sam.mufti@gmail.com[1], qi.civil@suit.edu.pk[2], engr_fazli@yahoo.com[3], babaralirabbani@yahoo.com[4], emalam82@gmail.com[5]
Received: 20 February, Revised: 26 February, Accepted: 04 March

***Abstract*—** Environmental and economic demands prompt to transportation agencies to increase in the use of Reclaimed Asphalt Pavement (RAP) in asphalt pavements. The use of RAP in pavements often require a rejuvenator to reduce the cracking. Estimating a best rejuvenator dosage is crucial to increase its advantages. Large quantity of waste oils from automobiles and restaurants can inflict adverse impact if it is not properly disposed. Recycling of these waste oils can be a suitable option, to reduce the use of natural resources and economic benefits. In this study, three rejuvenators were explored such as Waste Engine Oil (WEO), Waste Vegetable Oil (WVO) and Waste Brown Grease (WBG) with dosages of 5%, 10% and 15%. Physical testing (i.e. penetration, softening point, flash & fire point and ductility) were conducted in the lab on virgin and RAP binder with rejuvenators. WEO and WVO helps in softening when mixed with RAP binder. According to the results, both WEO and WVO can improve the properties of the RAP binder but WBG gives a little bit improvement.

***Keywords*—** reclaimed asphalt pavement, rejuvenators, physical testing.

I. Introduction

An Increase in the risk of crack formation is due to exposure to different temperatures, asphalt binders shift from ductile to brittle behavior [6]. This is even more damaging with reclaimed asphalt pavement (RAP) which is easily susceptible to cracking than virgin binders [8]. Reduction of brittleness, viscosity and stiffness of RAP binders can be done by adding rejuvenators that are available from natural resources [14]. Due to aging in asphalt, cracking resistance expected to have the worst impact on the asphalt because RAP becomes stiffer than virgin asphalt. The addition of rejuvenators helps in improving the mechanical properties of RAP [8]. The quality and effectiveness of rejuvenators can be compared with reference values of the virgin binders by comparing the standard tests such as softening point and penetration of the rejuvenator-aged bitumen [11]. In Pakistan, a large number of used engine oils from various sources are disposed into the rivers, lakes and Arabian Sea which not only contaminate water but are also harmful to marine life [12]. Approximately, one gallon of waste engine oil would pollute one million gallons of water [10]. From crude oil and derivatives, engine oils are prepared by the mixing process of other additives to gain certain properties. Essentially, engine oil is used to lubricate the engine parts. Waste Engine Oil (WEO) is capable of recycling RAP, protecting the environment, saving and reducing the resources as well as the cost of the project which can be signed for the road maintenance [13]. In order to minimize the use of bitumen in the binder content, the use of WEO has been studied with different compositions and resulted in promising performance by using the rejuvenators [9]. Due to the loss of high oil contents such as saturates aromatics resins and asphaltenes the process of asphalt aging started. So to reverse the asphalt aging process asphalt recycling is done in which rejuvenators are introduced to restore the properties of asphalt. As the increase in the dosage of WEO in aged asphalt, resulted in an increase in the ductility and decrease in the viscosity which has important significance in road maintenance [13]. Exposure to atmosphere asphalt aging takes place due to weathering and oxidation, which leads to cracking such as thermal and fatigue. Rejuvenating the aged asphalt by using Waste Cooking Oil (WCO) can have good results in enhancing the properties of RAP [7].

A. *Problem Statement:*

Aging of asphalt starts after the completion of its useful life. But after that, it is considered a worthless material which is a wasted resource. Loss of many essential components due to subjection of HMA to traffic and environmental conditions, stiffness occurs and which resulted in rutting and stripping of asphaltic roads and then which further leads to aging of asphalt. To enhance the properties of RAP and to recycle it, rejuvenation is done

B. *Objectives:*

Several rejuvenators such as WEO, WVO and WBG have been introduced in different proportions of 5%, 10% and 15% to evaluate and compared the properties of RAP binder.

II. METHODOLOGY

Extraction of bitumen is done according to [2] by using centrifuge method. Extraction bitumen was then collected and was compared with the properties of virgin bitumen as well rejuvenators were added in aged bitumen. Following are the physical tests performed on the samples.

A. Penetration Test:

Penetration test shows the grading index of asphalt. According to [5] the sample is kept in water bath at 25 °C temperature and test is done on penetrometer having a needle to penetrate in the sample.

Figure 1 Penetrometer

B. Softening Point Test:

According [4] asphalt's high temperature stability is reflect by softening point test in which two steel balls are placed on disk containing bitumen in it. It is an average temperature at which softening of bitumen take place and steel ball touches the surface.

Figure 2. Softening Point test

C. Ductility Test:

Elasticity of bitumen is measured by ductility test. This test is used to measure the stretching length of bitumen sample under standard testing condition before breaking (50mm/min stretching speed at 25 °C) according to [1].

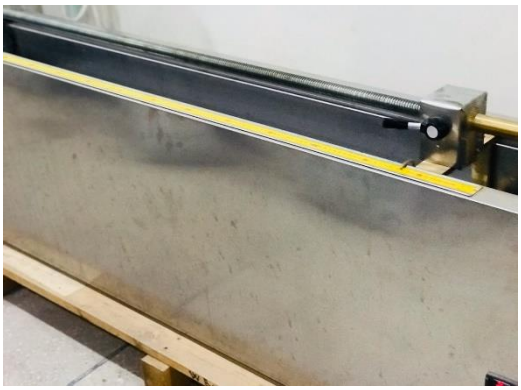

Figure 3. Ductility test

D. Flash and Fire Point Test:

According to [3] safety of asphalt can be measured by one of the test called flash and fire point test in which sample is heated and test flame is passed across the centre of the test cup. Test result are recorded when the sample at certain temperature distinct flash in the test cup.

Figure 4. Flash & Fire Point test

III. RESULTS

Table 1 shows the overall results of properites of rejuvenators in which it includes different physical testings. In which the values of penetration and Duciltiy of virgin and aged bitumen with different rejuvenators increases with the increase in the percentage of rejuvenators while softening point and flash and fire point test results shows the decrease in the values as the percentage increases.

Table 1. Physical Testing Results of Virgin and Aged Bitumen with Rejuvenators

Properties	Sample Type									
	Virgin	Aged Bitumen	WEO + Aged Bitumen			WVO + Aged Bitumen			WBG + Aged Bitumen		
			5%	10%	15%	5%	10%	15%	5%	10%	15%
Penetration (mm) @ 25˚C	64	33	46	57	62	44	56	65	41	49	54
Softening point, °C	55	59	64	61	57	68	64	56	62	59	56
Flash point, °C	305	277	272	269	266	288	270	261	256	251	239
Fire point, °C	312	282	280	278	273	298	279	272	265	260	248
Ductility (25°C, 50mm/min)	103	21	31	44	53	35	49	61	25	32	36

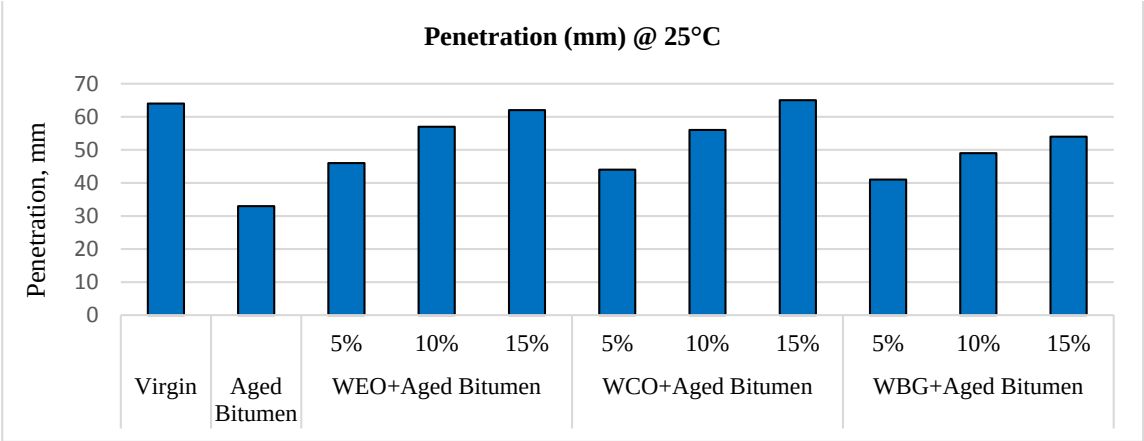

Figure 5. Graphs showing Penetration Test Results

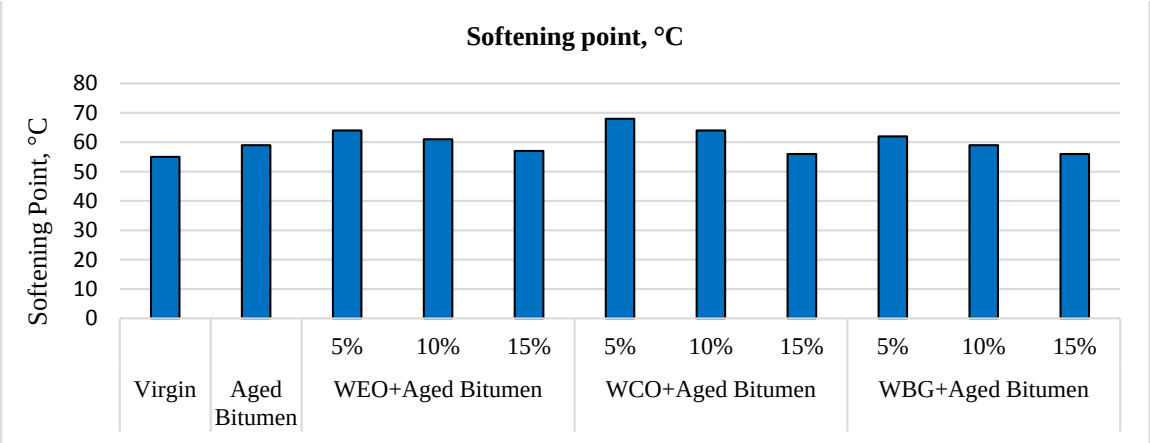

Figure 6. Graphs showing Softening Test Results

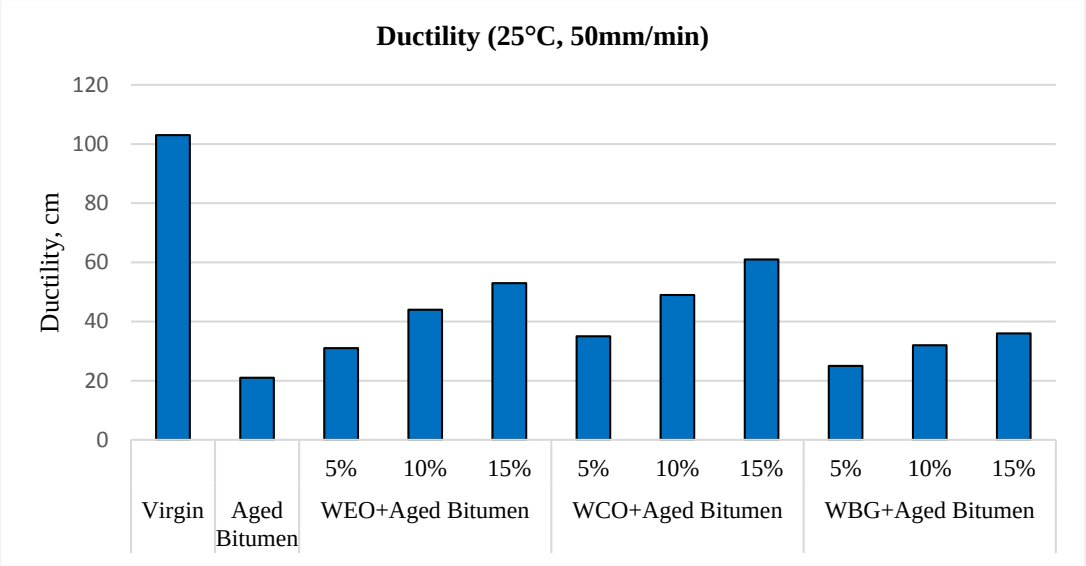

Figure 7. Graphs showing Ductility Test Results

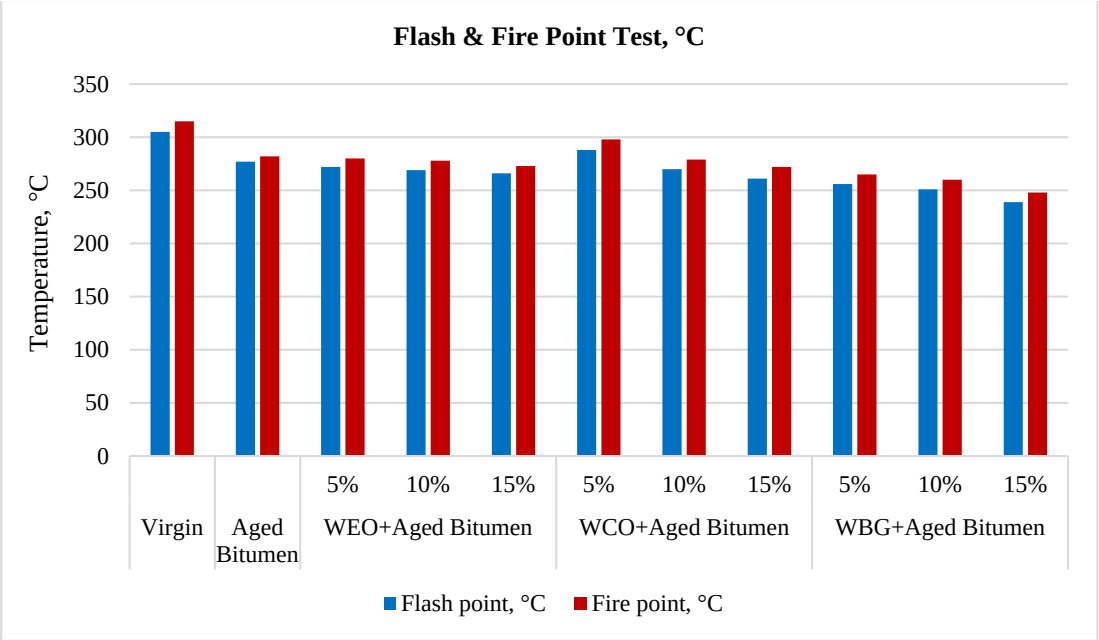

Figure 8. Graphs showing Flash & Fire Point Test Results

CONFLICT OF INTEREST

The contents of this study are free from plagiarism and therefore the study is original and is not copied from anywhere. Previous work of original authors has also been referenced.

CONCUSLION

The effects of WVO, WEO and WBG produced good effects to the binder. The values of penetration and ductility of rejuvenated asphalt increases as in the increase of dosages while the softening point and flash & fire point temperature values decreases.

REFERENCES

[1] "ASTM D 113-99, Standard Test Method for Ductility of Bituminous Materials."

[2] "ASTM D 2172 - 95, Standard Test Methods for Quantitative Extraction of Bitumen From Bituminous Paving MIxtures."

[3] "ASTM D 3143 - 92, Standard Test Method for Flash and Fire Points by Cleveland Open Cup."

[4] "ASTM D 36 - 95, Standard Test Method for Softening Point of Bitumen (RIng and Ball Appratus)."

[5] ASTM. "D5-97 Standard test method for penetration of bituminous materials." 1998 Annual Book of ASTM Standards, American Society for Testing and Materials, Philadelphia (1998): 19103-1187.

[6] "Baek, S.-H., Hong, J.-P., Kim, S.U., Choi, J.-S., Kim, K.-W., 2011. Evaluation of fracture toughness of semirigid asphalt concretes at low temperatures. Transp. Res. Rec."

[7] "Bailey, H. K., and S. E. Zoorob. "The use of vegetable oil as a rejuvenator for asphalt mixtures." Eurasphalt & Eurobitume Congress, 5th, 2012, Istanbul, Turkey. No. A5EE-161. 2012."

[8] "Cavalli, M.C., Zaumanis, M., Mazza, E., Partl, M.N., Poulikakos, L.D., 2018. Effect of ageing on the mechanical and chemical properties of binder from RAP treated with bio-based rejuvenators. Compos. B Eng. 141, 174e181."

[9] "Fernandes, Sara RM, Hugo MRD Silva, and Joel RM Oliveira. "Developing enhanced modified bitumens with waste engine oil products combined with polymers." Construction and Building Materials 160 (2018): 714-724."

[10] "J. L. A. Filho, L. G. M. Moura, and A. C. S. Ramos, "Liquid-liquid extraction and adsorption on solid surfaces applied to used lubricant oils recovery," Brazilian Journal of Chemical Engineering, vol. 27, no. 4, pp. 687–697, 2010."

[11] "Mangiafico, S., Sauz_eat, C., Benedetto, H.Di, Pouget, S., Olard, F., 2015. Influence of a recycling agent of vegetable origin on complex modulus and fatigue performances of bituminous mixtures produced with Reclaimed Asphalt Pavement, 629, 1-14."

[12] Shakirullah, Mohammad, et al. "Shakirullah, Mohammad, et al. "Environmentally friendly recovery and characterization of oil from used engine lubricants." Journal of the Chinese Chemical Society 53.2 (2006): 335-342."

[13] Wang, Fuyu, et al. "Effect of waste engine oil on asphalt reclaimed properties." AIP Conference Proceedings. Vol. 1973. No. 1. AIP Publishing, 2018."

[14] "Zhu, H., Xu, G., Gong, M., Yang, J., 2017. Recycling long-term-aged asphalts using bio-binder/plasticizer-based rejuvenator. Construct. Build. Mater. 147, 117-129."

International Journal of Engineering Works
ISSN-p: 2521-2419
ISSN-e: 2409-2770
Vol. 7, Issue 03, PP. 173-177, March 2020
https://www.ijew.io/
https://doi.org/10.34259/ijew.20.703173177

Significance of Power Quality in Power Systems

Muhammad Aamir
Department of Electrical Engineering
University of Engineering and Technology Peshawar
amirktk5593@gmail.com
Received: 19 January, Revised: 24 February, Accepted: 06 March

***Abstract*—** In this paper a review on power quality is discussed. Power quality is becoming a significant issue because of many reasons; few of these reasons are many instruments that are gaining familiarity in use to enhance the performance of energy system like advance power electronics and drivers of adjustable-speed motor. But the problem of using these instruments is that they enhance the level of harmonic components in distribution network.The control dependent devices and loads that relay on the microprocessor and microcontroller are most prone to problem of quality issue. Due to distortion in the system of energy there is severe effect on the interconnected networks that are common today. The reason behind it is the failure of an entire component. There is increasing growth of problems of voltages as voltage harmonics, over voltage, under voltage, etc. are causing awareness of issues in the power quality. So, the need of both better and high quality of power is increasing extremely among end users. Considering different cases any suitable option can be selected for power quality improvement.

***Keywords*—** Power Quality, Power Sytem

I. INTRODUCTION

The quality of power defined by international electrical and electronic engineering as sensitive load should be attached to a powering system such that the system is grounded and the supply power to the load is suitable for operation. Quality of power and reliability of power source are two aspects of any power system [1]. Earlier power quality was not considered is the main motto of the power system, continuity of electric supply was considered is the main concern. But nowadays the power system has changed to very complex networks. Nowadays the need of the time is it requires both the permanency of power supply and the power source quality.

II. POWER QUALITY

An ideal voltage or current signal is a signal with constant varying amplitude and constant frequency so that its shape is purely like sinusoidal signal. Current and voltage quality is defined as the load voltage or current must have the same waveform as the source. Any distortion in load voltage or current will be considered is the deviation from the source voltage or current is low power quality signal. Because of this deviation a device connected may produce less fruitful results than expected. The different meaning and importance of power quality is that the design of a device should be noise free in the grounding system and no voltage alteration should occur. However, the possibility of using the available power for processing of different types of loads is considered by the end users dependent on power quality. The issue of power quality can severely affect the distribution network system. Thus, the motive of our work is to enhance the power quality.
Quality of Power plays in important role in power system. Low power quality effect consumer in many ways [2], it causes distortion, electrical interruption in power appliances, decaying life of industrial equipment's, and more seriously it can be detrimental to life of human being. So power quality should be maintained in a best available limit to minimize loss and to keep electrical devices safe from contingencies and proper operation of electrical load.

Power quality issues have to be minimized using advance electronic based custom power devices [3]. There are many custom power devices which plays an important starring role for solving any desired solution for different problem in power quality. Dynamic voltage restorer (DVR) is a compensation device among different compensating devices, which can be used for unbalance load voltages, and voltage sage and swell problems [4]. DVR is only limited to voltage related problems. Power system is a complex network and any contingency in such a complex system is also complex so we need a custom device that can deal with different issues. One of these custom devices is Unified power quality conditioner (UPQC) [5]. Hirofumi Akagi designed this custom power device in 1995. This custom device can help us solve problems related to voltage sag, swell, current imbalance, reactive power, total harmonic distortion and flickering. UPQC is still in research and is very promising in solution to our problems.

Power quality as it is deal in most important aspect today was not given that much importance in past [1]. But it was not left as it has no importance. Solutions were designed accordingly to the problems that were persistent at that time. Passive elements were used by designer as solution which sometime work, if not then they had to be physically re-

operated manually. After the invention of semiconductor devices in 1932 the control of electrical power system became easy [6]. Large control systems were converted into portable control systems. For high electrical equipment's control system using semiconductor were designed, which were processing more fast, accurately and were more economical than previous system. So adaptation of these semiconductor devises introduces new problems and again using these semiconductor new solutions were presented.

Nowadays electrical devices made of semiconductor devices are very sensitive to many contingencies. Power electronic converters are non-linear devices, which enhances the reactive power capability of transmission network by introducing load current and voltage [2]. This load current and voltage introduces harmonic to the system, causing loss of power, abnormality in current and voltage waveform from ideal sine wave to distorted sine wave, and flickering. Overall power quality is reduced by these power electronic converters. Therefore compensation is required to avoid these contingencies and to recover the quality of power according to the standard set by IEEE.

III. Need of Better Power Quality

For every problem there is a solution. Power quality is becoming a significant issue because of many reasons; few of these reasons are discussed as follows

- There are many instruments that are gaining familiarity in use to enhance the performance of energy system like shunt capacitors and drivers of adjustable-speed motor. But the problem of using these instruments is that they enhance the level of harmonic components in distribution network.
- The control dependent devices and loads that relay on the microprocessor and microcontroller are most prone to problem of quality issue.
- Due to distortion in the system of energy there is severe effect on the interconnected networks that are common today. The reason behind it is the failure of an entire component.
- There is increasing growth of problems of voltages as over voltage, under voltage, voltage drop etc. is causing awareness of issues in the power quality. So, the need of both better and high quality of power is increasing extremely among end users.

IV. Motivation

For mitigating the issues regarding currents and voltages harmonics different custom devices has been introduced. Among these devices UPQC is preferred because of its hybrid APF. The series APF is used to compensate for the load voltages; it induces compensated voltage at the PCC. Where is shunt active power filtering induces current at PCC, eliminate distortion in current waveform, compensation of the load reactive power and the maintaining constant voltage of DC link capacitor. This gives me the motivation to investigate the total harmonic distortion in distributed power supply and improve it by using UPQC.

V. Impact of Power Quality on Load

Power electronic based devices have an advantage of cost reduction and disadvantage of sensitivity to reduction in power quality. Its impact is on both, the high power industrial load and on low power domestic load. Most of the loads are quite sensitive to the deviation in voltage or current waveform. Most common problems in power quality for both industrial and domestic load are low power factor, distortion and unbalance in supply voltage, DC components in load voltages and current (DC OFFSET) [1-3].

Power factor is because of increase in current in power appliances resulting in drawing more current from the source causing power loss and drop in line voltages [7]. Harmonics in current and voltage causes distortion in waveform and power losses and hence reduction in power quality. Current and voltage Harmonics have negative effect on protective devices e.g. tripping of relays and melting of fuses. Current harmonics especially of third order have very much negative impact of on transformer and neutral conductor. Third order current harmonic have interference effect on telecommunication signal. So as a protective step neutral conductor with larger cross sectional area is used in commercial places [8]. The DC component of current in transformer can cause disturbance in flux, resulting in excursion of flux which results in saturation of magnetic core of transformer. Also the return path for the dc current through earth sometime introduces corrosion to the metallic structure buried in earth [9]. Power quality also has impact on economic losses on both utilities and customer's side. Power quality impact on utility side is that it results in mal-operation of protective devices, metering devices and overheating of transmission cables. The assessed power losses in Pakistan are 30% of the total production [10].

VI. Custom Devices for Mitgation of Power Quality Problems

N.G. Hingorani in 1995 introduced custom power (CP) in [4]. Custom power device is a combination of different power electronic elements or a tool box that can be connected with transmission network to help in improving power quality of distribution system. The entities of CP are gate turn off Thyristors and insulated gate bipolar transistors (IGBTs) combined with microprocessor and different circuit elements.

Voltage sag is because of short circuiting. Excessiveness in voltage sag can be determined by fault time and magnitude of supplied current. Fault clearing time can be reduced consuming CLF (current limiting fuses) [5] and solid state circuit breaker [6]. A current limiting fuse has to be replaced after melting. CLF can remove the flaw in 1/2 cycle, where is solid state circuit breaker remove the flaw in one and 1/2 cycle but is a multipurpose device.

Quality of power is judged by the difference between the qualities of power supplied to the quality of power required for the safe operation of electrical load. So keeping this point in mind power quality problems can be resolved into main three ways

- Power supply disturbances should be reduced

- The immunity to disturbances at the load equipment should be reduced
- For sensitive load there must be some control unit to mitigate power quality problems between load side and source.

Considering different cases any suitable option can be selected. This proposed work focus on the third option.

The immunity to disturbances in load side can be mitigated using proper control and correcting devices, so that the load does not extract excessive current and excessive apparent power out of the supply. This is applicable to new devices, for old devices we cannot use the new control system [11]. Power quality problems are not new to this system but are existed from the time when voltages were transferred through feeders for the first time for long distances. Control system at that time were passive circuits at that power electronic were not invented [12]. They were named as conventional facilitation technique. The passive circuits were designed using inductors and capacitors. These passive circuits are currently utilized in transmission and distribution circuits for harmonics, reactive power, and voltage compensation, but special care should be taken while selecting these tuned circuits as they may add additional problems to the system. Passive circuits at high power level make a system bulky and prone to many problems.

For correction of power factor synchronous condensers, Capacitors bank, and SVCs are applied to distribution network [13]. Response of synchronous condenser and capacitor banks are slow. SVCs may add additional harmonics which need filtration. The advances in power electronics like digital signal processing (DSP) make this possible to achieve fast correcting response. These advance power electronic devices make this possible to achieve maximum improvement in quality of power and reducing the essential problems. These advance electronic power devices were named as custom power devices (CPD) [3].

CPDs can be categorized into two main groups, namely compensating devices and network-reconfiguring devices. The network-reconfiguring type has (SSCL) Solid State Current Limiter, (SSB) Solid State Breaker, (SSTS) Solid State Transfer Switch. Compensating type has (DSTATCOM) Distribution Static Compensator, (DVR) Dynamic Voltage Restorer, and (UPQC) Unified Power Quality Conditioner.

The compensating type controllers are used for compensation of reactive control, currents harmonics, voltage problems, power factor correction and THD. DSTATCOM can be utilized for the adjustment of Reactive control and current harmonic [14]. Voltage related problems can be compensated using Dynamic Voltage Restorer. UPQC is used for the compensation for both current and voltage. The proposed work relies on UPQC; this device is composed of both shunt and series power filtering. The reasons behind harmonic distortion describe in this paper are: extension in the network of power system, commonly used electrical devices made of advance power electronic and excessive use of non-linear loads. This paper also significantly improves the decrease in harmonics by employing D-STATCOM and DG. The measurements for total harmonic distortions are determined and their result for all buses is then presented. The result presented by author verify that DG and D-STATCOM optimal for decrease in harmonics. The efficiency in the voltage shape of a network, reduction in the system losses, and reduction in the disturbances of total harmonics are the results obtained by the use of D-STATCOM and DG. So THD is reduced to 6% [15]. In this paper author uses FACT device for mitigation of single line harmonics and three phase harmonics. The device used is static synchronous series compensator (SSSC). It also helps in mitigating noise from system voltages and currents. By the use of SSSC the THD has reduced to 6% from 16.6% [16].

For enhancing the decontrolled complex system is examined using genetic algorithm. For the assessment purposes two kinds of FACTS procedures are implemented, first TCSC (Thyristors-Controlled-Series-Capacitor) and second SVC (Static-VAR-Compensator), for the consistency of voltage, decrease in the line losses and minimization of congestion. The develop control algorithm is analyzed and applied to IEEE-30 bus transmission system. The study of transaction for bilateral and multilateral systems and issues like line outage and loading of uniform line has also been done. In this paper enhanced power system consistency and loss of power mitigation by introducing TCPS (Thyristors-Controlled Phase Shifter) is examined. The phase shifter distribution factor is the source of control of losses of energy [17]. In this paper clarified optimization technique by placing different Flexible alternating transmission system device on bus system of IEEE-57 is used as a base for propose technique. The propose system is tested on two conditions (1) normal condition and (2) line contingency condition in which FACTS devices were used. In this paper a Hybrid Fish method was used to manage complexity of the system that is called Bee Swarm Optimization technique. There are two basic methods of this technique: (1) Fish School Search (FSS) technique and (2) Artificial Bee Colony (ABC) technique. IEEE-30 bus transmission method was used to check the proposed technique, the result proved to be effective for the reduction of complexity [18].

To analyze bilateral and multilateral agreement there are two types of market models. For the management of congestion, researcher utilizes the association of the FACTS devices with transmission lines. There are two variable Reactance's that were modeled using FACT devices, TCSC and SVC. TCSC has the explanation of two situations or case. The settlement of TCSC for the congested line in the inductive mode is in the first case and settlement for slightly loaded buses in capacitive mode is the second case. By using the trial and error process normal settlement of TCSCs are applied. In this paper the researcher give detailed study of Genetic Algorithm based technique for the reduction of congestion by using specific settlement of FACTS device with transmission line [19]. In this paper author practically use a technique to mitigate the congestion. The technique used is called TCSC in series that is associated with transmission line for attaining the level of congestion called is Line Utilization Factor (LUF).

For controlling the active power flow and management for congestion an uncertain logic controller is utilized. Modified bus system of IEEE-14 is considered for analysis of suggested method. After that, comparison is done between the results of both uncertain logic and sensitivity process. So, the concluding studies showed that for the management of congestion process the most applicable method is uncertain method [20].

In this paper the author suggested a method for the mitigation of transmission line congestion that is called Particle Swarm Optimization (PSO). The settlement of proposed method of Unified Power Flow Controller (UPFC) is normally designed for specific size. For the special requirement of transmission line UPFC is personalized solutions. A test system of 5-bus is considered to be examined using UPFC method. Results obtained shows that the congestion problem has solved [29]. In this paper author analyzed the proper settlements for the FACTS devices to overcome the congestions in power supply lines. To determine the effectiveness the analysis of TCSC (Thyristors-Control-Series-Capacitor) and Statics-Synchronous-Series-Compensators devices has applied to modified bus test system of IEEE-14. Reduction in transmission line problems a comparison process has been used in this paper [21]. In this paper author uses an appropriate FACT devices for the settlement of reactive power. FACTS devices are used in appropriate location with specific index order to decrease maximum Reactive Power losses [31]. Author in this paper proposed a multi objective management method that is based on congestion management in power system. The functionality define by this method has three goals (1) operating cost, (2) voltage, and (3) transient stability margin, which is improved as proposed by author. The effective settlement and size of FACTS devices are managed by the suggested method based on congestion transmission line and by significance citation using LMP (Locational Marginal Prices) [22].

In this paper "current limiting fuses" is designed for fault clearing time and reduction in magnitude of fault current. The design helps in reduction of fault clearing time, and sag problem in voltage is limited to only half cycle. The disadvantage of this system is that after melting of fuse human intervention is necessary for the replacement of the fuse. In this paper solid state circuit breaker is proposed for fault clearing. It is a combination of Gate Turn off (GTO) and Thyristors switches. The design helps in clearing fault within half cycle. Solid state circuit breaker is a multifunction device and has an advantage over current limiting fuse of auto reclosing after fault clearance. This paper proposed solid-state-fault-current-limiter. This device is based on gate turn off circuitry which adds an inductor in series when fault is detected in power system. After clearing the faults the inductor is remove [23].

CONFLICT OF INTEREST

The author has no conflict of interest.

CONCUSLION

Quality of Power plays in important role in power system. Low power quality effect consumer in many ways , it causes distortion, electrical interruption in power appliances, decaying life of industrial equipment's, and more seriously it can be detrimental to life of human being. Considering different cases any suitable option can be selected for power quality improvement.

REFERENCES

[1] Sankaran, C., Power quality. 2001: CRC press.

[2] Bollen, M.H., Understanding power quality problems, in Voltage sags and Interruptions. 2000, IEEE press.

[3] Ghosh, A. and G. Ledwich, Power quality enhancement using custom power devices. 2012: Springer Science & Business Media.

[4] Zhang, S., et al., Control Strategy for Dynamic Voltage Restorer Under Distorted and Unbalanced Voltage Conditions. IEEE International Conference On Industrial Technology (ICIT), 2019: p. 411-416.

[5] Akagi, H., New trends in active filters for power conditioning. Industry Applications, 1996. **32**(6): p. 1312-1322.

[6] Alferov, Z.I., The history and future of semiconductor heterostructures. Semiconductors, 1998. **32**(1): p. 1-14.

[7] García, O., et al., Single phase power factor correction: A survey. IEEE Transactions on Power Electronics, 2003. **18**(3): p. 749-755.

[8] Grady, W.M. and S. Santoso, Understanding power system harmonics. IEEE Power Engineering Review, 2001. **21**(11): p. 8-11.

[9] Marketos, P., A.J. Moses, and J.P. Hall, Effect of DC voltage on AC magnetisation of transformer core steel. J. Elect. Eng, 2010. **61**: p. 123-125.B

[10] Hussain, Z., et al., Technical Losses Ratio: Analysis of Electric Power Transmission and Distribution Network. INTERNATIONAL JOURNAL OF COMPUTER SCIENCE AND NETWORK SECURITY, 2018. **18**(9): p. 131-136.

[11] Dugan, R.C., et al., Electric power systems quality. 2004, McGraw-hill.

[12] Myneni, H., G.S. Kumar, and D. Sreenivasarao, Dynamic dc voltage regulation of split-capacitor DSTATCOM for power quality improvement. IET Generation, Transmission & Distribution, 2017. **11**(17): p. 4373-4383.

[13] Ramachandaramurthy, V.K., et al., Supervisory control of dynamic voltage restorers. IEE Proceedings-Generation, Transmission and Distribution, 2004. **151**(4): p. 509-516.

[14] Gupta, A.R. Effect of optimal allocation of multiple DG and D-STATCOM in radial distribution system for minimizing losses and THD. in 2017 7th International Symposium on Embedded Computing and System Design (ISED). 2017. IEEE.

[15] Kullarkar, V.T. and V.K. Chandrakar. Power quality improvement in power system by using static synchronous series compensator. in 2017 2nd International Conference for Convergence in Technology (I2CT). 2017. IEEE.

[16] Esmaili, M., H.A. Shayanfar, and R. Moslemi, Locating series FACTS devices for multi-objective congestion management improving voltage and transient stability. European journal of operational research, 2014. **236**(2): p. 763-773.

[17] Kai, X. and G. Kusic, Application of thyristor-controlled phase shifters to minimize real power losses and augment stability of power systems. IEEE Transactions on Energy Conversion, 1988. **3**(4): p. 792-798.

[18] Rahimzadeh, S. and M.T. Bina, Looking for optimal number and placement of FACTS devices to manage the transmission congestion. Energy conversion and management, 2011. **52**(1): p. 437-446.

[19] Thangalakshmi, S. and P. Valsalal, CONGESTION MANAGEMENT USING HYBRID FISH BEE OPTIMIZATION. Journal of Theoretical & Applied Information Technology, 2013. **58**(2).

[20] Kulkarni, P.P. and N. Ghawghawe. Optimal placement and parameter setting of TCSC in power transmission system to increase the power

transfer capability. in 2015 International Conference on Energy Systems and Applications. 2015. IEEE.

[21] Dhansekar, P. and K. Elango, Congestion management in power system by optimal location and sizing of UPFC. IOSR Journal of Electrical and Electronics Engineering, 2013. **6**(1): p. 49-53.

[22] Kojovic, L. and S. Hassler, Application of current limiting fuses in distribution systems for improved power quality and protection. IEEE Transactions on Power Delivery, 1997. **12**(2): p. 791-800.

[23] Smith, R., et al., Solid-state distribution current limiter and circuit breaker: application requirements and control strategies. IEEE Transactions on Power Delivery, 1993. **8**(3): p. 1155-1164.

IJEW 国际工程期刊 International Journal of Engineering Works انجینئرنگ کاموں کا بین الاقوامی جرنل

International Journal of Engineering Works
ISSN-p: 2521-2419
ISSN-e: 2409-2770
Vol. 7, Issue 03, PP. 178-182, March 2020
https://www.ijew.io/
https://doi.org/10.34259/ijew.20.703178182

Operation and Fault Monitoring of Electric Generator using IOT

Jawad Ul Islam[1], Muhammad Azaz[1], Syed Abuzar Bacha[1], Sajad Ullah[1]
[1]Department of Electrical Engineering, University of Engineering and Technology Peshawar, Pakistan
Received: 05 March, Revised: 11 March, Accepted: 15 March

***Abstract*—** The reliable and quality power supply is vital for power system operation. Its importance become significant when dealing with sensitive load areas like hospitals, banks, airports, radar system, military offices and data centers. Their proper operation depends on uninterrupted and reliable power supply. In this regard, there is an emergent need to provide generator backup capacity in the events of power failure or blackout. These Generators can only be effective if they are maintained and operated properly. Problems like the remote monitoring of fuel tank, total load and the battery voltage of the generator are of main concern for better operation. To prevent these problems, the advance IOT based monitoring system is designed using an Arduino controller board. This system uses the fuel gauge for sensing the fuel level and a current transformer measures the load on generator, giving real time analogue data to the controller. The data is converted into digital through an ADC convertor and the instructions are programmed for every parameter in an IDE (Integrated Development Environment). This data can also be monitored on an android app or on laptop using esp8266 WIFI module as an interface between controller and clouds. A hardware based prototype is developed and installed on real generator. Results show real time remote monitoring of generator ensuring its reliable operation and timely indication of need of maintenance.

***Keywords*—** gaugel sensor, controller, reomote monitoring, WIFI module, temperature sensor.

I. INTRODUCTION

Power systems are needed to provide electricity to their consumers without any interruption. Sensitive departments like hospitals, schools, military offices, data centers and traffic system etc. require reliable and uninterrupted power supply. Grids are the main source to power all the passive infrastructures. However, due to energy crisis, power availability is not reliable in developing countries like Pakistan. To overcome this problem, one of the possible solution is to use diesel generator units as instant back up to power the loads ranging from small apartment to large industries. These generator units act as standby power source which are available at all the time to meet load in absence of main supply. Availability of these generators are subjected to their proper maintenance which can be ensured by an active monitoring system. Monitoring of generator is very important for its continuous operation. Fuel level in the tank, temperature, electrical load on the generator and battery voltage are the important parameters to be monitored. These parameters play an important role in timely maintenance of generator. Maintenance of generator improved the performance and life of the generator and reduces the probability of failure by increasing mean time between failures [1]. Beside this, fuel level monitoring in the tank can reduce the operational cost. Many of the generator are located at remote areas and remote monitoring of fuel tank, load on the generator, battery voltage and run hours are the main challenges in the proper operation of the generator. Moreover, monitoring of fuel level in tank can be helpful in fuel leakage and theft detection. The fuel theft and leakage from tanks is of main concern. Fuel theft is an international problem, with news of fuel theft coming from the modern countries like Australia, UK and New Zealand as well as across US etc. Hence, monitoring of generators improves efficiency and reliability while reducing the cost of operation.

Mohammad Asif khan et. al have already discussed the remote monitoring of fuel tank only through GSM based [1]. In [2] author designed, constructed and implemented the fuel level monitoring through GSM module and use a status messege to send information of fuel to mobile phone. The author disscused the real time monitoring of fuel level by ultrasound sensor with the help of data acquisition system in [3]. J.A Goundal et al have designed a system which is composed of a pressure sensor, microcontroller, solenoid valves and a liquid pump. The pressure sensor measures the pressure inside the air column submerged in the tank, which is then calibrated to display level [4]. The author in [5] design a fuel management system in which monitoring device built on the Raspberry-Pi computer, it takes information about tank's fuel level in real time through its sensor and live streaming of the site, then uploads it directly to the internet, where it can be read anytime and anywhere through web application. In the [6] the author proposed a system which monitors the fuel level of vehicles tank and the fuel consumption with distance covered. The measured values are send mobile user through SMS service using GSM technology. Authors of the work, [7], proposed a cloud based real time monitoring and control of diesel generator using IOT technology. The work is done by using an ultrasonic sensor for diesel level measuring, GSM shield for sending information of

the controller to clouds and Thing Speak clouds and app for real time monitoring of the data.

In this paper, Remote Generator Monitoring System (RGMS) is designed specifically for backup power generators to monitor generator operations remotely to ensure increased generator availability and efficiency by monitoring the fuel level, electric load and battery voltage of the generator. This system provides monitoring of fuel level, battery percentage, run hours and load on the generator with the help of IOT technology to monitor on mobile app through Wi-Fi based wireless communication. Here, we have used arduino microcontroller, esp8266 Wi-Fi module, fuel level sensor, current transformers and mobile app to design RGMS.

II. PROPOSED METHODOLOGY

Internet of Things (IOT) concept began as a simple idea of connected devices. The IOT promises to make our environment, homes, offices and vehicles smarter and more measurable. The IOT is being used in smart girds, smart city, industry, connected cars, automated industries, digital health and more others. IOT performs device-to-cloud communication. The IOT device connects directly to an Internet cloud are discussed in [8]. In [9] with the help of IOT, the different monitoring and controlling devices can generate, exchange and use data without or very little human intervention. For example, home and industry controlling and monitoring, human health (devices attached or placed inside human body to monitor human health, fitness and wellness), plant health (temperature, soil moisture, humidity, light intensity) enhanced learning are only a few examples of possible application scenarios in which the new technology IOT play a vital role. The most essential component of IOT is the cloud service where data are stored and analyzed. There are three types of services provided by cloud service providers and these include; Infrastructure as a service (IaaS), Platform as a service (PaaS), and Software as a service (SaaS) [10], [11, [12].

Proposed System Model is elaborated in Fig 1. The generator monitoring System is consists of the following three parts.

The System is consist mainly of

- Data Collection

  Sensors are placed to sense and measure required parameters. Different sensors collect data from generator and give this data to arduino control system.
- Controller

  Controller consists of an Arduino board and ESP8266 wifi module. Arduino take data from sensors, convert it into digital form, process and send to ESP8266 wifi module through TX and RX port.
- Thingspeek results

Thingspeek is a free cloud server. Wifi module of our controller send data to thingspeek server through Application Program Interface (API).

The arduino microcontroller is powered by a battery and this battery is charged when generator is running. The complete flow diagram of monitoring system is shown in fig.01. The data collection is done by current sensors and guage sensor which are connected to arduino microcontroller. The microcontroller is connected to IOT cloud through WIFI module esp8266. The data is visualized on the IOT web application as well as on smart phone app ThingView. The fuel consumed by the disesel generator in a specific time period is measured by both guage sensor as well as current sensors. The results of the sensors are compared, if there is a big difference between the two then there is a theft of fuel from the tank or the tank is leaked.

III. BLOCK DIAGRAM

The block digram is shown in Fig. 1.

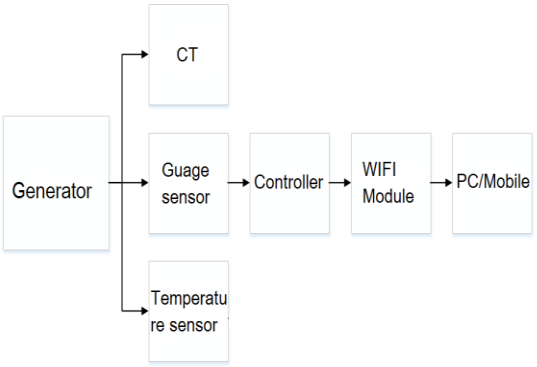

Figure 1: Flow Diagram of Proposed System

A. Fuel Level Sensor

A fuel gauge (or gas gauge) is an instrument used to indicate the level of fuel contained in a fuel tank. Commonly used in most motor vehicles, these may also be used for any tank including underground storage tanks. The gauge consists of two parts, sensing unit which is in the tank and indicatory unit which is on dashboard (serial monitor in this case).

The sensing part consists of a float which is connected to a thin, metallic rod. A variable resistor is connected to the end of the rod. As resistor opposes the flow of current, the more resistance there is, the less current will flow and vice versa. The variable resistor consists of a strip of resistive material whose one side is grounded. A wiper connected to the gauge slides along this strip of material, conducting the current from the gauge to the resistor. If the wiper is close to the grounded side of the strip, there is less resistive material in the path of the current and therefore, resistance is small. If the wiper is at the other end of the strip, there is more resistive material in the current's path and resistance is large. In the sensing unit, fuel has to drop below a certain level before the float starts to drop. When the float is near to the top of the tank, wiper on the variable resistor rests close to the grounded side, which means that the resistance is small and a relatively large amount of current passes through the sensing unit. As the level in the tank drops, the float sinks and wiper moves downward. As a result, resistance increases and the amount of current decreases. Indicating part measure and display the current flowing through the sensing part. If maximum current is flowing, the tank level is high and serial monitor shows a full tank. When lesser current is flowing as compared to maximum current, level of tank is

indicated correspondingly lower depending on amount of current flowing.

B. Generator load measurement

i. Current Measurement

Current transformer (CT) is used to measure large magnitude of alternating currents such as current from large generators or heavy loads. The split core type CT is particularly suitable for this purpose. They are clipped either the live or neutral wire for curent measurements. It has a primary winding, a secondary winding and a magnetic core. In proposed system, yhdc 100A current transformer is used.

The measured current is alternative, and CT is calibrated to measure a maximum of 100A RMS value of current. Transformation ratio of used CT is 1:2000. Hence, peak-peak current can be calculated by simple relation:

$I_{peak} = \sqrt{2} * I_{RMS}$ (i)

Output current of CT can be calculated as:

$I_{out} = I_{in} / (ns)$ (ii)

Where ns is number of turns at secondary side of CT.

a. CT-Arduino Interfacing

Output of CT is alternating current while Arduino is designed to accept analogue & digital voltage signal as input. A circuit shown in Fig. 2 is designed to interface CT and Arduino. First, it convert current signal into voltage using a burden resistor R13. Then AC signal is converted into analogue by adding 5V dc offset to make it compatible to use as Arduino input.

For the battery voltage measurement, circuit shown in Fig. 3 is designed. The D1 is use for reverse flow protection whereas R1 and R2 work as voltage divider and C1 is for purpose of noise removing. Arduino IN port will give status of the battery voltage to the Arduino controller.

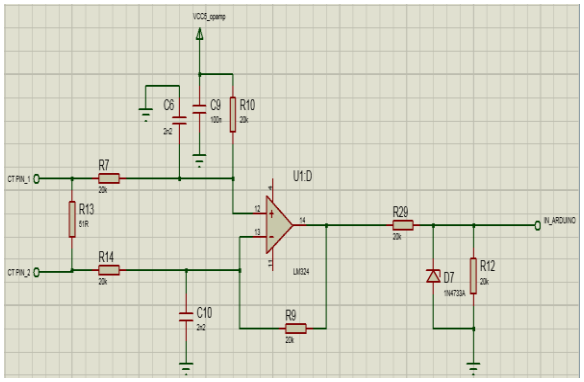

Figure 2: CT-Arduino Interface Circuit

ii. Battery Status

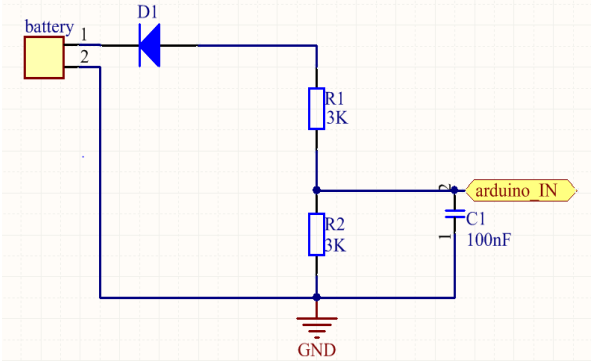

Figure 3: Circuit diagram for battery status

iii. Arduino Uno

Arduino Uno is a microcontroller board based on the ATmega328P controller. It has 14 digital input/output pins (of which 6 can be used as PWM outputs), 6 analog inputs and a 16 MHz quartz crystal. It can be powered by USB cable connection, by an AC-to-DC adapter or a 12V battery.

It is an open-source electronics platform based on easy-to-use hardware and software. Arduino boards are able to read inputs i.e. light on a sensor, a finger on a button, or a Twitter message and turn it into an output i.e. activating a motor, turning on an LED or publishing something online. Arduino Integrated Development Environment (IDE) is used to program the controller to perform different tasks.

iv. Module - ESP8266

The ESP8266 WiFi Module is a self contained system on chip (SOC). It is integrated with different protocols like TCP/IP that can give access any microcontroller to your WiFi network. The ESP8266 has capablability of sending and receiving data and commands to/from clouds and a microcontroller. The ESP8266 module is a small and cost effective board with multifunctionalities.

The ESP8266 module send and receive inforamtion through TX and RX pin. When we interface the module with Arduino and upload a programm to scan different networks and connect it to desire one. Service Set Identification (IEEE 802.11 wireless networks) and password is provided in the code for connection.

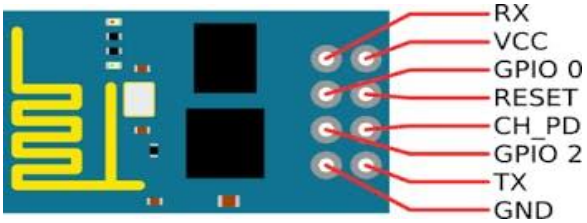

v. Uploading data to IOT Cloud

In the proposed system, WIFI module ESP8266 is used to upload data to IOT cloud (ThingSpeak). ThingSpeak provide

free cloud service to read/write and visualize data. Establishing connection of ThingSpeak with Arduino require channel ID and read/write API key which is provided by ThingSpeak to individual user.

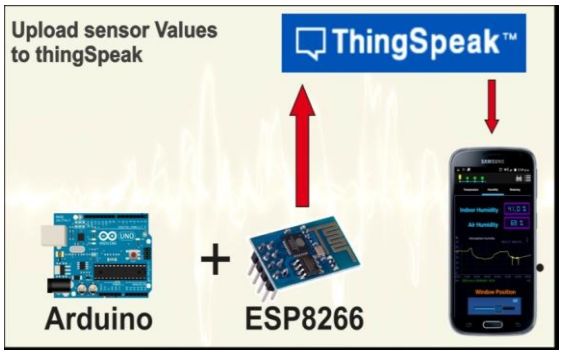

IV. RESULTS

A hardware is developed based on proposed solution and installed on 200kVA backup generator for a distribuiton network. Generator load, temperature, fule consumption and battery charging status are monitored for different times. These monitored parameters can be observed at any device using internet. Results show a great degree of easeness in remotely monitoring of generator parameters. Fig.4 show generator fuel level against time. Fuel tank is filled up to its maximum level in start and checked remotely to see its status. Then, fuel tank is made full empty and status is observed to check if it is following real status of tank. This sudden change may represent theft of fuel and using our remote monitoring system it can be easily and timely detected. Moreover, gradual change in fuel level represents fuel usage by generator to meet load.

As shown in Fig.5, there is no laod on generator in start. After some time the back up generator is on and load is added to generator. Maximum load on generator phases is 70 ampere. Load is monitored at different running time of generator.

In Fig 6 battery SOC is shown against time. The columns show state of charge of generator battery in percentage. Fig. 7 shows the temperature of generator with time. It can be clearly concluded that temperature of generator increases with its running time. Rise in temperature above its allowed limit can cause severe damage and should be avoided. This increases the importance of its monitoring and designed system is able to remotely monitor temperature with other important parameters.

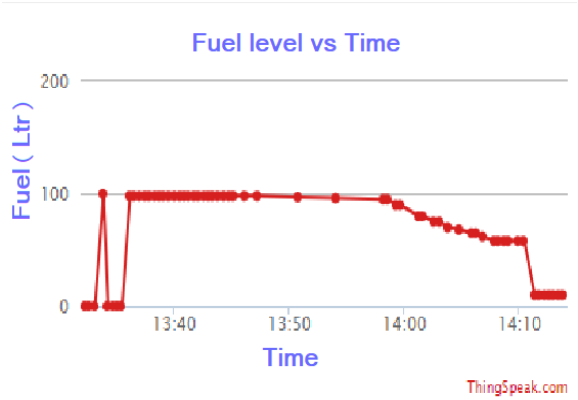

Figure 4: Fuel Level Vs. Time

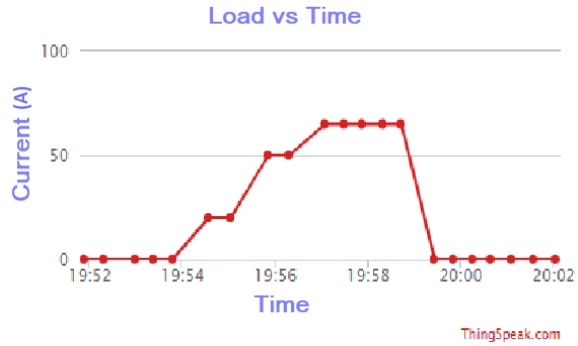

Figure 5: Generator load at different time

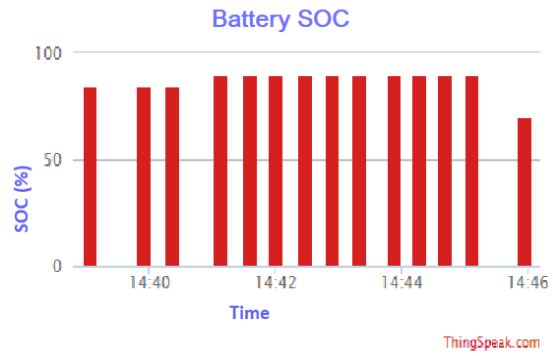

Figure 6: State of Charge (SOC) of Battery

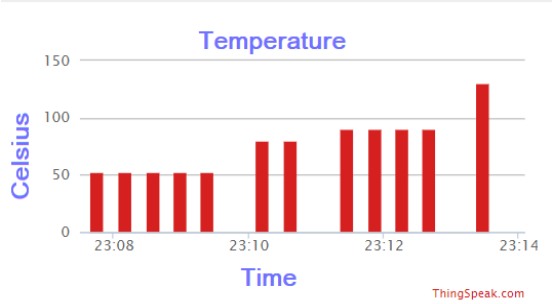

Figure 7: Generator Temperature in Celsius

CONCLUSION

Current work has focused on monitor of generator through two parameters tank and load on the generator so it is very limited to give information about generator there are so many important paramter like temprature ,rpm and mobile oil quality and remote on off of the generator to monitor through thingspeak. The sensors efficiently measure different paramter and send it to controller. The controller read the signals and convert it into useful meaning for further processing. The main focus of this work is to provide information about fuel level in the generator tank and can easily monitored from mobile App or computer. The proposed work will detect the fuel theft from the tank and leakage in case of tank crack. The proposed solution is much intelligent to differentiate the leakage and fuel theft from tank. Battery voltage and temperature is easily monitored to keep the generator healthy. The whole system ensure high level of maintenance and proper operation of generator.

REFERENCES

[1] Muhammad Asif et al "*Context Aware Fuel Monitoring System for Cellular Sites"* International Journal of Advanced Computer Science and Applications 8(8):281-285 · September 2017.

[2] Gbenga et al "*Design, construction, and implementation of remote fuel-level monitor system*" in *EURASIP Journal on Wireless Communications and Networking*2014:76

[3] Sadeque Reza Khan et al "*Real Time Generator Fuel Level Measurement Meter Embedded with Ultrasound Sensor and Data Acquisition System*" in Journal of Automation and Control Engineering Vol. 1, No. 4, December 2013.

[4] J A Gundar et al "*Mechatronic design solution for fuel level monitoring using pressure sensor"* **Published in:** Asia-Pacific World Congress on Computer Science and Engineering **IEEE *Xplore*:** 05 March 2015.

[5] Areeg Abubakr Ibrahim Ahmed et al "Fuel management system" **Published in:** 2017 International Conference on Communication, Control, Computing and Electronics Engineering (ICCCCEE) **on** 02 March 2017.

[6] Senthil Raja et al "*DETECTION OF FUEL THEFT IN HEAVY VEHICLE*" International Journal of Advanced Engineering Technology E-ISSN 0976-3945.

[7] Abel Avitesh Chandra et al "*Cloud Based Real-time Monitoring and Control of Diesel Generator using the IoT Technology*".

[8] An Introduction to the Internet of Things (IoT)', Lopez Research, 2013.

[9] Madakam, S., Ramaswamy, R., and Tripathi, S.: 'Internet of Things (IoT): A literature review', Journal of Computer and Communications, 2015, 3, (05), pp. 164.

[10] Sushil Bhardwaj et al "*A STUDY OF INFRASTRUCTURE AS A SERVICE (IAAS)"* published in IJEIT 2010, 2(1), 60-6.

[11] N. Khan and S. A. Bacha, "Proposing Optimal ARMA Based Model for Measurement Compensation in the State Estimation," 2017 International Conference on Frontiers of Information Technology (FIT), Islamabad, 2017, pp. 299-304.

[12] Naeem Khan, Syed Abuzar Bacha, Shahrukh Ahmad, Afrasiab, "Improvement of compensated closed-loop Kalman filtering using autoregressive moving average model", Measurement 134(2019) 266-279.

IJEW 国际工程期刊 International Journal of Engineering Works انجینئرنگ کاموں کا بین الاقوامی جرنل

International Journal of Engineering Works
ISSN-p: 2521-2419
ISSN-e: 2409-2770
Vol. 7, Issue 03, PP. 183-188, March 2020
https://www.ijew.io/
https://doi.org/10.34259/ijew.20.703183188

Adaptive Under-Frequency Load Shedding Scheme for Islanded Distribution Network based on Swing Equation

Nauman Ahmed[1], Dr. Muhammad Naeem Arbab[2], Hammad Israil Awan[3], Shehla Noor[4]
[1,3,4]PG Research student, Dept. of EEE, University of Engineering and technology Peshawar, KP, Pakistan
[2]Research scholar, Dept. of EEE, University of Engineering and technology Peshawar, KP, Pakistan
Received: 14 March, Revised: 19 March, Accepted: 20 March

***Abstract*—** Power system stable operation requires, generating power of the system equivalent to the sum of all losses and affiliated load. Therefore, excess of load needs to be shed especially in islanding mode because generators are running at rated capacity. Different factors e.g. over current, low voltage level and frequency affect system performance but among them constant frequency is imperative for the steady functioning of power system because frequency is constant at every voltage level and hence, a dependable and reliable parameter to show imbalance situation. Additionally, active power deficit. System frequency is very sensitive to disturbance specially in islanding mode and is severely affected by the power imbalance between power generation and load which leads to overload or power generation loss. To shed excess load, U.F.L.S. (Under Frequency Load Shedding Scheme) is implemented. This research here presents Under Frequency Load Shedding Scheme for islanded distribution network. This proposed adaptive U.F.L.S scheme use swing equation to find power imbalance. It takes into consideration ROCOF (rate of change of frequency) and power imbalance and based on this data load is shed in single step which is better than cascading as other traditional U.F.L.S implements cascading steps and the response time to any magnitude of disturbance is also better than others. The adaptive U.F.L.S scheme is tested in Simscape Power System and Simulink (Software Packages in MATLAB) and the results shows that it stabilized the frequency thus stabilizing the system by shedding the right amount of imbalance load.

***Keywords*—** Load Shedding, ROCOF (Rate Change of Frequency), Adaptive U.F.L.S, Islanding and Overload.

I. INTRODUCTION

Electrical power system stable operation requires, generating power of the system equivalent to the sum of all losses and affiliated load. Different factors e.g. over current, low voltage level, under & over frequency affects the stability of power system. Extreme example is complete blackout/collapse of the system. Large generators are considered economical to operate. however, in the event of instability huge number of consumers are affected. In any particular system, instability is a constant threat to the system. Usually in power system, the power house is at a very large distance from the load and there is a chance that the whole system collapse if the power station trips and therefore, needs real time system measurement parameters to change power generation accordingly so that the system remains stable.

While it is not completely possible to eliminate faults and failures from a power system however, it can be minimized and if not minimized and controlled properly, it can lead to severe blackouts and even system collapse. As a result, consumers will be affected and the utility in financial terms. Hence, it is imperative to design a system to cope with abrupt/unforeseen faults and continue to function with minimal disturbance in delivering of power to the consumer.

Stable frequency is imperative for the steady functioning of power system. Frequency is constant at every voltage level and hence, a dependable and reliable parameter to indicate imbalance situation. In electrical power system, frequency shows us the active power deficit. To sustain the frequency of electrical power system, mechanical-power input to the prime movers of alternators must be equivalent to the aggregate of all affiliated load and associated power losses of the system. Equilibrium/stability is disturbed when input or output are changed. Mathematically, a stable state is:

Power Generation = Connected load + Associated losses. (1)

The unexpected loss of transmission line, transformer, and alternator create an imbalance condition in which load will become more than the power generation, leading to frequency decline. The usage of Distributed Generation (DG) is going to expand with each passing day. Thus, islanding operation at distribution level will grow. It's quite a possibility that in future the entire region (national grid) is partitioned in to a number of islanded region and operate each and every region individually. Islanded region needs an effective and efficient protection scheme just like a national grid (inter connected system), For stability reasons, the power generation and affiliated load of an islanded region must be well-balanced. The most essential protection strategy for islanded distributed network is under frequency load-shedding scheme. Additionally, the reliability of islanded area/region can be enhanced by constantly supplying electrical power from Distributed Generation.

II. DESCRIPTION

A. Objective

- Nearly constant frequency for stable operation of an islanded region
- Stability in terms of power system protection, especially generators and turbines.

B. Islanding

An area or a region with one or two generating units serving local load of that area is known as islanded region. This local generation is known as DG. Main power source in this region is DG. Possibly it can be solar or wind or small hydro. The owner of DG earns more by selling power apart from having continuous supply and with time, power quality enhances because of the competition. All power utilities presently, turn off power when distribution system detects islanding. In accordance to IEEE-1547-2003 established standard, in case islanding detected, power must be cut off within 2 secs and this is also started in IEC 61727 [1]. In Denmark it is avoided to have maximum of 25MW utilization of generations units while islanding [2]. Power service providers/Utilities avoid this situation because;

- It possibly puts line workers life in danger if DG powers islanded region. if not properly grounded, un-faulted phase lines have very high voltage during earth faults [3].
- For protection reasons, the DG's power failure assistance probably not enough for reliable functioning as a result continued fault current [4].
- Most important point, the power utility companies avoid islanding because they are of the opinion that DG probably not capable to keep frequency and voltage inside required range during islanded mode [4].
- For reconnecting transmission and distribution system, most of the power utility companies utilize an instant recloser-breaker which results in out-of-phase closing. Thus, creating currents and mechanical torques which may damage the prime movers/generating units [5].
- At distribution level the usage of DG has increased sharply. It is inefficient to use traditional methods to turn off DG. In islanding mode, among the power providers the competition is growing, enhancing the reliability and quality [6].

C. U.F.L.S schemes

- **Traditional/Conventional UFLS Scheme**; Load first block is shed at 49.5 Hz as most power utilities exercise 49.5 as the 1st limitation/threshold. A particular magnitude of load is removed at a number of determined frequency thresholds between 49.5 - 47.5 Hz. Between two thresholds a proper amount of pause is necessary to examine the effect of load-shedding on frequency. Also, important to check if successive shedding sheds large amount of load without checking, frequency may overshoot its normal value. Frequency declines fast if disturbance is huge. Therefore, it may not be enough to shed just specified load compared to the frequency fast decline rate. This type of scheme has several disadvantages; one such is — load that is shed is pre-determined without taking into account the amount of power deficiency and intensity of turbulence. This scheme /strategy is ordinary & complex relay systems is not necessary. Frequency threshold and value of load for shedding is pre specified & fed to relay on the basis of experience [7]. If frequency continues to drop after first threshold, the process of load shedding continues at each threshold until it reaches its normal value.
- **Semi adaptive UFLS Scheme**; This type of scheme and traditional U.F.L.S are somewhat different. In this type of scheme, the first block of load is shed by determining ROCOF (rate of change of frequency). ROCOF may not always be the same because it relies on the value of load varied. So, for the load first block to shed, three or four different levels of frequency threshold is specified along with amount of load for each and whichever frequency threshold ROCOF matches its corresponding load is shed. For instance, ROCOF is -0.40 Hz/sec. then predefined load of 110MW is shed & if -0.90 Hz/sec. then 170 MW of pre-determined load-shedding. It only checks the speed of frequency variation; speedier the variation, greater the load-shedding. So, this schema only relies on ROCOF but just for the first step and after that it follows the same traditional U.F.L.S scheme [5].
- **Adaptive UFLS Scheme**; Using swing equation, this adaptive/dynamic U.F.L.S schema shed varied value of load every step by determining the magnitude of disturbance. When the disturbance is very high, a significant amount of load is disconnected but when less then small volume of load is shed. Therefore, the amount/volume of load to be disconnected is not predefined or fixed and is dependent on the amount of load as well frequency Due to this, this adaptive scheme stabilizes frequency faster than the other two schemes previously mentioned. Moreover, rather than a stepping/cascading scheme, a single step scheme produces better response of frequency Therefore, this scheme is preferred over other two schemes [8].

$$\Delta P = 2 * H * (\frac{df}{dt}) \quad (2)$$

Wherein;
df/dt — ROCOF (Rate of change of Frequency)
ΔP— Power Deficiency
H — Inertia-constant (in seconds)

Definition of H as the ratio of rotating components of alternator's moment of inertia to a unit capacity. Bigger values of H, slower the frequency fall for a given overload. Old generators like the water wheel units had H as big as 10 secs but the modern turbine units have H value of 2-3secs. because the

tendency is having smaller rotor masses resulting bigger output.

III. PROPOSED WORK IMPLEMENTATION AND RESULTS

The problem of maintaining Frequency in desired range is solved by dividing into three sections

- Mechanical torque control
- Calculating imbalance power
- Providing an extra power when load increases

A. Mechanical Torque Control

Islanding system with DG distribution network is first run without mechanical torque control to show the adverse effects of not having mechanical torque. If load is shed then frequency will rise. Also, the rotor speed which may run so faster that may damage the alternator. That's why system with mechanical torque is preferred. After this, mechanical torque control is introduced into the system. Once there, it can detect the frequency rise or depress and changes the mechanical shaft input accordingly to maintain frequency in desired range. Generator ratings;

- Generator of 4MVA
- Output (O/P) power = 3200.0kW (0.8 power-factor)
- Frequency (f) = 50.0Hz
- Total no. of poles (P) = 2.0
- Speed = 3000.0rpm
- Initial Load = 3200.0KW

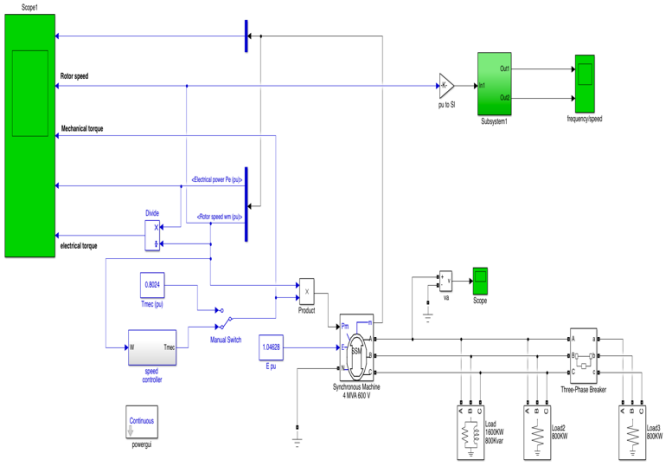

Figure 1. Schematic of system with & without mechanical torque control

The initial load is divided into three blocks i.e. 1600KW & two 800KW blocks each. Schematics shown in figure 1. At 0.2 seconds, load of 800KW is shed from the system and after the simulations, graphs are taken from both to show the difference that how important it is to maintain the frequency. Figure 2 shows frequency having no mechanical torque control and figure 3 shows frequency having mechanical torque and figure 4 show controlled mechanical torque response.

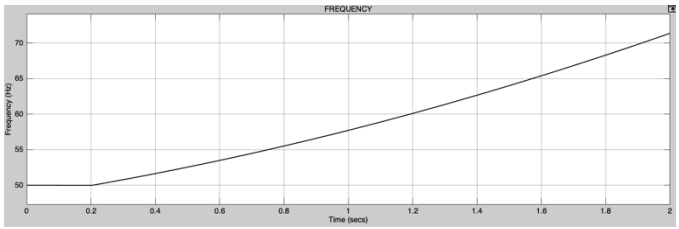

Figure 2. Frequency without mechanical torque control

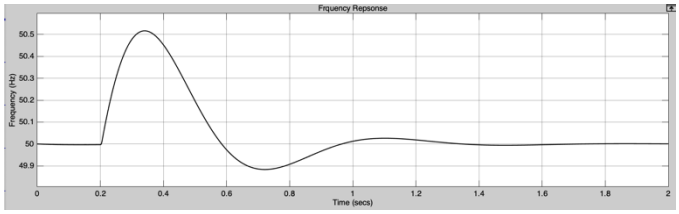

Figure 3. Frequency with mechanical torque control

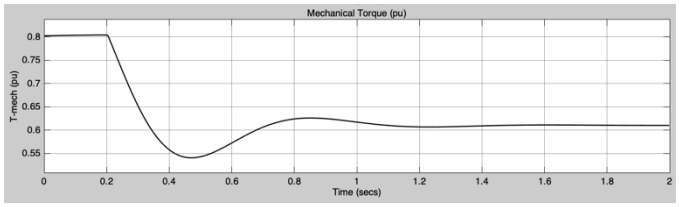

Figure 4. Controlled mechanical torque response

B. Calculating an imbalance power

To deal with system that is under frequency depress or on frequency rise, it is necessary to shed right amount of load. To maintain stable frequency in desired under load and overload both conditions are considered. Generator ratings:

- 125kVA Generator
- O/P Power = 100.0kW (0.8 power-factor)
- Frequency (f) = 50.0Hz
- Total no. of Poles (P) = 2.0
- Speed = 3000.0 rpm
- Initial Load = 100.0kW

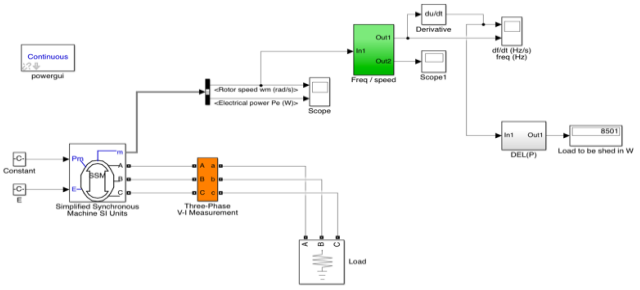

Figure 5. Calculating an imbalance power of system

Schematics for both conditions are designed accordingly, shown in figure 5. Firstly, an overload conditioned is implemented which calculates the excess load and then the

system sheds that load, then an under-load condition is implemented which again calculates the amount of load necessary to be added to the system and after the calculation, adds to the system right way. Graphs for both scenarios are taken to show the frequency depress and stabilize and again frequency rise.

At first the entire load of 100kW is on generator. It is then incremented from 100 to 108.5kW, that additional load leading to frequency depreciation as shown in figure 6. Swing-equation is applied to find the power difference between power produced and power demand/load. Frequency normalizes after load-shedding of 8.5KW load & comes back to rated value as shown figure 7. Also, the power station is tested in a condition when the power generation is more than power demand (load) as shown in figure 8. -9400W is shown as an imbalance power. The negative sign shows that this much of a load is less than power generated or need to be added to the system or the mechanical power input need to be lowered in accordance with the load on system. Table 1 summarize imbalance power situatuin.

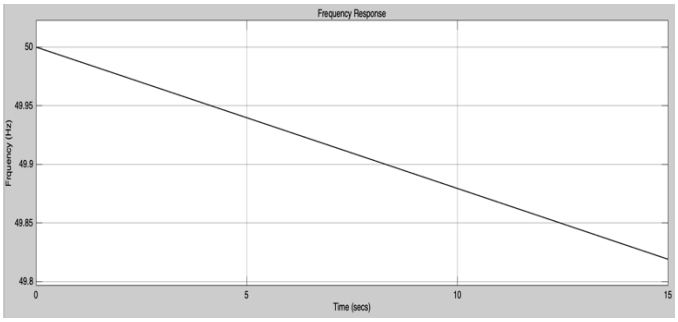

Figure 6. Frequency before load shedding

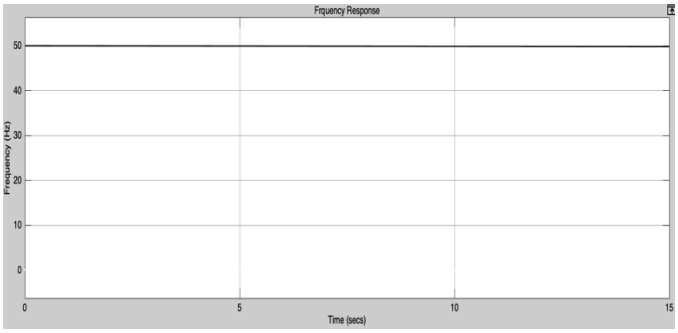

Figure 7. Frequency after load shedding

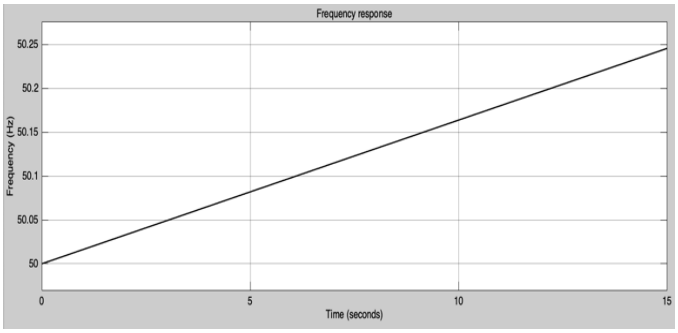

Figure 8. Frequency at small load

TABLE I. TO DETERMINE AN IMBALANCE POWER

Load (KW)	Frequency (f)(Hz)	ΔP (power imbalance) (W)
100.0KW	50 Hz	0.0
108.50 KW	Fall from 50 Hz to 49.8 Hz	8500 W
91.0 KW	Rose from 50 Hz to 50.25 Hz	-9400.0 W

C. Automatically adding a generator with increase in load

Generator power rating:

- 500 kVA generator each (three generators)
- Total Power Output = 1500.0kW
- Frequency (f) = 50Hz
- No. of Poles (P) = 2.0
- Speed = 3000.0rpm
- Initial Load = 1000.0kW

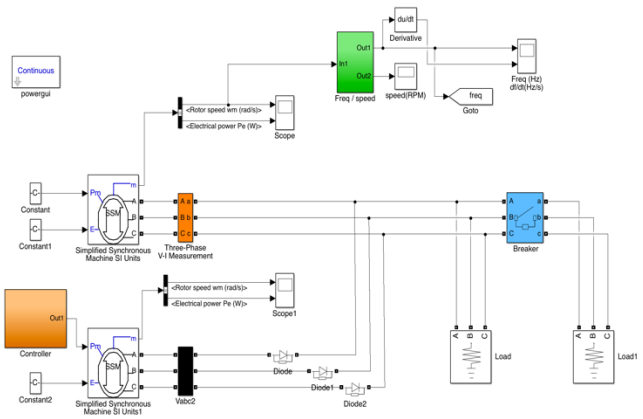

Figure 9. Automatically adding a generator

At first load of 1MW is attached as shown figure 9. only one generator is on standby while the other is contributing to generation. Circuit-breaker closes at t=4 sec; incrementing the net load to 1500kW from 1000kW. To maintain the frequency at rated value/constant a controller links the second standby generator to system. Second generator starts up when it receives a signal as mech-power input from controller which determines the power difference btw power demand & power generators capacity.

Figure 10 shows frequency response when load is increases and then a standby generator is added to the system to stabilize the frequency of the sytem.

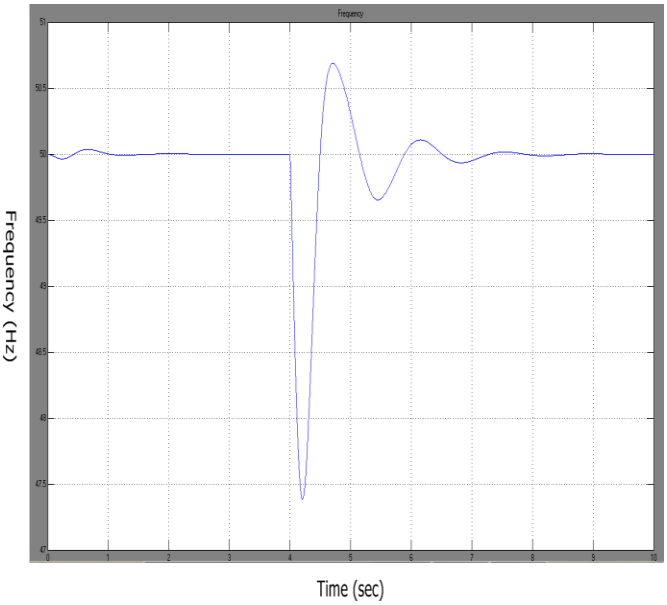

Figure 10. frequency after additional load is added as well an additional generator

CONCUSLION

A traditional load shedding scheme is depicted in table 2, in which percentage of load is shed according to frequency threshold are presented. Traditional load shedding scheme does not take into account the power deficit and magnitude of disturbance, value of load to disconnect is pre-determined. An incident of huge disruption, frequency fall is very sudden and disengaging pre-determined load may not be of great use to stabilize frequency from decline. The adaptive UFLS scheme discussed in this research consider the level of disturbance & sheds load depending upon the frequency & the rate of change of frequency.

TABLE II. A TRADITIONAL UFLS SCHEME

Threshold frequency	49.50Hz	49.00Hz	48.50Hz
Load that is to be shed in percent	40 %	30 %	30 %

The method implemented in this research is very advantageous because not only take care of the system, when there is an overload, but also when the generation is greater than the load (in this situation frequency rises than the nominal value, 50Hz which is also an unstable and unwanted condition). Moreover, load is shed in just one stepping as compared to other traditional schemes and as a result of one stepping, response time to stabilize frequency is less compared to other traditional schemes.

TABLE III. COMPARISON BTW STATE ESTIMATION VS ADAPTIVE UFLS

Power Imbalance Calculation Comparison			
Method presented in a Paper [9], ULFS & state estimation scheme		Method presented in this research	
Power imbalance (KW)	Load shed (KW)	Power imbalance (KW)	Load shed (KW)
300	113	8.5	8.5
450	284	-9.4	-9.4

From the above table, it is obvious that this proposed adaptive UFLS schemes works accurately and is better. Furthermore, the response time is excellent. Its response time from cascading UFLS is much better.

It is a common knowledge that the general grid is much bigger than the islanded region and hence it has much bigger system inertia as well spinning reserve, therefore during frequency depress situation the general grid response time will be slower as compared to islanded region.

A. Future Work

In this research only the simulations are carried out to implement the proposed methods to maintain frequency in desired range however its scope can be further extended by;

- Protection of reverse power flow from islanding region to the main grid.
- Preferential load shedding scheme to shed low priority load first and high priority load last.
- Fine tuning this existing scheme to improve its response time.
- Economical aspect of the work done.
- Hardware based implementation.

REFERENCES

[1] Photovoltaic (PV) systems Characteristics of the utility interface, IEC 61727 Standard, December 2004.

[2] K. Christensen, "Technical Regulation for Thermal Power Station Units of 1.5 MW and higher," Energinet.dk, Fredericia, Denmark, Regulation for grid connection TF 3.2.3, 2008.

[3] P. P. Barker and R. W. de Mello, "Determining the Impact of Distributed Generation on Power Systems 1 – Radial Distributed Systems," IEEE Power Engineering Society Summer Meeting, vol. 3, pp. 1645-1656, 2000.

[4] S. P. Chowdhury, S. Chowdhury, P. A. Crossley, and C. T. Gaunt, "UK scenario of islanded operation of active distribution networks with renewable distributed generators," International Journal of Electrical Power & Energy Systems 33, vol. 34, no. 12, pp. 2585-2591, 2011.

[5] R. A. Walling and N. W. Miller, "Distributed Generation Islanding Implications on Power System Dynamic Performance," IEEE Power Engineering Society Summer Meeting, vol.1, pp. 92-96, 2002.

[6] IEEE Standard for Interconnecting Distributed Resources into Electric Power Systems, IEEE Standard 1547TM, 2003.

[7] Md. Quamrul, Ahsan, A. H. Chowdhury, S. S. Nawaz, I. H. Bhuyan, M. A. Haque, and H. Rahman, "Technique to Develop Auto Load Shedding and Islanding Scheme to Prevent Power System Blackout," IEEE Transactions on Power Systems, pp. 198–205, 2012.

[8] X. Cao, I. Abdulhadi, C. Booth and G. Burt, "Defining the Role of Wide Area Adaptive Protection in Future Networks," IEEE international Universities Power Engineering Conference (UPEC), pp.1-6, 2012.

[9] J. A. Laghari, H. Mokhlis, A. B. Halim, A. Bakar, M. Karimi and A. Shahriari, "A New Under-Frequency Load Shedding Scheme for Islanded Distribution Network" IEEE Innovative Smart Grid Technologies (ISGT), pp. 1–6, 2013.

Nauman Ahmed (Peshawar, DOB 07/05/1990) received the B.Sc degree from the Department of Electrical and Electronics, University of Engineering and Technology Peshawar, Khyber Pakhtunkhwa, Pakistan, in 2014. He is doing his Master from the UET Peshawar with specialization in Electrical Power. His research interests are Under Frequency Load Shedding Scheme for Islanding Distribution Network. His email address is nauman236@gmail.com.

Professor Dr. Muhammad Naeem Arbab is a Professor in University of Engineering and Technology Peshawar in Electrical Department. He got his Ph.D. from UK and is an author of two engineering books i.e., High Voltage Engineering and Electrical Power Generation and published more than 25 research papers. His email address is mnarbab@gmail.com.

Hammad Israil Awan (Peshawar, DOB 18/12/1988) Received the B.Sc degree from the Department of Electrical & Electronics, University of Engineering & Technology Peshawar, Khyber Pakhtunkhwa, Pakistan, in 2014. He is doing his Master from UET Peshawar with Specialization in Electrical Power. His research interests are design & fabrication of novel power point tracking (MPPT) based charged controller for enhanced electrical performance. His email address is hammy_awan@hotmail.com.

Shehla Noor (Peshawar, DOB 10/02/1994) received the B.Sc degree from the Department of Electrical & Electronics, University of Engineering & Technology Peshawar, Khyber Pakhtunkhwa, Pakistan, in 2016. She is doing her Master from UET Peshawar with Specialization in Energy System Engineering. Her research interests are Analyzing Cost optimization techniques for electrification of grid connected and islanded micro grid. Her email address is shehlanoor231@yahoo.com.

International Journal of Engineering Works
ISSN-p: 2521-2419
ISSN-e: 2409-2770
Vol. 7, Issue 03, PP. 189-196, March 2020
https://www.ijew.io/
https://doi.org/10.34259/ijew.20.703189196

Multi-Robot Exploration in Unstructured and Dynamic Environments

Saad Javed[1], Muhammad Tahir Khan[2], Yasim Ahmad[3]
[1,2]Institute of Mechatronics Engineering, UET Peshawar, Pakistan
[3]Department of Mechatronics Engineering, Air University Islamabad, Pakistan
saad_cu09@yahoo.com[1], tahir@uetpeshawar.edu.pk[2], Yasim.ahmed63@yahoo.com[3]
Received: 15 March, Revised: 20 March, Accepted: 21 March

***Abstract*—** This paper deals with exploration by team of multi-robots in unknown, unstructured and dynamic environments at the same time. The goal of the research is to minimize the total exploration time taken by team of robots to complete the mission and to achieve faster re-planning of their planned path in case of sudden changes in the environment as robots move through the environment. The proposed exploration approach is fully distributive in the sense that all robots are assigned separate regions in an unknown environment with each robot exploring its assigned region. As a first step the environment is partitioned into different regions as available number of robots and then each robot in a team is assigned its separate region for exploration. The proposed approach has been tested in different simulation environments with varying number of robots. Comparison with another approach proves the superiority of the approach in terms of reduction of exploration time in unstructured and changing environments.

***Keywords*—** Region Assignment, Unknown environment, Un-structured environment, Dynamic environment, Re-planning.

I. Introduction

Exploration by a team of robots in unknown environment is a interesting field that is demanding research efforts by researchers as single robot is not capable of exploring whole environment efficiently [1][2]. Multi-robot teams are more fault tolerant than a single robot, thus robust to failure of a teammate during mission. Furthermore, multi-robots which perform exploration can save precious human lives as they can protect them by inspecting dangerous and life threatening environments instead of direct inspection by humans. Environment exploration carries out work by exploring all unknown regions with generating maps of these regions as multi-robots move in the environment. Robots in exploration maintains a map of their world and keep on updating it as unknown areas are explored by them. Applications of the field includes search and rescue operations, reconnaissance, surveillance and planetary exploration missions.

There are different kind of environments for achieving exploration. Some are structured [3], while some lack a defined structure i.e unstructured [4]. Another point of consideration is that not all environments are static, changes in environment are likely to occur, so multi-robot exploration should also be robust to any kind of environmental change [5][6] like moving people and obstacles while robots are performing exploration and other kinds of dynamics.

In order to reap benefits of exploration, researchers have provided novel ideas from time to time. Yamauchi [7] introduced the concept of frontiers for the first time between open and unexplored space for robotic exploration of unknown environment. Concept of frontiers is given as areas on the borderline between open space and unknown space. Some authors presented centralized approach in exploration in which supervisor makes the routing decisions based on status of robots regarding frontier exploration [8]. Burgard et al came up with an approach in which robots selected their target frontiers based on cost to reach frontiers and its utility and shared their positions with respect to team mates by simultaneous localization and mapping [9][10].

Work presented here applies a distributed approach which enables the complete dispersion of the team members in unpredictable environments. In the past, several researchers have carried out work on dispersing robots in exploring missions. Some have performed unsupervised clustering [11][12], While others have partitioned the environment into segments considering structure of the world [3][13].

In our method, we have highlighted an issue of efficient exploration by groups of mobile robots seeking for reduction in mission accomplishment time and energy consumption by each robot. Also we have taken into account sudden changes in the environment in the sense of unknown obstruction in planned path of a robot and how robot cope with these changes in an efficient manner. Our exploration methodology can be divided into three parts. First one is the partitioning of the environment. Second one is to assign regions to all robots. Third one is to plan a path for reaching assigned regions.

II. Literature Survey

A. Exploration and Mapping

The field of exploration has undergone developments year after year and still improving for benefit of science and technology. Yamauchi [14] came up with an exploration

strategy in which each robot tracked the frontier cell which it could approach with minimum cost. That strategy lacked coordination during exploration. Stachniss and Burgard came up with an idea of building and updating maps with mobile robots from sensor information [1]. Centralized approach for mapping [9] was also presented in which central executive robot received local maps generated by teammate robots and constructed a global map by integrating all local maps. Based on global map central executive assigned targets location for each robot. The drawback of centralized approach is that if central agent becomes faulty whole mission fails as a result. Another similar approach was used that maximized information gain and reduced cost through Auction Negotiation Process [15].

B. Other Approaches

Authors have also focused their work on behavior based approaches such as potential field that takes into consideration several behaviors to generate a resultant potential field. It works by planning path for robots by combined influence of attractive and repulsive potentials acting on robots. Robots are attracted towards frontiers and repelled by obstacles and fellow robots while navigating towards their goal [16][17]. The drawback of potential field approach is the problem of local minima i.e attractive and repulsive forces become balanced making resultant force zero. J. De Hogg, Cameron and Visser proposed Role based exploration approach [18] which is a centralized approach ,it gives importance to communication between robots when exploring distant regions in the environments. It is suitable in environments where communication drop out is an issue. Shortcoming of this approach lies in the fact that it requires separate explorer robots, relay robots and a central station, thus consuming much resources. Role-based method is also prune to complete failure in case of central station going down.

C. Distributed Approaches

Authors have also taken into consideration approaches that leads to faster distribution of robots in environments which is ideal for saving exploration time as well as power consumption by robots. Researchers have applied various techniques. Unsupervised clustering technique using k-means algorithm as proposed by Solanas and Garcia [11], divided the explored area into as many clusters as available robots. Also segmentation based approach was adapted by Wurm, Stachniss and Burgard [3] where robots were assigned different regions in an environment to explore using graph partitioning and Hungarian algorithm. Arezoumand, Mashohor and Marhaban, came up with an another segmentation approach which aimed at finding objects in exploration mission [19]. Lopez-Perez et al [20] proposed idea of splitting of the scene by assigning frontiers their weights for each robot to explore different regions.

Nowadays a key objective in exploration is planning an optimal path for robots in dynamic environments. In dynamic environments, robots have to deal with unknown obstructions in their planned path during navigation which we have considered here. This makes exploration mission really challenging. In such manner [21] thought of an algorithm that looked through a few way portions to make robot move towards its goal. Tazir et al [22] used static and dynamic modules to integrate two navigation methods by using prior information to find a global path in an efficient manner by applying a combination of Genetic algorithms and Dijkstra algorithm. In [23], adaptive dimensionality algorithm was applied to speed up path planning in changing environments for a robot without any assumptions on its motion model.

III. Environment Model

2D occupancy grid model of environment is considered here representing status of cells as free, occupied, unknown (frontiers). Status of the cell is determined by sensor information of robots.

A. Assumptions

- Every robot possess skills to map the environment and localize itself in it.
- Environment to be mapped is globally known and locally unknown.
- Multi-Robots can occupy a single grid.
- All robots are assumed to be holonomic (can move in all directions)
- The simulated robots are homogeneous with same sensing capabilities.
- Dynamic environment means only changing position of obstacles in the environment and not failure of robots.

B. Objectives

- To explore the whole environment in minimum time.
- Robots should consume less energy in mission.
- Robots should quickly overcome dynamics of the environment.

C. Terminologies used

- FREE CELL – Robot detected from sensors that the cell is free from obstacle but has not visited neither explored that cell.
- OCCUPIED CELL– Robot detected that the cell is occupied by obstacle or explored by another robot.
- UNKNOWN CELL – Robot has not detected neither explored that cell.
- FRONTIER CELL: Boundary between free and unknown space.
- SEGMENT: Separate portion of an environment for each robot to explore.

D. Significance of work

- Exploration approach is fully distributive.
- Approach deals with unstructured environments which are complex instead of simple structured ones.

- In addition to unstructured, dynamics of environment is also highlighted at the same time.
- Fast re-planning is applied in unpredictable scenarios.

IV. METHODOLOGY

Operational flow of our methodology is illustrated in Fig 1.

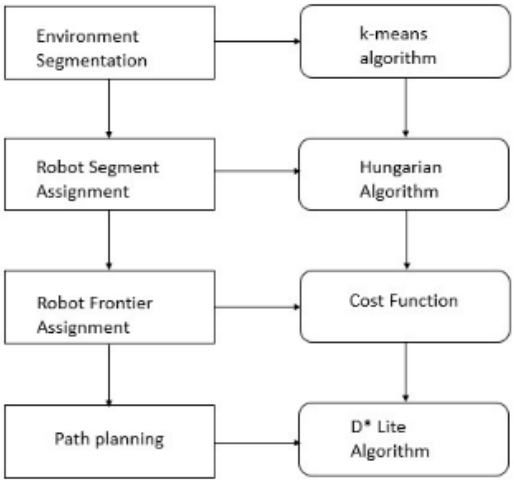

Figure 1. Methodology

A. Environment Segmentation

Unexplored space is divided into same number of segments as team members involved by the application of k-means algorithm [24]. Here, K corresponds to total team members involved in exploration and objects represent unknown cells which are expressed in 2D coordinates. The centroids of the k clusters are haphazardly set at start. Afterwards the algorithm makes modifications to centroids at every iteration till convergence condition is achieved, thus resulting in a group of k different clusters (segments) having center of mass as resulting centroids [11].

B. Robot Segment Assignment

After division of environment into segments, the approach decides for assignment of segments to each member in the team. The target is to choose such an optimal assignment so that total travelling cost of the team is reduced efficiently. Therefore, it is essential to architect a good solution to assign robots to their segments efficiently. We have used Hungarian method for this purpose [25]. This method handovers optimal assignment of robots to their segments, thus reducing travelling cost of robots in terms of distance.

Assignment is written in the form of 'n * n' cost matrix in (1) [12] which denotes the cost of all personal assignments of team members to their segments.

$$\begin{vmatrix} C11 & C12 & C13 & C1n \\ C21 & C22 & C23 & C2n \\ C31 & C32 & C33 & C3n \\ Cn1 & Cn2 & Cn3 & Cnn \end{vmatrix} \quad (1)$$

Here, each Ci value in the matrix denotes the travelling path the concerned robot has to pass through for reaching its assigned goal. Here position of robots are the source and centroid of a region are goals. The planning of path from a robot to reach its goal is accomplished by applying D* lite path planning algorithm [26] which is also well suited for re-planning in dynamic environments.

Steps of the Hungarian method [3] are as following:

1. Compute a reduced cost matrix by subtracting from each element the minimum element in its row. Afterwards do the same with the minimal element in each column.

2. Find the minimal number of horizontal and vertical lines required to cover all the zeros in the matrix. In case, exactly n lines are required, the optimal assignment is given by the zeros covered by n lines. Otherwise, continue with step 3.

3. Find the smallest non-zero element in the reduced cost matrix that is not covered by a horizontal or vertical line. Subtract this value from each uncovered element in the matrix. Furthermore, add this value to each element in the reduced cost matrix that is covered by a horizontal and a vertical line, continue with step 2.

C. Frontier Assignment using minimum cost

Here we choose those frontier cells as target points that can produce lowest costs. Here cost is defined in terms of distance to travel and is determined with the help of path planning algorithm.

Cost function is represented as:

$$Costij = \begin{cases} Cij + pj & Fj \in ri \\ \Delta + d(Fj, ci) + pj & Fj \notin ri \end{cases} \quad (2)$$

Terms used in (2) are specified in Table 1.

TABLE I. TERMS AND SPECIFICATIONS

Terms	Specifications
Fj	Frontier cell under consideration by a robot
ri	Region allotted to robot
Δ	Constant denoting the largest distance that can be measured on the map
ci	Centroid of the region
d	Euclidean separation between two points
pj	Penalization term of a frontier initially set to zero

The above cost function in (2) keeps robots dispersed while exploring and also assigns them frontier cells having the least cost. According to (2) frontier cells which are not related to the segment allotted to a robot are penalized by huge value Δ. Furthermore this condition assures that robots will go on

exploring their assigned segments. As a robot arrive at a target frontier, it start scanning the environment and updating the whole map, after that another goal is selected by repeating the same phenomenon and so on, As soon as detection of predefined number of unknown frontier cells is completed by robots, k means clustering process is applied to redistribute the rest of the cells and it stops until all cells are known in the environment.

D. Path-Planning

We have used D* Lite algorithm for calculating the shortest collision free path for all robots. It is fast re-planning methods which calculates most optimal paths between the present state of the robot and destination state again and again as variations come in graph,s edge cost as the robot advances towards the destination state [26]. Algorithm uses heuristic functions for restricting re-planning process to only states that are relevant for repairing the path. Thus it is well suited for dynamic environments. This algorithm searches from the destination state towards the present state of a robot.

A* algorithm used by researchers [12] for finding shortest path is suitable for those environments whose complete topography is known and will remain known throughout exploration. On the other hand D* Lite as used in our approach can plan a path efficiently in environments where topography is not completely known and is changing with time.

V. EXPERIMENTATION

We executed our methodology using Python based simulator running under operating system Ubuntu 16.04. For visualization we used cv2 python library. Robots used in simulation were holonomic robots (which can move in any direction) equipped with range sensors having a sensing range of 45 pixels in each direction. Environment in which experiments were performed consisted of three difficult levels with varying complexities as shown in Fig 2.

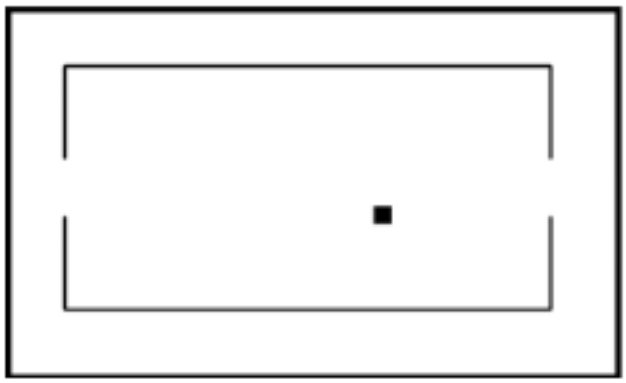

(a) Occupancy grid easy

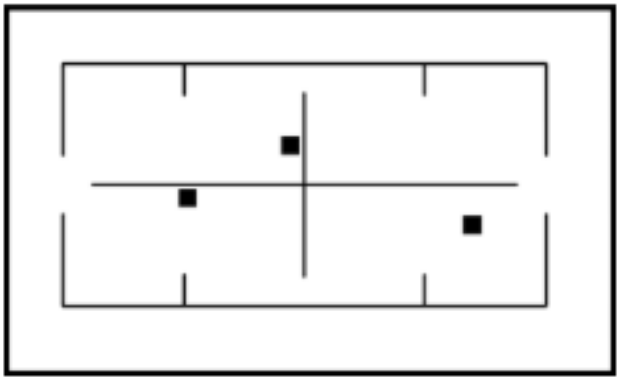

(b) Occupancy grid moderate

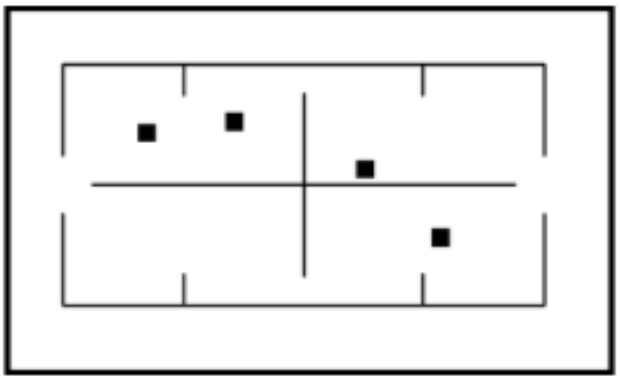

(c) Occupancy grid difficult

Figure 2. Simulation environments

We conducted experiments by varying team sizes from 1 to 8 robots in all environments. Size of the all three environments was set to 632×1044 pixels. During exploration we also changed position of obstacles in every iteration in environments given in Fig 2 to check robustness of our methodology. Our performance indicator was total time (in seconds) taken by robots to complete the exploration.

VI. RESULTS

As described in section 5, we check robustness of our approach in three different simulation environments with changing obstacle positions for each simulation run. We compared results of proposed method with Pruned Frontier method [12]. As stated earlier we assume here that all robots possess mapping, localization and communication capabilities.

For difficulty level easy, our complete exploration trajectories for team consisting of 4, 6, 8 robots is illustrated in Fig 3.

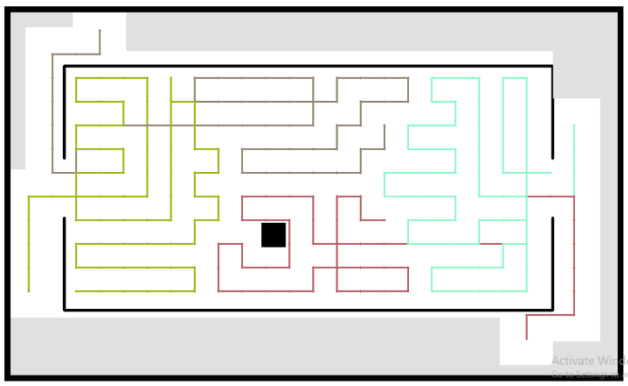

(a) Exploration by 4 robots

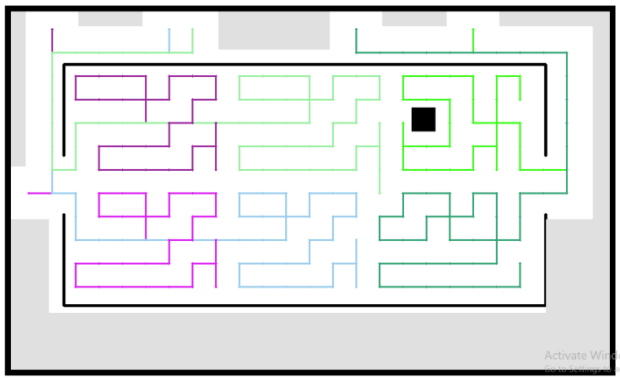

(b) Exploration by 6 robots

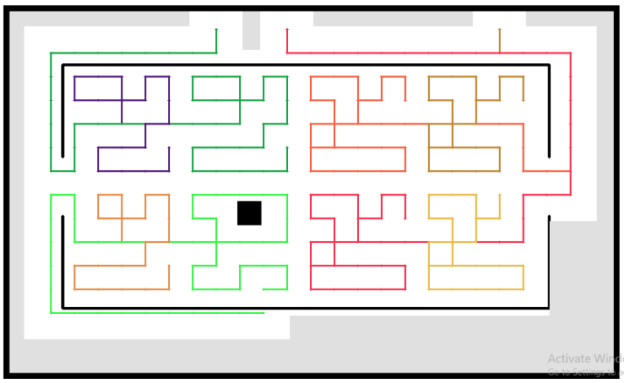

(c) Exploration by 8 robots

Figure 3. Exploration trajectories in occupancy grid easy

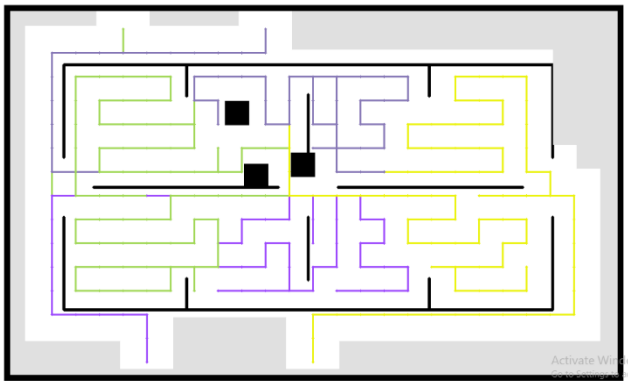

(a) Exploration by 4 robots

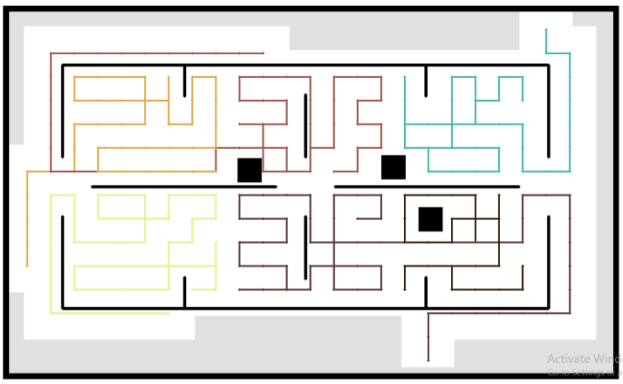

(b) Exploration by 6 robots

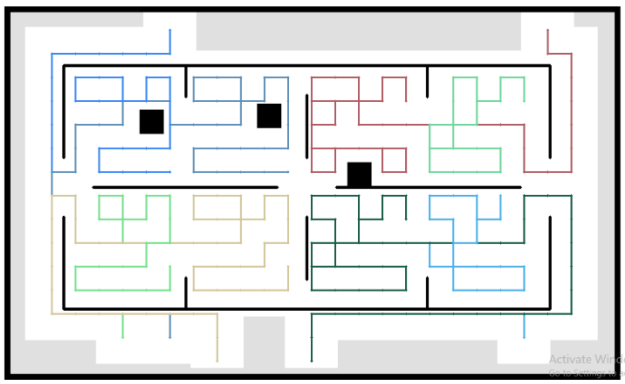

(c) Exploration by 8 robots

Figure 4. Exploration trajectories in occupancy grid moderate

From Fig 3(a), 3(b) and 3(c), it can be seen that position of obstacle is changing at every iteration.

For difficulty level moderate, the complete exploration trajectories for team consisting of 4, 6, 8 robots is illustrated in Fig 4.

Similarly for difficulty level difficult, the complete exploration trajectories for team consisting of 4, 6, 8 robots is illustrated in Fig 5.

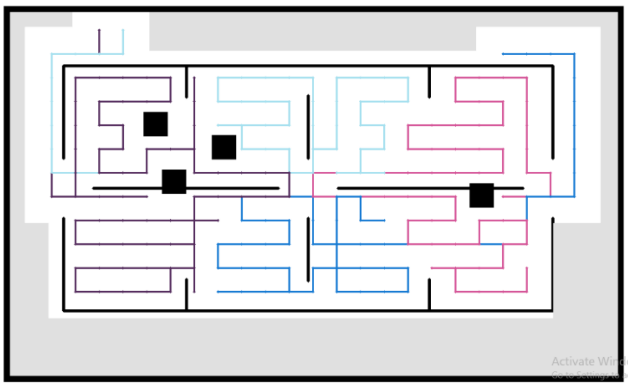

(a) Exploration by 4 robot

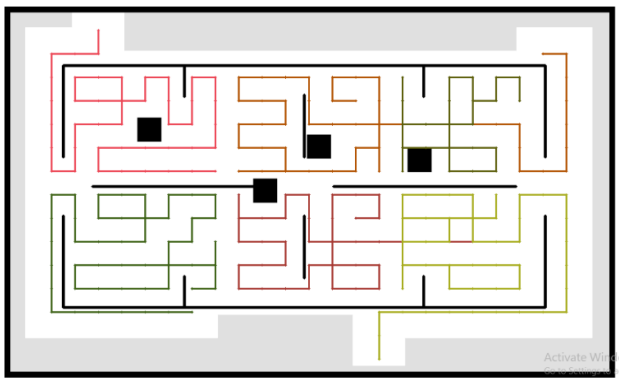

(a) Exploration by 6 robots

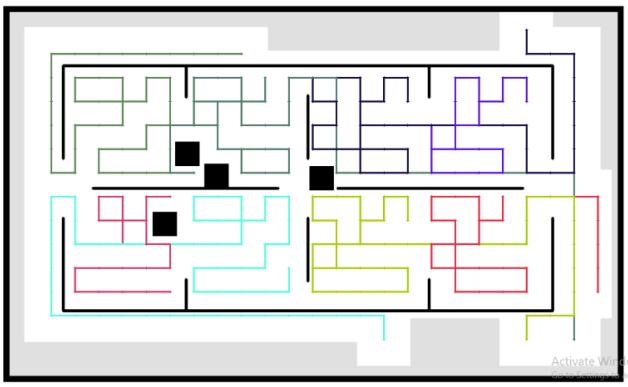

(b) Exploration by 8 robots

Figure 5. Exploration trajectories in occupancy grid difficult

We selected performance indicator as exploration time in seconds in simulation runs. Exploration time graph vs number of robots is plotted for teams of 1-8 robots in all three difficulty levels as illustrated in Fig 6.

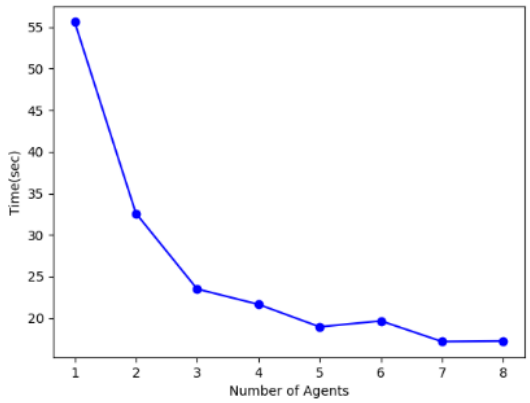

(a) Occupancy grid easy

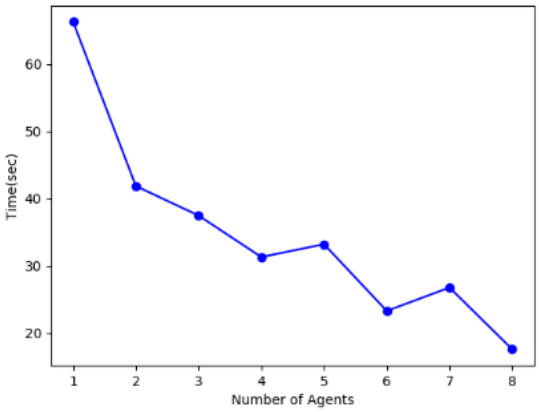

(b) Occupancy grid moderate

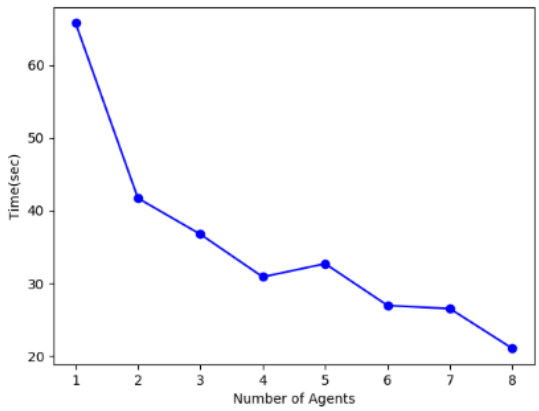

(c) Occupancy grid difficult

Figure 6. No of robots vs exploration time graphs

We cor
in terms
environment sizes were very large as compared to our maps, we scaled their exploration time according to our environment size. Results comparison in difficulty levels moderate and difficult are shown in Fig 7.

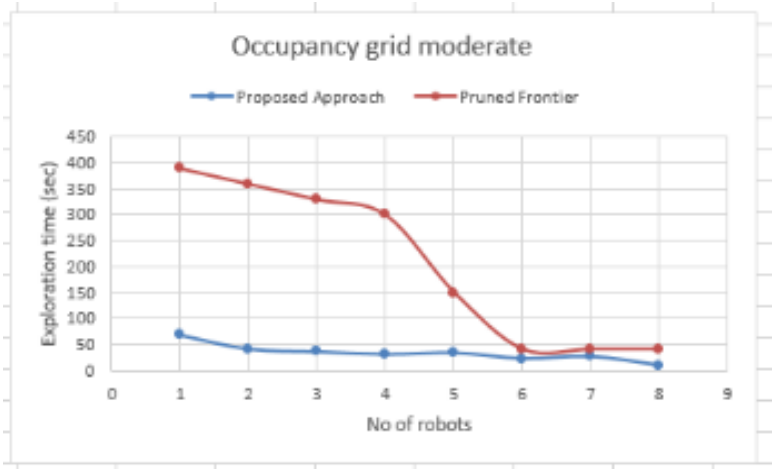

(a) Occupancy grid moderate

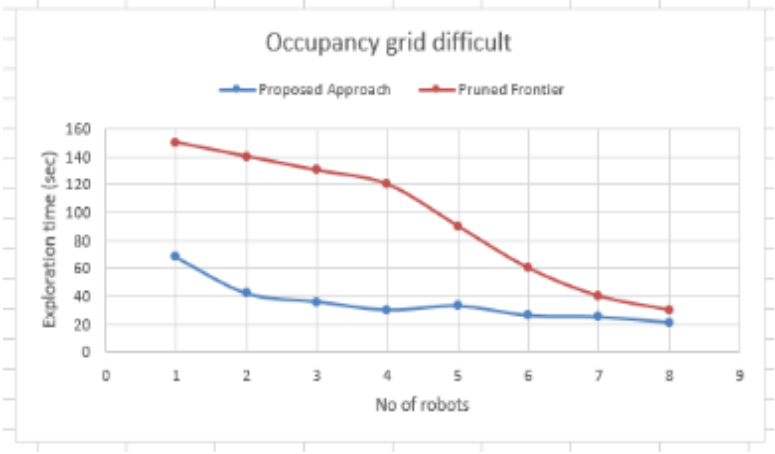

(b) Occupancy grid difficult

Figure 7. Comparison of results

From these results, it is very clear that our approach is time efficient in both difficulty levels moderate as well as difficult. For team size of 1-5 robots our approach is far superior in both environments, while for 6-8 robots, pruned frontier is nearly as good as our method.

CONCUSLION

The work presents exploration by a team of holonomic robots in an unknown environment which assures full distribution of robots in the environment by assigning them separate portions, thus making exploration time efficient. The work also highlights faster re-planning of multi-robots in unstructured and dynamic environments at the same time. As an additional factor, this approach also saves energy consumption by all robots because as time is reduced, power is also less consumed by each robot. We also tested our methodology by varying difficulty levels during experimentation and compared our approach with one approach in different environments and results proved the domination of our methodology in terms of exploration time.

REFERENCES

[1] C. Stachniss and W. Burgard, "Exploring unknown environments with mobile robots using coverage maps," *IJCAI Int. Jt. Conf. Artif. Intell.*, pp. 1127–1132, 2003.

[2] L. Bravo, U. Ruiz, R. Murrieta-cid, G. Aguilar, and E. Chavez, "A distributed exploration algorithm for unknown environments with multiple obstacles by multiple robots A distributed exploration algorithm for unknown environments with multiple obstacles by multiple robots," no. December, 2017.

[3] K. M. Wurm, C. Stachniss, and W. Burgard, "Coordinated multi- robot exploration using a segmentation of the environment," in *2008 IEEE/RSJ International Conference on Intelligent Robots and Systems, IROS*, 2008, pp. 1160–1165.

[4] P. G. C. N. Senarathne and D. Wang, "A two-level approach formulti-robot coordinated exploration of unstructured environments," *Proc. ACM Symp. Appl. Comput.*, pp. 274–279, 2012.

[5] F. Abrate, B. Bona, and M. Indri, "Map updating in dynamic environments," *Robot. (ISR), 2010 …*, vol. 83, pp. 296–303, 2010.

[6] C. P. Mcmillen, P. E. Rybski, and M. M. Veloso, "LEVELS OF MULTI-ROBOT COORDINATION FOR DYNAMIC ENVIRONMENTS," pp. 1–12.

[7] B. Yamauchi, “Yamauchi-frontierExploration98,” no. May, 1998.

[8] R. Sharma K., D. Honc, F. Dusek, and G. Kumar T., “Frontier Based Multi Robot Area Exploration Using Prioritized Routing,” pp. 25–30, 2016.

[9] R. Simmons *et al.*, “Coordination for Multi-Robot Exploration and Mapping,” *Proc. Natl. Conf. Artif. Intell.*, pp. 852–858, 2000.

[10] J. A. Castellanos, J. M. M. Montiel, J. Neira, and J. D. Tardós, “The SPmap: A probabilistic framework for simultaneous localization and map building,” *IEEE Trans. Robot. Autom.*, vol. 15, no. 5, pp. 948–952, 1999.

[11] A. Solanas and M. A. Garcia, “Coordinated multi-robot exploration through unsupervised clustering of unknown space,” pp. 717–721, 2005.

[12] A. Pal, R. Tiwari, and A. Shukla, “Multi robot exploration using a modified A* algorithm,” *Lect. Notes Comput. Sci. (including Subser. Lect. Notes Artif. Intell. Lect. Notes Bioinformatics)*, vol. 6591 LNAI, no. PART 1, pp. 506–516, 2011.

[13] A. Pal, R. Tiwari, and A. Shukla, “Multi robot exploration through pruning frontiers,” *Adv. Mater. Res.*, vol. 462, pp. 609–616, 2012.

[14] B. Yamauchi, “Frontier-based exploration using multiple robots,” no. May, pp. 47–53, 2004.

[15] R. Zlot, A. Stentz, M. B. Dias, and S. Thayer, “Multi-robot exploration controlled by a market economy,” pp. 3016–3023, 2003.

[16] H. Lau, “Behavioural approach for multi-robot exploration,” *Australas. Conf. Robot. Autom.*, pp. 1–7, 2003.

[17] A. Renzaglia and A. Martinelli, “Potential field based approach for coordinate exploration with a multi-robot team,” *8th IEEE Int. Work. Safety, Secur. Rescue Robot. SSRR-2010*, 2010.

[18] J. De Hoog and S. Cameron, “<Dynamic Team Hierarchies in.pdf>.”

[19] R. Arezoumand, S. Mashohor, and M. H. Marhaban, “Finding Objects with Segmentation Strategy based Multi Robot Exploration in Unknown Environment,” *Procedia - Soc. Behav. Sci.*, vol. 97, pp. 580–586, 2013.

[20] J. J. Lopez-perez, U. H. Hernandez-belmonte, M. A. Contreras-cruz, and V. Ayala-ramirez, “Distributed Multirobot Exploration Based on Scene Partitioning and Frontier Selection,” vol. 2018, 2018.

[21] H. Liu, H. Wen, and Y. Li, “Path Planning in Changing Environments by Using Optimal Path Segment Search,” pp. 1439–1445, 2009.

[22] M. L. Tazir, O. Azouaoui, M. Hazerchi, and M. Brahimi, “Mobile Robot Path Planning for Complex Dynamic Environments,” 2015.

[23] A. Vemula, K. Muelling, and J. Oh, “Path Planning in Dynamic Environments with Adaptive Dimensionality.”

[24] R. S. Society, R. S. Society, and A. Statistics, “Algorithm AS 136 A K-Means Clustering Algorithm,” vol. 28, no. 1, pp. 100–108, 2012.

[25] Harvard University, “The Assignment Problem and the Hungarian Method,” *Introd. to Linear Algebr. Multivariable Calc.*, 2005.

[26] S. Koenig and M. Likhachev, “D* Lite,” *Proc. Natl. Conf. Artif. Intell.*, pp. 476–483, 2002.

IJEW 国际工程期刊 International Journal of Engineering Works انجینئرنگ کاموں کا بین الاقوامی جرنل

International Journal of Engineering Works
ISSN-p: 2521-2419
ISSN-e: 2409-2770
Vol. 7, Issue 04, PP. 197-202, April 2020
https://www.ijew.io/
https://doi.org/10.34259/ijew.20.704197202

Simulation and Design of CIGS thin Film Solar Cell using Distributed Bragg Reflector

Muhammad Awais[1], Saddam Hussain[2], Muhammad Babar Iqbal[3]
[1,2,3] Department of Renewable Energy Engineering, U.S Pakistan Center for Advance Studies in Energy, University of Engineering and Technology Peshawar, Pakistan
qari2162@gmail.com[1], saddamahmad313@gmail.com[2], engr.mbabariqbal@gmail.com[3]
Received: 20 March, Revised: 26 March, Accepted: 31 March

***Abstract*—** CIGS is a better replacement of Si solar cell having low possibility of damage different layers is used for CIGS cell which decreases short current losses. CIGS solar cell technology is a very highly competitive and also need less raw material as well as low cost of fabrication. As compared to C-Si (~11000C) thermal budge is very low for the production of CIGS modules about (~550 0C approximately). The comparison of weight C-Si solar panels have lesser weight than CIGS because in CIGS solar panels there are two glass panes and in C-Si there is only one pane of glass are used. The absorption coefficient of CIGS is high as compare to C-Si because CIGS solar cells using direct band gap materials and C-Si included in indirect band gap material and having lower absorption coefficient property (104/cm) that's why CIGS solar cell thickness is 100 times lesser than as compare to C-Si solar cells. There are a lot of techniques to increase the efficiency and decrease transmission losses but the scope of this work covers how to use DBR (Distributed Bragg Reflector) as a back reflector and also examining its effect on decreasing thickness of the absorber layer. In real world it is not possible to reduce the transmission losses approximately equal to zero because some part of the light is absorbed and lost in metal used at the rear surface of the cell in the form of heat but reflection losses can be reduced up to zero. It is seen that mostly in conventional thin film solar cells thick metal plate is used at the rear surface of the solar cell for increasing reflection and decreasing transmission losses at the back surface of the cell. A huge proportion of heat is lost due to the collision of incident photons with metallic surfaces. However, DBR is tested in CIGS solar cell for increasing back surface reflection and increasing light trapping by this research work.

Keywords: Buffer layer, window layer, Independent Spectroscopy, Distributed Bragg Reflector, Soda lime glass.

I. INTRODUCTION

Direct solar energy is a type of renewable energy in which electrical energy generated based on utilizing solar irradiance in the form of light or heat. Some green and clean energy technologies are indirectly dependent on sunlight and solar irradiance for generation of electric power such as tidal and wind energy technologies. Different amount of thermal energy absorbed by several materials on earth's surface such as water, oceans, ground, etc. which has the capability to cause variation in thermal potential. Thus when wind blows it is important for normalize the temperature variance. Solar PV technology uses solar irradiance and changes it to Electrical power using photovoltaic (PV) [1]. However there are several technologies of solar cells but amongst them thin film is the most active option because they are flexible nature and light weight. Among thin film solar cells CIGS (copper indium gallium Selenide) is the leading technology in the market thin film solar cells are the leading thin film due to its mechanical flexibility and durability cost effective and reliable fabrication process. It is a compound related to the quaternary Selenide semiconductor alloy.

However the efficiency and performance of CIGS solar cell is not larger than much advanced multijunction cells or C-Si based solar cell but research work is in progress to reduce this efficiency gap. Many methods have been examined to increase the efficiency of CIGS solar cell the performance parameter of cell on depends on thickness, band gap and doping each portion of the cell. Word direct solar means those renewable energy technologies which based on solar energy from sun directly. Among all other technologies of solar cells thin film is the most attractive option because they are flexible nature and light weight. CIGS (copper indium gallium Selenide) thin film solar cells are the leading thin film technology in market it is a compound similar to quaternary semiconductor alloy. The properties like durability and mechanical flexibility presents attractive features for both military and civilian these properties are because of material properties used in CIGS solar cells [2].

As declare by the world energy council the total energy reaching on the earth is 7500 times' excess than the total world energy consumption [3]. Copper indium gallium di-seleniod (CIGS) based thin film cells are drawing worldwide attention and focus they are efficient for solar based power generation and has achieved 20.7% quantum Efficiency as associated to crystalline carbon silicon wafer based solar cell. CIGS is good absorber material which have attracted a good attention because of its band gap (~1.0-1.12ev) and having appropriate absorption coefficient (105/cm) and after usage very minor material

wastage Unit cell of CIGS has tetragonal geometry [4, 5]. Focus was given to its efficiency the modern of these with using a few years of research behind them changed 22% of incoming solar power to electrical power [6]. When thickness of the absorber layer decreases from 1500m to 600nm and the use of In2O3: H (IOH) both as back and front TCO, combined with a unique 2-D grating structure, led to increase and shows improvement up to 25% optical performance as compared to equally thick flat device [7]. Optoelectronic nano patterning path to reduce material consumption and increase efficiency of the cells [8]. Transparent conductive oxide (TCO) used as a front electrode for thin film solar cells and plays a major role in defining the maximum efficiency. Doped ZnO is a prominent TCO material which is extensively used in (a-Si) and CIGS thin film solar cells [9]. Combining nano-sized local point's contacts and rear surface passivation layer is one of them. For generation point contact openings atomic layer deposition (ALD) of Al2O3 is used for CIGS surface passivation and generate nano-sphere precipitates. The nano-sized local rear point contacts with Al2O3 rear surface passivated CIGS cell shows a significant development in open circuit voltage (Voc) as compared to an unpassivated reference cells [10]. The cost of CuInGeSe2 (CIGS) have already arrived in to the market having cost almost equal or lower than the conventional Si based solar cells [11].

The cells performance has been considering impact changes in hole or electron minority carrier life time and carrier density and efficiency record [12]. Now the first company of solar cell has stated recently maximum cell efficiency by 20.4% and a module efficiency reaching by 13.9% noted in laboratory conditions [13]. Explicitly metallic back reflectors would also act as electrodes for a cell, metals damage and suffer from intrinsic absorption losses incurred at the interface and surface. This absorption would be reduced by adding and inserting an optical spacing layer [14]. For all conductive webs would be used for both a- Si and CuInSe2, so a single cell is designed by edging and cutting the web then put on a metal grid manufacturing structure for developing the front contact to the cell and then assembling in group series manner to C- Si module [15]. That time it was the first thin film company which expresses "reliability and performance of thin film PV" which assist large scale PV modules and significantly decrease PV module cost and has attained the smallest manufacturing and power generation cost particularly for industry about 1$ per watt [16].

CIGS is one of the three mainstreamed thin film technology the other two technologies are CdTe and amorphous Silicon (a-Si). CIGS layer is flexible, thin and would be able to be deposited on a very flexible material. Earth receives huge amount of energy from sun for millions of years. The sun is just like of a fusion reactor and provides incredible amount of energy to earth. The evaluation and history of the cell is very dramatic [17]. CIGS has maximum absorption coefficient material of 10^5/cm so a film of thickness 1-2 µm very suitable for absorption most of the light which is altered from Si solar cell having cell thickness 200-300 µm. The required layer of CIGS is so thin, flexible and confirmed as a stable device outside, inside testing and is more trustworthy to high energy radiation as match to other thin film solar cell devices [18].

II. METHODOLOGY

The research work explains numerous methods unified to reflection losses in photovoltaic solar cell. At the very first stage we have explained some old methods then in second stage we associate new methods and techniques to the existing ones and have used PV Light house online software for consistent and advance results. PV light house software most possibly used for simulation and designing purposes to find optical and electrical properties of solar cell devices. The university of New South Wales (UNSW) PV light house and have officially publicized major free access solar cell fabrication simulator online. PV factory have said that all physics processes integrate in to a software package which is easy to understand, practice and which has been treated by over 500000 virtual cells throughout data testing. Improvements are likely to include more recording process steps and adding production lines.

The main resolve of the research is to minimize reflection losses by a special technique introducing Distributed Bragg Reflector (DBR) with different materials and then examined its efficiency for solar cells. This work also explains the variation of size and its effect on active region of thin film solar cell. However, we have used different software in this research work such as (originpro, SunSolve, webplot digitilizer) mostly concentrated on solar cell simulation processes, so we would associate new materials for DBR as a back reflector and at last relate these results for a specific range of DBR. The paper has given information about electrical properties of the materials so one can extent current and voltage (I-V) curve, short circuit current density (Jsc) and fill factor (FF) from (I-V) curve also can extent open circuit voltage (Voc), then at the end External quantum efficiency (EQE) of the solar cell was noted.

This research described various means associated to optical and reflection losses in photovoltaic. In the beginning we explained some old methods then in second stages we correlate new approaches and results to the current ones and have used PV Light house online software for reliable results. During simulation of various materials the optical and electrical properties of materials must kept in record so that it would be easily recognized that how efficiently photons or light energy transmuted in to electrical energy. Sun-Solve simulator contains both electrical and optical prototypes to produce extrapolative and precise device simulation. The model solves and processes the equation in 2D or1D this may be in time domain or steady state. The model described the transfer of charge within the device by solve hole and drift –diffusion and carrier continuity equations exactly in position space. Using Sun-Solve simulator we fabricated a design of CIGS solar cell involving DBR (distributed Bragg reflector) Fig.1 shows a solar cell in Sun-Solve simulator.

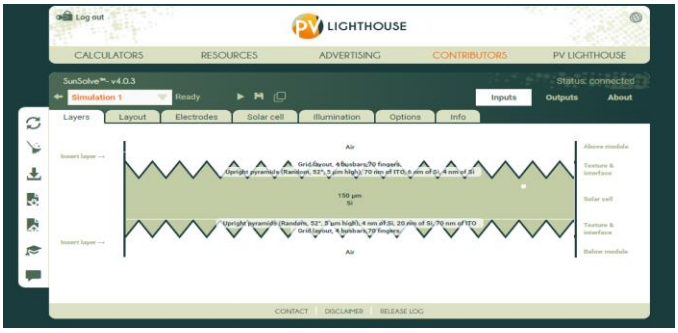

Figure 1. Sun-Solve simulator window

After getting access to the software and login to the software and then further select C-Si HJ cell so we could see a prototype solar cell. We have to select explicitly the upper most layer and then introducing films according to the desire and exact model of CIGS thin film solar cell and enlarge thickness of each film by giving electrical and optical details of layer, in second layer we add-on glass which act as a transparent layer and after this layer we add-on reflectors that in Ag (silver) or inserting DBR (distributed Bragg reflector), DBR contain alternate layers of Si and SiO2layer.

III. Discussion and Results

This Paper have publicized that PV lighthouse software has been used for simulation and designing of CIGS solar cell. After officially login to the Sun-Solve ray tracer module of sun solve simulator to process and simulate our CIGS model. There are various kinds of cells but for CIGS thin film select c-Si HJ solar cell and it generates a new model with different layers. Modern commercially and industrially formed CIGS cells containing six specific layers and hence each layer has specific function and parameters first of all substrate is essential then various layers are placed through various commercial methods. The model of CIGS cell is shown in Fig.2.

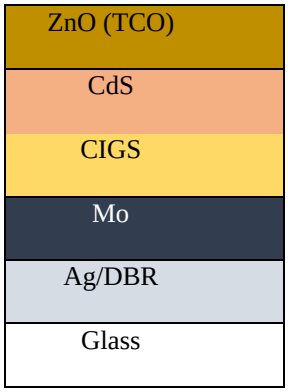

Figure 2. Sun-Solve model of CIGS thin film cell during Simulation

Several techniques have been recognized for fabrication CIGS solar cell. However, we have deliberated several layers and its optimization and fabrication for different layers. The first layer of CIGS solar cell is substrate which shows that the solar cell is may be rigid and flexible. Glass are the most frankly and commonly available substrate because of resist to corrosion and low cost. Commonly soda lime glass (SLG) usedfor increasing manufacturing and performance. However, we have used Glass in Sun-Solve CIGS model having thickness of 1000 nm. Which is to be found just beneath the ITO layer? It is thin and light weight. Generally back contact of the CIGS cell is reserved below the active layer and above the back reflector. It is fabricated especially for the collecting of carriers which are generated in the absorber layer. Typically Back contact is a metal serves as anode or positive lead having low resistivity. Though, in CIGS cells, most of the situations molybdenum (Mo) is used because of its compatibility and flexibility in the fabrication process. As long as during optimization deviation in the thickness of back contact current density in the absorber layer also varies shown in the Table I.

TABLE I. VARIATION OF JSC IN THE ACTIVE LAYER BY CHANGING THICKNESS OF BACK CONTACT (MO) THICKNESS

Back Contact (Mo) Thickness	**Current density in the absorber layer (J_{sc}) mA/cm^2**
10m	335
20m	336
30m	336
40m	337
50m	337
60m	338
70m	338

Hence in 10 nm thickness is chosen for the model so at this thickness average current density (Jsc) is 33.5 mA/cm2 which is appropriate for the absorber layer. Active layer is the key layer where majority of carrier generation occur. Though, CIGS also documented as chalcopyrite is an I-III-VI semiconductor. Essentially CIGS (copper indium gallium di-Seleniod) also an alloy consist of CuInSe2 (CIS) &CuGaSe2 (CGS) having direct band gap materials and excessive absorption coefficient with band gap having range of 1.07eV to 1.75 eV. However, values of the band gap has mostly covered the higher energies and infrared range of the solar spectrum so that most of the incoming light being entranced close to the P-n hetero junction molded with the CdS film. Hence, this characteristic permits the active layer CIGS with more thickness than traditional C-Si solar cells. The thickness of the active layer changes from 200 nm to 800 nm and current density (Jsc) also varies from 23.7 to 30.4mA/cm2 as we can see from the Table II.

TABLE II. VARIATION OF (JSC) IN THE ABSORBER LAYER BY CHANGING THICKNESS OF THE CIGS.

Absorber Thickness (CIGS)	Current density(J_{sc})mA/cm^2
200 nm	23.6
250 nm	24.7
300 nm	25.2
350 nm	26.4
400 nm	27.5
500 nm	28.1
550 nm	28.4
600 nm	28.6
650 nm	29.1
700 nm	29.4

Hence, from the above argument it is clear that after optimization we fixed thickness of the absorber layer on 670 nm having current density (Jsc) of 29.5mA/cm2. Definitely, Buffer layer provide n-type hetero junction of CIGS solar cell. However, thin film of CdS having most possibly band gap of 2.4 eV may allow maximum amount of the usable photons to conduct through. Though Cd is toxic but there is no suitable alternative that has same level of performance so here, varying the thickness of CdS buffer layer and tested for performance and current density at the absorber layer as shown in the Table III.

TABLE III. VARIATION OF JSC IN ACTIVE LAYER BY CHANGING THICKNESS OF CDS

CdS Buffer layer	Current density J_{sc} in absorber layer
5 nm	33.6
10 nm	33.7
20 nm	32.9
30 nm	32.1
40 nm	32.2

However, by changing the thickness of buffer layer current density and efficiency varies that's why buffer layer thickness has been fixed at 10 nm thickness. Window layer is fabricated with a comparable function as the back contact. This window layer collects the carriers which are basically generated in the active layer and transmit it to the load. This layer is the upper layer of the so it should be transparent to the maximum range of light spectrum so that is essential for generation of carriers and photoelectric effect. Mostly transparent conductive oxide (TCO) has used as a window layer an effective TCO having broad band gap and permits large number of photons to go in to the active layer. This is also essential that the TCO layer has low resistivity and low recombination losses. Normally CIGScells use ZnO for TCO layer having range of band gap 3.3 eV. However, ZnO is experienced for a series of its thickness as shown in the Table IV.

TABLE IV. DEVIATION OF (JSC) IN ABSORBER LAYER BY CHANGING THICKNESS OF WINDOW LAYER.

TCO (ZnO) Thickness	current Density (J_{sc}) of Active layer
10 nm	27.8
20 nm	27.8
30 nm	27.9
40 nm	28.2
50 nm	28.3
60 nm	28.8
70 nm	29.1
80 nm	29.3
90 nm	29.9
100 nm	30.1
110 nm	30.1

Hence, 90 nm thickness of ZnO is secure in the window layer having current density is 29.9 nm which is a very competent value.

Results with using (Ag) as a Back reflector:

As mentioned above different results of the simulated model it is essential to check absorption of photons when using silver (Ag) as a back contact then examine the efficiency and absorption using DBR as a back reflector in term of absorption and reflection loss. Hence using Ag as a back reflector the number of the photons are captivated by the Silver and losses occurs that's why current density (Jsc) comes to 29.6 mA/cm2 as we can see in Fig. 3 external quantum efficiency (%EQE) goes decreasing after 400nm wavelength, because some of photons are absorbed by the Silver and eventually produce heat.

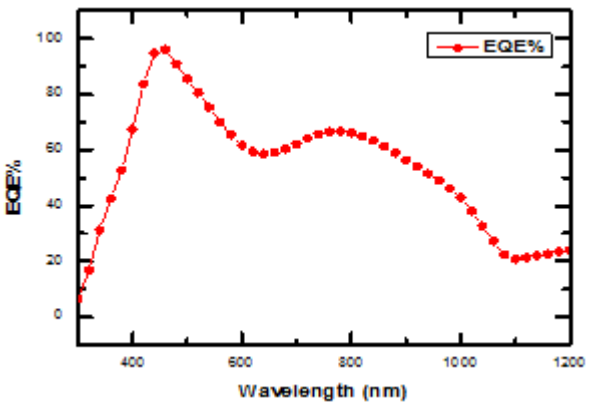

Figure 3. External quantum efficiency (%EQE) with silver as back reflector.

After using silver (Ag) as a back reflector replacing (Ag) with 1 DBR (distributed Bragg Reflector) as a back surface reflector in model. DBR consist of synchronized SiO2 and Si layers. DBR is a material containing of alternate high and low refractive index in the subsequent graph it is exposed that the overall performance of the cell has been upgraded, and photons captivation also have altered across the wavelength. Therefore, current density has upraised up to 30.3mA/cm2 as shown in Fig 4.

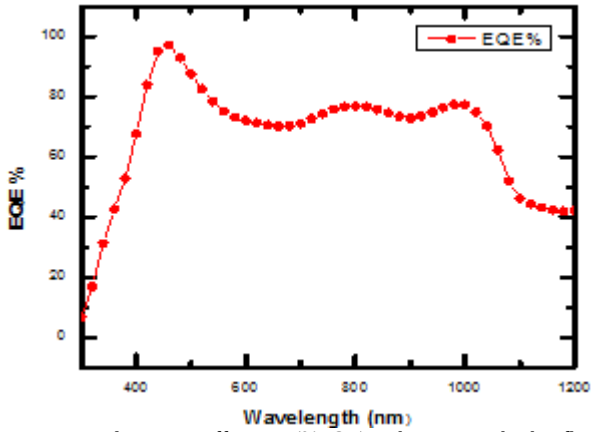

Figure 4. External quantum efficiency (%EQE) with 1 DBR as back reflector.

Hence, after using 1 DBR act as a back reflector replacing it with 2 DBR and it has seen that the cell performance and external quantum efficiency (EQE%) also changed, and definitely current density of the absorber layer amplified up to 32.2 mA/cm2 as shown in Fig 5.

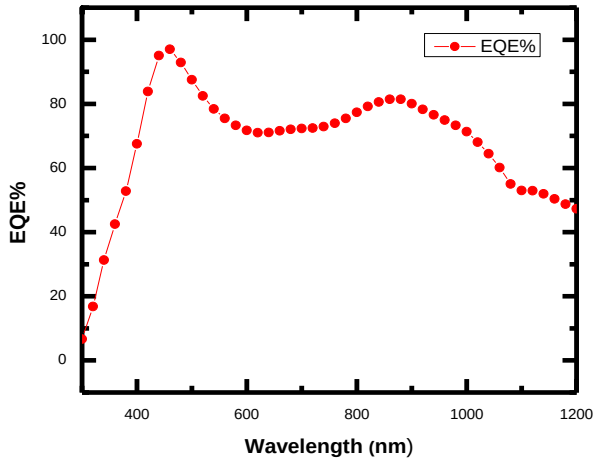

Figure 5. Variation in External quantum efficiency (%EQE) with 2 DBRs as back reflector.

After all for further simulations replacing back reflector 2 DBR with 3 DBR it is has shown from the following graph that the performance and external quantum efficiency upgraded overall the spectrum and the current density (Jsc) also varies to 33.4 mA/cm2 as shown in the Fig 6.

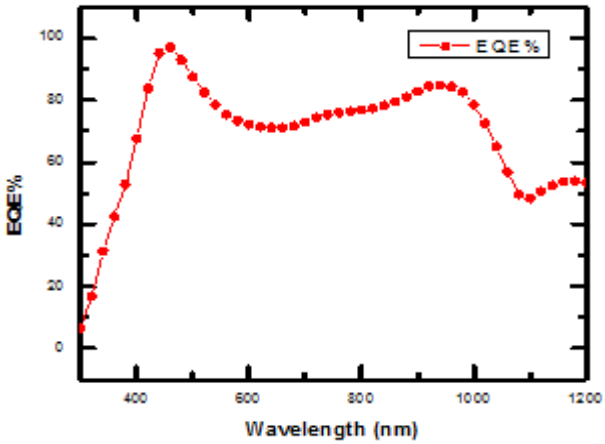

Figure 6. Variation in External quantum efficiency with 3 DBRs as back reflector.

Hence, by changing 3 DBR with 4 DBR act as a back reflector it is clear that the cell (EQE %) has enhanced performance and current density of the cell also promoted to 34.7 mA/cm2 so attraction of the active layer increases as shown in the Fig. 7.

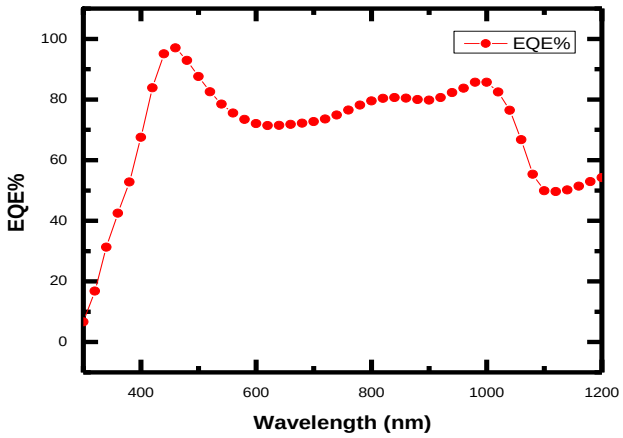

Figure 7. Variation in External quantum efficiency 4 DBRs as back reflector.

However, comparing both the graphs of 4 DBR and Ag the curve shows 4 DBR improved EQE% and performance however, black curve shows Ag EQE% and performance of the absorber layer at larger wavelengths while keeping thickness of the active layer constant. It shows that the cell performance and EQE% has improved at higher wavelengths with 4 DBR as compare to Silver (Ag) as a back reflector in case of 4 DBR more absorption of photons have occurred as shown in Fig.8 .

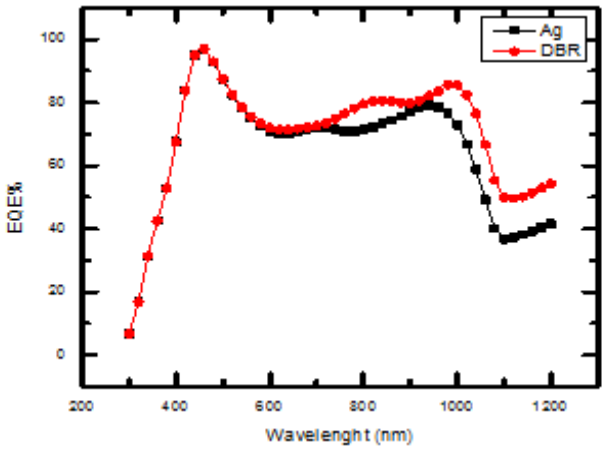

Figure 8. External quantum efficiency comparison using silver and four DBRs as a back reflector.

CONCLUSION

This paper, have revealed work on fabrication and designing of CIGS thin film solar cell though, its illustrations exposed the potential of improved efficiency among the thin film solar cells. As long as the efficiency of the CIGS increases becoming better and near to the C-Si based solar cell. However, there is need to carry out a lot of research work for future to rise its EQE % value close to Shockley queisser limit. This work shows high current density in the active layer that is 34.7 mA/cm2as compared to ideal calculation which is of 37mA/cm2 when all incoming photons transformed in to electron-hole pair generation. However, by inserting several DBR films as a back reflector in place of silver (Ag) therefore can potentially enhance its current density Jsc and EQE % value. This paper mainly focused on optimizing thickness of the CIGS, ZnO and CdS semiconductor layers. CIGS would diverge in band gap so several models would be tested to achieve higher efficiency. An effort would be done by insertion of higher band gap CIGS material above a lower band gap one and generate a dual junction CIGS solar cell.

REFERENCES

[1] S.&.0.P.A.Asumadu-Sarkodie, "The potential of ecnomic vibility of solar photovoltic in Ghana," Energy Sources, Part A: Recovery, Utilization , and Environmental Effects, 2016d.

[2] O.P.M.R.S.Y.S.K. Edenhofer, "Renewable Energy Sources and climate change mitigation," Cambridge: Cambridge University press, 2011.

[3] F.&.M.T.Urban, "Climate, disaster and electricity generation," 2011.

[4] J.F.Guillemoles, in "Thin solid Films", 2002, pp. p.p.404-409.

[5] M.B.F.E.H.a.A.V.P.J.Srour, in "in Phy.Status Solidi", 2016, pp. p.p.1472-1475.

[6] US National Renewable Energy Laboratory, "Best research- Cell efficiencie", 2016.

[7] R.V.Chidozie Onwudinanti, "Advance light management based on peroidic textures for Cu(In,Ga)Se2 thin film solar cells.",Optic Express, vol. vol.24, 2016.

[8] Guanchao Yin, "Optoelectronic Enhancement of Ultrathin CuInGaSe2 solar cells by nano-photonic contact,"Advance optical Materials,2016.

[9] S.Y.Guo, "Textured, doped, ZnO thin films produced by a new process for a-Si and CIGS solar cell application.",Energy Photovoltics,2007.

[10] B.Vermang, "Development of rear surface passivated Cu(In,Ga)Se2 thin film solar cells with non-sized local rear point contacts,"Solar Energy and Solar cells,2013.

[11] W.B.Zentrum, "CIGS-White paper. White paper for thin film solar cell Technology.",2015.

[12] A.a.T.AGESSERT, "Optimization of CdTe Solar cell performance impact of variation of minority carrier life time and carrier density profile,"IEEEJ Photonics1 (1), pp. P.P.99-103, 2011A.

[13] R.Birkmire, "In 33rd IEEE Photovoltic Specialist conf.paper 370," in In conference Rec, 2008.

[14] G.O.D.R.A.i.C.a.C.X.Meng, "Absorbing photonic crystals for silicon thin film solar cells design", fabrication and experimental investigation," Sol Energy Matter. Sol Cells 95, pp. p.p.S32-S38, 2011.

[15] B.J.a.T.A.M.Brnett, "Methods for the continuous manufacture of thin film solar cells,". US Patent 4318938, 9 March 1982.

[16] "First Solar quantity report for 2009," 2009.

[17] J.Perlin, "From Space to earth, study of solar electricity," MI,ATTEC,Publications, 1990.

[18] U. R. K. W. I. M. K. G. H. G. V. M. P. H. W. S. J. H. W. A. Jasenek, "Radiation resistance of Cu(In,Ga)Se2 solar cells under 1MeV Electron Irradiation,"Thin Solid Films, vol. Vols. no. 387, pp. pp. pp. 228-230, 2001.

Muhammad Awais received B.Sc. degree in Electrical (communication) Engineering from University of Engineering and Technology, Peshawar, Pakistan in 2016. He is currently pursuing his Master degree in Renewable Energy Engineering from U.S-Pakistan Center for Advance Studies in Energy, University of Engineering and Technology, Peshawar, Pakistan. His research interests include Power Electronics, wind Turbines, Renewable Energy Materials and Modeling, Photovoltaic Devices.

International Journal of Engineering Works
ISSN-p: 2521-2419
ISSN-e: 2409-2770
Vol. 7, Issue 04, PP. 203-206, April 2020
https://www.ijew.io/
https://doi.org/10.34259/ijew.20.704203206

A Revolution in Health Sector using Wireless Body Area Networks

Sajjad Hussain[1], Majid Ashraf[2]
[1,2] Department of Electrical Engineering, UET Peshawar
engr.sajjadhussain@yahoo.com[1], majid@uetpeshawar.edu.pk[2]
Received: 28 January, Revised: 28 March, Accepted: 30 March

***Abstract*—** Our world has been changed a lot over the past few years. Only a few decades back and you will see that communication among people was not an easy task at all. Thanks to the advancement in technologies especially the networking techniques that have made the lives of the people so comfortable. Now due to these computer networks, communication with your family, friends, and colleagues is so easy all across the globe. This communication is not only limited to the entertainment or information anymore. Wireless Body Area Networks has made it possible for the doctors to keep in touch with their patients and check their health conditions while staying miles away from them physically. This application of Computer Networks is impacting so many lives in the world in a very positive way. This technology is helping people in getting better health services without taking the time to go to their doctor or changing their daily routine. This application has so many benefits but at the same time it is also facing challenges and secure transfer of the data is one of the challenges and researchers are working to make sure to keep data of the patients secure.

***Keywords*—**Wireless Body Area Networks, Wireless Sensor Networks, Quality of Service, Security.

I. Introduction

Recent developments in technologies have made computer networks so complex. We just need to look at the basics first in order to get the idea that how smaller and simple networks have now become so large and how useful they are in connecting people with one another. The application of computer networks has tremendously expanded and now almost every person living on the planet earth is somehow connected to the world and is a part of the computer network. The computer networks were initially used for very low-level communications. People in the sitting in the same room were connected using computer networks. This was considered to be a huge success as people sitting nearby were been able to send and receive files from their computers. Then a point came when people started connecting different rooms and different floors of the building and they were able to communicate with each other through these networks. Besides this, the connections among different buildings were made to communicate and share the data. This was the time when people started thinking that different cities and even countries can be connected by using the concept of Computer Networks. Gradually networking among different cities was made possible and a time came when all the countries of the world were connected through the computer networks [1]. Now not only people living on the globe are connected to each other but these networks have made people connected in the space and under the water in the oceans. Computer Networks are benefitting mankind through its applications and Wireless Body Area Networks has also brought a revolution in the healthcare as its services are expanding and helping both the patients and doctors while not affecting their daily lives. We will start with the basics of computer networks and their geographical scaling.

II. Geographic Scaling of a Computer Network

A. Nano-Scale Network

Communication at the minor scale is taken place at the Nanoscale network. It is clear from its name that very small actuators and sensors are used at the Nanoscale Network. The category of body area networks also falls under the category of nanoscale networks as these sensors and actuators are the backbones of biological systems.

B. Personal Area Network

This type of network is used for the transfer of data among the computers and devices placed around a human being. The maximum area that can be covered under Personal Area Network is around 10 meters. The devices used in this type of network are printers, scanners, fax machines, personal computers and mobile phones. The network can be in the form of a wired network or it can be a wireless network.

C. Local Area Network

The most common and popular network that we have listened to so far is the Local Area Network. Computers and other devices within a range of less than 1 kilometer can be connected through this type of Network. This type of network is used to connect the offices or any other place which falls in the area of fewer than 1000 meters. These networks can be experienced mostly inside the buildings connecting different rooms or floors of a building. These sorts of networks are largely based on Ethernet technology. Wireless Local Area Network or commonly known as WLAN is the wireless form of this network.

D. Wide Area Network

These types of networks were previously known as Metropolitan Area Network or MAN. These are the networks which in those days was thought to be a network which can cover the whole town or a big locality. The population of the cities increased, this leads to the expansion of cities with the passage of time. The communication between the different cities started and that is why it is now known as Wide Area Network [2]. Three layers known as the Physical layer, Data link layer and Network Layer of the OSI model are used in these Wide Area Networks.

E. Global Area Network

The scope of communication becomes vast and now the whole world is a Global Village. Satellite communication is one of the most important factors for this type of network. Mobile or portable devices are used in the areas where there is an availability of satellite signals. Broadband Global Area Network is a well-known example of such a network. Both telephone and internet services fall under such type of network. Moreover, line of sight communication to the satellite signals is an important factor for the communication as the data cannot be transfer without the line of sight communication.

III. Wireless Sensor Network

Before Wireless Sensor Networks (WSNs) are the key factors in bringing the upcoming technological revolution in the world. WSNs are easing the ways for human beings and machines to link with their surrounding environment and to understand and react to the real-world problems that we face on a daily basis. WSNs are made up of nodes and these nodes are actually formed by the combination of micro-electronic mechanical systems, wireless communications, and digital electronics. These nodes are smart enough and have the ability to sense their environment, not only they sense their environment but they can also perform computations and communicate [3].

The WSN network is made up of a few nodes to as many as hundreds or thousands of nodes. These nodes are connected to the sensors. The complexity of the environment is the reason due to which the size of the sensor may vary. Sensors are found from a very small size to a large size. A sensor can be as small as a dust particle and can be as big as the size of the shoebox or even bigger. The price of the sensor nodes also varies. They can be very expensive as much as hundreds of dollars and can be cheap as a few dollars only depending upon the size and complexity of the sensor. Every node consists of some essential parts i.e.

- Radio transceiver
- An internal or an external antenna
- A battery
- Microcontroller
- Electronic circuit

WSNs have seen very fast and rapid growth over the past few years. It is assumed that in the coming 10-15 years the world will be full of WSNs and all these networks will be reached via the Internet. WSN is a very big field, it is also expanding at a high rate and it has too many applications covering different fields. A few of the applications are given below.

IV. Applications of WSNs

A. Military Purposes

The major application of WSNs development is military utilization. It was used mainly for surveillance purposes during battlefield activities. WSNs technology is helpful in intelligence as well as in commutations activities whereas WSNs detect the existence of military forces and war vehicles and in the tracking of their movements. The WSNs are also utilized for applications such as geo-fencing of oil as well as of the gas pipelines.

B. Domestic Uses

Wireless Sensor Networks are also utilized to facilitate household residents. It can be very helpful in making people's life easy and smooth. The Application mechanism of WSNs utilization is to install WSNs nodes at various locations at home and get control of various devices [4].

C. Industrial Uses

Wireless Sensor Networks are also utilized to facilitate household residents. It can be very helpful in making people's life easy and smooth. The Application mechanism of WSNs utilization is to install WSNs nodes at various locations at home and get control of various devices [5].

D. Agricultural Uses

The WSNs have wide usage in the agriculture field where the statistics of the water used in the fields are communicated through WSNs wireless systems to the control center where their billing amounts are calculated. These systems are providing a wide help inefficient utilization of water and avoid its wastage.

E. Environmental Uses

WSNs are utilized for the monitoring of harmful and poisonous gases present in the atmosphere. WSNs have been deployed in most of the advanced cities to monitor air pollution e.g. Brisbane, Stockholm, London.Landslides can be detected by using WSNs systems which will help to detect the movements going on in the soil by installing WSNs units in rocky and mountainous locations. Thus by timely detection of landslides through WSNs utilization, the severe damage caused by it can be avoided [6].A comprehensive analysis should be carried out while designing the security protocols of WBANs with the following three features to be highly prioritized.

- Security Attacks
- Security Requirements
- Existing Security Mechanisms

WSNs can be very helpful in flood prevention. The WSNs units can wirelessly communicate the water level information to the central location, thereby preventing the flood by advanced

detection. This advance detection will help the officials to relocate the inhabitants and goods to a safe place in time.In the current era, the most useful application of WSNs is in the underwater. There are various underwater parameters that can be detected by the installation of WSNs units, such as the water temperature and pressure, the salinity, turbidity and oxygen density can be measured.

During the past decade, the applications of WSNs in the health area has been increased many folds and is gaining more popularity amongst scientists and engineers. Various new techniques and inventions have been developed in the research field of WSNs that enables the patients to cope with the diseases effectively. Wireless Body Area Network is one of the applications of WSNs which is discussed in detail below.

V. WIRELESS BODY AREA NETWORKS

Wireless Body Area Network (WBAN) or Wireless Body Sensor Network (WBSN) is one of the major applications of WSNs in the field of healthcare. This technique has proved to be a revolution in this field as it provides efficient methods for healthcare and related issues. By using WSNs wireless devices a patient has the freedom to wander freely without being bound to stay at the bed at the hospital. WSNs help records the data and saves/wirelessly transmit the data of various parameters in a continuous way. This data is available to the concerned physician as well as for the consideration of the patient to monitor the patient's health regularly. WBAN is composed of various tiny devices implanted along with the human body. Various tasks are performed by these WBAN devices [7]. These devices help to establish the wireless link and perform un-interrupted health supervision. The most significant feature of WBANs is that they can perform continuously for 24 hours every day and perform the recording and storage of data in a periodic way. In general, the two significant types of WBANs devices used in general practice are sensors as well as actuators. The major task of the sensors is to measure various parameters. Contrarily, the function of the actuators is to carry out important steps as a response to the recorded data of the sensors. As an example, in case a sensor records a high level of diabetes, then the function of the actuator is to find out the proper dose of insulin. One requirement of WBANs is that it has to be very efficient in terms of energy consumption. Also, it should have good Quality of Service (QoS) [8]. Furthermore, the patient's privacy, as well as security, must be ensured. A wide range of work is carried out by the scientists as well as the engineers across the world, on various aspects of WBANs in order to improve the standard of services towards the patients. WBANs are categorized in a number of research areas, including energy efficiency, improving QoS as well as the routing of various WBANs nodes etc. Since the WBANs sensors are utilized such as they are embedded inside the body of the humans, and thereby replacing the sensors frequently is not easy. Therefore, the shortest possible time of these sensors is around 5 years nowadays [9]. Because of this necessity, most of the research is going on increasing the lifetime of these devices. Another most challenging factor is the Security of WBANs. The data transfer towards the destination from sensors is carried out in various ways. Our research is based on this issue and has proposed various optimal solutions for the secure transfer of finalized results towards the related receiver. One of the most important parameters of WBANs is to take care of the privacy as well as the security of the patients. Because in the case of tampered reading or malfunctioned measurement will result in a false dosage regarding medicine. All this will put the patient's life in extreme danger [10]. The major WBANs security factors are Confidentiality, Integrity and Availability of recorded data. In addition to these, the various other factors are also important while working on the security of the WBANs, like authentication as well as the fresh updates of the received results. The management is also important in terms of security because it serves as the keys distributor to the various nodes for the purpose of encryption as well as decryption. Similarly, the technique of secure localization helps in the estimation of the accurate localization of the target patient. This counts as an essential factor in terms of the security of the patient. Contrarily, scalability, as well as the flexibility, should also be considered vital in securing the WBANs. The data that is recorded may travel along a short route of a long route in order to be received by the doctor or a physician. Thus various people as diversified distances might attempt to tamper data thereby breaching the WBANs security. Mainly the internal and external sources are involved in the threats as well as attacks on the data. The classification is based on the type of attack carried out. For instance, if an attempt is carried out to attach the data for the purpose to illegally hack the data for changing it, then this type of attack is usually carried out through internal sources. Such sources are normally in the close proximity of the patient and thus can access the WBANs nodes of the patients physically. Contrarily, an outsider attacker breaches the WBANs security through passive eavesdropping, refusal of the demanded service as well as the replay attack to ignore the process of authentication. Such attackers don't have physical access to the patients and thus use such techniques for breaching WBANs security [11].

CONCLUSION

We discussed the geographical scaling of a network in detail and then we also discussed the applications of the computer networks in detail. While discussing all the other applications of the computer networks, we focused on one of the very important applications and it was the Wireless Body Area Networks. We discussed how this application is useful for the patients but besides other challenges one very important challenge that this application is the security, confidentiality and integrity of the data. We just need to carry out our research work in order to make the communication among stakeholders more secure and must not leave any loophole while designing the protocols from which the life of the patient could be at risk.

REFERENCES

[1] Queiroz-Sousa, Paulo Orlando, and Ana Carolina Salgado. "A Review on OLAP Technologies Applied to Information Networks." *ACM Transactions on Knowledge Discovery from Data (TKDD)* 14, no. 1 (2019): 1-25.

[2] Qin, Zhijin, Frank Y. Li, Geoffrey Ye Li, Julie A. McCann, and Qiang Ni. "Low-power wide-area networks for sustainable IoT." *IEEE Wireless Communications* 26, no. 3 (2019): 140-145.

[3] Gilbert, Edwin Prem Kumar, K. Baskaran, Elijah Blessing Rajsingh, M. Lydia, and A. Immanuel Selvakumar. "Trust aware nature-inspired

optimised routing in clustered wireless sensor networks." *International Journal of Bio-Inspired Computation* 14, no. 2 (2019): 103-113.

[4] Kashyap, Ramgopal. "Applications of Wireless Sensor Networks in Healthcare." In *IoT and WSN Applications for Modern Agricultural Advancements: Emerging Research and Opportunities*, pp. 8-40. IGI Global, 2020.

[5] Gope, Prosanta, Ashok Kumar Das, Neeraj Kumar, and Yongqiang Cheng. "Lightweight and physically secure anonymous mutual authentication protocol for real-time data access in industrial wireless sensor networks." *IEEE transactions on industrial informatics* 15, no. 9 (2019): 4957-4968.

[6] Shu, Tongxin, Jiahong Chen, Vijay K. Bhargava, and Clarence W. de Silva. "An energy-efficient dual prediction scheme using LMS filter and LSTM in wireless sensor networks for environment monitoring." *IEEE Internet of Things Journal* 6, no. 4 (2019): 6736-6747.

[7] Ohri, Kriti, R. Vijaya Saraswathi, and L. Jai Vinita. "Performance analysis of wireless body area sensor analytics using clustering technique." In *2019 International Conference on Communication and Signal Processing (ICCSP)*, pp. 0278-0281. IEEE, 2019.

[8] Tseng, Hsueh-Wen, Yu-Bin Wang, Yi Yang, and Ru-Xin Wang. "An Adaptive Channel Hopping and Dynamic Superframe Selection Scheme with QoS Considerations for Emergency Traffic Transmission in IEEE 802.15. 6-Based Wireless Body Area Networks." *IEEE Sensors Journal* (2019).

[9] Bai, Tong, Jinzhao Lin, Guoquan Li, Huiqian Wang, Peng Ran, Zhangyong Li, Yu Pang, Wei Wu, and Gwanggil Jeon. "An optimized protocol for QoS and energy efficiency on wireless body area networks." *Peer-to-Peer Networking and Applications* 12, no. 2 (2019): 326-336.

[10] Shim, Kyung-Ah. "Universal Forgery Attacks on Remote Authentication Schemes for Wireless Body Area Networks Based on Internet of Things." *IEEE Internet of Things Journal* 6, no. 5 (2019): 9211-9212.

[11] Paul, Pangkaj Chandra, John Loane, Gilbert Regan, and Fergal McCaffery. "Analysis of Attacks and Security Requirements for Wireless Body Area Networks-A Systematic Literature Review." In *European Conference on Software Process Improvement*, pp. 439-452. Springer, Cham, 2019.

International Journal of Engineering Works
ISSN-p: 2521-2419
ISSN-e: 2409-2770
Vol. 7, Issue 04, PP. 207-210, April 2020
https://www.ijew.io/
https://doi.org/10.34259/ijew.20.704207210

Spatial Variation of Temperature and Rainfall Trends in Kabul River Basin

Saadia Rehman[1*], M. Shahzad Khattak[2], Amjad Khan[3], Sajjad Ahmed[4]
[1,2,,3,4] Department of Agricultural Engineering, University of Engineering & Technology Peshawar
saadiarehman93@yahoo.com[1], shahzadkk2004@gmail.com[2], amjad_uet91@yahoo.com[3], sajjadahmed@uetpeshawar.edu.pk[4]
Received: 06 March, Revised: 16 March, Accepted: 20 March

***Abstract*—** Knowledge of temperature and rainfall periodicity is needed for urban and rural land-use and infrastructure planning, and their flood protection. In this study temperature and rainfall data from Climatic Research Unit Time Series version 4.03 (CRU TS4.03) was downloaded and inverse distance weighted (IDW) were made to analyze the temperature and precipitation variations in Kabul river basin (KRB). Interpolation maps were made using ArcMap 10.4.1. Analysis was done for period from 2004 to 2018. Annually for 15-year period, mean temperature variation can be noted as, upper part of the basin has minimum temperature of -1.2 °C while part of the study basin that lies in Pakistan has maximum temperature of 19 °C. Rainfall varies from 380 mm to 793 mm annually for 15-years. Due to increasing trend of both temperature and rainfall for KRB suitable methods should be applied for water management and flood risk reduction.

***Keywords*—** Temperature, Kabul River Basin, CRU, IDW, ArcMap 10.4.1

I. Introduction

Temperature and rainfall are key elements in hydrological cycle that plays an important role in water allocation. About one sixth (1/6th) of world's population depends upon water coming from frozen sources as their water resource [1]. This melting of water is influenced by temperature variations thus affecting the dependents. KRB is having its upper part covered with snow throughout the year. Thus, variation in temperature and rainfall analysis is necessary for the basin for better water distribution [2].

Higher temperature over a region is the feature of global warming. The global average temperature has increased by an average of 0.85 °C during 1800–2012 relative to 1961–1990 [3] and 0.74 °C (1906-2005) [4]. This increasing temperature ultimately rises the flow of water coming from frozen sources and results in changing the water distribution.

For the study climatic component of water balance approach was acquired from Climatic Research Unit Time Series version 4.03(CRU TS4.03), produced by University of East Anglia, England. It includes various variables like rainfall, cloud cover, temperature, potential evapotranspiration, vapor pressure, and frost day frequency on monthly basis from January 1901 to December 2018. Station anomalies are interpolated into 0.50 x 0.50 (latitude-longitude) grid cells covering entire land surface globally [5].

II. Data and Methodology

A. Study Area

The study is carried out on the Kabul river basin that lies between longitude 67040/ to 75042/ east and latitude 33033/ to 36002/ north [6]. Kabul river, 700 km long, has its origin from the Sanglakh Range of the Hindu Kush Mountains in Afghanistan, passes through Nowshera, Pakistan and ends in the Indus river near Attock [7]. Kabul river basin is in south-east of Afghanistan also is the portion of Indus river catchments. The catchment area of basin is 68040 km2 i.e. 78% area lies in Afghanistan while 22% area is in Pakistan boundaries, as depicted in Figure 1. The eastern portion of the basin that emerges from Pakistan has higher elevation and is covered by snow in most part of the year [8].

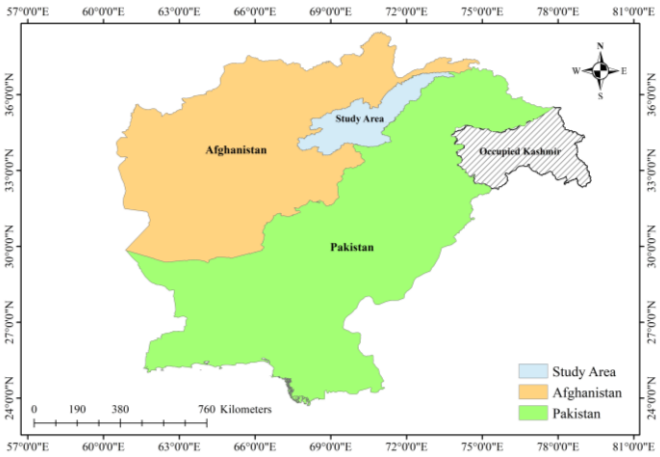

Figure 1. Study Area Map

B. *Temperature and Rainfall Data*

Monthly temperature and rainfall data of spatial resolution 0.50 was downloaded from CRU TS4.03 http://www.cru.uea.ac.uk/data from January 2004 to December 2018. Data was acquired for each grid made in study area and exported to excel spreadsheet. After that average of all grids were calculated to get temperature and rainfall data for entire basin.

C. *Methodology*

Entire study basin was divided into grid cells of 0.50 x 0.50 resolution. Data from each grid cell was obtained and then mean value for the basin was calculated using the weighted mean technique.

$$\bar{x} = \frac{\sum_{i=1}^{n}(x_i \times w_i)}{\sum_{i=1}^{n} w_i}$$

where, w = weights,
x = value

Inverse distance weighted maps were made using commands of GIS software ArcMap 10.4.1. Downloaded climatic data was arranged in excel spreadsheets and opened in ArcMap. Then after interpolation of data, monthly IDW maps for temperature and rainfall from 2004 to 2018 were made.

III. Results and Discussion

A. *Spatial Analysis of Temperature and Rainfall*

Spatial analysis of temperature and rainfall data, that was downloaded from CRU was done on ArcMap. Monthly IDW maps were made to inspect temperature and rainfall variations in KRB. Annually it can be noted that temperature ranges from -1.2 °C to 18.9 °C, as shown in figure 4 (a). the upper part of the basin was having negative temperature thus covered with snow throughout the year and serves as source of frozen waters. While lower part that lies in Pakistan boundary has maximum temperature of 18.9 °C i.e. plain area. Monthly maps shown in Figure 2 depicts that in January temperature of the study basin falls to minimum of -13 °C that follows the rainfall in upper part as snow at this minimum temperature. In June, the temperature rises maximum to 28 °C that results in snow melting and causes the stream flow to reach its peak rate.

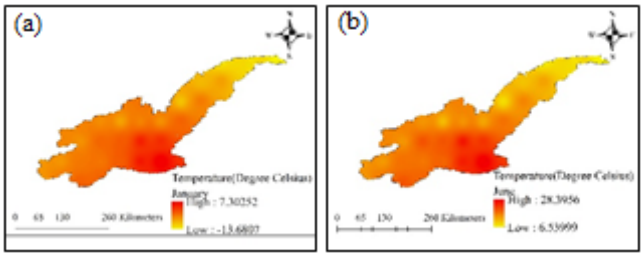

Figure 2. Spatial Analysis of Temperature over KRB (a) January and (b) June

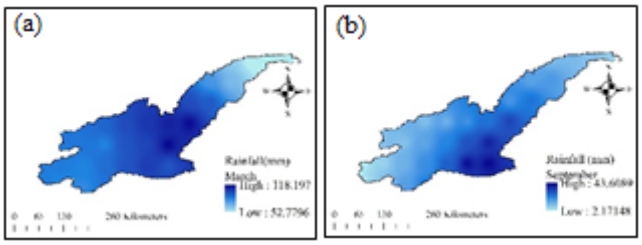

Figure 3. Spatial Analysis of Rainfall over KRB (a) March and (b) September

Rainfall map divides the entire basin into two zones, semi-arid and sub-humid. Semi- arid is the zone with annual rainfall of 300 to 600 mm, 70% of area lies in it. While other 30% lies in sub-humid zone with 600 to 1000 mm annual rainfall shown in figure 4 (b). Rainfall spatial analysis shows the minimum rainfall of 380 mm to maximum of 793 mm. the upper part of basin is having rain falling as snow. March is having maximum rainfall of 118 mm over the basin while in September has minimum rainfall of 2 mm (figure 3).

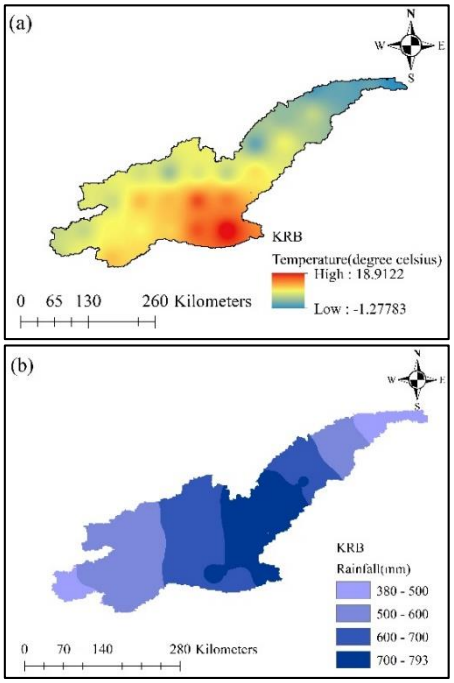

Figure 4. Annual Variation of (a) Temperature and (b) Rainfall in KRB

B. *Trend Analysis of Temperature and Rainfall*

Graphs were made to examine the trend for temperature and rainfall in KRB. Figure 5 gives the trendline for seasonal as well as annual temperature and rainfall. It can be observed that in summer temperature trendline is increasing. Same trend can be seen for annual temperature for 15-year i.e. from 2004 to 2018. This increasing temperature is affecting the snow budget as the basin comprise some of its part as snow. And this change influences the downstream water allocation.

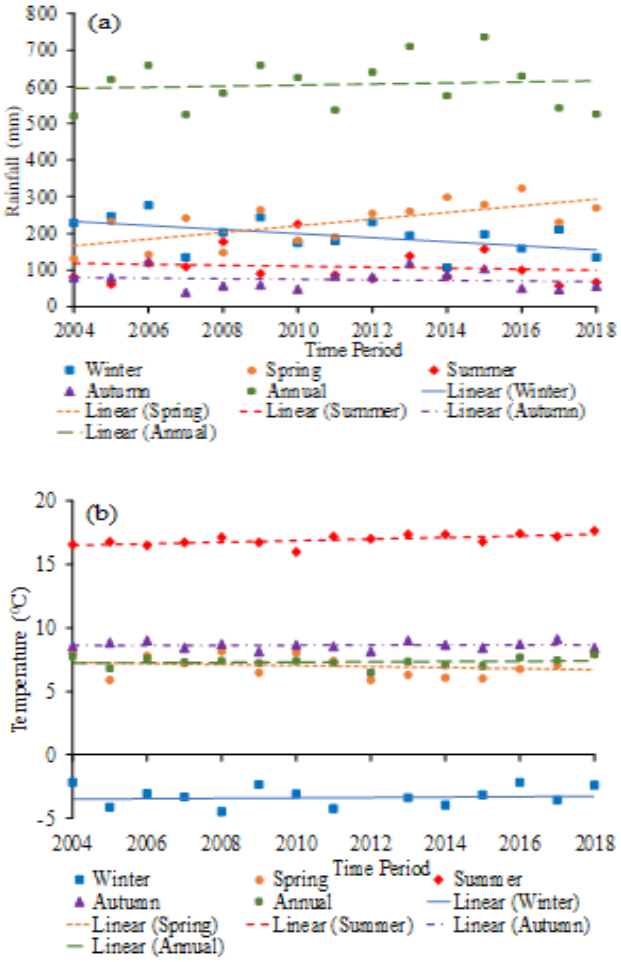

Figure 5. Trend Analysis for (a) Rainfall and (b) Temperature data for 15-Years.

Similarly, for rainfall trend estimation graph was developed and trendline was analyzed on seasonal and annual basis. Winter season is having decline in trendline for study period. That demands the proper management of water resources to be used by dependents. While annually, slight increasing trend line is observed.

CONCLUSIONS

The study concluded that the temperature has increasing trend for summer while on annual basis trend is also increasing slightly. The mean maximum annual temperature of the basin for 15-years was 19 °C and minimum was – 1.2 °C. Seasonally, temperature falls to -13 °C in January and rises to 28 °C in June. Rainfall range for the basin for 15-year period on annual base is 380 mm to 793 mm. Monthly analyses concluded that March has maximum rainfall of 118 mm and September has minimum 2 mm rainfall.

REFERENCES

[1] Barnett, T.P., Adam, J.C. and Lettenmaier, D.P., 2005. "Potential impacts of a warming climate on water availability in snow-dominated regions". Nature, 438(7066): 303.

[2] Flint, R.F., 1971. "Glacial and Quaternary Geology". New York. John Wiley and Sons,Inc., 892

[3] IPCC, "Climate Change: The Physical Science Basis; Contribution of Working Group I to the Fifth Assessment Report of the Intergovernmental Panel on Climate Change," Cambridge University Press: Cambridge, UK; New York, NY, USA. 1535, 2013.

[4] IPCC, "Climate change 2007: The Physical Science Basis. Contribution of Working Group I to the 4th Assessment Report of the Intergovernmental Panel on the climate change". Cambridge and New York: Cambridge University Press, 2007. 996, 2007.

[5] Shi, H., Li, T. and Wei, J., 2017. "Evaluation of the gridded CRU TS precipitation dataset with the point raingauge records over the Three-River Headwaters region". Journal of Hydrology, 548: 322-332.

[6] Lashkaripour, G.R. and Hussaini, S., 2008. "Water resource management in Kabul River Basin, Eastern Afghanistan". Environmnetalist, 28(3): 253-260.

[7] Khattak, M.S., Anwar, F., Saeed, T.U., Sharif, M., Sheraz, K., Ahmed, A., 2016. "Floodplain mapping using HEC-RAS and ArcGIS: A Case Study of Kabul River". Arabian Journal for Science and Engineering, 41(4): 1375-1390.

[8] Rasooli, A. and Kang, D., 2015. "Assessment of potential dam sites in the Kabul River Basin using GIS". International Journal of Advanced Computer Science and Applications, 6(2).

Saadia Rehman born in Peshawar, Khyber Pakhtunkhwa, Pakistan on 09th October 1993. Has got bachelor degree in Agricultural Engineering, from University of Engineering and Technology, Peshawar, Pakistan in 2015. Currently enrolled in MS program of Soil and Water Engineering in University of Engineering and Technology, Peshawar, Pakistan. Research interests include, Hydrology, GIS and Water Resource Management.

IJEW 国际工程期刊 International Journal of Engineering Works انجینئرنگ کاموں کا بین الاقوامی جرنل

International Journal of Engineering Works
ISSN-p: 2521-2419
ISSN-e: 2409-2770
Vol. 7, Issue 04, PP. 211-216, April 2020
https://www.ijew.io/
https://doi.org/10.34259/ijew.20.704211216

Frequencies Dominations for Different Rating of Distribution Transformer under Transients

Haseeb Faisal[1], Dr. Kashif Imdad[2], Najeeb Hussain[3], Faisal Sharif[4],
[1,2,3]Department of Electrical Engineering, HITEC University Taxila, Punjab, Pakistan
[4]WAPDA, Islamabad, Pakistan.
haseebf1@hitecuni.edu.pk[1], engr.kashif@hitecuni.edu.pk[2], najeebhussain@hitecuni.edu.pk[3]
faisalsharifch@gmail.com[4]

Received: 26 March, Revised: 04 April, Accepted 06 April

Abstract**—**Power transients faults on high voltage lines are prominently due to high frequency transients. These transients affect the predicted life and efficiency of equipment. The Fast Fourier Transform (FFT) is helpful in analysing the effect of high frequencies and Frequency Response Analysis (FRA) provide support in diagnosis and detection of deformation in a transformers. The major aim of this study is to analyse the incorporation of frequencies based on resonating core of a particular transformer. Using transfer function method an impedance change in transformer has been observed when equipment is subjected to high voltage transients. The effect of change in impedance is that it degrade the life of a core with respect to time. In this paper, research that has been done already on Transformers of different ratings i.e. 100, 50 and 30 kVA are studied and then an experiment is performed on 50-kVA transformer. It was concluded that the core of a transformer having rating equal or less than 50 kVA practically shows single resonance behavior while above 50 kVA for instance 100-kVA transformer core resonates twice. In actual, result defines the core deviating frequency with respect to the rating of a transformer.

Keywords**—** Frequency dominations, transients, Fast Fourier Transform, distribution transformer, high frequency modelling.

I. INTRODUCTION

A transformer is one of the expensive component in the power industry. Due to transients the efficiency of a transformer decreased and not effectively perform its function on the distribution side of a power system. In order to provide protection to the equipment; power transient measurement and analysis through high frequency modeling and study of frequency dominations is important. In literature, it was came into consideration that transformer winding has been the integral point of focus with respect to different faults for example, transformer winding deformation. Transformer winding deformation mainly occurred when transformer relocated from manufacturing plant to the operational area as in [1] [5]. Diagnoses on the bases of inter-turn faults need modeling of transformer winding. The modeling of transformer winding depend on its construction and study of the electrical stresses. In transformer diagnosis, reverse engineering method was adopted in general using black box analysis and its input and output (voltages, currents) were measured. Transformer models were developed to estimate transferred surges from High Voltage (HV) and Low Voltage (LV) line. These Models were valid for unloaded conditions [6] [8]. However, there are models that were functional for both loaded and unloaded conditions as described by [9] [10], they introduced an efficient model under electromagnetic transients. To calculate the transferred surges, distributed and lumped parameters models were used as in the paper [11] [19]. With the bandwidth up to 1MHz lumped parameters analysis were used; comparatively for satisfactory results, distributed parameter models were preferred. Problem is that, [8] defined dual resonance, while [7] presented single resonance behavior. However, no one clearly elaborated the dual and single core resonating frequencies exactly with respect to the rating of the transformer. Reference [20] described the sweep frequency analysis, to assess the mechanical deformation of a transformer core and found that the frequencies less than kHz are much more effective in enhancing mechanical efficiency of a transformer.

In this paper, a concept has been develop to examine the effect of high frequencies on the core in the form of resonance under the influence of high transient fault. The idea is based on the modeling of the equivalent circuit at low frequencies. In open circuit test of a transformer at low frequencies, core resistance and reactance are calculated. The output of an experiment was observe at open circuit noting that under the impulse voltage injection on primary and secondary side the core voltage is resonating and its characteristics are changing.

An experiment is performed on a distribution transformer aiming to define dominating frequencies for transformers of

different kVA rating. This research is two dimension in nature. In first dimension, an experimental approach is developed and secondly based on the past-published researches a comparison has been made with addition of experimental results that validates domination of the frequencies. This concept is competitive in term of defining single or dual resonance with respect to transformer ratings.

II. RESEARCH METHODOLOGY

A. *Experimental Setup*

The initial setup as shown in Fig.1 is comprised of a distribution transformer of 50 kVA (11 kV/440V), 3-phase; delta-star connection was designed in Universitat Politècnica de Catalunaya Barcelona, Spain.

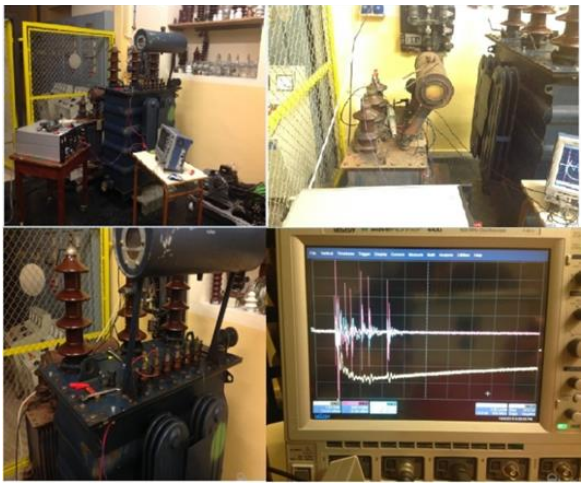

Fig. 1. Experimental Setup for 50kVA transformer.

To determine input and output values, 3-channel oscilloscope is used having a sampling time of 2×10^{-9}. The experimental configuration of the transformer is based on the model presented as in Fig. 2. All phases of the primary side of a transformer are kept short circuit so that each phase have same behavior as other. Corresponding phase input voltage and currents are measured to see the impedance change in core. In actual the mutual induction phenomenon in all phases affects the core but here it is assumed that all phase has similar windings in magnetizing the core. Secondary is open to analyze the behavior of a core under open circuit test. Finally, different values for transfer function method: I of primary and V of secondary under the influence of impulse voltage injection at primary are found out.

At the high voltage (primary) and on the low voltage side (secondary) side of the transformer, a surge voltage is applied. Output voltage is measured by the help of configuration as shown in Fig. 2. On different magnitude of surge voltages at the HV side, different current injections and output voltages are observed. Channel 1 (CH1) is used for the measurement of V_1, Channel 2 (CH2) is used for the measurement of I_1 and channel 3 (CH3) is used for the V_2. Secondary current is not measured because secondary is open so I_2 is equal to zero. The injected voltages and currents are shown in the Fig. 3. And Fig. 4.

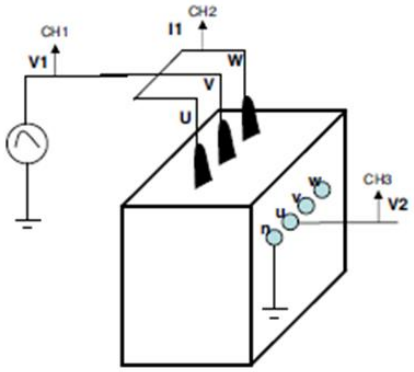

Fig. 2. Experimental configuration of 50kVA transformer.

B. *Transfer Function Method*

Impulse test has been performed by using two-port network theory. Secondly, transfer function is applied in term of impedance to see the core impedance behavior.

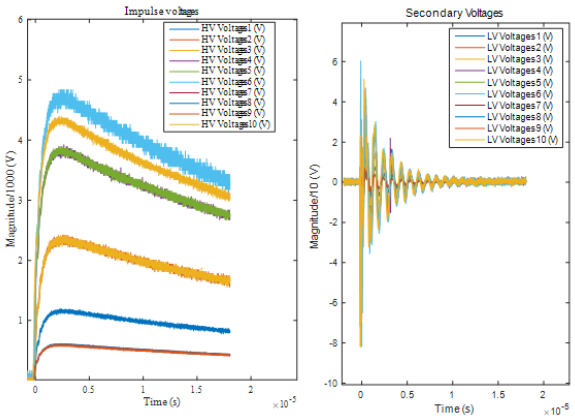

Fig. 3. Different impulse voltages at HV and secondary voltages at LV side.

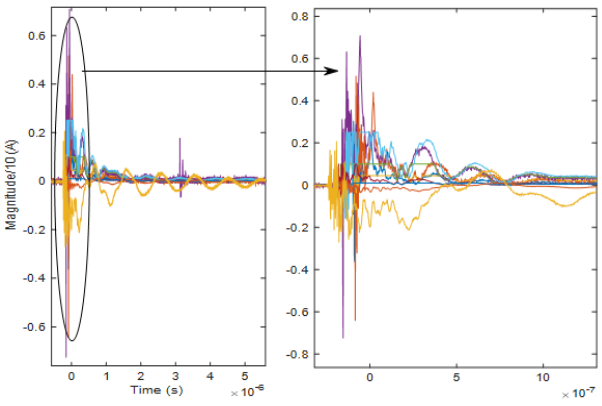

Fig. 4. Different injected currents on primary side.

The purpose of using transfer function method is to identify how much input (impulse voltage) is transferred towards output

and under these constraints what will be the behavior of the core. This transfer function *TF* as in (9) describes the effective transformation of output voltage in term of input current that is known as transformed impedance. The equations for the two-port network theory are:

$$V_p = Z_{11} \times I_P + Z_{12} \times I_S \quad (1)$$
$$V_S = Z_{21} \times I_P + Z_{22} \times I_S \quad (2)$$

$$Z_{12} = \frac{V_P}{I_S} \qquad \therefore I_P = 0 \quad (3)$$
$$Z_{21} = \frac{V_S}{I_P} \qquad \therefore I_S = 0 \quad (4)$$
$$Z_{11} = \frac{V_P}{I_P} \qquad \therefore I_S = 0 \quad (5)$$
$$Z_{12} = \frac{V_S}{I_S} \qquad \therefore I_S = 0 \quad (6)$$

For the analysis of the digital tested data under open circuit test, frequency domain analysis are performed under the transfer function method by using Fast Fourier transform as followed by the equation:

$$X(k) = \sum_{i=1}^{n} x(j)\omega_n^{(j-1)(k-1)} \quad (7)$$

Where,

$$\omega_n = e^{\frac{-2\pi i}{N}} \quad (8)$$
$$TF = \frac{V_{out}}{I_{in}} = \frac{V_{secondary}}{I_{primary}} \quad (9)$$

Here, T_{sample} is the sampling time, which is dependent on the selection of the samples matched closely to each other; in actual it is dependent on the required resolution, so that the outcome should be good.

$$T_{sample} = \frac{L}{N} \quad (10)$$

Where *L* is the length of a signal and *N* representing the number of samples.

C. Frequency Analysis & Discussion

The reason of this analysis is to observe that how many times core will resonate, when fault occurs at the HV side of the 50 kVA or less than 50 kVA transformer. Another issue is to see the dominating resonance frequencies because the resonating frequencies having low weight will not affect the core and hence their effect cannot incorporate as far the concern of developing a protection scheme model.

The obtained discrete data is imported to MATLAB, then Fast Fourier Transform algorithm is applied to recognize the behavior of core in term of core resonance. Analysis was done on frequency bandwidth of 100 kHz and 1 MHz as in [7] [8].

On single resonating response of transformer core, there are three zones. In zone one, on primary side of a transformer the highest current injection at which core resonates is at frequency

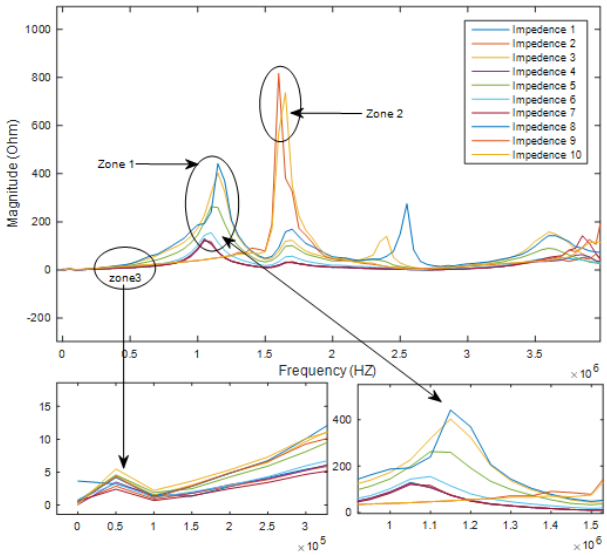

Fig. 5. Frequency vs magnitude response of transfer impedance.

of 1.05×10^6 having Z equal to 130 Ω As in Fig. 5.

Decreasing the value of injecting current an impedance increases and due to this frequencies are increasing; frequency is 1.15×10^6 having Z is 441.9 Ω.

In the zone 2, when we decrease the current at HV side then frequency response move towards dominating resonance frequency and impedance are also increased; *f* is 1.65×10^6 while Z equal to 736.7Ω.

In zone 3, there is resonating frequency for every value of injected current but the frequency involvement in term of its weight is too low that it has no effect on the core. At frequency *f* equal to 1.277×10^5 transformer core resonate and its response changed from capacitive to inductive behavior. It is very clear from above figure that domination of high frequency is only for the core resonance. The relation between impedance and current is inverse in nature so current is decreasing while impedance is increasing and high frequency is moving ahead.

From frequency response, it has been observed that there is only single core resonating frequency, which is dominating over all other frequencies and affects the core in terms of deviating the response and resonating the core.

For different transfer impedances, three edges are considered for analysis of core resonance in between frequency vs phase angle response as in Fig. 6. Edge one, show that response of core is shifting from inductive to capacitive; which is for the low resonating frequencies. Magnitude response is describing, that resonance is negligible when resonating frequencies have low weights in term of magnitude.

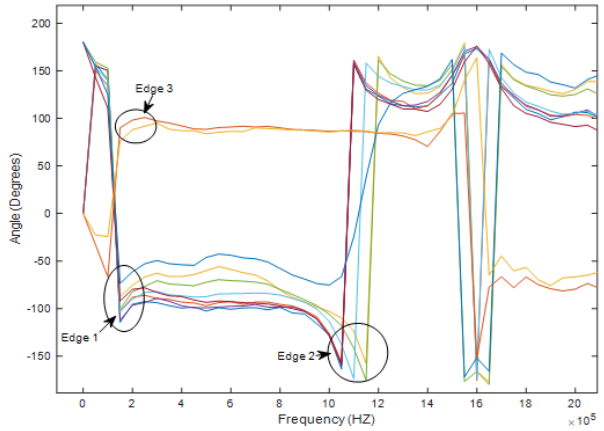

Fig. 6. Frequency vs phase angle response of transfer impedance.

Edge 2 is representing the response for frequency greater than 1 MHz dominating frequencies. The response of these dominating frequencies is changing from capacitive to inductive. This resonance is responsible in increasing the aging of transformer in term of core.

Edge 3 is describe the values or limit of current injection at High Voltage (HV). On this point current is very low, surge voltages and impedances are high. Dominating resonance is also high with respect to previous ones.

So, from the phase angle response it is very clear that in all entire defined bandwidth there is just single dominating resonance frequency for 50-kVA transformer.

D. Concept justification by literature investigation

In this part of the research, we are actually interested in elaborating and justifying our concept. The investigated research was presented in Finland and in Brazil at 100 kVA, 50 kVA and 30 kVA rating transformers.

Fig. 7. Represents the transfer impedance magnitude and phase angle of 100 kVA transformer. In the characteristic impedance figure dual resonance occurring. F_1 which is 374 kHz approximate, occurred at low frequency having a weight of 550Ω approx. and it resonate the core from inductive to capacitive, due to this heavy weight of low frequency was kept in consideration for modelling purposes. While F_2 was 1.36 MHz approximate, occurring at high frequency having an equivalent weight and it is resonating the core from capacitive to inductive. At F_2 the core was at high frequencies but it was responsible to switch the response in actual way normally inductive and at very high frequencies response become capacitive. Fig. 8. displaying a characteristics transfer impedance of 50 kVA transformer.

In Fig 8. Two frequencies were occurring which resonate the core consequently at F_1 and F_2. F_1 is low resonating frequency, its weight is 40Ω approximate and it resonate the core from inductive to capacitive but the response is much fluctuating and inductive response is dominating over capacitive. F_2 was the

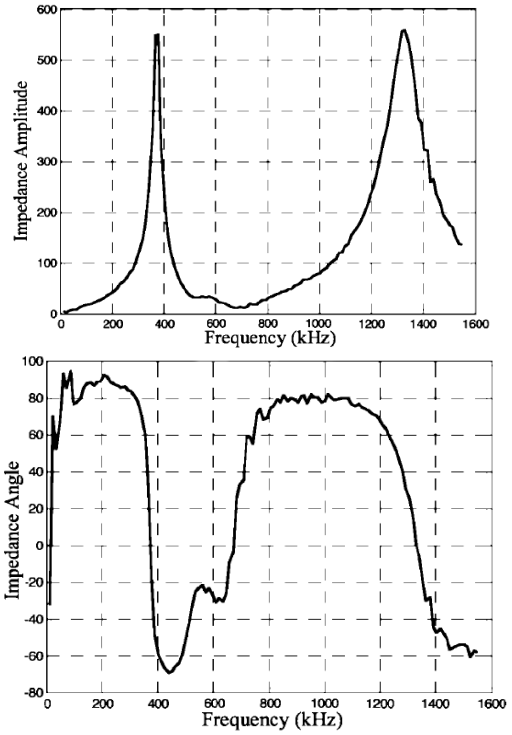

Fig. 7. 100-kVA transformer transfer impedance (reprinted form [8])

highest dominating frequency having weight was 500Ω approx. and response was resonating from inductive to capacitive. The below mentioned result and previous results in Fig. 4. And Fig. 5. Have relevancy, the reason is that both transformer have same ratings.

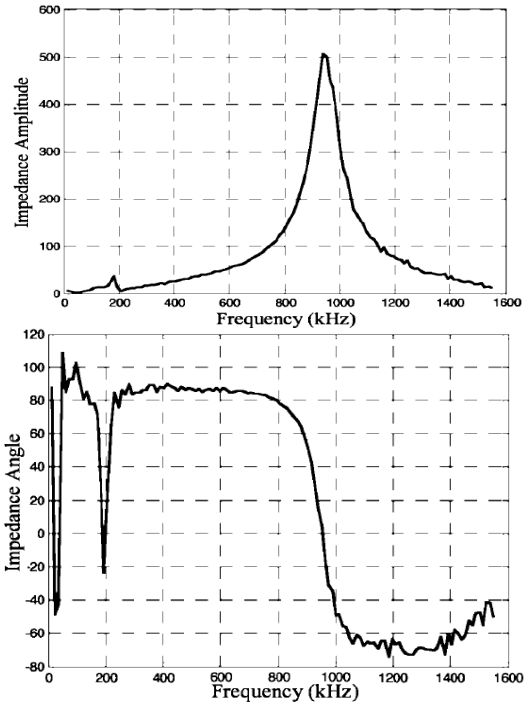

Fig. 8. 50-kVA transformer transfer impedance (reprinted from [8])

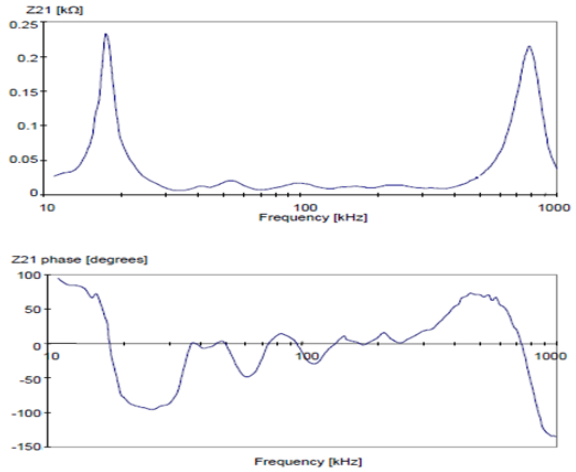

Fig. 9. 30-kVA transformer transfer impedance as in [7]

In the Fig. 9. Characteristic impedance is for 30-kVA transformer tested in Brazil. F_1 is occurring below bandwidth. Therefore, there is only single dominating frequency, which is high frequency.

It is the key indicating fact that in Fig. 8. at low frequency, capacitive response is very low and inductive is dominating; ultimately means that this frequency resonate the core in a very short band width. F_1 contains low magnitude and shorter band of frequencies having a less incorporation in the core resonating response. So this frequency will not affect the response of core and only one high frequency is dominating which validates the proposed concept.

CONCLUSION

The transformer models, which were investigated in previous research, were of 30 kVA, 50 kVA and 100 kVA. It was come into consideration that the discussions on those Transformer models was based on winding and were tested at no load condition. However, in this paper, the Transformer model of 50 kVA was selected and tested at load and no load conditions considering transformer rating and focusing on the core of a transformer. After theoretical analysis of past researches and experimental study of 50-kVA transformer, it is concluded that at 50 kVA and less ratings transformer core resonates at single frequency but above 50 kVA to higher ratings transformers core resonates two times. The model studied in literature investigation also validates the results of the model discussed in this paper. Proposed technique can be used in neural network to specify the specimen and patterns with respect to the characteristics frequencies to define the actual condition of the transformer in term of aging and efficiency.

REFERENCES

[1] S. Okabe, M. Koutou, T. Teranishi, S. Takeda, and T. Saida**,** A High Frequency Model of an Oil-Immersed Transformer, and its use in Lightning Surge Analysis, Elect. Eng. Jpn. vol. 134 (1), 2001.

[2] Y. Shibuya and S. Fujita, High frequency model and transient response of transformer windings, in Proc. IEEE Power Eng. Soc. Transmission and Distribution Conf. Exhibit., Asia Pacific, Vol. 3, pp. 1839–1844, 2002.

[3] Y. Shibuya and S. Fujita, High frequency model of transformer winding, Elect. Eng. Jpn. Vol. 146(3), 2004.

[4] M. Popov, L. Van der Sluis, R. P. P. Smeets, J. Lopez-Roldan, and V. V. Terzija, Modelling, simulation and measurement of fast transients in transformer windings with consideration of frequency-dependent losses, Inst. Eng. Technol. Electr. Power Appl., vol. 1(1), 2007. Y. Yorozu, M. Hirano, K. Oka, and Y. Tagawa, Electron spectroscopy studies on magneto-optical media and plastic substrate interface, IEEE Transl. J. Magn. Japan, Vol. 2, pp. 740–741, 1987.

[5] Y. Wang, W. Chen, C. Wang, L. Du, and J. Hu, A hybrid model of transformer windings for very fast transient analysis based on quasi-stationary electromagnetic fields, Elect. Power Components Syst., Vol. 36, pp. 540–554, 2008.

[6] P. T. M. Vaessen, Transformer model for high frequencies, IEEE Trans. Power Del., Vol. 3(4), pp. 1761–1768, 1988.

[7] A. Piantini and C. V. S. Malagodi, "Modeling of three-phase distribution transformers for calculating lightning induced voltages transferred to the secondary," presented at the IEEE 5th Int. Symp. Lightning Protection, Sao Paulo, Brazil, 1999.

[8] N. A. Sabiha and M. Lehtonen, Experimental verification of distribution transformer model under lightning strokes, presented at the IEEE Power Eng. Soc. Power Syst. Conf. Expo., pp. 15–18, 2009.

[9] T. Noda, H. Nakamoto, and S. Yokoyama, Accurate modeling of core-type distribution transformers for electromagnetic transient studies, IEEE Trans. Power Del., Vol. 17(4), pp. 969–976, 2002.

[10] T. Noda, M. Sakae, and S. Yokoyama, Simulation of lightning surge propagation from distribution line to consumer entrance via pole-mounted transformer, IEEE Trans. Power Del., Vol. 19(1), pp. 442–444, 2004.

[11] M. H. Nazemi and G. B. Gharehpetian, Influence of mutual inductance between HV and LV windings on transferred overvoltages, presented at the XIVth ISH Conf., Beijing, 2005.

[12] P. Mitra, A. De, and A. Chakrabarti, Resonant behavior of EHV transformer windings under system originated oscillatory transient over voltages, Int. J. Elect. Power Energy Syst., Vol. 33(1), pp. 1760–1766, 2011.

[13] A. N. de Souza, M. G. Zago, O. R. Saavedra, C. C. Oba Ramos, and K. Ferraz, A computational tool to assist the analysis of the transformer behavior related to lightning, Int. J. Elect. Power Energy Syst., vol. 33(3), pp. 556–561, 2011.

[14] K. Ragavan and L. Satish, An efficient method to compute transfer function of a transformer from its equivalent circuit, IEEE Trans. Power Del., Vol. 20(2), pp. 780–788, 2005.

[15] A. Miki, T. Hosoya, and K. Okuyama, A calculation method for impulse voltage distribution and transferred voltage in transformer windings, IEEE Trans. Power App. Syst., Vol. 3, pp. 930–939, 1978.

[16] P. G. Blanken, A lumped winding model for use in transformer models for circuit simulation, IEEE Trans. Power Electron., Vol. 16(3), pp. 445–460, 2001.

[17] R. C. Dugan, R. Gabrick, J. C. Wright, and K. V. Pattern, Validated techniques for modeling shell-form EHV transformers, IEEE Trans. Power Del., Vol. 4(2), pp. 1070–1078, 1989.

[18] R. C. Degeneff, W. J. McNutt, W. Neugebauer, J. Panek, M. E. Mc-Callum, and C. C. Honey, Transformer response to system switching voltage, IEEE Trans. Power App. Syst., Vol. (6), pp. 1457–1470, 1982.

[19] R. C. Degeneff, W. J. McNutt, W. Neugebauer, J. Panek, M. E. Mc-Callum, and C. C. Honey, Transformer response to system switching voltage, IEEE Trans. Power App. Syst., Vol. (6), pp. 1457–1470, 1982.

[20] G. M. Kennedy, Transformer Sweep Frequency Response Analysis, energize, pp. 28-33, 2007.

Haseeb Faisal received his BS Degree from COMSATS University Islamabad and currently persuing his MSc. Degree from Wah Engineering College. He is a research fellow at HITEC University Taxila. His major field of interest are High Voltage and Dielectrics materials.

Kashif Imdad received his BSc. Degree from UET Peshawer and then MSc. Degree from UET Taxila. He completed his PhD from Universitat Politècnica de Catalunya, Spain. Currently, serving HITEC University Taxila as an Assistant Professor. His major field of interest are High Voltage, Electrical Power Systems and Dielectrics.

Najeeb Hussain received his BS degree from HITEC University Taxila. He is attached with industry from Past two years.

Faisal Sharif BSc.(Pb), BS Engg. (Electr). Currently he is serving WAPDA as an Executive Engineer. He has an experience in Power Operations, maintenance and distribution.

IJEW 国际工程期刊 International Journal of Engineering Works انجینئرنگ کاموں کا بین الاقوامی جرنل

International Journal of Engineering Works
ISSN-p: 2521-2419
ISSN-e: 2409-2770
Vol. 7, Issue 04, PP. 217-220, April 2020
https://www.ijew.io/
https://doi.org/10.34259/ijew.20.704217220

Methodology of Material Selection for Evaporator Coil in Air Conditioning System

Wiqas Alam[1], Aamer Ullah Khan[2], Dr. Abdul Shakoor[3]
[1,2,3] Mechanical Engineering Department, Post-graduate Researcher, Professor
wiqassuit17@gmail.com[1], aamerkhan706@gmail.com[2], shakoor@uetpeshawar.edu.pk[3]
Received: 18 March, Revised: 25 March, Accepted 01 April

Abstract— The ever-growing demand of air conditioning system in commercial and household application's emphasis on long-term material's stability. Material's failure in air conditioning system due to temperature variance and heat flow causing reduction in cooling effect of the system. Considerable amount of heat waste in evaporator coil as a result of low thermal transitions through coil's material resulting reduction in overall efficiency of the system. This paper provide a CES Granta's design software-based approach being followed to select appropriate material for evaporator coil in air conditioning system. Cast iron, pure titanium, copper, low alloy steel, Stainless steel, and nickel-chromium alloys are the shortlisted candidate for evaporator coil based on design and functional requirements. Low alloy steel, titanium, and stainless steel are the top suitable candidate among which stainless steel shows promising attributes for evaporator coil in air conditioning system. This paper will help the researchers, engineers, and designers to better understand the methodology of selecting a stainless steel in evaporator system to control corrosion and provide high- temperature-resistance.

Keywords— Material Selection, Evaporator, Granta's Design CES software

I. INTRODUCTION

Evaporation process are commonly practice in various Industries viz, food, beverages, paper, petrochemical, and water treatment in order to remove moister from the products. Evaporator technology has been around for many years as a variant technology. Concentration on pollution control and energy conservation are the main causes for variation in evaporator technology. In past various problems in evaporator system encountered by engineers either by adjustment of operation temperature and pressure or complete transformation of existing system into efficient one. The concentration of aggressive elements increase with discharge of waste stream causing corrosion and premature system failure [1]. Material selection is more critical for evaporator coil provided efficient cooling system and pollution control by the process engineer. Low alloy steel has been used as an evaporator material but need to be upgraded in order to control corrosion problem. Stainless steels have been and will continue to be used in many industries for evaporation purposes. Stainless steel provide effective corrosion resistance, excellent thermal properties from very low to high temperature applications. Evaporating service having wider applications now utilize stainless steel due to high-temperature resistance and corrosion care.

Material plays important role in engineering design. Without proper material, design product leads to pre-mature failure during operation. Each material has its own properties due to which one can differ it from other. Material selection is a process of finding best match material for an engineering product. Granta's design CES (Cambridge engineering selector) provide a detail strategy and approach for materials selection introduced by Ashby et al., 2002 [2].

Ashby et al, 2009 [3] utilizing Cambridge Engineering Selector software compared various materials based on design and functional attribute's requirements. The methodology followed the basic principle of defining function, constrains, objectives, and free variables for specific applications. All the materials present in the universe are considered as a candidate materials for the applications. Applying design and functional requirements screen out the failed materials. The remaining material ranked based on material indices. Weight property index method calculate the performance value of each shortlisted candidate's material. Material with highest performance is the final selected material.

Evaporator Coil is the most important component in air conditioning system. Refrigerants is heated in the coil and transmitting the heat away in order to cool the room air. Refrigerants varies based on operation conditions. Evaporator material must have corrosive resistant, higher tensile strength and high melting point because the refrigerant conversion into vapor due to high temperature must not exceed the material's melting point in order to have heat transformation with an environment [4].

Shanian et al, 2004 [5] utilized CES approach for material's selection based on production cost analysis. Multiple decision making properties were investigated for selecting material for engineering products. Materials were ranked from best to poor

for covering cylinder to withstand static load and control conditions to room temperature.

Sommariva et al, 2003 [6] generated database for phase changing materials using CES edupack. The software listed the commercial and non-commercial phase changing materials based on temperature ranges from -50 ℃ to 150 ℃. Callister et al, 2012 [7] made selection of phase change materials such as 88Al-22Si for higher temperature applications considered thermal properties and environmental performance.

Heating, Ventilation, and Air conditioning (HVAC) coils utilized aluminum and copper tubes due to higher thermal conductance and lower cost. Stainless steel offers durable and corrosion resistance attributes, making them a wise choice for corrosive surroundings. Stainless steel has high strength but cannot transfer heat as effectively as aluminum tubes. Combining stainless steel tubes with aluminum fins are a future recommendation for effective heat transfer and lower cost in evaporator system [8].

Salty water or refrigerants that cause corrosion and leakage to the evaporator system can be reduced by utilizing stainless steel because of higher corrosion resistance offered by stainless steel. The Cambridge Engineering Selector approach used in this project will provides detail methodology for selecting stainless steel in evaporator's coils in HVAC system.

II. Methodology for Material Selection

Granta Design Selector (CES) is used to give a methodology for selecting a suitable material for any product design. Design and functional attributes are considered for selection purposes. Evaporator coil perform the function of extracting heat and transfer it outside to provide cooling effect to the conditioning systems. Design attributes include thermal, mechanical and corrosive properties. Thermal properties includes higher melting points, thermal conductance, and service temperature. Other attributes such as mechanical consists tensile strength and toughness, and corrosion resistance. The salty water and refrigerants causing corrosion to the evaporator coils need to be controlled by selecting higher corrosion resistance materials. The evaporator coils required attributes are given in Table 1. Based on the CES classification of material's universe into six categories are metals, polymers, ceramics, composites, elastomers and glasses, materials with higher melting point compared to evaporation system, having higher thermal conductance. Corrosion resistance, toughness and tensile strength would be the most promising material. Specifications and attributes specified for evaporator coil given in Table 1 identified the metals as a promising category out of six.

Table 1: Evaporator coil materials desirable properties

Property	**Desirable Categorizations**
Thermal	Higher melting point >730 ℃, higher thermal conductivity.
Mechanical	Higher Strength and Toughness
Corrosion	Must have higher corrosion resistance

The evaporator turns the liquid substance into gaseous or vapor form by absorbing heat from the system. Material must follow the emphasis constrains by the designer for effective evaporation systems. These restrictions are high melting pint, thermal conductivity, service temperature durability without corrosion, toughness and higher strength. The main goal is to achieve effective evaporation system for conditioning system. Material and dimension can be varied freely as a choice of designer. Table 2 describes the detail function, objectives, constrains, and free variables of evaporator coils in air conditioning systems.

Table 2: Function, objectives, constraints, free variable for evaporator coil's material

Function	• Evaporation
Constraints	• Higher melting point • Strong i.e. tensile strength • Greater Fracture Toughness • High Thermal conductivity
Objectives	• Maximize thermal conductivity • Minimize corrosion • Maximize strength • Minimize mass
Free Variables	• Choice of material • Dimension of coil

Following the Fig.1 to Fig. 4, illustrates various attributes such as melting points, thermal conductivity, tensile strength, and toughness of the metal alloys. Based on these properties, material is shortlisted for evaporator coil in conditioning system. Figures clearly shows the stainless steel, low alloy steel, titanium, nickel chromium, copper, and cast iron comes within the range specified after application of conditions and constraints. Apart from the above attributes, other properties that needs to be considered are service temperature, thermal diffusivity, and durability. Selecting the most promising material for evaporator system from the shortlisted candidate is the main challenge for designer.

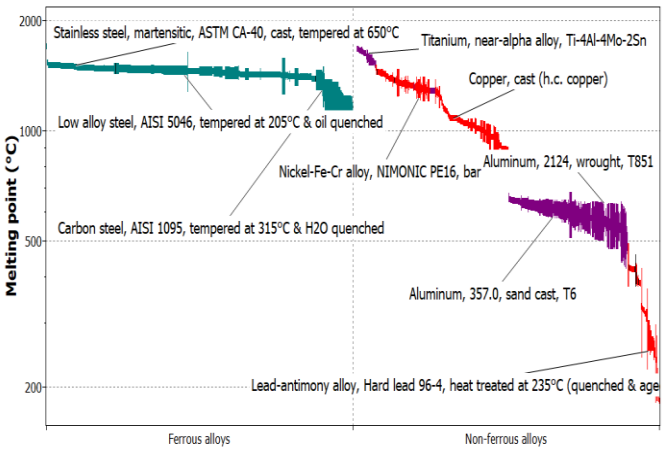

Figure 1; illustrate the melting points (℃) plotted on x-axis against the ferrous and non-ferrous alloys on y-axis.

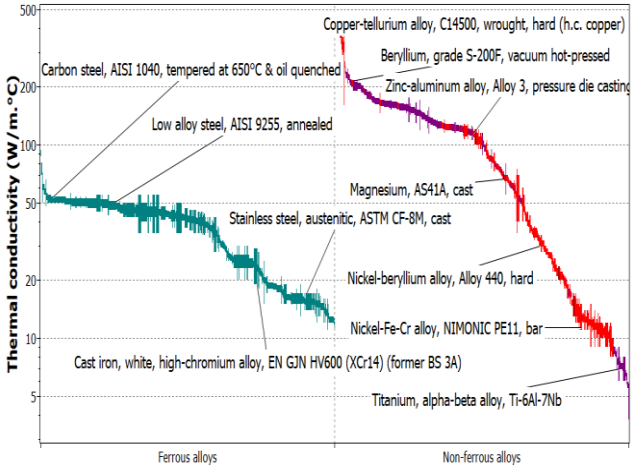

Figure 2; preview the thermal conductivity (W/m.°C) of ferrous and non-ferrous alloys plotted on x-axis and y-axis respectively using CES software.

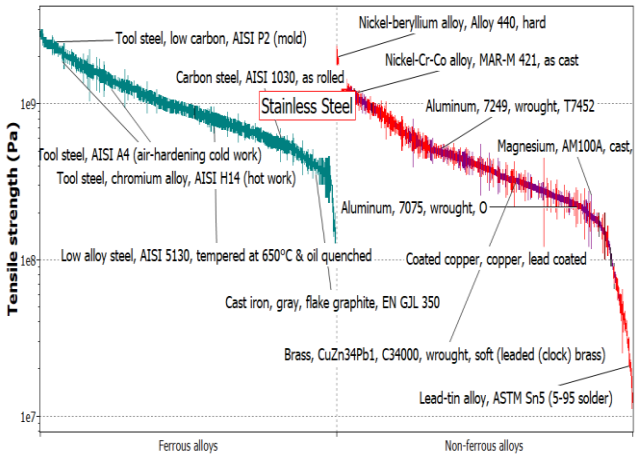

Figure 3; Tensile strength (Pa) plotted on y-axis against the metal alloys mentioning the shortlisted materials for evaporator coil operating conditions.

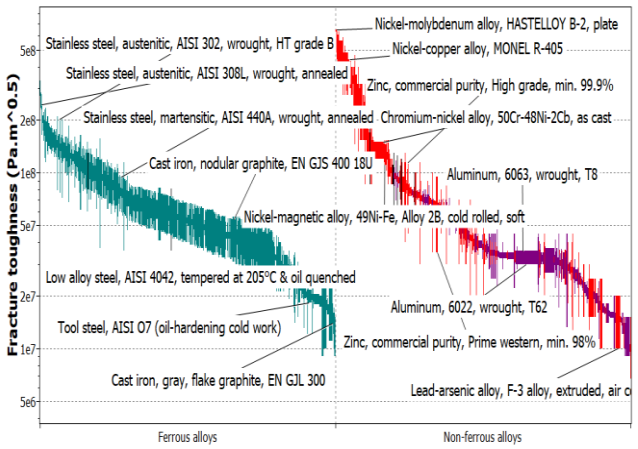

Figure; 4 Illustrate the fracture toughness (Pa.m^0.5) against the metal alloys.

From Figure 1-4, the following materials are listed as the promising candidate for evaporator system in air conditioning systems. The various attributes of the shortlisted candidate are given in Table 3.

TABLE 3: SHORTLISTED CANDIDATE FOR EVAPORATOR COILS IN AIR CONDITIONING SYSTEM

Materials	Comment
Cast iron	Cheap, easily available but corrosive
Commercially pure titanium	Lighter, high tensile strength but expensive
Copper	High thermal conductivity but expensive
Low alloy steel	Heavy but greater toughness
Stainless steel	Benchmark
Nickel Chromium Alloy	Corrosive resistant

Table 3 enlisted the cast iron, copper, low alloy steel, stainless steel and nickel-chromium steel selected from the Figure 1 to 4 based on design and functional requirements of the evaporator coil in conditioning system. Titanium addition to the list in Table 3 is because of the additional and supportive information gathered according to the application specifications.

III. PERFORMANCE CALCULATION (WEIGHT INDEX PROPERTY METHOD)

Material indices is a general expression of the parameters that optimize the desire performance based on the dependable factors. A brazed plate heat exchangers designed as an evaporator is used to transfer heat between the refrigerant and heat transfer fluid. Heat flux through evaporator is basically the heat transfer per unit area also known as heat exchanger's density. The equation (1) and (2) gives the required parameters for effective heat transfer between heat transfer fluid and refrigerants.

$$Q = k.\ A.\ MTD \quad (1)$$

$$Q/A = k.\ MTD \quad [W/m^2] \quad (2)$$

Where:
Q= Capacity [W]
A= Heat transfer area [m^2]
k= Overall heat transfer Coefficient [W/m. K]
MTD= Mean Temperature Difference [K]

The heat transfer density depend upon the mean temperature difference and overall coefficient which is thermal conductivity. To maximize the evaporator capacity, temperature difference and thermal conductivity should be higher. Material with high thermal conductance, melting points, and corrosion resistance will be prefer over the rest of the candidate materials.

TABLE 4: PROPERTIES OF SHORTLISTED CANDIDATE MATERIALS TAKEN FROM CES DATABASE

Material	Property			
	Melting Point (℃)	Thermal Conductivity (W/m.℃)	Tensile Strength (Pa) e^8	Toughness (Pa.m^0.5) e^7
Cast Iron	1200-1430	37-40	1.1-1.4	1-1.6
Titanium	1660-1680	20.4-22.1	2.4-5.5	5-5.5
Low Alloy Steel	1460-1510	41-45	6.52-7.20	1.03-1.17

Stainless Steel	1430-1470	12-15	5.15-7.15	1.32
Nickel-Chromium Steel	1320	9-12	9.05-10.02	10.02
Copper	1030-1050	65-70	5-5.9	5.43

Two different scales are set for calculation of performance criteria. Ascending order of the attribute from most important to less importance is arranged based on design and functional requirements of the evaporator coil in conditioning system. The scale vary from 1 to 5. The property nature is assigned from excellent to poor value on scale 0 to 1. Melting point is at the top of the scale and toughness is the least important one. The summation of importance on scale 1 to 5 against the property is represented by $\sum r = 14$. While performance weightage calculated is shown in Table 5.

TABLE 5. PERFORMANCE WEIGHTAGE OF SHORTLISTED CANDIDATE FOR EVAPORATOR COIL

Material	**Property**						
	Corrosion resistance	M.P (℃)	K (W/m.℃)	Tensile Strength (Pa) e^8	Toughness (Pa.m^0.5)ve^7	∑R	∑R/r
Cast Iron	X	5*0.4= 2.0	4*0.8= 3.2	3* 0.1= 0.3	2*0.4= 0.8	6.3	0.45
Titanium	S	5*0.6=3	4*0.6= 2.4	3*0.8= 2.4	2*0.6= 1.2	9	0.64
Copper	S	5*0.1= 0.5	4*1= 4	3* 0.6= 1.8	2* 0.8= 1.6	7.9	0.56
Low Alloy Steel	S	5*1= 5	4*0.6= 2.4	3* 0.4= 1.2	2*0.8= 1.6	10.2	0.729
Stainless Steel	S	5*0.8= 4.0	4*0.8= 4.0	3*0.8= 2.8	2*0.4= 0.8	10.4	0.74
Nickel Chromium Alloy	S	5*0.4= 2.0	4*0.4= 1.6	3*1= 3	2*1= 2	8.6	0.61

CONCLUSION

Evaporators are widely employed in most industries that depend on a constant supply of fluids or chemicals, and ideal for very low temperature applications in the food and pharmaceutical industries. Evaporator material failure occurs due to heat and aggressive particle present inside the conditioning system. Pitting corrosion take place inside the evaporator tubes because of chlorine and salty water circulating through the tubes. Stainless steel offer high strength along with higher corrosion resistance. Stainless steel gives promising performance in evaporating coils. The long-term stability of stainless steel over lower alloy steel and titanium made it final choice for evaporator coil in air conditioning system.

REFERENCES

[1] Wiqas Alam Material Selection for Micro Channel Heat Exchangers for Industrial Waste Heat Recovery International Journal of Engineering Works Vol. 6 Issue 11 PP. 406-413 November 2019

[2] Zupan, Marc, Mike F. Ashby, and Norman A. Fleck. "Actuator classification and selection—the development of a database." Advanced engineering materials 4.12 (2002): 933-940

[3] Schodek, Daniel L., Paulo Ferreira, and Michael F. Ashby. Nanomaterials, nanotechnologies and design: an introduction for engineers and architects. Butterworth-Heinemann, 2009.

[4] Reddy, G. Prashant, and Navneet Gupta. "Material selection for microelectronic heat sinks: an application of the Ashby approach." Materials & Design 31.1 (2010): 113-117.

[5] Shanian, A., and O. Savadogo. "A methodological concept for material selection of highly sensitive components based on multiple criteria decision analysis." Expert Systems with Applications 36.2 (2009): 1362-1370.

[6] Sommariva, Corrado, Harry Hogg, and Keith Callister. "Cost reduction and design lifetime increase in thermal desalination plants: thermodynamic and corrosion resistance combined analysis for heat exchange tubes material selection." Desalination 158.1-3 (2003): 17-21.

[7] Sommariva, Corrado, H. Hogg, and K. Callister. "Forty-year design life: the next target Material selection and operating conditions in thermal desalination plants." Desalination 136.1-3 (2001): 169-176.

[8] Anojkumar, L., M. Ilangkumaran, and V. Sasirekha. "Comparative analysis of MCDM methods for pipe material selection in sugar industry." Expert systems with applications 41.6 (2014): 2964-2980.).

IJEW 国际工程期刊 International Journal of Engineering Works انجینئرنگ کاموں کا بین الاقوامی جرنل

International Journal of Engineering Works
ISSN-p: 2521-2419
ISSN-e: 2409-2770
Vol. 7, Issue 05, PP. 221-227, May 2020
https://www.ijew.io/
https://doi.org/10.34259/ijew.20.705221227

Check for updates

Causes of Delay in the Establishment of Public Sector University in Newly Merged District's of KP, Pakistan

Mirza Ali[1], Dr. Shahid Iqbal[2], Dr. Qaiser Iqbal[3]
[1]Department of Works, FATA University, Newly Merged District Darra Adam Khel, Kohat
[2,3]Department of Civil Engineering, Sarhad University of Science and Information Technology, Peshawar
mirza.ali@fu.edu.pk[1], shahid.civil@suit.edu.pk[2], qi.civil@suit.edu.pk[3]
Received: 29 March, Revised: 07April, Accepted: 06 May

***Abstract*—**Delays are one of the major issues in the development venture. Because of this, projects surpass projected time and cost. Retardation in the project can be reduced only when its reasons are determined and evaluated. The main focus of this research study was to determine the delaying causes in the establishment of FATA University. The study follows a quantitative approach where a well-defined questionnaire was distributed among the experts directly managing the construction project of FATA University, i.e. the consultant, the contractor, and the client for the data collection. Relative Important Index (RII) was employed in the research methodology to determine the significance of each delaying factor. Top five delaying causes in the establishment of FATA University project were recorded as (1) client having risk attitudes, (2) Lack of coordination between client, contractor, and consultant, (3) slow decision effects, (4) consultant supervisory staff size and (5) frequent changes in design documents by the consultant. The efficient management and planning of these delaying factors will positively affect the project completion time and its overall cost.

***Keywords*—** Establishment of public sector University, Newly merged district of KP, Causes of delays, Public sector construction projects.

I. INTRODUCTION

The tribal districts and tribal sub-divisions (TSD) of the present-day of Khyber Pakhtunkhwa (KP) were the erstwhile Federally Administered Tribal Areas (FATA) of KP, Pakistan. The erstwhile FATA was consisting of seven (07) tribal districts and six (6) sub-tribal divisions. The seven tribal districts are District Malakand, District Mohmand, District Bajaur, District Khyber, District Kurram, and District North Waziristan and South Waziristan. The six (6) sub tribal divisions were located in the adjoining areas of the settled district of Peshawar, Kohat, Bannu, Tank, Dera Ismail Khan, and Lakki Marwat. The Sub-tribal divisions were also known as Frontier Region (FR). To the north and east of erstwhile FATA, Khyber Pakhtunkhwa is located, while in the south is the province of Baluchistan. In the southeast, erstwhile FATA districts join the Punjab province. To the west is the Durand Line, separating the Khyber Pakhtunkhwa (KP) province from the neighboring country of Pakistan is Afghanistan [1].

Erstwhile FATA districts, the total area is 27,220 square kilometer (m2) and according to the census 2017, the overall population is five (5) million and the population growth rate in erstwhile FATA is 3.8 percent (%) per year. Across FATA Population density under the 2017 census stands at 184 persons per square kilometers (p/m2). Newly merged districts of FATA are buffer areas between Afghanistan and Pakistan in the province of Khyber Pakhtunkhwa (KP). Moreover, the literacy rate is varying across FATA; it is 45 percent (%) for males and 7.8 percent (%) for females under the year of 2017 census of Pakistan. Overall, in erstwhile FATA the adult literacy rate is very low its 28.4 percent. This low literacy rate or low student engagement in education is a very alarming situation for the forthcoming generations of KP as well as for Pakistan [2].

Figure 1. Blue Area indicates the Erstwhile FATA Region of Pakistan

For the advancement of any nation, construction industries play a very significant role. The physical advancement of construction projects such as power stations, bridges, buildings, and roads are signs of economic upward movement of a nation

via which a society or nation achieves its aims and purposes of urban and rural development[4]. Usually, projects in public education sectors are planned for the undertaking. However, the delay may occur in the life cycle of the project. Delays of the project are a condition in which a contractor and the possessor bilaterally or individually add to the lack of complete execution of the construction project as mentioned in the original accorded period [5]. The retardation in the completion of the project can be reduced if the linked causes are unambiguously determined [6, 7]. The key focus of the current research study is to resolve the issue of retardation in the PSDP funded project of the establishment of FATA University.

The tribal districts and tribal subdivision (TSD) or the formerly federally administered tribal areas (FATA) of Pakistan are currently complete part of Khyber Pakhtunkhwa (KP) province after a twenty-fifth (25th) constitutional amendment in the constitution of Pakistan. This erstwhile FATA region is socio-economically very backward within Pakistan. The reasons are that the federal government kept the area deliberately under-developed for vested interest. Other reasons include dry or semi-dry weather conditions, mountainous regions, geographical remoteness, and lack of education. Contemporarily, the government of Pakistan has introduced numerous reforms in FATA, one of including the establishment of FATA University.

The delay in the construction of an agreed project is very undesirable especially for developing countries and areas like the backward erstwhile FATA of Pakistan. However, no meaningful research has been carried out for the concerned people to determine the associated causes of retardation in the completion of the establishment of the FATA university construction project within a specified time. The first public sector university construction project in erstwhile FATA is managed by the Higher Education Commission (HEC) by the sponsorship of the Planning Commission (PC) of Pakistan, which is fundamentally authorized for the design-bid-build construction. The government of Pakistan has allocated 4.7 billion (4700 Million) Pakistani Rupees (PKR) for this construction project, titled "Establishment of FATA University" in PSDP (HEC) 2015-16 (1 US $ = 100.52 PKR in January 2015) for the construction of first-ever public sector university in erstwhile FATA region. The government has released funds for the construction of FATA University for the first phase of Rs.1592 million rupees. The KP government also contributed to the erstwhile FATA educational development in various ways to sustain and benefit the educational need of the FATA underprivileged people [8]. The government of Pakistan usually allocates special budgets for the development of public-sector education projects in erstwhile FATA to develop the standard of life of residents of erstwhile FATA of Pakistan [17].

The proposed establishment of FATA University in Darra Adam Khel will extend an opportunity of higher education to the local peoples at the doorstep as was the vision 2025 of the government of Pakistan to give a good educational system as well as an efficient education service in the erstwhile FATA region. However, the project's delays are not an unusual phenomenon in the erstwhile FATA region; it is very common in the case of FATA districts. The general reasons for delays in project completion are the unstable economy, remoteness of the area, terrorism, militancy, and political instability. In case of FATA University project, it is significant to inquire the associated stakeholders (sponsor, contractor, and consultant) of the project to improve, strengthen the execution of the project so that it can be completed, not only within time but also within the stipulated cost and at the time maintaining the quality of structure as well. Further, it is also essential to discover the possible reasons of retardation in the construction project execution/construction phase. The fundamental focus of this research study is to determine the factors that are solely responsible for the retardation of the construction work of FATA University.

Figure 2. Proposed Main Gate of FATA University

II. JUSTIFICATION OF PROPOSED FATA UNIVERSITY

Presently, no higher learning Institute is operating in the erstwhile FATA region. This is the first public sector university in this region. Some of the graduates from the local postgraduate colleges were used to quite an education due to the unavailability of higher education facilities locally. While others used to migrate to areas outside the FATA region to avail higher education. There the students of the FATA region have to face tough competition in admission due to the presence of a lot of other talented students seeking the same admission. The proposed FATA University will assist in reducing the number of students who quit education after completing education from the post-graduate colleges. Further, through the establishment of FATA University provided the higher education facilities are at the doorstep, it will significantly reduce the competition of admission for the education of socially and economically backward erstwhile FATA region of Pakistan.

III. PROJECT BENEFITS AND ANALYSIS

A. Financial Benefits

The financial benefit cannot be quantified in the first phase of FATA University. However, FATA University's having the capability to provide admission to students is about 2000 students. Surely, the number will increase with the establishment of new departments, availability of resources, infrastructure, and success of existing programs. The quality of education is likely to improve with time.

B. Social Benefits

The establishment of FATA University will be a great source of a quality increase in education of the local peoples and at the same time and would escalate the male and female literacy rates in the erstwhile FATA region. This education ratio will directly affect the reduction of social evils and employments of the FATA peoples.

C. Enviromental impact

The establishment of the FATA University Project has no negative effect on the surrounding environment of the area. Rather, it would positively affect the environment in the sense that some areas under the university will be developed and environmentally be planting abundant trees and water availability provisions.

IV. LITERATURE REVIEW

At present education is considered a basic right of human beings and is considered key for social, economic, political development, and human freedom. Basic education was denied to the residents of erstwhile FATA which was not only gendered discrimination but was also an incorrect economic and social policy [2]. Pakistan is located in a region where almost 48% of the Illiterate population lives. The majority of these illiterates are women. Since independence, Pakistan is facing the education problem, despite a long period of 72 years of its existence; the literacy rate is still 58 percent (%) of the total population [3].

Identification of the delaying factors enables the contractors, sponsors, and consultants to minimize the effective delays in the project implementation process. This determination and evaluation of delaying factors are very essential, though it's very challenging. The need is to give priority to delaying factors for the purpose at least to decrease their impact. The retardation in the execution of construction projects is defined simply as an event, process, or acts that extend the budget and time duration agreed in the contract of the concerned contracting parties. [9-10].

Numerous research studies are available in various countries regarding construction projects and the factors solely responsible for the retardation in the completion of construction project [11-12]. Widely mentioned causes of delay in the construction works are; lack of financing or payment on the part of sponsor to the contractor, absence of contractor experience in the concerned construction field, change in the design, improper site selection, lack of proper supervision by contractor, as well as often contradictory order by owner. A significant number of research studies argue that delays in construction projects generate costs, schedules, and time escalation. Argue, it is necessary to improve the quality and efficiency of construction companies. Despite regional, administrative, and geographical differences, the researchers are struggling to suitably report the factors of project delay [6, 10]. Thus, researchers have determined distinct patterns of delaying factors in various research projects. Some studies have focused on general construction projects [10, 11, 14]. Very few research studies concentration of attention is on the government-funded projects [15, 16, 17]. Thus, public-funded university construction projects are not previously researched, hence, thus, this research study has surveyed, inquired about the reasons responsible for the retardation in the completion of the establishment of FATA University in Darra Adam Khel, Kohat. So this research study fills the gap in the literature regarding the construction phase of the FATA university project. There was a considerable requirement of such type of research study, because the project is still incomplete, and there is a need to finish the construction project as soon as possible. This is not the only project that faces delay, numerous other projects have frequently observed, experienced delay in the construction works, escalation in cost and budget in erstwhile FATA region. The frequently occurring delays stimulate the researcher to undertake a research study of the newly launched FATA university construction project to determine the delaying factors. Further, this research provides detailed information regarding all linked aspects of the construction project with the purpose to provide productive ideas for the improvement in the construction project. Surly, the research finding and proposal regarding the project extend valuable knowledge for the stakeholders to finish the project.

V. RESEARCH OBJECTIVES

The key purposes of this research study were to assess and identify the major factors which contributed to the delay of the FATA university construction project.

1. To establish a University in erstwhile FATA to provide equal opportunity to the students of FATA to acquire higher education in a conducive environment to lead enlightened and modern society.

2. To envisages establishing of FATA University, physical and academic infrastructure, are a deliberate attempt on the part of the Government to provide a very pleasant, conducive learning environment to fulfill the intended purpose of establishing and advancing the higher education opportunities for the people of FATA as well as to the whole country.

3. To make progress and survive competitively, the government of Pakistan's objective is to develop human resources by escalating investment in the higher education sector so that they can perform a productive function in the growth of education based economy in this highly competitive world.

4. Ensuring the availability of young talent in FATA peoples and skilled professionals in Pakistan is also the priority of the government.

VI. RESEARCH METHODOLOGY

The data collection method involved in three main phases, as shown in Figure-3. In the first phase, the researcher obtained the initial causes of affecting the establishment of the FATA university project. In the second phase, the researcher conducted a pilot study to gain a better understanding and completeness as well as modification of the questionnaire. In the final phase of the research, the researcher carried out a questionnaire survey to check the important degrees of the different causes and respondent perceptions.

To determine the Relatively Important Index (RII) factors affecting the FATA university construction project, a Relative Importance Index (RII) method is used in the research. The factors were divided into three main categories namely consultant related factors, contractor related factors, and client related factors. The RII index was ranked group wise as well overall for the selected factors. The five points Likert scale was employed ranges from (1=Not Important) to (5 = Extremely Important) and transformed to RII for each cause in a group as well overall follows:

$$RII = \Sigma W / A^* N$$

W = weighting given to each factor by respondents (1 to 5)

A = high weight (i.e. 5 in this case)

N = total number of respondent

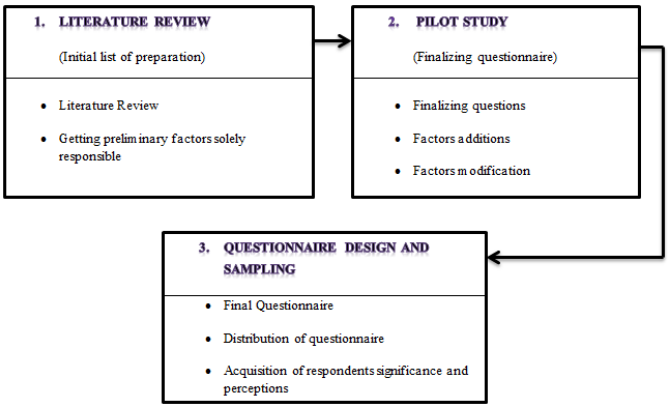

Figure 3. Data Collection Process

VII. RESULTS

TABLE I. OVERALL RANKING OF CAUSES AFFECTING TO CONSULTAN

Rank	ID	Causes	RII
1	1-2	Slow decision effects	0.900
2	1-6	Consultant Supervisory staff size	0.896
3	1-1	Frequent changes in design documents	0.887
4	1-3	Relevant past experiences in the complex projects	0.858
5	1-4	Inexperienced personnel in the consultant team	0.848
6	1-5	Lack of timely payments to the consultant	0.225

TABLE II. OVERALL RANKING OF CAUSES AFFECTING TO CONTRACTOR

Rank	ID	Causes	RII
1	2-5	Lack of high technology mechanical construction equipment's	0.880

2	2-1	Frequent changes of the sub-contractor	0.877
3	2-3	Lack of relevant experience	0.706
4	2-6	Lack of skilled labors work efficiency	0.332
5	2-8	Bid winning on the lowest price	0.283
6	2-4/2-7	Equipment's breakdown/ Lack of timely payment to the contractor	0.264
7	2-2	Lack of professional staff	0.258

TABLE III. OVERALL RANKING OF CAUSES AFFECTING TO CLIENT

Rank	ID	Causes	RII
1	3-7	Client having risk attitudes	0.941
2	3-4	Lack of coordination between client, contractor, and consultant	0.912
3	3-3	Inability to make a timely decision	0.883
4	3-2	Lack of client staff size	0.845
5	3-5	Lack of ability to cover the various construction packages by the client	0.377
6	3-1	Lack of relevant experience of the client	0.300
7	3-6	Shortages of fund	0.277

TABLE IV. OVERALL RANKING OF CAUSES

Rank	ID	Causes	RII
1	3-7	Client having risk attitudes	0.941
2	3-4	Lack of coordination between client, contractor, and consultant	0.912
3	1-2	Slow decision effects	0.900
4	1-6	Consultant supervisory staff size	0.896
5	1-1	Frequent changes in design documents	0.887
6	3-3	Inability to make a timely decision	0.883
7	2-5	Lack of high technology mechanical construction equipment's	0.880
8	2-1	Frequent changes of the sub-contractor	0.877

9	1-3	Relevant past experiences in the complex projects	0.858
10	1-4	Inexperienced personnel in the consultant team	0.848
11	3-2	Lack of client staff size	0.845
12	2-3	Lack of relevant experience	0.706
13	3-5	Lack of ability to cover the various construction packages by the client	0.377
14	2-6	Lack of skilled labors work efficiency	0.332
15	3-1	Lack of relevant experience of the client	0.300
16	2-8	Bid winning on the lowest price	0.283
17	3-6	Shortages of fund	0.277
18	2-4/2-7	Equipment's breakdown/ Lack of timely payment to the contractor	0.264
19	2-2	Lack of professional staff	0.258
20	1-5	Lack of timely payments to the consultant	0.225

CONCLUSION & RECOMMENDATIONS

The Relative Importance Index (RII) method enabled the researcher to identify the key causes of different construction project delays of FATA University of group-wise and as a whole as well. Three top causes linked to consultant were noted (1) slow decision effects, (2) consultant supervisory staff size, and (3) frequent changes in design documents. Contractor related factors the top three causes were (1) Lack of high technology mechanical construction equipment's (2) frequent change in sub-contractor and (3) Lack of relevant experience. Client related factors; the main three causes were (1) client having risk attitudes, (2) Lack of coordination between client, contractor, and consultant and (3) Lack of ability to make a timely decision. However top five overall causes are (1) client having risk attitudes, (2) coordination between client, contractor, and consultant, (3) slow decision effect, (4) consultant supervisory staff size, and (5) frequent changes in design documents by the consultant.

FATA University is the first varsity in the newly merged districts of Khyber Pakhtunkhwa.

Although FATA University is now establishing in Darra Adam khel, Kohat region, it compasses the direct benefits only to the students of Tribal subdivision Darra Adam khel, Tribal subdivision Peshawar and district Khyber. Due to the aftermath, in future FATA University should expand its campuses in the other newly merged districts of KP, like North and South Waziristan districts, district Kurrum, and Mohmand and Bajaur districts of KP.

1. It is suggested that the estimated cost and time of the forthcoming campuses should be accurate, and that can be done on the proper planning, designing, and scheduling of estimates.

2. All the changes should be done before the starting of construction works, because of the change of orders and changes in design documents on the spot, the construction works should be deferral.

3. It is suggested that during the planning and scheduling of detail designing of the upcoming campuses, the organization should be careful to hire the most relevant and having complex nature experience consultant.

4. It is suggested that during the preparation of the Master Plan, the consultant should focus on the detailed estimation and proper planning of the forthcoming campuses and if the Master Plan approved then avoid the self-made changes.

5. It is further suggested that the proper action should be taken into account to warn and forfeit the construction securities to solve and lessen the delays in the completion of large and complex educational institutions projects of Pakistan.

CONFLICT OF INTEREST

I declare that there is no conflict of interest and the previous work of the original author has been properly cited

REFERENCES

[1] Government of Pakistan, Planning and Development Department, Federally Administered Tribal Areas (FATA) Pakistan (Peshawar: FATA Secretariat, Warsak Road, 2009), p.vii http://fata.gov.pk/files/MICS.pdf (Accessed 17th August 2013).

[2] "In pictures: Census teams go door-to-door for Pakistan's first nationwide headcount in 19 years". DAWN.COM. 15 March 2017. Retrieved 21 March 2017.

[3] Social Policy and Development in Pakistan: The State of Education, Annual Review 2002-2003, Social Policy and Development Centre, Karachi, Pakistan, 2003. P.7.

[4] Alzahrani, J. I., & Emsley, M. W. (2013). The impact of contractors' attributes on construction project success: A post construction evaluation. International journal of project management, 31(2), 313-322.

[5] Aibinu, A. A., & Odeyinka, H. A. (2006). Construction Delays and Their Causative Factors in Nigeria. *Journal of Construction Engineering and Management*, *132*(7), 667–677. https://doi.org/10.1061.

[6] Santoso, D. S., & Soeng, S. (2016). Analyzing delays of road construction projects in Cambodia: Causes and effects. Journal of Management in Engineering, 32(6), 05016020.

[7] Awan, N. (2013). Education in FATA. Pakistan annual research journal, 49, 163-170.

[8] Assaf, S. A., & Al-Hejji, S. (2006). Causes of delay in large construction projects. *International Journal of Project Management*, *24*(4), 349–357. https://doi.org/10.1016/j.ijproman.2005.11.010.

[9] Lo, T. Y., Fung, I. W., & Tung, K. C. (2006). Construction Delays in Hong Kong Civil Engineering Projects. Journal of Construction Engineering and Management, 132(6), 636–649. https://doi.org/10.1061/(ASCE)0733-9364(2006)132:6(636)

[10] Gunduz, M., Nielsen, Y., & Ozdemir, M. (2015). Fuzzy Assessment Model to Estimate the Probability of Delay in Turkish Construction Projects. *Journal of Management in Engineering*, *31*(4), 04014055. https://doi.org/10.1061/(ASCE)ME.1943-5479.0000261

[11] Marzouk, M. M., & El-Rasas, T. I. (2014). Analyzing delay causes in Egyptian construction projects. Journal of advanced research, 5(1), 49-55.

[12] Al-Momani, A. H. (2000). Construction delay: a quantitative analysis. International journal of project management, 18(1), 51-59.

[13] Sambasivan, M., & Soon, Y. W. (2007). Causes and effects of delays in the Malaysian construction industry. *International Journal of Project Management*, *25*(5), 517–526. https://doi.org/10.1016/j.ijproman.2006.11.007

[14] Hwang, B.-G., Zhao, X., & Ng, S. Y. (2013). Identifying the critical factors affecting schedule performance of public housing projects. Habitat International, 38, 214–221. https://doi.org/10.1016/j.habitatint.2012.06.008

[15] Zaneldin, E. K. (2006). Construction claims in United Arab Emirates: Types, causes, and frequency. International journal of project management, 24(5), 453-459

[16] Hussain, S., Zhu, F., Ali, Z., Danial Aslam, H., & Hussain, A. (2018). Critical delaying factors: Public sector building projects in Gilgit-Baltistan, Pakistan. 8(1), 6.

[17] Hussain, S., Zhu, F., Ali, Z., & Xu, X. (2017). Rural residents' perception of construction project delays in Pakistan. Sustainability, 9(11), 2018.

Mirza Ali is the resident of Peshawar Khyber Pakhtunkhwa, Pakistan. He did his Bachelor of Technology from the Sarhad University of science and information technology Peshawar, Pakistan in 2015. Currently enrolled in the MS program of Construction Engineering and Management at Sarhad University of science and information technology Peshawar, Pakistan (SUIT). The paper is the research article of the scholar in the Master's Degree. Research interests include Construction Engineering Management, Material Management, and Risk Management.

IJEW 国际工程期刊 International Journal of Engineering Works انجینئرنگ کاموں کا بین الاقوامی جرنل

International Journal of Engineering Works
ISSN-p: 2521-2419
ISSN-e: 2409-2770
Vol. 7, Issue 05, PP. 228-232, May 2020
https://www.ijew.io/
https://doi.org/10.34259/ijew.20.705228232

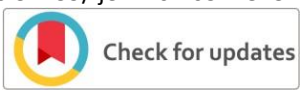

Implementation of Mobility Model for V2V Communication on LTE using NS3 and SUMO

Haseeb Jan[1], Dr. Mohammad Inayatullah Khan Babar[2]
[1,2]Department of Electrical Engineering, University of Engineering and Technology Peshawar, Pakistan
14pwele4534@uetpeshawar.edu.pk[1], babar@gwu.edu[2]
Received: 19 April, Revised: 04 May, Accepted: 11 May

***Abstract*—** Ad hoc network is a type of network in which there is no center node or center entity. So, there are two type of ad hoc network MANET and VANET. MANET (Mobile Ad Hoc Network) is a type of ad hoc network in which the nodes are connecting wirelessly and have some random mobility. But VANET (Vehicular Ad Hoc Network) are different in traditional MANET due to high mobility of nodes but the realistic vehicle can't be traced by using random mobility model and way point mobility model. So, for this purpose SUMO (Simulation of Urban Mobility) tool is used for vehicular mobility models and we successfully implement that model in NS3 and use a device to device feature (proximity sensor) of LTE module in NS3 for connected nodes (Vehicles) directly. And the aim of this project is to reduce the overload on infrastructural network and overhead in vehicular communication to avoid infrastructure and by connecting vehicles directly.

***Keywords*—** Vehicles, Roads, Trafic, LTE, Device-to-device, NS3, SUMO, OpenStreetMap, TraCI.

I. Introduction

Vehicle-to-vehicle (V2V) based on device-to-device (D2D) communication on LTE is seen as a promising technology to fulfill latency, reliability and capacity required by future wireless communication. Vehicular Ad-hoc Network (VANET) is a type of Ad-hoc Network that is used to provide communications between nearby vehicles, and between vehicles and fixed infrastructure on the roadside.

For defining mobility, we have two types of mobility models that is low mobility models and high mobility models. Low mobility models are used for user equipment's like mobile and this mobility is fully random. And on the second side we have high mobility which is used by vehicles on high speed which follows some architectural paths or patterns. There is a lot contribution present in telecommunication networks for low mobility networks, but no work done on high mobility infrastructure control mechanisms.

Deploying and testing these high mobility networks, usually known as Vehicular Ad-hoc Networks (VANETs), involves a high cost in the real world, so simulation is a useful alternative in research. Different simulation tools are available in the market to simulate these networks. But for mobility model implementation we use SUMO (Simulation of Urban Mobility) because of it is an open source tool which give us a good urban mobility model. And NS3 for simulating the network part of simulation are also open sourced tool having module for LTE.

A. Organization of paper

This paper follows the traditional paper flow of IEEE papers. There are five sections. First section is introduction in which I explain the various aspect of title and explain why we chose simulation. In the second section of paper I introduce the problem and literature review with various work done on this side with solution of problem in third section. Fourth section have two subsections, first subsection is about SUMO simulation and second subsection is about NS3. Finally, fifth section is a conclusion and future work.

II. PROBLEM STATEMENT

So, our aim to simulate mobility models for VANETS on LTE using SUMO and NS3. That of to provide path to practical demonstration in future.

A. Problem explanation

There are many ways to find the mobility of nodes in the network. In this project we will be using SUMO to define the mobility for the nodes in the network. To study different parameters of the LTE standard based network under different mobility models defined by SUMO we will be using NS3. The NS3 by itself cannot define Vehicular mobility for the nodes(it just have some random mobility models) that is why SUMO is used to generate the trace file of mobility for nodes which then will be imported in the context of NS3. *Automated cleaning.*

III. Literature Review

The literature is divided into three sections. In Section one we are going to study VANETs Models, then in section two we study mobility models and finally we study LTE in Vehicular communication [1].

A. VANETs Models

Figure 1. explaining that there are mainly three type of research area in VANETs Vehicles-to-Vehicles(V2V), V-to-RSU (V2I) and RSU-to-RSU(I2I). RSU also known as Road Side Unit and in VANETs it is also called OBU (On-Board Unit).

Vehicular network is expected to deploy variety of advanced wireless technologies such as Dedicated Short-Range Communication. The DSRC is created to support the data transfer in rapidly changing communication environments. DSRC is effective for short range communication and good for fulfilling the VANETs application for safety that is, Cooperative Collision Avoidance (CCA), Emergency Warning Messages (EWM), Cooperative Intersection Collision Avoidance (CICA), Traffic Managements, Advertisements entertainment and comfort application like Electronic toll collection. But due to low bandwidth DSRC is not applicable for user-based applications like data transmission and video conferencing so therefore we tried to replace it by LTE [2].

B. VANETs Mobility Models

There are two type of mobility models macroscopic and microscopic. Macroscopic models consider constrains at a higher level like road crossing, intersections, streets, roads and traffic lights. While microscopic models take the behavior of individual vehicle with respect to road architecture and other vehicles.

"The development of modern vehicular mobility models may be classified in four different classes: Synthetic Models wrapping all models based on mathematical models, Traffic Simulator-based Models where the vehicular mobility models are extracted from detailed traffic simulator, Survey-based Models extracting mobility patterns from surveys, and finally Traced-based Models which generate mobility patterns from real mobility traces [3]."

"Vehicles follow a trail or certain mobility pattern which is a function of the underlying roads, the traffic lights, the speed limits, traffic condition and driving behaviors of drivers. Because of the particular mobility pattern, evaluation of VANET protocols only makes sense from traces obtained from the pattern [3]."

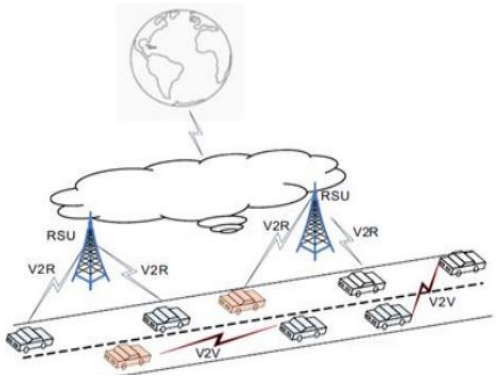

Figure 1. VENATs Model [1]

Different methods of configuration for mobility of Vehicles are advised which are classified as follows:" Entity Mobility Models (that represents mobile nodes whose movements are independent of each other), Group Mobility Models (that represent mobile nodes whose movements are dependent on each other), Urban Mobility Models, City section Mobility models (which are grid based models) and Realistic Mobility Models (that are based on realistic mobility patterns of mobile nodes) [5].

There are different factors which greatly affect the mobility of Vehicles on the roads. The foremost constraint is the presence of streets which restrict vehicular motion to well-defined paths. This makes the areas topology crucial because the same mobility model might lead to drastically different network performance under different topologies. "In short there five main factors which affect the mobility of Vehicles: Layout of Streets, Traffic control mechanisms, Interdependent vehicular motion, Average speed and Block size [5]."

[6] Has compared the performance of VANETs communication under the two mobility models i.e. MOVE and City Mob. According to [6] "Simulation analysis using realistic mobility model for VANET environment show that the performance of the protocol is greatly affected by the mobility model. The performance of an ad hoc network protocol can vary significantly with different mobility models then, the choice of mobility model in simulating VANET is very important. The mobility models for VANET should be most closely matching the expected real-world scenario. In fact, the anticipated real world scenario can aid the development of the ad hoc network protocol significantly.

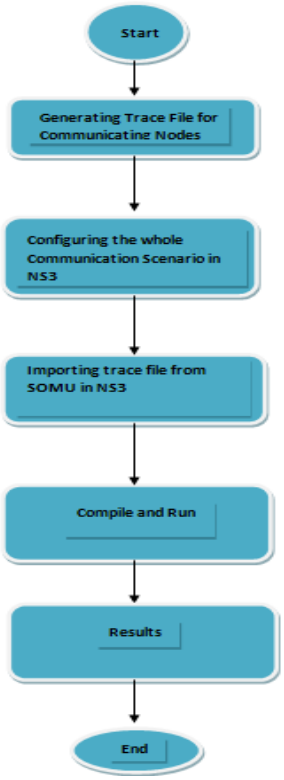

Figure 2. Block Diagram

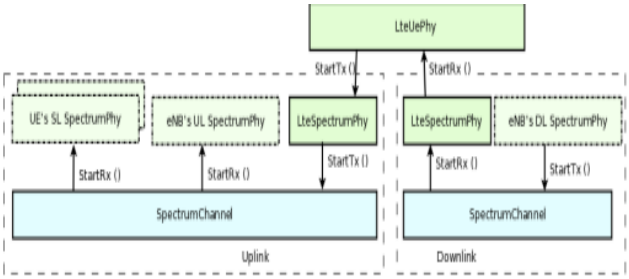

Figure 3: New PHY and Channel Model Architecture for the UE

IV. METHODOLOGY

As the main purpose of this project is to study the throughput for V2V for different mobility models using SUMO and NS3.Therefor we are going to use two major simulation tools to look for the desired results. The figure 2 shows the whole process of execution of this project.

For the movable communicating nodes first, it needs to be configured under specific communication standard protocol-in this case it is LTE. The second important parameter it must be provided with certain mobility pattern either to follow probabilistic pattern or deterministic pattern of motion. Figure 2 is flow chart we first study how we got the trace file out of SUMO. Export that trace file into ns3 adding LTE configuration.

A. Generating mobility model using SUMO

Before going into the steps we have taken for generating mobility in SUMO, we must mention that here we are using Ubuntu as an operating system platform for both NS3 and SUMO, also it is worth mentioning that SUMO could also be used in windows. And SUMO uses XML language for generating mobility scenario.

The following steps were taken to generate mobility in SUMO.

1. Generating Physical infrastructure: In this step we are going to generate physical infrastructure for mobility model that is roads and side buildings. For roads we have nodes (point where change in parameters of road occur) and links (connection between nodes). And also we used Open Street Map (OSM) for cloning maps for this purpose. After mentioning all parameter than we have to compile it by using SUMO pre define script that is "netconvert" which give us one file which contain full architecture and its attribute defined.
2. Dynamic of Traffic: Now we need to define number of vehicles its attribute and its mobility. Here we defined traffic and linked it with physical infrastructure. And for defining traffic we used both approach that define vehicles its sources and sink and its full path and time to start and end or we also used probabilistic approach which only need time to start and number of vehicles.
3. Then we converted that mobility to NS3 compatible trace file by using SUMO python script name "traceExport.py".

B. Putting all togather in NS3..

Now the trace file is created. It's time to configure the network of the communicating nodes in NS3. The whole process is divided into the following steps:

1. We created the lteHelper as an LTE object. Which includes our whole scenario. Then in the second and third line, we are going to create a core network, called PointToPointEpcHelper in the form of an object called epcHelper.
2. Now we configure the LTE scenario which consists of configuring eNbRrc in the transmission mode =2. As part of configuration, we create communication nodes, UE and eNB. we configure our scenario as default that is uplink bandwidth and download bandwidth is 50mbps default transmission mode of EnbRrc as 2. Their transmission and receiving power is 23dB and 46dB respectively.
3. Now attach the trace file generated by SUMO to the UEs. After this, we install the communication devices on UEs and eNbs. We attach the SUMO generated trace file named "examplemobility.tcl" as a mobility file of our scenario (SUMO generates NS2 support trace file which is also supported by NS3 using "ns2-mobility-helper.h" and install it to our scenario. The main limitation in NS3 in mobility models is that you can't specify the exact nodes for mobility. Because SUMO mobility should be installed to all nodes. So, making enb and epc static we do some changes that defining the position of those nodes in trace file at the last and make epc and enb nodes after UE nodes.
4. UEs are configured with side links with the default configuration. Now install internet devices on each UE and eNb and assigning IPs by epc (core network). We configured sidelink at Radio Resource Code level as preconfigure mode in this mode the UE's uses its configuration stored as a default in UE's this mode is used in out of coverage areas or we used here in V2V scenario. (that carrier frequency of sidelink is 23330Hz of the bandwidth of 50Mhz we make one pool of nodes that is every node are in the same network. And after that, we configure the parameter of the pool.) And after that we are going to install that default configuration to ueDevs(vehicles.)
5. Finally, we install application on the devices and run the simulation for particular duration. And enabled all traces of LTE. And enable animation interface on named "anim.xml." after all of that run simulator and end.

V. RESULTS AND DISCUSSION

As we have been using simulation tools in this entire project, therefore the results are presented in the form of the snapshots from the interfaces of these simulating tools. The simulating tools are SUMO and NS3 which had been discussed in great detail in the previous Section of methods.

We can see in figure 4a where the vehicles start to be generated by SUMO at the lower left corner and moving toward the right. In this topology of roads, there are three lanes defined in each segment of the road. Every vehicle follows its corresponding lane on which it is generated by the simulator.

In figure 4b Vehicles also generated from the second segment (the second left side vertex) also we can see that vehicles from the lower left side are taking turns in the intersection. This decision of taking turns is totally probabilistic, every vehicle takes a turn on the intersection they encounter is probable by a certain level of probability defined to the vehicles.

In figure 4c the vehicles are finally approaching for their defined destination. This locomotion of vehicles from start to their destination is logged by the simulator in the form of a trace file which is then exported to the Network nodes in the simulator, here in this project in NS3.

Now we are going to show the same movement of nodes in the network simulator, NS3. Where these vehicles will look like simple dots moving on the defined grid. The full scenario is expressed through the following figures. The sequence of the figures shows the progression in the motion of nodes toward the defined destination.

Figure 5a is the start of mobility and figure 5b is random clicks of scenarios in movements. In these figures, we only install the mobility of SUMO on nodes to validate the SUMO mobility in NS3. In NS3 comparing NS3 mobility to SUMO mobility animation file, we get that in NS3 origin of the plane is up-left while in SUMO it is down left.

Now after this we have installed the communication devices on each node so that they could communicate with each other. The next figure that is figure 6a and figure 6b is going to show how these moving nodes (vehicles) transmit message packets to each other on the shared medium.

The direction of arrows toward nodes shows the direction of communication. Also, the radius of the circles shows the transmission range of the individual node. So, from here we clearly see that every nod is communicating with each other.

VANETs and LTE protocol to have the maximum throughput. We didn't get to our goal during this short period of time as compared to the level of this project. Therefore, we only validated the D2D or ProSe functionality in LTE for VANETS.

As most part of this project has been completed, therefore the future of this project will be the achievement of the goal, to have the best-case scenario for the maximum throughput, for which this project had been started.

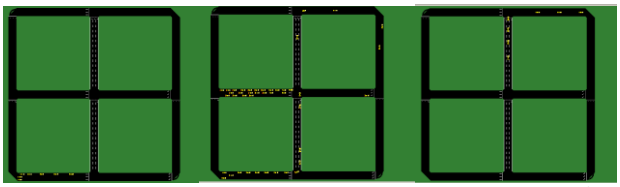

Figure 4a: Vehicles Start Moving

Figure 4b Vehicles Turns take on Intersection

Figure 4c: End of Simulaion

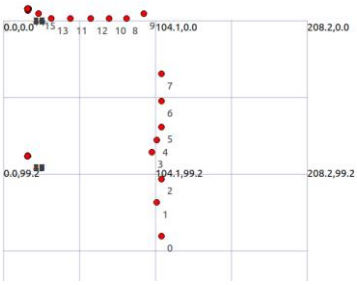

Figure 5a: Random click of NS3 Simulation

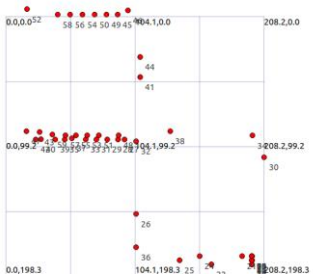

Figure 5b: Random click of NS3 Simulation

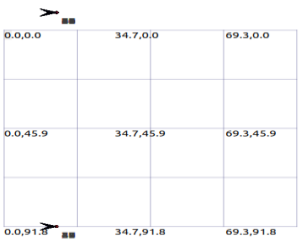

Figure 6a: communication between nodes

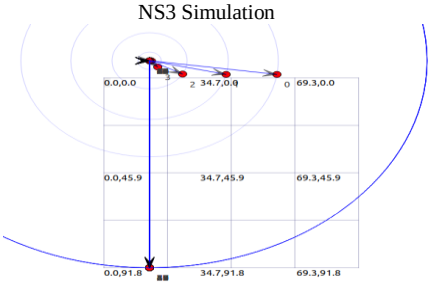

Figure 6b: communication between nodes

REFERENCES

[1] Deshmukh, Rajvardhan Somraj, Tushar Singh Chouhan, and P. Vetrivelan. "VANETS Model: Vehicle-to-Vehicle, Infrastructure-to-Infrastructure and Vehicle-to-Infrastructure Communication using NS-3." International Journal of Current Engineering and Technology, E-ISSN (2015): 2277-4106.

[2] HadiArbabi Michele C. Weigle (2010), Old Dominion University, Department of Computer Science Norfolk, VA 23529, USA, Highway Mobility And Vehicular Ad-Hoc Networks In Ns-3, Proceedings of the Winter Simulation Conference IEEE.

[3] Harri, Jerome, Fethi Filali, and Christian Bonnet. "Mobility models for vehicular ad hoc networks: a survey and taxonomy." IEEE Communications Surveys & Tutorials 11, no. 4 (2009).

[4] 3. J.G. Jetcheva, Y.C. Hu, S. PalChaudhuri, A.K. Saha D.B. Johnson, "Design and evaluation of a metropolitan area multitier wireless Ad-hoc network architecture," Mobile Computing Systems and Applications, 2003. Proceedings Fifth IEEE Workshop on, vol., no., pp. 32-43, 9-10 Oct. 2003.

[5] Rupinder, Kaur, and Singh Gurpreet. "Survey of various mobility models in VANETs." International Journal Of Engineering And Computer Science 3, no. 03 (2014).

[6] Feham, Mohammed & Bahidja, Boukenadil. (2015). Mobility Models for VANET simulation.

[7] Mir, Zeeshan Hameed, and Fethi Filali. "LTE and IEEE 802.11 p for vehicular networking: a performance evaluation." EURASIP Journal on Wireless Communications and Networking 2014, no. 1 (2014): 89.

[8] Rouil, Richard, Fernando Cintrón, Aziza Ben Mosbah, and Samantha Gamboa Quintiliani. "A Long Term Evolution (LTE) device-to-device module for ns-3." In The Workshop on ns-3 (WNS3). 2016.

IJEW 国际工程期刊 International Journal of Engineering Works انجینئرنگ کاموں کا بین الاقوامی جرنل

International Journal of Engineering Works
ISSN-p: 2521-2419
ISSN-e: 2409-2770
Vol. 7, Issue 06, PP. 233-237, June 2020
https://www.ijew.io/
https://doi.org/10.34259/ijew.20.706233237

Analysis of Energy Performance and Application of Wall Insulation on an Academic Building using EQUEST

Umair Abbas Shah
Department of Thermal Engineering Systems, U.S.-Pakistan Center for Advance Studies in Energy, University of Engineering & Technology, Peshawar, Pakistan,
umair.abbas@msn.com

Received: 19 May, Revised: 28 May, Accepted: 01 June

***Abstract*—**Building sector is one of the major consumers of energy produced in the country. This study was carried out to assess the energy performance of a typical academic building and to analyze the effect of energy efficiency measures on energy consumption for space cooling. EQuest software was used to model the year round energy performance. The simulation results were compared with annual metered energy usage. Moreover, a standard wall insulation was simulated in order to analyze its effect on energy saving. The results showed a considerable energy saving potential.

***Keywords*—** Energy performance, Energy efficiency, academic building, insulation

I. INTRODUCTION

Energy performance is a term use to access the quality of energy usage in buildings [1], [2]. Approaches of building energy assessment can be classified into two major types, i.e. performance-based approach & feature-based approach. In performance based approach, different indicators can be established to compare the performance among buildings like energy utilization index per unit area EUI, carbon dioxide CO2 emissions etc. While in feature-based assessment credit can be awarded for specific features. Hence, an overall score can be calculated by integrating the above two performances [3]. Performance-based assessment is more preferable as it is easily quantifiable and then comparable. Wang et al [4] divided energy quantification approaches into three types i.e. measurement based approach which uses sub-meters to calculate the energy consumption for specific tasks, calculation based approach which uses simulation techniques to simulate the energy usage while hybrid approach combines the features of above two methods. He also ascertained the importance of energy performance assessment of existing buildings. Different market available simulation tools were used which allowed detailed data input and hence comprehensive results, which proved helpful in assessing the energy performance. Yan et al [5] simplified the energy performance assessment procedure by disintegrating the energy bill into three end-uses and then comparing it with the respective domain-wise simulated energy results. Baig et al [6] modelled the energy performance of a library building using eQuest, one of the available simulation tool. Energy simulation was carried for three consecutive years and later compared with the metered energy usage. Overall simulated energy consumption was accurately in compliance with actual energy usage with only 2% difference. Jinghua et al [7] used eQuest software to analyze factors, thermal insulation of exterior walls, glazing of shades, window to wall ratio, which effect on energy savings of air conditioner. Energy savings of cooling and heating load was recorded and analyzed while changing the thermal insulation envelop configuration [8]. Another study was carried out to determine the effect of heating and cooling load in comparison to the exterior insulations on residential facility [9]. Bolatturk [10] carried out study to analyze the extent of heating & cooling savings with respect to the optimum insulation thickness. Payback period was also calculated to figure out the overall feasibility of this energy efficiency measure. Another approach was carried out by Hasan et al by using overall cost analyzes for optimum insulation thickness [11]. Bokos et al [12] established a comparison between the energy savings before and after the installation of thermal insulation in building's envelop. Mohammad et al [13] analyzed the optimum insulation thickness for building in hot climatic zone. It was also concluded that the maximum heat transfer was due to the solar thermal radiations. Dombayaci et al [14] analyzed the mitigation of environmental impact with thermal insulation installation. Coal was used as energy source while expanded polystyrene as insulation material.

II. METHODOLOGY

This chapter describes the experimental methodology of the research. Following tasks were carried out in chronological order with details.

- Data Collection

- Energy Simulation of Academic Building using eQuest
- Application of Thermal Insulation in eQuest

A. *Data Collection*

The eQuest is an energy simulation tool used to calculate yearly energy performance of a building by the input of certain required parameters. It is a highly efficient simulation tool also on the recommended by DOE (Department of Energy) [15].The collected data of the actual building parameters is fed into the simulation tool. The data is further processed by eQuest to generate yearly energy performance on the basis of data input. Data regarding the insulation thickness, glass type, door type, wall thickness & ceiling parameters are also taken from the detailed drawings. HVAC data was also collected from the relevant drawings so that installed HVAC can be modelled in eQuest with required accuracy. Internal load other than HVAC, was characterized into three portions i.e. lightning, occupancy load & appliances load. Figure 1 shows the two dimensional layout of the academic building under consideration while Figure 2 shows the building shell in eQuest after collecting the required data.

B. *Energy simulation of Academic Building using eQuest*

After getting the building envelop configuration from collected data, building was divided into different thermal zones as required. In academic building under consideration, split and window air conditioning units of various models were installed in different thermal zones. EQuest supports designing of the installed system directly as single packaged unit for each respective thermal zone.

Lighting, fan and other installed load were recorded through walk through energy audit and entered in eQuest model. Afterwards, building energy was simulated for the whole year. At the end, simulated energy usage was compared with the metered energy usage of the building, first to validate the energy simulation and as well as to deduce useful deductions in terms of energy efficiency.

C. *Application of Thermal Insulation in eQuest*

After simulating the energy performance of academic building as present, polystyrene having thickness of 4 in. was incorporated in the walls as thermal insulation in eQuest against the losses occurred during cooling the space.

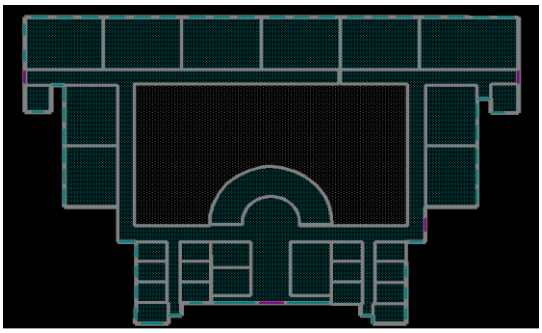

Figure 1: Two-Dimensional Layout of Academic Building in eQuest

As during heating days, natural gas was used in burners instead of electricity, so energy usage for heating was not included in this study. Later, energy usage of cooling space was compared as of before and after the installation of thermal insulation.

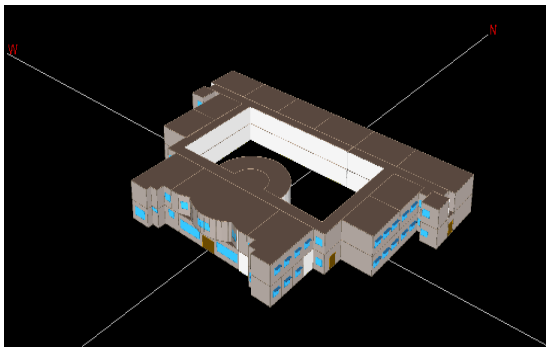

Figure 2: Academic Building Shell in eQuest

III. RESULTS & DISCUSSION

A. *Energy Simulation of academic building using eQuest*

Energy simulation of academic building situated in Peshawar was carried out using eQuest to determine its yearly energy usage of 2019 electricity by end use & ancess its energy performance. Results show that the building used total of 59.4 MWh of energy during the year 2019. Lighting consumed the maximum portion of load among the subcategories i.e. 27.47 MWh, 45.7% of the total, varing from monthly extremes of 2.41 MWh & 2.11 MWh. . It was also recorded that by the end use, cooling space used the second maximum portion of electricity i.e. 36.7%. Cooling space accounted 22.05 MWh energy usage of that year. Least energy by cooling space was used during the month of February i.e. 2.57 MWh while the maximum was recorded in July i.e. 8.07 MWh. This behavior was recorded as the tmeperatures kept increasing from February till July & then started decreasing subsequently. Apart from the above stated two major subcategories of energy usage, various other usages were recorded and are shown in Figure 3.

B. *Comparison between Actual Energy Consumption and Simulated Energy Consumption*

Figure 4 establishes a comparison between the yearly energy consumption of academic building under consideration situated in Peshawar, Pakistan. For the first four months of the year, both graphs depict almost same energy consumption. During the cooling season the difference starts increasing with maximum difference being recorded in the month of August. Split ACs were installed in different zones with varying EER (Energy Efficiency Ratio) values. Although overall energy consumption for the period of year 2019 from both graphs shows a mere change of 4.2%.

C. Comparsion of Simulated Energy Results of Cooling Space, before & after the Application of Thermal Insulation

After applying thermal insulation of 4 inch polystyrene with thermal conductivity 0.030W/m·K on all the walls, cooling space load was considerably reduced. Following Figure 5 establishes a comparison of cooling space load before and after the application of polystyrene 4 in. thermal insulation. 22% difference of yearly energy usage of cooling space was recorded before and after the application of energy efficiency measure.

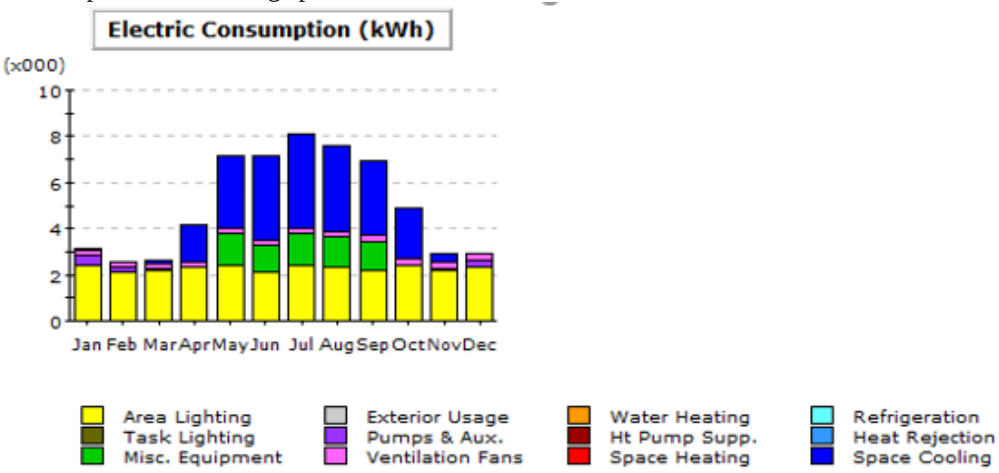

Figure 3: Whole year 2019 energy modelling of Academic building using eQuest

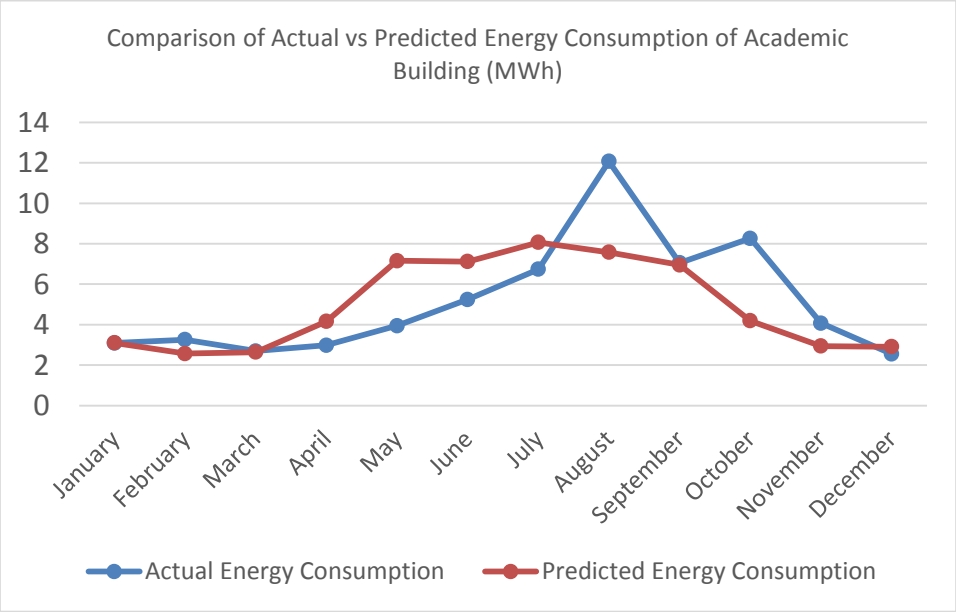

Figure 4: Actual & Simulated Energy Consumption Comparison

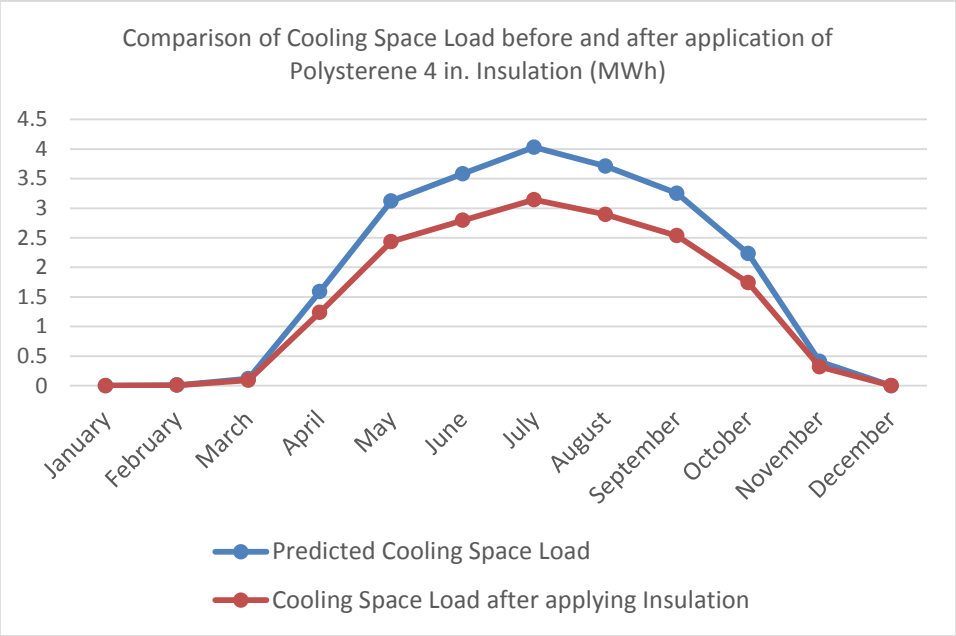

Figure 5: Cooling Space Load Comparison

CONCLUSIONS

This research was carried out to access an academic building energy performance located in Peshawar, Pakistan.
EQuest was used as a modelling tool to simulate the building energy performance. Actual building was modelled for whole year. The model design was validated by first recording the actual HVAC temperatures of each respective thermal zones. Also, lightning and other load schedules were monitored for the selected period to ensure maximum accuracy. Difference of only 4.2% was recorded while comparing actual metered energy consumption and the modelled energy consumption, thus validating our designed model after simulation. Hence, results show that energy simulation of buildings using eQuest can be used with much accuracy to predict the energy performance, having enough data input, hence getting in a better position for the formulation of energy efficiency measures.

By end use, cooling space used the maximum proportion of electricity. Maximum & minimum monthly values of 8.07 MWh and 2.57 MWh were recorded during the months of July and February respectively. In fact, cooling space accounted for 36.7% of the total energy usage, with no thermal insulation installed, pointing out the effectiveness of any proposed energy efficieny measure regarding thermal insulation.

After simulating the building energy performance and getting the end usage, an energy efficiency measure was proposed by applying a market available thermal wall insulation to lower the energy consumption of cooling space. It can be seen that by installing wall insulation of 4 inch polystyrene, this proposed energy efficiency measure reduced 22% of the overall energy usage of cooling space i.e. 4.85 MWh of energy can be saved yearly.

Different insulation materials can be simulated in future simultaneously using eQuest with varied thickness to get the optimum results. Furthermore, cost benefit analysis can also be performed while incorporating market related constraints.

Overall sustainability of the building needs to be quantified with better understanding to achieve effective results. Future research should also focus on other areas of building's overall sustainability as well i.e. Indoor air quality, onsite renewable energy, transport, etc.

REFERENCES

[1] CEN, E.J.B.E.S.O., EN 15217, Energy performance of buildings-Methods for expressing energy performance and for energy certification of buildings. 2007.

[2] Poel, B., et al., Energy performance assessment of existing dwellings. 2007. 39(4): p. 393-403.

[3] Lee, W., et al., A method to assess the energy performance of existing commercial complexes. 2003. 12(5): p. 311-327.

[4] Wang, S., et al., Quantitative energy performance assessment methods for existing buildings. 2012. 55: p. 873-888.

[5] Yan, C., et al., A simplified energy performance assessment method for existing buildings based on energy bill disaggregation. 2012. 55: p. 563-574.

[6] Baig, A.A. and A.S. Fung. A Case Study in Energy Modeling of an Energy Efficient Building with Gas Driven Absorption Heat Pump System in eQUEST. in Proceedings of the eSim Building Performance Simulation Conference, Hamilton, ON, Canada. 2016.

[7] Xiangzhao, H.Y.F.J.A.T., AFFECTION OF WINDOW-WALL RATIO ON ENERGY CONSUMPTION IN REGION OF HOT SUMMER AND COLD WINTER. 2001(10): p. 3.

[8] Shihuai, Z., H. Xiadong, and W.J.C.C.M.S. Xinyun, Analysis the effect of heat insulating on heating and cooling energy consumption of residential buildings in hot summer and cold winter zone. 2006. 1: p. 26-29.

[9] NING, Y.-f., Z.-h. LIU, and G.J.J.o.H.U. CHEN, The influence of residential air conditioning load on the exterior wall heat insulation in hot summer and cold winter zone. 2006. 5.

[10] Bolattürk, A.J.A.t.e., Determination of optimum insulation thickness for building walls with respect to various fuels and climate zones in Turkey. 2006. 26(11-12): p. 1301-1309.

[11] Hasan, A.J.A.e., Optimizing insulation thickness for buildings using life cycle cost. 1999. 63(2): p. 115-124.

[12] Bakos, G.J.E. and buildings, Insulation protection studies for energy saving in residential and tertiary sector. 2000. 31(3): p. 251-259.

[13] Al-Khawaja, M.J.J.A.t.e., Determination and selecting the optimum thickness of insulation for buildings in hot countries by accounting for solar radiation. 2004. 24(17-18): p. 2601-2610.

[14] Dombaycı, Ö.A.J.B. and Environment, The environmental impact of optimum insulation thickness for external walls of buildings. 2007. 42(11): p. 3855-3859.

[15] Hirsch, C.-J.J. [cited 2019; Available from: doe2.com.

International Journal of Engineering Works
ISSN-p: 2521-2419
ISSN-e: 2409-2770
Vol. 7, Issue 06, PP. 238-246, June 2020
https://www.ijew.io/
https://doi.org/10.34259/ijew.20.706238246

Micro Grid Automation with Unique Features of Power Flow Control by using SCADA

Farrukh Kamal[1], Dr. Naeem Arbab[2]
[1,2] US Pakistan Center for Advance studies in Energy, University of Engineering and Technology, Peshawar, Pakistan
farrukhkamal440@gmail.com[1] , mnarbab@gmail.com[2]
Received: 17 May, Revised: 29 May, Accepted: 01 June

***Abstract*—** Now a days, the load demand of the world is dramatically increasing day by day. This situation creates a big gap between the energy production and the energy consumption. The conventional energy sources are depleting globally. So it is a global phenomenon to restore the power energy and to look forward the other means of energy production. The load demand and power production gap can be reduced by Micro Grid. Micro grids is a group of localized electricity units and load that operates both in islanded mode/ autonomously or in grid connected mode. Grid connected mode is a small power generating unit that is connected with conventional grid system. Grid connected mode is a small power generating unit that is being connected with conventional grid system. Micro grid mostly utilizes the renewable sources of energy such as solar energy, wind energy, geo thermal energy and the other sources of distributed generation. While operating a power system in micro grid, the maintenance and flow of electricity is not simple task as compared to the unidirectional power flow in case of conventional grid station. Another problem is the identification of fault in power system in case of micro grids detection of fault location and its recovery is not an easy task. In this research work, I have developed a SCADA module through which fault location is detected automatically, by observing the power at different feeders and its dial recovery is done by supply the power from other nearby power generating station. This is only possible when the system has ability to operate in ring main system, but it normally operates in radial configuration.

***Keywords*—** Smart Grid, Micro Grid, Power System, Power Transmission, SCADA, PLC.

I. INTRODUCTION

Micro grid is a group of localized electricity units and load that either operates in islanded mode/autonomously or in grid connected mode (small power generation unit connected with conventional grid system) [1].

When micro grid operates in islanded mode it works like an isolated system. It reduces transmission cost, because no transmission line is required. There should be only generating units and distribution system for it [2].

Reliability of system is main issue for both consumers and the power producers. In case of occurrence of fault in distribution line, whole system or in a part of system power becomes disconnected, which further produce black out condition at some feeders. In order to compensate the fault usually the system is operated with radial configuration but when fault occurs at any point of circuit, the configuration of system would be changed to ring main in order to restore the system with minimum possible load disconnected [2][3].

In this research project, algorithm has been developed in order to automatically change the system configuration in case of fault and detection of fault location. The hardware that should be used for this purpose was programmable logic controller and smart meters. The PLC collect reading from smart meters and then decision has to make about logical and mathematical operation of system configuration according to the developed algorithm.

II. MICRO GRID AUTOMATION WITH POWER FLOW CONTROL BY USING SCADA

In case of conventional grid station power flow usually occurs from generating station to load center. But in case of micro grid station power flow occurs in both directions and its power flow control is also not an easy task. In this research work a SCADA system is introduced, through which the fault location will be automatically detected by monitoring power at different feeders. The second problem that is also solved by using same scenario is the recovery of fault, which is only possible if nearby generating station has spare power to feed that feeder. The whole scheme is implemented by considering that the system has ability to operate in ring main system, but normally operates in radial configuration.

A. Automation with PLC & SCADA Softwares

Programmable logic Controller (PLC) is controlling unit. The fault detection and decision how and when system configuration change will be decided by PLC.

- Two software's are used in order to operate them. "WinLog Lite" software is used to operate SCADA system and "GX.

Developer" is used for programing of Programmable Logic Controller.

Winlog Lite is very convenient for utilization, more reliable and easier to use software package in formation of the SCADA/ HMI techniques along with the supportive nature of Web Server.

GX Developer and simulator is software use to develop program for Programmable logic controller (PLC). The whole logic operation is programed in GX Developer. This Software is usually utilized as a single program debugging element using the PLC for debugging in advance and conventional way required not just the Programmable Logic Controller but also I/O and special modules and external use devices.

B. Inter Connection Scheme

In this research, a new idea has been proposed, in which the system is operated in islanded mode but in condition of fault at generator side or in condition of line fault, the system has ability to convert from islanded mode to ring main system.

The whole scenario can be described with the help of figure 1.1.

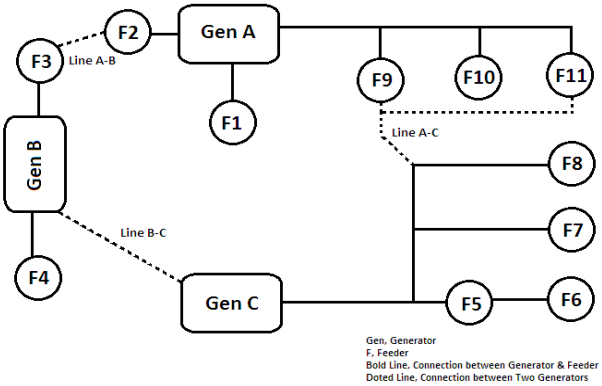

Figure 1.1: Ring main system

The above mentioned system is ring main distribution system. There are total 11 feeders as shown in the system, which is supplied by three different power sources. Initially the system is worked as radial system with lines A-B, A-C and B-C are not energized.

In the case of fault at any generator, the system configuration will change from radial to ring main and power supply will be provided by nearby generator. It can only be possible if the nearby generator has spare power and concern transmission line has capacity to transmit power.

The change of system configuration from radial to ring main is controlled and monitored by SCADA and PLC system. The PLC (Programmable Logic Controller) takes all the decisions, regarding fault detection, change of system configuration and restoration of system. On the other hand, the SCADA (Supervisory Control and Data Acquisition) provides human machine interface. SCADA provides visual display of whole scenario.

C. Condition of Lines at different conditions of Generators

At different condition of generators (either they are normal or in faulted condition) the line would be energized or not depending upon particular situation. The isolator and circuit breaker are installed at both ends of all lines connected to all generators and feeders. With the help of PLC that circuit breakers would be ON/OFF, which further maintain the condition of line (energized/ de-energized). The figure 1.2 shows the whole scenario of system with three generators and eleven feeders.

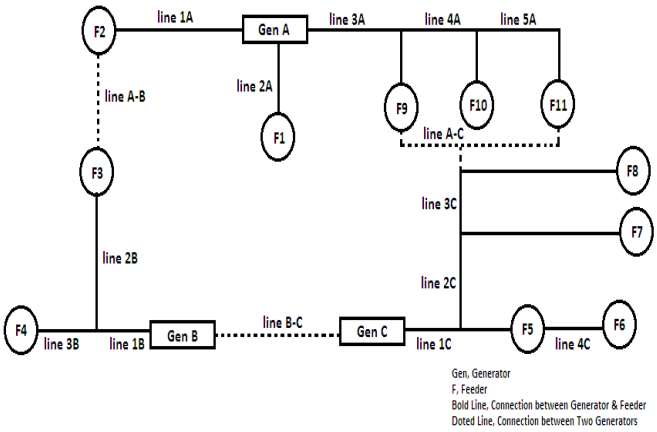

Figure 1.2 Power System with three Generators & Eleven Feeders.

In normal case, all generators are in operating condition, so all lines are energized except that lines which connect two generators (line 'A-B', 'A-C' & 'B-C'), because in this condition system work in radial fashion shown in figure 4.1.

In second case fault occur at generator 'C'. In this condition all lines remain energized except line '2C', line '4C' and line 'A-B', which become de-energized. The

The all cases are summarized into a table form and given below, where '1' represent energized state and '0' represent off/ de-energized state.

Table 1.1 (a) Condition of Lines at different conditions of Generators

Sr #	Gen A Y100	Gen B Y200	Gen C Y300	Line 1A Y101	Line 2A Y102	Line 3A Y103	Line 4A Y104	Line 5A Y105	Line 1B Y201	Line 2B Y202	Line 3B Y203
1	1	1	1	1	1	1	1	1	1	1	1
2	1	1	0	1	1	1	1	1	1	1	1
3	1	0	1	1	1	1	1	1	0	1	1
4	1	0	0	1	1	1	1	1	0	1	1
5	0	1	1	1	1	0	0	0	1	1	1
6	0	1	0	1	1	0	0	0	1	1	1
7	0	0	1	0	0	0	0	0	0	0	0
8	0	0	0	0	0	0	0	0	0	0	0

Table 1.1 (b) Condition of Lines at differentConditions of Generators

Sr #	Gen A Y100	Gen B Y200	Gen C Y300	Line 1C Y301	Line 2C Y302	Line 3C Y303	Line 4C Y304	Line A-B Y401	Line A-C Y402	Line B-C Y403
1	1	1	1	1	1	1	1	0	0	0
2	1	1	0	1	0	1	0	0	1	1
3	1	0	1	1	1	1	1	1	0	0
4	1	0	0	0	0	1	0	1	1	0
5	0	1	1	1	1	1	1	1	1	0
6	0	1	0	1	0	0	0	1	0	1
7	0	0	1	1	1	1	1	0	1	0

D. Condition of feeders at different condition of Generators

At different condition of generators (either they are normal or in faulted condition) the line would be energized or not depending upon particular situation, which further decide whether a particular feeder should be loaded or not. The different conditions of feeder at different condition of generator is given below. The whole scenario can be understand with the help of figure 4.1.

In first case there is no fault occur at any generator. In this condition all feeders remain in normal/ operating condition.

In second case fault occur at generator 'C', which results in shut down at feeder 6, while all other feeders remain in its normal state. Feeder 5 of generator 'C' will be supplied by generator 'B' through line 'B-C' and feeder 7, 8 of generator 'C' is supplied by generator 'A' through line 'A-C'.

The all other cases at different condition of fault is summarized in tabular form and given below, where '1' represent energized state and '0' represent off/ de-energized state. The feeder & generator are represented by 'F' & 'Gen' respectively.

Table 1.2 (a) Condition of Feeders at different conditions of Generators

Sr #	Gen A Y100	Gen B Y200	Gen C Y300	F 1 Y1	F 2 Y2	F 3 Y3	F 4 Y4	F 5 Y5	F 6 Y6
1	1	1	1	1	1	1	1	1	1
2	1	1	0	1	1	1	1	1	0
3	1	0	1	1	1	1	1	1	1
4	1	0	0	1	1	1	1	0	0
5	0	1	1	1	1	1	1	1	1
6	0	1	0	1	1	1	1	1	0
7	0	0	1	0	0	0	0	1	1

Table 1.2 (b) Condition of Feeders at different conditions of Generators

Sr #	Gen A Y100	Gen B Y200	Gen C Y300	F 7 Y7	F 8 Y8	F 9 Y9	F 10 Y10	F 11 Y11
1	1	1	1	1	1	1	1	1
2	1	1	0	1	1	1	1	1
3	1	0	1	1	1	1	1	1
4	1	0	0	1	1	1	1	1
5	0	1	1	1	1	1	0	1
6	0	1	0	0	0	0	0	0
7	0	0	1	1	1	1	0	1

E. PLC Program (Develop on GX Developer)

The Programmable Logic Controller (PLC) is decision making device. The program is written in GX Developer software and then burn in PLC module.

In this program Part 1 'X0' is input switch to ON the power system and 'X1' is used to shut down the whole power system. The 'Y0' coil shows the output status of system.

If system is in normal condition, then after switch on the power system the all generators should be start working. 'Y100', 'Y200' and 'Y300' represents the generator 'A', 'B' and 'C' respectively. Whereas normally closed switches 'X100', 'X200' and 'X300' represents fault at generator 'A', 'B' and 'C' respectively.

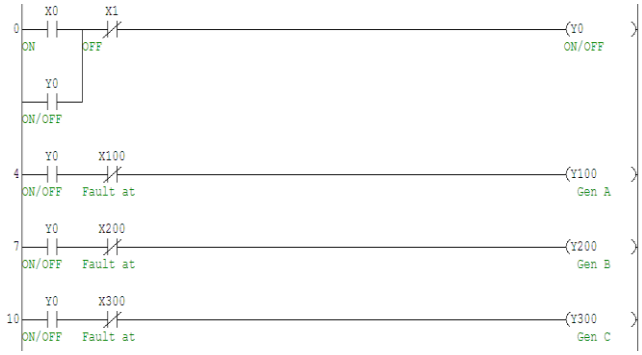

GX Developer Program Part: 1

In part 2 of program the conditions of operation of lines '1A' and '2A' associated with generator 'A' is describe according to table 4.1. The program is written only for those cases, when there is '1' (ON State) at output of line, with particular condition of generator.

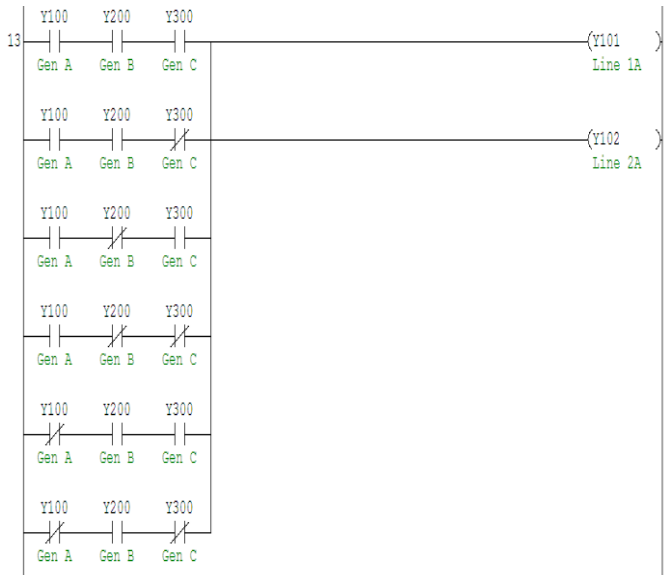

GX Developer Program Part: 2

Similarly in part 3 of program the conditions of operation of lines '3A', '4A', '5A' and '1B' associated with generator 'A' and 'B' is describe according to table 4.1. The program is

written only for those cases, when there is ‘1’ at output of line, with particular condition of generator.

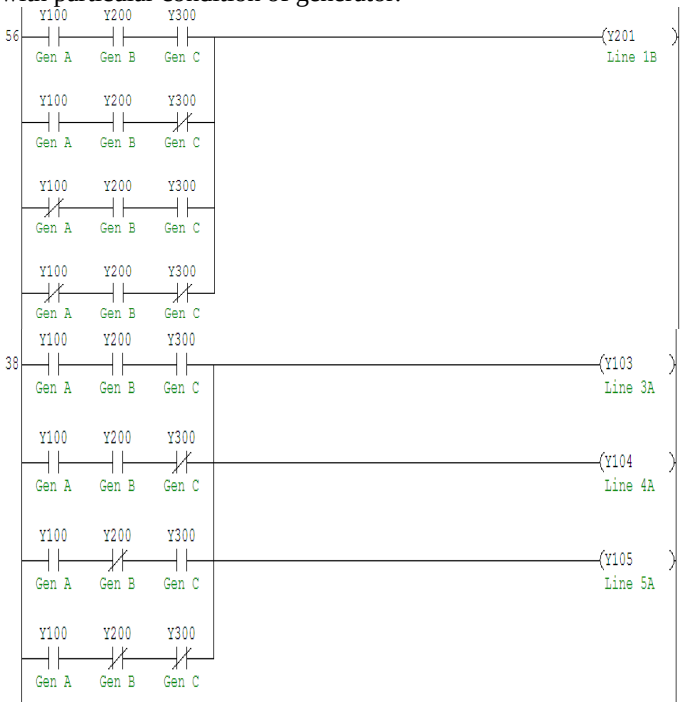

GX Developer Program Part: 3

In part 4 of program the conditions of operation of lines ‘2B’, ‘3B’, ‘1C’, and ‘2C’ associated with generator ‘B’ and ‘C’ is mentioned with respect to table 4.1. The program is written only for those cases, when there is ‘1’ at output of line, with particular condition of generator.

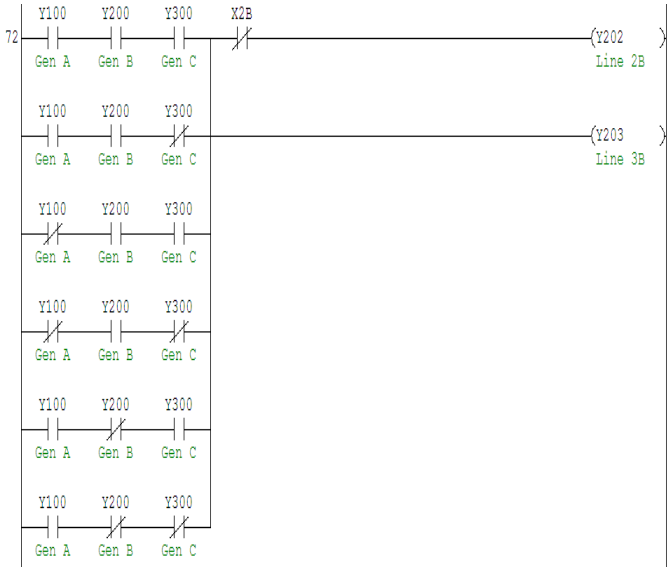

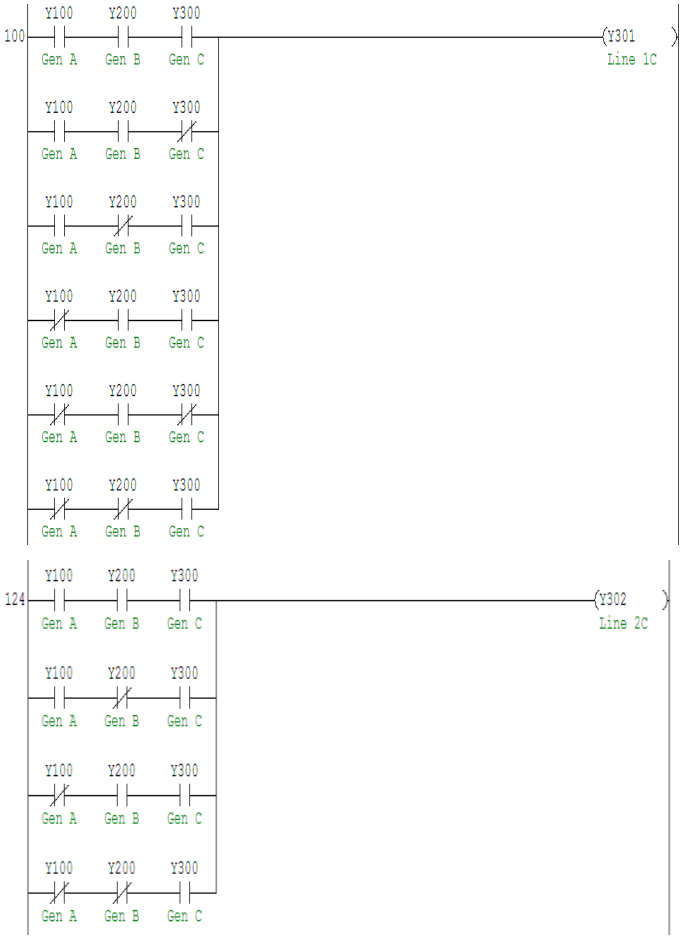

GX Developer Program Part: 4

In part 5 of program the conditions of operation of lines ‘3C’ and ‘4C’ associated with generator ‘C’ is mentioned with respect to table 4.1. The program is written only for those cases, when there is ‘1’ at output of line, with particular condition of generator.

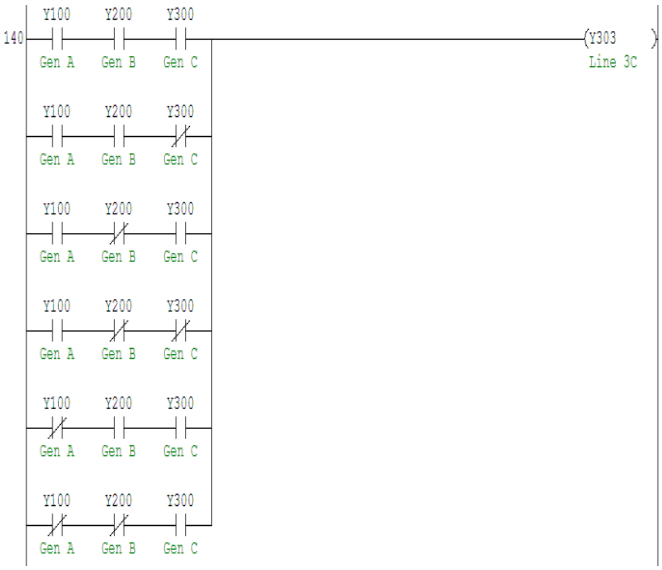

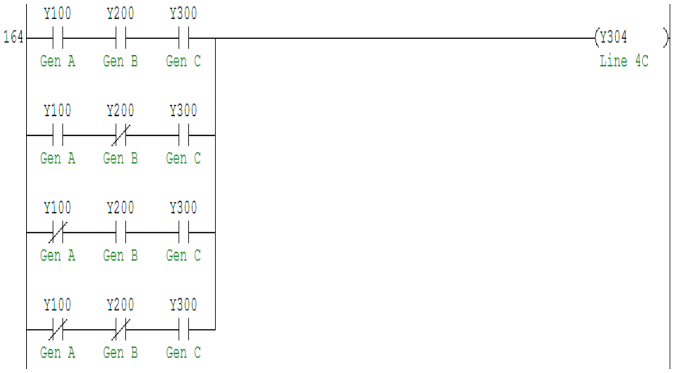

GX Developer Program Part: 5

In part 6 of program condition of operation of line ‘D1-2’ is mentioned by considering table 4.1. The line ‘D1-2’ connects generator ‘A’ and generator ‘B’ in the condition of fault at either generator or in condition of line fault. The last line of part 6 of program only operate when a line fault at line ‘2B’ occur.

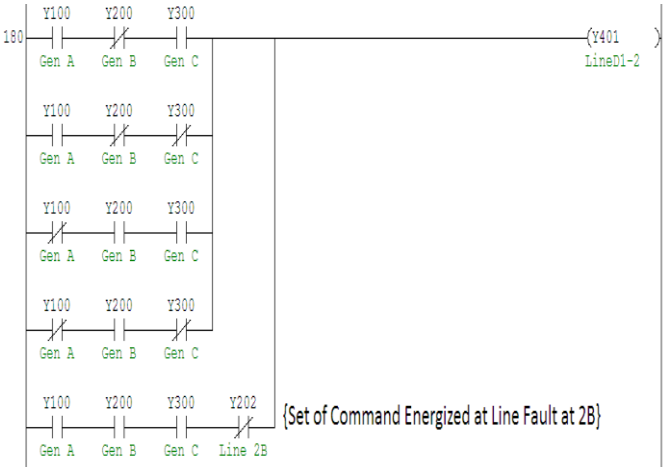

GX Developer Program Part: 6

In part seven of the program condition of operation of line ‘D2-3’ and line ‘D2-3’ is given. The line ‘D2-3’ connects generator ‘B’ and ‘C’ in the condition of fault and ‘D2-3’ connects generator ‘B’ and ‘C’ in the condition of fault. While developing the algorithm, the table 4.1 should kept in mind. The whole algorithm is according to table 4.1.

In part seven the operating status of feeder 1 and 2 is also mentioned. The operating status of feeder is not just depend upon condition of generator (table 4.2), but it is also depend upon actual configuration of system. For example the feeder 1 operate in two conditions. Feeder 1 operates when there is generator ‘A’ in system along with line ‘2A’ because line ‘2A’ connects feeder 1 with generator ‘A’. The other condition of operation of feeder 1 is presence of generator ‘B’ along with line ‘1B’, ‘2B’, ‘D1-2’, ‘2A’ and line ‘1A’.

The operating condition of feeder 2 is either presence of generator ‘A’ along with line ‘1A’ and other condition is presence of generator ‘B’ along with line ‘1B’, ‘2B’ and line ‘D1-2’ (connect generator A and B).

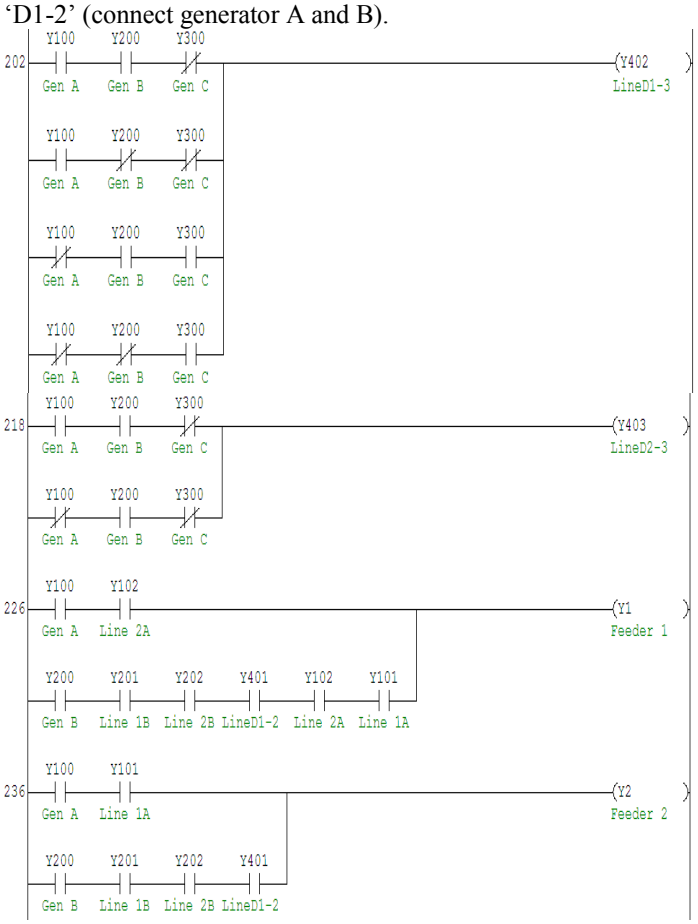

GX Developer Program Part: 7

The operating condition of feeder 3 is either presence of generator ‘B’ along with line ‘1B’ and line ‘2B’. The second condition of feeder 3 operation is presence of generator ‘A’ along with line ‘1A’ and line ‘D1-2’.

In case of feeder 4, the operation can be done either through generator ‘B’ along with line ‘1B’ and ‘3B’. Other condition of operation regarding feeder 4 is presence of generator ‘A’ along with line ‘1A’, ‘D1-2’, ‘2B’ and ‘3B’.

In part 8 of program the operating condition of feeder 5 is presence of generator ‘C’ along with line ‘1C’. The other condition of operation is presence of generator ‘B’ along with line ‘D2-3’ and ‘1C’.

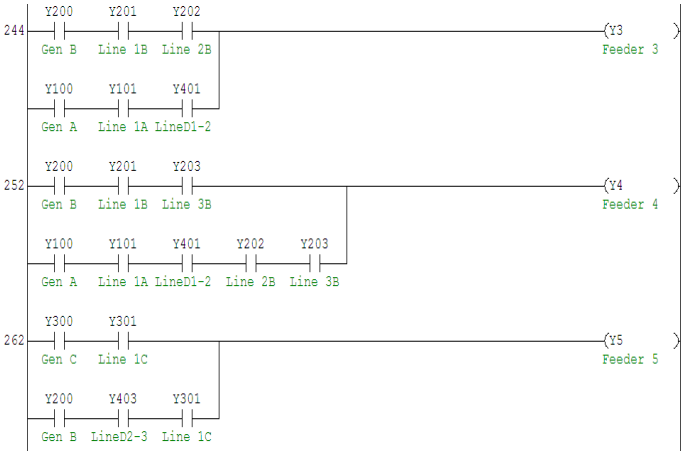

GX Developer Program Part: 8

In part 9 of program the operational condition of feeder 6 is presence of generator 'C' along with line '1C' and '4C'.

The feeder 7 operate in two conditions. The first condition of operation is presence of generator 'C; along with line '1C' and '2C'. The second condition of operation of feeder 7 is presence of generator 'A' along with line '3A', 'D1-3' and line '3C'.

The condition of operation of feeder 8 is either generator 'C' is in operation along with line '1C', '2C' and '3C'. The other condition of operation is energization of generator 'A' along with line '3A' and 'D1-3'.

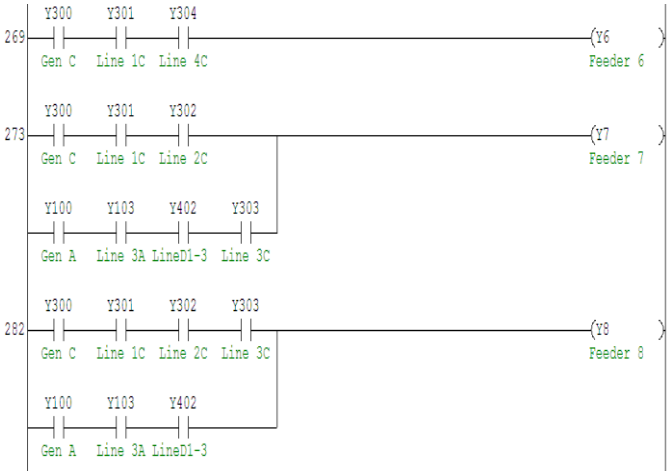

GX Developer Program Part: 9

In part 10 of program, the feeder 9 operates when there is generator 'A' in operation along with line '3A'. The other condition of operation is presence of generator 'C' along with line '1C', '2C', '3C' and 'D1-3'.

The operational condition of feeder 10 is energization of generator 'A' along with line '3A' and '4A'.

The feeder 11 operates when there is generator 'A' is energized along with line '3A', '4A' and '5A'. The other condition of operation is presence of generator 'C' along with line '1C', '2C', '3C' and line 'D1-3'.

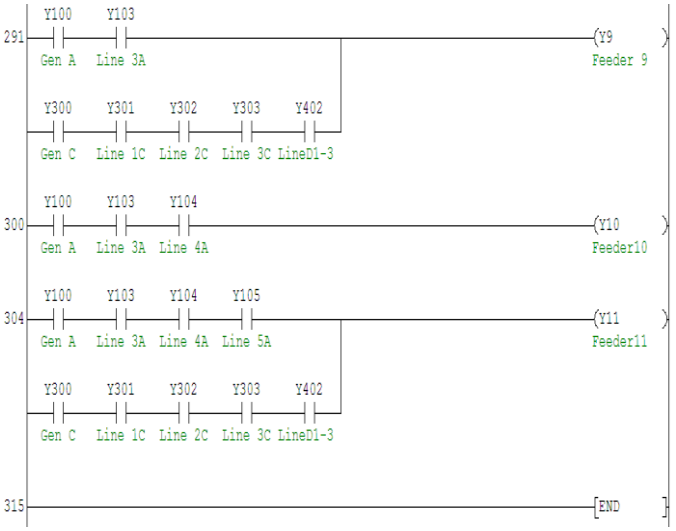

GX Developer Program Part: 10

III. RESULTS AND OUTPUTS

In order to demonstrate whole scenario, how SCADA software change/ shift the load from one generator to other or in case line fault, consider a small distribution system, supplied power to small area working in racial fashion. Total three number of generator are present in system: Generator A 500 KVA, Generator B 200 KVA, Generator C 400 KVA. There are total eleven (11) fearers feed the load center and connected to different generators. The feeder demand is given as: feeder-1 55 KVA, feeder-2 20 KVA, feeder-3 45 KVA, feeder-4 40 KVA, feeder-5 70 KVA, feeder-6 110 KVA, feeder-7 95 KVA, feeder-8 15 KVA, feeder-9 60 KVA, feeder-10 80 KVA and feeder-11 50 KVA. The feeders 1, 2,9,10 and 11 are connected with generator A. The feeders 3 and 4 are connected with generator B. The feeders 5, 6, 7 and 8 are connected with generator C.

A. Case A (Normal Operation/ All Generator ON)

The system configuration in normal condition is given below:

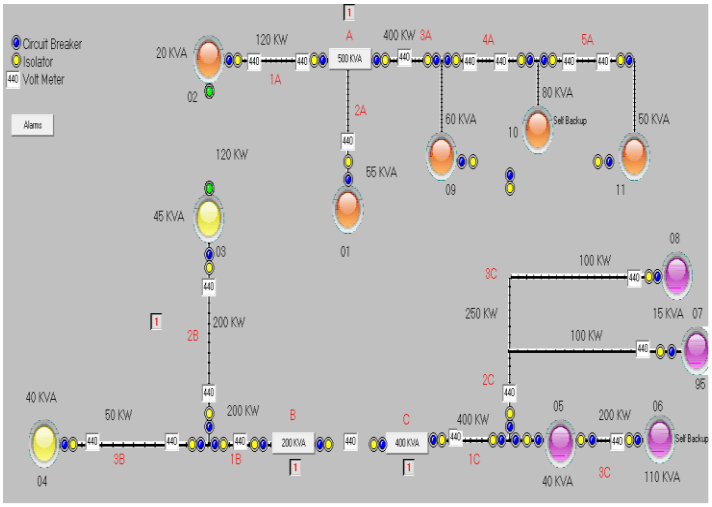

Figure 1.3: System configuration in normal condition

The suffix "1' along with generator show on condition and suffix "0" shows off condition of generator. The "MW" capacity of each line is also mention along with line.

B. Case B (Fault at Generator A)

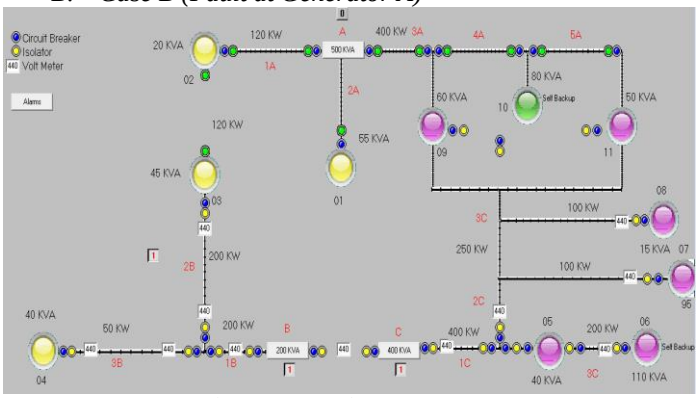

Figure 1.4: Fault at generator "A"

The above figure shows a faulty condition at generator "A". In this condition feeder 1, 2, 9, 10 and 11 become out of order. The total demand of feeder connected to generator A is 265 kilowatt. The maximum spare power, which can be produce by generator B would be 115 kilowatt and generator C has total spare power of 140 kilowatt.

C. Case C (Fault at Generator B)

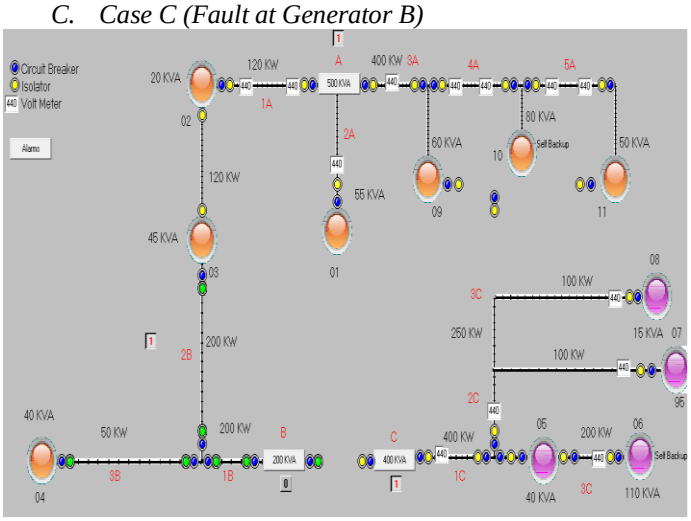

Figure 1.5: Fault at Generator B

The total power demand of feeders connected to generator B is 85 Kilowatts. The spare power that can be produced by generator A would be 235 kilowatts. The generator 'A' provided the power through line, which connect feeder '8' and '2'.

D. Case D (Fault at Generator C)

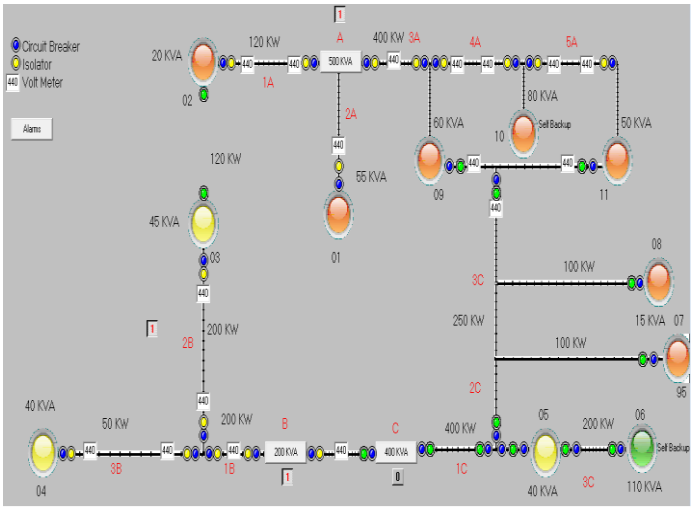

Figure 1.6: fault at generator C

The faulted condition is shown above, when fault occur at generator C. the total demand of all the feeders connected to generator C would be 260 kilowatts. The spare power that can be supplied by generator A would be 235 kilowatt and the power delivered by generator B would be 115 kilowatts. So in this condition one generator can't fulfill the demand of all the feeders connected to generator C.

E. Case E (Fault at Generator A & B)

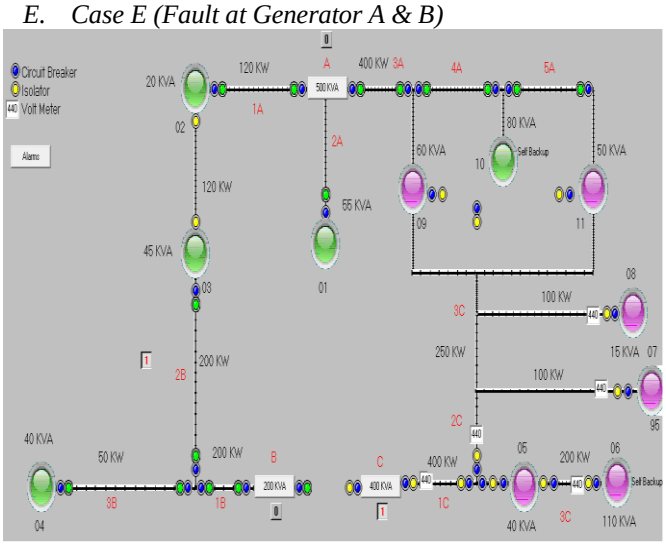

Figure 1.7: faulty at Generator A and B

The condition of fault when fault occur at generator A and generator B. In this condition majority of system will be disturb. Total seven number of feeders would be disturb. The total demand of all seven feeders would be 350 kilowatt. The spare power that can be produced by generator C is totally 140 kilowatt. So it is clear that only generator C can't fulfill the demand of all feeders connected to generator A and generator B.

F. Case F (Fault at Generator B & C)

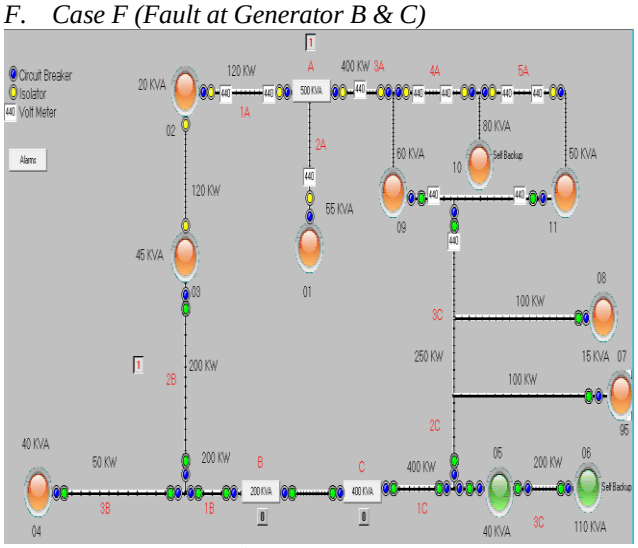

Figure 1.8: fault at generator B and C

The above mention figure show fault at generator B and generator C. In this condition total 6 number of feeders would be disturbed. The only generator that can feed in this condition is generator A. as generating capacity of generator A is 500 KVA and spare capacity of generator A would be 235 kilowatt. The total demand of all feeder connected to generator B and C would be 345 kilowatt, that can't be fulfil by generator A alone.

G. Case G (Fault at Generator A & C)

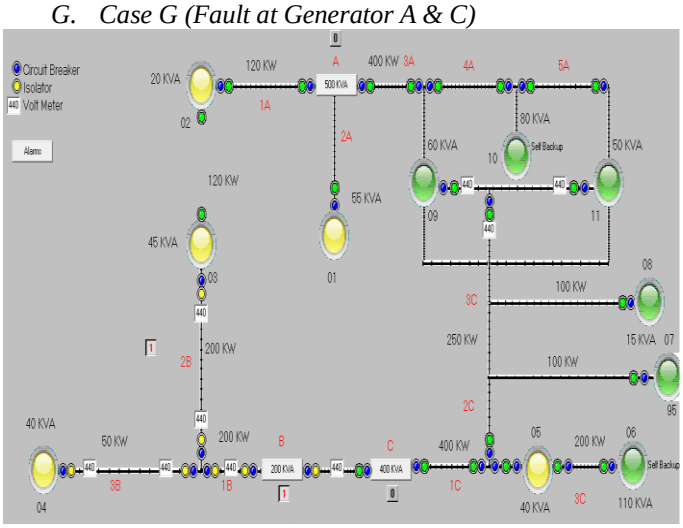

Figure 1.9: fault at generator A and C

The condition of fault at generator number A and C given below. In this condition only generator B is in working condition. It is not possible for generator B to fulfil demand of all feeders connected to generator A and B.

In this condition only limited generates would be supplied by generator B. the total generating capacity of generator B is 200 kilowatt and it has 115 kilowatt of spare power that can be supplied to feeders connected to generator A and C.

H. Case H (Fault at Line 2B)

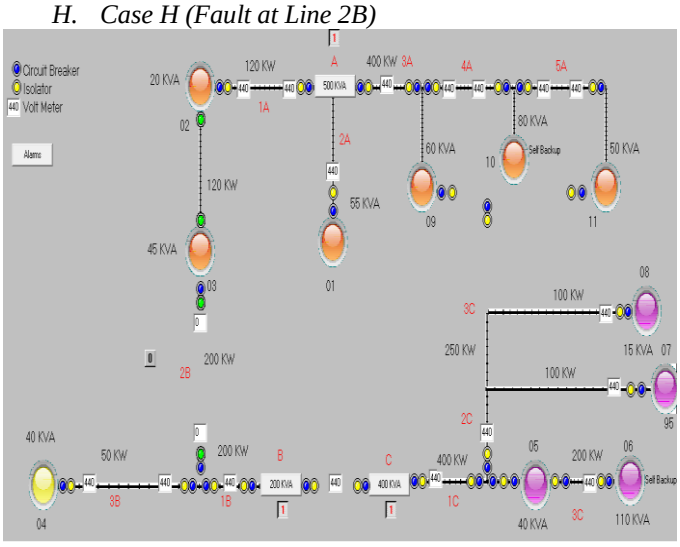

Figure 1.10: Line fault

A fault occur at line 2B, a line connect generator B with feeder number 3. In this condition only power flow to feeder 3 will be interrupted.

In this condition system consideration should be (a) is generator A has spare power to fulfil demands of feeder 3 and (b) line capacity.

CONCLUTION

The following conclusions are formulated from results obtained after implementation of proposed scheme.

- Using radial system for distribution system is more economical, but not feasible. In condition of fault majority of system would intercepted. By adopting proposed scheme a more reliable system can be built with system ability to change configuration from radial to ring main system.
- The fault clearance (line fault) would be done automatic fashion, which is less time consuming and more efficient and reduce human effort.
- More advance system can be obtained by using recommended policy, with better human interference.

ACKNOWLEDGMENT

I am extremely thankful to Almighty ALLAH, The most beneficent and merciful who helped me a lot in every moment of my life and blessed me with all successes. I offer my humblest thanks to The Holy Prophet "Hazrat Mohammad"ﷺWho is forever a torch for guidance, knowledge and inspiration for humanity.

I would like to express my deepest gratitude to my supervisor Sir Muhammad Naeem Arbab for his critical guidance, advices and invaluable assistance.

Last but not least, I would like to pay thanks from the core of my heart to my parents, brother, sister and all family members for their love and support throughout my M. Sc. program.

REFERENCES

[1] Michael, S., Goncalo, C., and Salman, M. Distribution energy resources and micro grid modelling.

[2] (2015). A survey of techniques for designing and managing micro grids. IEEE PES GM.

[3] (2011). DOE micro grid workshop report. IEEE.

[4] Hatziargyriou, N. (2014). Micro grids architectures and control. John Wiley and Sons (pp. 4).

[5] Salam, A. A., Mohamed, A., and Hannan, M. A. (2008). Technical challenges on micro grids. ARPN Journal of Engineering and Applied Sciences, 3: 64.

International Journal of Engineering Works
ISSN-p: 2521-2419
ISSN-e: 2409-2770
Vol. 7, Issue 06, PP. 247-252, June 2020
https://www.ijew.io/
https://doi.org/10.34259/ijew.20.706247252

A Fast and Efficient Absorbant BYW-01 and its Applications in Coking Plant Wastewater Treatment

Walzli Yousaf [1], Yueli Wen[2], Bin Wang[3], Faraz Ahmad[4], Wei Huang[5], Tauseef Khaliq[6], Mudassir Habib[7]
[1,2,3,4,5,6,7] College of Environmental Science and Engineering, Taiyuan University of Technology, Taiyuan, Shanxi, 030024, P/R China.
wenyueli@tyut.edu.cn[2], walzliyousaf@yahoo.com[1], tauseefkhaliq87@gmail.com[6], uetian92@yahoo.com[4], madsir55@gmail.com[7]
Received: 21 May, Revised: 03 June, Accepted: 09 June

***Abstract*—** Coking plant wastewater is well-known for its excessive NH3-N and COD content, for which it is difficult to meet emission standards even by using the biological treatment process. In this paper, a fast and efficient BYW-01 was prepared and used to remove NH3-N and COD in coking plant wastewater from different biological treatment processes.Combined with the characterization of XRD, BET, FTIR, SEM etc, it was found that the abundant –OH and C=O functional groups on the surface of the mesoporous structure absorbent was beneficial to NH3-N and COD capture. The NH3-N and COD removal rate could reach about 50 %, 66 % respectively in 5 minutes. The possible adsorption mechanism was proposed.

***Keywords*—** BYW-01 absorbent, Ammonia nitrogen, Chemical oxygen demand, Coking wastewater, Fast and efficient.

I. INTRODUCTION

Water resources are quickly polluted by human actions over the latest years. About 80% of the world population is exposed by water scarcity [1]. It is estimated that about 1.5 billion world population will face water scarcity by 2025 [2,3]. China becomes the second-largest industrial power in the world [4]. Rapid urbanization, economic development, and industrialization in China have been accompanied by significant water pollution. In 2015 China Ministry of environmental protection, 2017 classified water into quality classes I-III, VI-V and <V accounted for 64.5 %, 26.7 % and 8.8 % of the surface water, and the distribution of wastewater, COD and NH3-N emissions among this categories was 73,530, 22.2 and 2.3 million ton of the industrial pollution accounted for 27.1 %, 13.2 % and 9.4 % [5,6].

Ammonia nitrogen (NH3-N) and chemical oxygen demand (COD) are two core industrial water pollutants [7]. In the nitrogen cycle, ammonia nitrogen in the form of NH4+ and NH3 is present, mainly in natural water [8,9]. Nitrogen is an essential nutrimental element for all life forms. One of the major causes of eutrophication is a high amount of nitrogen, especially total ammonia nitrogen (NH3, NH4+, and TAN), in receiving waters [10].COD representing organic load in the water body, which leads to oxygen depletion and threatens to aquatic life. Generally, Industrial wastewaters such as coke-plant, textile, coal gas purification, refining, tannery, and fertilizer wastewater contain a high concentration of ammonia nitrogen [11]. Wastewater contains phenol, ammonia (NH3), carbon dioxide (CO2), hydrogen sulfide (H2S), tar, etc. [12]. Determination of Nitrogen from industrial wastewater is vital for pollution control because ammonia, nitrites, nitrates, and many other nitrogenous compounds act as nutrients for algae and other aquatic plants [13]. One of the major sources of ammonia nitrogen is the discharge of these industrial wastewaters [14]. Ammonium is predominant when the pH is below 8.75, and ammonia is predominant when the pH is above 9.75 [15,16].

In the past years, various analytical techniques have been proposed for the treatment of NH3-N and COD. Traditional methods for the determination of high concentration of ammonia nitrogen contain biological system [17], Chemical precipitation [18], supercritical water oxidation [19,20], steam-stripping [21], microwave (MW), Ion exchange, reverse osmosis, Electrochemical, Folding point chlorination, Solvent extraction [22] and so on.

After biological treatment, the ammonia concentration is still high because of the high ammonia concentration leads to a low ratio of C/N [23]. Further purified wastewater is using the microbial growth process to make sure a degree of purification meets the discharge standards. It is very effective and economical, but it is time taking. Chemical precipitation requires extra reagents, which may produce new pollutants. Supercritical water oxidation needs high temperature and high pressure in Steam-stripping high energy required for stripping tower. Microwave is still having no clear idea for the full-scale application. Ion exchange and reverse osmosis incur large operation costs due to resin preparation and pressure driving [24,25]. Electrochemical and folding point chlorination is used only for low concentration ammonia nitrogen [26]. Solvent

extraction is costly, requires high input, and may not substantially decrease pollutant concentration [27].

This study introduced a new BYW-01 absorbent, which is very fast and efficient to remove NH3-N and COD from the coking wastewater plant in 5 minutes.

II. EXPERIMENTAL

A. Absorbent preparation

All the chemicals used in this study were of analytical grade and purchased from chinese chemical reagent company.

The absorbent were made from coal ash, and some chemicals were used for modification. First, 1 mol crylic acid and 0.5 mol diethanol amine mixed well with 0.5 mol ethylene glycol, then 2 mol concentrated sulfate acid was added in the mixed solution. After reluxating the obtained mixed solution for 4 hours, 3.5 mol NaOH was used to neutralize it, and solution B was obtained. Second, 1 mol acrylic amide was added in B, after mixing well, N2 was bubled in at 25℃. After reacting with 0.007 mol sodium bisulfite and 0.006 mol ammonium persulfate at 40℃ for 8 hours, 70 g coal ash was added in and kept reacting for another 6 hours at 50℃ with continous stirring. Washed the obtained solid with distilled water for several times and dried at room temperature. The obtained solid was named as BYW-01.

B. Characterization

UV752N UV- Visible Spectrophotometer (Shanghai YOKE instrument CO., Ltd.) was used do the absorption spectral scanning,and it was quantified by absorbance of 425 nm. HCA-100 COD auto-digestion reflux instrument (Taizhoumeixu instrument equipment Co.,Ltd.) was used to digest wastewater samples.

X-ray diffraction (XRD) patterns were performed on a DX-2700 X-ray diffractometer for continuous scanning, using Cu Kα as the radiation source. The scanning range was 5°-85°, and the scanning rate was 8°/min.

Nitrogen adsorption-desorption characterization was performed on a Quantachrome SI gas adsorption analyzer (product from Conta, USA). The samples were degassed at 200°C under vacuum for 6 h prior to characterization. The specific surface area of the catalyst was calculated by using the BET method, and the pore volume and pore size were calculated by the BJH formula.

Fourier transform infrared (FT-IR) spectra were collected by using a Thermo Nicolet 6700 instrument with a measurement range of 400-4000 cm-1.

Surface morphology of the absorbents was observed by scanning electron microscopy (SEM) using Quanta 400 FEG type instrument of American FEI Company , and the acceleration voltage was 20 kV.

C. Sample collection

The wastewater used in the experiments was taken from different biological treatment processes of a coking plant located at Taiyuan, Shanxi, China. The wastewater treatment plant process for coking plant was shown in Fig. 1.

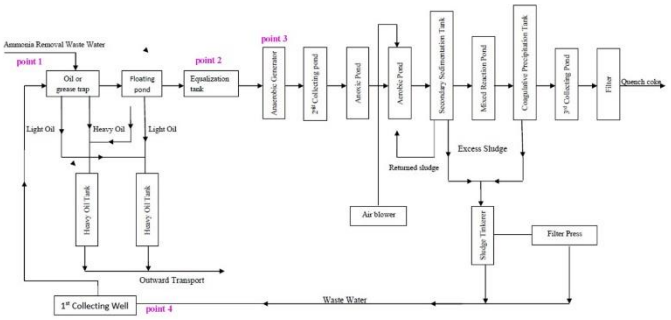

Figure 1. Wastewater treatment process flow chart of a coking plant

The sample collection plan was designed to cover almost all essential processes points of the coking plant.Four samples were taken from different sampling points (Point 01- Steamed Ammonia wastewater, point 02- Equalization tank wastewater, point 03- Anoxic tank wastewater, and point 04- collecting well wastewater.) and named as point 1-4. These samples contained a significant amount of ammonia nitrogen (NH3-N) concentrations, and chemical oxygen demand (COD) as shown in Table I.

TABLE I. THE NH3-N AND COD CONCENTRATIONS OF THE WASTEWATER SAMPLES

Samples	Point 1	Point 2	Point 3	Point 4
NH3-N (mg/L)	56.14	98.25	10.08	215.59
COD (mg/L)	4400.00	1080.00	600.00	1440.00

D. Wastewater treatment procedure and analytical methods

i. Wastewater treatment procedure

25 g absorbent was added in 25, 50,100,150, and 200 mL volume of wastewater for which the ratio of wastewater volume to absorbent mass was 1, 2, 4, 6, 8 mL/g respectively. The mixture was stirred continuously for 5 minutes. After that, the absorbent was separated by filtration, and then was ready for NH3-N and COD determination.

Figure 2. The flow chart for NH3-N treatment and determination

ii. Analytical methods

For determination of ammonia nitrogen: 2 mL sample before and after treatment was taken in a colorimetric tube, and shaken well after diluted with distilled water to the mark. Then 1 mL potassium sodium tartrate and 1.5 mL Nessler's reagent was

added in. After shaking well and waiting for 30 minutes, the samples were taken in 1 cm cuvette and the absorbance was tested by the spectrophotometer at wavelength of 425 nm by using amminia free distilled water as reference. The detailed procedure was shown in Fig.2.

For determination of COD: 1 mL sample before and after treatment was taken in 250 mL conical flask and diluted with 20 mL distilled water and followed by adding 3 mL potassium dichromate. Auto-digestion reflux was used to digest the organic substances. 5 mL of mercury sulfate-sulfuric acid was added to mask the chlorine ion. The mixture was heated and refluxed for 150 minutes. After standing for 3 hours at room temperature (22° to 27°), the solution was diluted in 150 mL distilled water, 3 drops of ferroin indicator were added in. And then the solution was titrated with 0.05 mol/L ammonium ferrous sulfate until the color changed. The detailed steps was shown in Fig.3

Figure 3. The flow chart for COD treatment and determination.

III. RESULTS AND DISCUSSION

A. Characterization of absorbent BYW-01

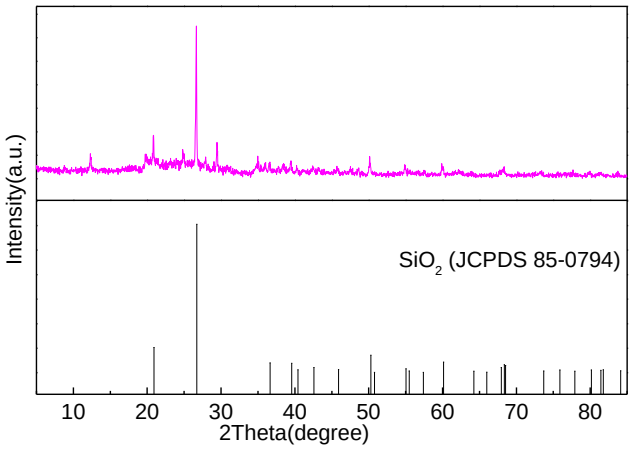

Figure 4. XRD pattern of absorbent BYW-01

Fig. 4 shows the XRD pattern of BYW-01, the peaks at 20.9°, 26.7 °, 50.3°could be attributed to the (100), (011), (11-2) crystal face of SiO2(JCPDS 85-0794). No other substances were detected.

Fig.5 displays the N2 adsorption-desorption isotherms and corresponding pore size distribution curve of BWY-01(the inset image). According to the IUPAC classification, the isotherms exhibited Ⅳ with H3-type hysteresis loop. It had a relative large adsorbance of N2 with a broad htsteresis loop at a relative pressure p/p0 of 0.10-0.95 and a bimodal pore diameter distribution concentrating on 3.8 nm and 7.7 nm. The N2 adsorption-desorption isotherms and pore size distribution revealed that the absorbent BWY-01 were of mesopore structure. It was noting that the broad hysteresis loop was due to the strong capillarity phenomena exsiting within the compact structure.As shown in the table in Fig.5, the multipoint BET specific surface of area was 11.78 m2/g and the pore volume was 0.02 cm3/g.

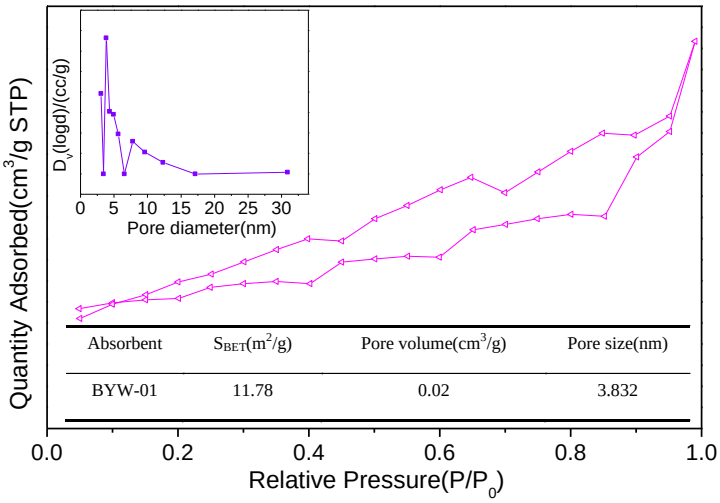

Absorbent	S_{BET}(m^2/g)	Pore volume(cm^3/g)	Pore size(nm)
BYW-01	11.78	0.02	3.832

Figure 5. N2 adsorption-desorption isotherms and corresponding pore size distribution of BWY-01.

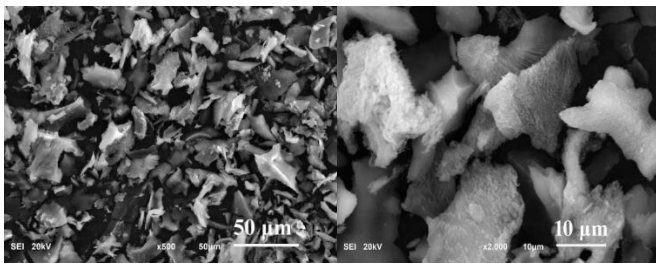

Figure 6. SEM spectra of BYW-01

Fig. 6 shows the SEM spectra of BYW-01. As shown in the inset graph of Fig. 6 b, the absorbent was composed of small spherical particles, which were self-organized as leaf-like microstructure as shown in Fig 6a. And there were many pores on every leaf as shown in Fig.6b, which was agree with BET characterization and contributed to the good performance for NH3-N and COD removal.

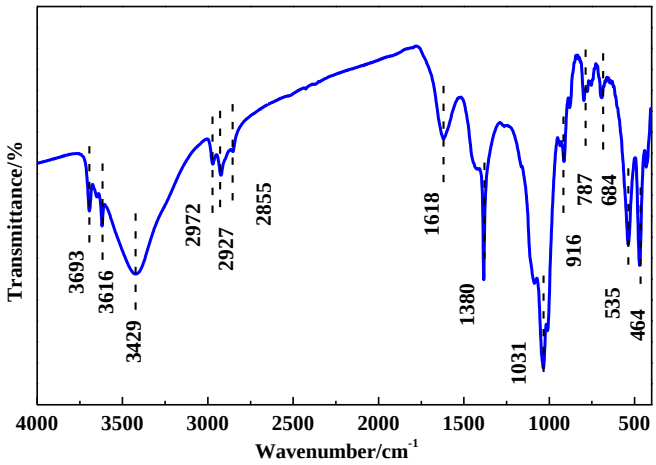

Figure 7. FTIR spectrum of BYW-01

Fig.7 gives the information about functional groups on the surface of BYW-01 by FTIR spectrum. The bands at 2927cm-1 and 2855 cm-1 could be attributed to C-H asymmetric and symmetric stretching vibration absorption of CH2 and the shoulder at 2972 cm-1 prepresented the asymmetric C-H stretching of vibration absorption CH3[28]. The band at 464 cm−1 was caused by Si−O bending vibrations[29]; and the bands at 916 cm−1and 1380 cm−1 were ascribed to bending vibration absorption of OH in carboxylic acid. The bands at 1031 cm−1 could be assigned to C-O-C asymmetric stretching vibration absorption of aromatic compounds. In addition, the band at 535 cm-1could be ascribed to in-plane bending vibration of C-C=O in aliphatic ketone. The intensity and shape of the band at 3429 cm-1 and 3616 cm-1 were assigned to dissociated and intramolecular associated OH groups, which derived from water absorbed from air. In summary, the absorbent BYW-01 exibited good adsorptive property for NH3-N and COD partly because of the abundant of –OH and C=O functional groups on the surface of the absorbent.

B. Adsorption performance

i. Effect of V/m ratio on NH3-N removal rate

The effect of the ratio of wastewater volume to absorbent mass (V/m) on the NH3-N removal rate was investigated, as shown in Table II and Fig. 8. It was observed that for different wastewater taken from various points of a coking plant wastewater treatment process, the removal rate has the same trend, in which the NH3-N removal decreased with V/m increasing from 1to 8 mL/g. The results showed that for different types of wastewater like steamed ammonia wastewater, equalization tank wastewater, anoxic pond wastewater, and collecting well wastewater, BYW-01 showed excellent performance for NH3-N removal in very short contact time (5 minutes). The best removal rate could reach to 48.67 % for collecting well wastewater in point 4. Combined with the original concentration of NH3-N listed in Table I, it was also observed that the removal rate increased with the concentration increasing (point 3-1-2-4) even for different V/m.

TABLE II. THE NH3-N REMOVAL RATE FOR WASTEWATER FROM DIFFERENT SAMPLING POINTS

Sample volume (mL)	Absorbent mass (g)	V/m (mL/g)	Removal rate %			
			Point 1	Point 2	Point 3	Point 4
25	25	1	29.85	30.37	24.32	48.67
50	25	2	28.64	29.95	18.92	48.35
100	25	4	18.64	29.40	17.57	40.51
150	25	6	13.10	19.69	14.86	40.13
200	25	8	10.19	18.30	12.16	36.40

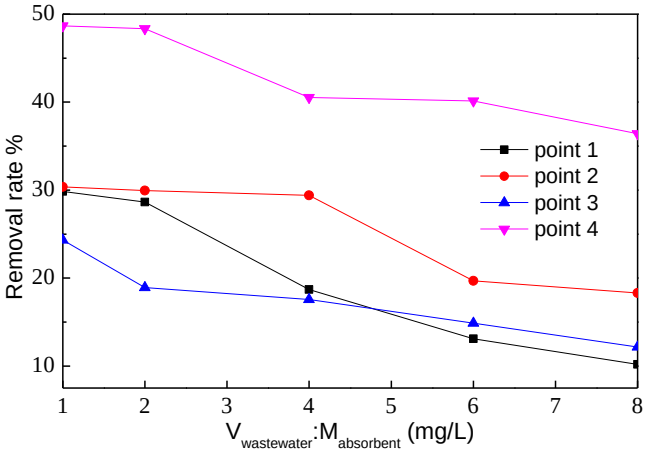

Figure 8. Effect of V/m on NH3-N removal rate at different sampling points

ii. Effect of V/m ratio on COD removal rate

The effect of the ratio of wastewater volume to absorbent mass (V/m) on the COD removal rate was also investigated, as shown in Table III and Fig. 9. Samples before treatment with different volumes (25, 50, 100, 150, 200) were treated with 25 g absorbent, so the V/m ratio was 1, 2, 4, 6, 8 mL/g respectively. The results showed that with the V/m ratio increasing, the COD removal rate was generally decreasing for wastewater from different coking plant processes. The best removal rate could reach near to 70 % for anoxic pond wastewater at point 3 with the COD concentration of 600 mg/L. But when the V/m ratio was more than 6 mL/g, the removal rate reduced slightly or kept constant.This might because the COD concentration was too high, and the absorbent could not absorb them in such a short time (5 minutes) for a lower COD concentration ratio below 1080 mg/L (anoxic pond wastewater and equalization tank wastewater). This might because the amount of absorbent was not sufficient to capture the COD anymore.

TABLE III. THE COD REMOVAL RATE FOR WASTEWATER FROM DIFFERENT SAMPLING POINTS.

Sample volume (mL)	Absorbent mass (g)	V/m (mL/g)	Removal rate %			
			Point 1	Point 2	Point3	Point 4
25	25	1	50.45	59.00	66.66	55.55
50	25	2	19.81	25.00	46.66	30.55
100	25	4	14.41	7.40	33.33	22.22
150	25	6	10.81	3.70	20.00	8.32
200	25	8	8.10	3.70	20.00	2.77

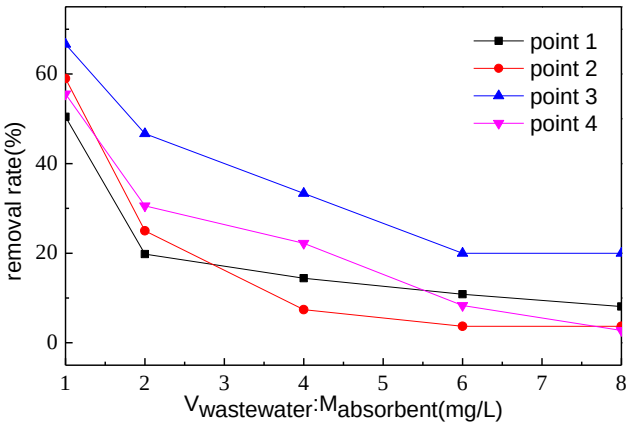

Figure 9. Effect of V/m on COD removal rate at different sampling points

TABLE IV. THE NH3-N AND COD CONCENTRATION BEFORE AND AFTER TREATMENT AND THEIR REMOVAL RATES AT V/M=1 ML/G

Concentration (mg/L)	Point 1	Point 2	Point 3	Point 4
NH_3-N before treatment	56.14	98.25	10.08	215.59
NH_3-N after treatment	39.38	68.41	7.63	110.65
Removal rate (%)	29.85	30.37	24.32	48.67
COD before treatment	4400.00	1080.00	600.00	1440.00
COD after treatment	2200.00	440.00	200.00	640.00
Removal rate (%)	50.45	59.00	66.66	55.55

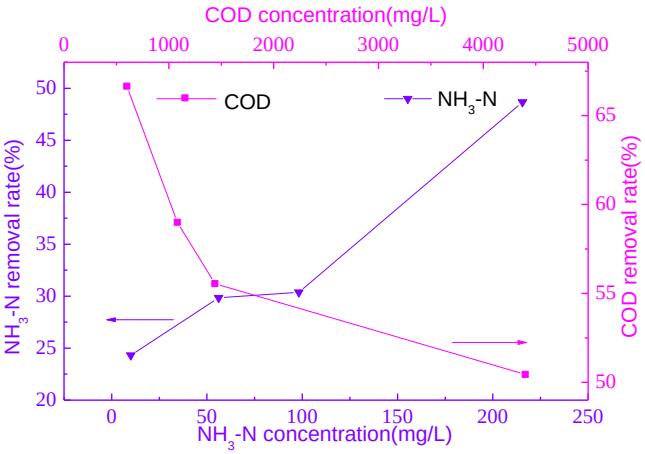

Figure 10. The effect of NH3-N and COD concentration on the removal rate

Table IV and Fig.10 shows NH3-N and COD concentration before and after treatment and the corresponding removal rates at V/m=1 mL/g. The removal rate variation trends with the concentration before treatment for COD and NH3-N at V/m=1 mL/g were completely different as shown in Fig. 7. For NH3-N, the removal rate increased with its concentration before treatment decreasing in the sequence of point 4-2-1-3, while the COD removal rate decreased with its concentration before treatment decreasing in the sequence of point 3-2-4-1 .That mainly because that NH3-N concentration was relatively lower than COD and the absorbent was sufficient to capture them so the higher NH3-N concentration was, the more NH3-N molecules were captured. But for COD, the concentration was too high to be absorbed, and only a small percentage of COD around the absorbent could be captured, which lead to a lower removal rate.

Fig. 11 displays the proposed adsorption mechanism of BYW-01.The coal ash had plentiful pores, which would do good to absorb the NH3-N and COD and let them get close to the absorbent. Furthermore,the coal ash after modification had abundant –OH and C=O functional groups on the surface, which would interact with NH3-N and COD, and capture them tightly.

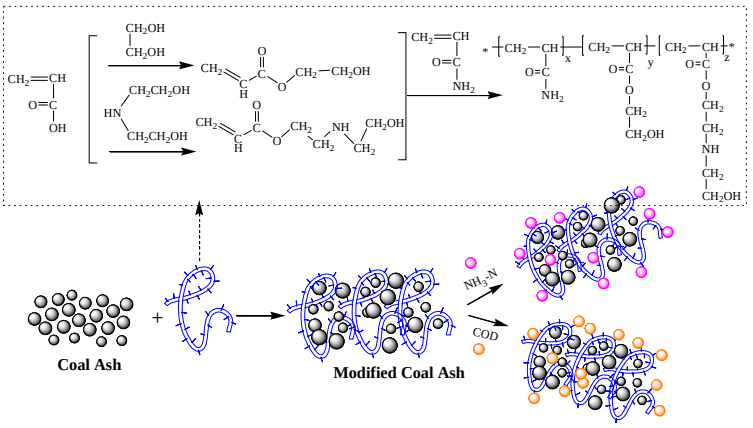

Figure 11. The proposed adsorption mechanism of BYW-01

CONCLUSION

A new, fast, and efficient absorbent was prepared by using coal ash and applied in NH3-N and COD removal in coking plant wastewater in this work, which contained a high amount of NH3-N and COD concentration. The NH3-N removal rate reached about 50% for collecting well wastewater(point 04), and the COD removal rate achieved about 66% for anoxic pond wastewater(point 03) in 5 minutes by using this absorbent partly because of the abundant –OH and C=O functional groups on the surface of the absorbent and partly because of the mesoporous structure of the absorbent. The wastewater volume and concentration affected the removal rate greatly. With the volume of raw water and the concentration of NH3-N and COD increasing before treatment, the removal rate decreased.

REFERENCES

[1] Chen, Bo, Wang, Meng, Duan, Mingxiao, Ma, Xiaotian, Hong, Jinglan, Xie, Fei, . . . Li, Xiangzhi. In search of key: Protecting human health and the ecosystem from water pollution in China. Journal of Cleaner Production, 228, 2019: 101-111.

[2] Hasan, Md Khalid, Shahriar, Abrar, & Jim, Kudrat Ullah. Water pollution in Bangladesh and its impact on public health. Heliyon, 5(8), e02145. (2019).

[3] WWAP, U. World Water Assessment Programme: The United Nations World Water Development Report 4: Managing Water under Uncertainty and Risk: Paris: UNESCO, 2012.

[4] Liang, Ying, Yan, Chunmei, Guo, Qing, Xu, Jin, & Hu, Hongzhi. Spectrophotometric determination of ammonia nitrogen in water by flow injection analysis based on NH3-o-phthalaldehyde-Na2SO3 reaction. Analytical chemistry research, 10, 2016: 1-8.

[5] Long, Sha, Zhao, Lin, Shi, Tongtong, Li, Jingchen, Yang, Jiangye, Liu, Hongbo, . . . Yang, Yongkui. Pollution control and cost analysis of wastewater treatment at industrial parks in Taihu and Haihe water basins, China. Journal of cleaner production, 172, 2018: 2435-2442.

[6] Long, S., Zhao, L., Shi, T., Li, J., Yang, J., Liu, H., & Yang, Y. Pollution control and cost analysis of wastewater treatment at industrial parks in Taihu and Haihe water basins, China. Journal of Cleaner Production, 172, 2018:2435-2442.

[7] Wang, Meicheng, He, Lizhi, Wang, Min, Chen, Lin, Yao, Sicong, Jiang, Wenju, & Chen, Yao. Simultaneous removal of NH3-N and COD from shale gas distillate via an integration of adsorption and photo-catalysis: A hybrid approach. Journal of environmental management, 249, 109342 ,2019.

[8] Zadorojny, C, Saxton, S, & Finger, R. Spectrophotometric determination of ammonia. Journal (Water Pollution Control Federation), 1973: 905-912.

[9] Šraj, Lenka O'Connor, Almeida, M Inês GS, Swearer, Stephen E, Kolev, Spas D, & McKelvie, Ian D. Analytical challenges and advantages of using flow-based methodologies for ammonia determination in estuarine and marine waters. TrAC Trends in Analytical Chemistry, 59, 2014: 83-92.

[10] Huang, Haiming, Liu, Jiahui, Xiao, Jing, Zhang, Peng, & Gao, Faming. Highly efficient recovery of ammonium nitrogen from coking wastewater by coupling struvite precipitation and microwave radiation technology. ACS Sustainable Chemistry & Engineering, 4(7), 2016: 3688-3696.

[11] Jung, Jin-Young, Chung, Yun-Chul, Shin, Hang-Sik, & Son, Dae-Hee. Enhanced ammonia nitrogen removal using consistent biological regeneration and ammonium exchange of zeolite in modified SBR process. Water Research, 38(2), 2004: 347-354.

[12] Yu, Zhenjiang, Chen, Yun, Feng, Dachun, & Qian, Yu. Process development, simulation, and industrial implementation of a new coal-gasification wastewater treatment installation for phenol and ammonia removal. Industrial & Engineering Chemistry Research, 49(6), 2010: 2874-2881.

[13] Albert, DK, Stoffer, RL, Oita, IJ, & Wise, RH. Rapid determination of ammonia and total nitrogen in municipal waste water by microcoulometry. Analytical chemistry, 41(11), 1969: 1500-1504.

[14] Lin, Li, Yuan, Songhu, Chen, Jing, Xu, Zuqun, & Lu, Xiaohua.Removal of ammonia nitrogen in wastewater by microwave radiation. Journal of hazardous materials, 161(2-3), 2009: 1063-1068.

[15] Li, Lan-Bing, Hu, Jin-Li, & Xia, Nian-Cheng. Industrial energy-pollution performance of regions in China based on a unified framework combining static and dynamic indexes. Journal of cleaner production, 131, 2016: 341-350.

[16] Molins-Legua, C, Meseguer-Lloret, S, Moliner-Martinez, Y, & Campíns-Falcó, P. A guide for selecting the most appropriate method for ammonium determination in water analysis. TrAC Trends in Analytical Chemistry, 25(3), 2006: 282-290.

[17] Yu, Hanqing, Gu, Guowei, & Song, Leping. Posttreatment of effluent from coke-plant wastewater treatment system in sequencing batch reactors. Journal of Environmental Engineering, 123(3), 1997: 305-308.

[18] Uludag-Demirer, S, Demirer, GN, & Chen, SJPB. Ammonia removal from anaerobically digested dairy manure by struvite precipitation. Process Biochemistry, 40(12), 2005: 3667-3674.

[19] Bermejo, MD, Cantero, F, & Cocero, MJ. Supercritical water oxidation of feeds with high ammonia concentrations: Pilot plant experimental results and modeling. Chemical Engineering Journal, 137(3), 2008: 542-549.

[20] Segond, Nathalie, Matsumura, Yukihiko, & Yamamoto, Kazuo. Determination of ammonia oxidation rate in sub-and supercritical water. Industrial & engineering chemistry research, 41(24), 2002: 6020-6027.

[21] Ghose, MK. Complete physico-chemical treatment for coke plant effluents. Water Research, 36(5), 2002: 1127-1134.

[22] Chan, Alison, Salsali, Hamidreza, & McBean, Ed. Heavy metal removal (copper and zinc) in secondary effluent from wastewater treatment plants by microalgae. ACS Sustainable Chemistry & Engineering, 2(2), 2013: 130-137.

[23] Melcer, Henryk, Nutt, Stephen, Marvan, Igor, & Sutton, Paul. Combined treatment of coke plant wastewater and blast furnace blowdown water in a coupled biological fluidized bed system. Journal (Water Pollution Control Federation), 1984: 192-198.

[24] Park, Man Ho, Jeong, Sangjae, & Kim, Jae Young. Adsorption of NH3-N onto rice straw-derived biochar. Journal of Environmental Chemical Engineering, 7(2), 103039, 2019

[25] Tchobanoglous, George, Burton, Franklin L, & Stensel, H David. Metcalf & Eddy wastewater engineering: treatment and reuse. International Edition. McGrawHill, 4, 2003: 361-411.

[26] Tian, Yang, Shu, Jiancheng, Chen, Mengjun, Wang, Jianyi, Wang, Yao, Luo, Zhenggang, . . . Sun, Zhi. Manganese and ammonia nitrogen recovery from electrolytic manganese residue by electric field enhanced leaching. Journal of Cleaner Production, 236, 117708, 2019.

[27] Jacinto, Maria Lourdes JAJ, David, Carlos Primo C, Perez, Teresita R, & De Jesus, Benjamin R. Comparative efficiency of algal biofilters in the removal of chromium and copper from wastewater. Ecological Engineering, 35(5), 2009: 856-860.

[28] Grehk, T M, Berger, R, Bexell, U. Investigation of the drying process of linseed oil using FTIR and ToF-SIMS, Journal of Physics:Conference Series 2008. 100, 012019-012023, 2009.

[29] Huirong Zhang, Jin Bai, Lingxue Kong, Xiaoming Li, ZongqingBai, and Wen Li.Behavior of Minerals in Typical Shanxi Coking Coal during Pyrolysis,Energy &Fuels, 29, 2015: 6912−6919

IJEW 国际工程期刊 International Journal of Engineering Works انجینئرنگ کاموں کا بین الاقوامی جرنل

International Journal of Engineering Works
ISSN-p: 2521-2419
ISSN-e: 2409-2770
Vol. 7, Issue 07, PP. 251-254, July 2020
https://www.ijew.io/
https://doi.org/10.34259/ijew.20.707251254

Design and Analysis of Dual Band Circular Slotted Patch Antenna at 2.45GHZ and 5.8GHZ for RFID Applications

N.A Khattak[1], M.I. Khattak[2]
[1]Department of Electrical Engineering, University of Engineering and Technology Peshawar, 25000 Pakistan.
[2]University of Engineering and Technology Peshawar, (Kohat Campus) Pakistan.
naveedakbarkhattak@gmail.com[1]

Received: 31 May, Revised: 15 June, Accepted: 25 June

***Abstract*—**In this project patch antenna has been used for Radio Frequency Identification (RFID) applications. Due to the advancement in the field of wireless communications day by day, RFID is the most attractive technology being used as an identification technology and is far better than other sources of identification and tracking i.e. Bar code technology. Different frequency bands are assigned for RFID antenna. But in this project work has been made in Microwave band ranging from (2.400- 2.483) GHz and (5.7250- 5.8750) GHz due to a number of applications and due to the higher transfer rate. In order to design slotted dual band patch for RFID 2.45GHz and 5.800 Ghz applications, a 1.58 mm thicker RT/duroid-5880 is selected for substrate material having a relative permittivity and loss tangent of ε_r=2.2 and δ=0.0009 respectively. To achieve dual band response different techniques can be adopted. First a conventional patch for 2.45GHz has been designed and then with the help of slotting techniques another frequency band was achieved that was radiating at 5.8 GHz. The dual band frequency of the antenna has been achieved by introducing the slot in the upper most layer patch with coaxial feed. The gain, efficiency and bandwidth of the antenna at (2.45 and 5.80) GHz are {6.661 dB, 89 %, 36 MHz} and {6.661 dB, 97 % and 341MHz}, respectively. The antenna can be potentially use for RFID and WLAN applications. All the simulations are carried out using CST MWS. The prototype has been fabricated to validate the results.**

***Keywords*—** Radio Frequency Identification (RFID), Giga hertz (GHz), Wireless lan (WLAN), Computer Simulation Technology Microwave Studio (CST MWS), Decibel (dB).

I. INTRODUCTION

Wireless communication is replacing the wired technologies. System antenna is an important module, without antenna wireless communication is impossible. Therefore the antenna must be more efficient to perform in a better way. Networked physical objects provide a great global infrastructure that connects virtually physical world with objects. Internet of Thing (IoT) is now a day's most emerging technology with very vast futuristic vision in which internet embed itself with every objects through RFID in a transparent way [1].

The clue of the identification of things and the control of remote devices through Radio frequency identifiers, (RFID's) was presented by H. Stockman in year 1948 [2]. RFID is an automated technology used for proof of identity and improved tracking of human as well as animals. It is also used for healthcare, security purposes, robotics, and collecting toll electronically vehicle speed measuring, and bioengineering [3]. It can identify, sensed object by sending a signal emerging from reader and ending at tag antenna where in the tag there is an integrated circuit (IC) where the information is stored so upon receiving an appropriate signal the information stored in the IC will send back through the tag antenna to the reader [4].

Antenna being a metallic device (as a wire or rod) while having the functionality of both receiving and transmitting electromagnetic energy. It can also be defined as something which can receive radio waves and can also radiate them [5].

According to the figure 1 ideal generator is the source.The impedance of antenna is signified by load ZA and transmission line bear connection with it, losses with in antenna is represented by RL known as dielectric losses and conduction, radiation resistance is denoted by Rr, and Xa also called reactance[5]. In ideal condition maximum power is transferred to the antenna from transmitting source. In applied systems, dielectric-losses appear in transmission line and mismatches appear between antenna impedances and antenna transmission line, which results in originating standing waves [5].

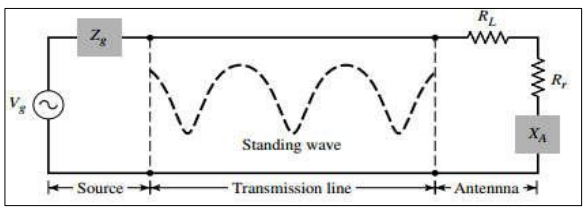

Figure 1. Thevenin & Norton of Antenna system

Less weight, small size, high performance, conformability and low cost are the key requirements of modern age and Patch antenna is the right choice. patch (antenna) contains a radiating-patch which is then attached on a dielectric layer (substrate) consequently supported by ground plane as yx

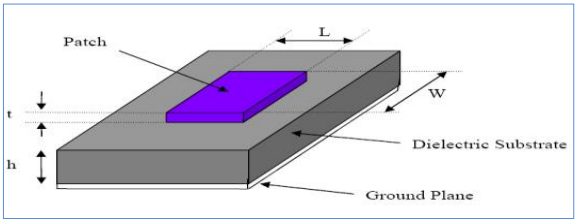

Figure 2. Microstrip patch Antenna

presented in the figure 2. Metals like copper metals or gold can be used as a patch of any shape.

The operation of conventional patch antenna can be modified also by applying the techniques of slotting in the patch. The insertion of slot will introduce perturbation of different modes. In some extent the effect of modes are dependent upon the slot shape, size and the position of the slot. As a result of inserting slot in some certain position there will be produced some more modes. Compact linear and circular polarised antennas, dual band and wideband antennas can be produce by perturbing the correct modes. There are different ways to make slots in patch [6-7].

II. ANTENNA DESIGN AND ANALYSIS

Figure 3 and 4 shows the layout and aspects of dual-band patch (antenna) for RFID 2.45 GHz and 5.8 GHz related applications. In this design a Rogers RT5880 (lossy) is used as a substrate. Relative permittivity, thickness and tangent loss of the substrate are 1.575 mm, $\varepsilon_r = 2.2$ and $\delta = 0.0009$ respectively. The conducting material of the radiating ground and patch plane is taken as low loss copper metal to get better radiation efficiency. The proposed antenna is excited by 50 Ω, 4.5 mm wide coaxial feed line. The width & length of the feed-line as shown are calculated using the standard Transmission-line theory. Slots we introduced to get the desired frequencies, dimensions of the slots can be seen in the same figure [8].

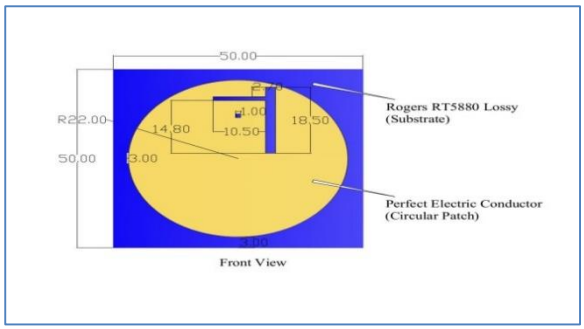

Figure 3. Front View of Antenna

Width equation:

$$W = \frac{c}{2f_r}\sqrt{\frac{2}{\varepsilon_r + 1}} \tag{1}$$

Length equation:

$$L = \frac{c}{2f_r\sqrt{\varepsilon_{reff}}} - 2\Delta L \tag{2}$$

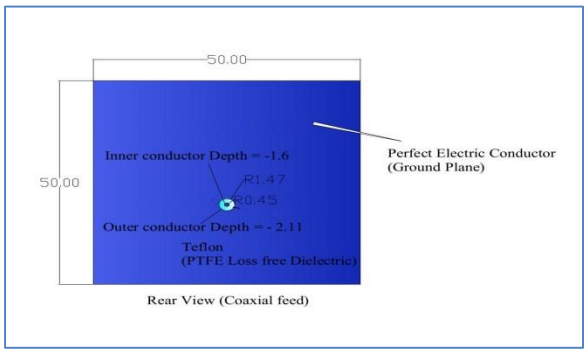

Figure 4. Rear View of Antenna

Frequency equation:

$$f_r = \frac{c}{2L\sqrt{\varepsilon_r + 1}} \tag{3}$$

Coaxial feed line characteristic impedance:

$$Z_{0\infty} = {}^{60}/_{\sqrt{\varepsilon_r}}\, ln\, {}^{D_e}/_{d_e} = {}^{138}/_{\sqrt{\varepsilon_r}}\, log_{10}\, {}^{D_e}/_{d_e}\ \Omega \tag{4}$$

III. RESULT AND DISCUSSION

Slotted dual-band circular patch antenna is simulated and designed in CST MWS and then fabricated. The Return loss is -31dB at 2.45 GHz and -23.7dB at 5.8 GHz as shown in the figure 5.

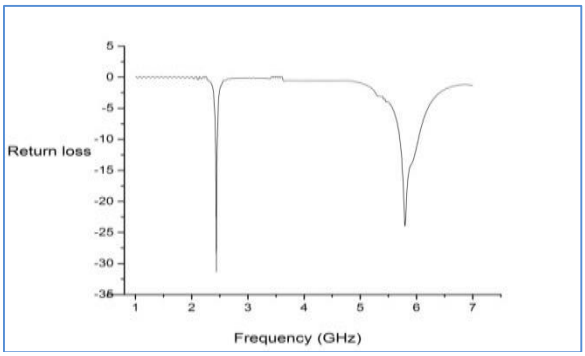

Figure 5. Return loss simulated result

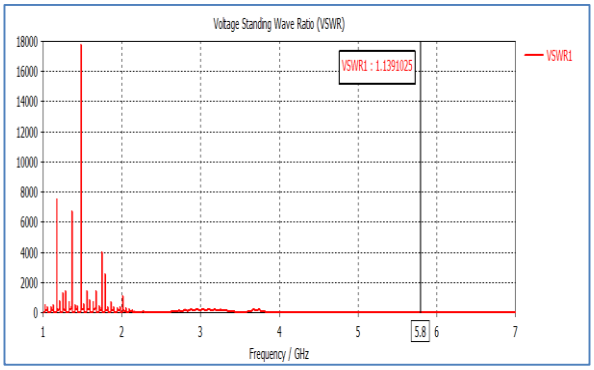

Figure 6. VSWR simulated antenna result

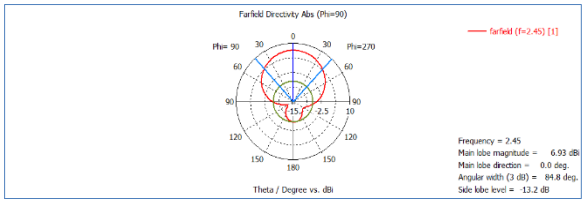

Figure 7. Radiation Pattern 2.45GHz

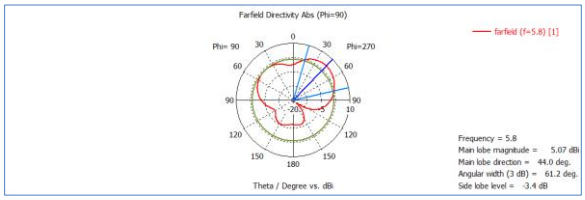

Figure 8. Radiation Pattern 5.8GHz

According to figure 6 The Voltage standing wave ratio of proposed antenna is 1.5 and 1.135 at 2.45GHz and 5.8GHz respectively. Radiation Pattern Plots of proposed antenna can be seen in figure 7 and 8 for frequency 2.45 and 5.8 GHz respectively.3-D gain patterns of simulated antenna can be seen in figure 9 and 10 for frequency 2.45 and 5.8 GHz respectively

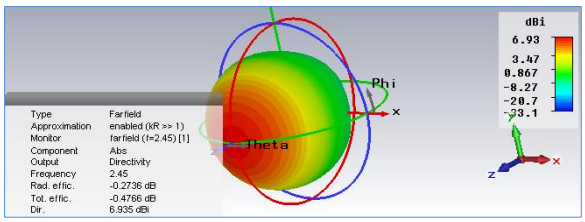

Figure 9. Radiation Pattern at 2.45GHz

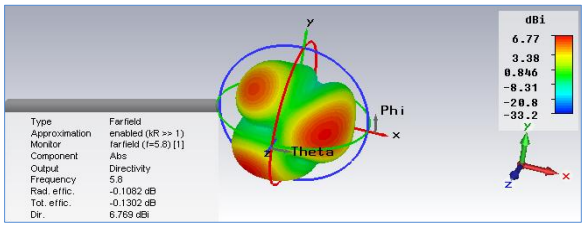

Figure 10. Radiation Pattern at 5.8GHz

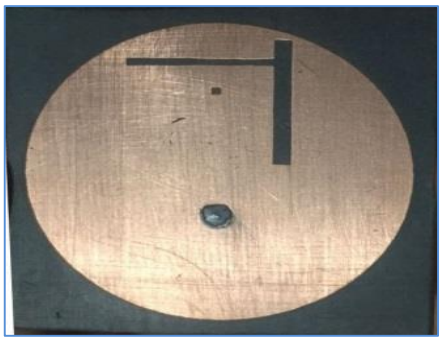

Figure 11. Front View

Figure 12. The Rear View

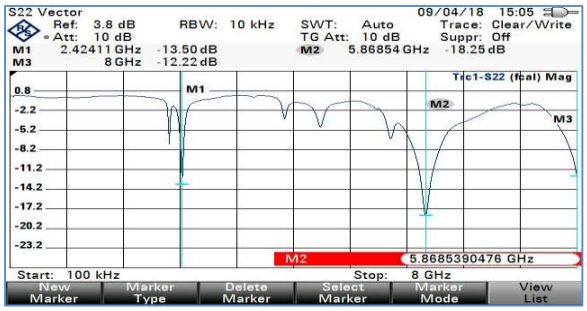

Figure 13. Return loss fabricated antenna result

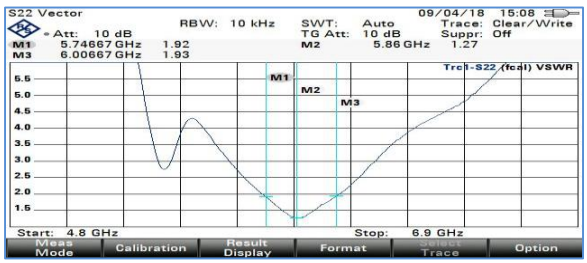

Figure 14. VSWR fabricated antenna result

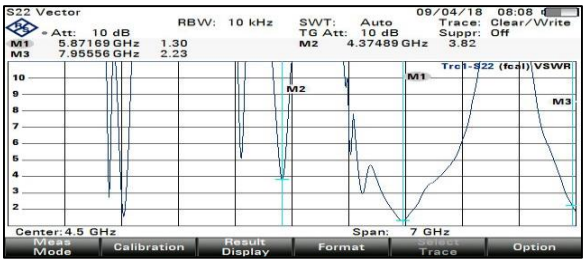

Figure 15. VSWR fabricated antenna result

The antenna is then fabricated and can be seen in figure 11 The front view and figure 12 The rear view. Return loss of fabricated antenna can be seen in figure 13. Fabricated antenna results of VSWR can be seen from the figure 14 and 15 at 5.8 GHz.It is quite evident from both the simulated and fabricated antenna results that the antenna has dual band characteristics with less than -10db (BW of 36MHz, gain of 6.661db, total efficiency of 89%) and (BW of 341MHz, gain of 6.661db, Total efficiency of 97%) for 2.4GHz and 5.8GHz respectively which is attained through famous slotting technique.

CONCLUSION

Numerous parameters of the antenna discussed and analyzed like radiation pattern, gain, return loss and finally analysis of VSWR both through simulation and fabricated results for design's complete understanding. The results shows that gain and bandwidth for both 2.45GHz and 5.8GHz is much high and it makes the antenna in heavy competition with those in the field for the different RFID applications

REFERENCES

[1] S. Mangal, Y.J. Kang and H. J. Lee. "Survey on security in Internet of Things: State of the art and challenges." Advanced Communication Technology (ICACT), 2017 19th International Conference on. IEEE, 2017.

[2] M. Gaetano. "The art of UHF RFID antenna design: impedance matching and size-reduction techniques." IEEE Antennas and Propagation Magazine, pp. 66-79, 2008

[3] A. Ren; C. Wu; T. Wang; B. Yao, "A novel design for UHF near-field RFID reader antenna based on traveling wave," Communication Technology (ICCT), 2010 12th IEEE International Conference on , vol., no., pp.239,242, 11-14 Nov. 2010

[4] A.Iqbal, S.Shah, M. Amir, "Investigating Universal Filtered Multi-Carrier (UFMC) Performance analysis in 5G cognitive Radio Based Sensor Network (CSNs)" *International Journal of Engineering Works*,Vol. 4, Issue 1, PP. 5-9, Jan 2017.

[5] Z. N. Chen Fellow IEEE; X. Qing; Member IEEE and H. L. Chung, "A Universal UHF RFID Reader Antenna" IEEE Transactions on Microwave Theory and Techniques, vol.57, no.5, pp.1275, 1282, 27 March 2009

[6] C. A. Balanis Antenna Theory: analysis and design. Wiley-interscience, 2012.

[7] E. Michael. An investigation of reduced size planer fed microstrip patch antennas. Doctoral thesis Northumbria University, 2005.

[8] W.S. Chen, "Single-feed dual-frequency rectangular microstrip antenna with square slot," Researcher own contribution – May 2019.

International Journal of Engineering Works
ISSN-p: 2521-2419
ISSN-e: 2409-2770
Vol. 7, Issue 07, PP. 255-258, July 2020
https://www.ijew.io/
https://doi.org/10.34259/ijew.20.707255258

Policy Analysis of Thermal Power Generation in Pakistan

Khalil Ullah
(Thermal System Engineering, U.S.-Pakistan Center for Advanced Studies in Energy (USPCAS-E), University of Engineering and Technology Peshawar, Pakistan,)
fkhalilu@asu.edu
Received: 23 June, Revised: 28 June, Accepted: 04 July

***Abstract*—** Provision of affordable and environmental friendly energy is a national concern. Pakistan is not endowed sufficiently with energy resources and has to import energy resources from the gulf countries mainly from the kingdom of Saudi Arabia. Energy policy has been the less researched field in Pkaistan. It is believed to be a ministerial subject with least or no input from other stakeholders like academia, industry and general populace. Under this research we have conducted a detailed survey amongst all the above mentioned stakeholders. The survey comprised of the following five aspects, that were focused in detail i.e. thermal power generation capability and suitability with refrence to Pakistani energy and climate scenarios, legislation capability and local capacity, social awareness and subsidy, energy efficiency and energy audit, industry academia collaboration. Regular policy making was started in mid 1990s. before that there has been no regular power policy and major mpart of the electric power came through the hydel power generation. Since only hydel was not enough to cater to the needs of a growing economy, injection of thermal became necessary. Afterwards i.e the first formal power policy of 1994 the power generation shifted more towards thermal power mode and by this day Pakistan has 62% of power generating from thermal power i.e. fossil fuels like oil, coal and natural gas. Pakistan is one of the most seriously affected country with climate change effects. Climate change effects and availability of power should be traded off to have a workable solution.

***Keywords*—** thermal power, power policy, climate change, fossil fuels, Stakeholders.

I. INTRODUCTION

Pakistan has been under severe energy crisis since early 1990. A need for a workable power policy was felt at this moment. Before the stated period the energy mix of the country abundantly consisted of hydel and less thermal. From that time onwards the energy mix became more oil dependent and less hydel or renewable. By now Pakistan is fulfilling 64% of energy needs via thermal power generation.

In 1947 for a population of 31.5 million Pakistan had 60 MW of generation i.e. 4.5 kWh of consumption per capita. In the year 1952 the government of Pakistan (GoP) had acquired major shareholding of the Karachi electric supply company (here after KESC) which was responsible for generation distribution and transmission of electrical power to all the commercial, domestic, and industrial facilities. In the year 1958 water and power development authority (hereafter WAPDA) was created which helped reach the power generation to 119MW. By now the country had entered into the development phase. The authority of power development was then undertaken by WAPDA. It had many hydel and thermal power generating units, transmission and distribution to cater to the needs of a fast growing demand, under its control.

After five years of operation the total capacity of the power generation rose to 636 MW from 119MW. This increase in the provision of electricity had a very positive impact on the overall life style of the country, mechanized agriculture, industrialization took pace and overall life quality improved. The increase in power generation kept the pace up and by the year 1970 the total generation capacity had reached to 1331MW by installing different thermal and hydel power generation plants. This increase in power generation kept on increasing and every time supply exceeded one step ahead of the demand until year 1990-91, when the power generation touched 7000MW. But in the years to come after 1990 supply lost the pace to demand and there started the gap between demand and supply. The demand was growing consistently with 9-10% annually. In early 90s peak demand exceeded supply by 15-25% resulting in load shedding of about 1500-2000MW [1]. At this moment power policy 1994 was announced and from this time onward the power parity shifted from hydel to thermal. This shift had profound effects on the state of economy and energy market.

II. NEED FOR POWER POLICY

To overcome the growing demand of power, need was felt for a workable policy that could help reduce/eliminate the gap between demand and supply. An energy task force was created in 1993 to come up with a policy which could eliminate power shortage in the minimum possible time [2]. This policy stressed upon the inclusion of private investment into the power sector. Since thermal power generation plant installation takes relatively less time in setting up so it attracted more investment relative to hydel power generation, hence disturbing the hydel

thermal parity. This was the time more thermal power was injected into the country power mix.

First formal power policy of Pakistan was introduced 25 years ago i.e. in 1994. That time 40% of the population had access to electricity and the total capacity stood at 10800MW. That time the load-shedding was weather dependent as in summers it was relatively in check due to high amount of availability of water in the rivers. The power policy adopted in 1994 envisaged 8% annual increase in demand meaning 54000MW would be needed by the year 2018 [2].

Power policy 1998 envisaged a competitive power market in Pakistan. This policy laid down a base for restructuring and privatizing thermal power plants, power transmission, and power distribution of the public sector utilities (WAPDA/KESC). National electric power regulatory authority (NEPRA) was created under power policy 1998. As per the policy once NEPRA becomes fully operational the power sector will become more competitive [3].

Another power policy came in 2002 where again the privatization and decentralization of power systems with separate generation, transmission and distribution exists. More private ownership and management were envisaged under this policy draft [4].

To meet the current and future needs of the country the Government of Pakistan came up with an ambitious power policy 2013. Policies are always made with a positive and constructive intent, what hampers the achievements of those policies is its implementation in true letter and spirit. Power policy 2013 identified four major challenges i.e. demand-supply gap, inefficiencies in distribution and transmission systems, highly expensive generation electricity, and subsidies and subsequent circular debt.

To achieve the long term vision and provide a sustainable power supply to common citizens of Pakistan the policy 2013 set nine goals to achieve i.e. creating power generation capacity, promoting a culture of conservation, inexpensive electric supply to domestic, commercial and industrial facilities, minimize pilferage and adulteration of fuel, world class efficient generation, a cutting edge transmission, minimize financial losses, and improve the governance of all the federal and provincial ministries and regulators [5].

III. PAKISTAN ENERGY SCENARIO

Pakistan is facing serious energy crisis since long. In 2011 Pakistan had a short fall of 4000-5000 MW in summer while 2000-3000 MW in winters. Also there is a about 2 billion cubic foot shortfall in energy [6]. Curerently Pakistan is also facing serious climate change effects. Currently thermal power generation also adds to this serious issue since there are toxic gases in the emission of thermal power plants.

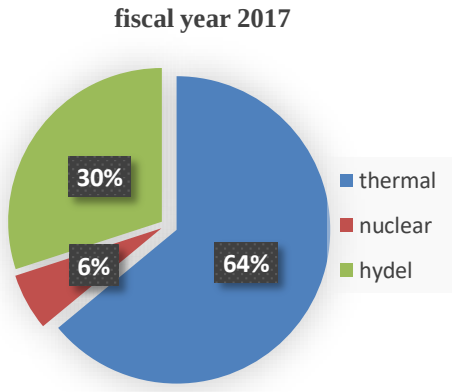

Figure.1 Pakistan energy mix

As depicted by the picture above the energy mix is heavily dependant on fossil energy fuels which are mainly to be imported from the gulf countries like KSA, Qatar and UAE. In order to invoke public, academia and investers perspective a detailed survey has been conducted to address the concerns of all the stakeholders.

IV. THERMAL ENERGY SUITABILITY

As per the survey conducted and in relation to the Pakistan energy enviromnet a response was recorded regarding the suitability of thermal power generation. Such response would give us an insight and a future road map whether to continue with thermal power genertation or if not where we should invest our energy efforts.

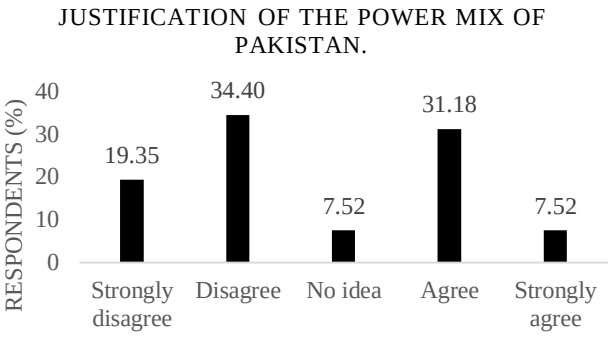

Figure. 2 Power mix Justification

As its obvious from the responses there is quite a parity between those who agree and those who does not. Since it could not be decided on the basis of this very response so we shall have to look somewhere else i.e. acceptability.

V. RENEWABLE ENERGY FUTURE AND ACCEPTABILITY

Renewable energy is a bussing word every where. It is enviromentall very compitable but not yet mature enough to cater to all the needs and without thermal power it can not cater to the needs of all the customers. It is indeed an environmentally accepted but it need to be improved further to replace all the thermal power with renewable energy. As long

as the acceptability is concerned it is hugely accepted and this is obvious from the over whelming response of the repondents

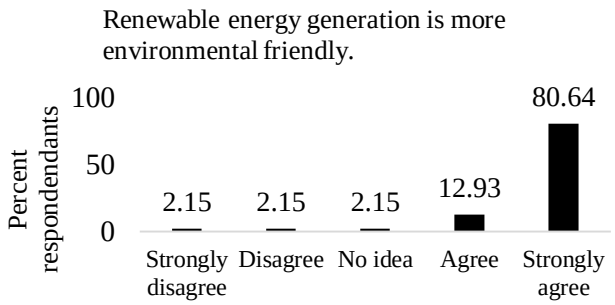

Figure. 3 Renewable energy acvironmental friendliness

From this response it is easy to predict the future of clean renewable technologies in coming time. Times when availability of energy and climate would equally matter then it would be renewable to fit into the market and fulfill the needs alongwith least harm to the environment.

SWOT Analysis of renewable energy in Pakistan

Strengths

i. Pakistan has got an overall sunny climate.
ii. Pakistan being 7th most affected country by the climate change makes it a valuable spot for injecting more renewable energy into her energy mix.
iii. With the help of Chines technology much of the renewable energy devices like solar cells are locally manufactured here in Pakistan.
iv. Globally climate change is hot issue and discussed at higher level and it has got even more centralized position after KYOTO protocol and Paris climate change agreement, this encourages further inclusion to power mix.
v. Exclusive renewable energy policy is 2019 to be announced soon.
vi. Pakistan envisaging complete phase-out of thermal power plants by 2040.

Weaknesses

i. Solar is not a reliable source for sustainable power supply.
ii. With ever increasing power deficit Pakistan energy sector cannot afford directing more funds towards a non-reliable energy source.
iii. Enough skilled workforce is not yet available and thus causes a huge loss to the national exchequer, Quaid e Azam solar park is one such example.

Opportunities

i. In Pakistan there are huge opportunities available for renewable energy provided its geography and climate.
ii. Pakistan being adversely affected would pay more attention to renewable environmental friendly technologies.

Threats

i. The ever increasing gap between demand and supply is a big threat to inclusion of renewable energy as it's not yet capable enough to suffice the need of the market.
ii. In order to sell back the electricity generated at homes or other facilities to the national grid requires net metering which is not yet introduced in Pakistan.

VI. Thermal Power Relaibilty

As thermal power is incredibly reliable and currently 80% of the global energy needs are fullfiled via thermal power generation[7].

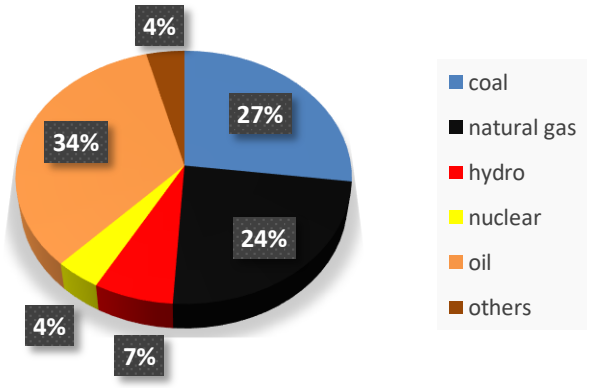

Figure. 4 World total primary energy consumption by fuel in 2018

Same response was recorded from the questtionaire respondents. Henced thermal is largely reliable and peak loads can only be met with thermal power generation.

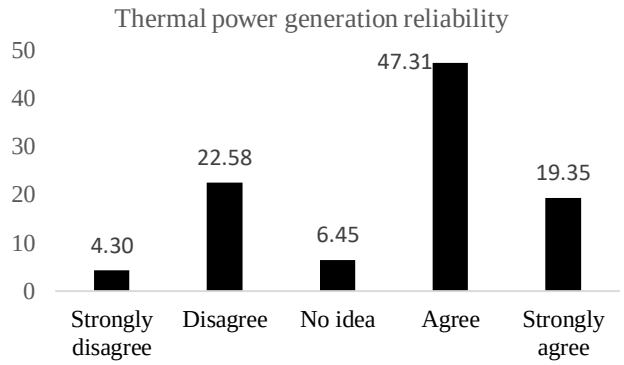

Figure. 5 Thermal Power generation reliability

SWOT Analysis of Thermal power

Since major part of our power comes from thermal sources like fossil fuels which include oil and gas and coal. Pakistan is a country blessed with huge reserves of coal which accounts for sixth largest globally. Such huge amount of coal gives thermal power generation a huge boost in order to arrest our energy deficit. Thermal power got its boost from power policy 1994 and the parity between thermal and hydel got unequal. Policy 1994 encouraged private investment in power sector and the investor finding the thermal power generation to be more and quick rewarding invested in thermal power sector in the

form of IPPs and public private partnerships. Here we are presenting a SWOT analysis of thermal power with contemporary climate change scenario.

Strengths

i. Globally no source is more reliable than thermal power. Major part i.e. around 80% of the global power around the world is produced thermally.
ii. As far as Pakistan energy environment is concerned which is heavily energy deficient only thermal energy inclusion can alleviate the issue.
iii. Since Pakistan is heavily blessed with coal reserves it is our extreme hard luck that despite the huge resources we still lack hundred percent energy access. Had this much energy resource in any other country, they would be exporting electricity.
iv. Pakistan is an under developed country which has the highest need of energy, and which can be achieved only with thermal power generation.
v. Under CPEC Pakistan has signed multiple MOUs with partner country china for power generation and recently Thar coal based two power generating units have been commissioned, each 660MW.

Weaknesses

i. Thermal power is regarded to be dirty i.e. polluting the environment. This makes this type of power generation less competitive.
ii. Fluctuations of fossil fuels in international market makes it an expensive fuel to generate power.
iii. Expensive fuel has resulted in accumulation of a mammoth of circular debt which is nearly RS 900 billion.

Opportunities

i. The major opportunity in this sector is the huge presence of coal reserves in the country which makes is a viable source for power generation.
ii. The deficit in demand-supply is itself a bigger opportunity as in a short span of time the gap can be bridged only via thermal; power generation.
iii. We have countries like Afghanistan and India, where too power shortage is a problem and we have a bigger opportunity exporting them electricity provided the political landscape allows it.

Threats

i. The major threat comes to thermal power generation from the proposed policy to oust it completely in 2040.
ii. The animosity between environment and thermal power generation makes it the last choice for many
iii. The power generated via thermal process is relatively expensive to the power generated via hydel.
iv. A threat to thermal power can also be envisaged from the survey we conducted, where we asked them whether they would like more inclusion of thermal power in their mix or not. The responses came mostly in the negative, which means the general public also does not want it anymore.

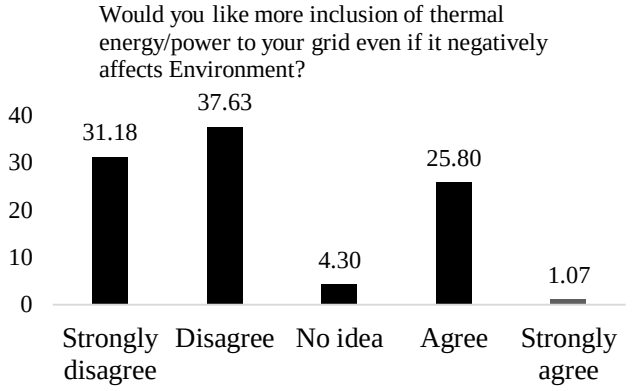

Figure.6 thermal power inclusion into power mix

Moreover, when we asked them about technologies having low carbon foot print, again the responses were overwhelming and almost all of the respondents either agreed or strongly agreed for advocating the inclusion of technologies that can lower the carbon from an already overburden upper atmosphere.

CONCUSLION

Based on the responses recorded from the diffderent respondents like academia, investors, government and common people there is huge likelihood that there is no immediate replacement fro thermal power but alongside it would be detremintal both for ec onomy and climate to go with thermal for long time. There should be timely replacement of thermal power generation with renewable technologies like solar, hydel, solar and wind. This will trade-off the harsh effects pof thermal power generation with provision of electricity across the board.

ACKNOWLEDGEMENTS

The authors are grateful to the U.S.-Pakistan Center for advanced studies in Energy (USPCAS-E) UET Peshawar for the financial support of current work.

REFERENCES

[1] M. A. Javaid, S. Hussain, Z. Arshad, Ma. Arshad, and M. Idrees, “Electrical Energy Crisis in Pakistan and Their Possible Solutions,” Int. J. Basic Appl. Sci. IJBAS-IJENS, vol. 11, no. 5, pp. 5–38, 2011.
[2] “75Aceb87369D3C696Ad46C349Aaa8D5B4Ec1D7C3.Pdf.” .
[3] S. No, Government of Pakistan Notification. 2004.
[4] “Policy For Power Generation Projects Year 2002,” Policy, 2002.
[5] J. Vinanchiarachi, N ational P ower P olicy, 2013th ed., no. September. government of pakistan, 2013.
[6] muhammad adnan, “Energy crisis in Pakistan and its issues,” 2011.
[7] “world energy usage by fuel,” 2018. [Online]. Available: https://en.wikipedia.org/wiki/World_energy_consumption.

IJEW 国际工程期刊 International Journal of Engineering Works انجینئرنگ کاموں کا بین الاقوامی جرنل

International Journal of Engineering Works
ISSN-p: 2521-2419
ISSN-e: 2409-2770
Vol. 7, Issue 07, PP. 259-263, July 2020
https://www.ijew.io/
https://doi.org/10.34259/ijew.20.707259263

Analysis of Green Technologies for Motorway Interchange

Muhammad Jamal Farooq[1], Tayyaba Sony[2], Nisar Ahmed[3],Khurram Shahzad Ali[4]
[1,2,3,4]Department of Electrical Energy System Engineering US-Pak Center for Advanced Studies in Energy (USPCAS-E), UET, Peshawar, Pakistan
engr.jamal.farooq@gmail.com[1], tayyaba_sony@yahoo.com[2]
Received: 01 July, Revised: 09 July, Accepted: 11 July

***Abstract*—** Pakistan is in phase of increasing economic growth which is also giving people to raise their standard of living which is growing in building construction. This is further rising the demand of electricity which is a big challenge for Pakistan. The energy savings made at load sites are nowadays regarded as energy generation. Taking all this parameter into account, there is an urge for alternative way to minimize the energy consumption in order to overcome the electricity shortfall in Pakistan.

A detailed analysis has been conducted to lower the annual energy requirements of the test site. The optimization strategy mainly involves (i) energy audit, (ii) retrofitting technique .An important finding is that the payback period of all technique is less than seven years. The results indicate that when 3 inch polystyrene insulation is internally employed along with the energy efficient appliances, an electricity saving up to 22% with a payback period of 4.96 years can be achieved.

***Keywords*—** Green technologies, Retrofitting, Energy Efficiency, LEB.

I. INTRODUCTION

Building is consuming one third of the total world of energy consumption [1] and the building construction is on rise and which is associated with energy consumption. Energy is basic need of life. Pakistan at the time of dependence only got 60 MW. At early Pakistan made some remarkable growth but it doesn't continue in positive manner [2] Energy sector of Pakistan is facing a severe shortfall form last decade. Rapid urbanization led to shortfall problems plus theft, loses and low energy mechanism took out major portion leaving shortfall up to 5000 MW during summer [3]. In 2009 the electricity shortage led to loss of 3.9 billion dollar which is 2.5% of Pakistan GDP [4].

Pakistan has great potential in field of renewable energy which can generate huge amount of energy.[5]. And also when we talk about on consumption side residential and commercial buildings use huge amount of energy

Due to crises of energy in Pakistan there is intense need to design new building in such a way that it consume less energy or the existing building should be retrofitted to such a design that it consumes less energy which can help to reduce the shortfall. Pakistan has neglected the green building topic which can lead to save huge amount of energy. Commercial and residential consumes a lot of power and has ability to save energy just by following basic steps like selecting right design of building and choosing right electrical appliances. Building design which can save energy can cost 15-20% extra in Pakistan[6]. Various estimate shows that by using energy efficient product can save 30% of energy consumption. Enercon estimated shows that by using efficient appliances can save in utility bills up to 50% while building design can save 15% of utility bills[6].

The difference between supply and demand of energy in Pakistan causes shortfall of electricity, this gap between demand and supply causes load shedding in urban and rural areas. The supply from generating station is 15,700MW while the requirement of energy is 20,223 MW per day, the country is facing approximately 5000 MW of energy per day[7]. Due to this gap of electricity in supply and demand, load shedding occurs for about 15 hours in rural areas, while 8-10 hour load shedding in urban areas, which is badly affecting all spheres of life [8]. To overcome load shedding there is intense need to increase the generation of energy, while on demand side the consumption should optimized. the demand of energy increases every year and hence the associated cost also increases, there is a need to minimize the existing energy consumption in an efficient way, so that the end consumer will fulfill their energy requirements at minimum price.

In this paper analysis has been done on motorway interchange of an existing building. Different type of insulation has been used while also energy efficient equipments are also been used

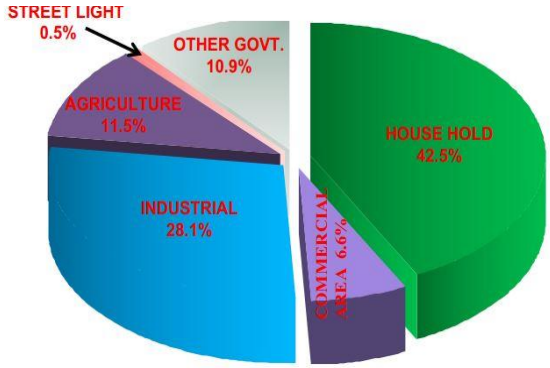

Figure 1. Consumption of electricity in various sectors of Pakistan [3]

II. GREEN BUILDINGS

Green buildings are those buildings which consume less energy as compare to conventional buildings. It can be achieved by using certain passive techniques like selection of site for buildings, windows position, using of materials, green roofing, shading etc[9]. While net zero energy building are those buildings which can generate all of its energy on site by renewable resources with no or zero emission of carbon dioxide. Retrofitting is a technique used to convert a existing building into energy efficient one. Retrofitting is cost effective as compare to build a new one. The goal of retrofitting to lower down the energy requirement for space heating without affecting the human comfort [10].

III. SYSTEM COMPONENTS

A. *Insulation Material*

The use of insulation in the building can significantly minimize the consumption of energy. Initially the building was examined for two different types of insulation i.e. for Polystyrene and Polyurethane. Results were in favor of polystyrene. thermally insulated model consist different size and different arrangement that has applied on the walls. the different location i.e. insulation on the outer surface of wall termed as external insulation, insulation on the inner wall known as internal insulation and combination on both external and internal known as mixed insulation.

B. *Energy Efficient Appliances*

By incorporating the energy efficient appliances, the energy consumption can be definitely low down as compared to the conventional appliances, so in this model the energy efficient appliances were considered and reduction in the energy consumption was noticed.

In this model the tube lights are to be replaced with energy saver bulbs or LED, conventional AC with inverter type etc.

C. *Combination of Insulation Material And Energy Efficient Appliances*

In this technique as the name suggests combination of insulation that is Polystyrene and energy efficient appliances was proposed. A significant reduction in consumption of electricity was observed.

IV. SYSTEM CONFIGURATIONS

The residential building was analyzed for different energy efficient strategies in the form of different scenarios. All these scenarios are discussed below.

A. *Scenario-I Insulation Using Polystyrene*

When pentane is added to Polystyrene grains and evaporated from which white, rigid and closed-cell foam is formed having thermal conductivity from 0.031 to 0.037 W/ mK, .In this model polystyrene is used against the 8 inch brick having 0.25 inch mortar on both sides. Insulation is used for wall and roofs.

- Cement mortar 0.25 inch
- Common brick
- Polystyrene 3 inch
- Cement mortar 0.25 inch

B. *Using Energy Efficient Appliances*

The appliances which are for conventional use consumed considerable amount of energy so for reducing consumption of electricity, energy efficient appliances are used in this model. For instance tube light which has consumption of 60 watt can be replaced by energy saver light which has consumption of only 25 watt. Likewise desktop computer replaced by laptop. And air conditioner is replaced by dc invertors air conditioner.

C. *Scenario-III Insulation using 1-inch Internal Polystyrene with EEA*

In this scenario insulation of Polystyrene of 1inch applied on wall and roof internally and also energy efficient appliances is used. The construction material is given as

- Cement mortar 0.25 inch
- Common Brick
- Polystyrene 1 inch
- Cement mortar 0.25 inch

D. *Scenario-IV Insulation using 1.5 inch internal polystyrene with EEA*

In this scenario Polystyrene of one and half inch is applied on the roof and walls internally and energy efficient appliances is also used. The construction material is given below.

- Cement mortar 0.25 inch
- Common brick
- Polystyrene 1.50 inch
- Cement mortar 0.25 inch

E. *Scenario-V Insulation using 3 inch internal polystyrene with EEA*

In this scenario Polystyrene of 3 inch is used internally on the walls and roofs. And also energy efficient appliances are considered. The construction material for this case is given below.

- Cement mortar 0.25 inch
- Common brick
- Polystyrene 3 inch
- Cement mortar 0.25 inch

F. Scenario-VI Insulation using 3 inch polystyrene external with EEA

In this scenario insulation of three-inch Polystyrene is used externally on the walls and roofs with the use of energy efficient appliances. The construction materials are given below.

- Cement mortar 0.25 inch
- Polystyrene 3 inch
- Common brick
- Cement mortar0.25

G. Scenario-VII Mixed Insulation with EEA

When insulation is used on both side internally and externally known as mixed insulation. In this scenario insulation of polystyrene is applied internally and externally and also energy efficient appliances are considered. The construction materials are given as.

- Cement mortar 0.25 inch
- Polystyrene 0.25 inch
- Common brick
- Polystyrene 0.25 inch
- Cement mortar

V. RESULTS

Results are discussed briefly in this section which is obtained as analysis and simulation were done for different cases. Which are given below.

A. Scenario-I Insulation using Polystyrene

When Polystyrene is applied on roof and walls the total energy consumption is reduced from 68,801 kWh to 59878 kWh. The comparison graph between baseline and insulation of Polystyrene is given below.

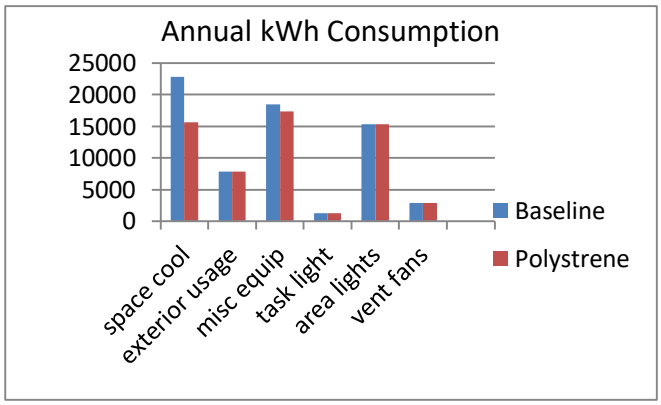

Figure 2. Comparison between Baseline and Scenario-I

B. Using Energy Efficient Appliances(EEA)

When conventional appliances is replaced by energy efficient appliances. The consumption of total energy is reduced to 57774 kWh per annum. Which is 17% of the total energy .the graph is given below.

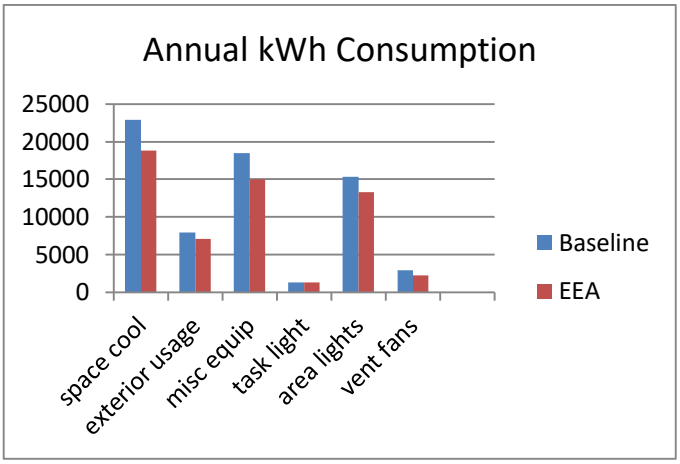

Figure 3. Comparison between Baseline and Scenario-II

C. Scenario-III Insulation using 1-inch internal Polystyrene with EEA

When 1 inch Polystyrene is used internally the total load in this case is lower down to 56,078 when insulation of Polystyrene is used in thickness of 1inch almost 19% of the saving. In this case mixture of insulation is used with energy efficient loads so the saving in loads will occur.

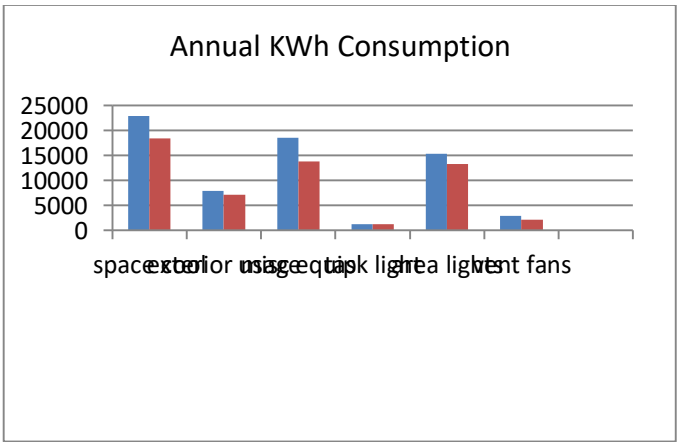

Figure 2. Comparison between Baseline and Scenario-III

D. Scenario-IV Insulation using 1.5 inch internal Polystyrene with EEA

When the diameter of insulation is increased from 1 to 1.5 inch of Polystyrene. Which show that consuming energy becomes lower in every sector. The total saving in kWh is given 13215 kWh of the unit almost 20% of the total.

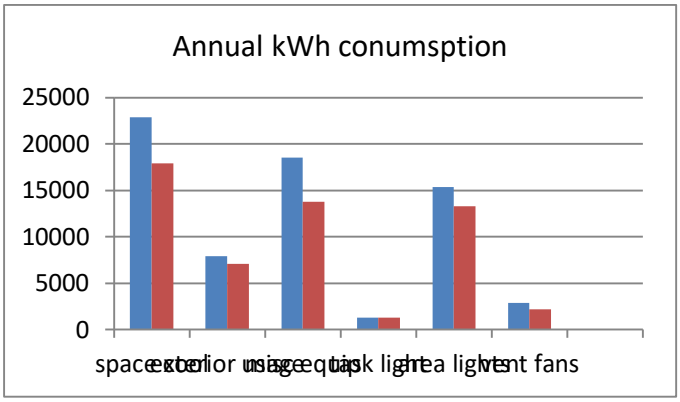

Figure 5. Comparison between Baseline and Scenario-IV

E. Scenario-V Insulation using 3 inch internal polystyrene with EEA

In this case insulation of Polystyrene is increased from 1.5 to 3 inch along with energy efficient appliances. The total saving in this case is 15389 kWh per annum which is almost 23% of the total.

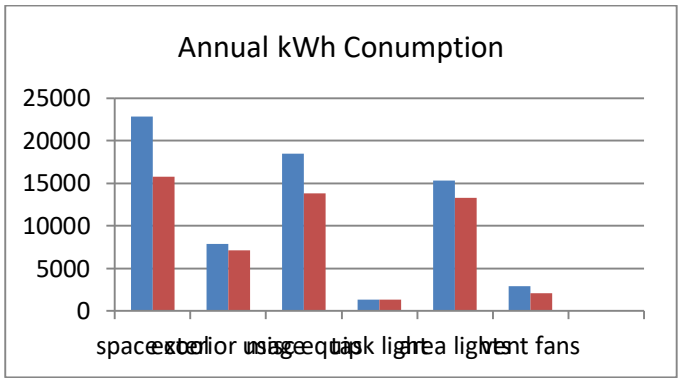

Figure 6. Comparison between Baseline and Scenario-V

F. Scenario-VI Insulation using 3 inch Polystyrene external with EEA

When 3 inch Polystyrene is taken externally along with energy efficient appliances the result shows that it lower down space cooling from22877 kWh to 14304 kWh per year. The total saving in this case is 17115kWh per annum which is almost 25% of the total power.

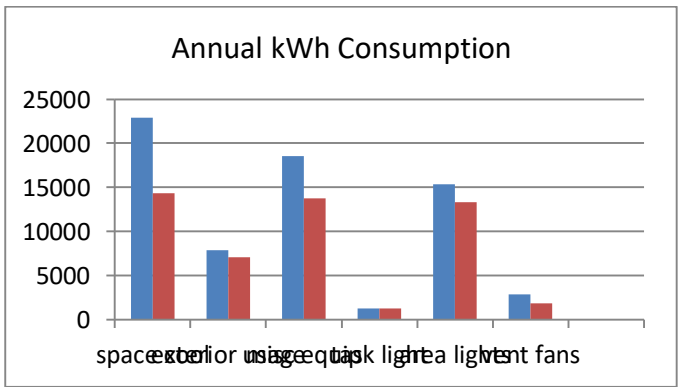

Figure 7. Comparison between Baseline and Scenario-VI

G. Scenario-VII Mixed Insulation with EEA

When insulation of Polystyrene is used internally and externally with energy efficient appliances space cooling loads is lower down to 22877 to 11384kWh unit. The total saving in this case is 20573 which are almost 30% of the saving in a year.

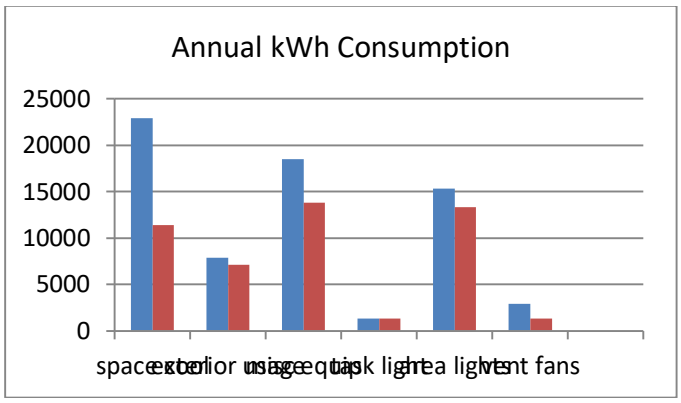

Figure 8. Comparison between Baseline and Scenario-VII

VI. COMPARISON

The comparative graphs of all scenarios are given below by line graph. The vertical showing per year kWh saving while in horizontal different scenarios is given.

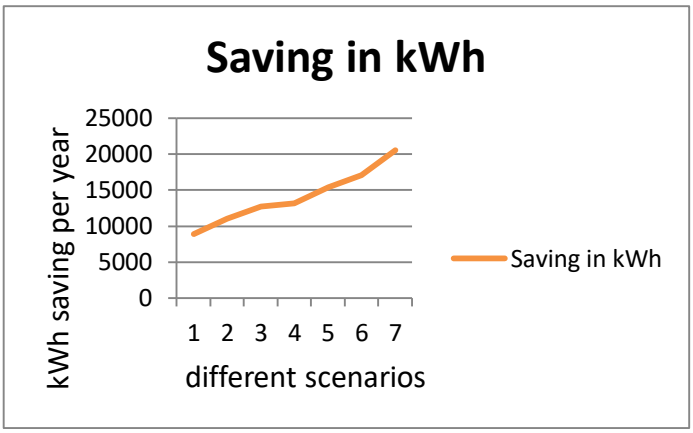

CONCLUSION

Pakistan is facing energy crises like other developing countries. Pakistan has strong growth of economy and demand of energy is rising but despite of this Pakistan has not given full attention to install new capacity for generation. So Pakistan is facing shortfall from past decade. To tackle this problem on distribution site people awareness is required to build such type of building which uses less amount of energy as compared to conventional building numerous potential is available in this regard. The strategies described in the above section are analyzed individually on the basis on insulation of polystyrene and also with energy efficient appliances and it is also analyzed mixture of both to lower down the use of electricity consumption with baseline model. The result shows that the insulation model taken lower down the kWh consumption to some extent but energy efficient equipments help to save kWh units in greater amount as the equipments used in building are not energy

efficient. The economical and easy way to lower down electricity consumption are the use of energy efficient appliances. And the payback will not be more than five years in this case and also lower down electricity consumption by 20-30% of kWh units.

In this research motorway interchanges has been taken and different technique has been applied to show how much energy can be saved. As there exists a lot of interchanges and new motorway are underway and will be completed. If we follow the way mentioned can save a lot of energy. The best technique is insulation of 3 inch polystyrene with energy efficient appliances as the pay back is period is 4.96 years. while other scenario Polystyrene external and mixed insulation with energy efficient appliances is not only costly but payback period of those model are above five years. And the second most important thing is that the appliances we are using are not as efficient. Switching to energy efficient appliances can have huge impact in our daily life in saving of energy.

References

[1] Karkare, A., Dhariwal, A., Puradbhat, S., & Jain, M. Evaluating retrofit strategies for greening existing buildings by energy modelling & data analytics. In *Intelligent Green Building and Smart Grid (IGBSG), 2014 International Conference* , pp. 1-4,2014, April. IEEE.

[2] Irfan, M., Abas, N., & Saleem, M. S. Net Zero Energy Buildings (NZEB): A Case Study of Net Zero Energy Home in Pakistan

[3] Rafique, M. M., & Rehman, S. National energy scenario of Pakistan–Current status, future alternatives, and institutional infrastructure: An overview. *Renewable and Sustainable Energy Reviews*, vol. *69*, pp.156-167, Mar 2017

[4] S. Aziz, S. J. Burki, A. Ghaus-Pasha, S. Hamid, P. Hasan, A. Hussain, H. A. Pasha, and A. Z. K.

a. Sherdil. "Third Annual Report—State of the Economy: Pulling back from the abyss

b. (Lahore)", Pakistan: Beaconhouse National University, Institute of Public Policy: 66

[5] F. Jan, A. Mutalib. "Mitigation of Energy Crisis in Pakistan through Energy Conservationin Residential Sector" *International Journal of Research in Engineering and Technology (IJRET*) 2, no.4(2013):169

[6] Malik, A. M., & Awan, M. Y. (2018). Need for Energy Proficient Buildings as Solution towards Energy Stability in Pakistan. *Technical Journal*, *23*(01), 1-8

[7] K. kiani, DAWN NEWS, May 2017.

[8] Valasai, Gordhan Das, et al. "Overcoming electricity crisis in Pakistan: A review of sustainable electricity options." *Renewable and Sustainable Energy Reviews* 72 (2017): 734-745.

[9] Asimakopoulos, D. A., et al. "Modelling the energy demand projection of the building sector in Greece in the 21st century." *Energy and Buildings* 49 (2012): 488-498.

[10] Zhang, Tao, Peer-Olaf Siebers, and Uwe Aickelin. "Modelling electricity consumption in office buildings: An agent based approach." *Energy and Buildings* 43.10 (2011): 2882-2892.

IJEW 国际工程期刊 International Journal of Engineering Works انجینئرنگ کاموں کا بین الاقوامی جرنل

International Journal of Engineering Works
ISSN-p: 2521-2419
ISSN-e: 2409-2770
Vol. 7, Issue 07, PP. 264-267, July 2020
https://www.ijew.io/
https://doi.org/10.34259/ijew.20.707264267

Ceramic Membrane Coating with Graphene Oxide for Tannery Wastewater Treatment

Ahmad Sher Khan Marwat[1], Waqar Shahbaz[2], Aizaz Ali Farman[3]
[1,3] Department of Chemical Engineering, University of Engineering and Technology Peshawar.
[2]Centre for Advanced Studies in Energy, UET Peshawar
ahmadsher0724@gmail.com[1], waqekhan@gmail.com[2], aixax26@gmail.com[3]
Received: 30 June, Revised: 07 July, Accepted: 13 July

***Abstract*—** Treatment of tannery wastewater produced from an ingeniously leather industry was carried out using a ceramic membrane coated with graphene oxide. The effluent was highly contaminated and thus posed a great threat to the terrestrial and aquatic life by polluting the environment. The current study proposed treatment of aforementioned wastewater with graphene oxide coated ceramic membrane. Graphene Oxide, synthesized by Modified Hummer's method, was coated on the inner surface of tubular ceramic membrane with a suspension of 5 mg/ml using dip-coating technique. Experiments were performed at different transmembrane pressures ranging from 0.7 bar to 3 bar while keeping the temperature and crossflow velocity constant. Rejection values for total solids, total dissolved solids, total suspended solids, salinity and conductivity were determined to evaluate the efficiency of the coated membrane.

***Keywords*—** Ultrafiltration, tannery wastewater treatment, ceramic membrane, Graphene Oxide, dip-coating.

I. INTRODUCTION

A major threat with increasing industrialization is the discharge of huge quantity of wastewater polluted with dyes. These wastewaters containing many toxic chemicals become part of streams, canals, rivers and seas, thus polluting the environment [1, 2]. Two types of industries including textile and dye manufacturing industries are contributing majorly in this regard. The wastewater coming out of these industries contain a large quantity of carcinogenic and toxic chemical additives. The reason is that these dyes are made-up of chemical such as benzidine and other aromatic compounds, which are carcinogenic in nature and may be reformed due to microbial metabolism. Among these, azo and nitro compounds has the ability to reduce in sediments and intestinal environment, resulting in reformation of toxic amines [3]. For this purpose, the treatment of such wastewater is of the primary concern to minimize the problems arising from the prescribed industries.

Among all the processes available for water treatment, membrane filtration is rated to be the most economical and efficient one. Membrane filtration is relatively a simple process and requires less energy [4-6].

Selection of membrane in this process is one of the most important steps that defines stability and viability of the process. Of all the different types of membranes, polymeric and ceramic membranes are used more commonly. Polymeric membranes have more flexibility, easier preparation process and less costly, but these membranes have some disadvantages including fouling, poor chemical and thermal resistance and short lifespans. On the other hand, inorganic ceramic membranes have higher strength, thermal stability, chemical resistance, and long lifetime. Their drawbacks include high costs, complex preparation methods and brittleness. An ideal membrane will be the one having both the desired properties of polymeric and ceramic membrane [7, 8].

The discovery of carbon nanotubes (CNTs) created the possibilities of achieving ideal membranes as they have flexibility like polymeric and stability like ceramic membrane [9]. Some theoretical studies were carried out which were in favor of using these 1-D tubes in water treatment, but the complications in preparation of CNT based membranes and their high costs diminished researcher interests in these tubes [10, 11]. Besides, the oxidized form of graphene, known as graphene oxide (GO), has attracted scientists due to its tremendous properties [12, 13]. GO is a well-emerged two dimensional material with O functional groups decorating the sp2 C basal plane. The presence of O functional group makes GO hydrophilic due to which it can be dispersed in water, contrary to graphene which is hydrophobic. The size of the GO flakes can be also tuned and varied from a few nm to mm. The tunability of both its chemical composition and flakes size makes GO an appealing material in many fields: electronics (sensors and transparent conductive films), composites materials, clean energy devices, biology, medicine and watertreatment[14]. In the present work, tubular ceramic membrane has been coated with a suspension of 5 mg/ml using dip-coating technique for wastewater treatment.

II. MATERIALS AND METHODS

A. Microfiltration Ceramic Membrane

The membrane used in this work was imported from Toho Ceramic Technology Co., Ltd, China. Table 1 shows characteristics of membrane used for coating purpose.

TABLE 1: CHARACTERISTICS OF CERAMIC MEMBRANE USED FOR GO COATING

Parameter	Value
Length	250 mm
Outer Diameter	10 mm
Internal Diameter	06 mm
Thickness of membrane	04 mm
Surface Area (internal)	47.7 cm2
Surface Area (external)	80.1 cm2
Pore size	50 nm
Membrane Type	TOHO01*10
Membrane Material	Alumina Ceramic

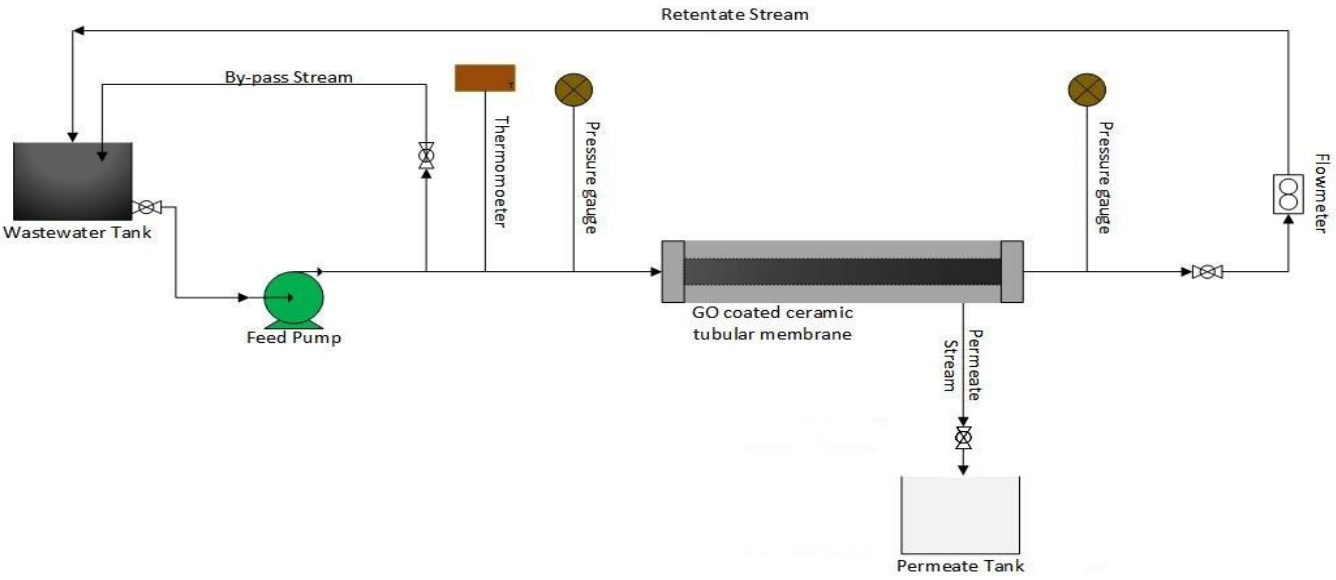

Figure 1: Cross-flow Tubular Membrane Filtration Unit

B. Ceramic Membrane Coating with Graphene Oxide

Graphene oxide was synthesized by Modified Hummer's method [15]. Following that, 5 mg/ml suspension of GO was prepared by mixing 0.5 g of GO powder in deionized water to make 100 ml of suspension. The suspension was then subjected to sonication for 30 minutes to make a homogenous and stable dispersion of GO nanosheets [16]. Following that, a thin layer of GO was coated over the surface of ceramic membrane using dip coating technique. For this purpose, the ceramic membrane was soaked in water for 2 hours to saturate the pores with water. Then the membrane coating was done in such a way that outer side of the membrane was covered with aluminum foil while GO dispersion was poured inside the tube. The GO dispersion was let for 10 minutes inside the membrane to form a uniform layer on ceramic membrane. The membrane was then subjected to heating at 100°C in furnace for strengthening of the covalent bonds between GO and the ceramic membrane [17].

C. Cross-Flow Membrane Filtration Unit

The experiments were performed on a lab scale cross-flow membrane unit, the diagram of which is shown in figure 1. A diaphragm pump with a capacity of 1.8 L/min was used to circulate the effluent though the unit. A thermometer, flowmeter and two pressure guages were installed to measure the temperature, flowrate and pressures respectively. The crossflow velocities and transmembrane pressure were adjusted through the flow control valves installed on the main stream and by-pass stream. A stainless steel tubular membrane pressure vessel was present for holding the membrane.

All the experiments were carried out under total recycle mode with both the retentate and permeate returning to the feed tank. Permeate samples were collected after every 5 minutes for one hour. The flux and rejection was calculated using the equations (i) and (ii) respectively:

$$J = \frac{Q}{A \times t} \quad \text{(i)}$$

$$R\% = \frac{C_f - C_p}{C_f} \times 100\% \quad \text{(ii)}$$

Where,
$\boldsymbol{J}$ is the permeate flux,
$\boldsymbol{Q}$ is the permeate flowrate,
$\boldsymbol{t}$ is the time taken by each experiment,
$\boldsymbol{A}$ is the effective membrane area,
$\boldsymbol{R\%}$ is the rejection percentage,
$\boldsymbol{C_f}$ and $\boldsymbol{C_p}$ is the concentration of feed and permeate respectively [**Error! Reference source not found.**

III. RESULTS AND DISCUSSIONS

A. Membrane Permeability Test

Membrane permeability tests were performed at constant temperature of 25°C, constant feed flux of 1 L/min and different transmembrane pressures ranging from 0.2 to 3 bar. From Figure 2, it can be seen that water flux approximately takes 30 minutes to get stabilized.

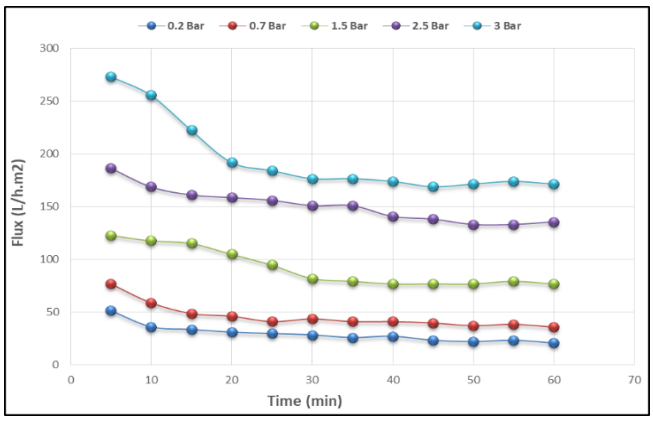

Figure 2: Deionized water flux vs operating time

It can also be observed that the water flux through the membrane is heavily depended upon the applied pressure and shows a linear relation with the transmembrane pressure. As shown in Figure 3, the value of membrane permeability using deionized water was noted to be 63.029 L/hr.m^2.bar.

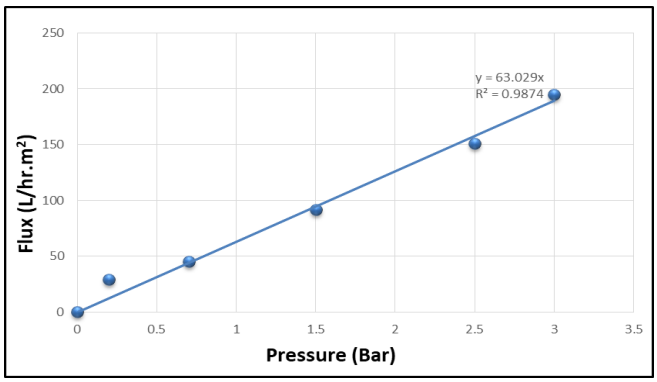

Figure 3: Deionized water flux variation with pressure

B. Effluent Properties

A sample of wastewater was collected from a locally situated dyes industry in Lahore. The characteristics of the collected effluent is given in table 2.

TABLE 2: EFFLUENT PROPERTIES

Effluent Property	Amount
Chemical Name	Acid Black 234
Chemical Formula	$C_{34}H_{26}N_{10}Na_2O_9S_3$
Molecular Weight	860.81
Total Dissolved Solids (TDS)	47.0 g/L
Total Suspneded Solids (TSS)	30 g/L
Total Solids (TS)	77 g/L
pH	8.8
Color	Brownish black
Conductivity	72 mS
Salinity	62.6 ppt

C. Effluent Permeate Flux

Experiments were performed using the GO coated ceramic membrane for dyes industries wastewater at room temperature i.e. 25°C, constant feed flowrate of 1 L/min and different transmembrane pressures i.e. 0.7, 1.5, 2.5 and 3 bar. Each experiment was performed for 65 minutes which were enough to reach the steady state. Permeate flux was monitored continuously and collected to find out its characteristics.

From Figure 4, it can be observed that the flux was high initially but then showed a sudden decline. This decline in flux can be associated to concentration polarization, which is the build-up of the solute particles near the membrane surface resisting the passage of solvent through the membrane.

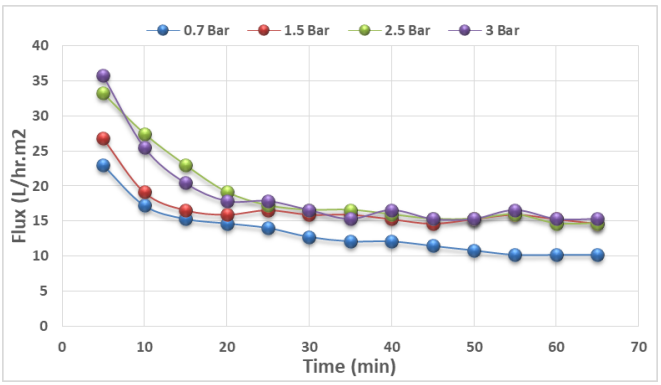

Figure 4: Effluent permeate flux vs operating time

Figure 5 shows that the flux increases exponentially by increasing transmembrane pressure till 2.5 bar, where it reaches its limiting value known as the limiting flux. Behind this pressure, the flux slightly decreased as a consequence of membrane compaction. The phenomena of membrane compaction does not usually occur in ceramic membrane, but the presence of GO layers made it applicable here. GO layers has the trait of getting compact at higher pressures and this was the main reason of flux decline over 2.5 bar [20].

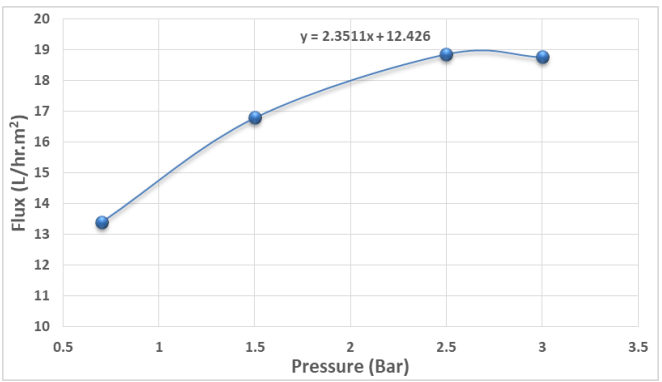

Figure 5: Variation of permeate flux with pressure

The average permeate flux of the membrane for dyes industries wastewater is noted to be 2.35 L/hr.m^2, which is very low in comparison with the one obtained for deionized water, hence confirms the polluting properties of the wastewater.

TABLE 3: MEMBRANE REJECTION PERFORMANCE AS AN EFFECT OF TRANSMEMBRANE PRESSURE

Effluent characteristics	**0.7 bar**	**1.5 bar**	**2.5 bar**	**3.0 bar**
Flux (L/hr.m^2)	13.40	16.79	18.85	18.76
TDS Rejection % (g/L)	82.69	80.34	79.62	80.05
TSS Rejection % (g/L)	92.78	91.07	89.16	92.24
TS Rejection % (g/L)	85.95	83.80	82.70	83.98
Conductivity Rejection % (mS)	83.90	81.55	80.83	81.26
Salinity Rejection % (ppt)	85.70	83.35	82.63	83.06

Table 3 shows the relationship between membrane rejection performance and transmembrane pressure. The percentage removal of different feed characteristics i.e. TDS, TSS, TS, conductivity and salinity are shown as an effect of the transmembrane pressure. For instance, TDS rejection has been maximum at 0.7 bar and shows a decreasing trend till membrane compaction at 2.5 bar. Membrane compaction narrows down the path for the particles due to which rejection increases and this has been observed in this case too. A reasonable rejection values are obtained for all parameters.

CONCLUSIONS

GO was synthesized through Modified Hummer's method. It was then coated on the inside of a ceramic membrane to enhance its separation ability. Water permeation tests under different transmembrane pressures were performed to find the permeability of the modified membrane. Finally, effluent permeate tests were carried out to find out the permeate flux and rejection. A limiting flux of 18.85 L/hr.m^2 was obtained at 2.5 bar. The membrane provided satisfactory results for the treatment of the effluent taken from dyes industry. These results can further be improved by optimizing GO layer thickness over ceramic membrane.

REFERENCES

[1] U. Pagga and D. Brown, "The degradation of dyestuffs: Part II Behaviour of dyestuffs in aerobic biodegradation tests," Chemosphere, pp. 479-491, 1986.

[2] M. F. Abid, M. A. Zablouk and A. M. Abid-Alameer, "Experimental study of dye removal from industrial wastewater by membrane technologies of reverse osmosis and nanofiltration," Iranian Journal of Environmental Health Science & Engineering, pp. 9-17, 2012.

[3] E. Clarke and R. Anliker, Organic Dyes and Pigments, Berlin; Heidelberg: Springer Verlag, 1980.

[4] K. O. Agenson, J.I. Oh and T. Urase, "Retention of a wide variety of organic pollutants by different nanofiltration/reverse osmosis membranes: controlling parameters of process," Journal of Membrane Science, pp. 91-103, 2003.

[5] J. Schaep, B. Van der Bruggen, C. Vandec and D. Wilms, "Influence of ion size and charge in nanofiltration," Separation and Purification Technology, pp. 155-162, 1998.

[6] K. Kimura, G. Amy, J. E. Drewes, T. Heberer, T. U. Kim and Y. Watanabe, "Rejection of organic micropollutants (disinfection by-products, endocrine disrupting compounds, and pharmaceutically active compounds) by NF/RO membranes," Journal of membrane science, pp. 113-121, 2003.

[7] L. Cot, A. Ayral , J. Durand , C. Guizard , N. Hovnanian , A. Julbe and A. Larbot , "Inorganic Membrane and Solid State Sciences," Solid State Sciences, pp. 313-334, 2000.

[8] S. Benfer, P. Arki and G. Tomandl, "Ceramic Membranes for Filtration Applications — Preparation and Characterization," Advanced Engineering Materials, pp. 495-500, 2004.

[9] L. F. Dumée, K. Sears, J. Schütz, N. Finn, C. Huynh, S. Hawkins , M. Duke and S. Gray, "Characterization and evaluation of carbon nanotube Bucky-Paper membranes for direct contact membrane distillation," Journal of Membrane Science, pp. 36-43, 2010.

[10] M. Yu, H. H. Funke, J. L. Falconer and R. D. Noble, "High density, vertically-aligned carbon nanotube membranes," Nano Letters, pp. 225-229, 2009.

[11] S. Kim, J. R. Jinschek, H. Chen, D. S. Sholl and E. Marand, "Scalable fabrication of carbon nanotube/polymer nanocomposite membranes for high flux gas transport," Nano Letters, pp. 2806-2811, 2007.

[12] A. K. Geim and K. S. Novoselov, "The rise of graphene," Nat Mater, pp. 183-191, 2007.

[13] D. R. Dreyer, S. Park, C. W. Bielawski and R. S. Ruof, "The chemistry of graphene oxide," The Royal Society of Chemistry, p. 228–240, 2010.

[14] F. Perrozzi, S. Prezioso and L. Ottaviano, "Graphene oxide: from fundamentals to applications," Journal of Physics Condensed Matter, 2014.

[15] K. Narasimharao, G. Venkata Ramana, D. Sreedhar and V. Vasudevarao, "Synthesis of Graphene Oxide by Modified Hummers Method and Hydrothermal Synthesis of Graphene-NiO Nano Composite for Supercapacitor Application," Journal of Material Sciences & Engineering, 2016.

[16] Kang Huang, Gongping Liu, Yueyun Lou, Ziye Dong, Jie Shen and Wanqin Jin, "A Graphene Oxide Membrane with Highly Selective Molecular Separation of Aqueous Organic Solution," Angewandte Chemie International Edition, p. 6929 –6932, 2014.

[17] S. Nataraj, S. Roy, M. B. Patil, M. N. Nadagouda, W. E. Rudzinski and T. M. Aminabhavi, "Cellulose acetate-coated α-alumina ceramic composite tubular membranes for wastewater treatment," Desalination, pp. 348-353, 2011.

[18] Xuebing Hu, Yun Yu, Jianer Zhou, Yongqing Wang, Jian Liang, Xiaozhen Zhang, Qibing Chang and Lixin Song, "The improved oil/water separation performance of graphene oxide modified Al2O3 microfiltration membrane," Journal of Membrane Science, pp. 200-204, 2015.

[19] Y. Lou, G. Liu, S. Liu and J. Shen, "A facile way to prepare ceramic-supported graphene oxide composite membrane via silane-graft modification," Applied Surface Science, pp. 631-637, 2014.

[20] Jeng Yi Chong, Bo Wang, Cecilia Mattevi and Kang Li, "Dynamic microstructure of graphene oxide membranes and the permeation flux," Journal of Membrane Science, vol. 549, pp. 385-392, 2018

International Journal of Engineering Works
ISSN-p: 2521-2419
ISSN-e: 2409-2770
Vol. 7, Issue 08, PP. 268-273, August 2020
https://www.ijew.io/
https://doi.org/10.34259/ijew.20.708268273

Comparasion of Different Configuration of Hybrid Electrical Power System – A Case Study of a Site in Peshawar

Raheemullah khan[1], Jehan Parvez[2], Abdur Rehman[3], Muhammad Ibrahim[4]
[1,2,3,4] US Pakistan Center for Advance Study in Energy, University of Engineering and Technology Peshawar
raheem38k@gmail.com[1], jehanparvezcecos@gmail.com[2], engrrahman756@gmail.com[3], ibrahim_492@yahoo.com[4]
Received: 13 July, Revised: 20 July, Accepted: 27 July

***Abstract*--** Instructions are this paper is the cost analysis of different sources of electricity for an educational institute in Peshawar. The technical and cost analysis of different system is done for the case study so that a system could be recommended for the site which can fulfill the demand requirement by least net present cost. By using HOMER software load profile is created and cost analysis is done for a project life time of 15 years. Five different configurations is studied in this paper for techno economic analysis of the system. These configurations are made by selected different combination of solar, generator, battery storage and diesel generator. HOMER software simulate these configuration find out a system which have least net present cost.

By analysis of result obtain from different configuration a hybrid system consists of solar photo voltaic cells of 77 Kw, diesel generator of 50kva, a battery storage of 8 strings of 4 batteries can fulfill our need a least net present which is the recommended system to be install for our system. The system will have a net present cost of 24.6 million, level zed cost of energy is 29.04Rs.

***Keywords*—** electricity, educational institute, loads shedding, HOMER software, net present cost, level zed cost of energy.

I. Introduction

This template Economic devolvement of a country is mainly concern with production and use of electricity. In this modern society living without electricity is very difficult. In flied of life we see electricity is used I-e in daily life we use electricity for lighting for running fans, ironing our cloths, washing cloths using refrigerator or running a television or a computer. On commercial side it is used in decoration and lighting of building and running different electrical machine. While on industrial side it is used in manufacture of various materials used in our daily life. So electricity is backbone of industrial area.

In developing countries like Pakistan there is a lot of energy crisis which have created many problems for the people of Pakistan [1]. Load shielding become the common phenomena in Pakistan. People uses their own solution for load shielding some people uses generator other use solar system [2]. But they don't know what the best solution is for them.

In this research we study hybrid of solar, grid, battery storage and diesel generator. We will find the optimum way to utilize these resources in order to satisfy the diversified load of a commercial building on both optimization of generation sources and also strategy of changing load according to the cost of the source in order to gain maximum economic benefits[3][4].

Literature review shows a lot of been done in this area including current load shielding situation in Pakistan. Potential of renewable energy in Pakistan. A lot similar work in which the feasibility of hybrid system is studded. The techno economic evaluation is also studded by different author by using the HOMER as tool different configuration is consider and their comparison is carried out by their net present cost and cost of energy[5].

Another good research has been carried out by Saleh at all, for Malaysia for PV diesel and unreliable grid. The methodology[7] he used in work nearly similarly to my work. During his work four scenario were investigated and simulation has been carried out through HOMER software and found that there is 13% reduction in net present cost, 10% cost of energy and 50% reduction in carbon dioxide.

In Dhaka city a design implementation and experimental analysis is similar work related to my study[8]. A PV diesel based hybrid is taken as the configuration and the result show that by optimization techniques in HOMER software PV diesel system can reduce the because of dependence of fuel is reduced. The cost of energy of this system is .36 USD/KWH and net present cost is 164106 USD. The installation of PV will save 18440 USD annually. The 30 year revenue will be 553200 USD[8]

Another research is carried out by Deepak Kumar Lal for optimization of PV/wind micro hydro/diesel generator system by using HOMER for a rural area in Sundergah district Orissa state of India various alternative is used to see the see the result. He carried out different simulation in HOMER by changing different load condition on hourly bases and found that a hybrid renewable energy can replace the conventional grid and thus the

transmission and distribution losses can be reduce by using this method[9][10].

J. B. Fulzeli has done his research on optimization of PV wind hybrid system with some battery back. In his research he has done the best way to select to component and used it the site. HOMER has done various optimization process and finally select the best way to optimize these resources so the least net present cost could be obtain. During his research he conclude the contribution of each components in portion of PV is 16.5% battery has 3.8% and generator has largest portion which 76.8% of the total cost [11].

II. ROSPOSED LOCATION

The case study is a college (NIMS) which is under construction. There are three floors in the college and we are going to design a hybrid economical system which can fulfil the demand. According to the owner in 2019 and 2020 we need only ground floor and library on first floor and rest will be needed in future so we have to design a hybrid system which has a demand of ground floor and library.

III. METHODOLOGY

This section describes the procedure implemented throughout this study. An investigation was done to assess the load of selected site. Different possible sources of electricity were observed and HOMER Pro software is used to do the techno-economic comparison of different models for the system. The different steps taken for this research is given bellow.

A. Sessional condition of load

In this section we will start a pre design preparation by making load profile. For this perfuse we visit the site and gain the information of connected load also interview the owner of the site and make a table of the connected load which is given. The case study is a college which is under construction. The load of the site seasonally according to the table shown.

TABLE 1 SEASONAL LOAD CONDITION OF SITE

Months	Dec, Jan, Feb	March, April, May	Jun, July, Aug	Sep, Oct, Nov
Air conditions	Off	Off	On	Off
Fans	Off	On	On	On
Water cooler	Off	On	On	On
Other loads	On	On	On	On
Total connected Load	14.65 KW	20.55KW	30.35 KW	19.55KW

B. Modelling of system

For modelling the system, we use simulation software called hybrid optimization model for multiple energy resource HOMER. Homer software do simulation, optimization and sensitivity analysis of different configuration. It will determine the technical feasible and more economical system among the given configuration the daily load data is obtain through as shown in fig.

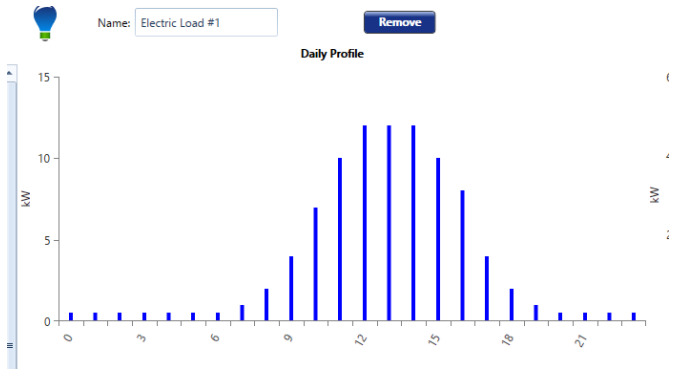

Figure 1 daily load profile

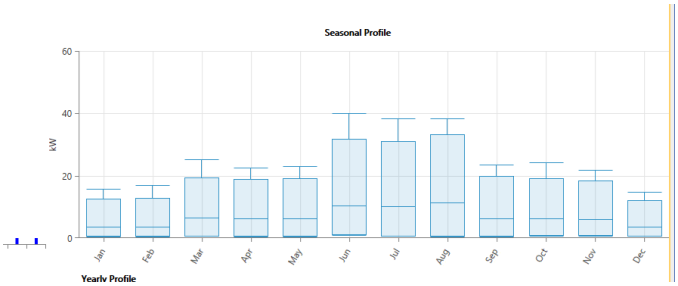

Figure 2 monthly load profile

IV. SIMULATION AND RESULTS

For simulation we take different possible configuration and compare them on technical economical basses and find the best possible configuration for them.

- Reliable grid connected system
- Grid and photo voltaic system
- reliable Grid, PV, storage system
- un reliable Grid, PV, storage system
- unreliable grid, PV, storage and generator system

A. Relaible grid connected system

In this system we will study that how much bill is to paid when the load we created is connected to the system and taking the ideal situation that no load shielding is consider.

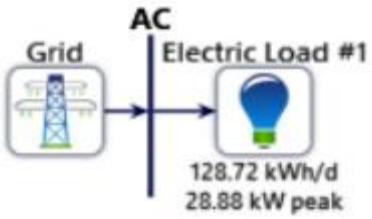

Figure 3 reliable grid connected system

The net present cost of this system is 14.6M which is taken as reference for comparison of other configuration

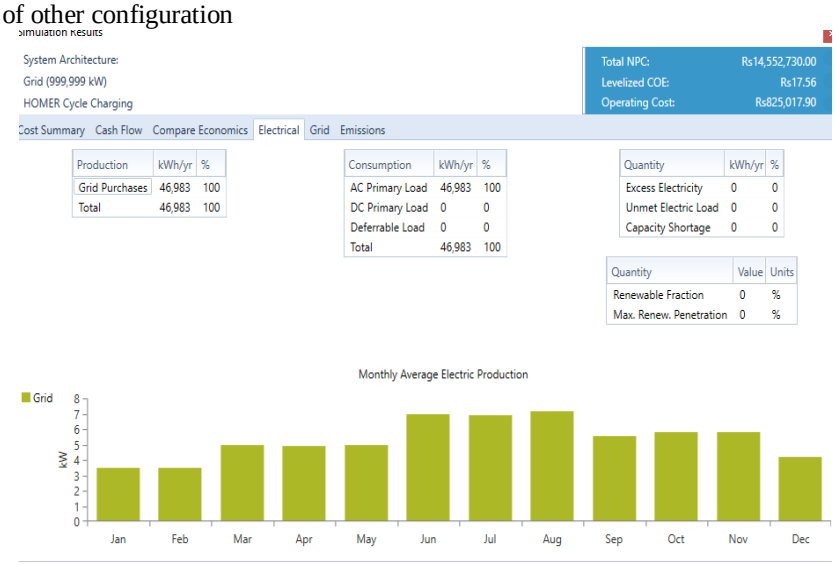

Figure 4 result of reliable grid connected system

B. Reliable grid connected pv system

This system is also an ideal model so that no load shielding is consider. But the study of this system is to investigate the system that how a how a solar system can reduce the level cost of energy and net present cost.

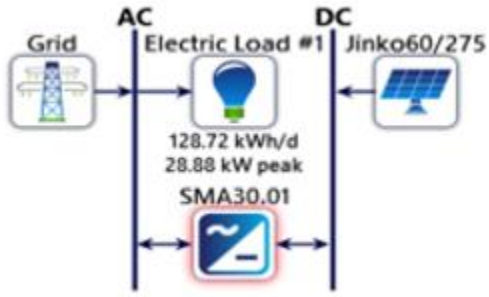

Figure 5 reliable grid with PV system

The net present cost of this system is reduce 9.1M, decrease the cost of the system up to 37 percent.

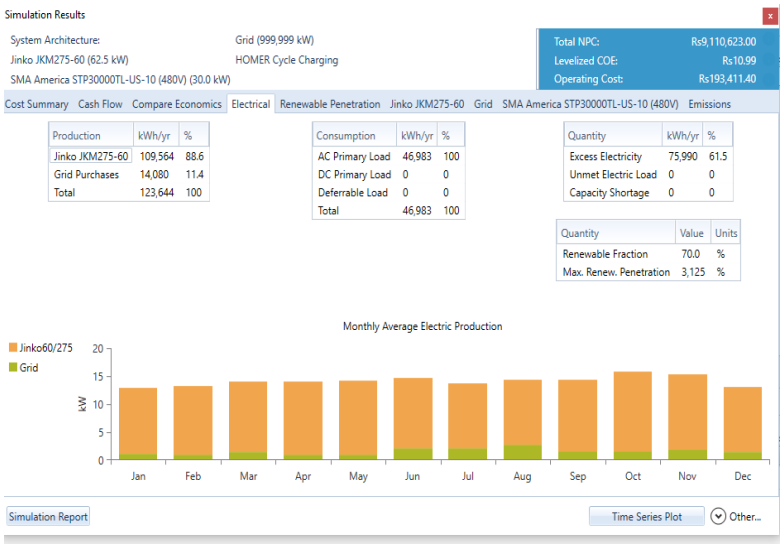

Figure 6 reliable grid with PV

C. Reliable grid, PV, and storage system

in this system the effect of adding a storage battery is study that how it effect the net present cost and cost of energy provided that there is no load shielding is consider the battery will store energy from solar during peak sun hours and use it during off sun hours

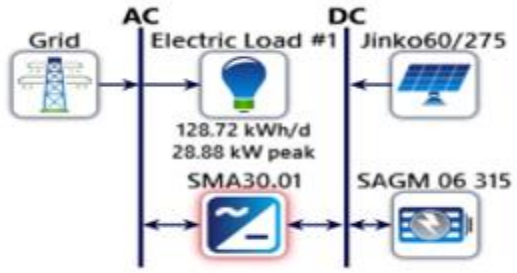

Figure 7 reliable grid, PV and storage

In this system we have a storage system to see its effects on technical and economic evaluation. As there was a lot of excess energy which we lose but by connecting a storage source we can decrease the excess energy to 64,386 kwh/year. The net energy production by solar panels is 98,961 Kwh per year.

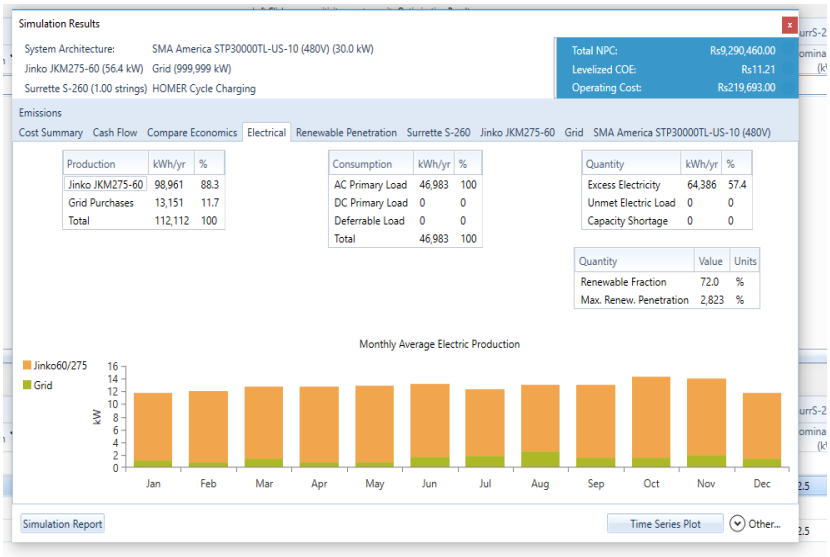

Figure 8 result of reliable grid, PV and storage

The economic analysis of the system obtain from the result of simulation is the LCOE is 11.2Rs while NPC of the system is 9.29 million as shown in fig 23 and table 8. For economic evaluation the net present cost of the system is increased to 9.29 million from 9.15million.

D. UN reliable grid, PV, storage system

Gradually we are coming to our real time situation in which the grid is unreliable. There is none schedule load shielding in our study site. So we simulate the system according to our observation and prediction of hours in which grid is present and hours in which grid is absent we will compare the study to precious system that cost is effected when the grid become un reliable.

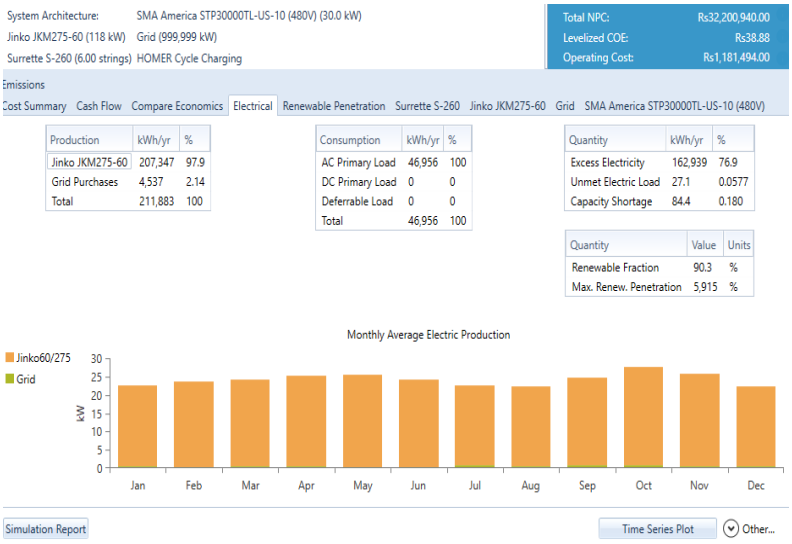

Figure 9 result of unreliable grid PV and storage

The net present cost of the system is 32.2M which 112percent of net present of reliable grid connected system, which is because we make our unreliable system reliable by compromising on economy.

E. Unreliable grid, PV, storage and generator system

The 5th system that is unreliable grid, photo voltaic cells, battery storage and a generator. This system is the most used situation in Pakistan which is our real scenario. The simulation result of the system.

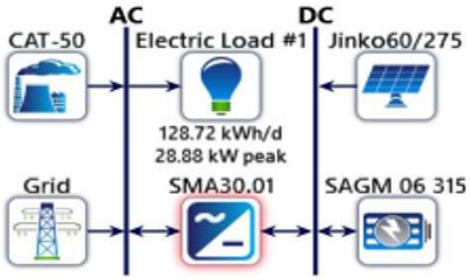

Figure 10 unreliable grid, PV, storage and generator

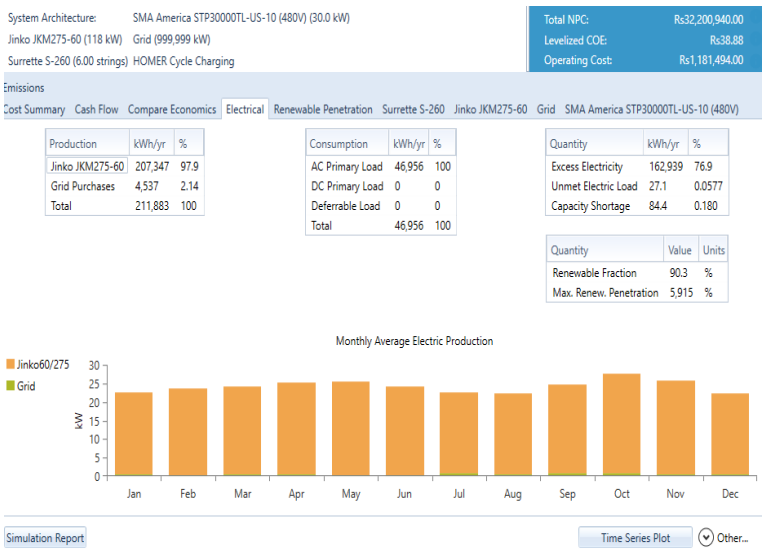

Figure 11 result of unreliable grid, PV, storage and generator

The net present cost of this system is 24.1M. Which is 65 percent of the net present cost of reliable grid connected system.

CONCUSLION

The final conclusion of work is that we simulate different configuration for the system so that an optimize configuration could be obtain. The result of different system by HOMER software. By comparison of different system on the basis of net present cost, level zed cost of energy, excess amount of energy, unmet capacity of energy is calculated and a decision is taken and found out that a grid connected PV, battery storage with diesel generator is the more suitable option for the case study. The optimize values of these component are PV of 77kW, battery storage of 24 and a diesel generator 50 kVA which give us net present cost of 24.6M at LCOE of 29.04Rs per kWh which is recommended system to be install on case study.

ACKNOWLEDGMENT

We would like to acknowledge Assistant Professor Dr. Arif Khattak for his valuable knowledge and experience which helped us in achieving this milestone. We are thankful to our fellow students, faculty and all the staff members of United States Pakistan Center for Advanced Studies in Energy at UET Peshawar for their support in this work. We are also thankful to USAID for providing us financial support in our MS studies.

REFERENCES

[1] M. J. O. C. Asif, "Energy crisis in Pakistan: Origins, challenges, and sustainable solutions," 2012.
[2] M. A. Javaid, S. Hussain, A. Maqsood, Z. Arshad, A. Arshad, and M. J. I. J. B. A. S. Idrees, "Electrical energy crisis in Pakistan and their possible solutions," vol. 11, pp. 38-52, 2011.
[3] U. K. Mirza, M. M. Maroto-Valer, N. J. R. Ahmad, and S. E. Reviews, "Status and outlook of solar energy use in Pakistan," vol. 7, no. 6, pp. 501-514, 2003.
[4] H. B. Khalil, S. J. H. J. R. Zaidi, and S. E. Reviews, "Energy crisis and potential of solar energy in Pakistan," vol. 31, pp. 194-201, 2014.
[5] M. A. J. R. Sheikh and S. E. Reviews, "Energy and renewable energy scenario of Pakistan," vol. 14, no. 1, pp. 354-363, 2010.
[6] S. Alayan, "Design of a PV-Diesel Hybrid System with Unreliable Grid Connection in Lebanon," ed, 2016.
[7] S. A. Almajdup, M. Z. Akop, M. A. Salim, M. R. Mansor, and M. A. M. J. P. o. M. E. R. D. Rosli, "Design of photovoltaic (PV)-diesel hybrid system with unreliable grid connection in Kampung LB Johnson, Malaysia by HOMER," vol. 2018, pp. 106-107, 2018.
[8] M. T. Riasat, M. A. Ahmed, S. Tasin, M. A. Nabil, and S. Andalib, "Designand performance analysis for hybrid PV-Diesel-Battery power system for residential area in Dhaka city," in 2013 IEEE 39th Photovoltaic Specialists Conference (PVSC), 2013, pp. 1515-1520: IEEE.
[9] N. M. Isa, C. W. Tan, and A. Yatim, "A techno-economic assessment of grid connected photovoltaic system for hospital building in Malaysia," in IOP Conference Series: Materials Science and Engineering, 2017, vol. 217, no. 1, p. 012016: IOP Publishing.
[10] D. K. Lal, B. B. Dash, A. J. I. J. o. E. E. Akella, and Informatics, "Optimization of PV/wind/micro-hydro/diesel hybrid power system in HOMER for the study area," vol. 3, no. 3, p. 307, 2011.
[11] J. Fulzele, S. J. I. J. o. E. Dutt, and C. Engineering, "Optimium planning of hybrid renewable energy system using HOMER," vol. 2, no. 1, p. 68, 2012.

Raheemullah khan has received BSc Electrical Engineering (Power) degree from department of Electrical Engineering University of Engineering and Technology Peshawar, Pakistan in 2016. He is currently pursuing MSc degree in Electrical Energy Systems Engineering from United States Pakistan Center for Advanced Studies in Energy (USPCAS-E) at University of Engineering and Technology Peshawar.

Abdur Rehman has received BSc Electrical Engineering (Power) degree from department of Electrical Engineering University of Engineering and Technology Peshawar, Pakistan in 2016. He is currently pursuing MSc degree in Electrical Energy Systems Engineering from United States Pakistan Center for Advanced Studies in Energy (USPCAS-E) at University of Engineering and Technology Peshawar.

IJEW 国际工程期刊 International Journal of Engineering Works انجینئرنگ کاموں کا بین الاقوامی جرنل

International Journal of Engineering Works
ISSN-p: 2521-2419
ISSN-e: 2409-2770
Vol. 7, Issue 08, PP. 274-281, August 2020
https://www.ijew.io/
https://doi.org/10.34259/ijew.20.708274281

Reliability Improvement of Micro-Inverter through AC-Ripples Voltage Compensator

Siraj ud Din
Department of Electrical Energy System Engineering, US-Pakistan Center for Advanced Studies in Energy, University of Engineering and Technology Peshawar, Pakistan
siraj8575025@gmail.com
Received: 22 July, Revised: 27 July, Accepted: 10 August

***Abstract*—** In this paper the resiliency improvement of micro inverter is considered. Its life degrades mainly due to failure of DC link capacitor. The inherent 100 Hz ripples from inverter stage causes excess heat in capacitor. Consequently, the electrolyte dries out quickly and its lifespan decreases. The objective of this paper is to mitigate such AC harmonics on DC link capacitor. A compensator or active power decoupling circuit, APD, is designed in PSIM. The APD circuit is a combination of film capacitor, H-bridge and control circuit. Second frequency AC ripples are converted into DC by actively controlling the capacitor. In this manner AC harmonics are mitigated at the DC link capacitor. Firstly, a benchmark micro inverter is designed and simulated without using APD circuit. Secondly, active power decoupling is used by designing APD circuit. The simulation results show that there is a decrease in AC ripples from 9.4% to 3.2% by using series voltage compensator as compared to passive power decoupling i.e. only a bulk capacitor. The capacitor life is increased up to 19 years and hence of micro-inverter. The total harmonics distortion (THD) analysis shows that by using active power decoupling, system injects 2.7% THD as compared to passive decoupling which is 1.69%. which is still in bellow the IEEE standard of allowable 5% THD.

***Keywords*—** Micro inverter, Reliability, Active Power Decoupling APD, PV system, AC Ripples.

I. INTRODUCTION

With the decrease in fossil fuel reserves and environmental impacts, world has got a trend to use green energy resources. These energy resources include solar energy, wind energy, micro hydro energy and fuel cell energy etc. The power plants for these green energy resources sometime produce DC power especially the solar panel which needs to be converted into AC power for connecting to grid and AC loads. Conversion to AC is required because the infrastructure already exists is AC. For this conversion we need an interface between DC power of the solar panel and the grid or AC loads. This interface is called inverter. A typical inverter is an electronic device which converts unidirectional or direct current (DC) into alternating current or AC current. On the basis of power rating and installation, inverters have two types. One is called central inverter and second one is called micro inverter. Central inverter is connected to series string of solar panels with high voltage and power ratings of 400V-600V and above 1000W respectively [2]. On another hand micro inverter is a type of inverter with power rating of about 300W and voltage rating of 220V RMS for Asia and Europe and 120V for America and Canada. Micro inverters are connected at the back of each solar panel and feed the load or grid in parallel manner [2]. [3] Shows that micro inverter produces 3.7%, 7.8% and 12.3% more energy in case of light, moderate and heavy shading respectively, as compared to string inverter.

Most of the manufacturers of solar panels offer guarantee of 20 to 25 years of life on their solar panels. As for every panel there is a single micro inverter, and comes in embedded form in some cases, so it has to have a life span of 25 years. But in practice its life span is about 5 to 10 years and needs to be replaced which increases the cost of the system. There are many reasons for life degradation of micro inverter. One reason is the frequent failure of the DC link electrolytic Capacitor which contributes 30% to overall failures in the system [4]. The electrolyte of the capacitor wears due to temperature which is caused by the AC and DC current ripples. DC ripples comes from PV panel side due to variation in irradiance. AC ripples reflects from inverter having frequency of 100Hz. Both of these ripples increases the temperature of the capacitor and degrades its life. The aim of this thesis is to minimize the AC ripples by bypassing them through a compensator.

The main objective of this thesis is to design a voltage compensator for double line frequency AC ripples in PSIM software using active power decoupling APD techniques. First off a complete micro inverter is designed in PSIM using passive decoupling (only DC link capacitor) technique and amount of ripples on DC link capacitor are observed through wave form. Then using the noted value of ripples, life of capacitor is calculated. Secondly, active power decoupling circuit is designed in PSIM and is connected in series between converter and inverter stage and is examined to find how much ripples are

reduced on DC link capacitor. Based on these values (passive decoupling and active power decoupling), a graphical analysis is carried out which represents improvement in life of micro inverter.This paper is structured as Section II provides an overview about the background of the research, Section III presents a methodology and system description, Section IV describes the simulation results and deiscussion, whereas, the last section i.e. Section V portrays the conclusion of this research article.

II. BACKGROUND

Decoupling is actually the process of eliminating DC or AC ripples present in DC/AC or AC/DC power converters. In both of these converters both AC and DC ripples exists. In case of micro inverters, DC ripples comes from boost converter stage and AC ripples comes from inverter stage. As inverter is a bidirectional circuit it acts as a rectifier for DC link stage and inverter for grid or AC load side. That is why 2nd frequency AC (100Hz in this case) ripples comes from inverter to DC link capacitor as shown in figure 1.

$$P(t) = 0.5VI + 0.5COS(2\omega t) \quad (1)$$

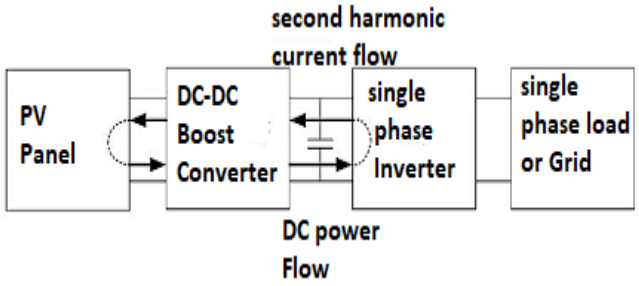

Figure 1. Second harmonics flow in micro-inverter

A. *Passive Decoupling*

The simplest solution to AC ripples is to use an electrolytic capacitor at DC link stage as shown in figure 1. Advantage of this type of decoupling is simplicity and cost. But the disadvantage of this decoupling technique is that it requires a large size capacitor to ensure complete elimination of AC ripples and this big size leads to thermal losses and life degradation of capacitor and hence of micro inverter [6]. [7] talks about the placement of capacitor and suggest three positions as PV side decoupling, DC side decoupling and AC side decoupling. They conclude that PV side position requires large size of capacitor as compared to DC side. On another hand if we do decoupling at AC side there will be required an additional capacitor on DC side. So if we do decoupling at DC link side, it will cover both AC and DC ripples and thecomplexity and cost reduces. The required size of the capacitor can be calculated by equation (2). where Po is inverter output power, Fline is the system frequency (50Hz), Vdc is inverter Input voltage and ΔV is ripple voltage [7]. David William et al in [7] mentions another passive decoupling technique which has another passive element of coupled inductor with the capacitor. In this method the series combination of capacitor and inductor is connected in parallel with another inductor. This method has the ability that it completely directs the ripples to the capacitor with little impact on DC side. However, this method requires precise calculation of inductance values and require magnetic circuit understanding. Equation (1) is the governing equation for second frequency harmonics reflected from AC side of inverter. Where the first term shows the DC power from converter stage and second term shows double frequency harmonics which comes from AC side of the inverter. This entire research is based on the mitigation of AC ripples on DC link capacitor.

$$C = \frac{Po}{2\pi flineVdc\Delta V} \quad (2)$$

B. *Active Power Decoupling*

In active power decoupling technique, an active element or switch such as MOSFET switch or an IGBT switch is used along with passive element as capacitor or inductor. In active power decoupling the AC ripple energy is temporarily stored in actively controlled capacitor for short time and then released to the load in next cycle. In this type of decoupling the bulk DC link capacitor is split into two small capacitors. One is placed at DC link side and accommodates DC ripples from boost converter output. The other part is controlled through switches and takes responsibility of only AC ripples. This splitting is done because as the size of capacitor increases its ESR equivalent series resistance increases, consequently thermal losses increases and its life degrades quickly [7]. So we connect a relatively small size film capacitor at DC link and other film capacitor is controlled through switches. This technique leads to different types of switching circuit, switching signal generation and topologies. According to [8] the switching circuit has two types, independent and dependent. In independent topology, the capacitor is controlled by a separate full H-bridge or half bridge circuit connected in series or parallel to DC port. For dependent technique, the inverter bridge is time multiplexed or shared with circuit of AC rippled compensator.

1). H-bridge topology

In this topology the capacitor (and inductor for smoothing out current) is controlled through H-bridge circuit as shown in figure 2, in which plus and minus terminals are connected across A and B or in series between A and P. switch S1~S4 are controlled by a reference signal which is extracted from the DC link voltage. When DC link voltage is positive, the capacitor is Directed to store energy and give it back to load when voltage is negative. The advantage of this technique is that it effectively controls the energy flow with less amount of harmonics. But the limitation of this topology is that the voltage of APD port must be less than the DC port voltage [7].

2) . Buck, Boost and Buck-boost based APD

The drawback of full bridge APD circuit is that it requires more components. [9] [10] and [11] propose other models based on converters, buck, boost and buck-boost. The voltage across capacitor in these circuits is unipolar. Figure 3 shows the buck converter based APD, connected across DC link capacitor, in which the ripples are compensated by capacitor through switches. The drawback of this method is that the capacitor

voltage is less than DC bus voltage, this may sometimes lead to the discontinuity of current which will contribute harmonics to the system. Other solution to AC ripples mitigation is boost converter based APD which do the same job as buck based APD, but here it gives the advantage of making the requirement of capacitor size lesser than any other topology because the voltage at capacitor is greater than DC bus voltage. The disadvantage of this method is it produces higher voltage stress on capacitor and causes safety hazards. Another solution is based on buck-boost converter topology as shown in figure 5, this APD technique allows for more reduction in capacitance requirement as compared to buck or boost converter topology because high voltage fluctuates about DC bus voltage [7]. The main limitation of this technique is discontinuity in current which injects high order harmonics in the system and degrade the efficiency.

3). Split capacitor based APD

The split capacitor APD is proposed in [12] where DC port capacitor is split into two parts. One acts as main DC filter and other part is actively controlled through switches S1 and S2 which compensate for AC ripples from inverter stage as shown in figure 6. The advantage of this method is that there is no need of extra capacitor for DC bus. This give the simplicity and makes it cost effective. Difficulty with this technique is that it requires that the values of Cr1 and Cr2 should be precisely identical. If these values are not equal, then the control system parameters will get complicated. And algorithm for controlling parameters will not easy to handle.

C. Our Proposed Design

An AC series compensator is an active filter which is connected in between DC bus and inverter which filters AC harmonics coming from inverter side to stop it from going into DC link capacitor. These ripples, if goes into DC electrolytic capacitor, degrade its life by thermally deteriorates its electrolyte. This compensator is proposed by [13] and mentioned by [7]. It consists of an H-bridge circuit and for its switchhing, it is controlled by a PWM (pulse width modulation) switching pattern. The benefit of this technique is that it introduces very low harmonics as compared other techniques which is a very important consideration. The drawback of this technique is complexity, more components compared to others, but its advantage is more than its limitations. This thesis also considers this technique with the innovation in circuitry in PWM switching techniques. [13] uses bipolar PWM technique which produces more harmonics as compared to unipolar PWM considered in this thesis. This thesis considers open loop control to decrease the overall complexity of the system. Active power decoupling based on series voltage compensator is shown in figure 7.

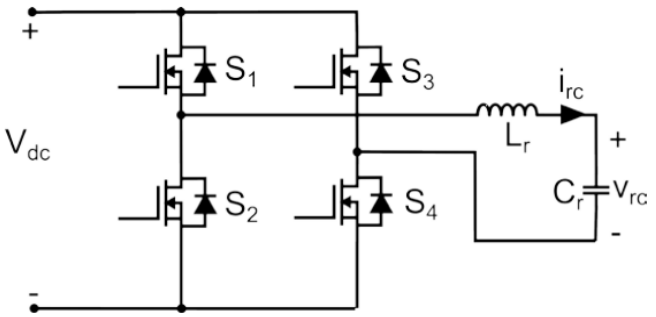

Figure 2. H-bridge topology

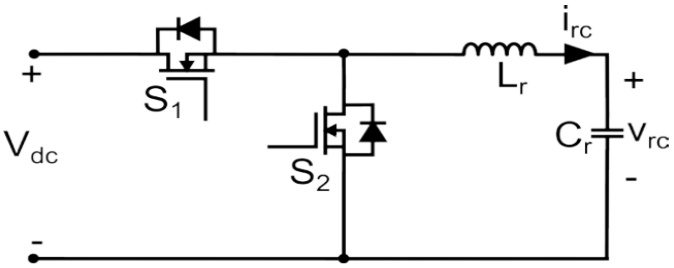

Figure 3. Buck converter based APD circuit

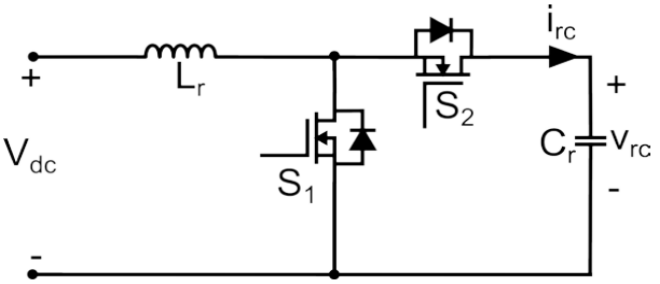

Figure 4. Boost converter based APD circuit

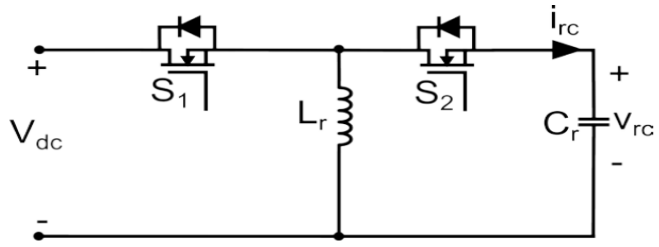

Figure 5. Buck-boost converter based APD circuit

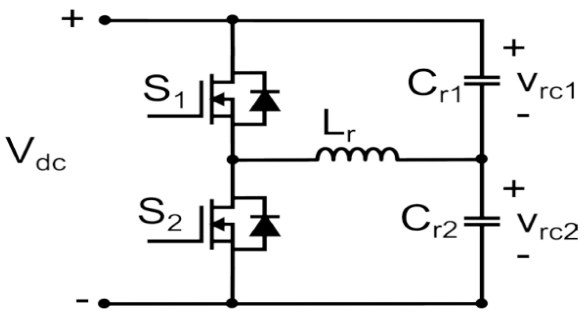

Figure 6. Split capacitor based APD circuit

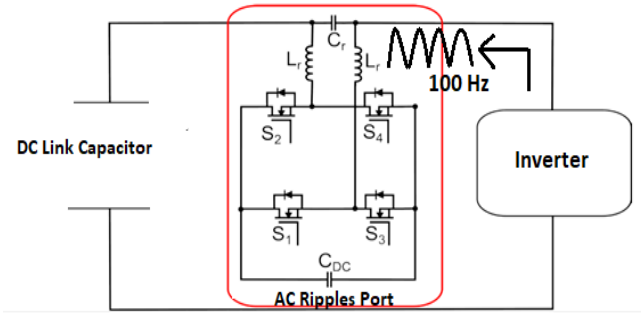

Figure 7. Series compensator based APD

III. METHODOLOGY

The reliability of micro inverter is degraded mainly due to failure of electrolytic capacitor. The capacitor burns out due to heat which is caused mainly by AC voltage ripples coming from inverter AC side. The aim of this research is to bypass these AC ripples from electrolytic capacitor. For this purpose, we design an active filter or active power decoupling circuit abbreviated as APD which is actively operated through switches. First of all, a specific power and voltage rating for micro inverter is considered. Before designing, all parameters are calculated through formulas. For this project a PV module of 300 watts of power and 40 volts is considered. The designing of micro inverter is done in PSIM software starting from boost converter. The capacitance and inductance values of boost converter are calculated by using equation (3) and (4). The switching frequency of the MOSFET is 20k Hz and duty is found from equation 5 using desired values of input and output voltages. The inverter stage is made up of four IGBT switches which are operated by SPWM circuit based on unipolar SPWM which is three level modulation scheme and using switching frequency of 20k Hz. For pure sine wave at the output an AC filter is used whose values of inductance and capacitance are calculated using equation (6) and (7) respectively. In first case for power decoupling, a simple capacitor is used and the circuit is simulated. Based on the capacitance of decoupling capacitor, the magnitude of AC ripples is measured as benchmark value from the graph of voltage at DC link bus. After this active power decoupling APD circuit is designed for compensation of AC ripples which is main objective of this thesis. This circuit consists of H-bridge, capacitor and filters. After designing series compensator, it is connected in series between the inverter stage and DC link capacitor. The circuit is simulated again and the AC ripple voltage at DC bus is measured. Now the measured AC ripple voltage is very less than the benchmark value. Based on mitigated voltage value, life of capacitor and hence life of micro inverter is calculated and is graphically represented. Methodology of the research is shown in figure 8 through a flow chart and complete simulation circuit in figure 9.The circuitry of series active power decoupling circuit consists of differentiator, unipolar sinusoidal pulse width modulator SPWM circuit and H-bridge circuit. Differentiator sense the voltage at DC bus having a signa consistsl of DC voltage and second harmonic frequency voltage. Differentiator extracts the 100 Hz AC component and gives it to SPWM generator as reference voltage wave. SPWM generator compares this reference wave with 20k Hz triangular wave and generates switching patterns. This switching signal is given to H-bridge circuit connected in series to DC bus. The H-bridge is controlled through switching in such a way that it converts 100 Hz AC ripple signal to a DC signal because the H-bridge in this case is bidirectional, it acts like a full wave rectifier circuit operated in reverse directional. The output of H-bridge is a pure DC voltage (in ideal condition, but it still have some small amount of AC ripples) which is added to DC bus. DC link capacitor in this way is protected from AC ripples.

$$L = \frac{\mathrm{d(1-d)\^{}2RTs}}{\%\mathrm{ripples}} \quad (3)$$

$$C = \frac{\mathrm{dTs}}{\mathrm{R\%ripples}} \quad (4)$$

$$\mathrm{d} = 1 - \frac{Vin}{Vo} \quad (5)$$

$$L = \frac{Vdc}{8\,\Delta ripples\ fsw} \quad (6)$$

$$\mathrm{C}= \frac{\emptyset\ Prt}{2\pi Fline\ V\^{}2} \quad (7)$$

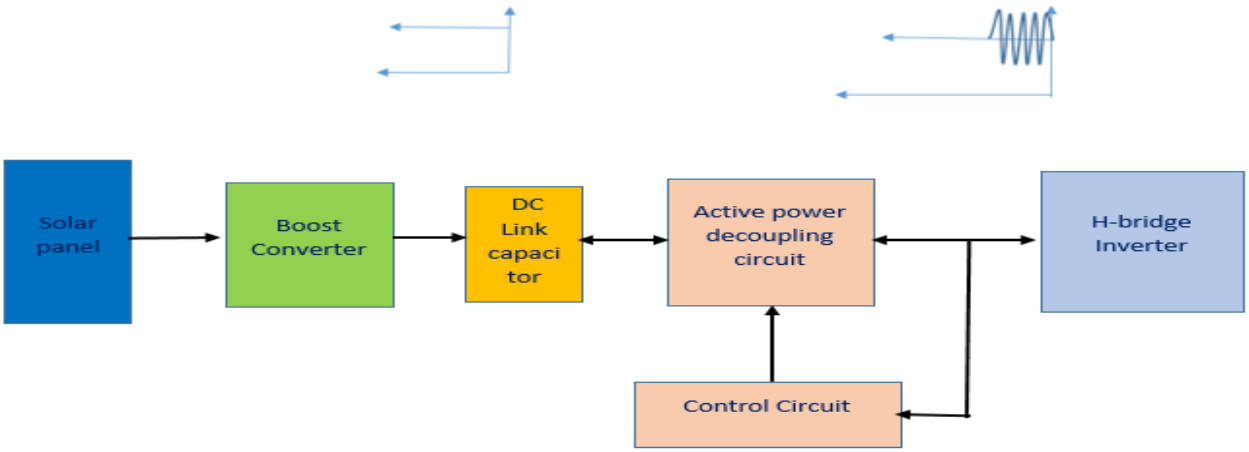

Figure 8. Flow diagram for series compensator

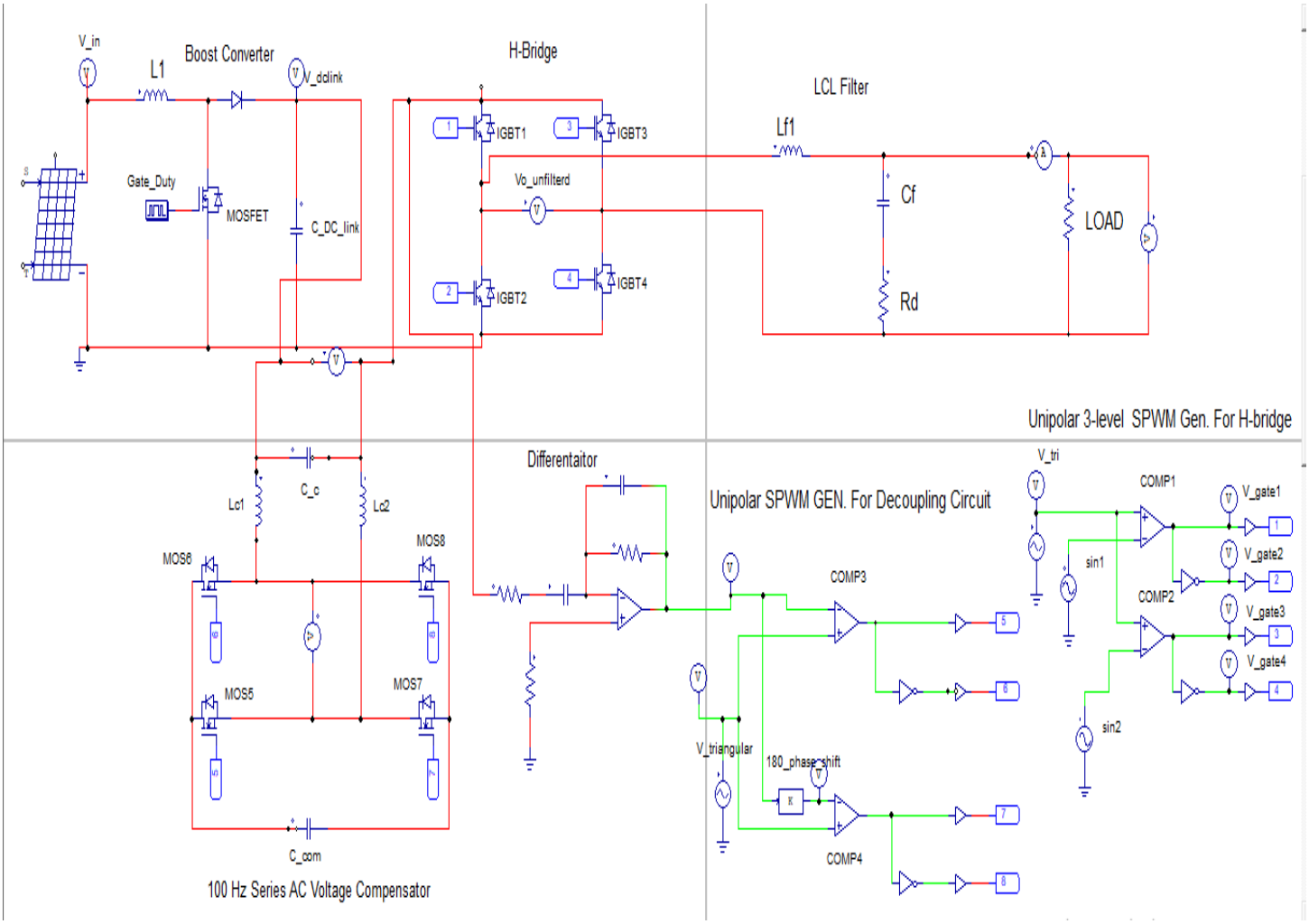

Figure 9. Complete circuit diagram of micro-inverter with APD circuit in PSIM

IV. RESULTS AND DISCUSSION

The life span of an electrolytic capacitor is effected due to external and internal environmental factor. External factor maybe ambient temperature, humidity, pressure, and vibration. The impact of external factor on life of electrolytic capacitor is minimum and can be neglected. But internal factors have significant impact on life of capacitor. These factors include operating voltage, charging and discharging and the more important one is the ripple current through the capacitor [7]. The equivalent series resistance(ESR) of electrolytic capacitor is relatively higher than other type of capacitor. Due to this, when ripple current passes through capacitor, it causes heat dissipation inside capacitor which is shown by equation (8).

$$H = Irip^2 \times ESR \qquad (8)$$

Equation (8) shows that for constant value of ESR, heat generated inside the capacitor is proportional to the square of ripple current. This shows a significant contribution to inside temperature of electrolytic capacitor by the ripple current. This temperature rise (ΔT) can be approximated by equation (9).

$$\Delta T = \frac{Irip^2 \times ESR}{\beta A} \qquad (9)$$

Where, Irip is ripple current ESR is equivalent series resistance β is heat radiation factor and A is surface area. Electrolytic capacitor is an electro-chemical device. Due to high temperature, the rate of chemical reactions inside it increases which ultimately degrade life of capacitor. In [7] this life degradation due to ripples and operating voltage can be calculated by using Arrhenius law in equation (10).

$$L = Lo * 2^{0.1(Tm-Ta)} * Mv * 2^{\frac{\Delta Tr - \Delta T}{\Delta Tr}} \qquad (10)$$

Where ΔT is temperature developed due to ripples ΔTr is rated ripple temperature L is expected life and Lo is base life calculated by manufacturer. Tm is maximum allowable temperature, Ta is actual operating temperature. Mv is voltage multiplier and is given by equation (11).

$$Mv = 4.3 - 3.3\frac{Va}{Vr} \qquad (11)$$

Vr is rated voltage and Va is the applied voltage. The value of Mv is 1 when capacitor is operated at rated DC voltage and greater than 1 when it is operated at less than rated DC voltage. Now using PSIM we simulate two systems to show their life span due to AC ripples.

A. Ripples on DC bus in Benchmark Micro inverter.

In this benchmark micro inverter system, the circuit is simulated in PSIM without using series AC voltage compensator. The peak to peak voltage ripples in this system were 28V as shown in figure 10. In the circuit for this benchmark system, only an electrolytic capacitor of 400uF capacitance is used to decouple the DC voltage variations. Voltage at the DC link bus consists of two components, one component is 310V DC voltage comes from boost converter and along with it another voltage component which is 100Hz AC ripples come from inverter side.

B. Ripples in Proposed Micro inverter.

In the proposed micro inverter whose schematics is given in figure 9, an h-bridge is controlling the charging and discharging of capacitor C_com. This h-bridge is controlled by SPWM generator circuit. This h-bridge is actually works in opposite manner (converts AC ripples to DC voltage) as compared to inverter h-bridge which converts DC into AC voltage. the wave form of this proposed micro inverter is shown in figure 11. This shows that AC ripples in proposed system are 3.6V peak to peak which is considerable reduction as compared to benchmark system which are 28V peak to peak. These results shows that ripples in benchmark system are 9% but in proposed system it is 1.1%. which is a reasonable reduction achieved by the proposed system. For IEEE standard the allowable ripples are 5%. Then using equation (10) the capacitor life graphs for benchmark micro inverter and proposed micro inverter is plotted in figure 12. Expected life of capacitor for different decoupling techniques are summarized in comparison table 1. Although a lillte complex but the our proposed design enhance life expectancy of the capacitor.

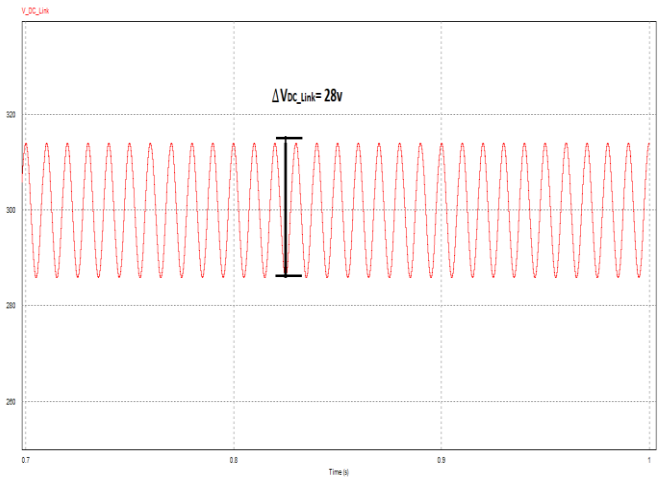

Figure 10. AC Ripples On DC Bus In Benchmark System

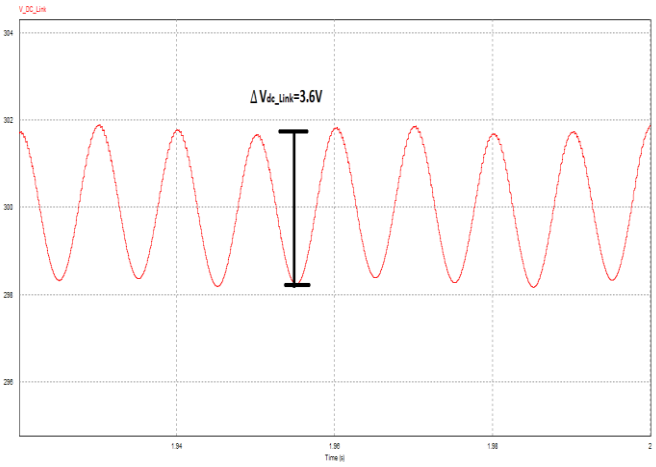

Figure 11. Ripples on DC link Capacitor in Proposed Micro inverter

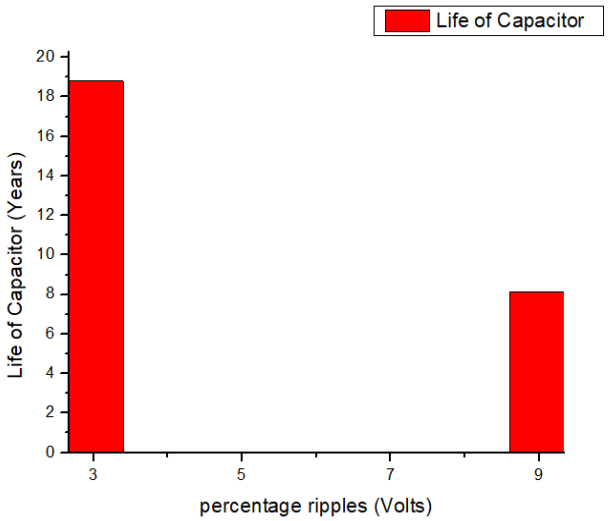

Figure 12. Capacitor Life Graphs Proposed (left) Benchmark(right)

TABLE I. CAPACITOR LIFE COMPARISN

S No	Reference	Decoupling technique	%age Ripples	Capacitor Life(years)
1	Haibing et al	PV side passive decoupling with no ripples compensation on DC link side.	31 %	1.5 yr.
2	Our benchmark	Small capacitor	9%	6 yrs.
3	R. Wang et al	Buck-boost based APD	4.4 %	11 yrs.
4	Y. Tang et al	Half bridge APD	3.2 %	12 yrs.
5	Our proposed design	H-bridge unipolar SPWM based APD	1.1 %	19 yrs.

C.Total Harmonics Distortion THD

The allowable amount of total harmonics distortion THD by IEEE is 5%. Figure 13 shows the simulation results for total harmonics distortion for micro inverter system with only capacitor as decoupling element which are only 1.7% and figure 14 shows result for THD when active power decoupling circuit is inserted along with DC link capacitor which increases the distortion only up to 2.7% which is still very less than the IEEE standard. Table 1. Capacitor life comparison.

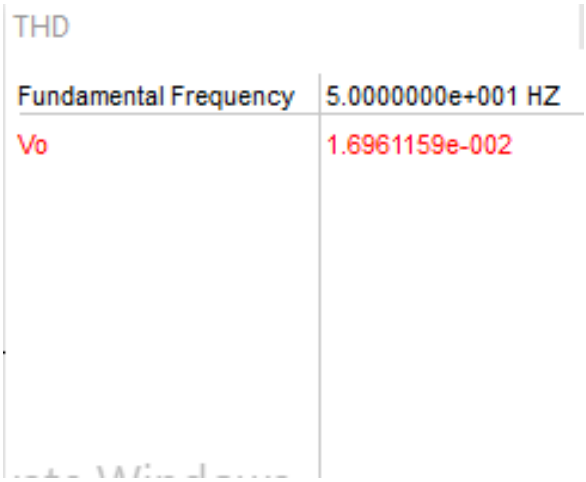

Figure 13. THD without compensator

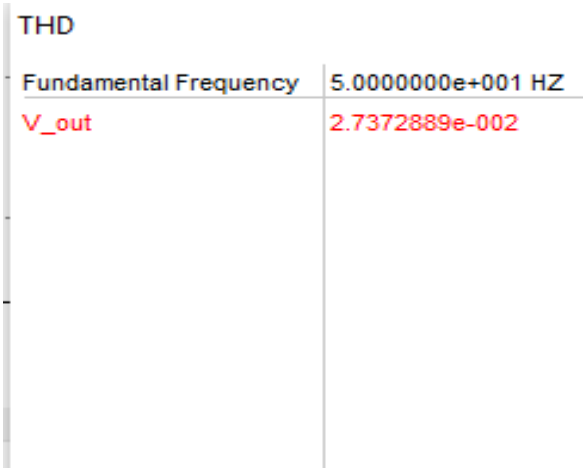

Figure 14. THD with Compensator

CONCUSLION

Solar energy is one the renewable energies which is available in abundance but to harvest it requires a system of PV modules. Like many other renewable sources e.g. fuel cell, micro hydro and small wind generator, PV module generates a DC power. This DC power is need to be converted into AC power as more than 95% of loads and generators already installed produces or consume AC power. For this conversion we need an electronic device called inverter which converts unidirectional or DC current to alternating or AC current. On the bases of power rating and configuration inverters can be a central or conventional inverter which is connected to a series string of PV modules and it can be of small rating called micro inverter. Micro inverter has about 300 Watts of rating and connected at the back of each and every PV module and all of them are connected to a common bus. In certain small scale application such as residential, small industries, labs, electric car etc. micro inverters outperform central inverters. In such cases a match between life of micro inverter and PV module is necessary to reduce maintenance cost. As most of the PV manufacturers offer

20 to 25 years of guarantee on their modules, so it is necessary for micro inverter to have a life of 20 to 25 years. But in practice it is not the case as it has hardly a life span of 5 to 10 years. The reason for its short life is electrolytic capacitor, connected at DC link for power decoupling, burns due heat which is caused by AC ripples coming from inverter side. This thesis mainly focused how to mitigate these ripples by using another film, long life capacitor actively controlled by an h-bridge circuit which converts AC ripples into DC voltage at the DC link bus. For this purpose, this thesis developed an active power decoupling ADP circuit which is connected in series between boost converter and inverter stage. This research work develops the model in PSIM environment. Two model of micro inverters has been simulated one is a benchmark system without ADP series compensator which gives 28V peak to peak ripples at DC link capacitor. And other system is proposed micro inverter with series compensator which gives 3.6V ripples at DC link capacitor. Using Arrhenius equation, the life graphs of capacitor for both system has plotted which shows that reducing ripples from 9% to 3.6%, increases life from 8.16 year to 18.8 years.

REFERENCES

[1] Arráez-Cancelliere, Oswaldo A., Nicolás Muñoz-Galeano, and Jesús M. Lopez-Lezama. "Performance and economical comparison between micro-inverter and string inverter in a 5, 1 kWp residential PV-system in Colombia." In *2017 IEEE Workshop on Power Electronics and Power Quality Applications (PEPQA)*, pp. 1-5. IEEE, 2017.

[2] https://en.wikipedia.org/wiki/Solar_micro-inverter

[3] Harb, Souhib, et al. "Micro inverter and string inverter grid-connected photovoltaic system—A comprehensive study." *2013 IEEE 39th Photovoltaic Specialists Conference (PVSC)*. IEEE, 2013.

[4] "Examples for failures in power electronics system", *European Center for Power Electronics (ECPE)*, tutorial, April, 2007

[5] S. B. Kjaer, J. K. Pedersen, and F. Blaabjerg, "A Review of Single-phase Gridconnected Inverters for Photovoltaic Modules," IEEE Transactions on Industry Applications, vol. 41, pp. 1292-1306, 2005.

[6] Williams, David. Active power decoupling for a boost power factor correction circuit. Diss. University of British Columbia, 2016.

[7] Hu, H., Harb, S., Kutkut, N., Batarseh, I., & Shen, Z. J. (2012). A review of power decoupling techniques for microinverters with three different decoupling capacitor locations in PV systems. *IEEE Transactions on Power Electronics*, *28*(6), 2711-2726.

[8] Sun, Yao, Yonglu Liu, Mei Su, Xin Li, and Jian Yang. "Active power decoupling method for single-phase current-source rectifier with no additional active switches." *IEEE Transactions on Power Electronics* 31, no. 8 (2015): 5644-5654.

[9] K.-H. Chao, P.-T. Cheng and T. Shimizu, "New Control Methods for Single Phase PWM Regenerative Rectifier with Power Decoupling Functions," in *International Conference on Power Electronics and Drive Systems*, Taipei, Taiwan, 2009.

[10] B. Tian, S. Harb and R. Balog, "Ripple-port integrated PFC rectifier with fast dynamic response," in *IEEE 57th International Midwest Symposium on Circuits and Systems*, College Station, Tx, 2014.

[11] M. Saito and N. Matsui, "Modeling and Control Strategy for a Single-Phase PWM Rectifier Using a Single-Phase Instantaneous active/reactive Power Theory," in *Telecommunications*

[12] C. Wang, Y. Zou, Y. Zhang and Y. Xu, "Research on the single-phase PWM rectifier basedon the repetitive control," in *IEEE International Conference on Industrial Technology*, Chengu, 2008.

[13] h. Wang, H. S.-H. Chung and W. Liu, "Use of a Series Voltage Compensator for Reduction of the DC-Link Capacitance in a Capacitor Supported System," *IEEE Transactions on Power Electronics*, vol. 29, no. 3, pp. 1163-1175, 2014.

[14] https://energyinformative.org/best-solar-panel-monocrystalline-polycrystalline-thin-film/

[15] Joshi, Mahendra Chandra, and Susovon Samanta. "Modeling and control of bidirectional DC-DC converter fed PMDC motor for electric vehicles." In *2013 Annual IEEE India Conference (INDICON)*, pp. 1-6. IEEE, 2013.

[16] Hu, Haibing, Souhib Harb, Nasser Kutkut, Issa Batarseh, and Z. John Shen. "A review of power decoupling techniques for microinverters with three different decoupling capacitor locations in PV systems." *IEEE Transactions on Power Electronics* 28, no. 6 (2012): 2711-2726.

[17] Namboodiri, Anuja, and Harshal S. Wani. "Unipolar and bipolar PWM inverter." *International Journal for Innovative Research in Science & Technology* 1, no. 7 (2014): 237-243.

[18] Azri, Maaspaliza, and Nasrudin Abd Rahim. "Design analysis of low-pass passive filter in single-phase grid-connected transformerless inverter." In *2011 IEEE Conference on Clean Energy and Technology (CET)*, pp. 348-353. IEEE, 2011.

Siraj Ud Din was born in district Lower Dir of Khyber pakhtoonkhwa, Pakistan in April 4th, 1994. He has received his BSc Electrical Engineering degree from the University of Engineering and Technology Peshawar, Pakistan in 2016. He has completed his MSc in Electrical Energy System from US-Pakistan Center for Advanced Studies in Energy, University of Engineering and Technology Peshawar, Pakistan in 2019. His major fields of research are smart grid, cost optimization of hybrid energy system and photovoltaics.

IJEW 国际工程期刊 International Journal of Engineering Works انجینئرنگ کاموں کا بین الاقوامی جرنل

International Journal of Engineering Works
ISSN-p: 2521-2419
ISSN-e: 2409-2770
Vol. 7, Issue 08, PP. 282-285, August 2020
https://www.ijew.io/
https://doi.org/10.34259/ijew.20.708282285

Analysis of Conventional and Microwave Assisted Technique for the Extraction of Concentrated oils from Citrus Peel

Uzair Tariq[1]*, Syed Mustafa Shah[2]*, Mian Yahya Gul[3]
[1,2,3] Department of Chemical Engineering, University of Engineering and Technology Peshawar
*Corresponding Author
uzairtariq_67@outlook.com[1]*, mustafa.baharshah@gmail.com[2]*, kakakhel49@yahoo.com[3]
Received: 26 July, Revised: 03 July, Accepted: 11 August

***Abstract*—** Citrus peel belongs to orange and lemon plant that contains concentrated oils. Oil from citrus peel is widely used in foods, perfumes and pharmaceutical industry worldwide. In this study, the advantages of citrus concentrated oil extracted by conventional and novel techniques were studied. Microwave extraction techniques have come out as new alternatives to conventional techniques (hydro distillation) for extraction of oils. This paper reviews the novel separation technique with the conventional techniques in terms of extraction time, yields and energy. Extraction of oils with solvent free microwave extraction (SFME) was comparatively better in terms of extraction time that is 50 minutes while for microwave assisted hydro distillation (MAHD) is 60 minutes and for hydro distillation (HD) it is 3 hours. Yields percentage was almost same for the three processes that are 1.67%. Energy savings were greater in both MAD and SFME that is 0.4 kWh while in Hydro distillation it is 1.3 kWh. Overall MAD was better in performance than other techniques.

Keywords: Citrus Peels essential oil, Hydro Distillation, Microwave Assisted Distillation, Solvent-Free Microwave Extraction.

I. INTRODUCTION

Citrus fruits including types of oranges and lemons are largely grown in different regions of the world [1]. It is one of the major crops in Pakistan. The annual production of citrus fruit in Pakistan is about 2000 k. tons [2] while global production of lemon is about 7.3 million tons and that for oranges are 2.4 million tons [3]. Citrus fruits are largely consumed for juice Besides these conventional methods, solvent extraction is also used for extracting essential oils. In the experiment of Lopresto et. al. found that a yield of 0.95% (v/w%) was observed for Lemonene through solvent extraction in Soxhlet apparatus. Hexane was used as solvent [13]. Other solvents used for extraction of oils from citrus peels include: Methyl Alcohol, Methylene Chloride, Ethyl Alcohol and Acetone etc. [14-17]. These conventional techniques provide good basis for extraction but on expense of energy and time.

Here in this research article experiments are done for the comparison and analyzing microwave assisted distillation (MAD) with the conventional techniques. The main difference is in heating mechanism. In microwave heat in the molecules are generated through waves, these waves vibrate the molecules and thus heat is produced so in MAD heat generation takes place from inside of body while in the steam and hydro distillation heat transfer occurs from out to inside of the body [18].

extraction so it leaves a lot of waste in the form of its peels. About 50% of wet fruit waste is of citrus peels [4]. These waste products are used to feed animals or a major portion of it is directly dumped into open-air, which causes adverse effects on the environment. Citrus fruits are rich in vitamin C, carotenoids and bioactive compounds [5].

Citrus peels are rich in essential oils that contain some significant compound good for skin and health and are widely used for flavoring, in perfumery, cosmetics, medicine and pharmaceuticals [6]. Many essential compounds can efficiently be extracted from citrus peels. Citrus peels have bio-active phenols i-e flavonoids and phenolic acids. These phenols have significant properties like antioxidants, antiviral, antimicrobial, anti-inflammatory and neuroprotective, etc. [7]. Therefore, it is very important to use this waste to extract these valuable compounds from it.

The extraction of essential oils from citrus peels is done conventionally by two methods. 1. Hydro distillation and 2. Steam Distillation. In hydro distillation, dry peels are subjected to heat along with some ratio of water in a specific Clevenger type apparatus for several hours. Water and essential oils evaporate out and then condensed through the condenser in a separate flask where it is left for phasing out from water and thus collected for further analysis. Salma et. al. in their experiments found that after 4 hours extraction of essential oils from clementine the yield obtained was about 0.73% (v/w%) [8]. In one other experiment by Mohamed et. al. obtained yield of 0.24% (v/w%) from 3-hour long hydro distillation [9]. 0.42% (w/w%) yield was obtained in similar experiment performed by Uysal et. al. [10].

Steam distillation is still widely used for extraction of oils. In its steam is passed through the material from which oils are to be extracted and the rest of the process is same as of hydro distillation. Some times third solvent is used for layer separation of extracted oil from water and then heat treatment is done to vaporize the concentrated oil leaving behind. In one such experiment performed by Pauline et. al. They extracted oil by steam distillation in two-hour long process and at temperature of just above 100 oC, then sodium chloride and chloroform were added to the separating funnel and shaken back and forth several times and thus layer separation occurs. A yield of 2.475% (w/w%) was observed [11]. Kusuma et. al. obtained a yield of 0.59% (v/w%) by steam distilling citrus peels for 7 hours [12].

II. Materials and Methods

Citrus Limonum peels were used for extraction of oil along with water. Sodium sulphate was used to remove any water present in essential oils.

For hydro distillation Clevenger type apparatus was used. 100 g of citrus peels cut in 3-5 mm in size were taken in 500 ml flask with 200 ml of water. This flask was connected to Clevenger type apparatus through special connector. A temperature was kept at 120 oC. Hydro distillation was performed from 3 hours. Oil obtained was dehydrated with sodium sulphate and then kept in air tight bottle in freezer. Hydro distillation setup is shown in figure 1.

Figure 1: Hydro Distillation

For Microwave assisted distillation modification to Whirlpool VIP 34 microwave oven was done. A hole was made at top of the oven to hold a special connector that is then connected with condenser. Oven has a wave frequency of 2.45 GHz. It can deliver a maximum power of 1100 Watts. Flat bottom flask was used with 500 ml capacity. The setup is shown in figure 2. For microwave assisted hydro distillation (MAHD) the time range was 45 to 75 minutes with 15-minute interval and the ratio of peels to water was 1:2 (w:v). While for Solvent free microwave extraction (SFME) dry peels were subjected for extraction with a time range of 40 to 60 minutes with 10-minute interval. Energy calculations were done through digital clamp meter by measuring the drawing current.

Figure 2: Microwave Assisted Distillation

III. Results and Discussions

Experimental results for MAHD show that a yield of 1.2%, 1.7% and 1.8% was observed at 45 to 75 minutes time range with 15-minute interval respectively. A total increase of 34% was observed from initial reading, at 60 minutes while 6% increment occurs in yield from 60 to 75-minute time. Power consumption per gram was 0.42, 0.44 and 0.51 kWh/g for 45-, 60- and 75-minutes time. The increase in power consumption is very high for 75-minutes time i-e. about 16% as shown in table 1.

SFME results observed a yield of 1.4%, 1.7% and ≈1.7% for 40-, 50- and 60-minutes time with a yield increment of 22% and 4.2% for 50- and 60-minutes respectively. Power consumed per gram for 50-minute was 0.38 kWh/g with 11% increase while for 60-minute an increase of 10% i-e 0.04kWh/g was observed. For hydro distillation a experiment was conducted for 3-hours until a yield of 1.7% was obtained. Power consumed per gram of essential oil was the higher of all which is 1.3 kWh/g. As presented in table 2.

TABEL 1. RESUTLS FOR MIRCOWAVE ASSISTED HYDRO DISTILLATION IN COMPARISON TO HYDRO DISTILLATION

Parameter/Sample	1	2	3	Hydro Distillation
Time (min)	45	60	75	180
%Yield (% Increased)	1.2	1.7 (34%)	1.8 (6%)	1.7
kWh/g (% Increased)	0.42	0.44 (5%)	0.51 (16%)	1.3

TABLE 2. RESULTS OF SOLVENT FREE MICROWAVE EXTRACTION IN COMPARISON WITH HYDRO DISTILLATIO

Parameter/Sample	1	2	3	Hydro Distillation
Time (min)	40	50	60	180
%Yield (% Increased)	1.4	1.7 (22%)	1.8 (4.2%)	1.7
kWh/g (% Increased)	0.34	0.38 (11%)	0.42 (10%)	1.3

CONCLUSIONS

The aim of this research was to investigate the effectiveness of MAD. It was observed that MAD provides higher yields with less extraction time and low power consumption per gram of essential oil. Yield with connection to time and power consumption for SFME per gram was slightly and significantly better than MAHD and hydro distillation respectively. As shown in figure 3(a) and (b).

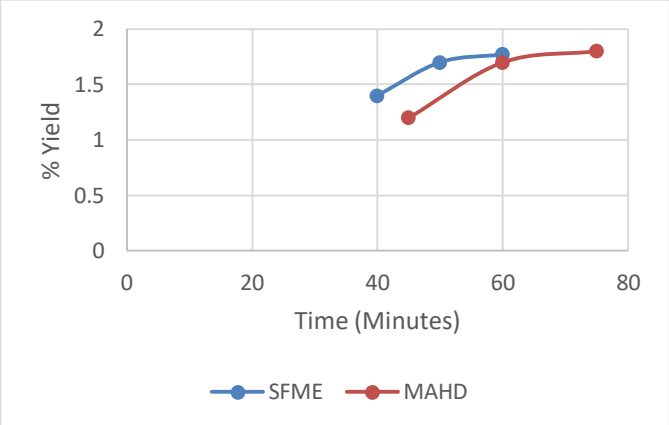

Figure 3 (a): Time vs % Yield of SFME and MAHD

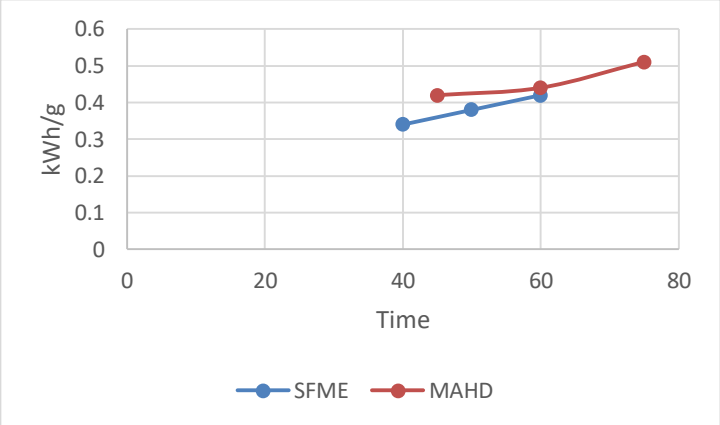

Figure 3(b): Time vs kWh/g of SFME and MAHD

REFERENCES

[1] A. K. Maurya, S. Mohanty, A. Pal, C. S. Chanotiya and D. U. Bawankule, " The essential oil from Citrus limetta Risso alleviates skin inflammation: in-vitro and in-vivo study", Journal of Enthnopharmacology, https://doi.org/10.1016/j.jep.2017.10.018

[2] M. Abbas, M. M. Khan, S. M. Mughal and P. Ji, "Comparison of infection of Citrus tristeza closterovirus in Kinnow mandarin (Citrus reticulata) and Mosambi sweet orange (Citrus sinesis) in Pakistan", Crop Protection, Vol. 78, 2015, pp. 146-150.

[3] S. E. Kantar, N. Boussetta, N. Lebovka, F. Foucart, H. N. Rajha, R. G. Maroun, N. Louka and E. Vorobiev, "Pulsed electric field treatment of citrus fruits: Improvement of juice and polyphenols extraction", Innovative Food Science and Emerging Technologies, Vol. 46, 2018, pp. 153-161.

[4] L. Zuo, Y. Hu, Y. Sun, W. Xue, L. Zhou and X. Zhang, "Rapid determination of 30 bioactive constituents in XueBiJing injection using ultra high-performance liquid chromatography-high resolution hybrid quadrupole-orbitrap mass spectrometry coupled with principal component analysis", Journal of Pharmaceutical and Biomedical Analysis, Vol. 137, 2017, pp. 220-228.

[5] F. J. Barba, O. Parniakov, M. Koubaa, and N. Lebovaka, "Pulse electric fields assisted extraction from exotic fruit residues. In D. Miklavcic (Ed.)", Handbook of electroporation, Cham: Springer International Publishing, 2017, pp. 1-18.

[6] M. A. Desai, J. Parikh, and A. K. De, "Modelling and optimization studies on extraction of lemongrass oil from Cymbopogon flexuosus (steud.) Wats.", Chem. Eng. Res. Des., Vol. 92, No. 5, 2014, pp. 793-803.

[7] E. G. Mejia, N. R. Conrado, M. E. Leon-Gonzalez and Y. Madrid, "Citrus peels waste as a source of value-added compounds: Extraction and quantification of bioactive polyphenols", Food Chemistry, Vol. 295, 2019, pp. 289-299.

[8] S. A. El-Sawi, M. E. Ibrahim, K. G. El-Rokiek, and S. A. El-Din, "Allelopathic potential of essential oils isolated from peels of three species.", Annals of Agricultureal Sciences, Vol. 64, 2019, pp. 89-94.

[9] M. A. Ferhat, B. Y. Meklati and F. Chemat, "Comparison of different isolation methods of essential oil from citrus fruits: cold pressing, hydrodistillation and microwave 'dry' distillation.", Flavour Fragr. J., Vol. 22, 2007, pp. 494-504.

[10] B. Uysal, F. Sozmen, O. Aktas, B. S. Oksal and E. O. Kose, "Essential oil composition and antibacterial activity of the grapefruit (Citrus Paradisi. L) peel essential oils obtained by solvent-free microwave extraction: comparison with hydrodistillation.", International Journal of Food and Technology, Vol. 46, 2011, 1455-1461.

[11] M. N. Pauline, B. Nithyalakshmi and R. A. Lakshmi, "Extraction of Orange Oil by Improved Steam Distillation and its Characterization Studies", International Journal of Engineering Technology, Management and Applied Sciences, Vol. 3, No. 2, 2015, pp. 1-8.

[12] H. S. Kusuma. A. F. P. Putra and M. Mahfud, "Comparison of Two Isolation Methods for Essential Oils from Orange Peel (Citrus auranticum L) as a Growth Promoter for Fish: Microwave Steam Distillation and Conventional Steam Distillation", Journal of Aquaculture Res. Development, Vol. 7, No. 2, 2016, pp. 1-5.

[13] C. G. Lopresto, F. Petrillo, A. A. Casazza, B. Aliakbarian, P. Perego and V. Calabro, "A non-conventional method to extract D-limonene from waste lemon peels and comparison with traditional Soxhlet extraction", Separation and Purification Technology, Vol. 137, 2014, pp. 13-20.

[14] Y. Ma, X. Ye, Y. Hao, G. Xu and D. Liu, "Ultrasound-assisted extraction of hesperidin from Penggan (Citrus reticulata) peel", Ultrasonics Sonochemistry, Vol. 15, No. 3, 2008, pp. 227-232.

[15] K. Xhaxhiu, A. Korpa, A. Mele and T. Kota, "Ultrasonic and Soxhlet Extraction Characteristics of the Orange Peel from "Moro" Cultivars Grown in Albania", Journal of Essential Oil Bearing Plants, Vol. 16, No. 2, 2013, pp. 421-428.

[16] B. B. Li, B. Smith and Md. M. Hossain, "Extraction of phenolics from citrus peels I. Solvent extraction method", Separation and Purification Technology, Vol. 48, 2006, pp. 182-188.

[17] B. Nayak, F. Dahmoune, K. Moussi, H. Remini, S. Dairi, O. Aoun and M. Khodir, "Comparison of microwave, ultrasound and accelerated-assisted solvent extraction for recovery of polyphenols from Citrus sinensis peels", Food Chemistry, Vol. 187, 2015, pp. 507-516.

[18] H. S. Kusuma and M. Mahfud, "Comparison of conventional and microwave-assisted distillation of essential oil from Pogostemon cablin leaves: Analysis and modelling of heat and mass transfer", Journal of Applied Research on Medicinal and Aromatic Plants, Vol. 4, 2017, pp. 55-65.

International Journal of Engineering Works
ISSN-p: 2521-2419
ISSN-e: 2409-2770
Vol. 7, Issue 08, PP. 286-292, August 2020
https://www.ijew.io/
https://doi.org/10.34259/ijew.20.708286292

Role of Women in Energy Management at Household level in Peshawar, Pakistan

Naseha Wafa Qammar[1], Shamaima Wafa Qammar[2]
[1] US- Pakistan Center for Advanced Studies in Energy, University of Engineering & Technology, Peshawar
[2] Civil Engineering Department, University of Engineering & Technology, Peshawar
nasehaqammar@gmail.com[1]
Received: 10 August, Revised: 19 August, Accepted: 25 August

***Abstract*—** Pakistan is an energy stressed nation and is currently facing short-fall of power output around 6500 MW and is among those countries which are mostly affected from climatic changes in the past ten past years i.e. from 1998 to 2017. To cater the aforementioned energy and environmental concerns, this research study is fabricated to (1) figure out the awareness level of females in regards to energy management (2) women behavior towards utilization of renewable energy resources in the households (3) females response to the changing energy conditions as a result of power outages in the household setting and (4) energy management strategies conducted at the households. The scope of the study is Peshawar district, Pakistan. To investigate the queries discussed above, a research questionnaire with a random sample of (n=121) is devised and analysed. Major conclusions drawn from this survey are (1) About (54.5%) of women are aware of energy savings by doing proper management (2) Females are also wise in decision making at households. (3) About (55.3%) of the womens are aware of peak hours unit and (48.4%) of females are aware of hours of electricity and gas load shedding and in lieu of waiting for electricity and gas recovery, women know how to manage routine chores but yet 52.6% gap leaves a pace for policy makers to integrate social and behavioral aspects of energy consumers and move toward energy efficient and sustainable solutions of energy management at residential sector.

***Keywords*—** energy management, residential sector, females, Peshawar.

I. INTRODUCTION

Different energy management practices are being applied in different parts of world. One of the most effective energy management strategies is energy conservation as discussed in most of the literature. The consumption of energy at demand side especially at households solely involves the proper decision making as human activities are being carried out the full day at home. According to the recent global gender gap report index, the study shows that less than seven percent of the women are at managerial positions in the four worst performing countries including Pakistan and also the women spend on average twice more time in contrast to men on the household and other unpaid activities [1]. Contrarily the Pakistan across its length and breadth is in complete energy crisis. The full-fledged energy shortage levy discomfort, water and food scarcity, electricity cut off and thousands of jobless people [2]. Currently Pakistan is facing short-fall of power output around 6500 MW except for the nonrenewable energy. Pakistan has renewable energy potential of 2,900,00 MW for solar, 346000 MW for wind 3000MW for biogas, 2000 for small hydropower and 1000MW for waste-to-energy, with its share in total present energy scenario being less than 1% [3]. According to the Pakistan energy year book data (2017) collectively oil and natural gas supply a bulk of 79.2% of Pakistan's energy need. The consumption of these energy sources tremendously cross the indigenous supply. This condition forecasts the dependency on LNG imports which is almost 5.6% making it an import economy which dramatically enhances the country's poor financial conditions. The Pakistan is now in import economy zone with its oil import bill prices are about 9.1 billion dollars as seen in

Figure *1*. Also the developing economies are fuel importing countries, and the process of fuel import is multifold given that transportability of fuel itself requires more fuel which counter attack the environment in one or the other way. At the same time the recent study of gender gap report (2018) reveals the fact that Pakistan is considered to be the worst performing country lying below the global average scale and ranked at 148 with 0.550 score out of (0-1) and in Economic Participation and Opportunity it is ranked at number 146 with score of 0.318 out of (0-1). However, Pakistan is closing the gender gap in the education achievement and wage equality [1]. Considering the aforementioned scenario of Pakistan in regards to severe energy crisis, the energy conservation is one of the most environment friendly solutions for fulfilling the energy crisis of a nation and meets the demand of increasing population. The conservation can be done in different ways but integrating the efforts of women in energy management practices, is not being fully evaluated in developing countries. Also the sector wise energy

consumption levy the fact that domestic sector in Pakistan consumes 22.6% energy as clear from

Figure 2. Thus relating the household sector, energy management and women participation in domestic sector can clarify the picture of behavior of women in regards to her awareness level with energy management. Prior to unfold the findings of this research, it is mandatory to understand the relation between (1) energy, gender and environment, (2) household economics (3) energy consumption at residential sector.

1.1 Interconnectivity of energy, gender and environment

Human activities are not solely for the purpose of living in a society but also to survive in an environment and thus energy enters into a physical and technical society in terms of food and its utilization and ultimately have unforeseen environmental consequences [4]. The typical energy resources human began to utilize were from fossil fuels at an appreciable rate of about 150 years ago [5]. Energy consumption is never ending and unstoppable phenomenon for the human survival and both developed and developing countries are using energy in different forms. One study shows that consumption of energy is not fully understood by the humans [6]. Similarly most of the times it happens that what people say is in converse with what people do in daily life in regards to energy use [7]. Gender, technology and sustainability are all interrelated terms with complex parameters that involve socio-physical, economical, behavorial factors [8]. However, on the other hand the developing and developed countries are concomitantly encountering the inauspicious environmental conditions. In order to enter into the market competitiveness, the developing countries are sparing no effort in order to increase their economic growths which ultimately lead those nations to utilize more energy. Utilizing energy in such a way to make it affordable can help to reduce poverty and enhance economic situation more better [9]. In an effort to enhance the economic growth, the consumption of energy is having adverse effects on environment in form of land derogation, air pollution, resource shear, water shortage, adapted climatic conditions (acid rain, greenhouse gas emissions etc.) and vulnerable wild life. With this, the domestic sector is also accountable for negative environmental effects [10]. For example rural household energy consumption contributes to climate risk conditions due to CO2 emissions because of their use of biogas, wood etc. [11]. Urban household women spend more time in kitchen than rural women [12]. One of the rural household energy consumption study in China shows the interesting findings by relating the household energy usage pattern and lifestyle with the amount of CO2 emitted into the environment by analyzing the real time data. The key findings shows that CO2 emissions increases with (1) the large number of people living in the house (2) where people are more educated, thus acquire to have better life standard and use more energy (3) households where people are getting more income can bear all expenses for leading a comfortable life [11]. Thus the energy has close relation with environment and its effect can be adverse or positive depending upon people's reliability on types of fuels and sources they use for energy utilization either directly like for space heating, cooling and comfort or indirectly like the tools used for mobility or delivery of materials from place to place. The lifestyle of people like the way they eat, live or use vehicles for mobility had its impact on surrounding and is not the only but one of the essential tool to look deep into it for energy saving as well as clean environment practices [10].

1.2 Energy utilization at residential sector

Energy is being utilized at different sectors like industrial, commercial, transport, domestic as seen in

Figure 2 and its consumption cum utilization depends upon the requirement of energy for that locale. Household energy consumption is a complex process driven by various individual and situational foretellers [13]. Residential sector has a major pace in energy utilization because it is the place where human needs are getting fulfilled and without using energy it is not possible to meet the demands of daily life [10].

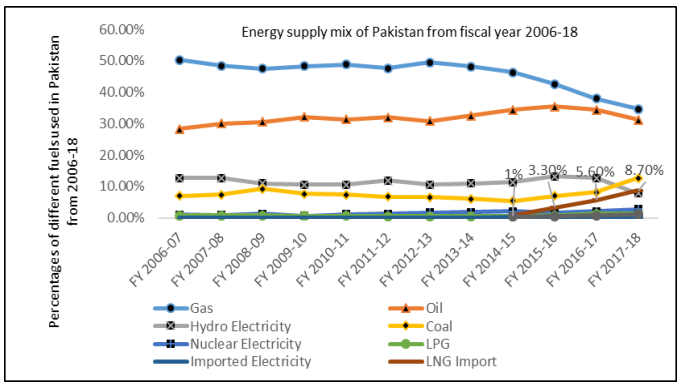

Figure 1 Pakistan's primary energy supply mix for the year 2006-2018 [14]

In a household system the men, women and children all are using energy or energy related technologies like fans, bulbs, refrigerators, washing machine, mobile phones, computers, laptops, microwave oven, air condition, television, iron etc. All these mentioned technologies are basic needs of life and everyone in the house has access to these gadgets according to their needs. For example men mostly use laptops or watch television whilst children may use toys that need charging and women has access to all kitchen related stuff as well as other tools as she is running the household all the day long. Behavioral aspect of personnel consuming energy is key factor in either saving energy or wasting energy by doubling its demand [12]. Water management by female in Tanzania, African country has also undergone through a research study and the case shows that females are recessive as compared to males [15]. The housing lifestyle in European countries exert influence on energy usage [10]. On the other side the physical environment is being affected by the cultural environment which includes all the correlated cultural, technological, behavioral and decision making factors of a cultural society consuming energy [12].

In the developing countries the energy consumption depends directly on increasing level of GDP, urbanization , level of income in contrast to depleting natural resources [16]. For example same level of urbanization in two cities might have different energy consumption which is a proof of other variables such as social, economic, and environmental aspects to be involved in changed energy usage pattern [16]. Viz a viz people with average income, spend more on energy related stuff as compared to the people having high level of income [16].

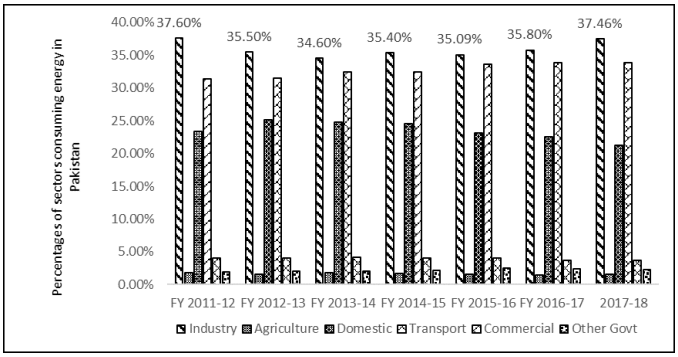

Figure 2 Sector wise energy consumption in Pakistan from year 2016-17 [3]

However, the location of the city does not account as the main perimeter for energy usage except the subtropical regions where the household energy consumption seasonally varies such as regions across Asian, European and American countries but it did not vary in tropical regions [16]. The same results were achieved when the study carried out among ten different European countries-the country of residence did not affect the energy saving efforts carried out daily [10].

1.3 Household economics and energy consumption

Household decision making process is complex and is individual's way of thinking [17]. Energy savings can be achieved by behavioral wise way of thinking [18]. It is an era when one need to move beyond gender differences to think optimistically about the social value of energy [19]. Keeping in mind all the factors related to energy and gender it is obvious that energy is purchased for getting some useful work done within the household, that energy can be in the form of electricity as well as fuel, there are respondents (the people living in a house) to use that energy, a part of that energy is wasted while consuming it, the output of that energy is needs of household are getting fulfilled and that energy also effects the environment. So there is services and good production inside the household by its members and commodities are meals, grocery, power utility and the labor is cooking, cleaning, ironing, and laundry [20]. As another argument sharing of house actually means the sharing of energy usage among personnel's and this also accounts for the consumption of energy being consumed more by the person living alone in a house with same living standard as two people house [21]. One of the study from Netherlands concluded that demographic and economics are the major constituents of the residential dwellings [22]. Another finding of the Bangladesh studies which measured the household electricity consumption using Multi-Tier framework formula reveals that electricity supply during the peak hours i.e. evening time is mostly subjected to outages [23]. The economy involved in household production is named as Gross Household Production. The unseen and unpaid human labor inside the house hold is basically the human capital and by using this capital the raw form materials or commodities are finalized into the physical forms like food , neat and clean living and others etc. [20]. 60% of GNP is covered with household purchases. According to a household study the effort done to earn money outside of house is less than effort done to satisfy households' tasks and it will surpass with the passage of time. To make women's unseen labor at household notable, the household production measurement is necessary.

1.4 Energy management practices at household level and policy implications

One of the research study in US unveil the fact that highly educates as well as married females cannot pay attention to both their work and household responsibilities [24]. The bulk of energy usage at household level is not ignorable and correlated to per capita energy consumption and Human Develop Indicator [9]. More people living in a house as an obvious discussion consumes more energy but energy used per capita in a house where multiple families are residing the energy is shared [13]. In female-headed houses in the rural areas 1.3 billion women are living in poverty [9]. In Asian countries, the problems related to energy consumption require an in depth study from the ground level to make changes in their policies [16]. Women needs to cope with not only the daily routine chores but also the childrearing and other responsibilities are at her shoulder each day and this burden indirectly matters a lot when it comes to success or failure of any policy. Engaging women from the household sector into the advanced energy management tools with new technology can help policy makers to set new foundations for energy saving techniques and economy enhancement of a nation. A range of multiple parameters can be crafted for creating awareness of energy management through these parameters [12]. According to a research study in United Kingdom the dwelling parameters of household such as size of house, total number of people living in the house, electricity and gas appliances used for space heating and cooling have been covered by many researchers and literatures but the factors related to ownership of appliances used in the household are paid least attention [25]. During the child rearing period in the house the energy use is more dominant as the household activities increased such as washing, cooking, cleaning etc. [13]. The multiple household related parameters and the gender role specially the women participation as described above from different studies through different parts of the world can help the policy makers to make changes or amend the existing policy structure already described for gender role to have a better energy saving methods. Most of the times females might be the victim of the poverty and thus they need different energy policy [9]. For instance 2.5 billion people use biomass fuels in developing nations and 1.6 billion people are without electricity due to non-availability and affordability [9]. Another study concluded that the residential sector is the primary area to target for energy management measures [25]. In a challenging era where the world is moving towards the energy deprivation the technical solutions are not enough to get rid of the underlying problems. The social value of energy and human behavior towards this, needs an in depth study and understanding. Therefore, the researchers and policy makers ought to integrate social and behavioral aspects of energy consumers and move toward energy efficient and sustainable solutions of energy management [13]. Awareness to home owned technologies for the home dwellers place an important role in analyzing energy conservation of household [13]. Invisible factors such as government policies for the environment and public,

infrastructure, role of media and others may participate to encourage household owners to opt for energy conservation tools while utilizing energy [13].

II. METHODOLOGY

2.1 Demographics of Khyber Pakhtunkhwa

Khyber Pakhtunkhwa formerly known as North West Frontier Province (N.W.F.P) shares its borders with other provinces of Pakistan to its south-east lies the Punjab , to its south-west lies the Baluchistan, to the west and north it shares a border with Afghanistan and to the east and northern areas it has the Azad Kashmir and Northern areas (Retrieved from: http://kp.gov.pk/).

2.2 Population overview of Khyber Pakhtunkhwa

With a population of 30,523,371 in Khyber Pakhtunkhwa it is divided further into hierarchy of Divisions, Tehsils, and Districts. The seven divisions of the Khyber Pakhtunkhwa are Malakand ,Hazara , Mardan, Peshawar, Kohat , Bannu and D.I Khan.

Figure *3* indicates that the Peshawar division has the population of 7,403,817 which is 24 percent of the entire population of KP province and is the second large division after Malakand division which is 25 percent. Our area of conducting research is Peshawar District-Tehsil that has the population of 4,269,079 (58%) [26]. Pakistan's sixth populated city is Peshawar with an area of 1257 kilo meter square. The counted number of the males in Peshawar is 2,201,257, and the females are 2,067,591 and average annual growth rate is 3.99% from 1998 to 2017 (Retrieved from: http://www.pakinformation.com/population/peshawar.html). This is an overview of population statics for the Peshawar city. The next section deals with the climate and weather of KP.

2.3 Climate and weather of Khyber Pakhtunkhwa

Khyber Pakhtunkhwa experiences four variety of seasons with most prominent are summer months start from May to September when an average weather approximately reaches to 40°C (104°F) and the winter month takes start from November and stay till February with average minimum temperature recorded as 4°C (39°F) (https://en.wikipedia.org/wiki/Climate_of_Peshawar). Speaking about the rainfall pattern in Peshawar, it comes under the Zone 2 area and has both hot and cold climate located in between 31 degree N to 34 degree N [27]. Conversely, hourly weather data can be obtained from Pakistan Meteorological Department which is the official website for getting weather updates (Retrieved from: http://www.pmd.gov.pk/).

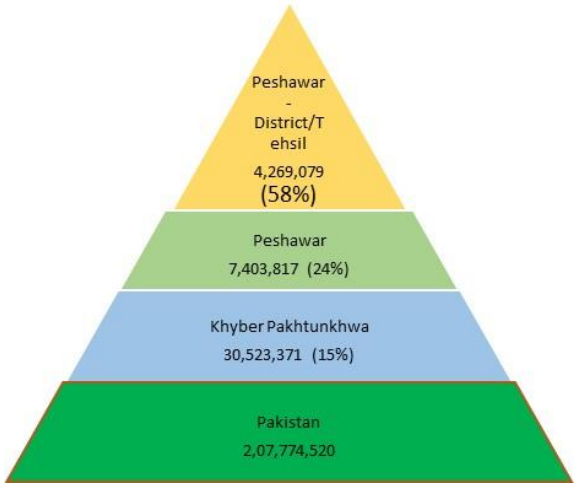

Figure 3 Pyramid showing the population of Pakistan from province level to tehsil level [26]

2.4 Questionnaire distribution and collection criteria

With an aim of procuring data of household women involvement in energy management practices, this research study was conducted in (2019) in Peshawar district. The survey query is randomly distributed by hands across the different areas of Peshawar and respondents were given a time of a week to respond and remit it back. The random selection criteria is adopted from similar research study carried out in Indonesia. The randomly selected houses are retrieved from the google map of Peshawar (https://www.google.com/maps). In a population of 4,269,079 with confidence level of 95% and 10% of error tolerance the expected sample size of questionnaire came out to be 125 and by this calculation a total of 200 questionnaire were distributed and about 121 responses were received. Table 1 indicates the details of the survey questions.

TABLE 1 DETAILS OF QUERY INVESTIGATED REGARDING ENERGY MANAGEMENT

S.No.	Question Investigated
1	Demographics of the respondents
2	Awareness level of respondents about energy management
3	Information about peak hours' unit
4	Awareness of advantage of using renewable energy resources
5	Specification of any renewable energy resource currently in use
6	Idea of energy consumption of electrical appliances
7	Idea of electricity load shedding pattern
8	Idea about the hours' of load shedding
9	Alternate source use in case of electricity load shedding
10	Time management criteria Vs routine chores
11	Idea about gas load shedding pattern
12	Idea about hours' of gas load shedding
13	Kitchen management criteria during gas load shedding
14	Awareness about high billing cost during peak hours
15	Awareness about energy saving initiatives
16	Participation interest in TV ads relating the energy management
17	Information about living room occupancy during night time
18	Information about responsibility to turn of fans and lights

2.5 Eliminating mischievous responses

In order to get stable and reliable results the survey questionnaire should be free from the different types of respondents like outliers, mischievous respondents, fake respondents etc. Either it is a paid survey questionnaire or unpaid there is always probability of having mischievous responses. To get the most accurate results and valid data an algorithm named as the distribution-free, sample-size- unconstrained, backward-stepping MR is applied here and two respondents were found to be mischevious [28]. For the data analysis and applied algorithm SPSS software and microsoft excel were used [10, 28, 29].

III. RESULTS AND DISCUSSIONS

The queries of this research deals with awareness level of respondents towards energy management. The scope of our research is Peshawar district mainly and targeted respondents are females which are mostly marginalized in society due to cultural, religious, social and other involving factors. To get an idea of female's interest level towards energy management a total of (18) questions are cross-examined. From Figure 4 it is deducted that average number of females are aware of the household energy management. 50% of the females wait for recovery of light to cover routine chores and about 47% of the females do the time management in case of electricity load shedding. Another important result is associated with the gas and electricity load shedding and alternate source used during these hours.

Figure 5 and Figure 6 enounces the fact that hours of load shedding in Peshawar district is maximum (04) hours and the alternate source used during gas load shedding is gas stove while that used during electricity load shedding is UPS. The results of closed ended questions are tabulated in Table 2, Table 3 and Table 4.

Fifty five percent of the females are aware of the peak hours' unit. 51% of the women are aware of high billing cost during peak hours. 54% of the respondents are aware of energy saving information provided on the utility bills, collectively these figures are clear indication of women role in the household energy management and the way she responds to energy changes as a result of blackout hours.

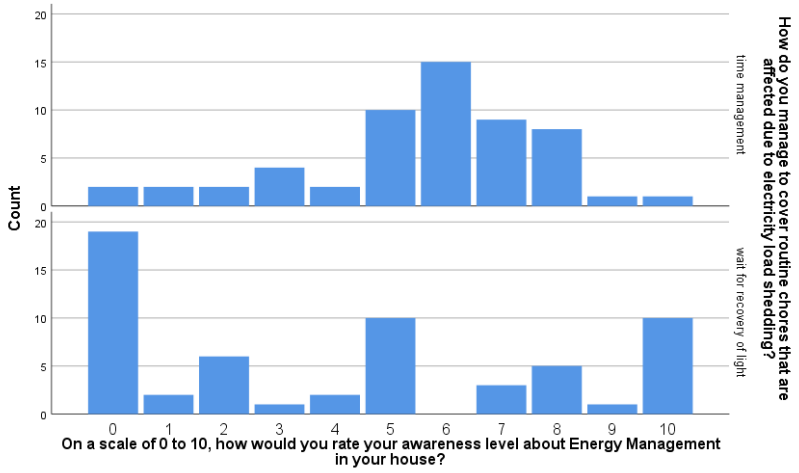

Figure 4. Comparison of awareness to energy management Vs. management of routine chores.

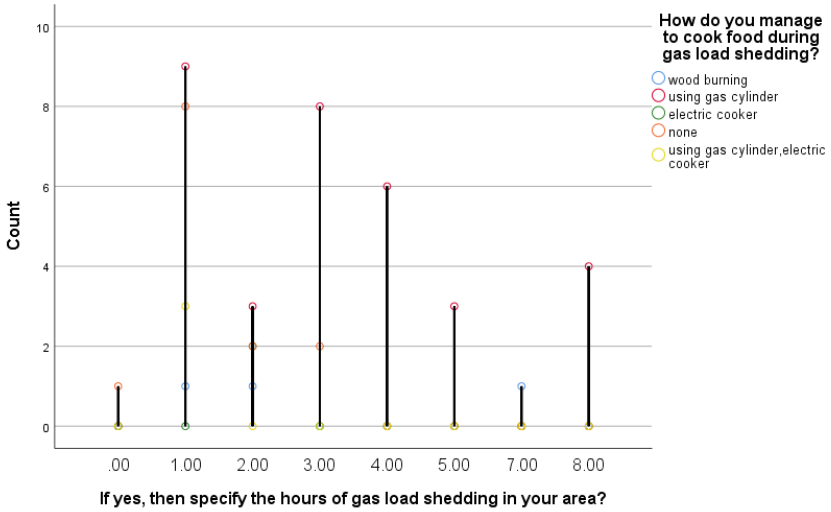

Figure 5. Hours of gas load shedding vs. alternate source used during load shedding

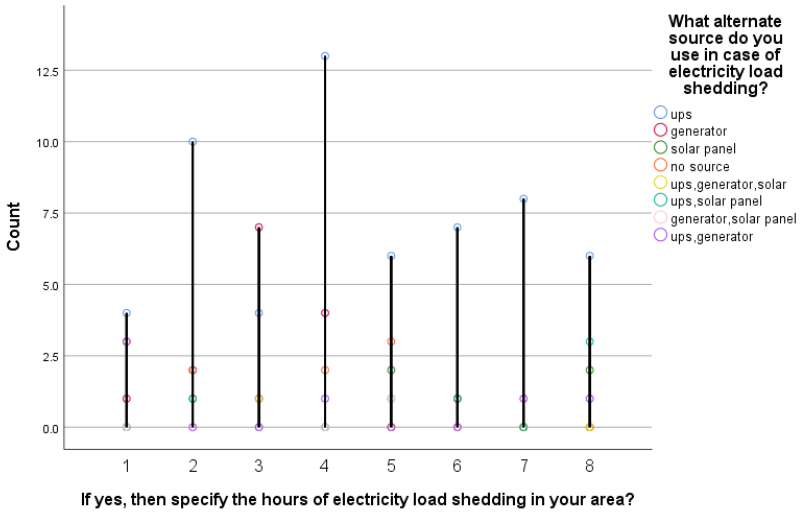

Figure 6. Hours of load electricity shedding vs. alternate source used during load shedding

TABLE 2 INFORMATION ABOUT PEAK HOUR'S UNIT

Do you know about the peak hour's unit?					
		Frequency	Percent	Valid Percent	Cumulative Percent
Valid	yes	68	55.3	55.3	56.8
	no	51	44.7	44.7	100.0
	Total	119	100.0	100.0	

TABLE 3 STATICS FOR THE AWARENESS OF HIGH BILLING COST PER UNIT OF ELECTRICITY

Are you aware of high billing cost per unit of electricity during the peak hours?					
		Frequency	Percent	Valid Percent	Cumulative Percent
Valid	yes	65	51.5	50.4	50.4
	no	54	48.5	49.6	100.0
	Total	119	97.7	100.0	
Total		119	100.0		

These results are also an indication of women working hours in the household with the elecricty and gas related chores, which indicates an indirect relation of females with the energy utilization and that is ultimately adding up into the economy of a nation.

TABLE 4 RESPONDENTS INFORMATION ABOUT ENERGY SAVINGS

Are you aware of energy saving information provided at the backside of utility bills?					
		Frequency	Percent	Valid Percent	Cumulative Percent
Valid	yes	72	54.5	55.8	55.8
	no	47	45.5	44.2	100.0
	Total	119	97.7	100.0	
Total		119	100.0		

CONCLUSION

Conclusions drawn from this survey research are women are aware of energy savings by doing proper management and wise decision making at households. This result is in line with a study that has already proved that the behavior of a person widely effects the household energy consumption [30]. Females are aware of hours of electricity and gas load shedding in their area so instead of waiting for electricity and gas recovery, women know how to manage routine chores. Women in the households also bear an idea of renewable energy resources but they are slowly moving towards renewables. Another positive indication by this research is that the females are aware of electricity consumption during the peak hours but an unexpected response against the same questions appears that 51.5% of the respondents know the high billing cost of electricity while 48.5% respondents denied to know the information about high billing cost. Again this 48.5% denial reveals the fact of keeping very low awareness of energy management at household level.

FUTURE WORK AND POLICY IMPLICATIONS

Before acquainting the policy suggestions, it is noticeable to know the limitations of this study. This sole study does not completely identify all the parameters which are accountable in energy management of household system. The religious norms are unquestionably the same for Muslims but demographics, psychographics and sociographic of Peshawar are quite different from those of other provinces like Punjab and Sindh therefore, similar study can have different emerging results from other parts of the country. Researchers are motivated to further dig deep into the gender, environment and energy nexus study within the other province of Pakistan and compare the results to come up with specified methodology and framework to evaluate the energy management practices at domestic sector. To find the missing links in the literature in between developing as well as developed nation relating gender, energy and environment studies.

This study has demonstrated very clearly that women's role in household energy management is remarkable and her efforts are uncountable. She is knowledgeable and it is necessary to integrate women's knowledge, skills, efforts and hard work into the society either explicitly-by doing job or implicitly- by better household management. Policy makers should not ignore the women's participation into the society as an essential tool for a successful developed nation by keeping in view the social, cultural and religious background of a homogenous society and this participation is not ignorable [29]. Policy makers are requested to raise the gender disparity issue on a forum and encourage women to participate in energy management schemes and educate women about the most updated and current technologies and their effective use which indirectly relates the energy use and energy saving. Researchers are encouraged to manipulate the gender inequality in society, energy consumption behavior and gender response to this behavior and household economy with different angles. For developing nations like Pakistan, it is necessary to conduct such research and make the women's participation as the strongest tool for the success of nation. In a challenging era where the world is moving towards the energy deprivation, the technical solutions are not enough to get rid of the underlying problems. The social value of energy and human behavior, needs an in depth study and understanding. Therefore, the researchers and policy makers ought to integrate social and behavioral aspects of energy consumers and move toward energy efficient and sustainable solutions of energy management.

AUTHOR CONTRIBUTIONS: Conceptualization: N.W.Q. and Z.R.A.; methodology: N.W.Q and Z.R.A.; software: N.W.Q. S.W.Q.; validation: N.W.Q. and Z.R.A.; formal analysis: N.W.Q. and S.W.Q.; writing—original draft preparation: N.W.Q. and S.W.Q.; supervision: Z.R.A.; project administration: Z.R.A.

CONFLICTS OF INTEREST

The authors declare no conflict of interest.

REFERENCES

[1] W. E. Forum. (2018, October 01). The Global Gender Gap Report. Available: http://www3.weforum.org/docs/WEF_GGGR_2018.pdf

[2] M. Kugelman and R. M. Hathaway, Powering Pakistan: Meeting Pakistan's Energy Needs in the 21st Century: Oxford University Press, 2009.

[3] M. Wakeel, B. Chen, and S. Jahangir, "Overview of energy portfolio in Pakistan," Energy Procedia, vol. 88, pp. 71-75, 2016.

[4] I. Hanif, "Economics-energy-environment nexus in Latin America and the Caribbean," Energy, vol. 141, pp. 170-178, 2017.

[5] J. P. K. Robert A. Ristinen Energy and the Environment, 2nd ed.: Wiley.

[6] R. Wilk, "Consumption, human needs, and global environmental change," Global environmental change, vol. 12, pp. 5-13, 2002.

[7] H. Wilhite Jr and R. Wilk, "A method for self-recording household energy-use behavior," Energy and Buildings, vol. 10, pp. 73-79, 1987.

[8] U. Offenberger and J. C. Nentwich, "Home heating and the co-construction of gender, technology and sustainability," Kvinder, Køn & Forskning, 2009.

[9] A. Rojas, F. Schmitt, and L. Aguilar, "Guidelines on Renewable Energy Technologies for Women in Rural and Informal Urban Areas," SanJose, Costa Rica: IUCN and ENERGIA http://genderand environment. org/resource/guidelines-on-renewable-energy-technologies-for-women-in-rural-andinformal-urban-areas, 2012.

[10] J. Thøgersen, "Housing-related lifestyle and energy saving: A multi-level approach," Energy Policy, vol. 102, pp. 73-87, 2017.

[11] W. Liu, G. Spaargaren, N. Heerink, A. P. Mol, and C. Wang, "Energy consumption practices of rural households in north China: Basic characteristics and potential for low carbon development," Energy Policy, vol. 55, pp. 128-138, 2013.

[12] A. Elnakat and J. D. Gomez, "Energy engenderment: An industrialized perspective assessing the importance of engaging women in residential energy consumption management," Energy Policy, vol. 82, pp. 166-177, 2015.

[13] E. Frederiks, K. Stenner, and E. Hobman, "The socio-demographic and psychological predictors of residential energy consumption: A comprehensive review," Energies, vol. 8, pp. 573-609, 2015.

[14] M. o. E. P. Division) and Hydrocarbon Development Institute of Pakistan, "Energy Year Book 2018," pp. 13-20, 2018.

[15] B. P. Michael, "The role of women in water resources management: the Tanzania case," International Journal of Water Resources Development, vol. 14, pp. 499-504, 1998.

[16] A. S. Permana, R. Perera, and S. Kumar, "Understanding energy consumption pattern of households in different urban development forms: A comparative study in Bandung City, Indonesia," Energy Policy, vol. 36, pp. 4287-4297, 2008.

[17] R. R. Wilk, "House, home, and consumer decision making in two cultures," ACR North American Advances, 1987.

[18] L. McClelland and S. W. Cook, "Energy conservation effects of continuous in-home feedback in all-electric homes," Journal of Environmental Systems, vol. 9, 1979.

[19] U. Offenberger and J. Nentwich, "Home heating, technology and gender: A qualitative analysis," in Sustainable energy consumption in residential buildings, ed: Springer, 2013, pp. 191-211.

[20] D. Ironmonger, Household production and the household economy, 2000.

[21] Y. He, B. O'Flaherty, and R. A. Rosenheck, "Is shared housing a way to reduce homelessness? The effect of household arrangements on formerly homeless people," Journal of Housing Economics, vol. 19, pp. 1-12, 2010.

[22] L. Karsten, "Housing as a way of life: Towards an understanding of middle-class families' preference for an urban residential location," Housing studies, vol. 22, pp. 83-98, 2007.

[23] S. Groh, S. Pachauri, and N. D. Rao, "What are we measuring? An empirical analysis of household electricity access metrics in rural Bangladesh," Energy for sustainable development, vol. 30, pp. 21-31, 2016.

[24] C. Hill, C. Corbett, and A. St Rose, Why so few? Women in science, technology, engineering, and mathematics: ERIC, 2010.

[25] R. McKenna, L. Hofmann, E. Merkel, W. Fichtner, and N. Strachan, "Analysing socioeconomic diversity and scaling effects on residential electricity load profiles in the context of low carbon technology uptake," Energy Policy, vol. 97, pp. 13-26, 2016.

[26] Pakistan Bureau of Statics Government of Pakistan, "PAKISTAN TEHSIL WISE FOR WEB CENSUS," p. 18, 2017.

[27] S. Salma, M. Shah, and S. Rehman, "Rainfall trends in different climate zones of Pakistan," Pakistan Journal of Meteorology, vol. 9, 2012.

[28] M. R. Hyman and J. J. Sierra, "Adjusting self-reported attitudinal data for mischievous respondents," International Journal of Market Research, vol. 54, pp. 129-145, 2012.

[29] A. S. Permana, N. A. Aziz, and H. C. Siong, "Is mom energy efficient? A study of gender, household energy consumption and family decision making in Indonesia," Energy research & social science, vol. 6, pp. 78-86, 2015.

[30] C. Wilson and H. Dowlatabadi, "Models of decision making and residential energy use," Annu. Rev. Environ. Resour., vol. 32, pp. 169-203, 2007.

IJEW 国际工程期刊 International Journal of Engineering Works انجینئرنگ کاموں کا بین الاقوامی جرنل

International Journal of Engineering Works
ISSN-p: 2521-2419
ISSN-e: 2409-2770
Vol. 7, Issue 09, PP. 293-297, September 2020
https://www.ijew.io/
https://doi.org/10.34259/ijew.20.709293297

Intrusion Detection System for SDN based IoT Devices using Deep Neural Network

Naqib Ullah[1], Dr. Abdus Salam[2]
[1,2]Abasyn University Peshawar
naqibullah14044@gmail.com[1]

Received: 16 August, Revised: 25 August, Accepted: 29 August

***Abstract*—** One of the emerging technologies in the field of networking is the Software Defined Networking (SDN). Since it is a centrally controlled networks, it provides us with a better control to improve the security within our network against the potential threats. In this work we are using Deep Neural Network (DNN) model to detect the flow-based anomaly within the network. The model was trained on NSL-KDD dataset and out of forty-one features only six of the most relevant features of NSL-KDD were used. The results show that Deep Learning approach shows some promising results in detecting the anomaly in the SDN environment.

***Keywords*—** Internet of Things, Software-defined networking, anomoly detection, machine learning

I. INTRODUCTION

Traditional Network Architectures have not changed much in the past decades but their use has exponentially increased. Providing the additional benefits like manageability, cost effectiveness, adaptability and being dynamic, Software Defined Networks (SDN) are emerging due to the dynamic applications of today's world [1]. SDN gives a higher degree of control to the programmers by decoupling control and data forwarding functions, hence enabling a better abstraction for applications. Due to the additional advantages OpenFlow and SDN is a centre of interest in both the industry and academic domains. Large enterprises and datacentres (e.g. Google B4, Huawei) are harnessing the promising advantages that SDN has to offer. A new market for SDN software providers like NOX, Floodlight and Ryu is also emerging. A variety of supporting hardware are also offered by mainstream vendors like HP, Cisco, Dell and Intel. The first communication interface standard between control and forwarding layer is OpenFlow protocol. In OpenFlow traffic of the network is identified using the concept of data flow. Counters are used to record information. Flow is referred to as IP packets having similar properties, that are passing from a specific point of observation. The dynamics of SDN makes it very venerable to attacks by foreign agents. Alongside, the decoupled control and centralized system architecture also makes it easy to detect and react to the attacks. As Kreutz states SDN contains seven threat vectors. Three of the seven vectors are related to the data control interface. A system named NIDS (Network Intrusion Detection System) guards the network against software attacks [2]. NIDS employs two strategies to detect network attacks. Among the two, the first one is signature-based detection. It uses a prebuilt data base for intrusion identification. Despite being unable to detect novel attacks, signature-based detection is the most common approach used. The second strategy uses a machine learning based approach, in this technique normal behaviour is compared with the new incoming data and the quantitative distance is used to detect anomaly. This strategy is referred to as anomaly-based detection and is able to detect zero-day attacks that system has not seen before. This second approach is usually combined with flow-based data monitoring system, when deploying NIDSs. Being based on packet header information, flow-based NIDSs has significantly less amount of data, if compared to payload-based NIDSs. Machine learning (ML) has been very popular in face detection and speech recognition but the domain of anomaly detection has not been explored extensively. Vern Paxson and Robin Sommer has described the factors that directly affects the use of ML in anomaly detection in networks [3-4]. Deep Learning is now emerging as a new standard for many of the computer science problems and is extensively in use for the vocal and visual data applications. Since deep learning offers the capabilities of corelating data, it displays itself as a potent standard for the upcoming generation of intrusion detections. Since the system can detect zero-day attacks, a high detection rate can easily be expected [5-8].

In this paper a flow-based intrusion detection using Deep Learning approach is proposed. We deploy a Deep Neural Network and use it for NIDS in the software defined network. The model is trained and tested using the NSL-KDD dataset. Optimal hyperparameters of the neural network are extracted by experimentation and performance results (false alarm rate and detection rate) are obtained. Performance accuracy of 75.75% is observed, which is a reasonable performance taking into consideration that only six network features were used.

Contribution:

1. Proposing a fully connected deep neural network for flow-based intrusion detection for IoT network.

2. The intelligent SDN orchestration is proposed that can monitor the network states globally for achieving better results.

Organization of the paper is as follows: section 2 displays related work; section 3 briefly explains the architecture of our deep learning model and introduces the NSL-KDD dataset; section 4 is dedicated to the performance analysis; section 5 states the conclusion and proposes our future work.

II. Related Work

The Flow based anomaly detection is particularly a centre of research now a days. Multi-layered Perceptron and Gravitational optimization-based algorithm was proposed by [11]. One-Class SVM (Support Vector Machine) was used for NIDS by [12], hence achieving a low false alarm rate. Anomaly detection systems in traditional networks are extensively studied and are applied to software defined networks. The privilege of programmability control in SDN is used by [13] to secure SOHO (Small Office, Home Office) network environments. Four of the most prominent anomaly detection algorithms are implemented in SDN using OpenFlow compatible switching and NOX controller. These detectors include Threshold Random Walk with credit-based rate limiting algorithm (TRW-CB), NETAD, Max. entropy detector and rate limiting algorithm. Experimentation has shown a significant improvement in accuracy, if compared to traditional Internet Service Provider (ISP) without introducing additional overhead on the network, especially for (SOHO) networks.

The will connected and centrally controlled architecture of SDN makes it venerable to DDoS (Distributed Denial of Services) attacks. The plot for DDoS attacks are to make the network resources scares for the potential user. The attack is attempted by two or more agents and launched to target application layer, control layer and infrastructure layer plane. These sorts of attacks are hard to identify but are easy to execute. DDoS are getting common due to the networks constructed by bots or machine containing malwares. [14] States the increase of DDoS attacks by 125.36% in one year in 2015. [15] Presents a light weight DDoS attack having 6-tuple features: Avg. duration per flow (ADF), Percentage of pair flow (PPF), Growth of single flow (GSF), Growth of Different Ports (GDP), Avg. bites per flow (ABF) and Avg. Packets per flow (APF). For calcification Self Organizing Maps (SOMs) are used. [16] proposes the combination of OpenFlow and s-Flow to effectively scale the intrusion detection and its mitigation. [17] uses the approach of combining the threshold detection and fuzzy inference system (FIS) for risk prediction of DDoS attacks. It uses three features for attack identification: Distribution of packet quantity per flow, interval time and flow quantity observed by the server. Other features are used by different researchers to improve detection accuracy.

We use Deep Neural Network for detection of the intrusion and the six basic features that we are using in order to detect the anomaly are as follows: srv_count, dst_bytes, count, src_bytes, protocol_type and duration. We are using simplex per-processing in SDN context, that makes our work different from the previous researchesThe will connected and centrally controlled architecture of SDN makes it venerable to DDoS (Distributed Denial of Services) attacks. The plot for DDoS attacks are to make the network resources scares for the potential user. The attack is attempted by two or more agents and launched to target application layer, control layer and infrastructure layer plane. These sorts of attacks are hard to identify but are easy to execute. DDoS are getting common due to the networks constructed by bots or machine containing malwares. [14] States the increase of DDoS attacks by 125.36% in one year in 2015. [15] Presents a light weight DDoS attack having 6-tuple features: Avg. duration per flow (ADF), Percentage of pair flow (PPF), Growth of single flow (GSF), Growth of Different Ports (GDP), Avg. bites per flow (ABF) and Avg. Packets per flow (APF). For calcification Self Organizing Maps (SOMs) are used. [16] proposes the combination of OpenFlow and s-Flow to effectively scale the intrusion detection and its mitigation. [17] uses the approach of combining the threshold detection and fuzzy inference system (FIS) for risk prediction of DDoS attacks. It uses three features for attack identification: Distribution of packet quantity per flow, interval time and flow quantity observed by the server. Other features are used by different researchers to improve detection accuracy.

We use Deep Neural Network for detection of the intrusion and the six basic features that we are using in order to detect the anomaly are as follows: srv_count, dst_bytes, count, src_bytes, protocol_type and duration. We are using simplex per-processing in SDN context, that makes our work different from the previous researches.

The above techniques perform well for small datasets. Nowadays, the IoT networks comprise of dynamic traffic generated from heterogeneous networks and it is not possible to detect the DDoS attacks from dynamic traffic. Thus, this study will use the DNN approach for improving the accuracy and reducing the FAR of highly dynamic IoT traffic. The proposed algorithm will be compared with the benchmark algorithm [15] using the Deep Neural Network (DNN) for intrusion detection.

III. Proposed Architecture

The proposed architecture is shown in Figure 3. The DNN algorithm will be implemented in the NIDS module in the SDN controller. The controller will have the global view of the network and will monitor the the states and traffic generated from the network. The network statistics will be forwarded to the SDN controller using the ofp_flow_stats_request request. The controller will forward the traffic to NIDS module that will correlate and analyze the forwarded traffic for network intrusion. The traffic forwarded from the SDN switches will be forwarded to the SDN controller that will be monitoring the

traffic using the DNN algorithm. If Intrusion detection is found in the traffic, it will be notified to the network administrator.

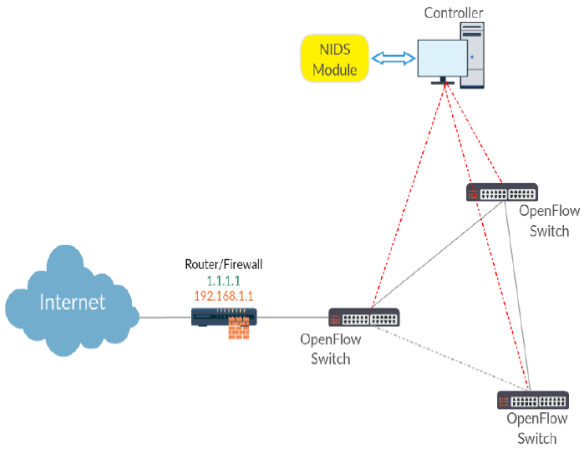

Figure 1. Proposed SDN-based architecture

IV. METHODOLOGY

a) Deep Learning Model

If we consider traditional machine learning model, important features are needed to be manually designed and then the system trains the model according to the provided features. In contrast to that deep learning multiple layers of features are automatically detected and are used to produce output. These features are hierarchically layered, which implies that features in later layers are discovered from previous layers. Our neural network is five layered networks containing three hidden layers and two input/output layers as shown in Fig.1. It has six input dimensions and two output dimensions. Hidden layers have twelve, six and three neurone layers respectively. Batch size of 10 and 100 epoch are used for model initialization. Learning rate is concluded after experimentation. The architecture of neural network can be seen in figure 1.

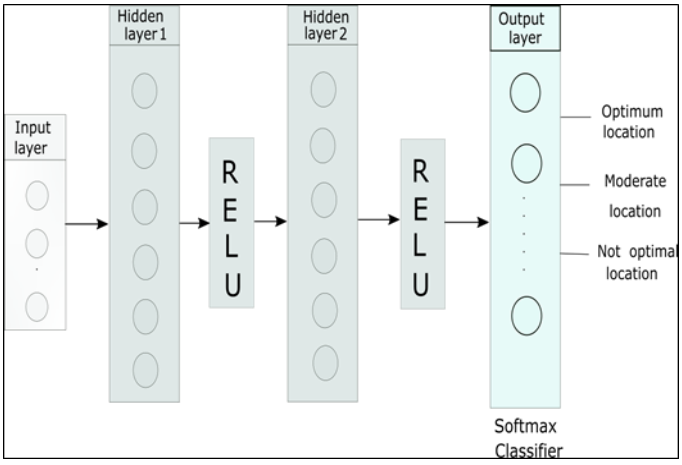

Figure 2. Architecture for Deep neural network

b) Dataset

NSL-KDD dataset is the perfect representation for the current real-world networks. The dataset was proposed for a data mining competition KDD Cup in 1999 [18]. It is used as a standard for NIDS benchmark for software defined networks in research, hence providing us with an ability to compare our performance with the previous work. KDDTrain+ contains 125,973 samples and 22,554 network traffic samples are available for KDDTest++. Each sample is defined by forty-one feature vector, that are divided into three following types: basic features, content- based features, traffic-based features. Similarly, attacks are also divided into for separate categories according to their characteristics. Table 1 describes the categories. Detection task is made more realistic due to the lack of some categories in the training dataset. Out of the forty-one available features in NSL-KDD Dataset six above mentioned features are used for our model. These features are traffic-based basic features that can be easily obtained in an SDN environment and are described in Table 2.

c) SDN-Based IDS Architecture:

As displayed in Fig.2 we proposed an SDN-based NIDS architecture. As the figure shows NIDS module is implemented inside the controller. As all the switch activity is monitored by the controller, we can leverage the global overview of the network for detecting the intrusions and anomalies in the network. In order to request the network statistics a request message of ofp_flow_stats_request is sent from controllers to all OpenFlow switches. A ofp_flow_stats_reply message is sent back to the controller that contains all the statistics. The centralized architecture is the key feature of the network that is put into use for analysing and detecting network intrusions. In case of a anomaly in the network flow table is modified in order to mitigate the intrusion and security policies are sent to the switches for the intrusion prevention.

V. PRELIMINARY EXPERIMENTAL RESULTS

1. Evaluation Metrices

The criteria for the performance evaluation are accuracy (AC), recall (R), precision (P) and F-measure (F). The target is to get high accuracy and detection rate while keeping the false alarm rate low. We use confusion matrix to converge to these parameters. True Positive (TP) and True Negatives (TN) refer to correctly classified attack and normal records. Similarly, False Positive (FP) and False Negative (FN) are the number of attacks and normal records incorrectly classified.

- The percentage of True detection is referred to as Accuracy (AC):
- Precision (P) is the ratio of True Positives with the total number of detections by the system:
- The percentage of predicted intrusion compared to all intrusions is displayed using Recall (R):

- F-measure (F) is for an improved measure of accuracy for NIDS, considering both the precision and recall:

2. Experimental Results

NIDS is initially implemented for two-way classification. Model performance is dependent on the initial hyperparameters. After optimizing the hyperparameters we obtained the optimal classification. Learning rate was varied by the following range {0.1, 0.01, 0.001, 0.0001}. The goal was to maximise the accuracy. Table I below, displays a comparison of accuracy for training phase and testing phase. We can observe accuracy has directly proportional relation with the learning rate respectively. While in testing phase the learning rate of 0.001 performs better than the learning rate of 0.0001. The reason is the model will be overfitted due to the very small learning rate. Hence, 0.0001 is the choice for the learning rate, so the generalizability of the model is not compromised. As a result, new intrusions could be caught by the system.

We also calculated precision, recall and f-measure of the model. The performance was evaluated using the provided test data, which is displayed in the Table II. It can be observed that the best results are obtained with 0.001 learning rate. Evaluation metrices are grown as we decrease learning rate from 0.1 to 0.001 but the performance deteriorates as it is further decreased to 0.0001.

TABLE I. ACCURACY FOR DIFFERENT LEARNING RATES

Learning rate	Train data Accuracy (%)	Test data Accuracy (%)
0.1	89	73
0.01	91	75
0.001	93	76
0.001	95	77

TABLE II. METRICS FOR DIFFERENT LEARNING RATES

Learning rate	Precision (%)	Recall (%)	F1-score
0.1	80	73	73
0.01	83	75	75
0.001	85	76	77
0.001	86	77	78

Comparison of our results with other machine learning algorithms was also conducted. As in [15] six features (APF, ABF, ADF, PPF, GSF and GDP) for DDoS were used and false alarm rate of 0.46% and detection rate of 99.11% was extracted. Results from our system were low if compared to their systems because of the features that we have selected for testing and training. The features that they have selected directly targets detection of DDoS attacks while we opted for the six very basic features. The future goal is to apply six features to our model for further evaluation. [10] uses machine learning algorithm using forty-one training and testing features.

TABLE III. ACCURACY COMPARISION WITH BENCHMARK

Algorithms	Precision (%)
SVM	74
Decision tree	76
Proposed DNN	85

Results of these experiments show the performance evaluation of these algorithm. As can be observed in Table III DNN approach performs best compared to benchmark algorithmns. It can be observed that Deep learning algorithms perform better than other algorithms. Our system performs more accurately, giving us low false positive if compared with other algorithms. Hence our system (DNN approach) is capable of genializing the characteristics of the network with reasonable accuracy using fewer number of features

CONCLUSION

The paper evaluates NIDS and implements deep learning algorithm for network intrusion detection. Despite our results not begin reliable enough for commercial purposes, our system yields significant advantages in certain areas and have scope for further improvements. Our paper shows the potential for deep learning in flow-based anomaly detection. Deep learning approach also has potential in the context of SDN, due to the centralized design of SDN. A deep learning model can easily extract real time basic features from the network controllers and analyse them. We plan to propose other types of features in order to improve our accuracy. The architecture of SDN gives us flexibility to use specific features for particular types of attacks, for example DDoS to increase the accuracy of NIDS. We will try to tune our DNN model for better performance and apply this approach to real SDN networks to extract the latency and throughput performances.

REFERENCES

[1] "Software Defined Networking Definition," Available:https://www.opennetworking.org/sdn-resources/sdn-definition,[Accessed 04 Jul. 2016].

[2] N. McKeown, T. Anderson, H. Balakrishnan, G. Parulkar, L. Peterson,J. Rexford, S. Shenker, and J. Turner, "Openflow: enabling innovation in campus networks," ACM SIGCOMM Computer Communication Review, vol. 38, no. 2, pp. 69–74, 2008

[3] S. Jain, A. Kumar, S. Mandal, J. Ong, L. Poutievski, A. Singh, S. Venkata, J. Wanderer, J. Zhou, M. Zhu et al., "B4: Experience witha globally-deployed software defined wan," ACM SIGCOMM Computer Communication Review, vol. 43, no. 4, pp. 3–14, 2013.

[4] C. T. Huawei Press Centre and H. unveil world's first commercial deployment of SDN in carrier networks, "[online]. available: pr.huawei.com/en/news/hw-332209-sdn.htm."

[5] N. Gude, T. Koponen, J. Pettit, B. Pfaff, M. Casado, N. McKeown, and S. Shenker, "Nox: towards an operating system for networks," ACM SIGCOMM Computer Communication Review, vol. 38, no. 3, pp. 105–110, 2008.

[6] "Ryu," Available: http://http://osrg.github.io/ryu/.

[7] "Floodlight," Available: http://www.projectfloodlight.org/.

[8] D. Kreutz, F. Ramos, and P. Verissimo, "Towards secure and dependable software-defined networks," in Proceedings of the second ACM SIGCOMM workshop on Hot topics in software defined networking.ACM, 2013, pp. 55–60.

[9] R. Sommer and V. Paxson, "Outside the closed world: On using machinelearning for network intrusion detection," in 2010 IEEE symposium onsecurity and privacy. IEEE, 2010, pp. 305–316.

[10] M. Tavallaee, E. Bagheri, W. Lu, and A.-A. Ghorbani, "A detailed analysis of the kdd cup 99 data set," in Proceedings of the Second IEEE Symposium on Computational Intelligence for Security and Defence Applications, 2009.

[11] Z. Jadidi, V. Muthukkumarasamy, E. Sithirasenan, and M. Sheikhan,"Flow-based anomaly detection using neural network optimized with gsa algorithm," in 2013 IEEE 33rd International Conference on Distributed Computing Systems Workshops, 2013, pp. 76–81.

[12] P. Winter, E. Hermann, and M. Zeilinger, "Inductive intrusion detection in flow-based network data using one-class support vector machines,"in New Technologies, Mobility and Security (NTMS), 2011 4th IFIPInternational Conference on. IEEE, 2011, pp. 1–5.

[13] S. A. Mehdi, J. Khalid, and S. A. Khayam, "Revisiting traffic anomaly detection using software defined networking," in International Workshop on Recent Advances in Intrusion Detection. Springer, 2011, pp. 161–180.

[14] "Q1 2016 State of the Internet / Security Report," Available: https://content.akamai.com/PG6301-SOTI-Security.html, [Accessed 07Jul. 2016].

[15] R. Braga, E. Mota, and A. Passito, "Lightweight ddos flooding attackdetection using nox/openflow," in Local Computer Networks (LCN),2010 IEEE 35th Conference on. IEEE, 2010, pp. 408–415.

[16] K. Giotis, C. Argyropoulos, G. Androulidakis, D. Kalogeras, and V. Maglaris, "Combining openflow and sflow for an effective and scalable anomaly detection and mitigation mechanism on sdn environments," Computer Networks, vol. 62, pp. 122–136, 2014.

[17] P. Van Trung, T. T. Huong, D. Van Tuyen, D. M. Duc, N. H. Thanh, and A. Marshall, "A multi-criteria-based ddos-attack prevention solution using software defined networking," in Advanced Technologies forCommunications (ATC), 2015 International Conference on. IEEE,2015, pp. 308–313.

[18] "KDD Cup 1999," Available: http://kdd.ics.uci.edu/databases/kddcup99/,[Accessed 04 Jul. 2016].

IJEW 国际工程期刊 International Journal of Engineering Works انجینئرنگ کاموں کا بین الاقوامی جرنل

International Journal of Engineering Works
ISSN-p: 2521-2419
ISSN-e: 2409-2770
Vol. 7, Issue 09, PP. 298-304, September 2020
https://www.ijew.io/
https://doi.org/10.34259/ijew.20.709298304

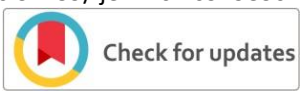

Economic Dispatch Solution for Generating units through Optimization

Muhammad Nazeer[1], Shazmina Jamil[2], Mohsin[3], Jibran Ullah Khan[4]
[1,2,3,4] Department of Electrical Energy System Engineering, US-Pakistan Center for Advanced Studies in Energy (US-PCASE), UET Peshawar
muhammadnaxeer@gmail.com[1], shazminajamil@yahoo.com[2], malakmohsin5533@gmail.com[3], jibrank787@gmail.com[4]
Received: 31 August, Revised: 07 September, Accepted: 15 September

***Abstract*—** The complex nature of the modern power system is because of the interconnection of the generating units and day by day increased load demand. The main purpose of the power system is to tantalize the load needs and generate reliable and cheap energy i.e. cost of generation should be optimum i.e. operating every generating unit in such a way to optimize the cost. The cost function of every generating unit is different from other generating unit, so load has to be divided among various generating units to obtain optimum generation. The optimization of power system is done by Economic load dispatch (ELD). ELD is of immense importance in power system operation and planning (PSOP). The primary purpose of ELD is to pacify the load needs at lowest cost while satiating all kind of equality and inequality constraints. Power system has highly non-linear input output characteristics because of different generation constraints. In ELD cost function of each and every generating unit is equated as quadratic function. Numerous methods have been devised to figure out ELD problem incorporating conventional methods like Lambda iteration method and Gradient method, and artificial intelligent method like Particle Swarm Optimization, Generic Algorithms etc.

In this thesis optimization of generating units is done through General Algebraic Modelling System (GAMS). GAMS is a modelling system used for mathematical programming and optimization on a large scale. It helps to develop a mathematical model similar to their corresponding mathematical expression and gives more accurate results.

Keywords— Optimization, ELD, GAMS.

I. INTRODUCTION

The one and only single most extremely important objective of the power system is to dispatch reliable and cheap energy to its consumer. In order to achieve that goal economic load dispatch (ELD) is very critical factor in power system operation and planning. Economic load dispatch is stated as the practice for the allocation of load to the generating units in order to satisfy the load demand in such a way to minimize the cost of energy generation while all the constraints either equality or inequality constraints are satisfied. In other words, it helps to achieve optimum generation schedule for every generating unit in power system.

In the beginning the economic load dispatch concept was developed to cater different load variations in a given period by running most efficient unit first until it reaches its maximum limits, after that second most efficient unit starts increasing its generation to pacify the load requirements in case of load increasing during peak hours' duration until its maximum range is reached, and so next most efficient unit will start increasing its generation and so on, the drawback of this logic was that was that the cost of operation increased as during light load hours the units were running at their lower efficiency causing more problems [1]. After that lots of approaches have been developed to figure out economic load dispatch problem. The traditional approach to figure out economic load dispatch problems are lambda iteration method, Newton Raphson method and gradient method, Participation Factor Method and Base Point Method [2]. The problem related to these methods are such that they used only for those generating whose fuel-cost characteristic curve is linear and increases in a monotonic way this leads to extremely high operating cost as because of different constraints the input/output characteristics is non-linear in nature [3]. The effective way to solve the ELD problem in an accurate way is to have the smoothly increasing and continuous nature of the cost curve [4]. Highly intelligent algorithms are used to solve constrained economic load dispatch problem which includes Particle Swarm Optimization, Genetic Algorithms (GA), Evolutionary programming, neural networks, Hopfield neural networks [5]. Some of these methods can result in slow convergence except Particle Swarm Optimization [6].

Different constraints such as transmission losses, load demand balance, quadratic nature of a cost functions, and valve point loading effect made the economic load dispatch

problem a nonlinear optimization problem in a power system operation and planning, conventional methods are not able to solve such a nonlinear problem so for that different techniques have been developed to figure out such complex problem while handling these constraints in order to get real time results [7].Further development in the solution of Economic load dispatch of thermal power unit have been made by considering the optimum amount of heat release, for that purpose different Heuristics and meta Heuristic techniques have been developed [8]. Optimum emission of flue gases in the air in order to maintain the environment clean and free from the oxides of carbon, sulphur and nitrogen [9]

In this proposed thesis Economic Load Dispatch is done through General Algebraic Modelling System (GAMS). GAMS helps to develop mathematical programming in a same way as that of system mathematical expression and performs the function of the optimization of linear, Non-linear and mixed integrals. GAMS used for a large scale optimization techniques and gives most accurate results.

II. RELATED WORK

Lots of work has been done on Economic load dispatch ranging from small scale to a large scale power system optimization. In this regard some of the work is mentioned here as a literature study.

In [10] a multi objective meta heuristic approach for dynamic ELD problem using multi objective PSO (MOPSO). Emission constrained Economic Load Dispatch problem is solved using differential evolution (DE), [11]. A comparative analysis of Genetic approach based on arithmetic crossover with the enhanced Hopfield Neural Network, Fuzzy logic controlled Genetic Algorithms (FLCGA) and advance Hopfield Neural Network, [12].

A Hybrid technique consisting Genetic Algorithm as an optimizer and SQP used for tuning purpose [13]. Θ-Particle swarm optimization technique is applied for optimization by changing traditional PSO to Θ-PSO by using phase angle vector [14].Another variant of PSO approach known as Adoptive PSO has been developed and implemented [15].A Heuristic approach consisting of Iteration PSO associated with variable acceleration coefficient by choosing a proper penalty factor [16]. In [17] above approach is used for combined heat power economic dispatch (CHPED) problem.

Artificial Immune System (AIS) based on evolutionary techniques and colonel selection approach [18]. An Encoding technique based on Genetic Algorithms used for global optimization [19]. A Hybrid Harmony Search (HHS) technique based on Swarm approach meta-heuristic algorithm for the optimization [20]. Other variant of HHS, which is tournament based THS [21].

An iterative PSO developed to get optimum scheduling of power, [22].In [23] Gravitational Search Algorithm related to law of gravity and mass interaction for the optimization. A hybrid system consists of PSO and SQP is used for optimization [24].

Hybrid approach consist of PSO, Gaussian probability distribution functions and chaotic sequence for power system optimization [25]. A hybrid system of GA with SQP and IPA (interior point algorithm) with their nine variants are implemented for optimization of thermal generating units [26]. In [27] a hybrid technique called Estimation of Distribution and Differential Evolution developed. Another variant of Differential evolutionary approach is developed which include restoration process in case if the constraints are disobeyed [28]. A self-adaptive DE along with GE is implemented for the solution of dynamic economic load dispatch problem [29]. DE practice is implemented on the optimization of thermal power plant along with the integration of renewable energy resource including wind energy in order to solve the combined economic emission dispatch [30].

A meta-heuristic approach based on the insect's casual nature like Cuckoo and Levy have been developed known as Cuckoo Search Algorithms (CSA), [31]. In [32] and [33] a detailed review of different modifications of Cuckoo algorithms discussed for the purpose of optimization and its significance in the research. to solve this complex nature of ELD a cuckoo algorithm is implemented [34].A variant of firefly algorithm (MFO) is implemented in [35] for optimization and a comparative analysis is made based on results with different algorithms used in a literature. A multi objective evolutionary technique called chemical reaction optimization has been implemented on DELD, the convergence of presented method is improved by hybridization with differential evolution to get rid of local minima [36].

In [37] different techniques and their hybrid combination based on different has been reviewed and addressed the complexity related to every computational techniques. A review of different hybrid approaches developed for the solution combined economic emission dispatch problem [38]. Another method known as flower pollination Algorithm is used to solve multi objective function of combined economic emission [39].A quadratic programming approach is presented and compared with different approaches like GAMS, GA, PSO and ED and also with hybrid technique consist of GA, ED and PS [40]. A Moth Flame Optimization (MFO) technique in [41]. A hybrid approach consist of Nelder Mead and pattern search algorithm in which the former performs the function of optimization and the later used to find the best optimum solution [42].An algorithm based technique known as Social Spider Optimization and its later version (SSSO and ISSO) is implemented in [43]. In [44] SSO is implemented on five models for constrained ELD problem. In [45] a modification of OLC called OLC swarm presented as optimization technique.

In [46] a modified HNN method uses two different practices to solve ELD problem in order to minimize the computational time. Differential Evolutionary approach is

implemented and results shown compatibility to those obtained by MHNN and MPSO [47]. The combined heat and power (CHP) day ahead optimization to improvise optimum cost and heat dissipation developed applied on two models which are Electric storage system and thermal storage system [48].Extension classical Bat Algorithm known as chaotic Bat Algorithm has the issue that operator has to tune the model in order to get the feasible results [49].An evolutionary approach known as Backtracking Search Algorithms is applies in [50] for optimization purpose. A Meta heuristic approach Grey wolf optimization approach is developed, [51]. In [52] Grey wolf optimization is used for solution of dynamic economic load. Exchange Market Algorithm to achieve globally optimized region [53]. A crisscross optimization approach is developed for optimization on large scale basis of generating units and to achieve better performance [54].

A comparison is made between General Algebraic Modelling System (GAMS) and the quadratic Programming is presented [55] and in [56] optimization is carried out through GAMS, initially ELD was solved using PWL and SOS algorithms which were unable to give optimum schedule for power system. An optimization for the dynamic economic load dispatch is done through GAMS, in results GAMS shown the upper hand over the other available approaches [57].

III. METHODOLOGY

In this paper, Optimization of different generating units is carried out using GAMS as optimization tool on different case studies along with load and generation profiling.

Case 1: this case study includes 26 generating units.

Case 2: Total of 35 generating units are used for optimum scheduling of different generating units.

A. generalAlgebric Modelling system

General algebraic modelling system commonly known as GAMS is a high level mathematical programming tool used to solve mathematical models according to the mathematical expressions of that model. Used by both commercial areas and academic institutions in different areas of research for optimization purposes varies from production planning to economic modelling. GAMS is developed to solve linear, nonlinear and mixed integral optimization problem. The basic coding structure of the GAMS comprises Sets, Data, Variable, Equations, Model and solve statement, Output. Different constraints and cost functions of generating units are given in the form of table.

TABLE I. UNITS CONSTRAINTS AND COST FUNCTION COEFFICIENTS.

Sr. No	Unit name	p_{max} (MW)	p_{min} (MW)	c_i	b_iP ($/MW)	a_iP^2 ($/MW^2)
1	G1	2170	217	2001.32	7.1	0.00277
2	G2	2402	520.5	2202.55	7.97	0.00313
3	G3	1638	350.7	1794.53	6.66	0.00284
4	G4	1370	274	1785.96	6.63	0.00298
5	G5	680	250	1247.83	7.97	0.00313
6	G6	665	222	1249.9	7.95	0.00313
7	G7	1320	264	1755.55	7.69	0.00294
8	G8	1292	274	1801.25	8.01	0.00125
9	G9	2200	450	2855.32	7.93	0.00235
10	G10	1320	374	1798.25	6.75	0.00196
11	G11	1320	375	1815.32	5.12	0.00149
12	G12	1320	256	1915.32	6.64	0.00155
13	G13	1320	275	1720.55	9.60	0.00160
14	G14	1320	200	1650.56	8.66	0.00187
15	G15	1320	295	2390.52	6.12	0.00785
16	G16	600	200	1113.4	8.5	0.00421
17	G17	660	254	1728.3	9.15	0.00708
18	G18	600	180	1285.25	8.25	0.00902
19	G19	450	195	635.5	11.154	0.00515
20	G20	330	99	287.71	8.03	0.00357
21	G21	330	135	455.76	6.6	0.00573
22	G22	330	110	391.93	7.01	0.00492
23	G23	1036	230	1247.15	8.15	0.00333
24	G24	727	250	460.32	7.26	0.00526
25	G25	216	100	107.87	8.95	0.0001
26	G26	175	50	222.21	6.45	0.0016
27	G27	3478	575	3354.96	14.36	0.00014
28	G28	1410	282	1954.96	8.8	0.00378
29	G29	1410	220	1830.85	7.8	0.00222
30	G30	1450	290	1949.72	9.18	0.00122
31	G31	669	134	969.8	7.05	0.00766
32	G32	121	24.2	694.26	4.84	0.00841
33	G33	96	20	278.16	4.18	0.00766

34	G34	500	125	766.32	6.8	0.00345
35	G35	1310	275	1550.32	6.78	0.00245

IV. RESULTS

The research work comprises of total 35 generating units to be economically dispatched in order to get the inexpensive energy from the traditional power system. in this work two case studies have been carried out on with 26 generting units and other with 35 generting units. The results are shown in the form of tables and graphs.

A. Optimization of 26 unitss at 15000MW load demand.

In this section the optimization of 26 generating units dispatched in order to meet the load of 15000 MW load including losses associated with power system is discussed. Table below shows the results of how much power should be generated from each unit on the basis of the cost function of individual generating unit given in table below.

Negative value of marginal cot shows that the unit is hitting the maximum range so its marginal cost will be less than that of the system marginal cost by an incremental cost of the unit. Zero or EPS shows that the generating unit is operating within the allowable range of generation so its incremental cost will be same as that of system marginal cost, the positive value shows that the generating unit is operating at its minimum allowable range of generation limit, so its marginal cost should be greater than that of system marginal cost by incremental cost of the generating units.

TABLE II. UNIT'S DISPATCHED GENERATION AND INCRIMENTAL COSTS

Unit	Generation (MW)	incremental cost $/MWh
g26	175	-4.21676630288306
g25	216	-2.23974630288306
g11	1320	-2.18366630288306
g22	330	-0.980066302883063
g21	330	-0.855466302883062
g20	330	-0.851066302883062
g12	1320	-0.505266302883063
g13	511.645719650957	0
g1	766.160426459827	EPS
g2	521.927524422215	EPS
g3	805.856743465328	EPS
g4	773.031258872997	EPS
g5	521.927524422215	EPS
g6	525.122412601128	EPS
g7	603.27658212297	EPS
g8	1290.90652115323	EPS
g9	703.673681464482	EPS
g10	1144.7107915518	EPS
g14	689.108637134509	EPS
g15	325.940528846055	EPS
g16	325.091009843594	EPS
g23	463.553498931391	EPS
g24	378.067139057326	EPS
g18	180	0.259933697116937
g17	254	1.50937369711694
g19	195	1.92523369711694

The table below gives the system marginal cost and the totl generation cost in order to meet the total load demand.

TABLE III. SYSTEM MARGINAL AND TOTAL GENERAATION COST

Load (MW)	System marginal cost	Generation (MW)	Total cost of generation in $
15000	11.237266302883 1	15000	173065.176140 111

The graphical representation shows the results from most economical generating unit at left and most expensive unit at right of the graph shown in Fig below.

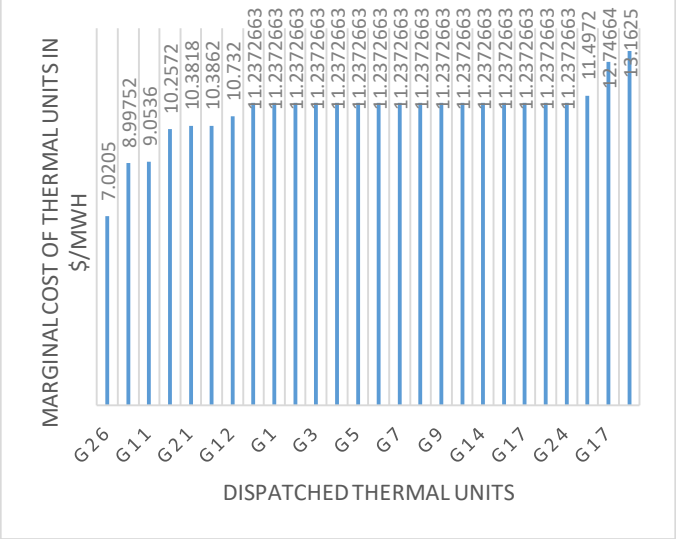

Figure 1. Units marginal cost.

B. Optimization of 35 unitss at 15000MW load demand.

Total of 35 generating units are used for optimum scheduling of these plants. The load along with losses is taken as the load demand 26359 MW. In below gives the optimum scheduling of the generating unit is illustrated.

The table below gives the optimum scheduelling nd incremental cost of each generating units.

TABLE IV. UNIT'S DISPATCHED GENERATION AND INCRIMENTAL COSTS

Unit name	Generation (MW)	Unit marginal cost
g33	96	-7.60739449154909
g32	121	-6.38289449154909
g26	175	-6.23761449154909
g25	216	-4.26059449154909
g11	1320	-4.20451449154909
g34	500	-3.00811449154909
g22	330	-3.00091449154909
g21	330	-2.87631449154909
g20	330	-2.87191449154909
g31	669	-2.78283449154909
g12	1320	-2.52611449154909
g8	1292	-2.01811449154909
g10	1320	-1.33371449154909
g6	665	-1.14521449154909
g5	680	-1.03131449154909
g30	1450	-0.54011449154909
g35	1310	-0.0591144915490904
g1	1140.39157250909	0
g13	1143.16077860909	EPS
g14	1229.44237741954	EPS
g15	454.656973984018	EPS
g16	565.096732963075	EPS
g17	290.121079911659	EPS
g18	277.611668045959	EPS
g19	204.282960344572	EPS
g2	844.746723889631	EPS
g23	766.984157890254	EPS
g24	570.162974481853	EPS
g28	589.697684067334	EPS
g29	1229.30506566421	EPS
g3	1161.639875272	EPS
	73	
g4	1112.09974690421	EPS
g7	946.958246862009	EPS
g9	1133.64138118066	EPS
g27	575	1.26288550845091

The table below gives the system marginal cost and the total cost of generation.

TABLE V. SYSTEM MARGINAL AND TOTAL GENERAATION COST

Load (MW)	**System marginal cost**	**Generation (MW)**	**Total generation cost in $**
26359	13.2581144915491	26359	313223.669360519

The graphical representation of each generating unit's marginal cost is give as,

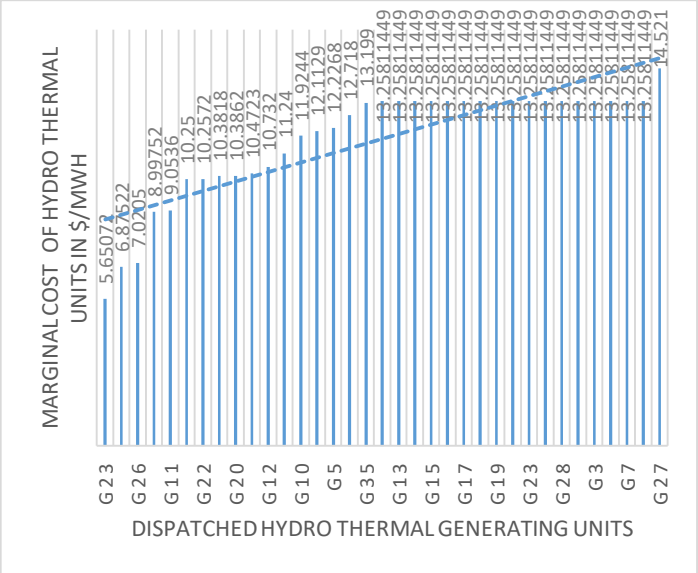

Figure 2. Units marginal cost.

CONCUSLION

One of the main objective of the power system is to provide cheaper and uninterrupted energy to its consumer and to reduce losses in associated with power system by economically dispatching generating units in a power system in order to meet the load requirements which should financially benefit both the generating utility and energy consumers. General Algebraic Modelling System is one of the most efficient and mathematical programming software for the optimization on large scale in which mathematical algorithm is defined based on the mathematical expressions of the system. GAMS used for the optimization purpose on a large

scale system is one of the easy software platform is user friendly, easy handling and takes less time for the execution of program and gives best results. Different scenarios for optimization of Pakistan power system is discussed in this work including optimum dispatching. At the end, results shown the dispatching of hydro-thermal generating units available in the research studies gives the most economical solution for optimization problem.

Future work on this area of study can be done by considering multi-objective function associated with power system. Research can be extended for the optimization of power system along with different constraints associated with unit commitment such as ramp rates etc. further extension can be made to consider the optimal power flow scenario for power system. Due to rapid trend towards renewable sources, Integration of renewable energy sources with the classical power system is one of the complex job. So solution can be developed for the optimum dispatching and integration of renewable energy resources with conventional grids.

REFERENCES

[1] T. Phase et al., "University of Nairobi School of Engineering Department of Electrical and Information Engineering," no. 100, 2015.

[2] P. Systems and E. Drives, "ANALYSIS AND COMPARISON OF ECONOMIC LOAD DISPATCH USING GENETIC ALGORITHM AND Master of Engineering," no. July, 2011.

[3] "SOULTION TO CONSTRAINED ECONOMIC LOAD DISPATCH SOLUTION TO CONSTRAINED ECONOMIC LOAD Department of Electrical Engineering National Institute of Technology Rourkela-769008 (ODISHA) May-2013."

[4] B. Sahu, A. Lall, S. Das, and T. Manoj Kumar Patra, "Economic Load Dispatch in Power System using Genetic Algorithm," Int. J. Comput. Appl., vol. 67, no. 7, pp. 17–22, 2013.

[5] P. Control, "Particle Swarm Optimisation Applied To Economic," Electr. Eng.

[6] E. Engineering, "Economic Load Dispatch for Ieee 30-Bus System Using Pso," pp. 1–40.

[7] C. Kuo, "A novel string structure for economic dispatch problems with practical constraints," Energy Convers. Manag., vol. 49, no. 12, pp. 3571–3577, 2008.

[8] M. Nazari-heris, B. Mohammadi-ivatloo, and G. B. Gharehpetian, "A comprehensive review of heuristic optimization algorithms for optimal combined heat and power dispatch from economic and environmental perspectives," Renew. Sustain. Energy Rev., no. April, pp. 1–16, 2017.

[9] Y. A. Gherbi, H. Bouzeboudja, and F. Z. Gherbi, "The combined economic environmental dispatch using new hybrid metaheuristic," Energy, vol. 115, pp. 468–477, 2016.

[10] H. Shayeghi and A. Ghasemi, "IJTPE Journal APPLICATION OF MOPSO FOR ECONOMIC LOAD DISPATCH SOLUTION WITH TRANSMISSION LOSSES," Int. J., no. March, pp. 27–34, 2012.

[11] A. A. Abou El Ela, M. A. Abido, and S. R. Spea, "Differential evolution algorithm for emission constrained economic power dispatch problem," Electr. Power Syst. Res., vol. 80, no. 10, pp. 1286–1292, 2010.

[12] T. Yalcinoz, H. Altun, and M. Uzam, "Economic dispatch solution using a genetic algorithm based on arithmetic crossover," 2001 IEEE Porto Power Tech Proc., vol. 2, no. 4, pp. 153–156, 2001.

[13] D. kuo He, F. li Wang, and Z. zhong Mao, "Hybrid genetic algorithm for economic dispatch with valve-point effect," Electr. Power Syst. Res., vol. 78, no. 4, pp. 626–633, 2008.

[14] V. Hosseinnezhad and E. Babaei, "Electrical Power and Energy Systems Economic load dispatch using h -PSO," Int. J. Electr. POWER ENERGY Syst., vol. 49, pp. 160–169, 2013.

[15] B. K. Panigrahi, V. R. Pandi, and S. Das, "Adaptive particle swarm optimization approach for static and dynamic economic load dispatch," vol. 49, pp. 1407–1415, 2008.

[16] B. Mohammadi-ivatloo, A. Rabiee, A. Soroudi, and M. Ehsan, "Electrical Power and Energy Systems Iteration PSO with time varying acceleration coefficients for solving non-convex economic dispatch problems," Int. J. Electr. Power Energy Syst., vol. 42, no. 1, pp. 508–516, 2012.

[17] B. Mohammadi-ivatloo, M. Moradi-dalvand, and A. Rabiee, "Combined heat and power economic dispatch problem solution using particle swarm optimization with time varying acceleration coefficients," Electr. Power Syst. Res., vol. 95, pp. 9–18, 2013.

[18] B. K. Panigrahi, S. R. Yadav, S. Agrawal, and M. K. Tiwari, "A clonal algorithm to solve economic load dispatch," vol. 77, pp. 1381–1389, 2007.

[19] P. Chen and H. Chang, "Large-scale economic dispatch by genetic algorithm," vol. 10, no. 4, pp. 1919–1926, 1995.

[20] V. R. Pandi and B. K. Panigrahi, "Expert Systems with Applications Dynamic economic load dispatch using hybrid swarm intelligence based harmony search algorithm," Expert Syst. Appl., vol. 38, no. 7, pp. 8509–8514, 2011.

[21] A. L. Bolaji, "Tournament-based harmony search algorithm for non-convex economic load dispatch problem," Appl. Soft Comput. J., pp. 1–11, 2016.

[22] A. Safari and H. Shayeghi, "Expert Systems with Applications Iteration particle swarm optimization procedure for economic load dispatch with generator constraints," Expert Syst. Appl., vol. 38, no. 5, pp. 6043–6048, 2011.

[23] R. K. Swain, N. C. Sahu, and P. K. Hota, "Gravitational Search Algorithm for Optimal Economic Dispatch," vol. 6, pp. 411–419, 2012.

[24] T. A. Albert and A. E. Jeyakumar, "Hybrid PSO – SQP for economic dispatch with valve-point effect," vol. 71, pp. 51–59, 2004.

[25] S. Coelho and C. Lee, "Solving economic load dispatch problems in power systems using chaotic and Gaussian particle swarm optimization approaches," vol. 30, pp. 297–307, 2008.

[26] M. Asif, Z. Raja, U. Ahmed, and A. Zameer, "Bio-inspired heuristics hybrid with sequential quadratic programming and interior-point methods for reliable treatment of economic load dispatch problem," 2017.

[27] Y. Wang, B. Li, and T. Weise, "Estimation of distribution and differential evolution cooperation for large scale economic load dispatch optimization of power systems," Inf. Sci. (Ny)., vol. 180, no. 12, pp. 2405–2420, 2010.

[28] D. Zou, S. Li, G. Wang, Z. Li, and H. Ouyang, "An improved differential evolution algorithm for the economic load dispatch problems with or without valve-point effects," Appl. Energy, vol. 181, pp. 375–390, 2016.

[29] M. F. Zaman, S. Member, S. M. Elsayed, T. Ray, and R. A. Sarker, "Economic Dispatch Problems," pp. 1–10, 2015.

[30] B. Y. Qu, J. J. Liang, Y. S. Zhu, Z. Y. Wang, and P. N. Suganthan, "Economic emission dispatch problems with stochastic wind power using summation based multi-objective evolutionary algorithm," pp. 1–19, 2016.

[31] C. D. Tran, T. T. Dao, V. S. Vo, and T. T. Nguyen, "Economic Load Dispatch with Multiple Fuel Options and Valve Point Effect Using Cuckoo Search Algorithm with Different Distributions," Int. J. Hybrid Inf. Technol., vol. 8, no. 1, pp. 305–316, 2015.

[32] S. Rakesh and S. Mahesh, "A comprehensive overview on variants of CUCKOO search algorithm and applications," Int. Conf. Electr. Electron. Commun. Comput. Technol. Optim. Tech. ICEECCOT 2017, vol. 2018-Janua, pp. 569–573, 2018.

[33] G. A. Ajenikoko, O. S. Olaniyan, and J. O. Adeniran, "Cuckoo Search Algorithm Optimization Approaches for Solving Economic Load Dispatch : A Review," vol. 1, no. 2, pp. 1–15, 2018.

[34] A. Gautam, A. Masih, and A. Ashok, "Implementation of Smooth and Non-Smooth Fuel Cost Function for Economic Load Dispatch using Cuckoo Search Method," vol. 8, no. 3, pp. 682–691, 2018.

[35] R. C. A. Subramanian, K. Thanushkodi, and A. Prakash, "An Efficient Meta Heuristic Algorithm to Solve Economic Load Dispatch Problems," vol. 9, no. 4, pp. 246–252, 2013.

[36] P. K. Roy and S. Bhui, "A multi-objective hybrid evolutionary algorithm for dynamic economic emission load dispatch," 2015.

[37] D. Santra, A. Mondal, and A. Mukherjee, Study of Economic Load Dispatch by Various Hybrid Optimization Techniques. .

[38] F. Parvez, P. Vasant, V. Kallimani, and J. Watada, "A holistic review on optimization strategies for combined economic emission dispatch problem," Renew. Sustain. Energy Rev., no. March, pp. 1–15, 2017.

[39] A. Y. Abdelaziz, E. S. Ali, and S. M. A. Elazim, "Electrical Power and Energy Systems Combined economic and emission dispatch solution using Flower Pollination Algorithm," Int. J. Electr. POWER ENERGY Syst., vol. 80, pp. 264–274, 2016.

[40] I. Ziane, F. Benhamida, and A. Graa, "Dynamic Economic Load dispatch Using Quadratic Programming : Application to Algerian Electrical Network," no. March, 2015.

[41] P. Tripati, U. Tomar, and A. K. Singhal, "Solving Economic Load Dispatch Problems through Moth Flame Optimization Algorithm," no. March, 2019.

[42] Z. C. Khalid, M. H. Muhammad, and A. Zahoor, "Design of reduced search space strategy based on integration of Nelder – Mead method and pattern search algorithm with application to economic load dispatch problem," Neural Comput. Appl., 2017.

[43] L. C. Kien, T. T. Nguyen, C. T. Hien, and M. Q. Duong, "A Novel Social Spider Optimization Algorithm for," pp. 1–26, 2019.

[44] J. J. Q. Yu and V. O. K. Li, "Neurocomputing A social spider algorithm for solving the non-convex economic load dispatch problem," Neurocomputing, pp. 1–11, 2015.

[45] G. Xiong and D. Shi, "SC," Appl. Soft Comput. J., 2018.

[46] K. Y. Lee, A. Sode-yome, and J. H. Park, "Neural Networks for Economic Load Dispatch," vol. 13, no. 2, pp. 519–526, 1998.

[47] N. Noman and H. Iba, "Differential evolution for economic load dispatch problems," vol. 78, pp. 1322–1331, 2008.

[48] M. Kia, M. S. Nazar, M. S. Sepasian, A. Heidari, and P. Siano, "Optimal day ahead scheduling of combined heat and power units with electrical and thermal storage considering security constraint of power system," Energy, vol. 120, pp. 241–252, 2017.

[49] B. R. Adarsh, T. Raghunathan, T. Jayabarathi, and X. Yang, "Economic dispatch using chaotic bat algorithm," Energy, vol. 96, pp. 666–675, 2016.

[50] M. Modiri-delshad, S. H. Aghay, E. Taslimi-renani, and N. Abd, "Backtracking search algorithm for solving economic dispatch problems with valve-point effects and multiple fuel options," Energy, vol. 116, pp. 637–649, 2016.

[51] T. Jayabarathi, T. Raghunathan, B. R. Adarsh, and P. Nagaratnam, "Economic dispatch using hybrid grey wolf optimizer," Energy, vol. 111, pp. 630–641, 2016.

[52] V. Kumar and K. S. K. Bath, "Solution of non-convex economic load dispatch problem using Grey Wolf Optimizer," Neural Comput. Appl., 2015.

[53] N. Ghorbani and E. Babaei, "Electrical Power and Energy Systems Exchange market algorithm for economic load dispatch," Int. J. Electr. POWER ENERGY Syst., vol. 75, pp. 19–27, 2016.

[54] A. Meng, J. Li, and H. Yin, "An ef fi cient crisscross optimization solution to large-scale non-convex economic load dispatch with multiple fuel types and valve-point effects," Energy, vol. 113, pp. 1147–1161, 2016.

[55] D. Bisen, H. M. Dubey, M. Pandit, and B. K. Panigrahi, "Solution of Large Scale Economic Load Dispatch Problem using Quadratic Programming and GAMS : A Comparative," vol. 7, no. 3, pp. 200–211, 2012.

[56] M. Javadi, T. Amraee, and S. Member, "Economic dispatch : A mixed-integer linear model for thermal generating units," 2018 IEEE Int. Conf. Environ. Electr. Eng. 2018 IEEE Ind. Commer. Power Syst. Eur. (EEEIC / I&CPS Eur., pp. 1–5, 2018.

[57] F. Benhamida, I. Ziane, B. Bouchiba, and G. Amel, "Dynamic Economic Load Dispatch Optimization with Ramp Rate Limit Using GAMS-CONOPT Solver," no. November, 2013.

IJEW 国际工程期刊 International Journal of Engineering Works انجینئرنگ کاموں کا بین الاقوامی جرنل

International Journal of Engineering Works
ISSN-p: 2521-2419
ISSN-e: 2409-2770
Vol. 7, Issue 09, PP. 305-311, September 2020
https://www.ijew.io/
https://doi.org/10.34259/ijew.20.709305311

Hindko Sign Language (HSL) Recognition using Convolutional Neural Network

Ali Raza[1], Dr.Syed Irfan Ullah[2]
[1,2] Department of Computing, Abasyn University Peshawar Pakistan
ali.raza@abasyn.edu.pk[1], syed.irfanullah@abasyn.edu.pk[2]
Received: 30 August, Revised: 14 September, Accepted: 20 September

***Abstract*—** Language has always played a significant role in Human to Human communication. In case of not knowing someone else's language, one can use hand gestures for communicating crudely but still be able to convey the message. Other than not knowing someone else's language there are millions of people in the world who have hearing or speaking disability. According to the World Health Organization (WHO), it has been estimated to be a population of 436 million (5% of the total world's population) people in the world who have hearing disabilities. Deaf people cannot use oral languages for communicating with other people. The source of their communication is Sign Language (SL) that conveys the message to the other person. In Computer Vision, there are different algorithms, which are used to interpret gestures and recognize them. The Deaf community of Pakistan uses its SL, like any other country in the world i.e., Pakistan Sign Language (PSL). There are around 60 local languages that are spoken in Pakistan including Hindko. Hindko and many other local languages spoken by minorities in Pakistan are on the brink of being endangered as the amount of research done on these languages is almost negligible. In this paper Convolutional Neural Network (CNN) is used for the recognition of Hindko Sign Language (HSL). Furthermore, we examine and analyze the recognition based on prediction to evaluate the efficiency of the utilized CNN. The methodology developed in this research work achieved an accuracy rate of 99.98%.

***Keywords*—** World Health Organization (WHO), Sign Language (SL), Gestures, Pakistan Sign Language (PSL), Convolutional Neural Network, Hindko Sign Language (HSL).

I. INTRODUCTION

The use of gestures and its applications are vast in number and are utilized in domains like gesture recognition, entertainment purposes, Video Games, Sports, etc. It has been observed that in recent years, Human-Computer Interaction (HCI) has moved to another level of popularity in such a way that humans can now interact with computers not only with mouse and keyboard, but with voice, body movements, hand gestures, etc. The basic aim of this type of interaction is to make the experience natural (without any additional hardware attached with the user's body) and user friendly, for which different types of environments have been developed like web browsers, video games, and Virtual Reality (VR) environments. This type of interface is known as Natural User Interface (NUI), where sensors are used to capture the user's interactions, and the system performs actions accordingly.

Gesture recognition systems have also proved to be very effective in the development of assistive technologies for old and handicapped people. For visually impaired or blind people, a lot of applications have been developed for indoor and outdoor navigation to improve the quality of their lives, e.g. on-device sensors to detect dead-reckoning in support with a web-based architecture, to easily create indoor maps for navigation and localization [1]. Several factors make the process of interpretation of gestures a critical one including type of gestures, background, illuminance, number of hands, and space. Gestures can be performed by humans, robots, or any other device. There can be different types of gestures one-handed, two-handed or in some cases you might need to wear gloves [2]. There are times when different parts of the body other than hands being used for making gestures [3]. Usually, arms and hands are the main focus of gesture recognition systems while they disregard the movement of the whole body.

Deaf people cannot use oral languages for communicating with other people. The source of their communication is SL (making different movements and shapes with hands). Facial expressions and body gestures also come into play when communicating through SL. It is considered to be a natural language by Linguists because it shares many commonalities with the oral language.

One misconception about the SL is that people consider it to be universal and deaf people belonging to any part of the world can communicate with people from other parts of the world. SL is mostly subjected to the country and within a country many local SLs' may exist. The exact number of existing SLs' is unknown, but according to a study conducted in 2015, Ethnology has listed them to be 137, which are known [4].

The deaf community of Pakistan uses its SL, like any other country in the world i.e. PSL. It has a distinct style of syntax,

grammar, and vocabulary. A point to understand is that SLs' vary depending upon the variability in regions e.g. American Sign Language (ASL) and British Sign Language (BSL). In the same manner, the PSL alphabet gestures are the exact depiction of the Urdu language alphabets (National Language of Pakistan) [5]. There are 37 alphabets in the Urdu language and each of them is represented by a unique PSL sign shown in Fig. 1.

Figure 1. SL Representation of Urdu Language Alphabets

Majority of the people with hearing disabilities belong to third world countries. These countries are mostly financially very unstable which results in poor services to the deaf community. According to the WHO, there are around 436 million people in the world with hearing disabilities [6

There are around 60 local languages that are spoken in Pakistan including Hindko. Hindko and many other local languages spoken by minorities in Pakistan are on the brink of being endangered because of a lack of developmental work to promote languages. In this research Hindko Language (a local language in Pakistan) is selected for research to revive the dying language. Hindko has a total of 50 alphabets, with 37 alphabets the same as in Urdu and the rest of them being new. Some of the alphabets in Hindko language [7], are shown in Fig. 2 for which there are no SL gestures available at present for blind people to understand. In this research not only, we developed gestures for new alphabets but have also generated a system to recognize all of them.

ٹ Tah	ٹھ Tha	ٹ Tah	پھ Pha	پ Pah	آ Aaa
ڻ Nra	کھ Kha	ک Kah	چھ Chhah	چ Chah	ٹھ Tha

Figure 2. Hindko Language Alphabets with No Sign Gestures

The scope of this research work is limited to HSL recognition by creating a recognition and classification system for which a new dataset had to be developed. The organization of the research work is as follows. Section 2 provides background information and research work done in SLR. Section 3 presents the methodology including the classification model and algorithm. Section 4 covers the discussion on results. Finally, section 5 presents the conclusions and future work.

II. Literature Review

Deep learning being a branch of machine learning works on the principle of the brain's neural networks and uses algorithms developed based on the brain's structure and function. The learning occurs either in a supervised or unsupervised manner. Supervised learning is based on making interpretations from labeled data, while unsupervised learning involves making interpretations from unlabeled data. This research work is based on supervised learning. The models in deep learning are defined as Artificial Neural Networks (ANNs'). ANN's structure is created based on a collection of connected units called neurons. Neurons can transmit signals with the help of connections between them. Typically, the organization of neurons is in the form of layers.

Recognition of bodies and body parts have been a widely studied topic, for which a variety of application have been developed. In this context the techniques used in deep learning have enhanced the capability of the systems to understand in an accurate and automated manner. Deep learning is also known as a convenient tool in image processing applications, computer vision, text classification, robotics and control, and so on [8]. CNN also has been popularly used for analyzing images, data analysis, and other related classification problems. CNNs' are known to have been designed in such a specialized manner that they can detect patterns and make sense of them. With the help of pattern detection, CNNs' are very useful for image analysis because they can be used on massive collections of images. CNNs' can learn valuable characteristic features for a huge database of images and outperforms traditional features like Histogram of Oriented Gradients (HOG), Local binary pattern (LBP), or Speeded Up Robust Features (SURF) [9].

An easy way to use CNN in a much more efficient manner to minimize the efforts and training time, is to utilize a pre-trained CNN for feature extraction. In this particular research work, a specific architecture of CNN has been used, named as "GoogLeNet [10]". The reuse of pre-trained networks is also known as transfer learning, in which weights from the pre-trained networks are used. Since, pre-trained networks have already detected the low-level features like edges, lines, and curves, which are frequently computationally expensive in terms of time, skipping over these parts helps the network to achieve an exceptional result in less time rather than starting the training process all over again. In this research paper, pre-trained GoogLeNet is used to recognize 50 different HSL alphabets shown in Fig. 3.

Figure 3. Sign Language Representation of Hindko Alphabets

People with hearing disability live a compromised life, to improve the standard of their lives a lot of different techniques can be implemented, one of them is the conversion of gesture to text and vice versa. A method to convert gesture to text and text to gesture for Hindi Language has been developed, the images of palm gestures were given as an input to extract the region of hand, based on skin color segmentation [11]. A 5-bit binary string to extract features was used to identify 32 different gestures. The algorithm proved to be robust to variability in hand orientation and changes in scale making the algorithm efficient in recognizing images accurately.

Hand Gesture Recognition (HGR) approach is the most appropriate way for recognition and acceptance. A method was proposed for ASL recognition using CNN for feature extraction using Hand Gestures and further classifying them based on Multi-Class Support Vector Machine (MCSVM) [12]. The model shows to perform satisfactorily in terms of classification accuracy, i.e., 94.57%. To support the argument a technique has been proposed in [13], in which the AdaBoost classifier based on Haar is used for the hand segmentation and discrimination of skin color respectively.

To minimize the barrier between deaf and normal people a technique is proposed for recognition of hand gestures for PSL alphabets in unobstructed scenarios [14]. To acquire images, a digital camera was used with a random background. After the images were acquired, they were are pre-processed for hand detection using skin classification filter. For feature extraction Discrete Wavelet Transform (DWT) was used and eventually for sign recognition ANN with backpropagation learning algorithm was used.

An application based on android platform for mobile phones to detect hand motion for the generation of basic mobile commands [15], stored the hand gestures in the application and were re-labelled. Kanade-Lucas-Tomasi (KLT) algorithm was then used for feature point extraction to detect the static gestures of the hand to call applications installed on the phone.

In another method, the authors introduced a system to capture an image using a webcam, removing the hand from the background by segmentation, extracting features using Principal Component Analysis (PCA), and finally classifying PSL gestures with the help of K Nearest Neighbors (KNN) [16].

In comparison to the previous work done in SL detection, the work done in this research opens new dimensions for a pre-trained GoogLeNet for the detection of HSL images and it has proved to be more accurate than other state-of-the-art machine learning algorithms [12, 14, 16, 17, 18, 19]. A detailed comparison is discussed in section 4. There has been a considerable amount of work done on PSL but it is very unfortunate that some of the local languages of Pakistan are yet to be explored. In this research work we have selected "Hindko" as a local language for which an automated gesture recognition system has been developed.

III. METHODOLOGY

CNNs' are different from regular neural networks in terms of architecture. Typically, a CNN comprises 3 architectural layers including convolutional, pooling, and fully connected layers. A feature map of the input data is generated after carrying out a series of steps involving convolution and pooling processes. Every feature map generated through the convolutional layer is combined together to form the final output. The convolutional layer plays an important role in building a CNN, hence results in high time costs for the training process. The convolutional layers have parameters in the form of shared sets of weights, having minimal receptive fields. In the pooling layer, the input is separated into 2 groups i.e. non-overlapping frames and the maximum for each group using nonlinear down sampling (Max pooling). The number of parameters, overfitting, and computational complexity is reduced by max-pooling layers. Hence, the max-pooling layer is normally placed between the convolutional layers. The dropout layer then drops neurons with a certain probability [20] and Non-saturating ReLU (Rectified Linear Unit) helps the network to learn complex patterns. Finally, fully connected layers work as a classifier having all of the neurons in a fully connected layer being fully connected to all of the outputs of the previous layer. Nevertheless, it is very important to mention that CNN training from the beginning is a time-consuming task on a very large training dataset, which is mostly unavailable and can cause overfitting. Hence, in this research paper, a pre-trained GoogLeNet architecture with proper fine-tuning was applied.

There are 3 different sizes of the filters used in GoogLeNet i.e. 1x1, 3x3 and 5x5 on the same image for dimensionality reduction shown in Fig. 4. Finally, for the same image all of the features are combined to produce a robust output. GoogLeNet comprises 22 layers and the number of parameters is reduced from 60 million to 4 million when compared to AlexNet [21].

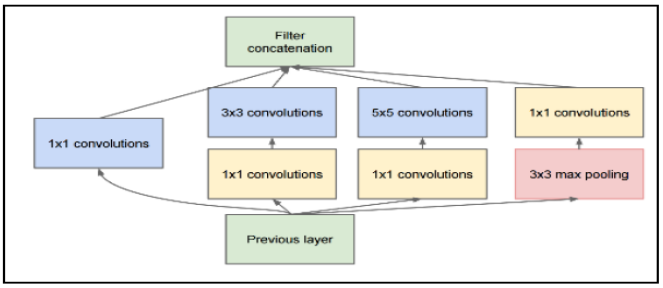

Figure 4. Multiple Convolutions for Dimension Reduction

The basic structure of GoogLeNet can be seen in [10]. It shows the overall network's architecture. Multiple Inception modules combined together form a deeper structure through which high accuracy is achieved.

A. *Pre-trained Networks*

A pre-trained network has pre-trained weights, these weights can be utilized in other similar tasks. A pre-trained network may also perform well in training CNNs where there is a limited sized dataset. In addition to that, training CNN from the beginning is time-consuming as well as computationally expensive. Rather than training the network from the beginning, the best way to retrain a network is to perform fine-tuning through which initial layers of the network are kept frozen and the last set of fully connected layers are replaced with the newly trained layers, so that errors cannot propagate backwards [22]. Stochastic gradient descent (SGD) algorithm was used for the initialization and training of weights in the network.

Each layer in GoogLeNet works as a filter. This formation improves the capability of GoogLeNet in better feature detection in images. Common features like blobs, edges, and colors are detected in the first layer, while high-level features are detected in the last layers. In this research work, the working procedure was divided into 2 phases (Training and Evaluation) is shown in Fig. 5. All of the training images were pre-processed for resizing and data augmentation, where operations like random reflection on the horizontal axis and 30-pixel range translation over the x and y axis to avoid overfitting and memorization of the exact details during the training process [23]. Following are the steps categorized in Training and Evaluation separately:

Training:

1. Pre-Trained Network Loading.
2. Final Layers Replacement.
3. Train Network with new pre-processed images.

Evaluation:

1. Give a pre-processed input image.
2. Extract the features using trained CNN.
3. Classify the image.

Let Z be a set of SL images, j representing the resized image z in set Z, G and G1 representing pre-trained and modified GoogLeNet network and ACC be the element representing accuracy. The methodology is depicted in the Algorithm.

B. *Algorithm*

Input: Input Image.
Output: Accuracy Achieved.

1. ∀ z ∈ Z, ∃ j ∈ Z: j be pre-processed z
2. Let G be a pretrained GoogLeNet network ∈ CNN
3. Modify G to G1 ∈ CNN
4. Train G1 ∀ j ∈ Z.
5. Let ACC be the accuracy
6. ∀ G1, ∃ ACC be the achieved accuracy → CNN (Z)

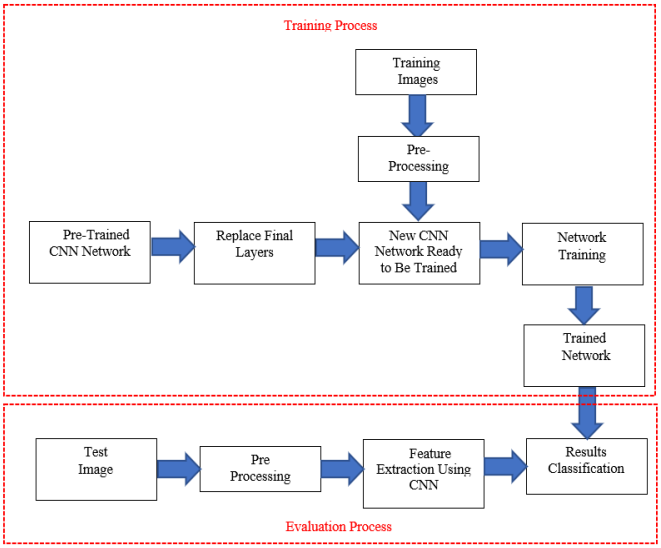

Figure 5. Working Procedure of The Model

IV. RESULTS

This section describes the results for the evaluation of 50 classes of HSL images. The Schematic diagram of the overall system is shown in Fig. 6. The performance of GoogLeNet is evaluated using the accuracy achieved. The accuracy was achieved by finding the number of correctly classified images.

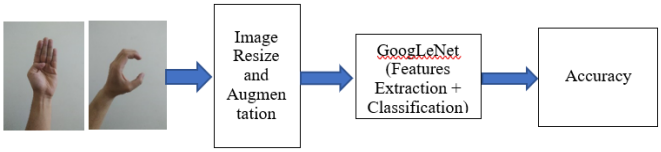

Figure 6. Schematic Diagram of The Overall System

To evaluate the most appropriate settings the experiments were performed for 3 different learning rates i.e., [0.01, 0.001, 0.0001], with the size of mini-batch and number of epochs set to 128 and 10 respectively.

The simulations were ran using MATLAB 2019a. The network was trained on an individual system with the specification of an Intel Core Processor i5-8250U with 4 cores at 1.6 GHz and 16 GB RAM.

The images were collected on our own. 16,500 images were captured using a mobile camera, including 330 instances of each alphabet. Images were divided into training and testing sets. 70% i.e. 11,550 images were used for the training process

and the remaining 30% i.e. 4,950 images for validation. The original images were of resolution 1080 × 1920 × 3 (1080 width, 1920 height, RGB). The images had to be resized to 224 × 224 × 3 pixels to fit in the GoogLeNet. It categorizes the input image in one of the 50 classes of HSL. Table 1 summarizes the evaluations of the network with different learning rates.

TABLE I. GoogLeNet Settings With 3 Different Learning Rates

Network Configuration and Accuracy Achieved	Learning Rates		
	0.01	**0.001**	**0.0001**
Mini-Batch Size	128	128	128
Epochs	10	10	10
Iterations	900	900	900
Iterations per Epoch	90	90	90
Validation Frequency	90	90	90
Time Consumption	240 minutes	245 minutes	250 minutes
Accuracy	99.98%	99.92%	99.78%

GoogLeNet trained with a learning rate of 0.01 achieved an accuracy of 99.98%. The value to be chosen for the learning rate requires some testing. We had to test and tune with each model before we knew exactly where we wanted to set it. The idea is to set the value somewhere from 0.01 to 0.0001. Fig. 7, 8, 9 shows the training processes of GoogLeNet with 3 different settings as shown in table 1. It can also be noticed that with decreasing the learning rate the accuracy has reduced and the time consumption has increased because with lower learning rate the system learns slowly and takes more time to complete.

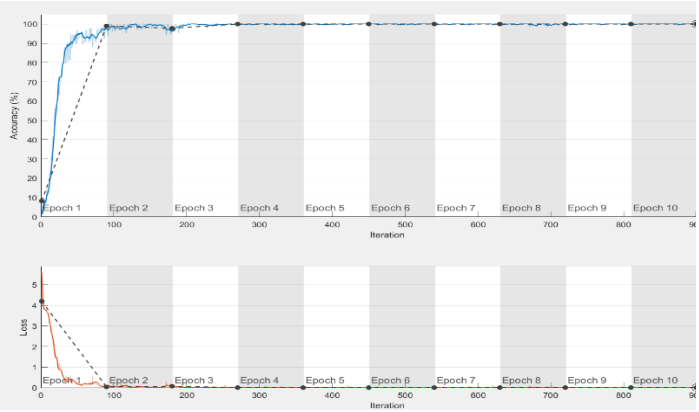

Figure 7. 99.98 % Accuracy Is Achieved With 0.001 Learning Rate

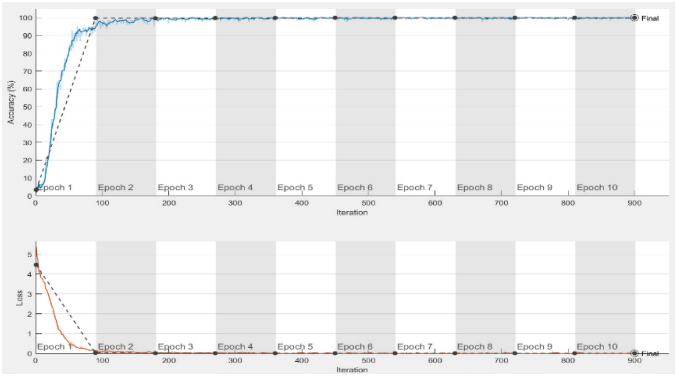

Figure 8. 98.92 % Accuracy Is Achieved With 0.001 Learning Rate

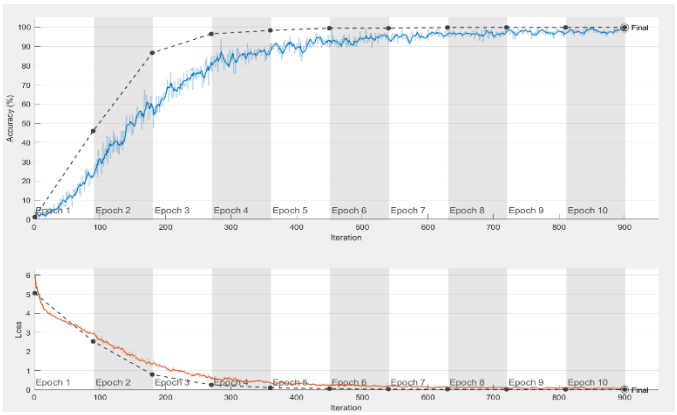

Figure 9. 99.78 % Accuracy Is Achieved With 0.001 Learning Rate

V. DISCUSSION

Based on the results, we came to the conclusion that for the method presented in this research paper, a high learning rate of 0.01 provides the best result. This is the best result achieved in SLR in comparison with other state-of-the-art techniques for classification of SLs', as shown in Figure 11. Detection of ASL signs Using the Leap Motion Controller with Machine Learning Approach achieved an accuracy of 93.81% [17]. Another methodology shows a simple algorithm, which was used for feature extraction to recognize ASL alphabets using hand gestures and then on the basis of the extracted features, ANN achieved 95% classification accuracy [18]. A pre-trained CNN using AlexNet architecture and MCSVM achieved an accuracy of 94.5% [12]. To detect PSL gestures, images were captured through a webcam, after that the images were segmented to separate hand from the background PCA and then finally classified the gesture feature by utilizing KNN achieved an accuracy of 85% [16]. A system using a DWT for feature extraction and ANN with a back-propagation learning algorithm is employed to recognize PSL alphabets achieved an accuracy of 86.40% [14]. In an automatic recognition system of PSL alphabets using MCSVMs' validated over the data set of 3414 PSL signs achieved 77.18% accuracy [19].

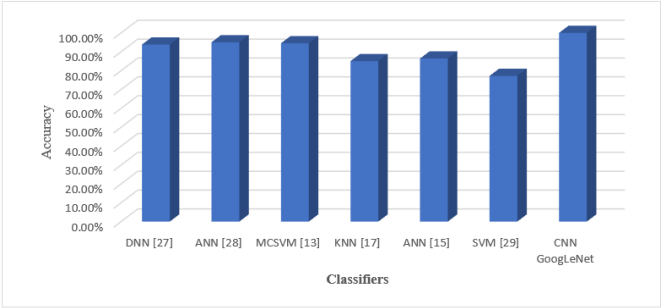

Figure 10. Comparison of State-Of-The-Art Techniques for Classification of SL's

The comparison shown in Fig. 10 indicates that the methodology implemented outperforms other state-of-the-art methods for sign language detection. The classification accuracy obtained satisfactorily, which is 99.98%. Fig. 11 shows the sign wise classification accuracy of HSL alphabets.

ت 99.9%	پھ 100%	پ 100%	پ 100%	ب 100%	ا 99.9%	آ 99.9%
ج 100%	ش 100%	ٹھ 100%	ٹ 100%	ٹ 99.9%	تھ 100%	ث 100%
ڈ 99.9%	د 100%	خ 100%	ح 100%	چھ 100%	چ 99.9%	چ 100%
ش 100%	س 100%	ژ 99.9%	ز 99.9%	ڑ 100%	ر 100%	ذ 100%
ف 100%	غ 98.9%	ع 99.7%	ظ 99.9%	ط 100%	ض 100%	ص 100%
م 99.9%	ل 100%	گ 100%	کھ 100%	ک 99.9%	ک 100%	ق 100%
ی 100%	ء 99.9%	ہ 100%	و 99.9%	ں 99.9%	ٹ 100%	ن 99.9%
						ے 100%

Figure 11. Classification Accuracy of HSL Alphabets

CONCLUSION

In recent times, deep learning has been frequently used in research which has yielded a significant improvement in automated analysis and recognition in comparison with traditional machine learning algorithms. The innovativeness of this research work lies in illustrating the use of pre-trained CNN network for recognition of SL images. A pre-trained GoogLeNet network model was modified according to the requirements of this particular work and achieved high accuracy ad excellent results. The exceptional detection rates in this research work are expected to reinforce its use in Sign Language Detection. Furthermore, for the first time, a pre-trained CNN is used for Hindko Sign Language recognition, which has the possibility to lay the foundation for employing pre-trained CNNs within a CAD system for accurate detection. In this paper static images have been used to recognize Hindko sign language. Hindko has 13 more alphabets than Urdu, and for these 13 alphabets new gestures have been developed, which will prove to be a valuable addition for further research. Since, this work is limited to static signs, in future this work can be given a more practical form by installing it into an embedded system with the webcam.

REFERENCES

[1] Verma, S., Omanwar, R., Sreejith V., and Meera, G. S., "A Smartphone Based Indoor Navigation System", 28th IEEE International Conference on Microelectronics, pp. 345-348, 2016.

[2] Varga, R., and Prekopcsák, Z., "Creating a Database for Objective Comparison of Gesture Recognition System", 15th International Student Conference on Electrical Engineering, pp. 1-6, 2011.

[3] Sigalas, M., Haris, B., and Panos, T., "Gesture Recognition Based on Arm Tracking for Human-Robot Interaction", IEEE International Conference on Intelligent Robots and Systems, pp. 5424-5429, 2010.

[4] Lewis, M. P., Simons, G. F., and Fennig, C. D., "Ethnologue: Languages of The World", Texas: SIL International, 2015. [Online]. Available: https://www.ethnologue.com/sites/default/files/Ethnologue-18-Honduras.pdf

[5] Sulman, D. N., and Zuberi, S., "Pakistan Sign Language–A Synopsis", Pakistan, June, 2000. [Online]. Available: https://www.academia.edu/2708088/Pakistan_Sign_Language_-_A_Synopsis

[6] Organization, W. H., "10 Facts About Deafness", Posje´ceno, Vol. 14, pp. 2017, 2017.

[7] Toker, H., "A Practical Guide to Hindko Grammar", Trafford Publishing, 2014. [Online]. Available: https://www.scribd.com/book/387784340/A-Practical-Guide-to-Hindko-Grammar

[8] Han, J., Zhang, D., Cheng, G., Liu, N. and Xu, D., "Advanced Deep-Learning Techniques for Salient and Category-Specific Object Detection: A Survey", IEEE Signal Process. Mag., Vol. 35, No. 1, pp. 84–100, 2018.

[9] Lee, A., "Comparing Deep Neural Networks and Traditional Vision Algorithms in Mobile Robotics," Traditional Vision Algorithms in Mobile Robotics", 2016.

[10] Krizhevsky, A., Sutskever, I., and Hinton, G., "Image Net Classification with Deep Convolutional Neural Networks", In Proceedings of The Advances in Neural Information Processing Systems, Lake Tahoe, NV, USA, pp. 1097–1105, 2012.

[11] Chaman, S., D'souza, D., D'mello, B., Bhavsar, K., and D'souza, T., "Real-Time Hand Gesture Communication System in Hindi for Speech and Hearing Impaired", IEEE International Conference on Intelligent Computing and Control Systems (ICICCS), pp. 1954-1958, 2018.

[12] Islam, M. R., Mitu, U.K., Bhuiyan R. A., and Shin, J., "Hand Gesture Feature Extraction Using Deep Convolutional Neural Network for Recognizing American Sign Language", IEEE 4th International Conference on Frontiers of Signal Processing (ICFSP), pp. 115-119, 2018.

[13] Sun, J. H., Ji, T. T., Zhang, S. B., Yang, J. K., and Ji, G. R., "Research on the Hand Gesture Recognition Based on Deep Learning", 12th IEEE International Symposium on Antennas, Propagation and EM Theory (ISAPE), pp. 1-4, December, 2018.

[14] Khan, N., Shahzada, A., Ata, S., Abid, A., Khan Y., and Farooq, M.S., "A Vision-Based Approach for Pakistan Sign Language Alphabets Recognition", Pensee, Vol. 76, No. 3, pp. 274-285, 2014.

[15] Dadiz, B.G., Abrasia, J. M. B., and Jimenez, J. L., "Go-Mo (Go-Motion): An Android Mobile Application Detecting Motion Gestures for Generating Basic Mobile Phone Commands Utilizing KLT Algorithm", IEEE 2nd International Conference on Signal and Image Processing (ICSIP), pp. 30-34, 2017.

[16] Malik, M. S. A., Kousar, N., Abdullah, T., Ahmed, M., Rasheed, F., and Awais, M., "Pakistan Sign Language Detection using PCA and KNN", International Journal of Advanced Computer Science and Applications, Vol. 9, No. 54, pp. 78-81, 2018.

[17] Chong T.W., and Lee, B.G., "American Sign Language Recognition Using Leap Motion Controller with Machine Learning Approach", Sensors, Vol. 18, No. 10, pp. 3554, 2018.

[18] Thongtawee, A., Onamon, P., and Yuttana, K., "A Novel Feature Extraction for American Sign Language Recognition Using Webcam", 11th IEEE Biomedical Engineering International Conference (BMEiCON), pp. 1-5, 2018.

[19] Shah, S. M. S., Naqvi, H. A., Khan, J. I., Ramzan, M., and Khan, H. U., "Shape Based Pakistan Sign Language Categorization Using Statistical

Features and Support Vector Machines", IEEE Access, Vol. 6, pp. 59242-59252, 2018.

[20] Goodfellow, I., Bengio Y., and Courville, A., “Deep Learning”, MIT Press: Cambridge, MA, USA, 2016. [Online]. Available: www.deeplearningbook.org

[21] Krizhevsky, A., Ilya, S., and Geoffrey, H. E., "ImageNet Classification with Deep Convolutional Neural Networks", Advances in neural information processing systems, pp. 1097-1105, 2012.

[22] Rumelhart, D., Hinton, G., and Williams, R., “Learning Representations by Back-Propagating Errors,” Nature, Vol. 323, pp. 533–536, 1986. [Online]. Available: https://www.iro.umontreal.ca/~vincentp/ift3395/lectures/backprop_old.pdf

[23] Mathworks, “Transfer Learning Using GoogLeNet - MATLAB Simulink - MathWorks United Kingdom”, 2018. [Online]. Available: https://uk.mathworks.com/help/nnet/examples/transfer-learning-using-googlenet.html

IJEW 国际工程期刊 International Journal of Engineering Works انجینئرنگ کاموں کا بین الاقوامی جرنل

International Journal of Engineering Works
ISSN-p: 2521-2419
ISSN-e: 2409-2770
Vol. 7, Issue 09, PP. 312-317, September 2020
https://www.ijew.io/
https://doi.org/10.34259/ijew.20.709312317

Check for updates

Novel Application of Whale-Optimization-Algorithm Integrated with Local Search Deterministic Techniques to Solve Economic-Load-Dispatch-Problem with Valve-Point-Loading-Effect and Gaseous Emission

Hafeez ullah Khan
Department of Electrical Energy System Engineering, US-Pakistan Center for Advanced Studies in Energy (USPCAS-E), UET, Peshawar, Pakistan
hafeezullahkhan273@gmail.com
Received: 13 September, Revised: 20 September, Accepted: 26 September

***Abstract*—** Amidst the prevailing energy crisis have thus pulled the thermal power plants to come into strike inorder to overcome the aforementioned issue seriously have invited ecological problem in parallel and is swelling day by day. Economic load dispatch (ELD) and economic emission dispatch (EED) are the Bi-objective opposite natured functions to each other which are brought into a single function with the aid of scaling factor (SF) and price penalty factor (PPF) to overcome the contradictory natures of fuel cost and emission levels at the same instant while keeping the alternators in their rated constraints of inequality in terms of maximum and minimum power levels and power balance constarint as well as including/excluding the phenomena of valve point loading effects (VPLE). Thus both the functions are balanced at specific single point which not only cuts down the fossil fuel cost but also keeps in parallel the emission level of gaseous products at minimum. Hybridized optimization technique is proposed in this research that carries the capability to combine the nature inspired Whale optimization algorithm with the three specific local search techniques i-e interior point algorithm (IPA), sequential quadratic programming (SQP) and active set (AS) and have been applied on two test cases for cost effective solution.

***Keywords*—** Thermal Power Plant, Economic Load Dispatch, Economic Emission Dispatch, Whale Optimization Algorithm, Local Search Techniques, Valve Point Loading Effect.

I. INTRODUCTION

Economic load dispatch is one of the major functions of electrical power management systems. In electric power industry efficient, high quality, reliable supply and optimum operation of electrical power generation is demanded by utilities so for this purpose the power production level of multiple coupled alternators in an interrelated power production system are scheduled in such a manner that the operating cost of the system is reduced and entire power demand is fulfilled subjected to satisfaction of all affiliated distinct constraints of power balance and generation capacity linked to electrical power generation units and plant are contented is called as problem of economic load dispatch [1]. The purpose of economic load dispatch is to find out the operating policy for "NG" number of generators that which generator will produce how much power. The following diagram clearly visualizes the scenario.

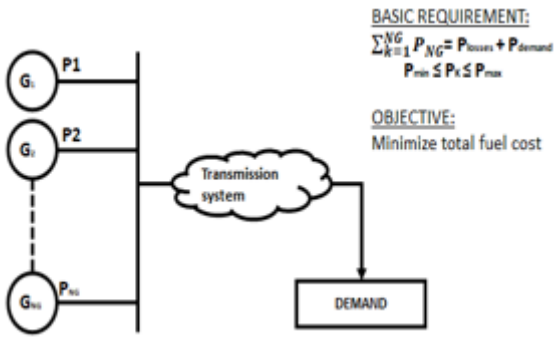

Figure 1: Policy of Economic Load Dispatch

With a rapid increase in population and commercialization, the electrical power demand raises day by day while fossil fuels are already high-priced so there should be an unavoidable need to cut down the operational cost of production in respect of fossil fuel cost. Fossil fuel are burnt in the furnace of thermal power plants emitting several toxic gases like carbon dioxide (CO2), silicon dioxide (SO2) and nitrogen dioxide (NO2) in the chimney promoting another serious issue called "global warming" when released into atmosphere. Due to the increased thermal power plants penetration, the level of gaseous emissions has been exponentially increased within no time [2].So In order to challenge the reduction of the operational cost concurrently with the level of gaseous emissions into the air

and afore said ecological effects, economic load dispatch concerned problem is reshaped into a latest expression and is labeled to be the problem of Combined Economic Emission Load Dispatch (CEELD).So this problem considering emissions not only reduces the level of gaseous emissions, but also have the ability to curtail the fuel cost magnificently.

Due to the involved natural complexities in traditional optimization techniques, a Hybridized optimization technique is developed that is capable to combine whale optimization algorithm with local search methods for cost effective solution.

II. SYSTEM MODE

A. Economic load dispatch Problem

The main objective of economic load dispatch problem is to schedule the generators power output at lower possible fuel cost. Characteristic equation of fuel cost as quadratic polynomial along with the valve point loading effect as sine term can be formulated as follws,

$$\boldsymbol{Min}\ \boldsymbol{C_V(P)} = \sum_{K}^{NG} \boldsymbol{C_K P_K} = \sum_{k=1}^{NG} (\boldsymbol{a_k P_k^2 + b_k P_k + c_k + |d_k \times \sin(e_k \times (P_k^{min} - P_k))|}) \quad (1)$$

Where ak, bk and ck are the related fuel cost coefficients of kth generator in $/MW2h, $/MW/h and $/h respectively while dk and ek are the related coefficients of valve point loading effect in $/h and rad. “Pk“ is the variable power output assigned to each ganarator in MW, Pkmin and Pkmax denoting maximum and minimum power output limits while C(P) on the left hand side of the above equation gives the specified total fuel cost of power system in $/h for “NG” generators [3].

B. Economic Emission Dispatch problem

Similarly economic emission dispatch is the function to curtail the level of gaseous emissions as minimum possible while satisfying the demanded load. EED problem can be expressed mathematically as follows,

$$\mathbf{Min}\ \mathbf{E_V(P)} = \sum_{\mathbf{k=1}}^{\mathbf{NG}} \mathbf{E_k(P_k)} = \sum_{\mathbf{k=1}}^{\mathbf{NG}} (\mathbf{ae_k P_k^2 + be_k P_k + ce_k + de_k \times \exp(fe_k \times P_k)}) \quad (2)$$

aek, bek, cek, dek and fek are the coefficients of gaseous emissions expressed in ton/MW2h,ton/MWh, ton/h respectively while Ev(P) on the left hand side is expressed as the total level of emission in tons/h.

C. Combined Economic Emission Load Dispatch problem

In need to reduce the fossil fuel cost and degree of gaseous discharge simultaneously while keeping in mind both the equality and inequality constraints, both the objective functions of ELD and EED are combined together by introduction of price penalty factor (PPF), whereas for their contradictory nature, scaling factor (SF) is inserted,the so called as problem of (CEELD), which is a real-world many-objective optimization problem shown below

$$\boldsymbol{Min}\ (\boldsymbol{F_{C.E.E.L.D}}) = \boldsymbol{W} * \boldsymbol{C_v(P)} + (\mathbf{1} - \boldsymbol{W})(\boldsymbol{P.P.F})_k * \boldsymbol{E_V(P)} \quad (3)$$

Where

$$(\boldsymbol{P.P.F})_k = \frac{\boldsymbol{C_V(P_k^{max})}}{\boldsymbol{E_V(P_k^{max})}} \quad (4)$$

III. HYBRIDIZED WOA TECHIQUE

Whales are considered to be the largest and longest amongst all the mammals and thus has been categorized into seven distinct species of blue, Minke, killer, finback, humpback, sei and right. These fancy gigantic mammals are assumed to be an intelligent and smart like a human being due to the presence of spindle cells in their brain twice in count than a human adult. They are responsible to develop their emotions, judgment and social behavior like a human being. Whales can live in a family or live alone depending upon the specie. Adult humpback whale is found to be a school bus Equivalent in length and are being grazed on krill and small fish herds present on the surface of water. The unique mechanism of Bubble_net_Feeding has been detected uniquely in humpback specie in which they start to dive about 12m deep inside the water when prey is sighted. Humpback then travel upward towards the targeted prey following two types of manevours [4].

A. Shrinking Surrounding Mechanism

This mechanism employs the following equation in which the value of “$\vec{a}$” is dropped down from 2 to 0 in iterations which in turn effects the value of arbitrary “$\vec{A}$” in interval [-a,a] decreased too. Thus mentioning the value of “$\vec{A}$” in [-1,1] any location can be achieved from the location of search agent towards the best agent location. The equations below shows the achievable position of search agent towards the best agent location in 2D between 0≤A≤1.

$$\vec{\boldsymbol{D}} = \left|\vec{\boldsymbol{C}}.\overrightarrow{\boldsymbol{X_{arb}}} - \vec{\boldsymbol{X}}\right| \quad \textbf{(4)}$$

$$\overrightarrow{\boldsymbol{X}}(\boldsymbol{t+1}) = \overrightarrow{\boldsymbol{X_{arb}}} - \vec{\boldsymbol{A}}.\vec{\boldsymbol{D}} \quad \textbf{(5)}$$

Vector $\vec{A}\ and\ \vec{C}$ can be find out with the help of equations given below.

$$\vec{\boldsymbol{A}} = \mathbf{2}\vec{\boldsymbol{a}}.\vec{\boldsymbol{r}} - \vec{\boldsymbol{a}} \quad (6)$$

$$\vec{\boldsymbol{C}} = \mathbf{2}.\vec{\boldsymbol{r}} \quad (7)$$

B. Spiral Updating Mechanism

A coil shaped path between the original position of whale and targeted position of prey is followed in this spiral updating mechanism with the help of a spiral equation subjected below,

$$\vec{X}(t+1) = \vec{F}.e^{cl}.\cos ine(2.\pi.l) + \overrightarrow{X*}(t) \quad (8)$$

"I" in [-1,1] denotes arbitrary number, "c" is a scalar identifying logarithmic spiral shape while $\vec{F} = \left|\overrightarrow{X*}(t) - \vec{X}(t)\right|$ describes gap between the targeted prey and the kth humpback.

Humpback whale while on its journey towards its targeted prey follow together their spiral shaped and shrinking encircling paths assumed to have 50% chances of selection each at the same time while designing their hunting technique mathematically expressed as follows

$$\vec{X}(t+1) = \begin{cases} \overrightarrow{X*}(t) - \vec{A}.\vec{D} & when\ q < 0.5 \\ \vec{F}.e^{cl}.\cos(2\pi l) + \overrightarrow{X*}(t) & when\ q \geq 0.5 \end{cases} \quad (9)$$

IV. Simulation Results and Discussion

This section illustrates the detailed results of simulation tested upon 2 cases discussed below.

A. Case 1: System of 3 Generators

In this case, 3 generator units for ELD problem subjected with and without valve point loading effect with load demand of 850 MW is examined. For the 2-test case systems i-e 3 and 6 units, their corresponding generation power limits and scalar coefficients of fuel cost and emission level have been obtained from [5]. Both the cases including and excluding the phenomena of valve point loading effect compiled for 100 independent runs limited to 500 iterations maximum per run where the search agents are kept to 15000 with VPLE phenomena whereas 7500 for without VPLE phenomena.

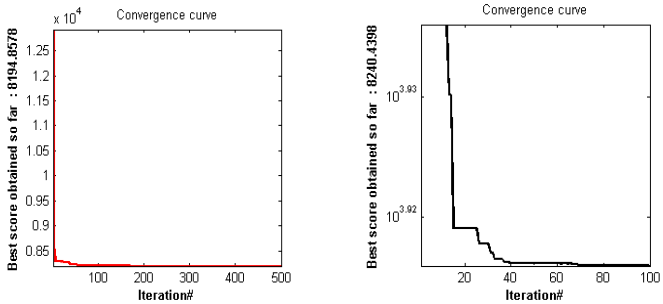

(a) Without VPLE (b) With VPLE

Figure 2: Learning curve for test case 1

TABLE 1: INEQUALITY CONSTRAINTS, FUEL COST AND VPLE COEFFICIENTS FOR SYSTEM OF 3-GENERATORS TEST

G.N	Generator Bound limits	a x10^{-3}	b	c x10^{2}	d	e x10^{-3}
G1	100-600	1.56	7.92	5.61	300	31.5
G2	100-400	1.94	7.85	3.10	200	42
G3	50-200	4.82	7.97	0.78	150	63

TABLE 2: COMBINED REFINED RESULTS OF TEST CASE 1 WITHOUT VPLE

Power (MW)	WOA			WOA Hybridized with		
	Best	Mean	worst	IPA	SQP	AS
P1	391.7667	400.0000	600.0000	393.1698	393.1698	393.1698
P2	344.1687	400.0000	100.0000	334.6038	334.6038	334.6038
P3	114.0646	50.0000	150.0000	122.2264	122.2264	122.2264
Total power	850.0000	850.0000	850.0000	850.0000	850.0000	850.0000
Cost $/h	8194.8578	8227.8700	8371.6700	8194.3561	8194.3561	8194.3561
T (sec)	0.7046	0.7400	0.7011	0.1005	0.0593	0.0357

Simulation results for whale optimization algorithm alone interms of best, mean and worst, and in hybridized form with three local search techniques are tabulated in table 2&3 along with levels of power assigned to each and every generator and execution time for the load demand of 850MW with and without considering the phenomena of valve point loading effect. Learning curve for test case 1 is shown in figure 2 whereas results for 100 independent runs for both the cases including/excluding VPLE Phenomena are showing in figure 3&4.

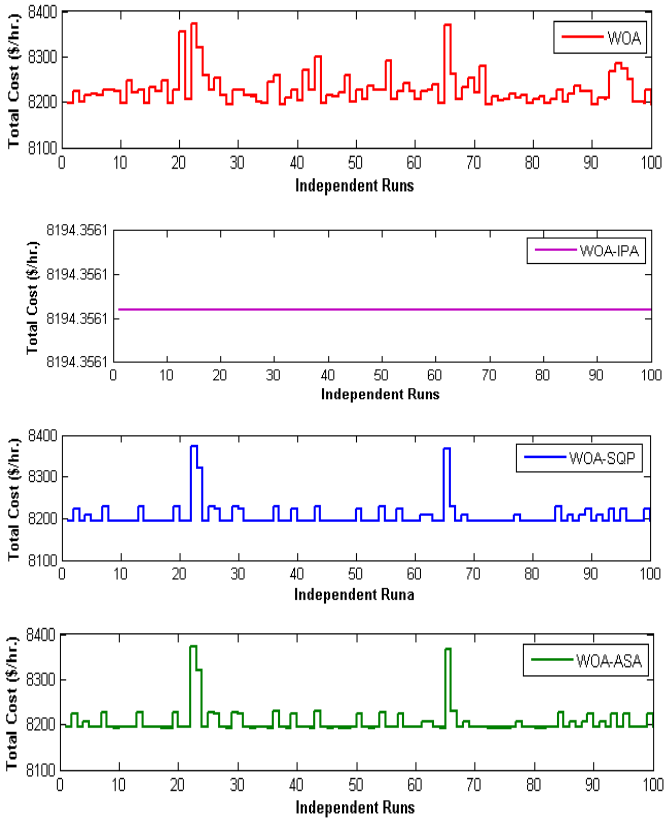

Figure 3:100 independent runs for test case 1 without VPLE.

TABLE 3: COMBINED REFINED RESULTS OF TEST CASE 1 WITH VPLE.

Power (MW)	WOA			WOA Hybridized with		
	Best	Medium	worst	IPA	SQP	AS
P1	300.6138	392.3836	423.5195	300.2668	300.2668	300.1957
P2	400.0000	257.6164	226.4805	400.0000	400.0000	400.0000
P3	149.3862	200.0000	200.0000	149.7332	149.7332	149.8043
Total Power	850	850	850	850	850	850
cost	8240.	8368.	8624.	8234.	8234.	8234.
$/h	4398	7836	4998	0718	0718	1115
T(sec)	0.2770	0.2800	0.2773	0.0838	0.0841	0.0490

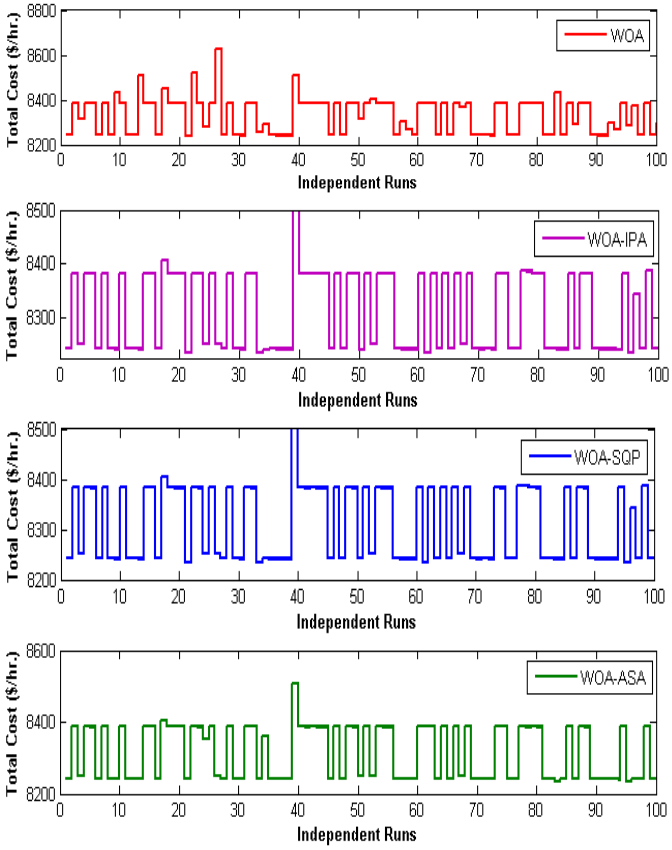

Figure 4: 100 independent runs for test case 1 with VPLE

B. Case 2: System of 6 Generators

This test case consists of 6 generator units for combined economic emission dispatch (CEELD) problem without valve point loading effect (VPLE) having the required power demand of 1000 MW.The required data has been tabulated below in table 4. At scaling factor SF=1, CEELD problem becomes economic load dispatch (ELD) problem which cuts down fuel cost to 5039.6315 $/h but increases emission levels to 978.8066 ton/h. Conversely at scaling factor SF=0, it becomes economic emission dispatch (EED) problem decreasing down emission level to 800.1264 ton/h but increases fuel cost to 5211.1423 $/h.

Learning curve for test case 2 is shown in figure 5 while the Simulation results relating the proposed Algorithm for the cost of fuel and gaseous emissions are mentioned in table 5.

TABLE 4: INEQUALITY CONSTRAINTS, FUEL COST COEFFICIENTS AND EMISSION COEFFICIENTS FOR SYSTEM OF 6-GENERATORS TEST

G.N	Generator Bound limits	a	b	c $x10^3$	ae	Be $x10^{-3}$	ce $x10^3$
G1	10-125	756.8	38.540	152.5	13.860	330	4.2
G2	10-150	451.325	46.160	106	13.860	330	4.2
G3	35-225	1050.0	40.400	28	40.267	545.5	6.8
G4	35-210	1243.53	38.310	35.5	40.267	545.5	6.8
G5	130-325	1658.57	36.328	21.1	42.900	511.2	4.6
G6	125-315	1356.66	38.270	18	42.900	511.2	4.6

TABLE 5: COMBINED REFINED RESULTS OF TEST CASE 2 WITHOUT VPLE

S.F	Megawatts allocated to each and every generator for P_D=1000MW						Cost $/h	EmissionTons/h
	G1	G2	G3	G4	G5	G6		
0	100.7180	104.5094	166.7849	166.9590	228.8116	232.2171	5211.1423	800.1264
.1	82.7954	95.7914	160.4211	146.5920	253.7708	260.6293	5150.5907	819.7198
.2	61.4815	92.3611	197.1234	148.0541	274.0373	226.9426	5128.4269	847.7854
.3	57.7113	120.0979	157.8813	165.8447	242.9844	255.4804	5175.4062	824.2638
.4	94.3480	73.5812	165.1936	159.1398	272.5470	235.1904	5138.9258	827.0479
.5	79.5469	73.4171	152.2838	164.0147	255.3650	275.3725	5111.7421	839.3119
.6	61.5374	59.9085	151.9599	172.4086	274.8620	279.3236	5073.9744	870.4544
.7	55.9275	88.6383	178.7685	151.6686	280.5957	244.4014	5110.9701	849.9554
.8	76.5679	59.3863	160.3021	177.2455	228.8013	297.6969	5099.6485	861.9298
.9	61.0173	31.5855	162.5899	169.4998	284.7081	290.5994	5052.2486	905.6545
1	30.7412	23.4987	173.4407	142.8450	319.6550	309.8194	5039.6315	978.8066

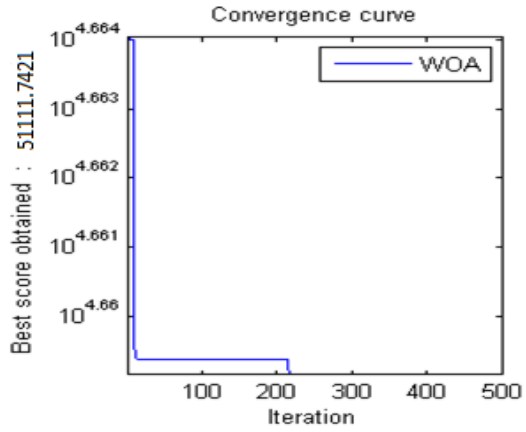

Figure 5: Learning curve for test case 2

CONCUSLION

This paper analyzes two test case systems for economic load dispatch and combined economic emission load dispatch problems having distinct power load demands. Test case 1 contains the proposed algorithm alone and in hybridized form both for the cases with and without VPLE Phenomena.Without considering the Valve point loading effect, above table 2 shows best, mean and worst fuel cost results for whale optimization algorithm and hybridized whale optimization algorithm showing that the best score achieved for W.O.A alone is 8194.8578 $/h.“S.Q.P”, “A.S” and “I.P.A” are known as local search techniques which have the capability to reduce down the cost more when hybridized with Whale algorithm of optimization. All the three local search techniques integrated with W.O.A tabulated the same fuel cost results of 8194.3561$/h and thus showed their optimality. On the other hand, Taking into account the phenomena of valve point loading effect, the simulation results are listed above in table 3 The best score achieved for W.O.A is 8240.4398 $/h executed in 0.2770 seconds Whale optimization algorithm admits 8234.0718 $/h hybridized with local search techniques I.P.A & S.Q.P while A.S hybridization admitted 8234.1115 $/h. Thus it is clear from the table that W.O.A-I.P.A & S.Q.P proved to be more cost effective and optimum compared to W.O.A by tailoring the fuel cost from 8240.4398 $/h to 8234.0718 $/h. Similarly in test case 2, at scaling factor 1 and 0, the established function converts wholy to ELD and EED problems respectively due to their contradictory natures thus to overcome the unbalanced phenomena between fuel cost and emission level

SF=0.5 is selected that makes the functions mutually stable to cut down the fuel cost and emissions volume at the same time.

REFERENCES

[1] S. Basak and S. Banerjee, "Adaptive Jaya Optimization Technique for Economic Load Dispatch Considering Valve Point Effect," in 2019 Devices for Integrated Circuit (DevIC), 2019, pp. 104-107.

[2] F. P. Mahdi, P. Vasant, M. Abdullah-Al-Wadud, V. Kallimani, and J. Watada, "Quantum-behaved bat algorithm for many-objective combined economic emission dispatch problem using cubic criterion function," Neural Computing and Applications, pp. 1-13, 2018.

[3] L. T. Al-Bahrani, J. C. Patra, and A. Stojcevski, "Solving economic dispatch problem under valve-point loading effects and generation constrains using a multi-gradient PSO algorithm," in 2018 International Joint Conference on Neural Networks (IJCNN), 2018, pp. 1-8.

[4] S. Mirjalili and A. Lewis, "The whale optimization algorithm," Advances in engineering software, vol. 95, pp. 51-67, 2016.

[5] T. M. Subhani, C. S. Babu, and A. S. Reddy, "Particle swarm optimization with time varying acceleration coefficents for economic

Hafeez ullah khan was born on September the 16th 1994 in district swabi Khyber pukhtoonkhwa Pakistan. He has received his BSc degree in electrical engineering (Power) back in 2016 from university of engineering and technology (UET) Peshawar Pakistan. He is a post graduate researcher in united states Pakistan centers for advanced studies in energy (US.-PCASE) university of engineering and technology peshawar and has completed his MS in Electrical Energy Systems Engineering from the same university in 2019. His major interest is to design algorithms for fuel cost optimization and emission reductions.

International Journal of Engineering Works
ISSN-p: 2521-2419
ISSN-e: 2409-2770
Vol. 7, Issue 10, PP. 318-325, October 2020
https://www.ijew.io/
https://doi.org/10.34259/ijew.20.710318325

Design of CZTS-Perovskite thin-film Hetero-Junction Solar Cell

Engr. Azeem Ullah[1], Engr. Aimal Daud Khan[2], Engr. Muhammad Awais[3]
[1,2,3] Department of Renewable Energy Engineering, U.S Pakistan Center for Advanced Studies in Energy, University of Engineering and Technology, Peshawar, Pakistan
aazeem2286@gmail.com[1], aimaldawoodkhan@gmail.com[2], qari2162@gmail.com[3]
Received: 22 August, Revised: 02 September, Accepted: 28 September

***Abstract*—**The Thin film technology is one of the fastest growing technologies because of the increase in energy demands and scarcity of energy materials. In thin film solar PVs PSC & CZTS are two of the most promising, abundant and efficient thin film solar PVs. They offer tunable band-gaps that can be adjusted for maximum PCE. Perovskite is one of the efficient solar PV material with a band-gap ranges between 1.55 to 2.3 eV which is too much close to the optimum photovoltaic conversion material. But it is less stable and vulnerable to environment while CZTS is more stable but have less band-gap as compared to perovskite. So, we make a tandem of perovskite & CZTS to utilize their efficiencies and durability. We simulate different thickness of layers and band-gaps of this tandem using SCAPS-1D, which is one of the best utilities for efficiency calculations of thin film solar PVs. We performed different simulations for that tandem while changing the allowable thickness of absorber layers & their band-gaps to obtain an optimum solution. During multiple simulations I obtained a better efficiency of 22.61% which was the greater efficiency during my simulations.I have used SCAPS-1D for modeling and simulations of thin film Perovskite and CZTS solar cells, calculated their I-V curve QE (quantum efficiency) for different thickness whose ranges are 200-500 nm for perovskite and 200nm to 1.2um for CZTS with step-length thickness of 25nm. I selected the best configuration for my simulations for better performance, on which I performed further simulations and chose model with efficiency of 22.61%. Which shows that a handsome amount of conversion efficiency is achievable for tandem solar cells consist of Perovskite and CZTS.

Keywords—
PSC Perovskite Solar Cell
CZTS Copper Zinc Tin Sulfide
QE Quantum efficiency
PCE Power conversion efficiency

I. INTRODUCTION

This We know a basic lawof energy which govern all the natural phenomena and is valid till date. which is known as “law of energy’s conservation”, which states - “energy can neither be generated nor destroyed but can be converted from one form to another and total quantity of energy does not change”.

There exist different forms of energy with definite formulae. These forms are energy due to motion known as kinetic energy, due to position-potential energy, other types of energies are heat, solar, electrical, chemical, nuclear, elastic. If we sum up the formulae for each of these contributed energies, then there is no difference except transfer of energy – going in or out of the system.

Energy is the basic need for the nature performance and sustainability. Every material object needs energy in one or the other form. Human itself work due to availability of energy. Human body maintain itself at constant temperature of 37 ^{o}C. So it contains energy. It is fact that body of the human body is regularly cooled by the surrounding-environment, so thermal energy is dissipated to the outside. More-over blood is pumped into the vessels of the blood. As this blood travels through the blood vessels, its kinetic energy is reduced due to friction with the walls of the vessels this kinetic energy which is lost is basically transformedinto heat energy. So to keep this blood circulation in the vessels the heart provides the required energy which further need energy which is supplied by food we eat in the form of chemical energy and that chemical energy is obtained from potential energy of the food. Which is basically conversion of different energy forms for specific purpose. Furthermore, human require energy for movement and brain consume a lot of energy. The calculated adult human consumes about 10,000 kJ or 2500 kcal every day[1]. Electricity is predicted to be lied between 8TW and 25 TW with growth of nearly 3.75-17.81% within 10 to 20 years[1]. Fossil-fuel i.e; natural-gas, oil and coal is dominating source worldwide which is 85% in 2008. But increase emissions of green-house gases are between factor of 5 and 35 is forecasted[1]. So transfer from fuel to renewable energy sources like wind, biomass, solar, hydropower and tidal is must and must be matured to face the future energy crises. Among other renewable energy sources sun energy is regarded as the most sustainable source due to its availability and cleanliness[1]. Besides this solar photovoltaics technology has emerged as the faster growing technology compared to other due to great amount of cost declination between 2008 and 2012, 60%reduction has been recorded in the price of PV modules per MW[1].

Sunlight is the most abundant and sustainable source of energy, but it is not divided evenly on the earth surface. Surfaces

with low latitude that is semi-arid and aridareas, in the range of 35LN to 35LS, collect the most normal direct irradiance (DNI). For example, the Desert named Mojave (latitude: 35LN) situated in the United States, and the Negev-Desert (latitude: 30.5LN) which is located in the southern Palestine receive 1921 kW-h-m^{-2}/ year and power of 2007 kW-h/m^2/year, respectively a report by NASA Solar Insolation, 2008[1]. All other deserts of the globe, are situated between these two latitudes and are able to obtain the require energy all over the globe with solar power generation technologies.

The name of the solar photo-voltaic is derived from a Greek word "Phos" which means light and word "voltaic" which means electricity and is given the name due to large contribution of an Italian scientist Allesandro Volta in this field.Photo-Voltaic effect which is the basis of photovoltaics is the conversion of light into electricity. A device that converts optical energy from sun to electrical energy using photo-voltaic by effect of semiconductors solar cell. This phenomenon is basically the optical and electricalcharacteristics of semiconductor. When a photon, having higher energy to band-gap energy of the semi-conductor material then this photon is absorbed so that it energizes electron to shift it from valence band (V_v) to conduction band (V_c) so electron&hole pair is formed which form electric field across the p-n junction. Due to inherent properties of semiconductor solar cell efficiency is limited to 15-20% [2]. Depending upon the design of the module, installation and environment, each PV panel have different performance level. A well-researched study by scientists and engineers it is deducted that the mean between fossil-fuels consumption and emission of carbon dioxide, it can now be estimated that for international community's target accomplishment of limitation of Carbon di Oxide emission and to control or lessen the harmful effects of climate change due to consumption of fossil fuel and production of CO_2, about 25,000 GW of clean energy is needed by 2050 [3]. By the virtue of decrease in system installation and increases in industrial experience,PV shall become a better economical source of electricity production. Other findings show that the predicted PV installation is 200GW in 2020 and 2TW in 2050 globally [4]. These statistics show that there will be a great reliance on PV technologies, in term of resources and production. In predicted power thin film solar-PVhas 10% more share which is expected to be increased in the next 10-12 years [4]. This is evident from the fact that due to advancement in PV technology and concentrated solar power (CSP), these technologies have been periodicallydominated the (IEA) projected targets made for different periods of time. For example, the 2006 International Energy Agency's (IEA) projection cumulative solar capacity in 2020 and 2011 IEA's projection for 2030 have been sur-passed in year 2012 and 2014 separately[3, 5]. It is evident that solar PV has emerged the resultant energy producers due to its high contribution in today's energy especially in the off-grid areas [6] and is considered one of the prominent RE for the future[7, 8]. That statistics of solar PV indicates the option that PV technology can supply handsome chunk of future energy- mix and make it an important technology for future energy's demand and sustainability and for better environment [9, 10]. It is therefore, evident that main focus of national and international energy policies is PV technology.

The journey of photo-voltaic starts from the 19th century discovery of Becquerel in which he discovered photo-voltage by the action of light on electrode immersed in electrolytic solution in the year 1839 A.D[11]. Table 1.1 shows the remarkable contribution after this discovery.

Despite the above contributions and improvements, electricity from a solar cell is still hard to afford by a common man. In this situation thin film solar cells make the choice based on cost-effective novel, ecofriendly and abundant material which shall make remarkable contributions. Hence improvement in this technology is need of the day. Major two types of thin film PV technology based on construction type. Which are categorized in the following table.

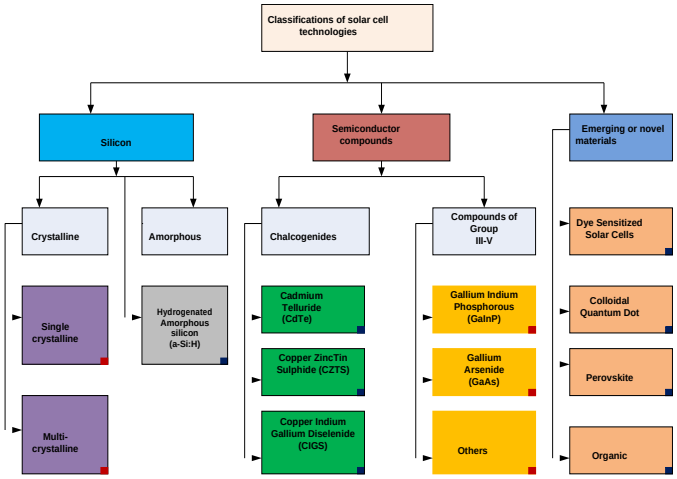

key: Represents thin-film PV Represents wafer-based PV

Fig.1 Division of PVbased onkey active material

The (1). Commercial thin film solar cell technology. It includes (CdTe), (a-Si:H), copper-indium-gallium deselenide (CIGS).

(2). Emerging or novel thin film -PV technology. Here we shall focus on evolving or novel technology of thin film- PV. It includes colloidal quantum dots PV (QDPV), Dye sensitized solar cells (DSSCs), Organic photovoltaic (OPV),Perovskite and (CZTS).

Developing or novel thin-film technology is under research stage and offer better properties which include visible transparency, high definite power in terms of watt/grams and novel form-factor [12]. In this chapter we shall discuss perovskite and CZTS under this emerging thin film technology. The origin of "Perovskite" from the calcium titanate crystal structure which was revealed by a German scientist named "Gustav-Rose" and this structure was given name by a Russian researcher named "Lev-Perovski". Which was modified to Perovskite with passage of time. Since that time the term "Perovskite" was raised to all such type of compounds which have similar crystal assembly of calcium-titanate.General formula deducted for perovskite light absorption layer is $AB\text{-}X_3$, where A is cation-organic (i.e; $CH_3NH_3^+$), B- is divalent cation-mate (i.e; Pb^{+2}, Sn^{+2}) and X which shows halide anion (i.e; Cl^-, Br^- ,I^-). Organic inorganic halide-perovskite CH_3NH_3I, photovoltaic turned great amount of attention of scientists and

engineers towards itself due to its steady and great amount of efficiency enhancement from 3.8 to 22.1 % since 2009 [13, 14], for applications in optoelectronic devices, highly efficient electroluminescence from visible range to near infrared range (NIR) light detector applications and lasers [15, 16]. Perovskite is regarded as one of the potential replacements of thin film silicon PV devices which prevail solar PV market with remarkable efficiency of 26% [17]. This small gap of efficiency between PSC and Silicon solar PV of scientists and engineers especially those who have experience in organic PV or (DSSCs) because its materials are used in engineering of PSC. Origin of (PSC) starts from the device structure of DSSCs [11].

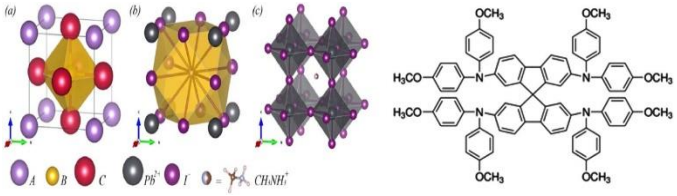

Fig. 2 Perovskite ABX_3 Construction (left) & SPIRO-OMeTAD Concluded from research ref [18] by © Copyright 2015 permission

Two of the important properties of perovskite is its largely tunable bandgap (i.e; PSC has a band-gap from 1.5 to 2.3 eV)[19]& high light captivation co-efficient which is larger than 10^4 cm^{-1}[20, 21] that is comparable to other thin film PV constituent ingredientsi.e; materials of CZTS and CdTe[22, 23]. Its suitable and low-cost fabrication techniques also play an important role as compared to Si-based fabrication that is costly and complex high vacuum deposition method. Although it has great amount of efficiency but have two major problems causing hurdle for its improvements which need attention, i.e; (i) device instability [24] and (ii) Hysteresis of J-V [25].

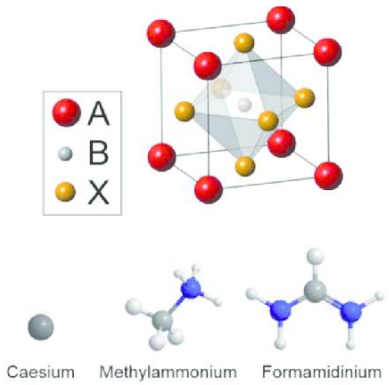

Fig. 3 A basic perovskite crystal of the form ABX3 [26]

For this purpose, we use CZTS-more stable, abundant, non-toxic light absorbing material with perovskite to make our thin film solar cell stable and efficient. For a long-term future development of PV technology, it is necessary to use such materials which are abundant, non-toxic and stable material just like silicon. For that purpose, CZTS (Kesterite -- quaternary compound) semiconductor has been developed as an owing postulant for such type of next-generation solar cell technology. It captivated attention of researchers owing to its three important properties, i.e; high efficiency, non-toxicity and low cost-earth abundant material [27,28]. Kesterite (CZTS) come-from chalcogenite family having diamond like structure and it is regarded as exact derivative of commercialized CIGSe (CuInG1-xSe2) and CdTe PV technology, which are known for complimentary electronic and optical properties which have demonstrated an efficiency of more than 22%[17]. The bandgap of CZTS is 1.5eV which is so close to optimum band-gap of a single junction PV. Furthermore, bandgap of it can be adjusted between (1.5 to 1.6 eV) during the process of fusing with other elements i.e; Ag,Ge, creating it an appropriate contender for uppermost cell bandgap goal for Si based tandem solar cell stacks[29]. Photovoltaic devices fabricated by CZTS absorber layer are one of most efficient, non-toxic andabundant thin-film PV cells under research by scientists and engineers at present time. Despite its useful properties its reported conversion efficiency so far is hardly 9% for number of years of research and development [30] which is far lower as compared to suggested efficiency limit of 33% [31], due to high deficiency in Vo (Eg/q-Vo; here Eg is bandgap, q is charge on electron[32]. Many types of preparation techniques have been implemented and employed for CZTS thin film solar cell preparation in different scientific literature [33]. In which highest solar conversion efficiency of CZTS based on solution process have been reported which is 10.1% [34]. For vacuum process based prepared pure CZTS PV cell, PCE of 8.4% have attained to date[29] while lab based fabricated solar cell have attained an attractive efficiency of 12.6% [35, 36]. In CZTS the major challenge is the management of disorder of cation defects, a phenomenon in which zinc and copper cations are internally substituted, which result into point defects and this point defect is the major cause in decrease of Voc[36].

II. METHODOLOGY

Model structure of hybrid CZTS Perovskite thin film solar cell

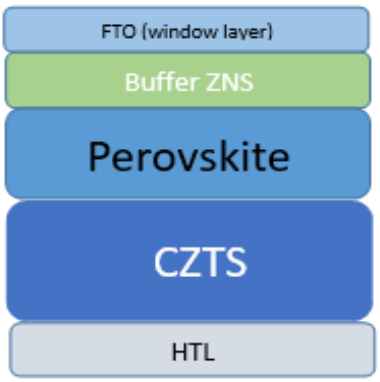

Fig. 4 proposed hybrid structure of Perovskite-CZTS solar cell

Fig. 4 displays the proposed hybrid structure of thin-film CZTS and Perovskite PV which consist of five layers. The top layer which can also be called as window layer I have used ITO (Indium Tin Oxide) that is primarily used as anti-reflection coating in opto-electronics such as liquid crystal displays (LCDs) and different kinds of electroluminescence, along this it has been used in thin film solar PVs[1,2] due to its two major qualities i.e.; high transmission efficiency of more than 85% and

low specific electrical resistivity of 1x10-4Ω-cm [3,4,5]. These properties make it one of the most suitable window layers for maximum light transmission. The second layer we installed in the structure is buffer layer made of zinc-sulfide which has a wider band-gap than subsequent layers of that model. This buffer layer along with absorption of highly energetic photons also improve conductivity of window layer, drop in its resistivity up to 50% in the window layer as well as make it crystalline. Next layer is copper zinc tin oxide (CZTS). It is known as kesterite also and chemical formula is Cu2ZnSnS4, it has attracted attention for manufacturing thin film solar PVs due to its abundance, huge efficiency, low price and non-toxicity[6,7]. After that we have PSC material which is organic inorganic lead halide perovskite, ABX3 where A is organic monovalent cation, B is lead or tin Sn(II) & X is the anion species like I- ,B-, Cl –[8]. Benefits of this type of semiconductor materials contain low material cost, low recombination-losses, large charge-carrier-diffusionlength and probability of anion and cation swap for band gap[9]. The main disadvantages of perovskite include control of properties of material and film morphology, high vulnerability to moisture, instability of cell and the use of toxic materiali.e; lead.

All simulations have been performed by SCAPS-1D which is frequently used for solar cells simulations it is free tool to measure important terms like Vo, short circuit current Is, fill factor FF and efficiency-η of PVs. Its simulations are based upon three important semiconductor equations for the study of the solar-cell routine parameters: Pioson's equation, continuity equation of holes and continuity equation of electrons. SCAPS-1D software solves these three partial differential equations in a numerical way for electrostatic potential of holes and electrons concentrations as a function of positions X.

Poisson's equation can be formulated as follows:

$$\frac{\partial}{\partial x}\left(\varepsilon\frac{(x)\partial\psi}{\partial x}\right)=\frac{-q}{\varepsilon_0}\left[p-n+N_D^{+}-N_A^{-}+\frac{\rho\, def(n,p)}{q}\right] \quad (1)$$

Where ϵ is the dielectric constant, Ψ is the electrostatic potential while q is charge on electron or electronic charge, p and n are the free charge-carriers/volume while N_D^+ and N_A^- are ionized-donor and acceptor type dopants, i.e; localized states &$\rho\, def$ is the defect of charge density. Now continuity equation for conservation of free holes and free electrons in a device are expressed as;

$$\frac{\partial p}{\partial x}=-\frac{\partial J_p}{\partial x}+G-U_p(np) \quad (2)$$

$$\frac{\partial n}{\partial t}=\frac{-J_n}{\partial x}+G-U_n(np) \quad (3)$$

Where n and p are free carrier conc, N_D and N_A are charged dopants, $\rho\, def(n,p)$ distribution of defects, J_p, J_n are the holes and electrons current densities, U_p, U_n are the recombination rates and generation rate is represented by G.

During simulations we changed some parameters while keeping other key parameters constant; i.e; absorber layer thickness was changed while keeping doping concentrations etc kept constant. In second step we changed doping concentration in the absorber layer and checked for their output key parameters. We performed simulations in the room temperature or ambient temperature (250C or 300K).At the final step we concluded the optimum thickness and doping concentration of absorber layer after several simulations results by observing Jsc,Voc, FF% and conversion efficiency percentage, performed by SCAPS-1D.

III. Results and Discussion

We observed different parameter values for different thickness of each layer as well as defects in respective layers. These parameters include voltage, current, fill-factor, efficiency. Which are described in the following manner:

Window layer:

We start with the top window layer whose thickness has been varied and observed the key parameters, where in our simulations optimum thickness value is 160nm where maximum open circuit voltage, short circuit current density, percentage fill-factor and conversion efficiency obtained with values of 0.8706 V, 24.55044 mA/cm2, 75.02% and 15.71% respectively as sown in fig.5.

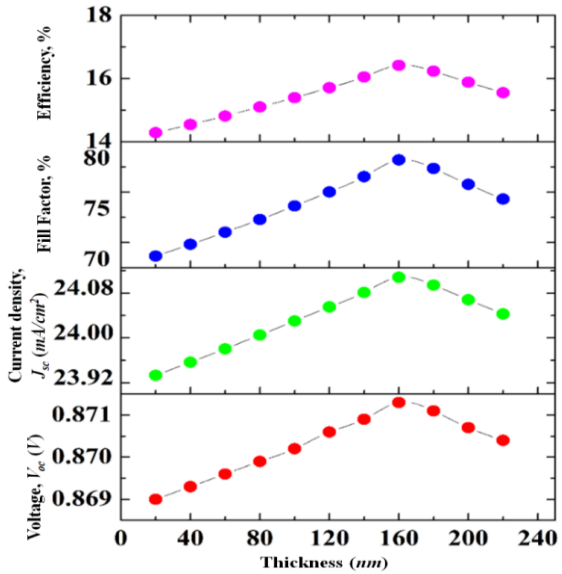

Fig. 5

Then we changed the doping concentration in the window layer and observed different values of performance parameters for different value of defect or doping values. During which we obtained an optimum value at 22 doping concentration/cm3 where performance parameters in term of Voc, Jsc, percentage fill-factor FF, and efficiency of the value of 0.8720 V, 23.081452 mA/cm3, 78.18% and 17.14% respectively as sown in fig.6.

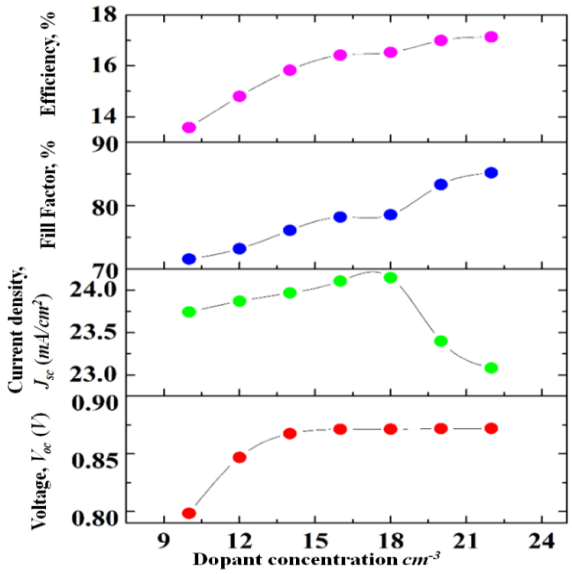

Fig. 6

Buffer layer:

The main function of the buffer layer in heterojunction thin film solar cell is to form such a junction layer which admit maximum number of light rays to absorber layer and junction layer [1]. Here we observed buffer layer by changing its width and doping concentration and observed different performance parameters of the thin film solar cell and we obtained the following result during the process. During simulations of buffer layers for different width, we obtained optimum solution at 220nm where we obtained, Voc,Jsc, fill-factor FF and efficiency ,ef of 0.8737 volt, 24.106716 mA/cm2, 85.37 % and 17.97% respectively as sown in fig. 7.

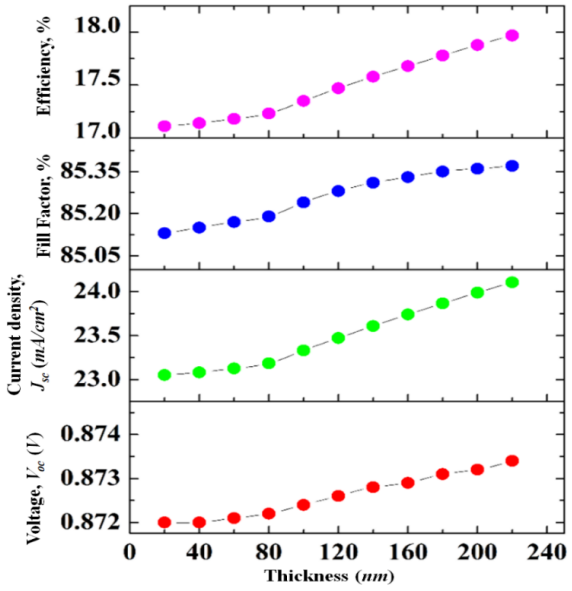

Fig. 7

Now by changing the doping concentration of the buffer layer we performed different simulations during which we obtained an optimum solution at defect value of 20/cm3 of buffer layer where we obtained maximum values of Voc, Jsc, fill-factor percentage and efficiency percentage of 0.8735 volt, 24.213276 Amp/cm2, 85.35% and 18.05 % respectively as sown in fig. 8.

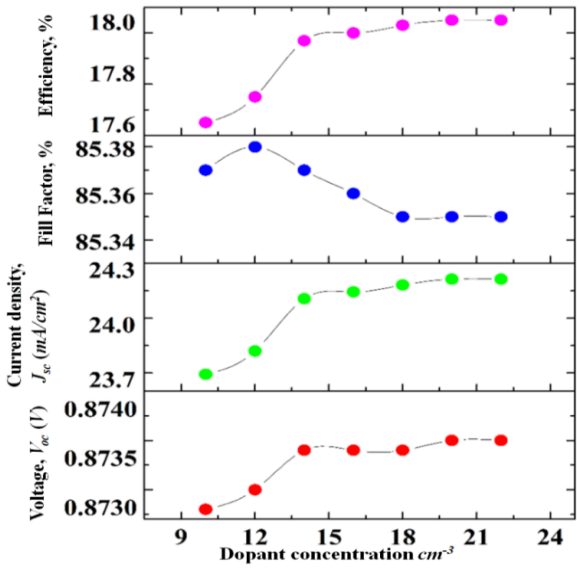

Fig. 8

Absorber layer1 (Abs1) or Perovskite layer:

Graph of Abs 1:

From the simulation graph it's is obvious that the optimum thickness is 400nm for which optimized cell performance parameters occur. Beyond this thickness, although there is increase in other parameters except fill-factor which decreases which largely effect cell performance as sown in fig. 9.

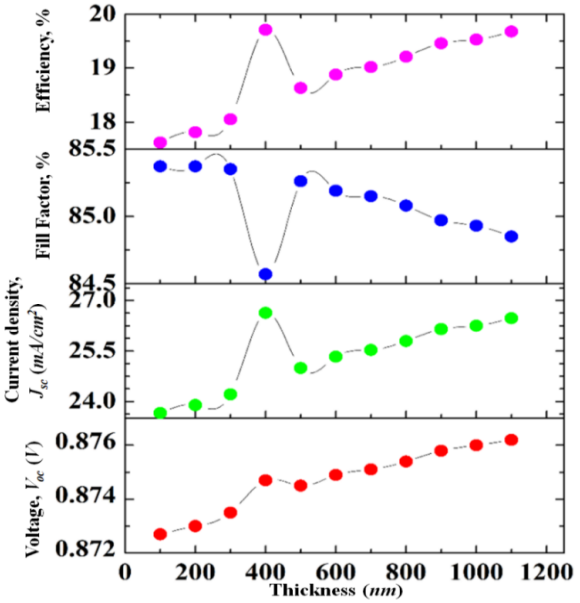

Fig. 9

Absorber layer 2 (Abs 2) or CZTS layer:

Then we observed absorber layer-2 or cupper zinc tin sulphide (CZTS). Whose simulations are stated in the following table which shows key performance parameters for different thickness of CZTS layer. During our simulations we obtained an optimum solution at thickness of 1000nm where we obtained Voc, short Jsc , fill-factor% and efficiency% of 0.8926 volt, 28.860649 A/cm2, 82.93% and 21.36% respectively as sown in fig. 10.

Furthermore, during simulations keeping I obtained efficiency of 22.6% for tandem Perovskite-CZTS solar cell by changing the band-gaps of perovskite and CZTS to 1.9 eV and 1.6 eV respectively as sown in fig. 11. For that formation I obtained an efficiency of 22.60%. This high efficiency is as a result of making high bandgap absorbing material where recombination losses are low. I took the sample of already made structure where efficiency was 22.57%[37].

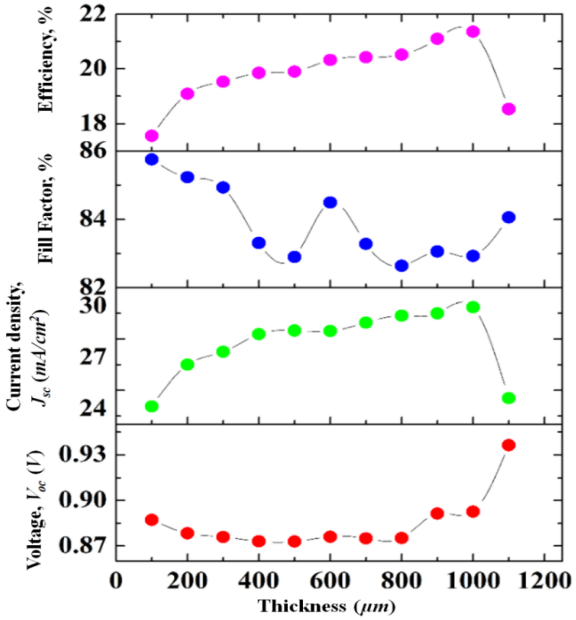

Fig. 10

BSF:

It is the last layer of the stack known as back surface field or hole transport layer- HTL in thin film solar cells. It's basically a p-type which serves as p-type dopant in the back surface. This layer controls recombination losses as well as keeping series resistance at low level by providing ease to mobile carriers to be collected at the back electrode, thus enhancing fell-factor. We had performed simulations on its thickness as well as defects and picked-up optimized solution of this layer through SCAPS-1D. Following are the tables showing optimum width and defect of back surface field. It shows that the optimum width of this layer is 440nm for which we have 0.9157 V-Voc, 29.142192 A/cm2 - Jsc , 82.99% fill-factor percentage and 22.15% conversion efficiency percentage. The following simulation diagram shows the performance parameters dependence on the thickness of the HTL material which about linearly increases by increasing its thickness up to 440nm and beyond this thickness series resistance increases which decreases fill-factor. Which can be easily seen from the following simulations diagram

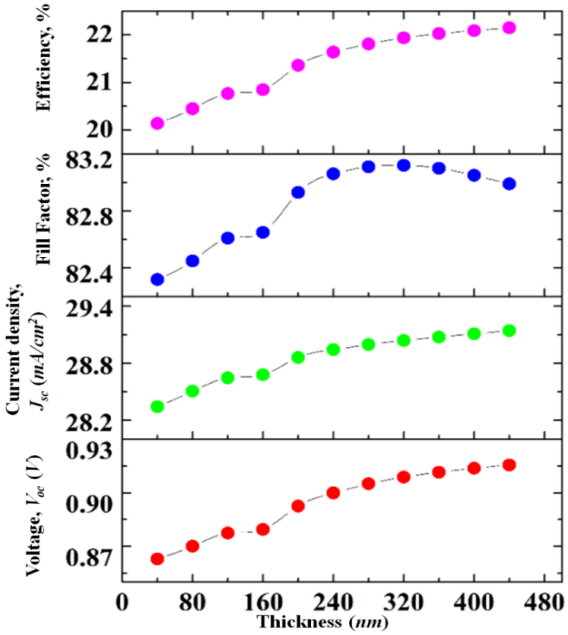

Fig. 11

The following figure shows the simulated program result of defect/ doping concentration which effects the performance parameters of thin film solar cell in which 21 mass/cm3 concentration which shows maximum EF% of 23.22%, FF of 83.87% , Jscof 29.139922 A/cm2 and Vocof 0.9750. After this, fill-factor declines due to due to increase in series resistance so optimum solution is that as sown in fig. 12.

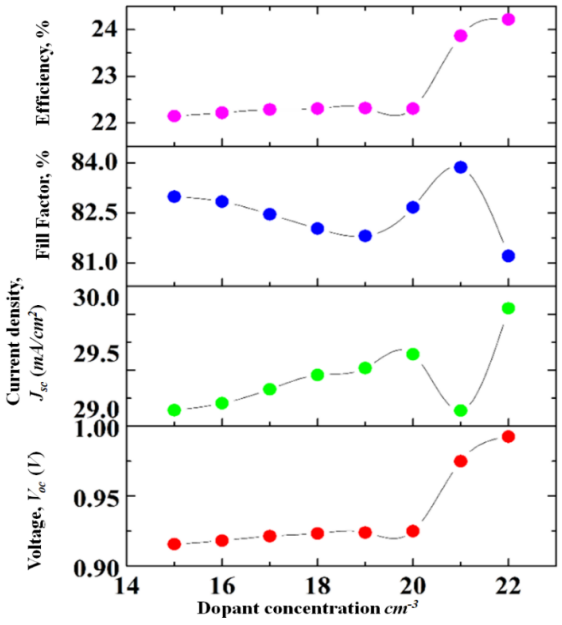

Fig. 12

CONCUSLION

I worked on the perovskite solar cell due to its organic inorganic properties and high conversion efficiency and abundancy. As its efficiency is high but its life time is so short and is vulnerable to environment so the need of tandem is felt for which CZTS an abundant, stable and non-toxic is the best material to make tandem with Perovskite cell to make it durable and efficient. As their bandgaps can be tuned to obtain high quantum efficiency. As Perovskite have high bandgap of 1.55 to 2.3 electron volts and CZTS have 1.45 to 1.6 electron volts. So for high energy photon i.e UV light we place Perovskite absorber layer and for low energy photons i.e; infrared we place CZTS as it has smaller bandgap.

From simulations keeping the bandgap and thickness of the absorber layers we obtain a best efficiency of the tandem which was 22.60%. For future works I shall recommend different fusions of absorber layers buffer layers and using tunnel junction between the perovskite-CZTS layers as well as keep changing bad-gap and thickness of the absorber layers we can obtain higher efficiencies.

REFERENCES

[1] A. H. Smets, K. Jäger, O. Isabella, R. van Swaaij, and M. Zeman, Solar Energy: The physics and engineering of photovoltaic conversion technologies and systems: UIT, 2016.

[2] T. Tiedje, E. Yablonovitch, G. D. Cody, and B. G. Brooks, "Limiting efficiency of silicon solar cells," *IEEE Transactions on electron devices*, vol. 31, pp. 711-716, 1984.

[3] R. C. Armstrong, C. Wolfram, K. P. De Jong, R. Gross, N. S. Lewis, B. Boardman, *et al.*, "The frontiers of energy," *Nature Energy*, vol. 1, p. 15020, 2016.

[4] A. Jäger-Waldau, "PV status report 2013," Institute for Energy and Transport, Renewable Energy Unit, p. 55, 2013.

[5] M. A. Green, "Crystalline and thin-film silicon solar cells: state of the art and future potential," *Solar energy*, vol. 74, pp. 181-192, 2003.

[6] P. V. Kamat, "Evolution of perovskite photovoltaics and decrease in energy payback time," ed: ACS Publications, 2013.

[7] S. Reichelstein and M. Yorston, "The prospects for cost competitive solar PV power," *Energy Policy*, vol. 55, pp. 117-127, 2013.

[8] F. Cucchiella, I. D'Adamo, and S. L. Koh, "Environmental and economic analysis of building integrated photovoltaic systems in Italian regions," *Journal of Cleaner Production*, vol. 98, pp. 241-252, 2015.

[9] P. FAQs, "Does the world have enough materials for PV to help address climate change," *US Department of Energy*, 2005.

[10] F. Cucchiella, I. D'adamo, M. Gastaldi, and S. L. Koh, "Renewable energy options for buildings: Performance evaluations of integrated photovoltaic systems," *Energy and Buildings*, vol. 55, pp. 208-217, 2012.

[11] M. Becquerel, "Mémoire sur les effets électriques produits sous l'influence des rayons solaires," *Comptes rendus hebdomadaires des séances de l'Académie des sciences*, vol. 9, pp. 561-567, 1839.

[12] J. Jean, P. R. Brown, R. L. Jaffe, T. Buonassisi, and V. Bulović, "Pathways for solar photovoltaics," *Energy & Environmental Science*, vol. 8, pp. 1200-1219, 2015.

[13] A. Kojima, K. Teshima, Y. Shirai, and T. Miyasaka, "Organometal halide perovskites as visible-light sensitizers for photovoltaic cells," *Journal of the American Chemical Society*, vol. 131, pp. 6050-6051, 2009.

[14] M. Saliba, T. Matsui, J.-Y. Seo, K. Domanski, J.-P. Correa-Baena, M. K. Nazeeruddin, *et al.*, "Cesium-containing triple cation perovskite solar cells: improved stability, reproducibility and high efficiency," *Energy & environmental science*, vol. 9, pp. 1989-1997, 2016.

[15] F. Deschler, M. Price, S. Pathak, L. E. Klintberg, D.-D. Jarausch, R. Higler, *et al.*, "High photoluminescence efficiency and optically pumped lasing in solution-processed mixed halide perovskite semiconductors," *J. Phys. Chem. Lett*, vol. 5, pp. 1421-1426, 2014.

[16] G. Xing, N. Mathews, S. S. Lim, N. Yantara, X. Liu, D. Sabba, *et al.*, "Low-temperature solution-processed wavelength-tunable perovskites for lasing," *Nature materials*, vol. 13, p. 476, 2014.

[17] K. Yoshikawa, H. Kawasaki, W. Yoshida, T. Irie, K. Konishi, K. Nakano, *et al.*, "Silicon heterojunction solar cell with interdigitated back contacts for a photoconversion efficiency over 26%," *Nature Energy*, vol. 2, p. 17032, 2017.

[18] T. J. Jacobsson, L. J. Schwan, M. Ottosson, A. Hagfeldt, and T. Edvinsson, "Determination of thermal expansion coefficients and locating the temperature-induced phase transition in methylammonium lead perovskites using x-ray diffraction," *Inorganic chemistry*, vol. 54, pp. 10678-10685, 2015.

[19] N. J. Jeon, J. H. Noh, W. S. Yang, Y. C. Kim, S. Ryu, J. Seo, *et al.*, "Compositional engineering of perovskite materials for high-performance solar cells," *Nature*, vol. 517, p. 476, 2015.

[20] N.-G. Park, "Perovskite solar cells: an emerging photovoltaic technology," *Materials today*, vol. 18, pp. 65-72, 2015.

[21] M. Zhang, J. S. Yun, Q. Ma, J. Zheng, C. F. J. Lau, X. Deng, *et al.*, "High-efficiency rubidium-incorporated perovskite solar cells by gas quenching," *ACS Energy Letters*, vol. 2, pp. 438-444, 2017.

[22] Z. Shi and A. H. Jayatissa, "One-pot hydrothermal synthesis and fabrication of kesterite Cu2ZnSn (S, Se) 4 thin films," *Progress in Natural Science: Materials International*, vol. 27, pp. 550-555, 2017.

[23] J. Rangel-Cárdenas and H. Sobral, "Optical absorption enhancement in CdTe thin films by microstructuration of the silicon substrate," *Materials*, vol. 10, p. 607, 2017.

[24] W. Chen, Y. Wu, Y. Yue, J. Liu, W. Zhang, X. Yang, *et al.*, "Efficient and stable large-area perovskite solar cells with inorganic charge extraction layers," *Science*, vol. 350, pp. 944-948, 2015.

[25] E. L. Unger, E. T. Hoke, C. D. Bailie, W. H. Nguyen, A. R. Bowring, T. Heumüller, *et al.*, "Hysteresis and transient behavior in current–voltage measurements of hybrid-perovskite absorber solar cells," *Energy & Environmental Science*, vol. 7, pp. 3690-3698, 2014.

[26] A. Jain, I. E. Castelli, G. Hautier, D. H. Bailey, and K. W. Jacobsen, "Performance of genetic algorithms in search for water splitting perovskites," *Journal of materials science*, vol. 48, pp. 6519-6534, 2013.

[27] M. A. Green, "Commercial progress and challenges for photovoltaics," *Nature Energy*, vol. 1, p. 15015, 2016.

[28] P. D. Antunez, D. M. Bishop, Y. Luo, and R. Haight, "Efficient kesterite solar cells with high open-circuit voltage for applications in powering distributed devices," *Nature Energy*, vol. 2, p. 884, 2017.

[29] B. Shin, O. Gunawan, Y. Zhu, N. A. Bojarczuk, S. J. Chey, and S. Guha, "Thin film solar cell with 8.4% power conversion efficiency using an earth-abundant Cu2ZnSnS4 absorber," *Progress in Photovoltaics: Research and Applications*, vol. 21, pp. 72-76, 2013.

[30] S. Tajima, M. Umehara, M. Hasegawa, T. Mise, and T. Itoh, "Cu2ZnSnS4 photovoltaic cell with improved efficiency fabricated by high-temperature annealing after CdS buffer-layer deposition," *Progress in Photovoltaics: Research and Applications*, vol. 25, pp. 14-22, 2017.

[31] A. Polman, M. Knight, E. C. Garnett, B. Ehrler, and W. C. Sinke, "Photovoltaic materials: Present efficiencies and future challenges," *Science*, vol. 352, p. aad4424, 2016.

[32] D. Shin, B. Saparov, and D. B. Mitzi, "Defect engineering in multinary earth-abundant chalcogenide photovoltaic materials," *Advanced Energy Materials*, vol. 7, p. 1602366, 2017.

[33] K. Ramasamy, M. A. Malik, and P. O'Brien, "Routes to copper zinc tin sulfide Cu 2 ZnSnS 4 a potential material for solar cells," *Chemical Communications*, vol. 48, pp. 5703-5714, 2012.

[34] D. A. R. Barkhouse, O. Gunawan, T. Gokmen, T. K. Todorov, and D. B. Mitzi, "Device characteristics of a 10.1% hydrazine-processed Cu2ZnSn (Se, S) 4 solar cell," *Progress in Photovoltaics: Research and Applications*, vol. 20, pp. 6-11, 2012.

[35] M. A. Green, K. Emery, Y. Hishikawa, W. Warta, and E. D. Dunlop, "Solar cell efficiency tables (Version 45)," *Progress in photovoltaics: research and applications*, vol. 23, pp. 1-9, 2015.

[36] W. Wang, M. T. Winkler, O. Gunawan, T. Gokmen, T. K. Todorov, Y. Zhu, *et al.*, "Device characteristics of CZTSSe thin-film solar cells with 12.6% efficiency," *Advanced Energy Materials*, vol. 4, p. 1301465, 2014.

[37] I. T. Bello, M. K. Awodele, O. Adedokun, O. Akinrinola, and A. O. Awodugba, "Modeling and simulation of CZTS-perovskite sandwiched tandem solar cell," *Turkish Journal of Physics*, vol. 42, pp. 321-328, 2018.

AzeemUllah received BSc. degree in Electrical (Power) Engineering from University of Engineering and Technology, Taxila, Pakistan in 2015. He is currently pursuing his Master Degree in Renewable energy Engineering from U.S-Pakistan Center for Advance Studies in Energy, University of Engineering and Technology, Peshawar, Pakistan. His research interests include Power System design, Solar Cells, Renewable Energy Materials and Modeling, Photovoltaic Devices.

International Journal of Engineering Works
ISSN-p: 2521-2419
ISSN-e: 2409-2770
Vol. 7, Issue 10, PP. 326-332, October 2020
https://www.ijew.io/
https://doi.org/10.34259/ijew.20.710326332

Machine Learning based Energy Consumption Prediction of Appliances in a Low Energy House

Samiullah[1], Muhammad Nazeer[2], Naveed Malik[3]
[1,2,3] Department of Electrical Energy System Engineering, US-Pakistan Center for Advanced Studies in Energy (US-PCASE), UET Peshawar
samiullahkhan4191@gmail.com[1], muhammadnaxeer@gmail.com[2], engrmalikuet@gmail.com[3]
Received: 22 September, Revised: 30 September, Accepted: 05 October

***Abstract*—**In reaction to the impacts of global warming, individuals are becoming increasingly conscious of their homes unchecked power usage, particularly the use of electrical energy for cooking, heating, refrigeration, dish-washing and drying. There is an increased concern about idle losses, expended by devices when not in use, which not only add to utility bills but also add to the waste of energy. Monitoring and controlling end-use electricity demand in residential buildings can have a significant impact on reducing peak demand and optimizing energy consumption that can be achieved in smart households with residential load control systems.
This study benchmarked eight Machine learning based algorithms: Linear, Ridge and LASSO regression; Support Vector Machine; Multilayer Perceptron; Nearest Neighbor regression; Extra-Trees and XG-Boost on a pre-collected "appliance energy" data-set. The specified algorithms were benchmarked on error metric of: training and testing set R-squared statistic; MAE; RMSE and also training time. Data-preprocessing and visualization was done to yield insight into data used. Firstly, un-tuned version of the eight algorithms were benchmarked, then model tuning via Grid-Search was carried for five algorithms and finally the effects of inclusion of certain features and varying parameters was tabulated and graphed. The least scores, on the specified error metrics, were obtained by the regression algorithms. The best scores were obtained by Extra-Trees and XG-Boost, which belong to ensemble algorithms of which Extra-Trees obtained best variance explanation (R-squared) scores of 98.94% on training set and 60.21% on testing set along with least scores on above specified error metrics.

***Keywords*—** Machine Learning, Regression, Prediction.

I. INTRODUCTION

Reduction of CO2 emissions is the need of the hour as excessive energy usage has led to increase of ill effects of green-house gas and has impacted various sectors of economy in the world[1]. Among the various sectors, the residential block remains a dominant consumer of electrical energy in each and every country and in need of special attention for the development of techniques to reduce energy consumption. In the U.S residential building consumes about 16-52% of all sectors combined and comes around a worldwide average of 30%[2]. In response to the effects of global warming, people are increasing becoming aware of the excessive energy consumption in their homes especially electrical energy use for cooking and heating[3]. They are now more conscience of the standby losses that appliances incur which not only increase utility bills but also contribute to energy wastage[4]. To help users in adopting renewable energy generation, implement demand side management, promote healthy energy consumption strategies and home automation infrastructure detailed models are need to capture the energy consumption habits of their home[5].

In general, the tentative estimate of complete energy usage in the housing industry is released by governments: compiling gross energy values presented by energy suppliers[6]. These estimates offer good indices of energy consumption in the incumbent sector but may be incorrect, since they do not cater for unreported energy or generation on-site

Techniques for modelling residential energy usage can be generally divided into two classifications: "top-down approach " and "bottom-up approach ". The top-down perspective treats the housing industry as an energy drain and individual uses does not differentiate energy usage because of personal end-use. The bottom-up method includes all models using input information below the level of the overall sector. Models can account for individual end-use power consumption; on the basis of the representative weight of the model sample, individual houses or groups of houses are then extrapolated to represent the region or nation

The approach taken in this study is that of a "Machine learning" model building approach. ML based energy consumption prediction methods have gained a lot popularity in recent years due to increase in computing power; especially increase in the processing power of graphic processing units (GPU), multi-core processors, open-source implementation of sophisticated algorithms and wide availability of data available

from various repositories that host data for ML model building purposes.

II. Related Work

Westergren et al.[7] Proposed a LR model which takes weather data as input and predicts electricity use of four homes located in Sweden. Three models were proposed for the prediction of electrical energy consumption per unit hour. The first two models were of the LR kind which took the mean of deviation of temperatures inside and outside the house. Al-Garni et al.[8] Developed a LR model to predict electricity consumption in Eastern Saudi Arabia by using environmental variables such the ambient temperature, humidity, solar irradiation. Model variables were selected using the step-wise regression technique. T.A Reddy et al.[9] Used synthetic data to develop a multiple regression and a Principle component analysis (PCA) based model to predict daily electricity consumption. Moletsane el al.[10] Implemented a LR model on real data collected over the period of two years from the sensors placed inside two houses. The electricity consumption data of a house was obtained every 30 minutes. The data was recorded using every wall socket plug in the house. Ambient temperature and outside weather conditions were used to develop the regression model. For home 1 an R-squared value of 0.67 was obtained which had not heating/cooling load control while for home 2 an R-squared value of 0.87 was obtained which had a better load control mechanism installed.

Kalogirou et al.[11] Used a multilayer recurrent neural network (RNN) with back-propagation for predicting the energy consumption of a passive solar house. Two cases were investigated: one with building walls fully insulated and one with partial insulation of building walls with thermal insulation and masonry. The effect of two seasons: summer and winter was also included in the experiment.The artificial neural network was trained on the simulated data using the variables listed above with the output being the building energy consumption in kWh. The model achieved an R-squared of 0.9975 on the training data and an R-squared value of 0.9911 on the test data which signals accuracy of the model in explaining the variance in the building energy consumptionon of a building. Neto et al.[12] Implemented feed-forward neural network (FFNN) with 11 neurons and 4 hidden layers to predict the energy consumption of an administration building of a University campus in Sao Paulo and compared the performance of the algorithm with a detailed building energy simulation software (Energy-Plus). The input or feature variables were meteorological data: humidity, temperature, atmospheric pressure, solar radiation; the occupant behavior (air-conditioning use);effect of weekdays and weekends; lighting use in the building and the seasonal affects: summer, winter The results showed that the detailed engineering approach to predicting building energy consumption that take building physical characteristics as input produced an error range of ±12% for 80% of the testing data while the neural network model produced an average error of about 9% on the test set including the effects of weekends.

Gonzalez et al.[13] Used a multilayer perceptron with feed-back to predict hourly electricity consumption of a building. The dataset used was divided into two parts to simulate two distinct building energy consumptions. The neural network was composed of one hidden layer, 25 neurons, and the tangent hyperbolic function was used as an activation function. The input features were environmental variables, building occupancy, time of day, hour of day, effect of public holidays. The predicted variable was total electricity consumed in an hour in the two building. The neural network was trained using a hybrid back-propagation method which had recursive feature. The trained neural network was able to achieve a coefficient of variation (CV) score of 1.4422, mean bias error (MBE) of 0.0332 and a mean absolute percentage error (MAPE) of 1.955. The authors used a training of 21 days to achieve the best results. The results showed that the training window was an important variable for increasing the algorithm's accuracy in forecasting electricity consumption

A Chae et al.[14] Implemented a neural network with Bayesian based regularization to predict energy usage of an office building. The data used consisted of 1000 sample point with 21 different types of measurements recorded at 15 minute intervals in (kWh).The variable used for the prediction were ambient conditions, weather variables, temperature, humid, time of the day, day of the week, operation cycle of the HVAC components especially chillers. The preliminary variable selection was performed using random forest (RF) algorithm. The algorithm was applied till 6 important variables were selected. A Bayesian regularized neural network was used to train on the reduced dataset. To select the optimal number of hidden layers and neurons the two were varied. The neurons were varied between 10 and 50 while number of hidden layer varied between 1 and 10. The best architecture had 6 hidden layers and 50 neurons with a sigmoidal activation. The trained network achieved an average of RMSE (RMSE) 10% and mean squared error (MSE) of 0.0099.

Biswas et al.[15] Applied feed-forward neural networks with two different kind optimization algorithms to train the network: the Levenberg-Marquardt (LM) and OWO-Newton to predict the energy consumption of an unoccupied house. Two cases were considered: one for predicting the overall energy consumption and the other for predicting the energy consumed by a heating pump. The model considered various weather parameters as input features: the dry bulb temperature, relative humidity and solar radiation. First an ANN was trained using the LM algorithm to predict the overall energy consumption of the unoccupied house. The data was collected during the summer from June 2013 to August 2013 with 60 sample points. 25% percent of the data was set aside for testing and rest for training. Using exploratory data analysis it was revealed that the overall energy consumed by the house was highly non-linear as compared to the energy consumption trend of heating pump. The ANN had one input layer, one hidden layer with 8 neurons and one output layer. The LM ANN was able to achieve an R-squared value 0.868 and the OWO-Newton ANN was achieved an R-squared value 0.871 with 1000 epochs. The same networks were used to predict energy consumption of heating

pump of the unoccupied house. The LM ANN predicated with an R-squared of 0.912 while the OWO-ANN achieved an R-squared of 0.886. From the results it was concluded that LM ANN performed had a slight edge over the OWO-Newton algorithm in terms of prediction accuracy

Dong et al.[16] Applied support vector regression to forecast the hourly energy consumption of four office buildings located in a tropical region in Singapore. The SVM used RBF as kernel and 4-fold CV was applied to find the Cost parameter (C) and epsilon error parameter (ε). A grid search was performed for the data of 4 buildings to estimate the value of C and ε. The C varied between 2-5 and 25 and ε varied from 0.001 to 0.1. The SVM with C = 2-5 and ε = 2-2 was able to achieve an MSE = 0.14, %Error = -1.89, CV = 99%..

III. METHODOLOGY

The approach taken in this study is that of a "Machine learning" model building approach. ML based energy consumption prediction methods have gained a lot popularity in recent years due to increase in computing power; especially increase in the processing power of graphic processing units (GPU), multi-core processors, open-source implementation of sophisticated algorithms and wide availability of data available from various repositories that host data for ML model building purposes. The seven steps are outlined below and are each explained in detail.

1. Data acquisition
2. Data Preparation or Pre-processing of data
3. Selecting algorithm
4. Training the algorithm
5. Testing the algorithm
6. Parameter tuning
7. Prediction

1. Data acquisition

The data used for this study was downloaded from "UCI ML Repository". The data-set consists of 19,735 sample points on 29 features. The data points comprised 10 minutes interval aggregated energy consumption data recorded by sensors placed in various rooms of a passive energy house. The data-set mostly consists of humidity and temperature conditions inside and outside house. The variable to be predicted is "appliance energy consumption", represent by "appliances" column, whose units are in Watt-h.

2. Data Preparation or Pre-processing of data

First, data is read using the "Pandas" library. The data-set is then split into training and testing set, in which, 75% is for training and 25% testing. After performing the split, the training data consisted of 14,801 sample points and 4,934 test sample points (Figure 1).

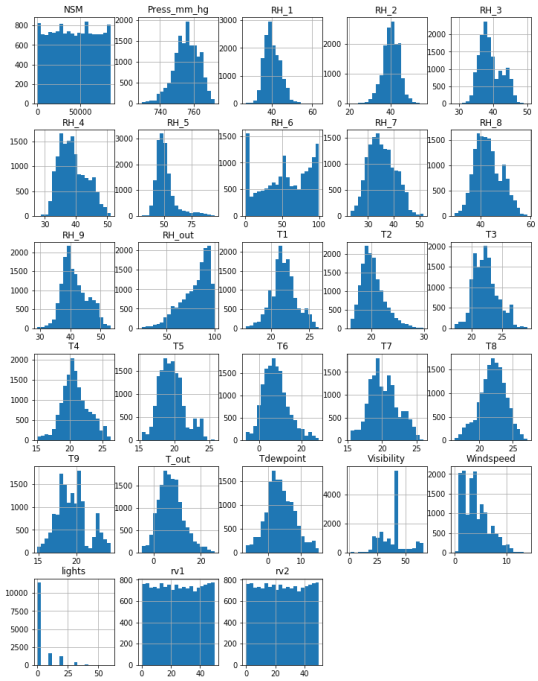

Figure 1. Distribution of predictors

To proceed with visualization of data, first the distribution of input features is plotted, the distribution of target variables and the correlation among them are also plotted, and finally some observations are made from visualization of data.

TABLE I. SUMMARY STATISTICS OF ENERGY USAGE

Count	14,801
Min value	10
Max value	1081
Mean	97.85
Standard error	102.93
25%	50
50%	60
75%	100

3. Selecting algorithm

Selection of particular algorithm depends on numerous considerations, some of which are consideredbelow:

Problem type: It is clear that algorithms were designed to solve specific instances of problems. It's important to know type of problem being dealt with and the type of algorithm used to solve that specific problem.it is vital to understand the nature of the problem and whether it yields itself to one of the following types of learning: Supervised, Unsupervised and Reinforcement learning.

Training data size: High bias and low variance classifiers (Naïve Bayes) have an edge over low bias and high variance classifiers (KNN) for a small training set, since the latter will start over-fitting. As high bias methods are not complex enough to provide accurate results, the low variance algorithms will start to show improved performance as the training set grows.

• Training time: Training time usually depends on the size of the dataset and the accuracy of output because algorithms have varying runtime.
• Parameter size: Parameters influence the behaviour of the algorithm, like tolerance for errors or number of iterations. Typically, in order to find a good mix, algorithms with a large number parameters require trial and error.
• Feature size: Compared to the amount of sample points, the amount of features in some datasets can be large. Often this situation has been observed in genetics and textual information. Some learning algorithms can be overwhelmed by the big amount of characteristics, making training time unfeasible. In this situation, certain algorithms such as SVM are especially suitable.
• Linearity assumption: Linear algorithms are good choice for first run of the data. This is the underlying assumption for many algorithms: LR, SVM, logistic regression, etc.it works well in some instances but may decrease the accuracy of the model in other situations.
• Accuracy: Approximation is sometimes sufficient, which can result in an enormous decrease in processing time. The desired accuracy is highly dependent on the ML problem. Approximation techniques are Nosie immune and robust to over-fitting.

4. Training the algorithm

The training process of an ML model includes providing sample data to learn from using an ML algorithm (learning algorithm). Training data should include the correct response, known as target attribute. Training data can be: collection of text, images, and that collected from individual processes by sampling. The learning algorithm discovers patterns in the sample data, mapping the target's input data features and yields an ML model capturing these patterns. The ML model is then employed to obtain predictions on news data for which the desired outcome is not known .Usually, 70% of the data is set aside of training.

5. Algorithm Testing

To this end, a test harness is defined which means that a data set is created on which an algorithm is trained and tested against set performance measure. Testing the algorithm on an instance of a problem should be the objective of the test harness. The result of testing various algorithms will be an estimate of how a multitude of algorithms benchmark on the selected performance measure. Performance measurement is a means of assessing a solution to particular problem. Standard performance measurements will provide with a score that is relevant to domain of problem (e.g. classification accuracy). Using the entire transformed data set to train and test a specified algorithm is a more advanced strategy called CV which involves dividing the dataset into a number of instance sets (folds) of equal size. The model will then be implemented on all handles except one the developed model will be validated on the left out fold. This process is iteratively repeated for each fold and eventually performance measurements are averaged among all folds to assess the performance of the algorithm. 30 to 25% of data is used for testing.

6. Parameter tuning

Hyper-parameters are external model settings variables whose values cannot be derived from data meaning in standard model training, they cannot be learned straight from the data-set.it is frequently specified prior to training by trial and error till best prediction performance measure is achieved by the algorithm. Grid Search is simply an exhaustive method of searching over a manually supplied subset of parameters in the hyper-parameter space.it has been the go to method for many researchers and been the conventional way of hyper-parameter tuning. The exhaustive search is tracked by a performance metric, usually training cross validation or test set evaluation score. It might needed to manually set the boundaries or do a discretization of search space because search space of ML algorithm might contain real numbers or values which are unbounded.

7. Prediction

After the model has been trained and cross validated the model is tested on 25% of data used for testing and the results are reported.

IV. RESULTS

ML-algorithm benchmarking was done in "Jupyter notebook" which is a part of "Anaconda distribution" for Python. "Jupyter" provides an interactive environment for programming rather than a "compiled" approach. The libraries used for carrying out visualization of data were mainly "Matplotlib" and "sea-born"; for data analysis "Pandas" and for core-ML algorithms, the "Sci-kit learn" library was used which are all open-source and freely available. The simulation was carried out on a core-i5 7th gen processor with @ 16GB DDR5 memory.

Exploratory Data Analysis.

Temperature t1 through tout, are normally distributed. The interval values for inside house t1 to tout except t6 varies as 14.79°C to 29.65°C and outside house, t6, -6.04°C to 28.20°C. This range was obtained from "pandas' feature describe" function. Outside temp variability is more than inside temp (Table I). Humidity markers, both inside and outside house are mostly normally distributed and varies inside the house, for rh1 through rh9, between 20.63% to 63.56% except rh5 taking values 29.72% to 96.52% and rh6 which ranges 1% to 98.9%. Wind-speed, lights, visibility, rh6 and rhout have irregular distributions.Wind-speed exhibits positive skew while Visibility negative skew.Appliance exhibits positive skew with strong outliers as marked by high values of 1081.The mean of appliance column is 97.85 with standard deviation of 102.93. 75% of values lie below 100 which indicates lower energy use most time. The temp t1 through tout have positive correlations with appliances (**Error! Reference source not found.**). All indoor temp variables have strong positive correlation as compared to outside temps. A high correlation (> 0.94) exists between column t9 and t3, t5, t7, and t8 as shown plotted, t6 and tout also exhibit high correlation. The humidity markers have mild positive (< 0.6) correlations. Visibility, Tdewpoint, and Pressure_mm_hg have low (< 1) correlation values. Rv1 and rv2, the random variables have no effect.There are no variables that indicate Weekend days' consumption.

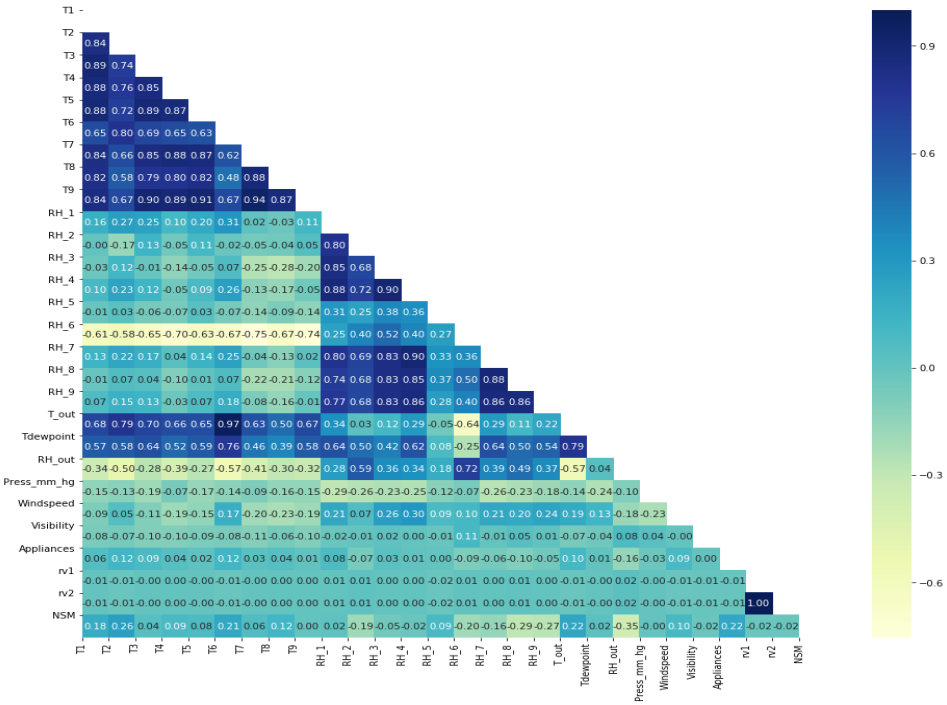

Figure 2. correltion among different predictors

Data Normalization

Data pre-processing is done to normalize values between -1 and 1. To achieve this, the standard-scalar function is used which transforms the data-set to range specified. The target "appliance" is separated from the training set. This step is done to ensure no missing, corrupted or high values bias algorithm performance.

Untuned models' results

The un-optimized versions of ML-algorithm yielded the following performance results:

TABLE II. UNTUNED ALGORITHMS' RESULTS

Name	Train R2	Test R2	Test Rmse	Mean absolute error	Train time
LASSO	0.0000	0.0000	1.000	0.5868	0.0050
RIDGE	0.1632	0.14522	0.9245	0.5522	0.0050
KNN	0.8410	0.4718	0.7267	0.3090	0.0471
SVR	0.2729	0.2403	0.8716	0.3610	6.5504
RF	0.91153	0.5073	0.7018	0.3397	1.7967
ET	1.0000	0.5436	0.6755	0.3149	0.6226
LR	0.1632	0.1452	0.9224	0.5229	0.0059
XGB	0.3603	0.2803	0.8483	0.4555	0.8302
MLP	0.4533	0.3576	0.8014	0.4545	4.5982

From the Table above (Table II), it can be seen that linear models: Linear, Ridge and LASSO regression have the least scores on RMSE, MAE and R-squared. Out of the regression models, LASSO was the poorest performer, indicating that constrained based regression models should not be used on this data-set.

Tuning via Grid Search

The KNN, MLP, SVR, XGB and DT algorithm wereselectedfor optimal parameter search. The optimal parameterGridSearch takes in a set of pre-specified set of values to gothrough in search of the best estimate. The parameter grid values for each of five ML-algorithms with 5-fold CV is given below:

1) KNN:
   i) 'No. neighbours':{ 2,4,6,8,10,15,20}
   ii) 'Leaf size':{ 15,20,25,30}
   iii) 'Metric' = 'Murkowski'
   iv) 'Weights' = 'uniform'
2) SVR:
   i) 'C':{ 1,5,10,15,20}
   ii) 'epsilon': { 0.1,0.2,0.3,0.4,0.5,0.6,0.8}
   iii) 'Kernel': 'rbf'
3) MLP:
   i) 'Max iteration':{ 1000,5000,8000,12000,15000}
   ii) 'No. of hidden layers':{ 50,100,200,300,500}
   iii) 'Activation'='relu'
   iv) 'momentum' = 'Nesterov'
   v) 'learning rate' = 0.001
   vi) 'momentum size' = 0.9
4) XGB:

i) 'No. of estimators':{1000,2000,4000,8000,12000}
ii) 'min child weight':{1,2,3,5}
iii) 'max depth':{5,10,15,20}
iv) 'booster'='gbtree'

5) ET:
i) 'max depth':{5,10,15,20}
ii) 'No. of estimators' :{1000,2000,4000,8000,12000}
iii) 'max features':{auto,log2,sqrt}

Tuned Algorithms Performance

After grid searching for optimal parameters, the select algorithms were trained and tested (Figure 2) on the data.

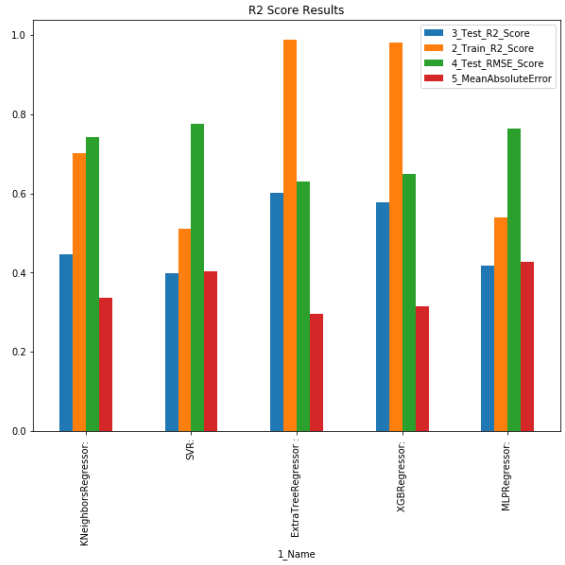

Figure 2. Tuned algorithms results

From tabulated error scores Table III , it is clear that the two best performing algorithms are XGB and ET.

TABLE III. TUNED ALGORITHMS' RESULTS

Name	Train R2	Test R2	Test Rmse	MAE	Train time
KNN	0.7027	0.4467	0.7438	0.3367	0.0508
SVR	0.5113	0.3987	0.7753	0.4033	5.4015
MLP	0.5402	0.4176	0.7631	0.4273	64.167
ET	0.9894	0.6021	0.6307	0.2953	629.3184
XGB	00.9820	0.55775	0.6500	0.3154	675.6424

CONCUSLION

One From data exploration, the results show that inside house temperature variable t1 through tout have more predicting power than outside temperature variable. Some temperature markers t3, t5, t7 and t8 had strong positive correlations with t9, so they were dropped. Humidity markers had mild correlations 0.3-0.6 with appliance variable while also exhibiting weak positive correlation 0.1-0.5 among itself. Lights variable was irregularly distributed with a lot of zero values. Target variable 'Appliance' exhibited strong positive skew indicating outliers while 75% of values (in Watt-h) fell below 100 Watt-h, indicating low energy use, usually.

Eight ML-algorithms Linear, Ridge, Lasso, KNN, SVR, MLP, XGB and ET regression were implemented. The worst performing algorithms belonged to regression family in which the least scores were obtained by Lasso: Train R2 =0; Test R2 =0; Test RMSE=1; MAE= 0.5868, indicating constrained regression models completely fail on this data-set. Out of the eight, five select ML-algorithms: KNN, SVR, MLP, XG-Boost and ET were chosen for model tuning. The algorithms were fit with best estimates of parameters returned by Grid-Search and the results were tabulated. Out of the five, two best scoring ML-algorithms belonged to ensemble family: XGB and ET, in which ET obtained best benchmarking scores of, Train R2 =0.9894; Test R2 =0.6021; Test RMSE=0.65; MAE=0.2953 and training time of 629 seconds, using 22 features. The effect of feature selection was observed which revealed that 'NSM','T3', 'lights' , 'RH3' and 'RHout' were the highest ranked. Reducing the feature set deteriorated algorithm's performance. A same result was obtained by reducing variable 'max depth' while keeping the number of iteration constant. The training time increased linearly with increase in max depth of trees.

This research used a relatively small set of parameters for the Grid Search to go through. Mostly the "number of estimators", "max-depth of leaves", "max-features" and "size of cross-validation" were changed for the best performing algorithms over a restricted set due computational and time constraints. Besides, there are other parameters like "leaf-weight", "minimum fraction of leafs" and "minimum impurity split", etc. that needs an exhaustive Grid-Search which may be considered in future work. The Grid-Search over the MLP was very limited; only the "number of iteration" and "number of hidden layers" was varied. For a more accurate model "solver for back-propagation", increasing the depth of hidden layers and momentum size etc. could be looked at.

REFERENCES

[1] M. H. Goldberg, S. Linden, E. Maibach, and A. Leiserowitz, 'Discussing global warming leads to greater acceptance of climate science'', Proc. Natl. Acad. Sci, vol. 116, no. 30, pp. 14804–14805, Jul. 2019.

[2] A. Sokolova and B. Aksanli, 'Demographical Energy Usage Analysis of Residential Buildings'', J. Energy Resour. Technol, vol. 141, no. 6, p. 062003, Jun. 2019.

[3] Q. Wang, M.-P. Kwan, K. Zhou, J. Fan, Y. Wang, and D. Zhan, 'Impacts of residential energy consumption on the health burden of household air pollution: Evidence from 135 countries', Energy Policy, vol. 128, pp. 284–295, May 2019.

[4] Q. Wang, M.-P. Kwan, K. Zhou, J. Fan, Y. Wang, and D. Zhan, 'Impacts of residential energy consumption on the health burden of household air pollution: Evidence from 135 countries'', Energy Policy, vol. 128, pp. 284–295, May 2019.

[5] P. S. Solanki, V. S. Mallela, and C. Zhou, 'An investigation of standby energy losses in residential sector: Solutions and policies', p. 10.

[6] C. Lee, J. Park, K. Lee, J. Y. Yang, and T. Roh, 'Energy Efficiency for Supplier and Sustainability for Demand: A Case of Heating Systems in South Korea'', Sustainability, vol. 11, no. 15, p. 4216, Aug. 2019.

[7] K.-E. Westergren, H. Hogberg, and U. Norlen, 'Monitoring energy consumption in single-family houses', p. 11, 1999.

[8] A. Al-Garni, ‘A regression model for electric-energy-consumption forecasting in Eastern Saudi Arabia’, Energy, vol. 19, no. 10, pp. 1043–1049, Oct. 1994.

[9] T. A. Reddy and D. E. Claridge, ‘Using synthetic data to evaluate multiple regression and principal component analyses for statistical modeling of daily building energy consumption’, Energy and Buildings, vol. 21, no. 1, pp. 35–44, Jan. 1994.

[10] P. P. Moletsane, T. J. Motlhamme, R. Malekian, and D. C. Bogatmoska, ‘Linear regression analysis of energy consumption data for smart homes’, in 2018 41st International Convention on Information and Communication Technology, Electronics and Microelectronics (MIPRO), Opatija, May 2018, pp. 0395–0399.

[11] S. A. Kalogirou and M. Bojic, ‘Artificial neural networks for the prediction of the energy consumption of a passive solar building’, p. 13, 2000.

[12] A. H. Neto and F. A. S. Fiorelli, ‘Comparison between detailed model simulation and artificial neural network for forecasting building energy consumption’, Energy and Buildings, vol. 40, no. 12, pp. 2169–2176, Jan. 2008.

[13] P. A. González and J. M. Zamarreño, ‘Prediction of hourly energy consumption in buildings based on a feedback artificial neural network’, Energy and Buildings, vol. 37, no. 6, pp. 595–601, Jun. 2005.

[14] Y. T. Chae, R. Horesh, Y. Hwang, and Y. M. Lee, ‘Artificial neural network model for forecasting sub-hourly electricity usage in commercial buildings’, Energy and Buildings, vol. 111, pp. 184–194, Jan. 2016.

[15] M. A. R. Biswas, M. D. Robinson, and N. Fumo, ‘Prediction of residential building energy consumption: A neural network approach’, Energy, vol. 117, pp. 84–92, Dec. 2016.

[16] B. Dong, C. Cao, and S. E. Lee, ‘Applying support vector machines to predict building energy consumption in tropical region’, Energy and Buildings, vol. 37, no. 5, pp. 545–553, May 2005.

International Journal of Engineering Works
ISSN-p: 2521-2419
ISSN-e: 2409-2770
Vol. 7, Issue 10, PP. 333-337, October 2020
https://www.ijew.io/
https://doi.org/10.34259/ijew.20.710333337

Role of Demand side Management in Reliability of Distribution Network

Sajad Ullah[1], Muhammd Azaz[2], Jawad Ul Islam[3]
[1,2,3] Department of Electrical Energy System Engineering, US-Pakistan Center for Advanced Studies in Energy (US-PCASE), UET Peshawar
sajad.ullah@yahoo.com[1], azazkhan8511@gmail.com[2], jawad_ulislam@ yahoo.com[3]
Received: 28 September, Revised: 07 October, Accepted: 10 October

***Abstract*—** Demand side management (DSM) is of the most important feature of modern smart grids, enable the utility companies and customers to efficiently use the available power. Load are shifted from peak demand hours to off peak hours, that minimize the pressure on grid and make it most efficient and reliable. In this paper the reliability of a distribution network is tested for different scenario. In first scenario, base case the reliability is tested without demand side management in term of different reliability parameters. In second case part of load which is noncritical load, is shifted to off peak hour and reliability is tested that shows improvement in reliability. In third scenario the percentage of load shifted is increased and reliability is calculated. Similarly, the reliability of system is tested for different percentage of noncritical load shifted to off peak hours. Based on calculation of different scenarios, the best DSM scenario is evaluated that gives the best reliability and high efficiency of the system.

Keywords: Demand side Management (DSM), Smart Grid, Distribution Network, Peak Demand.

I. INTRODUCTION

Demand side management is one of the most important features of smart grid that enable the electricity provider to manage high load demand within the available energy resources. Based on the daily load demand of consumer noncritical loads are shifted from peak hours to off peak hours, this make the load demand curve flattened and hence the pressure on grid is minimized. Distribution network is a key part of the power system that facilitate the energy supply to the consumer from distribution grids. The reliability of this network is very important for continuous supply of electricity. So applying demand side management to distribution system make it an efficient, robust and reliable [1]. Demand side management encourage renewable energy (RE) integration in the system. The demand response (DR) strategy is used based on day ahead electricity prices provided by the utility companies to shift load to the low prices hours while fulfilling the customers need that help electricity consumer to reduce their electricity bills[2]. The residential loads controllable, uncontrollable and electric vehicle (EVs) are optimized through particle warm optimization (PSO), considering the realistic constrains and then the electricity bills are compared for different DR which shows a significant reduction in electricity bill [3]. Demand side management is used for residential peak shaving with integration of demand response and vehicle to home (V2H) [4]. With the advancement in transportation system the conventional vehicles are being converted to electrical vehicle (EV). However, these vehicles bring more pressure to the power grid especially to the distribution level. Energy management system (EMS) equipped with energy meter used DSM and charge management scheme of EV to limit the peak energy consumption [5]. The communication infrastructure between the distribution operator and household consumer monitor the peak demand and charging status of the vehicle, peak shaving is done through V2H based on charging status of vehicle. Effective DSM reduce loading stress on distribution system and its components that improve system reliability and therefore reduces the probability of failure [6]. So, applying DSM make the distribution system reliable that benefit both the customer and electricity providers. Customer have the choice to manage electricity consumption and reduce their electricity bills. Similarly, peak demand is reduced that benefit the electricity provider in saving their capital and operational cost. Demand side management is used for efficient energy use and elimination of energy wastage in a photovoltaic wind hybrid energy system which are not connected to the grid [7]. The daily load profile and the climate data is carefully observed which gives the total energy demand and the energy generation. Based on this data energy is managed by shifting demand from peak hours or the time of energy use is shift to off peak hours using load management unit [8]. Therefore, this management system increases the power efficiency, increase system reliability and prevent system failure. Demand side management greatly improve power system small signal stability and improve the performance of transmission and distribution system [9]. The small signal stability problem occurs as the steady increase in rotor angle due to insufficient synchronizing and damping

torque. DSM is used to efficiently manage the available power by shifting loads from peak load time to offpeak time, so this ensure that total demand is managed and not to endanger the system performance in case of any fault. This improve distribution system performance, increase reliability and stability of the system [10].

II. METHADOLOGY

The methodology include a distribution system modeling in DIgSILENT, performing load flow analysis and reliability analysis. Demand side management is applied by shifting loads from peak hours to off-peak hours.

A. Modeling IEEE 33 Bus Distribution System

To assess the reliability of system a 33-bus model of distribution system is designed in DIgSILENT software which is an advance state of the art software for designing power system generation, transmission and distribution system. The propose system is a 1 MW radial distribution system and the power is supplied from an external grid. The external grid and main bus are slack (SL) bus that are taken as refence with voltage of 1 p.u and angle of zero degree. The system is designed such as it consists of three feeder and a total of 33 buses that distribute power to the consumer at 11KV. Distribution transformer of different rating based on consumer demand are installed on all buses to stepdown the voltage to the 400V and 230V for consumer use.

Table 1. System Components

No. of Busbars	34
No. of Lines	63
No. of Terminals	33
No. of Transformer	33
No. of Loads	66
No. of customer per load	2--16
Total Peak Load	1 MW
Total Losses in System	93KW

The loads consist of residential and small commercial load. Therefore, loads of different active and reactive power demand are connected to the system having total demand of 1MW. Load flow analysis is carried out to find the voltages magnitude, angle, currents, active and reactive power of all buses. Complete model of the system is shown the following figure.

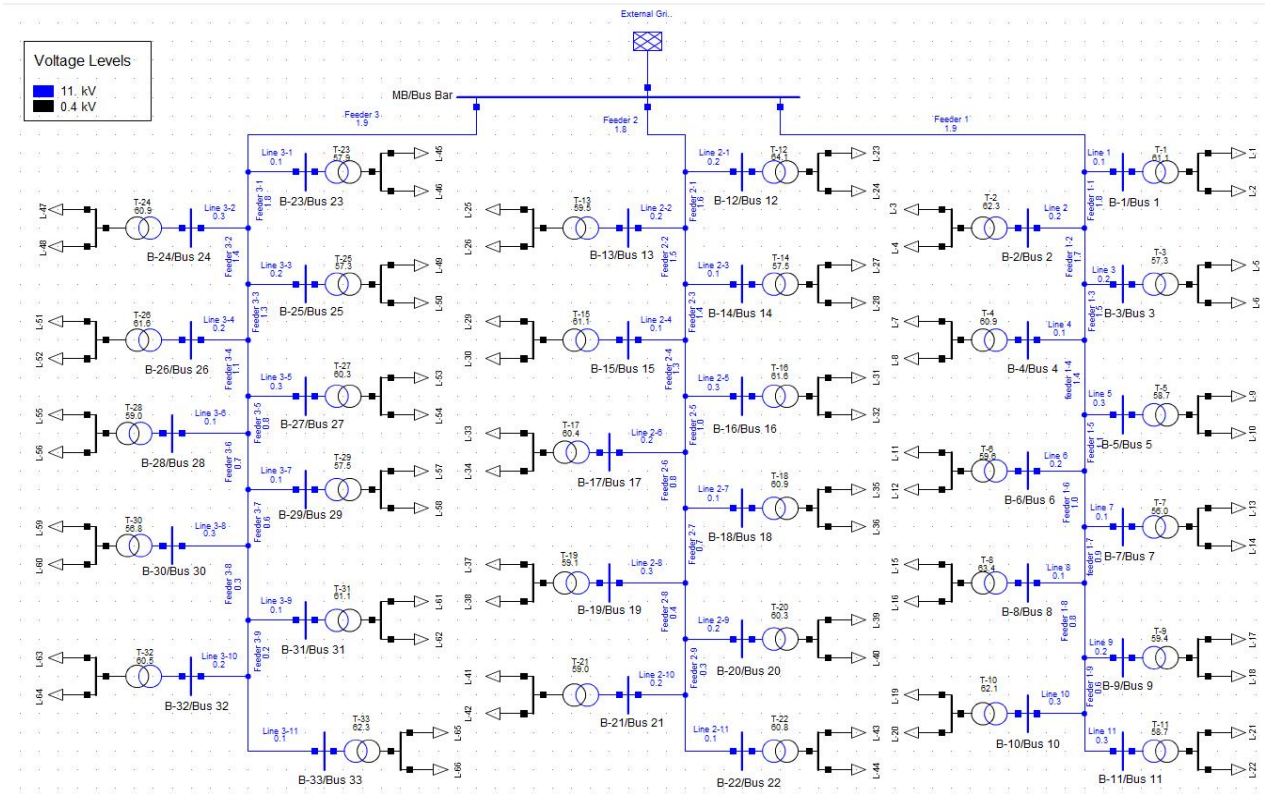

Figure 1. System Model

B. Load Flow Analysis

Load flow analysis is the most important and essential tool while doing power system planning and operation. The bus voltages, load angle, currents, active power and reactive power of the system is evaluated. That gives the loading condition of each component and ensure their operation within the optimum range. Moreover, the maximum capability of each component is finding, so that it can carry the load of adjacent component if it fails due to any faults. Load flow analysis is done by solving complex mathematical equations through an algorithm. Newton Raphson algorithm is used for load flow analysis which is built-in simulator in power factory.

1) Newton Raphson Method

Newton Raphson is an efficient load flow analysis algorithm based on solution set of simultaneous nonlinear equations. In power factory we define bus data, line data, generation data and load data, then load flow analysis calculate bus voltage, load angle, active and reactive power, current flow and the power losses in system.

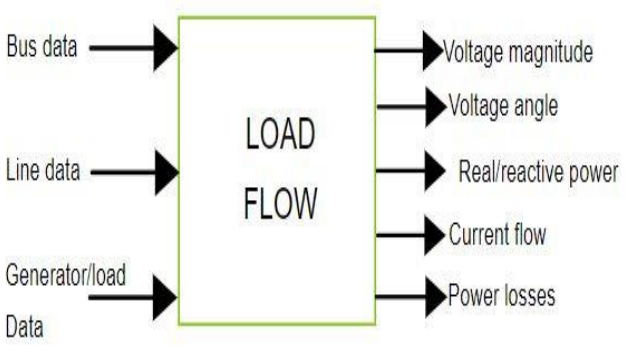

Figure 2. Load Flow

The iteration to solve the following mathematical equation of load flow analysis gives the active power, reactive power and load angle of the system.

$$S_i = VI^* = P + jQ \quad (1)$$

$$P - jQ = \sum_{j=1}^{n} Y_{ij}\, V_j V^* \quad (2)$$

Where Y_{ij} are the elements of bus admittance matrix

Here

$$Y_{ij} = |Y_{ij}|\angle Q_{ij} \;\; and \;\; V = |V|\angle\delta \quad (3)$$

$$P - jQ = \sum_{j=1}^{n} |Y_{ij}|\,|V_j||V|\angle(Q_{ij} + \delta_j - \delta) \quad (4)$$

$$P = \sum_{j=1}^{n} |Y_{ij}|\,|V_j||V|\, cos(Q_{ij} + \delta_j - \delta) \quad (5)$$

$$Q = -\sum_{j=1}^{n} |Y_{ij}|\,|V_j||V|\, Sin(Q_{ij} + \delta_j - \delta) \quad (6)$$

Where n is the number of buses and i= 1, 2, 3….n

After calculating the active power, reactive power and load angle the bus voltage, currents and power losses are calculated for the system.

C. Daily Load Demand

Daily load demand curve shows the hourly energy demand and consumption of power system. The proposed system is a distribution system, consist of residential and small commercial consumer. The load demand is low during daytime when peoples are in their workplaces, the demand increases when they arrive back and the system experience peak demand. Following figure shows the daily load demand of the system.

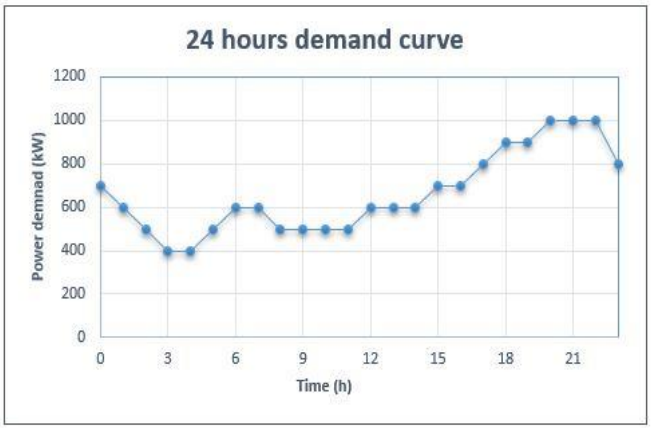

Figure 3. Daily Demand Curve

D. Reliability Analysis

Reliability analysis is a statistical method to determine the total load interruption in power system during certain period of operation. Load interruption are defined by several parameters that depend on number of customers, total connected load, duration of interruption, amount of power interrupted, frequency of interruption, repair time and probabilities of interruption. For reliability analysis in power factory, first a stochastic model is created for all components and for single line fault, then feeder is defined for reliability and switches are configured. Next the number of customers, interruption cost, priority, load transfer and shedding are defined, and reliability assessment is run.

Table 2.Reliability Analysis User Input Data

Component	Failure Rate	Mean Repair Time
Busbar	0.008/year for each terminal 0.015/year per connection	7 hours
Line	0.015/(km,year)	15 hours
Transformer	0.003/year	18 hours

III. Applying Demand Side Management

Demand side management is one of the important features of modern smart grid that enables electricity utilities to efficiently manage the available energy and fulfill customer demand without disturbing their life comfort. To apply DSM to the network, first the daily load demand curve is plotted based on power consumption of consumer. The major part of system consists of residential consumer that has low power demand during daytime because peoples went to their duties at that time and their demand increases in evening when they come back. Now to apply DSM, loads are shifted from peak demand hours to off-peak. Initially 5% load are shifted, and reliability of the system is analyzed. Then the percentage of load shifted is increased gradually to 7%, 10%, 15% and finally 20%, the reliability assessment is done for all DSM strategy in term of SAIDI, SAIFI and ENS.

IV. Results

The research work consists of reliability evaluation of the system. Reliability of the system is evaluated in term of SAIFI, SAIDI and ENS. Initially reliability analysis is done for base case without load shifting. After that different percentage of non-critical load are shifted from peak hours off peaks hours and reliability is analyzed. The results of reliability parameters obtained for different case are following.

A. System Average Interruption Frequency Index (SAIFI)

SAIFI indicates that how often a customer experience interruption during a specific defined period. So smaller is the SAIFI index less will be the interruption in system. The result of SAIFI obtained for different DSM scenarios are compared with base case of peak demand. The comparisons are shown in the following figure, when the load is shifted from peak demand hours the system interruption decreases. A point come where the SAIFI become minimum, which shows less interruption and high reliability. In our case SAIFI become minimum at 15% load shifting, that bring 14% reduction in SAIFI as shown below.

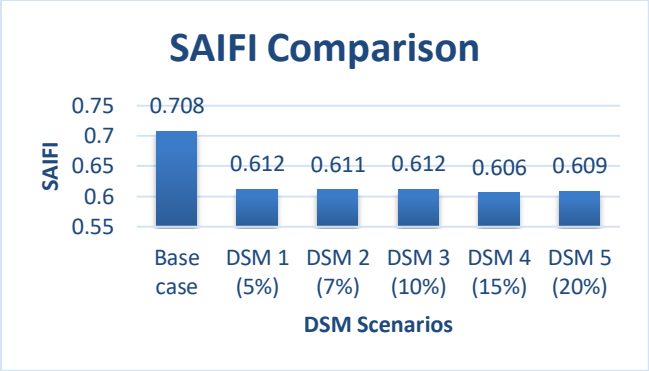

Figure 4. SAIFI Comparison

B. System Average Interruption Duration Index (SAIDI)

SAIDI indicates the interruption duration of a customer during a specific period. The result of SAIDI obtained for different DSM scenarios previously are compared with base case. The comparisons are shown in the following figure, when the load is shifted from peak demand hours the interruption duration decreases. At a specific point SAIDI become minimum, which shows less interruption duration and high reliability of the system. The SAIDI become minimum at 15% load shifting as shown in the following figure. This bring 14% reduction in SAIDI.

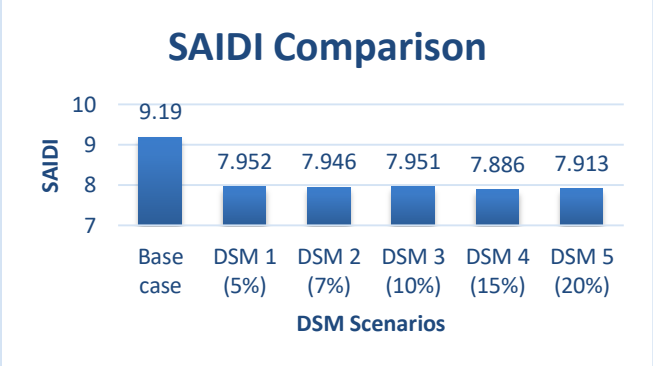

Figure 5. SAIDI Comparison

C. Energy Not Supplied (ENS)

ENS shows the energy not supplied to the load during a specified period. The result of ENS are obtained for different DSM scenarios and compared with base case. The comparisons are shown in the following figure, when the DSM is applied, and load are shifted from peak demand hours the ENS decreases. At 20% load shift its value is smallest, which shown the higher reliability of the system at that point.

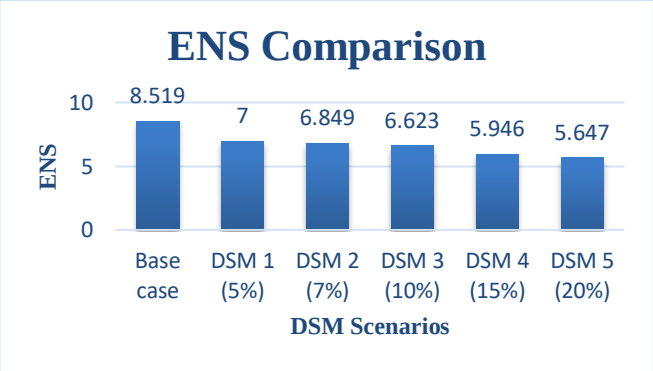

Figure 6. ENS Comparison

CONCLUSION

Distribution system is key part of power system that plays important role of transferring power to the customer premises. Reliability of this network is very important to ensure continuous power supply. The main objective of this research is o find most optimum and reliable operation of the proposed distribution system, for this a model is designed in DIgSILENT Power Factory. Load flow analysis is performed to find the loading of each component in the system and to ensure it safety. Load flow analysis is also used to find the maximum loading capability of the system. The reliability analysis of the system is performed for different casese. First the reliability analysis is done for base case. After that DSM is applied and different percentages of noncritical load is shifted from peak-hour to off-peak hours From reliability results it is concluded that for 15% of load shifting while applying DSM, the system have less interruption and reliability of the system is higher. So, the system operates in most optimum condition. This optimum operation condition is used for better system performance and high reliability.

In future, the proposed system can be modeled with the integration of renewable energy resources and distribution generation. The distributed generation will perform peak shaving and fulfill customer demand locally. This system can also be modeled with the integration of V2G and V2H. The vehicle will be charged during off peak hours and then used for peak shaving during peak hours of high demand.

REFERENCES

[1] S. Kahrobaee and S. Asgarpoor, "The effect of demand side management on reliability of automated distribution systems," in 2013 1st IEEE Conference on Technologies for Sustainability (SusTech), 2013, pp. 179-183.

[2] U. Akram, M. Khalid, and S. Shafiq, "A strategy for residential demand response management in modern electricity markets," in 2018 IEEE International Conference on Industrial Technology (ICIT), 2018, pp. 1138-1142.

[3] M. Tariq and M. Adnan, "Stabilizing Super Smart Grids Using V2G: A Probabilistic Analysis," in 2019 IEEE 89th Vehicular Technology Conference (VTC2019-Spring), 2019, pp. 1-5.

[4] Y. Liu, S. Gao, X. Zhao, S. Han, H. Wang, and Q. Zhang, "Demand response capability of V2G based electric vehicles in distribution networks," in 2017 IEEE PES Innovative Smart Grid Technologies Conference Europe (ISGT-Europe), 2017, pp. 1-6.

[5] L. Zhao and V. Aravinthan, "Strategies of residential peak shaving with integration of demand response and V2H," in 2013 IEEE PES Asia-Pacific Power and Energy Engineering Conference (APPEEC), 2013, pp. 1-5.

[6] A. Al Hourani and M. AlMuhaini, "Impact of Demand Side Management on the reliability performance of power distribution systems," in 2016 Saudi Arabia Smart Grid (SASG), 2016, pp. 1-5.

[7] T. Alnejaili, S. Drid, D. Mehdi, and L. Chrifi-Alaoui, "Advanced strategy of demand-side management for photovoltaic-wind energy system," in 2014 15th International Conference on Sciences and Techniques of Automatic Control and Computer Engineering (STA), 2014, pp. 797-802.

[8] O. Ayan and B. Turkay, "Energy Management Algorithm for Peak Demand Reduction," in 2018 20th International Symposium on Electrical Apparatus and Technologies (SIELA), 2018, pp. 1-4.

[9] X. Tang and J. V. Milanović, "Assessment of the impact of demand side management on power system small signal stability," in 2017 IEEE Manchester PowerTech, 2017, pp. 1-6.

[10] S. Jaiswal and M. Ballal, "Optimal load management of plug-in electric vehicles with demand side management in vehicle to grid application," in 2017 IEEE Transportation Electrification Conference (ITEC-India), 2017, pp. 1-5.

International Journal of Engineering Works
ISSN-p: 2521-2419
ISSN-e: 2409-2770
Vol. 7, Issue 10, PP. 338-341, October 2020
https://www.ijew.io/
https://doi.org/10.34259/ijew.20.710338341

Evaluation of PSD Models for the Estimation of Hydraulic Conductivity for Different Soil Textural Classes

Nazia Arfeen[*1], Taj Ali Khan[2]
[1,2] Department of Agricultural Engineering University of Engineering and Technology Peshawar, Pakistan
[*]Correspondence author: naziaarfeen@uetpeshawar.edu.pk
Received: 28 September, Revised: 07 September, Accepted: 10 October

***Abstract*—**The Hydraulic conductivity (K) of soil, is an important parameter that is used to predict the movement of water and the dissolved contaminants, if any, through it. It can be determined through different in-situ and lab methods; however, it can also be determined easily, using the PSD models or empirical equations developed for this purpose. These equations specifically utilize the particle size distribution (PSD) data of the soil, as movement of water, and hence the hydraulic conductivity depends upon the types and sizes of the soil particles. Most of these equations have been developed for the coarse-grained soil only like the sand and gravel, and some of them only consider the fine-textured soil. In actual condition, soil is not present only as the sand or gravel or as fine-textured only but is the combination of three important particles, which are sand, silt, and clay, due to which the permeability of the soil is affected. This research work is based on the hypothesis that the formulas developed for the estimation of K, the hydraulic conductivity of the soil, may not work properly due to the presence of other particles. For this, different empirical models were considered for only four textural classes of the soil i.e., sand, loamy sand, sandy loam, and silt loam. It was found that as the number of fine particles increases in the sand the formulas do not give a good estimate of the K value.

***Keywords*—** hydraulic conductivity, PSD model, effective size, soil texture.

I. Introduction

Soil is naturally a disperse, polyphasic, porous, and a diverse system. Innumerable discrete mineral particles of various sizes and composition naturally combine to make up the soil matrix [1]. These particles can be separated into groups to classify the soil in terms of relative proportions of its particle-size. The soil water filling the voids between the soil particles partially or completely makes its liquid phase, While the soil air or entrapped gases filling the soil voids, which are not occupied by soil water, is termed as the gaseous phase or the vapor phase [2]. The occurrence and movement of groundwater depends upon the porous media when it is completely saturated. As all the soils are permeable, water flows freely through their interconnected pores, even though it may be at a very slow rate in some soils [3]. The hydraulic conductivity (K) value is the key to the solution of several geotechnical engineering and hydrological problems like the modeling of underground flow of water, determination of the hydraulic properties of leachate water in waste disposal areas, calculation of the compressibility, and much more [4].

The 'K' value can be found by hydraulic methods or the correlation methods. The hydraulic methods can either be the field methods or the laboratory methods, while the correlation methods are based on relationships between hydraulic conductivity value and easily determining soil properties like texture, bulk density, etc., [5].

Different techniques are applied to find the K¬-value of the soil by field methods, depending upon the situation. For rapid testing, the small-scale methods are designed while the large-scale methods are used to get a representative K-value of soil body that is of a larger scale. Constant head and Falling head permeameter methods are based on Darcy's law of hydraulic conductivity to determine the K value in the laboratory of coarse and fine-grained soil, respectively [6].

Owing to the difficulties in the determination of the K value in the field and the laboratory different empirical formulas have been developed for the estimation of the K value Some of these are purely the PSD models as they consider the data of the particle-size distribution only, while other are the pedotransfer functions (PTFs) which not only consider some data of the PSD but also take into account some other properties of soil [7]. Where the permeability data is scarce and the region is comprised of a variety of soils making the direct measurements impractical for larger-scale studies, then these interrelationships can be useful and economically feasible for the estimation of K¬ values [8]. The determination of a relation between Ks and soil PSD data is dependent on the selection of a representative grain-size or particle size diameter, dn [9]. Later on, it was further concluded that the diameter of the pores also plays a more significant role in the estimation of K but their determination is a cumbersome job, therefore, the estimation of the hydraulic conductivity is mostly based on the particle size distribution (or PSD), which can be determine easily [10].

It was observed by the researchers that soil water retention characteristics are dependent upon the percentage of the soil particles i.e., sand, silt, and clay, the quantity of the organic matter, and the bulk density of the soils [11]. Mishra et. al. (1989), reported that as compared to the dynamic hydraulic data, the soil textural data can be a good alternative for estimating soil properties. It was further concluded that the ability of the PSD models to predict the hydraulic conductivity of the soil, was affected by the soil texture, which was generally neglected in those models [12].

The study objective was to check the effects of soil texture on the efficiency of some well-known PSD Models.

II. Materials and Methods

In this study, 25 sets of soil samples were collected to evaluate the PSD models. The samples selected had a high proportion of sand particles as the PSD models selected for this research work were developed for the sand texture. The texture of the soil samples was tested according to the USDA soil classification system, these belonged to sand, loamy sand, sandy loam, and silt loam textural classes. Standard methods were applied for the investigation of saturated hydraulic conductivity (K) in the laboratory, and to determine the particle size distribution (PSD) of these samples.

TABLE 1: LIST OF THE EQUATIONS USED TO ESTIMATE THE HYDRAULIC CONDUCTIVITY OF THE SOIL (K)

Equation/Researcher Name	Type	Equation	Reference
Hazen (1893)	Quadratic	$K = \frac{g}{\upsilon} C_h f(n) d_{10}^2$ $K = c d_{10}^2$	Sezer et al. (2009)
Slitcher (1899)	Rational	$K = 0.01 \frac{g}{\upsilon} n^{3.287} d_{10}^2$	Sezer et al. (2009)
Beyer (1998)	Logarithmic	$K = 6\times10^{-4} \times \frac{g}{\upsilon} \log \frac{500}{C_u} \times {d_{10}}^2$	Rosas et al. (2014)
Alyamini and Sen (1993)	Quadratic	$K = 1300\left[I_o + 0.025\left(d_{50} - d_{10}\right)\right]^2$	Alyamini and Sen, (1993).
Kozeny (1953)	Functional	$K = 8.3\times10^{-4} \frac{g}{\upsilon} \frac{n^3}{(1-n)^2} d_{10}^2$	Sezer et al. (2009)
Gustafson (1984)	Functional	$K = 10.2\times10^6 \times \frac{(0.8\times\frac{1}{2\times\ln(C_u)} - \frac{1}{(C_u)^2-1})^3}{1+(0.8\times\frac{1}{2\times\ln(C_u)} - \frac{1}{(C_u)^2-1})^3} \times \frac{1}{(\frac{1.3}{\log_{10} C_u} \times \frac{C_u^2-1}{C_u^{1.8}})^2} \times \left(\frac{d_{10}}{1000}\right)^2$	Svensson, (2014)

The PSD data was used to determine different soil parameters like, the grain diameters (mm) of which 10%, 30%, 50%, and 60% of all soil particles are finer by weight i.e., d10, d30, d50, and d60, respectively, also the coefficient of uniformity (Cu) of the soil. The soil porosity (η) and the bulk density (ρb) data were calculated using the general formulas proposed by Vukovic and Soro (1992). The mean values of all these soil properties are summarized in Table 1. It was clear that the most abundant particle of these soil samples was sand.

The data obtained by the soil tests were utilized in already developed empirical formulae and PSD models, given in Table 1, for estimating the K values, and the results were compared with experimental methods. The missing data like the porosity and bulk density of the soil, which are required in some equations were determined by using the general equation presented by Vukovic and Soro (1992).

TABLE 2: MEAN VALUES OF THE PARAMETERS OF THE SOIL USED IN THIS STUDY

Soil Class	Parameters										
	d_{10} (mm)	d_{30} (mm)	d_{50} (mm)	d_{60} (mm)	C_u	ρ_b (g/cm^3)	H	%Sand	%Silt	%Clay	K (cm/s)
Sand	0.202	0.300	0.487	0.483	2.51	1.66	0.37	89	7	4	$3.78*10^{-02}$
Loamy Sand	0.094	0.194	0.292	0.351	4.12	1.65	0.38	78	15	7	$4.44*10^{-03}$
Sandy Loam	0.042	0.115	0.179	0.232	8.53	1.75	0.34	68	25	7	$4.84*10^{-04}$
Silt Loam	0.015	0.073	0.222	0.333	20.13	1.88	0.29	32	58	10	$7.81*10^{-05}$

III. RESULTS AND DISCUSSION

In the original Hazen equation (Table 1), the constant c varies from 1 to 1.5, for the research work it was considered to be 1.25, and it was observed that the Hazen equation give a good result for the sand class but for the other three classes the estimated value of K by this equation was not satisfactory. The Slitcher equation cannot predict the K-value for medium-grained soils but overall, the result was satisfactory. The overall result by the Breyer equation was satisfactory but for the separate classes, it was not good in the estimation of the soil classes with a larger percentage of fine particles. The Alyamani and Sen equation was developed while testing the sandy soils therefore it was good in estimating the K-value of the sand and loamy sand, but as it incorporates the d50 value therefore as compared to the three classes, its prediction was relatively better for the other two classes as well. It was observed that the result of the Kozeny equation was similar to the Slitcher equation. The Gustafson equation also held good for the prediction of coarse-grained soils. Table 3 gives a clear picture of the r-square value of these equations.

CONCUSLION

It was concluded that the empirical equations which had been developed for the estimation of K generally considering the effective diameter along with other properties of soil predicted well about the saturated hydraulic conductivity of the soil having a larger amount of sand. Moreover, it was found that besides the Slitcher equation, the Gustafson equation also predicted well about the K value of the soil with an R-square value of 0.82, the reason was that, that the equation took use of the coefficient of uniformity of the soil (Cu). It was also observed that these models do not hold good for every texture of the soil, even if there is not a very large deviation of percentages of particles. It is therefore recommended to develop an equation which can be used for different soil classes with a wide range of percentage of the particles.

TABLE 3: MEAN VALUES OF THE PARAMETERS OF THE SOIL USED IN THIS STUDY

Equation	R^2 for Sand	R^2 for Loamy Sand	R^2 for Sandy Loam	R^2 for Silt Loam	R^2 for types of soils combined
Hazen Original	0.71	0.63	0.0007	0.0077	0.72
Slichter	0.68	0.68	0.010	0.001	0.88
Beyer	0.74	0.60	0.004	0.010	0.70
Alyamini and Sén	0.78	0.62	0.013	0.140	0.78
Kozeny	0.67	0.69	0.014	0.014	0.60
Gustafson	0.74	0.42	0.004	0.001	0.82

REFERENCES

[1] Petrich, C., Langhorne, P.J., Sun, Z.F. (2006). "Modelling the interrelationships between permeability, effective porosity and total porosity in sea ice". Cold Regions Science and Technology, 44(2), 131–144.

[2] Jarvis, N.J., Hollis, J.M., Nicholls, P.H., Mayr, T., Evans, S.P. (1997). "MACRO - DB: A decision-support tool for assessing pesticide fate and mobility in soils". Environmental Modelling and Software, 12(2–3), 251–265.

[3] Tietje, O., Hennings, V. (1996). "Accuracy of the saturated hydraulic conductivity prediction by pedo-transfer functions compared to the variability within FAO textural classes". Geoderma, 69(1–2), 71–84.

[4] Schwartz, F.W., and Zhang, H. (2004). Fundamentals of groundwater Singapore: John Wiley & Sons, 42-68.

[5] Schaap, M. and Leij, F.J. (1998). "Using neural networks to predict soil water retention and soil hydraulic conductivity". Soil and Tillage Research, 47(1–2), 37–42.

[6] Blott, S.J., and Pye, K. (2001). "GRADISTAT: A grain size distribution and statistics package for the analysis of unconsolidated sediment". Earth Surf. Process. Landforms 26, 1237–1248

[7] Alyamani, M.S. and Sen, Z. (1993). "Determination of hydraulic conductivity from complete grain-size distribution curves". Ground Water, 31(4), 551–555.

[8] Salarashayeri, A.F., and Siosemarde, M. (2012). "Prediction of soil hydraulic conductivity from particle-size distribution". World Academy of Science, Engineering and Technology, 6(1), 394-399.

[9] Gupta, S.C., and Larson, W.E. (2007). "Estimating Soil water retention characteristics from particle size distribution, organic matter content and bulk density". Water Resources Research, 15(6), 1–3.

[10] Hwang, S. (2004). “Effect of texture on the performance of soil particle-size distribution models”. Geoderma, 123(3–4), 363–371.

[11] Sezer, A., Göktepe, A.B., and Altun, S. (2009). “Estimation of the permeability of granular soils using neuro-fuzzy system”. CEUR Workshop Proceedings, 475, 333–342.

[12] Rosas, J., Lopez, O., Missimer, T.M., Coulibaly, K.M., Dehwah, A.H.A., Sesler, K., and Mantilla, D. (2014). “Determination of hydraulic conductivity from grain-size distribution for different depositional environments”. Groundwater, 52(3), 399–413.

[13] Svensson, A. (2014). “ Estimation of hydraulic conductivity from grain size analyses”. Chalmers University of Technology.

[14] Vuković, M,. and Soro, A. (1992). “Hydraulics and water wells: theory and application”. Water Resources Publications, Highlands Ranch, CO, USA.

Nazia Arfeen was born in Peshawar, Khyber Pakhtunkhwa, Pakistan. Has got her bachelor’s degree in Agricultural Engineering from University of Engineering and Technology Peshawar, Pakistan in 2011, and currently enrolled in MS program of Soil and Water Engineering in the same university. Research interests include, Hydrology, Soil and Water Management, and Environmental Engineering.

IJEW 国际工程期刊 International Journal of Engineering Works انجینئرنگ کاموں کا بین الاقوامی جرنل

International Journal of Engineering Works
ISSN-p: 2521-2419
ISSN-e: 2409-2770
Vol. 7, Issue 10, PP. 342-349, October 2020
https://www.ijew.io/
https://doi.org/10.34259/ijew.20.710342349

Application of Self-reported Drivers' Behavior Questionnaire in Private Vehicles (Motorcar) in Peshawar

Wajidullah[1], Safiullah[2], Muhmmad Adil Khan[3]
[1,2,3] National Institute of Urban Infrastructure Planning, University of Engineering & Technology Peshawar
wajidullah.momand@gmail.com[1]

Received: 29 September, Revised: 10 October, Accepted: 12 October

***Abstract*—** Transportation plays an essential role in our everyday lives. Transportation planners often looking for systems that are efficient, reliable, and safe. One of the most significant factors in road accidents and public safety is the behavior of drivers. The Driver Behavior Questionnaire (DBQ) has not been used in Peshawar to find driver behavior. The dream of a secure and effective transportation network seems to exacerbate these conditions. The complete DBQ method is essential to find the effectiveness of the DBQ. The Driver Behavior Questionnaire (DBQ) was split into four separate sections. There were three major categories of driver behavior: mistakes, slips and lapses, violations, and unintentional violations. The respondents had to rate themselves on a scale of 1 to 3, how good they think they are, how healthy they think they are. The report concludes with a list of recommendations on how drivers can improve their behavior. Survey was performed at colleges and public buildings in parking lots. Drivers were questioned directly in the parking lot. 250 questionnaires were filled out in total. Statistical Package for Social Sciences (SPSS) was mainly used for the analysis of the data. Almost 64% of people do not have a driving license. 62% consider the process of getting a license difficult while 29% consider it of no use, and they believe they do not need it. Drivers with no driving license do more speeding than those who have a license. Most of the respondents were of the opinion to have strict enforcement of traffic rules, mandatory training before issuing a driving license.

***Keywords*—** Accident, Driver, Behavior, DBQ, Traffic

I. INTRODUCTION

A. *Background*

Safety, in its entirety, is of great importance to us. Safety is part and parcel of the project, whether we are planning or designing. By moving goods and people from one location to another, transportation plays an essential role in our everyday lives. Transportation planners are often looking for systems that are efficient, reliable, and safe. Due to new technology, our daily lives have acquired more momentum. In addition, our road networks have also been affected by rapid urbanization, resulting in densely packed volumes of traffic. The dream of a secure and effective transportation network seems to exacerbate these conditions. Traditionally, road safety is accounted for by considering variables that may potentially affect driver behavior, such as weather, road conditions, and traffic conditions see Fig.1. The Driver Behavior Questionnaire (DBQ) is used to capture the behavior of drivers as a method originally formulated by the ref [4]. DBQ covers four major aspects of driver's behavior: Mistakes, lapses, violations, and Unintentional violations.

Drivers should be qualified and expected to drive according to the road conditions. Similarly, it is often part of the driver's actions to observe the gears and brakes of other traffic. One of the most significant factors in road accidents and public safety is the behavior of drivers.

Figure 1 Relation between road accidents, drivers behviour and other factors

When addressing behavior as an accident agent, we have to bear in mind that in the case of drivers, this is the most flexible aspect and even very complex. Does it, therefore, take extensive and laborious analysis to determine how the conduct of a driver results in different types of accidents? So observing the behavior of the driver in congested traffic such as Peshawar would lead us to formulate and quantify the involvement of the behavior of the driver in traffic accidents.

B. Problem Statement

The complete DBQ has not been used in Peshawar to find driver behavior, to 1) find the behavior of drivers through the behavior technique of self-reporting drivers and 2) the relationship of such driver behavior with the frequency of involvement in accidents. Given the enormous amount of ownership of private motor vehicles in Peshawar, it is clear that in evaluating driving conduct, it is essential to find the effectiveness of the DBQ method, in addition to finding the relationship between the DBQ and the traffic accident.

C. Objectives

In order to find the self-reported driving behavior in private cars, this research study suggests using the DBQ method. The research is more precisely targeted at:

- Compile a database of self-reported driver behavior factors and socio-economic data.

II. Literature Review

The death rate due to road traffic in South East Asia is 18.5 per 1 Lakh population, and this death rate is by far much higher than the death rate in the 1st Global Road Safety Report [6]. According to this report, the death rate is 16.6 per 1 lakh population due to road traffic [3]. Another National Highway Traffic Safety Administration (USA) study estimated that car accident happens every ten (10) seconds. Much of the deaths of older and younger individuals (35 years and below) in America were attributed to road accidents due to careless driving. According to the [3], approximately 98 percent of car accidents in 2013 is attributable to lower driver concentration.

[4] conducted a case study (DBQ, Driver Behavior Questionnaire) on driver behavior while driving. In the checklist, they listed fifty (50) different things concerning the most common mistakes during driving. Fifty (50) respondents/drivers were asked to state their actions with errors that they normally experienced when driving over the last year. The study results indicate that all the violations (attention, perception, etc.) were due to psychological reasons. Errors/violations simply explain the behaviors of drivers created by the same reluctant driving for years [7].

According to the findings of several studies, four causes are the fundamental reasons for violations while driving, i.e., violations, aggressive violations, errors, and lapses [1]. Almost all experiments used Linear / logistic regressions, using the factor scores, to find the best accident predictor [1], [7], [4]. 174 case studies were analyzed by the ref [7], and the findings revealed that individual/person difference us the basic application of the Driver Behavior Questionnaire, BDQ.

A study based on the Chernobyl and Zeebrugge study was conducted by the ref [4], their findings clearly showed that there is a difference between each and every violation of drivers during accidents. Errors can be identified based on each person's cognitive/mental state, according to the authors, while errors/violations cannot be represented in isolation from society. Violations can only be specified based on the social/environmental context, since this process would be administered in this way under codes of conduct, culture, norms, regulations, laws, and procedures, etc. Violations are those deviations from existing practices that involve safeguarding the minimum harmless activity from dangerous vulnerability.

The aim of the [4] analysis was to find out how far the distinction of mistakes and violations would lie through the research in the questionnaire on car drivers, in which drivers describe the number of occasions while driving on the road they perform bad or silly behavior.

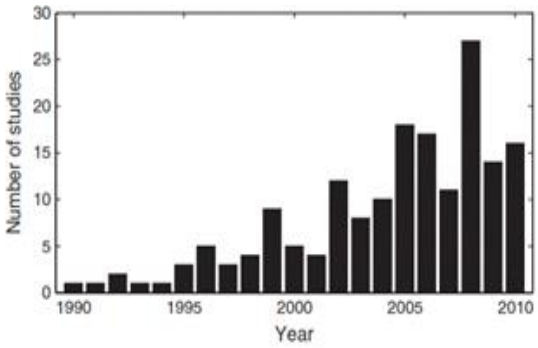

Number of English-written studies per year using the original DBQ or a modified version of it.

Figure 2 Number of English-written studies per year using DBQ

Due to the important findings of this method in different cognitive failure questionnaires, a self-reported questionnaire was used, answers to those questionnaire questions were usually positively associated. The Driver Behavior Questionnaire (DBQ) was based on fifty items used in this analysis. Slips, lapses, accidental violations, and intended violations were focused on objects. In the DBQ, Section 1 of the report, three sections were defined: information on personal data concerning age, occupation, marital status, driving experience, and mileage, etc. Section 2: 50 violation items in which they have to respond on a category scale of 05 points. In addition, these items were grouped into three categories of risk. Section 3 consisted of five questions in which drivers were questioned about their driving performance on a three-scale option. Results indicate that there is a lower violation rate for old age drivers. People with high annual mileage, who consider themselves to be better drivers, and more violations have been reported by those influenced by mood. More crimes are confessed by men than women do. The mood was directly related to risky mistakes, while the use of motorways was inversely related. For researchers and traffic safety experts, this instrument turned out to be a landmark.

The questionnaire on driver conduct primarily used in Arab countries (Qatar and the United Arab Emirates) was based on the DBQ [1]. The main objective of the research was to establish the relationship between incidents in the UAE and Qatar and then to compare the findings between the two countries. Based on twenty (21) Primary Health Case Divisions in the province, Qatar was divided. Using nurses and health educators, 847 men and 263 women were approached to complete the questionnaire. 80.5% of drivers acknowledge that they have been involved in at least one traffic accident. A different sampling method was used for the UAE; instead,

during their renewal of car registration, random drivers, 992 males, and 294 females approached clinics. 55.8 percent of drivers admit that at least one traffic accident has involved them. A report on 'Aberrant driving behavior: mistakes and violations' by the ref [2], was also based on the analysis by the ref [4]. The study explains the violence and mistakes of drivers in Western Australia. As was the case in the overall sample of 135 (61 male and 74 female), the same number of items and methodology was used. Data reveals that most of the risky violations/errors are committed by young drivers relative to old drivers. Path visibility and speeding while driving is the most extreme offenses.

Many other experiments were conducted with minor modifications based on the research [4]. In ref [7] performed 174 studies to determine the correlation between errors and violations using DBQ. The relationship with self-reported injuries was found to have violations in 42 samples and errors in 32 samples. The findings indicate that age negatively correlates with mistakes and breaches, while the experience is positively linked. The authors affirm the validity of the DBQ tool and conclude that DBQ is a useful tool for predicting the actions of drivers in road accidents.

Lahore's city traffic police statistics indicate that 76,070 accidents occurred in Lahore between 2004-2010, while in 2010 alone, there were 31,717 accidents in Lahore. Approximately 86% of accidents in 2010 were due to careless driving, as seen in Figure 2. Of the 31717 accidents in 2010, 7950 occurred only because of the over-speed, While 12487 accidents occurred due to the driver's carelessness, 4658 occurred due to incorrect turnings, and 1950 U-turn accidents. 46 percent were motorbikes in these 31717 deaths, and 29 percent were motorcars. About 73 percent of the victims of accidents were under 40 years of age, and 31 percent were 20 years or younger. On the top, motorcycles are involved in traffic accidents, and on the second, cars are the same as in the rising vehicle rate, see [5].

In ref [8] quoted the data from Rescue 1122 concerning Peshawar city in a newspaper article that Rescue 1122 was busier in 2012 than in 2011. 4,639 people were rescued and hospitalized, and 1,014 have been involved in road accidents among those individuals [8].

All these figures highlight how important it is to observe the actions of the driver. The conduct of drivers is an essential factor influencing road safety, but other factors are primarily accounted for. There is a need to measure the impact of the actions of drivers on safety in a more transparent way. This will allow us to recognize the root causes of injuries and can also be used to enhance the traffic rules.

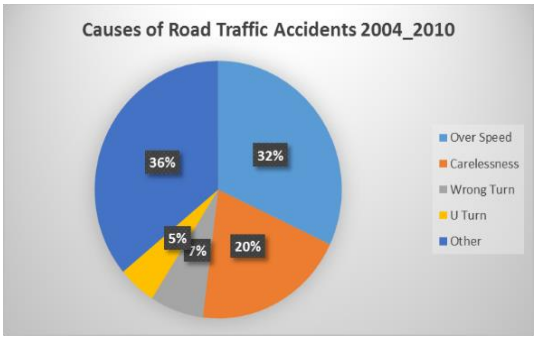

Figure 3 Causes of road traffic accidents 2004 to 2010

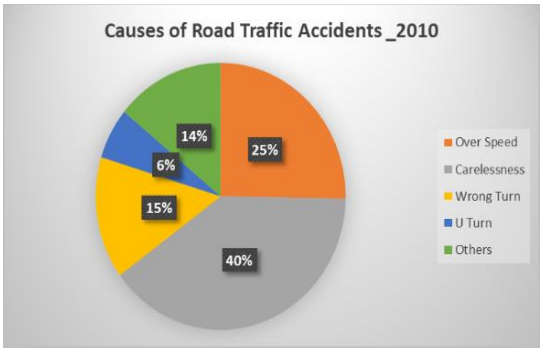

Figure 4 Causes of road traffic accidents 2010

III. METHODOLOGY

A. *Driver Behavior Questionnaire (DBQ) Construction*

The essential tool for the study of dissimilarity between aberrant driver behavior errors and violations was the driver behavior questionnaire. In terms of behavior, the Driver Behavior Questionnaire (DBQ) was split into four separate sections. The first part of the questionnaire included the socio-economic conditions of the driver and other information, i.e., age, gender, driving experience, level of education, respondents' monthly income, driving license, average mileage age of the car, frequency of motorway use, regular driving hours and past records of road accidents.

As in the [4] driver behavior questionnaire, the 2nd part of the questionnaire consisted of 50 different kinds of behavioral questions. Overall, in section 2, there were three major categories of driver behavior: mistakes, slips and lapses, violations, and unintentional violations. A total of twenty-one items of Slips and Lapses (When in 3rd gear and driving away from the traffic signal, switching windscreen wipers instead of headlights, etc.), 9 items of error (hitting a car in a car park when reversing, misjudging the entry), 3 Unintended violations (look at the speed meter when driving and find out that you are going faster than the speed limits permitted unwillingly.) and 17 intentional violations (overtake on the inner/left hand (wrong side) due to slow driving on the outer/fast lane of other cars (overtaking lane). Driving too close to the car and flashing the car to warn the front car to go fast or get off the front lane.). With five, most general self-assessment questions, section three contained the DBQ. The respondents had to rate themselves on a scale of 1 to 3, how good drivers they think they are, how healthy they think they are, how many mistakes

they think they are prone to drivers, how much compliant with the law they think they are as drivers, and to what degree their mood influenced their driving.Particular attention was paid to the direct opinion of people in the questionnaire analysis on why the Driver Conduct is bad and how it could be changed. Two logical categories were split into section four of the report. In the view of the respondent, the first focuses on the causes/reasons behind the bad conduct of the driver. Moreover, the second part comes from a detailed recommendations section, which covers some of the potential steps to change the conduct of the driver. The respondent was asked in section four to comment on the reasons for the aberrant conduct of the driver in general. The respondent has to give their opinion on the options provided for poor behavior, i.e., Lack of knowledge of traffic rules and regulations, lack of driving instruction, lack of enforcement of traffic regulations, low literacy rate, the weak signal system for traffic, and weak road signs. The respondent was also asked about the impact of the weather on the actions of the driver. Section four contained several questions concerning their views about strengthening the conduct of the driver, i.e., advertising campaigns via cable, national television, print media, the inclusion of some courses in academia, training, and seminars in educational institutions, etc.

After completing the questionnaire in English, it was translated to Urdu for keeping in mind the illiterate and even the lessor knowledge of traffic. The questionnaire was formatted in such a way that both English and Urdu were back-to-back lines, so if a person finds it difficult in one language, he may understand it from the other language.

B. Instructions

Every responded were given the following set of instructions:

There is no one flawless. At some point, the best drivers often make mistakes or commit violations in some situations. It is possible to consider most of them as inconsequential, but some are potentially very dangerous. The research is about analyzing the observations of drivers into their own aberrant behavior. This thesis is part of a Master of Science in Urban Infrastructure Planning research program at the National Institute for Urban Infrastructure Planning and Management. It is quite easy with the questionnaire in hand. Below is a range of things relating to violations and mistakes that you have encountered while driving. For each question, the respondent was to answer how much, if at all, the kind of thing listed in that question happened to you in the last year or so. The respondent was required to write the number range from 0-5 in the box on the right side of each question. The numbers with its meanings are; never=0, Hardly ever=1, Occasionally=2, Quite Often=4, Frequently=4, and Nearly all the time=5.

We recognize that it is impossible to provide specific answers, so we are only interested in your general opinion and interpretation of each item. So, spending too much time on each object is not appropriate. Easily write the number you think your best guess is most suitable as easily as possible. It is optional to include your name and contact numbers. Your answers to the items provided are anonymous and will be taken into account in the strictest confidence. However, we want to know a few information about your socio-economic profile and your driving experience. If you could fill in the things in section one before the central part and the rest of the pages, we will be obliged. It is a request to work as fast as possible through all the behavioral questions and write one number against each question. Please re-check it after completing all the questions to ensure that you do not miss the answer to any question. Please make sure that the questions are answered honestly. Your replies are anonymous. Thank you, and help in completing it for all your cooperation.

C. Survey

The survey was performed at colleges and public buildings in the parking lots. Drivers were questioned directly in the parking lot. After a brief introduction, they were given the option of filling it at home and then delivering it to the watchman in the parking lot or filling it on the spot either by himself or by the interviewer by verbally answering him. Three hundred and fifteen questionnaires were given to individuals who told the interviewer that after filling it in at home, they would send it back to the watchman. A total of 45 questionnaires, 4 of which were incomplete, were returned. Via an interview, an additional 110 questionnaires were completed by describing each object and then writing their responses. 250 questionnaires were filled out in total. In the study field, the number of female drivers was very small, and it was also difficult to approach females to fill out the questionnaire because of cultural restrictions, so only two questionnaires were filled out by female drivers, which is not appropriate for research, so they were removed from the research.

D. Data Analysis

Statistical Package for Social Sciences (SPSS) was mainly used for the analysis of the data. The collected data through 250 questionnaires were entered into SPSS for analysis.

E. Descriptive Statistics

The socio-economic characteristics of the surveyed drivers were determined. Descriptive Statistics analyses were determined for the DBQ items to know the mean, standard deviation, and frequencies of the data.

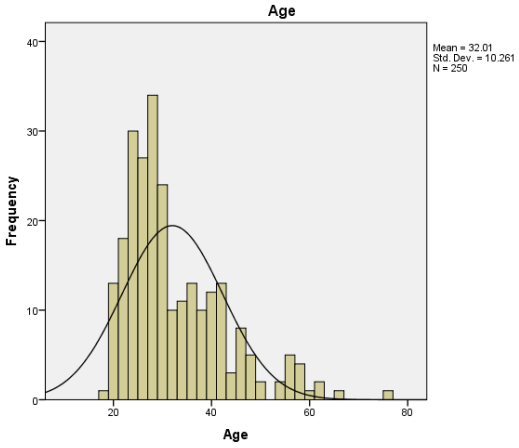

Figure 3 Age of respondents

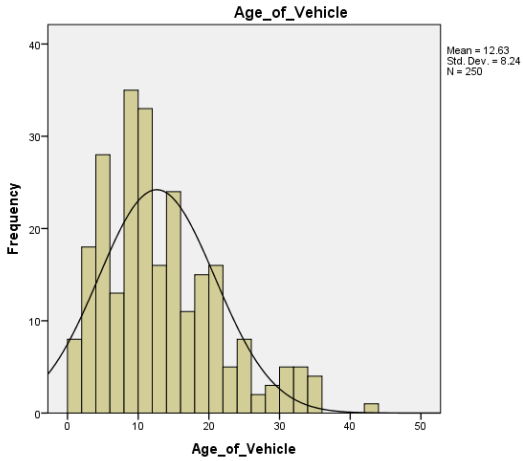

Figure 4 Age of vehicle

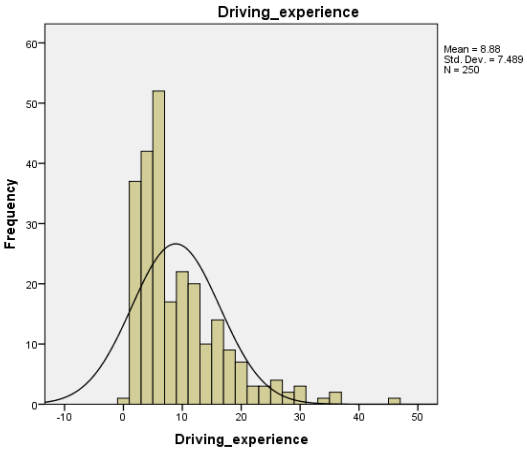

Figure 5 Driving experience of respondents

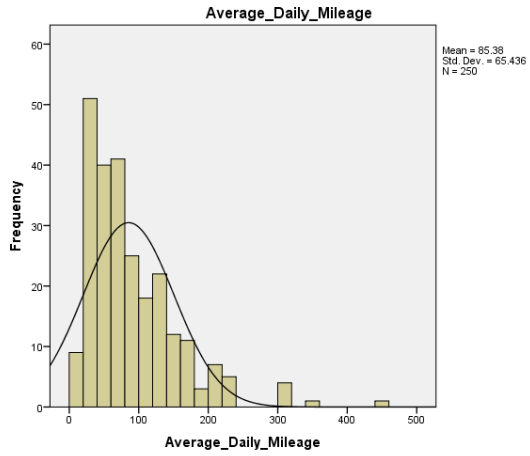

Figure 6 Average daily milage

F. Education Level

The level of education indicates that the sample size includes 51 percent of graduate or undergraduate students, 31 percent of intermediate and below, while 17 percent were illiterate, showing that the sample size includes all literacy sections. First of all, there were two reasons for most of the graduates this, as the study aims to find the difference in violations & errors in private car owners; thus, it was evident that educated people are mostly private car owners in the city; secondly, the study was conducted in the University of Peshawar car parking lot and some public offices, which also caters to educated people.

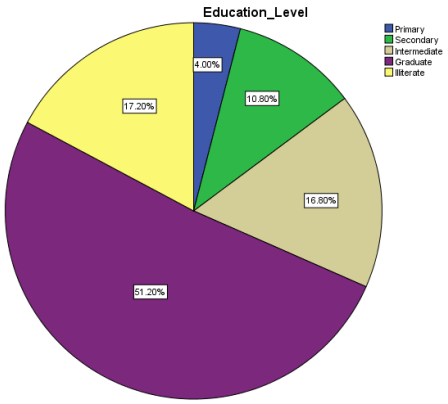

Figure 7 Educational level

G. Monthly Income

40 percent of individuals had an income of less than 10,000, which was attributed to the fact that most of these groups were university students. 38 percent of individuals have revenues between 10000 and 30000, mainly drivers of private drivers or drivers of public/private agencies, who are likely to earn salaries in that range. Although 21% of individuals had an income of more than 20%.

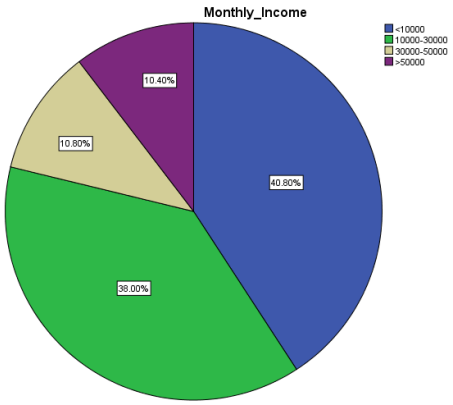

Figure 8 Monthly Income

H. Occupation of the respondent

The sample size was distributed, which is evident from the table, among all the occupations. 26 percent were teachers, 38 percent were in their own private company, 16 percent were government employees, and 15 percent were private employees.

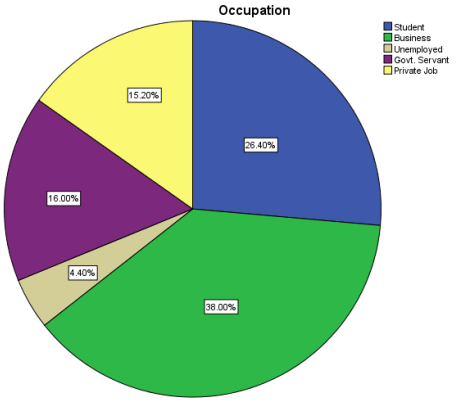

Figure 9 Occupation

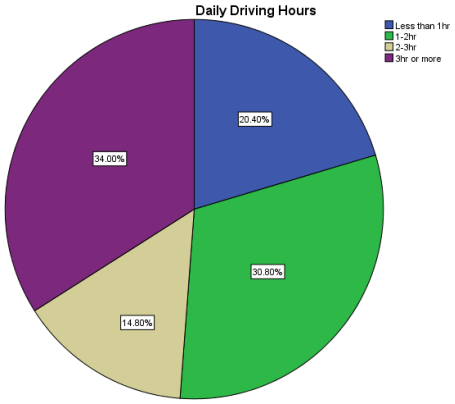

Figure 11 Daily driving hours

I. Frequency of Motorway use

Around 50% of respondents were using the motorway monthly or more. While 17% of respondent use motorway fortnightly. 32% of respondent were using the motorway weekly are daily.

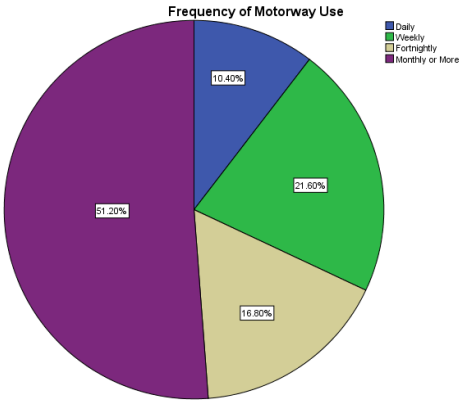

Figure 10 Frequency of motorway use

J. Daily Driving Hours

Daily driving activity indicates that 20 % of respondents have less than one hour of daily driving hours. In comparison, 31% have 1-2 hours of daily driving hours, while 46% have 2 hours or more than 2 hours, mainly drivers who come for work from outside the city or drivers of public/private departments or private taxi drivers who ride all day long. So, the sample for the analysis is well distributed.

K. Accidents

The respondents were asked regarding their accident history. The accident history of the drivers shows that 89% have experienced accidents in the past one year.

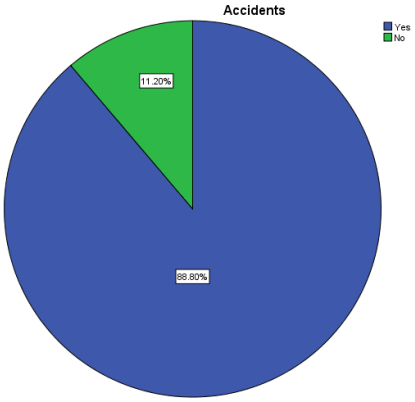

Figure 12 Accidents

L. Martial Status

54% were married while the remaining 46% were unmarried.

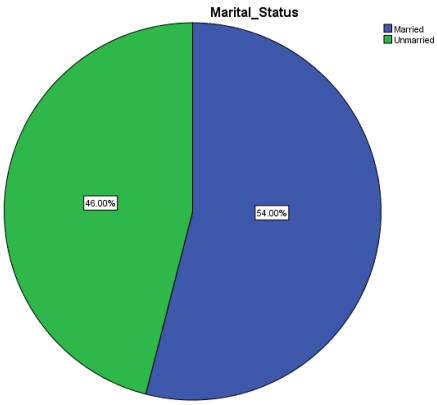

Figure 13 Marital status

M. Driving License

A license is an official identification document which states that a motorized vehicle and/or a motorbike may be driven by the recipient. The details relating to the possession of a license was reported in order to verify the legal driving status of the respondent. Twenty-seven percent of respondents do not have a driving license (27 percent).

To know the reasons why a person could not get the driving license, we have recorded the reasons. There are four main reasons for this problem.

- The person is underage and could not apply for the Driving License.
- Many people may find the licensing process difficult.
- The official has made it very expensive, or the person having the vehicle is very poor.
- Some careless people did not care to have a driving license due to the lake of enforcement.

Although the data from Figure 13 indicate that 50 percent of respondents consider the process complicated, it is evident that the licensing institutions that have established the process lack the power. 24 percent said they did not need a license. Whatever the legitimacy of the driving license process is, but the least that indicates the driver's legal status is that at least he is a driver and has been through a license obtaining process of written and realistic checks. It is worrying for both the top reporting reasons mentioned by the respondents.

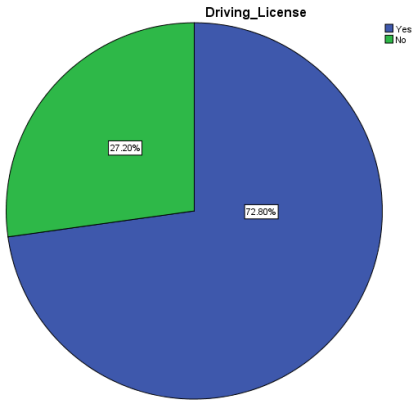

Figure 14 Driving license

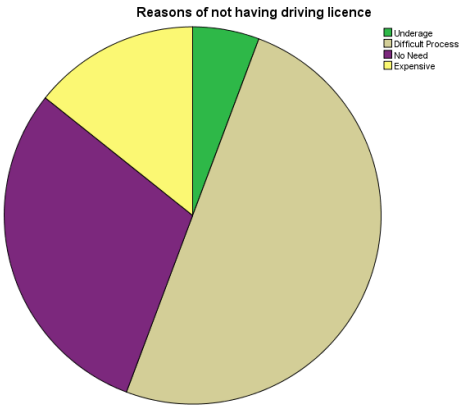

Figure 15 Resaons of not having driving license

IV. RESULTS

Primary data is collected in the field by means of a driver survey. In the four major structural groups, the data is broken. In section one, demographic data and the respondent's driving experience/history are addressed. The second segment illustrates the interpersonal elements of the pilot. Section 3 contains self-assessment questions.

- Socio-economic Profile and driving history
- Drivers behavior during driving
- Self-assessment
- Remedial Measures

A. Descriptive Statistics

Participants ranged from 18 to 53 years of age, with an average of 26.66 years (S.D. 8.05) and from 1 to 25 years of driving experience with an average of 6.20 years (S.D. 5.03). With a mean of 48.92, the average daily mileage ranged from 2 to 350 (S.D. 65.88). The level of use of the highway was almost weekly or longer. As the average vehicle age is 9.65 (S.D. 7.59), the age of the vehicle was also important.

Drink (Alcohol) and drive, Ignoring motorway exit, misjudging car gap while parking, attempting to drive away without switching ignition, While in 3rd gear and driving away from the traffic signal, forgetting car in parking are the least reported things while flashing the car to signal the car in front to go quickly or get off the front lane. The highest recorded things were being frustrated with a car in front and overtaking on the wrong side, disregarding red lights late at night, overtaking vehicle inside, and disregarding speed limits late at night or early in the morning. Due to the cultural and religious sense, the use of alcohol is a bit evident. The data showed that the respondents to this study do not regularly use motorways, so one of the least mentioned items is the missed exit on the motorway. As the replied were mainly younger, so the least reported stupid errors such as driving without ignition and/or in third gear were reported. Mean and standard deviations for socio-economic products can be seen in detail in the see Table 1.

TABLE 1 SOCIO-ECONOMIC CHARACTERISTICS OF DRIVERS SURVEYED IN PESHAWAR

	Age	Age_of_ Vehicle	Driving _ experience	Average_Daily_ Mileage
N Valid	250	250	250	250
Missing	0	0	0	0
Mean	32.01	12.63	8.88	85.38
Median	29.00	11.00	6.00	70.00
Mode	24	8a	5	50
Std. Deviation	10.26	8.24	7.48	65.43
Minimum	18	1	0	10
Maximum	76	42	45	450

B. Descriptive Statistics for The Behavior Items

The answers reported for section 2 were from Never (0) to Frequently (4). Drink (alcohol) and drive, missing motorway exit, misjudging car gap. In contrast, parking, attempting to drive away without switching ignition, attempting to drive away from the third gear traffic signal, forgetting car in parking were the least reported things while flashing the car in front as a signal to drive faster, the highest recorded items were to become aggressive with a car in front and overtake on the wrong side, pay no attention to red lights at night, overtake the vehicle on the inside and ignore speed limits late at night or early in the morning. Due to the cultural and religious sense, the use of alcohol is a bit evident. As the replied were mainly younger, so the least reported stupid errors such as driving without ignition and/or in third gear were reported.

CONCLUSION

The trend of people not having a driving license is very high, especially in young people. Almost 64% of people do not have a driving license. The reason for those not having the driving license is very alarming; as described by the respondents of these areas, 62% consider the process of getting a license difficult while 29% consider it of no use, and they believe they do not need it. This issue needs much importance because, on the one hand, getting a license is difficult. At the same time, on the other, a lot no of people think they do not need it, which shows poor enforcement and reliability of the public institutions. Drivers with no driving license do more pushing speeding than those who have a driving license.

Fifty percent of the respondent believes that the reason for the bad behavior of drivers is due to the lack of awareness about traffic guidelines and regulations and lack of regulations enforcement. The majority of the respondents believe that having awareness regarding safe driving behavior on national television will be effective. The respondents also believe in training and workshops on driver behavior at school and university level. Most of the respondents were of the opinion to have strict enforcement of traffic rules, mandatory training before issuing a driving license, improvement of traffic signal system, and improvement of road signs will help to improve the aberrant driving behavior.

REFERENCES

[1] Bener, A., Ozkan, T., & Lajunen, T. (2008). The Driver Behaviour Questionnaire in Arab Gulf Countries: Qatar and United Arab Emirates. Accident Analysis and Prevention, 1411-1417.

[2] Hartley, P. N. (1995). Aberrant driving behaviour: errors and violations. Ergonomics, VOL. 38(NO. 09), 1759-1771.

[3] NHTSA, N. (2013). Traffic Safety Facts. Washington, DC 20590: National Center for Statistics and Analysis, U.S. Department of Transportation.

[4] Reason, J., Manstead, A., Stradling, S., Baxter, J., & Campbell, K. (1990). Errors and violations on the roads: a real distintion? Ergonomics, 33, 1315-1332.

[5] Rescue 1122, P. (2011, March Saturday). Performance of Rescue 1122. Retrieved from Punjab Emergency Service: http://www.rescue.gov.pk/Performance.aspx

[6] WHO. (2013). Global status report on road safety. WHO.

[7] Winter, J. d., & Dodou, D. (2010). The Driver Behaviour Questionnaire as a predictor of accidents: A meta-analysis. Journal of Safety Research, 463-470.

[8] Zia, A. (2013, January Sunday). KP & Fata. Retrieved from The Express Tribune: http://tribune.com.pk/story/493217/rescue-1122-registers-busy-year-as-violence-soars/

Wajidullah: M.Sc. in Urban Infrastructure Planning from University of Engineering & Technology Peshawar. B.Sc. in City & Regional Planning from University of Engineering & Technology Lahore.

Safiullah
B.Sc. Civil Engineering, from CECOS University Peshawar

Muhammad Adil Khan
B.Sc. Civil Engineering, from CECOS University Peshawar

International Journal of Engineering Works
ISSN-p: 2521-2419
ISSN-e: 2409-2770
Vol. 7, Issue 10, PP. 350-355, October 2020
https://www.ijew.io/
https://doi.org/10.34259/ijew.20.710350355

Retrofitting of RC Beam Structure Member By Using CFRP

Ismail Shah[1], Li Jing[1]*, Shahid Ayaz*[2], Waqas Ali[3], Abdullah[4] and Nauman Khan[5].
[1]School of Architecture and Civil Engineering, Yunnan Agricultural University, 650000, Kunming China.
[2]MSCE scholar, Department of Civil Engineering, Abasyn University, Peshawar Pakistan.
[3]US-Pakistan Center for Advanced Study in Energy, National University of Science and Technology, Islamabad, Pakistan.
[4]Department of Civil Engineering, Sarhad University of Science & Information Technology, Peshawar Pakistan.
[5]School of Civil Engineering, Zhenjiang, Jiangsu University of Science and Technology Jiangsu China.
Corresponding authors
Li_jing69@163.com[1]*, shahid_ayaz92@gmail.com[2]*
Received: 01 October, Revised: 11 October, Accepted: 15 October

Abstract:- The research has been lead relating the use of carbon fibre-reinforced polymer (CFRP) sheets in retrofitting and strengthening of the reinforced concrete member. The present research was conducted by using the epoxy to reinforced concrete beams retrofitted and strengthened for flexural strength by using CFRP sheet. The selected cross-section of the beam having 2400 mm length with 150 mm width and 225 mm height and the beam tension reinforcement on the bottom was set on 2#4bar@1.5" with the 38.1 mm clear cover was set to the main flexural reinforcement. The studied beam was focused on flexural behavior. The experimental study has shown that while the using of CFRP with epoxy will improve the rigidity and durability of the concrete beam. Their great deformability greatly improves the seismic properties of the beam structures. Under the reinforced RC beams showed a very large deflection by control beam before their failure. By using CFRP externally the rigidity of retrofitted and strengthened beams can be improved.

Keywords— CFRP, Epoxy, Flexural strength, Retrofitting/ Rehabilitation.

I. INTRODUCTION

One of the most important and significant challenges in civil engineering has become the retrofitting and reinforcement existing structures. Generally encountered engineering issues such as increased in-service loads, structure usage changes, structural design and/or construction mistakes, and change in design codes, deterioration issues and the seismic retrofitting are some of the reasons for the need to repair/retrofitting of an existing structure. The most common solution is of rehabilitation and repairing is retrofitting for RC structures. This project has been chosen after the strong earthquake was felt with the M7.5 in Hindukush region on the 2015 October 26, with the epicenter of 45 kilometers, at the southwest of Jurm, Badakhshan Province Afghanistan. Above 280 persons were killed and 1,770 persons were injured and remarkable demolition about 109,123 building was recorded by that earthquake [1]. Earlier that on 8 October 2005 earthquake smash the northern Pakistan, Afghanistan, and India with the magnitude of 7.6. The epicenter city of the earthquake was the capital city of Azad Kashmir, named Muzaffarabad, throughout 19 days 978 shocks with ≥ 4.0 scale magnitudes shock were recorded in the region, 86,000 people were killed, 96,00 were hurt, 32,000 houses were demolished and 2.8 million peoples became emigrant [2, 3].

The modern rehabilitation techniques (ie expand current parts, add new structural components, glued steel plates etc.) encounter numerous shortcomings, e.g. problematic and slow application, and lack of durability [4]. A retrofitted beam with CFRP laminates can resist up to 170 % of the maximum load as compared to control beams [5]. Dong considered reinforced concrete beams longitudinal reinforcement with the different cross-section depths, thickness and concrete cover and different flexural properties. They determined that the retrofitted CFRP beam will increase the resistance by 41 to 125% and stated that the stiffness would not change with increasing of concrete cover thickness [6]. Kachlakev and McCurry confirmed that when the beam reinforced with FRP glass and CFRP laminate, respectively were enhanced in flexural and shearing, with maximum load increase to 150% [7]. In attempts to quantitatively increase the flexural and shear strength provided by externally bonded CFRP laminates [8, 9]. It has been confirmed that if FRP plates increase the stiffness, the capability of load and the cracks can be decreasing with on RC structures [10]. The consideration of retrofitted beams is smaller as compared to un-retrofitted beams due to the added toughness by FRP Sheets or plates [11]. With the increasing numbers of layers of the FRP, the sheet has significant effect toughness and an

extreme load of the RC structure beam. The load capacity will increase as the number of CFRP sheets increases, up to 6 sheets [12]. The strengthened beam by using CFRP sheets to superior load the stiffness will be increase and the cracking tension will be delayed [13]. The initial load of resistance during amplification is a key factor that affects the maximum strength of the RC retrofitted beam with FRP. A retrofitted beam lover level ultimate strength will produce a higher level of the load than a beam retrofitted with lover level of load [14]. On the continuous beams, the FRP can be used in the positive torque zone or the negative torque zone. Previous research studies confirm that the growing toughness and supreme carrying load carbon fiber reinforced polymer laminate can be used to RC beam, because the CFRP sheet increases the rigidity of the RC member, furthermore; the number of CFRP sheet has a significant impact on the maximum load and rigidity of a beam. The results show that the load carrying capacity increases as the number of CFRP sheets increase up to six, the early load during the reinforcement is also a main influence to affects the maximum strength of reinforced beams with CFRP. CFRP has the potential to apply on continuous beams, the use of CFRP laminates can effectively reduce deflection and increase beam load capacity [15, 16]. Repair and reinforcement of EB-FRP can be performed in three types of applications: holding, bending and shear reinforcement [17, 18].

The main objective of this experiment to study the flexural behaviors of RC concrete beams by using CFRP. In this experiment has shown the find-out contrast among the flexural strength of control and strengthen and retrofitted beams. The specimen cast in this experiment is to compare the retrofitted beams and non-retrofitted beams. Static load reactions of the RC beams structure under the two-point loading method was evaluated as a function of flexural strength, observation of crack, composite amongst concrete and CFRP, and the related failure approaches. Comparisons are made between the controlled beam and strengthened and retrofitted beam experimental results. excellent style manual for science writers is [7].

II. EXPERIMENTAL PROGRAM AND STRENGTHENING TECHNIQUES

In the present research work beams samples are tested under two-point loading situation. The beams were tested after 28 days of curing. The beams were tested in separately two groups. 1st group of beams are focused on flexural behavior and 2nd group of beams was focused on the shear behavior. The first group of beams in the experiment were labelled as control beams, and the other group was preloaded up to flexural cracks performed and after that strengthened these beams with CFRP. Lastly, the load was applied on the strengthened beam until they failed and the obtained results were matched with additional beams. In the total of two beams were cast in the 2nd group as control beams. Two beams were cast in 2nd group as well as two beams cast in control beams, and pre-loaded two beams until shear cracks appeared and after that the pre-loaded beams were retrofitted and lastly tested until their failure.

A. MANUFACTURING OF BEAMS

The beams cast having the cross-section area of 1960 mm length, 150 mm width, with the depth of 300 mm. The beams are considered to having insufficient bending strength to attain the pure bending failure, with compression reinforcement of (2@10) and tension reinforcement of (2@10) and along with the 8 mm strips c/c 100 mm are used to tie the steel bars together as shown the Figure 1. In all beams, the clear concrete cover of the central flexural bar was used to 25 mm. The reinforcement and geometry are shown in "Figure 1". All beams were tested after curing of 28 days. The laminate used in this research had 1.4 mm thickness, with the width of 50 mm and according to the manufacturer the elastic modulus 165 GPa.

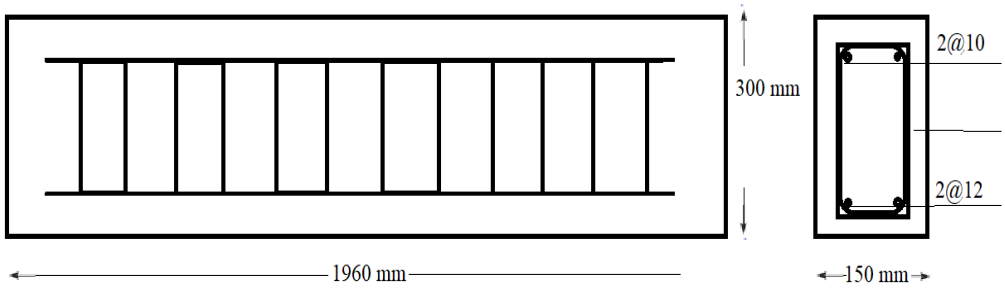

Figure 1. Beam Manufacturing with reinforced dimensions

The reinforcement geometry of beams shown in Figure 1. and the during the testing of control beams was tested by using the two-point bending load method. This load ratio was taken in the present the current study because it delivers a maximum force and as well zero cross-sectional shears between the loads, and delivers the maximum shear force among the load and supports. The beam supports span was kept 1560mm and the load was applied into equal parts as shown in Figure 2. over the width of the beams steel plates were used to distribute the load equally. The jacking machine in this test equipment has used the capacity of 1400 KN. To find out the deflection at the middle of the beam span, Linearly Variable Differential Transducer (LVDT) is used, as shown in Figure 2. the test arrangements of a beam.

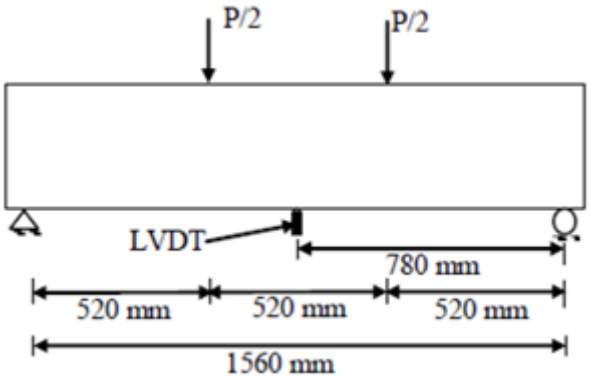

Figure 2. Loading, Position and Supports of LVDT

III. METHODOLOGY

In the present experiment, we will study about the CFRP as a building retrofitting material that used in RC beam structure member. The beams having the cross-section area of 1960 mm length, width were 150 mm and 300 mm height, with the tension reinforcement 2#4bar@1.5" as shown in Figure 1 and the bottom of the beams, the main flexural reinforcement clear cover was set 38.1 mm. in this experiment two beams cast by using 1:2:4 mix ratio as well as cured for 28 days. The grinder machine were used to make rough the surface of the beam and after that by using the surface cleaner the beam surface was cleaned to make it rough and level. After making the beam surface rough and clean mixed form of epoxy glue was applied to the rough and cleaned surface of the beam into two layers and then placed the CFRP sheet on the glued beam and kept on room temperature for 24 hours to get the strength. After 24 hours the bending test was scheduled for retrofitted beams and strengthened beam and the load was recorded until the failure of the beam.

A. TESTING OF CONTROL BEAMS

In the present study, the two-point bending test is carried out. This loading situation is selected because it provides a maximum shear force and zero shears in the cross-section between the loads. These moments vary linearly between the supports and the load. The load was applied at two positions that equally divided beams into three parts as shown in Figure 3. under the load steel plates were used to distribute the load equally over the beam width. The testing device of 200 KN capacity jack was used in this experiment. A linear variable differential transducer, LVDT was used to find out the deflection of the central span of beams. Load and Deflections were recorded throughout the examination.

B. TESTING OF RETROFITTING BEAMS

The grinder was used for rough surface of beams to coated CFRP sheets, applied CFRP sheets to the bottom of the entire beam as shown in the Figure 3. after that all the specimens were being exposed to negative moment allowing to its weight. This represents a minor pre-stressing effect; it can be found through a jack in the condition of onsite maintenance.


Figure 3. The surface of the beam roughened afore put on CFRP and applied CRFP Sheet on beam

IV. RESULTS AND DISCUSSION

In this experimental study, CFRP externally bonded was used to repair a reinforced beam structure. The reinforced beam structure deformation capability performance against the seismic was improved by using CFRP, by using CFRP is easy to apply with epoxy as a construction material. The CFRP with

epoxy has shown an improvement in strengthening the current construction practice results.

A. *Load Deflection Analysis*

The current assessment used data is obtained from the dialed reading which is attached with data logger placed at the middle span of the examined beam models and from the load chamber (applied load). At the load of the control beam as opposed to the deflection curves of the beam in the middle as shown in Figure 4. The beams performance in a yielding behavior and beam has shown large deflection before the final failure. RC structural beams should retrofit by using CFRC to meet the revised specification and change in the function of structures. Adsam et al. [19] investigated RC structural beams by using CFRC the retrofitted samples showed an increase in maximum load capacity and rigidity up to 53% and 61% respectively. They concluded that the CFRP laminates strengthened RC beams.

At the load of 1.7 tons, the first crack has appeared on retrofitted beam and middle span deflection curvature was noticeable the non-linearity of the cracking of reinforced beam. After 2.1 tons of load, flexural cracks found and became broad and open by increasing applying load. The maximum load of 2.7 tons was recorded.

The strengthened beam load versus middle span beam for strengthening beam load-deflection curves are shown in Figure 5. In the strengthened beam at the load of 3.4 tons, the first crack has appeared on strengthened beam and middle span deflection curvature was clear the non-linearity of the cracking of strengthened beam. The maximum load of 6.3 tons was recorded.

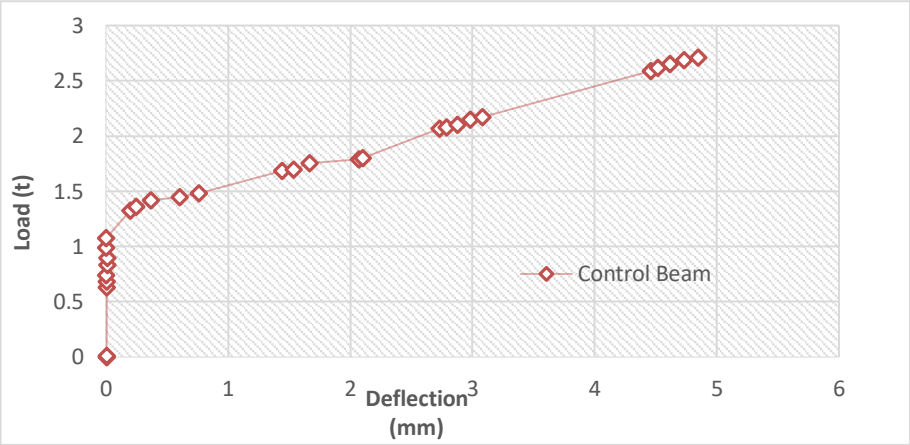

Figure 4. Control beam load vs. deflection

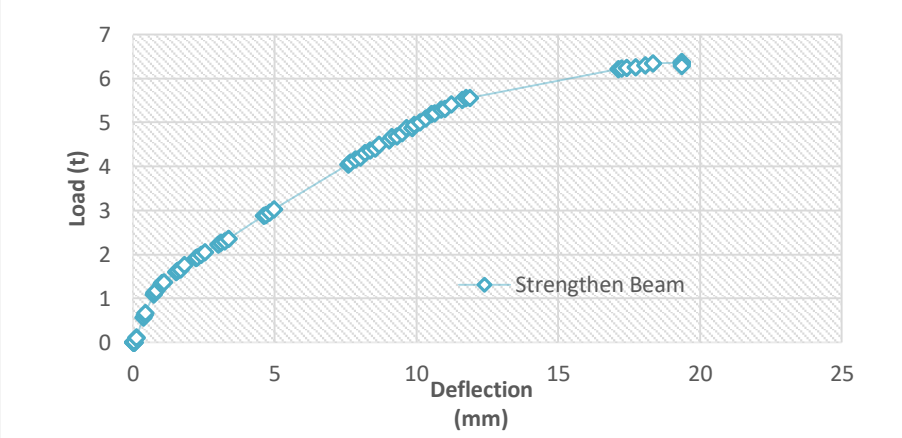

Figure 5. Strengthen beam load verse deflection

B. Comparison Between Control and Strengthen and Retrofitted Beams

The rigidness of the CFRP-reinforced (retrofitted) beam and strengthened beam was improved as a contrast to the control beams. By using the externally bonded CFRP results shown increases in the focused load of the CFRP-reinforced beam as well as strengthened beam specimens when contrasted to the control beams as shown in Figure 6.

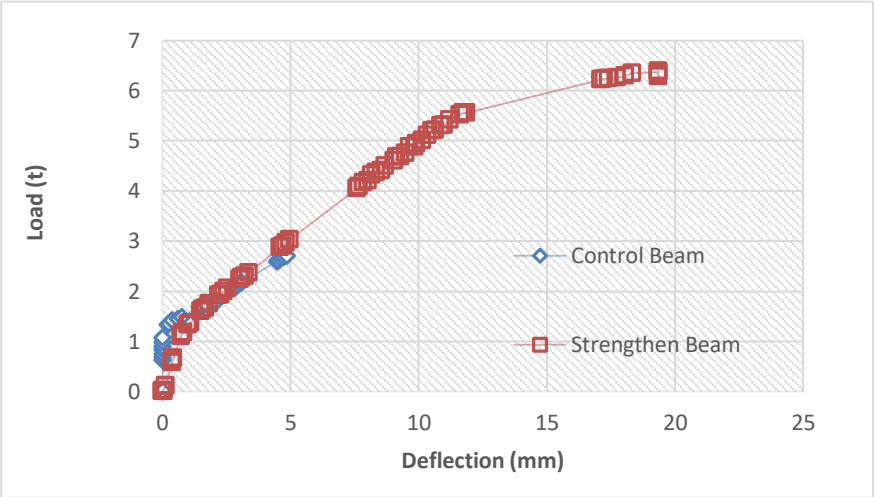

Figure 6. Comparison between control and strengthened and retrofitted beam

CONCLUSION

The purpose of this study is to investigate the rehabilitation performance of flexural strength by using CFRP retrofitting techniques. Experimental results have shown an increase in the length of CFRP in strengthened and flexural retrofitted can create the CFRP extra active in repairing and strengthening of concrete. This founds that unsatisfactory strengthening length does not yield the desired strengthening effect.

ACKNOWLEDGEMENT

The authors would like to thank Dr. Samiullah Khan for helping critical reading and editing of the manuscript.

REFERENCES

[1] Ismail, N. and N. Khattak, Building typologies prevalent in Northern Pakistan and their performance during the 2015 Hindu Kush Earthquake. Earthquake Spectra, 2016. 32(4): p. 2473-2493.

[2] Peiris, N., et al., Mission: October 8 2005 Kashmir earthquake, preliminary report. 2006.

[3] Peiris, N., et al., EEFIT mission: October 8, 2005 Kashmir earthquake. Published Report, The institution of structural engineers, London, 2006.

[4] Karzad, A.S., et al. Repair of reinforced concrete beams using carbon fiber reinforced polymer. in MATEC Web of Conferences. 2017. EDP Sciences.

[5] Toutanji, H., L. Zhao, and Y. Zhang, Flexural behavior of reinforced concrete beams externally strengthened with CFRP sheets bonded with an inorganic matrix. Engineering structures, 2006. 28(4): p. 557-566.

[6] Yang, D.-S. and S.-K. Park, An experimental study on the flexural behavior of RC beams with cementitious repair materials. KSCE Journal of Civil Engineering, 2002. 6(1): p. 11-17.

[7] Kachlakev, D. and D. McCurry, Behavior of full-scale reinforced concrete beams retrofitted for shear and flexural with FRP laminates. Composites Part B: Engineering, 2000. 31(6-7): p. 445-452.

[8] Khalifa, A. and A. Nanni, Rehabilitation of rectangular simply supported RC beams with shear deficiencies using CFRP composites. Construction and building materials, 2002. 16(3): p. 135-146.

[9] Shehata, I., E. Cerqueira, and C. Pinto. Strengthening of RC beams in flexure and shear using. in FRPRCS-5: Fibre-reinforced Plastics for Reinforced Concrete Structures: Proceedings of the Fifth International Conference on Fibre-Reinforced Plastics for Reinforced Concrete Structures, Cambridge, UK, 16-18 July 2001. 2001. Thomas Telford.

[10] Khalifa, A., et al. Shear strengthening of continuous RC beams using externally bonded CFRP sheets. in American Concrete Institute, Proc., 4th International Symposium on FRP for Reinforcement of Concrete Structures (FRPRCS4), Baltimore, MD. 1999. Citeseer.

[11] David, E., C. Djelal, and F. Buyle-Bodin, Repair and strengthening of reinforced concrete beams using composite materials. 2nd international PhD Symposiumin civil engineering, Budapest, 1998: p. 23-34.

[12] Shahawy, M., et al., Reinforced concrete rectangular beams strengthened with CFRP laminates. Composites Part B: Engineering, 1996. 27(3-4): p. 225-233.

[13] Ferreira, A., On the shear-deformation theories for the analysis of concrete shells reinforced with external composite laminates. Strength of materials, 2003. 35(2): p. 128-135.

[14] Wenwei, W. and L. Guo, Experimental study and analysis of RC beams strengthened with CFRP laminates under sustaining load. International Journal of Solids and Structures, 2006. 43(6): p. 1372-1387.

[15] Grace, N., et al., Strengthening of continuous beams using fiber reinforced polymer laminates. Special Publication, 1999. 188: p. 647-658.

[16] Aiello, M., L. Valente, and A. Rizzo, Moment redistribution in continuous reinforced concrete beams strengthened with carbon-fiber-reinforced polymer laminates. Mechanics of composite materials, 2007. 43(5): p. 453-466.

[17] Pellegrino, C. and M. Vasic, Assessment of design procedures for the use of externally bonded FRP composites in shear strengthening of reinforced concrete beams. Composites Part B: Engineering, 2013. 45(1): p. 727-741.

[18] 440, A.C.I.C. Guide for the Design and Construction of Externally Bonded FRP Systems for Strengthening Concrete Structures: ACI 440.2 R-08. 2008. American Concrete Institute.

[19] Adsam Gideon, D. and P. Alagusundaramoorthy, Flexural retrofit of RC beams using CFRP laminates. MS&E, 2018. 431(7): p. 072006.

Ismail Shah is the resident of Mardan Khyber Pakhtunkhwa, Pakistan. Have received his BSc. Degree from Abasyn University Peshawar, Pakistan and currently enrolled in the MS program of Construction Engineering and Management of Urban and Rural areas at Yunnan Agricultural University Kunming, China (YNAU). His major field of interest are Retrofitting/ Rehabilitation.

How to cite this article:

Ismail Shah, Li Jing, Shahid Ayaz, Waqas Ali, Abdullah and Nauman Khan "Retrofitting of RC Beam Structure Member by using CFRP" International Journal of Engineering Works, Vol. 7 Issue 10 PP. 350-354 October 2020, https://doi.org/10.34259/ijew.20.710350354.

International Journal of Engineering Works
ISSN-p: 2521-2419
ISSN-e: 2409-2770
Vol. 7, Issue 10, PP. 356-360, October 2020
https://www.ijew.io/
https://doi.org/10.34259/ijew.20.710356360

Serial Robot Collision Reaction Using Joints Data at Stationary Position

Omar Abdelaziz[1234] [0000-0002-2326-6333] and Minzhou Luo[24]
[1] Hefei Institute of Physical Science, Chinese Academy of Science, Hefei 230031, China
[2]University of Science and Technology of China, Hefei, China
[3] Egyptian Russian University, Egypt
[4] Institute of Intelligent Manufacturing Technology, Jiangsu Industrial Technology Research Institute, Nanjing, 211800, China.
Corresponding author: Omar Abdelaziz
Email:o0m_ziz@yahoo.com
Received: 03 October, Revised: 12 October, Accepted: 16 October

***Abstract*—** This paper present a method for detecting collision occurs in the robot manipulator and reacting according to collision direction. An experiment was conducted to read the joints speed during collision of the UR3 robot at static position, where the joints speeds are supposed to be zero. The experiment showed that when collision occurs within the manipulator there is oscillatory speed produced in joints, which is suggested to be duo to the stiffness of the harmonic drive. The harmonic drive is a flexible transmission generates stiffness behavior, as a spring, between the motor and the link. The collision is determined from the oscillatory speed produced in robot joints at static position. The method successfully identified the collision impact at joints, and reacted according to the collision direction. The experimental setup and the results are presented in this paper.

***Keywords*—** Collision Detection and Reaction, Flexible Robot, Harmonic Drive, Human Robot Interaction.

I. INTRODUCTION

This paper addresses a hot topic for robotics research in the recent years, which is the human robot collaboration. The coexistence of human in the robot workspace and interacting with it is not suitable in many of the existing robotics applications, particularly the robot manipulators, for several reasons. One of the most significant reasons is the safety factor[1]–[4]. Robots which have the capability of interacting and collaborating with Human should fulfill some parameters to achieve this task[5]. These robots should be flexible and compliant to achieve the collaboration and interaction. Therefore it needs some consideration in the mechanical structure design of the robot manipulator and in choosing the hardware devices. In the other side it requires implementing complex control techniques[6]. There should be certain control strategies to detect the physical collisions and interactions within the robot manipulator as to make it able to collaborate with humans physically. In this direction, there are several methods used for determining these actions. Some works in literature utilize external sensing such as using force sensors, tactile sensors, etc.[7]–[11]. There are also other detection collision/ interaction techniques without using external sensors, such as in[12], [13].These methods mainly based on the knowledge of robot model. Robot modeling can be separated into two main sectors; kinematics and dynamics. The kinematics describes the robot relative pose for each link to their coordinate frames, and consequently to the ground frame. Accurate kinematic model is the main factor for accurate motion control and better robot performance[14]. The dynamic model of the robot is very significant in advanced robotics applications such as working in unstructured or unknown environment, application that required force control and advanced human robot collaboration[1], [5], [15]. Other methods for collision detection without the need for robot modeling presented in [16]. Also we had the chance to present a method for collision detection in [4]. This paper discussing the collision behavior in a static position and reacting against, it consider an extension for the collision detection step. The proposed method in this paper would not require pre-knowledge about the robot dynamics. The method is based on the joints flexibility, this flexibility is due to harmonic drive. The harmonic drive is a flexible transmission produce stiffness behavior, as a spring, between the motor and the link[17]. The harmonic drive is widely used in serial manipulators due to negligible backlash, compact design, and a high torque-to-weight ratio[18]. Moreover it can achieve the desired flexibility in robot joints. Once we are able to detect the speed change from the robot real time interface, a control action is given to the robot to react. The UR3 robot, one of the popular human collaborative robots in the market[19], is used for the implementation of this work. A review for the robot design and its forward and inverse kinematics analysis are presented in[14], [20], [21]. The robot has a TCP/IP interface that allows accesses to some readings in real time. In this work the actual speed and position readings are used for the method implementation. This paper is arranged as follows; section 2 shows the robot joints structure. Section 3 explains the methodology for collision detection and reaction. Section 4 presents the implementation, includes the experimental setup and the results.

II. ROBOT JOINTS STRUCTURE

The UR robot has harmonic drive in each joint for achieving the compliance and flexibility required for interaction. The robot joints structure and its components are shown in Fig. 1. Modeling and controlling robot with flexible joints, as in this robot case, needs detection of the motor and link position. That is why they use two encoders, one for the motor and the other for link position. The flexibility in the harmonic drive system can be modeled as a spring with stiffness (k). Schematic for the joint with flexible transmission is illustrated in Fig. 2. The dynamic model for robots with flexible joints is represented as

$$M(q)\ddot{q} + \mathrm{C}(\mathrm{q},\dot{\mathrm{q}})\dot{\mathrm{q}} + \mathrm{G}(\mathrm{q}) = k(\theta - q) \quad (1)$$

$$I_m\ddot{\theta} + k(\theta - q) = \boldsymbol{\tau}_{\mathrm{m}} - \boldsymbol{\tau}_l \quad (2)$$

Equations (1) and (2) are referred to as the joint and the motor equations, respectively. Where $\mathrm{M}(\mathrm{q})$ is inertia matrix robot links, $\mathrm{C}(\mathrm{q},\dot{\mathrm{q}})$ is the Coriolis and centrifugal velocity terms, $\mathrm{G}(\mathrm{q})$ is gravitational terms, and $\boldsymbol{q}, \dot{\boldsymbol{q}}, \ddot{\boldsymbol{q}}$ respectively are the vector of generalized joints positions, velocities and accelerations. θ is the vector of motors position. I_m is the motors inertias matrix (reflected through the gear ratios), k is joints stiffness matrix, $\boldsymbol{\tau}_{\mathrm{m}}$ are the motor torques, and $\boldsymbol{\tau}_l$ are the losses and dissipative torques due to friction as seen from the motor side.

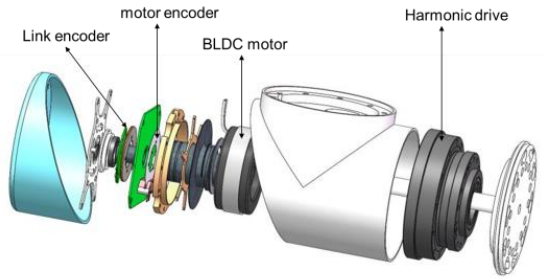

Fig. 1. Flexible joint structure and components

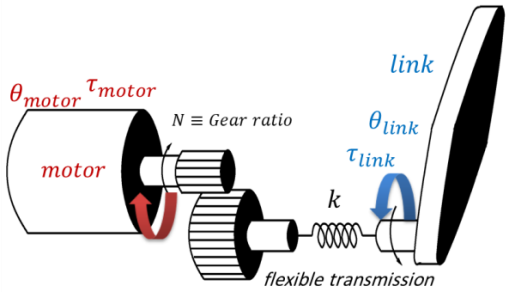

Fig. 2. Joint with flexible transmission schematic

However in our case, the information about the motors encoders is not available. As the robot controller is handling the relation between the encoders, and only provides the average between the two encoders without giving details about the model. Moreover the dynamic model is not required in this work, as we only use the kinematics information of the joints position and speed. The methodology for collision detection and reaction is presented in next section. More about modeling Robots with flexible elements can be found in [22], [23].

III. METHODOLOGY

The method utilized in this work based on the distribution of the collision force on the robot joints. This collision force produces moments at the joints. Hence the highest moment/ torque occur at the joints that have axis of rotation perpendicular to the force direction. Illustrating example is shown in Fig. 3. In Fig. 3(a) the force is applied on link 2 and it is perpendicular to the axes of rotation of joint1, hence the highest moment/torque is produced in joint 1. In Fig. 3(b) the force is applied on link 3 and it is perpendicular to the axes of rotation of joints 2 and 3, hence the moments/ torques produced in these joints higher than the other joints. Since the existence of the harmonic drive, these torques/moments generate oscillatory speed in the joints been impacted.

An experiment was conducted to read the joints speed during Collision while the robot at static position, from experiment we found that there is speed variation at the joints. Thus this information can be used for detecting the collision and its direction.

Since the robot at static position then the joints position $\mathrm{q}_{\mathrm{i},0}(\mathrm{i} = 1 \rightarrow 6)$ are known, and the joints speed $\dot{\mathrm{q}}_{\mathrm{i},0}$ $(\mathrm{i} = 1 \rightarrow 6)$ should be zero. But practically the $(\dot{\mathrm{q}}_{\mathrm{i},0})$ are not zero, it have very slight value around zero due to the noise, we give it a threshold value $\alpha_{\mathrm{thr}} \rightarrow (|\dot{\mathrm{q}}_{\mathrm{i},0}| \leq \alpha_{\mathrm{thr}})$. If the joints actual speed absolute value $|\dot{\mathrm{q}}_{\mathrm{i,act}}|$, from the real time interface, detected to be higher than α_{thr} this means that collision occurred. And from the $\mathrm{sign}(\dot{\mathrm{q}}_{\mathrm{i,act}})$ the direction of the collision can be determined. Such that if $(\dot{\mathrm{q}}_{\mathrm{i,act}} > 0)$ means the collision is in the forward direction, and if $(\dot{\mathrm{q}}_{\mathrm{i,act}} < 0)$ means the collision is in the backward direction. Then we can control the impacted joint position to move in the direction of the collision as

$$\mathrm{q}_{\mathrm{i,new}} = \mathrm{q}_{\mathrm{i},0} + \dot{\mathrm{q}}_{\mathrm{i,act}}.\Delta\mathrm{t} + \mathrm{sign}(\dot{\mathrm{q}}_{\mathrm{i,act}}) * \varphi \quad (3)$$

Where φ is the value of reaction in terms of position, this φ could be a variable that is adjusted relatively to the force impact. The integral term of the speed in the equation compensate the slight displacement occurred from collision impact due to joint flexibility. The reaction algorithm for instantaneous collision force at static position is shown in Fig. 4. As when collision occurs, the robot reacts by moving away of collision point. Thus φ should be proper value in (rad) to let the robot link move away from collision point. We means by instantaneous collision that it is discontinue force, and not persistent such as stuck object on the robot link. So that the algorithm assumes that while the robot is moving away of the collision point, the collision impact fades. In practice we found that the best range of φ that allows the robot to move away a proper distance from collision point is between $(5\sim10\ \mathrm{deg} \equiv 0.087\sim 0.17\ \mathrm{rad})$. The experimental setup for reading the data from the robot interface, and the procedures for collision detection are presented in Next section.

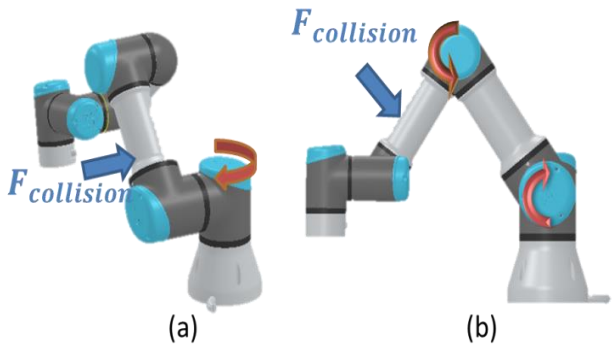

Fig. 3. Collision force that produces moments at the joints in two different examples (a) and (b)

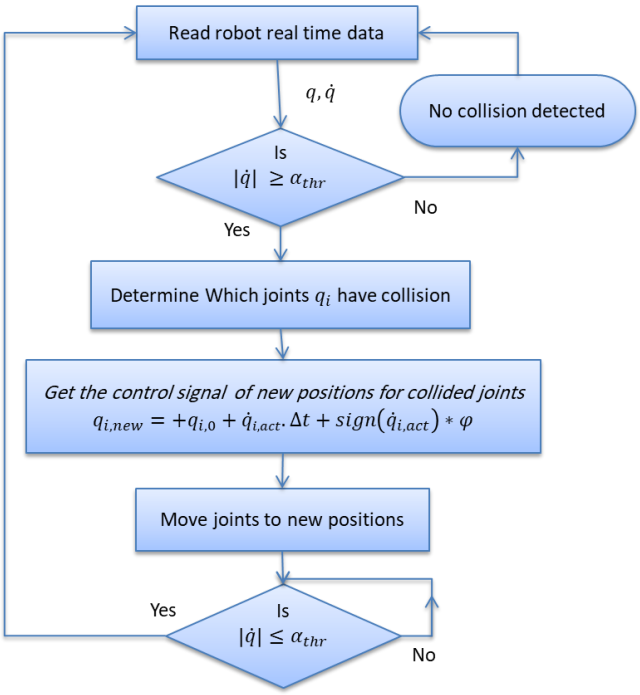

Fig. 4. Collision reaction algorithm at statistic position

IV. IMPLEMENTATION

In order to observe the collision impact on the robot joints, we carried out an experiment to record joints behavior during collision. The robot controller have TCP/IP real time interface at 125Hz. We developed a program to record the data and control the robot through the interface. The program architecture is shown in Fig. 5 . Communication with the robot controller implemented in Python. It is parallel Architecture, where receive socket thread is used to read the real time data in parallel to the main loop. A force applied to the robot manipulator, as shown in Fig. 6. The joints behaviors were plotted in real time. In this figure the force applied on link 2, but it produce torque at joint 1 and 2. In addition the direction of the collision could be detected. The collision force applied on link2 and the data recorded. Fig. 7 shows the response of the 6 joints for an instantaneous collision impact on link2 at the robot position shown in Fig. 6

From experiment results we can see that the collision force is not affecting only the joint have rotation axis perpendicular to the force, but also other joints got affected as shown in Fig. 7. Also the resonance of the joints speed is obvious, that during collision the speed is resonating around the zero value and return to rest again in nonlinear behavior, modeling this behavior is complicated. We take advantage from the behavior to detect collision occurrence and its direction and react to it. The collision is detected from the sudden joints speed variation if ($|\dot{q}_{i,act}| \geq \alpha_{thr}$), while the robot is at static. And the direction determined from the first peak of the speed. The reaction algorithm in Fig. 4 implemented successfully to react at instantaneous discontinuous collision force. In case of continuous collision such as stuck object on the link, which is not discussed in this work, identifying the collision direction using the speed readings might not be accurate because the oscillatory response of the speed is unpredictable. For that, more information should be involved for identifying the direction such as the torque or current information. Fig. 8 shows the current response for joint 1 and 2, the two joints that have collision impact. As it can be seen from the currents figure that the impact period is happened between the two peaks of the speed. The direction of impact of joint 1 and 2 are opposite to each other. The impact direction for joint 1 is in the +ve direction, while for joint 2 is in the –ve direction.

In addition, current readings can be used not only as a double check for the collision direction, but also for understanding the behavior of the impact. It can indicate if the impact is collision or interaction, continuous or instantaneous[4].

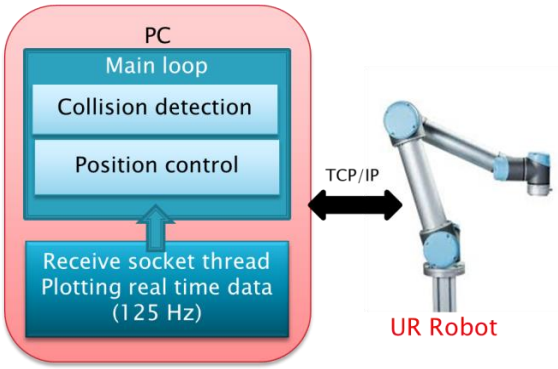

Fig. 5. Interface program architecture

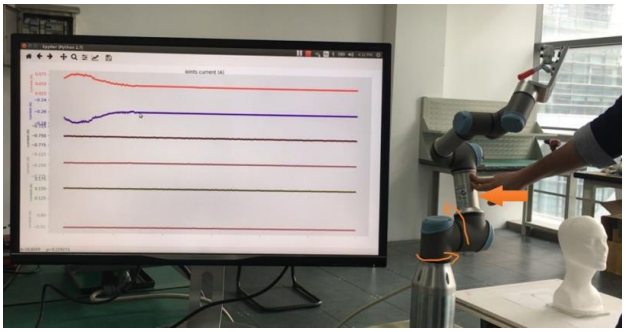

Fig. 6. Monitoring collision impact

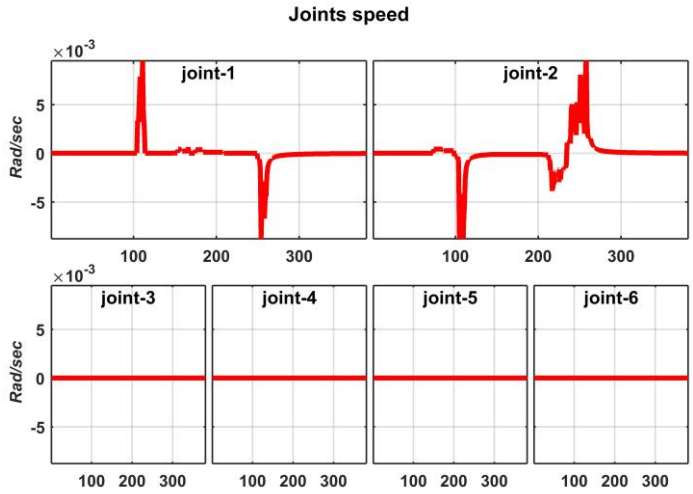

Fig. 7. Joints speed response at collision force applied on link2

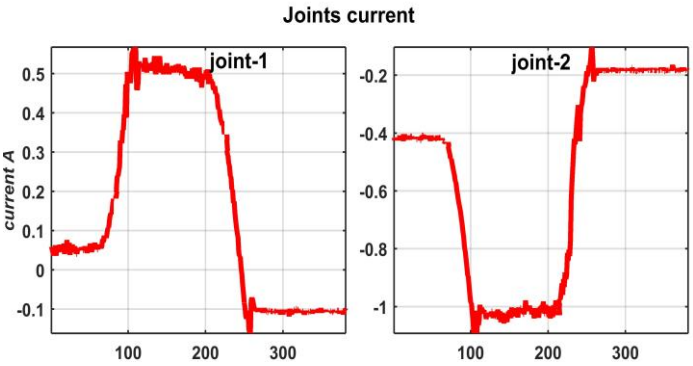

Fig. 8. Joints 1and 2 current response at collision force applied on link2

V. RESULTS

The results of the collision reaction algorithm are presented for two examples as follow; First example is illustrated in Fig. 9, where the robot is in collision in its second link, this collision impacted joint 2. Figure shows the sequence of the robot reaction by moving link 2 down, in the same direction of the collision, to escape the collision impact.

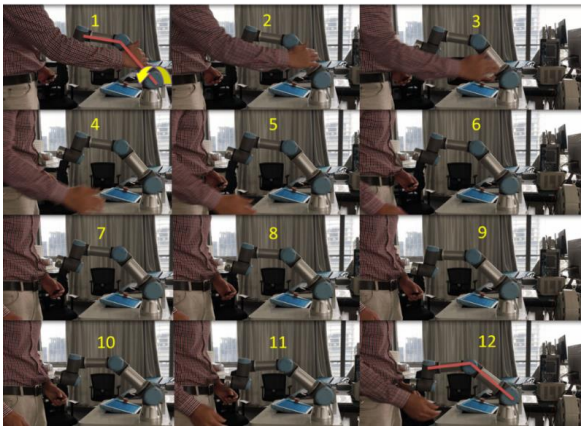

Fig. 9. Collision reaction illustration example 1

Second example is shown in Fig. 10 the robot is in collision the end effector and the highest impact of the collision is affecting joint 2, thus the reaction of the robot is in same direction of the impact by pulling down. More tests were been carried out, but it can't be presented in image format, videos for this work are available upon request

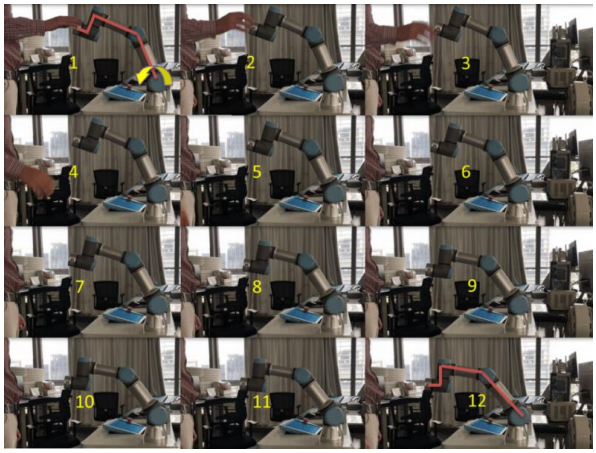

Fig. 10. Collision reaction illustration example 2

CONFLICT OF INTEREST

The authors declared that they have no conflicts of interest to this work

CONCLUSION

The paper presented an experimental setup for recording and plotting real time data from the UR3 interface. This data used for studying the behavior of the joints speed during collision. The experiments were carried out on the robot at static position. The results had shown that during collision there are speeds produced in the joints, and this speeds act in resonant way. This behavior was suggested to be resulting from the harmonic drive. The impacted joints from collision and the collision direction can be detected. This data used for taking a reaction as explained in the paper. The use case in this paper discussing the robot at static position, and the collision detection and reaction was successfully implemented at instantaneous discontinuous collision force.

REFERENCES

[1] I. Maurtua, A. Ibarguren, J. Kildal, L. Susperregi, and B. Sierra, "Human-robot collaboration in industrial applications: Safety, interaction and trust," Int. J. Adv. Robot. Syst., vol. 14, no. 4, pp. 1–10, 2017.

[2] P. A. Lasota, T. Fong, and J. A. Shah, "A Survey of Methods for Safe Human-Robot Interaction," Found. Trends Robot., vol. 5, no. 3, pp. 261–349, 2017.

[3] S. Haddadin, A. Albu-Schäffer, A. De Luca, and G. Hirzinger, "Collision detection and reaction: A contribution to safe physical human-robot interaction," in 2008 IEEE/RSJ International Conference on Intelligent Robots and Systems, IROS, 2008, pp. 3356–3363.

[4] O. Abdelaziz, M. Luo, G. Jiang, and S. Chen, "Adaptive threshold for robot manipulator collision detection using fuzzy system," SN Appl. Sci., vol. 2, no. 3, p. 319, Mar. 2020.

[5] X. Lamy, F. Colledani, F. Geffard, Y. Measson, and G. Morel, "Achieving efficient and stable comanipulation through adaptation to changes in human arm impedance," in Proceedings - IEEE International Conference on Robotics and Automation, 2009, pp. 265–271.

[6] D. J. Braun et al., “Robots driven by compliant actuators: Optimal control under actuation constraints,” IEEE Trans. Robot., vol. 29, no. 5, pp. 1085–1101, Oct. 2013.

[7] S. Lu, J. H. Chung, and S. A. Velinsky, “Human-robot collision detection and identification based on wrist and base force/torque sensors,” in Proceedings - IEEE International Conference on Robotics and Automation, 2005, vol. 2005, pp. 3796–3801.

[8] O. Sim, J. Oh, K. K. Lee, and J. H. Oh, “Collision Detection and Safe Reaction Algorithm for Non-backdrivable Manipulator with Single Force/Torque Sensor,” Journal of Intelligent and Robotic Systems: Theory and Applications, Springer Netherlands, pp. 1–10, 13-Oct-2017.

[9] M. Fritzsche, N. Elkmann, and E. Schulenburg, “Tactile Sensing : A Key Technology for Safe Physical Human Robot Interaction,” in Proceedings of the 6th international conference on Human-robot interaction, 2011, pp. 139–140.

[10] C. Bartolozzi, L. Natale, F. Nori, and G. Metta, “Robots with a sense of touch,” Nature Materials, vol. 15, no. 9. Springer Nature, pp. 921–925, 01-Sep-2016.

[11] J. Ulmen and M. Cutkosky, “A robust, low-cost and low-noise artificial skin for human-friendly robots,” in Proceedings - IEEE International Conference on Robotics and Automation, 2010, pp. 4836–4841.

[12] S. D. Lee, M. C. Kim, and J. B. Song, “Sensorless collision detection for safe human-robot collaboration,” in IEEE International Conference on Intelligent Robots and Systems, 2015, pp. 2392–2397.

[13] A. De Luca and R. Mattone, “Sensorless robot collision detection and hybrid force/motion control,” in Proceedings - IEEE International Conference on Robotics and Automation, 2005, no. April, pp. 999–1004.

[14] S. Chen, M. Luo, O. Abdelaziz, and G. Jiang, “A general analytical algorithm for collaborative robot (cobot) with 6 degree of freedom (DOF),” in Proceedings of the 2017 IEEE International Conference on Applied System Innovation: Applied System Innovation for Modern Technology, ICASI 2017, 2017, pp. 698–701.

[15] R. Cortesao, C. Sousa, and P. Queiros, “Active impedance control design for human-robot comanipulation,” in American Control Conference, 2010, pp. 2805–2810.

[16] S. Haddadin, “Towards Safe Robots: Approaching Asimov’s 1st Law,” Springer Tracts Adv. Robot., pp. 1–352, 2011.

[17] S. Chen, M. Luo, G. Jiang, and O. Abdelaziz, “Collaborative robot zero moment control for direct teaching based on self-measured gravity and friction,” Int. J. Adv. Robot. Syst., vol. 15, no. 6, 2018.

[18] H. D. Taghirad and P. R. Belanger, “An experimental study on modelling and identification of harmonic drive systems,” in Proceedings of 35th IEEE Conference on Decision and Control, 1996, pp. 4725–4730.

[19] Universal Robots, “UR3 Robot,” 2017. [Online]. Available: https://www.universal-robots.com/products/ur3-robot/. [Accessed: 14-May-2018].

[20] O. Abdelaziz, M. Luo, G. Jiang, and S. Chen, “Multiple configurations for puncturing robot positioning,” International Journal of Advance Robotics & Expert Systems (JARES), 06-Mar-2019. [Online]. Available: https://airccse.com/jares/papers/1419jares01.pdf. [Accessed: 01-Feb-2020].

[21] G. Jiang, M. Luo, L. Lu, K. Bai, O. Abdelaziz, and S. Chen, “Vision solution for an assisted puncture robotics system positioning,” Appl. Opt., vol. 57, no. 28, p. 8385, Oct. 2018.

[22] A. De Luca and W. J. Book, “Robots with Flexible Elements,” in Springer Handbook of Robotics, Berlin, Heidelberg: Springer Berlin Heidelberg, 2016, pp. 243–282.

[23] M. W. Spong, “Modeling and Control of Elastic Joint Robots,” J. Dyn. Syst. Meas. Control, vol. 109, no. 4, p. 310, Dec. 1987.

Omar Abdelaziz had recieved his PhD from University of science and technology of China. He is a lecturer in Egyptian Russian University, Egypt. And Researcher at Institute of intelligent Manufacturing Technology, Jiangsu industrial and technology research institute, China. In 2011 He had received master degree of mechanical engineering from UTHM, Malaysia. Omar’s research interest in robotics and intelligent technology. Including topics such as human robots collaboration, serial robots kinematics and dynamics, and Robot control.

Minzhou Luo had recieved his Ph.D. degree from University of Science and Technology in 2005. He had received his M.S. degree in Mechanical Engineering from Hefei University of Technology in 2002..he achieved the researcher of Hefei Institute of Physical Science, Chinese Academy of Science. His research direction is the humanoid robot, industrial robot, Mechatronics, intelligent machine etc,.

How to cite this article:

Omar Abdelaziz and Minzhou Luo, Serial Robot Collision Reaction using Joints Data at Stationary Position, International Journal of Engineering Works, Vol. 7, Issue 10, PP. 356-360, October 2020, https://doi.org/10.34259/ijew.20.710356360.

International Journal of Engineering Works
ISSN-p: 2521-2419
ISSN-e: 2409-2770
Vol. 7, Issue 10, PP. 361-368, October 2020
https://www.ijew.io/
https://doi.org/10.34259/ijew.20.710361368

Designing and Analysis of Single Stage and Two Stage PV Inverter Connected to Weak Grid System

Naveed Malik[1], Sami Ullah[2], Amir Khan[3], Farhan Ullah[4]
[1,2,3,4] Department of Electrical Energy System Engineering, US-Pakistan Center for Advanced Studies in Energy (USPCAS-E), UET Peshawar
engrmalikuet@gmail.com[1], samiullahkhan4191@gmail.com[2], amirkaahn@gmail.com[3], farhan.ullah58@gmail.com[4]
Received: 05 October, Revised: 13 October, Accepted: 17 October

***Abstract*—** In this research paper design, analysis and comparison of single stage and two stages Photovoltaic inverter connected to weak grid system is executed in terms of their maximum power point tracking, DC link voltage regulation, power factor and overall efficiency. Majority of the commercial and industrial loads are inductive in nature and result in a very low lagging power factor. However renewable energy sources have no reactive power generation and lagging power factor results in a weak grid system. For this purpose control mechanism comprises of three objectives is proposed in this research paper. These objectives are to obtain highest amount of power from photovoltaic array, the power must be deliver from photovoltaic array into the utility grid at unity power factor and to maintain desired voltage at the input of the inverter. In order to achieve these objectives nonlinear control mechanism of Photovoltaic inverter connected to weak grid system is established and implemented based on accurate mathematical modeling and by using Backstepping technique and Lyapunov Stability analysis. PI controller is used for the purpose to maintain desired voltage at input of the inverter according to the requirement of inverter. Both single stage and two stage models are developed and simulated in Simulink/Matlab environment.

***Keywords*—** Photovoltaic (PV), Maximum power point tracking (MPPT), Power factor control (PFC)

I. Introduction

There is a rapid increase in population and industrialization of the world and due to this increase demand for electrical energy increases exponentially. Majority of electrical power systems are aiming to reduce their dependency toward fossil fuels due to their growing concerns for environment, fuels prices and sustainable development. The research in renewable energy has become an increasingly important topic in the modern era with the problem of energy crisis becoming more and more aggravating, resulting in increased exploitation and research for new power energy resources such as wind, tide, geothermal and solar energy around the world [1].

Solar energy generators are extensively used to harness power from solar irradiation. Solar power is converted into electric power by photovoltaic (PV) panels. The output power of the PV panels depends on the surrounding weather conditions like sun irradiance levels and temperature. The electric characteristics of solar PV panel are affected by these conditions [2]. It can be observed that under certain irradiance levels, unique points exist where the output power from each solar panel is Maximum. These points on the P-V curves are known as the maximum power points (MPPs). The idea of MPPT is developed in the solar system to utilize PV panels at the optimal efficiency by tuning the duty cycles of the power converters inserted between PV source and the load. Different MPPT techniques have been proposed in the literature for PV power generation such as Perturb & Observe algorithm [3], incremental conductance, short circuit current, the hill climbing search and some other special methods such as fuzzy logic technique, neural network etc. The P&O method is mostly used due to its ease of implementation.

The global concern about climate change and the growing energy demand of industrialized countries have necessarily led to exploring other new sources like renewable energy. The main advantage of this type of renewable energy is that it results in reduction of pollution caused by production of greenhouse gases which alternately affects human health and ozone layer [4]–[6]. Among different type of renewable energies the photovoltaic energy has attained great attention. Photovoltaic power supplied to the utility grid is gaining more and more attention nowadays [7]. Numerous inverter circuits and control schemes can be used for PV power conditioning system. For residential PV power generation systems, single-phase utility interactive inverters are of particular interest [8]–[10].]. However, depending on the characteristics of the PV panels, the total output voltage from the PV panels varies greatly due to different temperature, irradiation conditions, and shading and clouding effects. Thus, the input voltage of a residential PV inverter can vary widely. Therefore, a dc–dc converter has been used. Such a dc–dc converter in conjunction with a dc–ac inverter arrangement has been widely used in the state-of-the-art PV power conditioning system. In

grid connected photovoltaic system, the photovoltaic system is connected to the grid through three phase or single phase inverter to deliver power directly to the utility grid.

However the effective use of solar energy in a grid connected system is a very big problem [11] and availability of solar energy depends on weather conditions and time of usage. Grid connected photovoltaic is widely used for projects producing bulk amount of power. Due to intermittent nature of Photovoltaic source, supplies from PV cells are variable in nature and must be conditioned as per the demand of the utility grid. This can be done in two ways i) Single stage operation and ii) Two stage operation[4]-[5]. Single stage operation consists of inverter that inverts the DC output voltage provided by the PV cells to AC as per the demand of utility grid [9]-[10]. Whereas in two stage operation the DC voltage provided by the PV cells are first step up by the boost converter and then inverted into AC as per demand of utility grid [16].

Single-phase grid-connected inverters with DC-links are widely used in residential PV systems. In such a PV inverter, the DC-link capacitor plays an important role of decoupling DC power and AC power and buffering energy to ride through power disturbances. Reducing the DC-link capacitance helps to lower the cost, improve reliability and increase power density of inverters, which, however, increases the voltage ripple and reduces the ride-through capability. Therefore, a high performance DC-link voltage controller with fast response is desirable to keep the voltage in a safe operating range when the DC-link capacity is small. Conventionally, a PI controller is adopted to regulate the DC-link voltage as the outer loop, and it provides the AC current reference to the current regulator that works as the inner loop.

Lyapunov stability analysis method is widely used for stability analysis of the equilibrium point, Lyapunov direct method is used to analyze the stability properties of the equilibrium point by studying the energy of the system [17].

Grid-connected inverter plays an important role in injecting high-quality power into the grid [18]. In the grid-connected inverter, an output filter is needed to attenuate the switching harmonics. Compared with an LCL filter, an L filter is considered to be a preferred option due to the resonance hazard of the LCL filter, damping solutions are required to stabilize the system [19].

II. Modelling of Grid Connected PV System

This section presents the equations used for modeling each component in the grid connected Photovoltaic system. The primary objective of grid connected PV system is to transform solar energy into electrical energy and to deliver this generated energy into utility grid efficiently. The grid connected system comprises of PV panels arranged in series or parallel fashion or combination of both for production of maximum power, DC/DC converter for power conditioning, DC/AC inverter and passive filter for reduction of harmonics. In this research paper the array consists of nine panels arranged in a series fashion, each of which are 213.15 Watts delivering total of 1916 Watts into the utility grid. To raise the output voltage, each panel comprises of 60 cells linked in a series fashion. The basic parameter temperature and irradiance of the solar panel is fixed and held constant at 25 0C and 1000 W/m2.

A. Single stage grid connected PV system

In single stage operation the photovoltaic array is directly connected with the utility power network through PV inverter as shown in Fig. 1. In this case the maximum power point tracking and delivery of real power to the grid is achieved by the inverter stage itself.

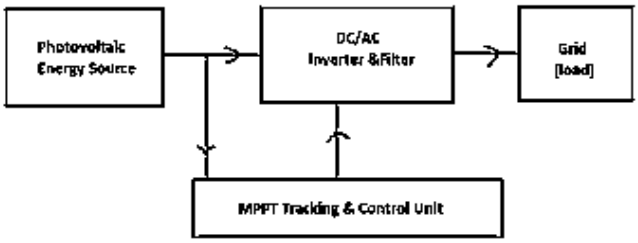

Fig. 1 Single stage grid connected PV system

B. Two stages grid connected PV System

In two stages operation the voltage from the PV generator is first step up through DC/DC boost converter and then the boost voltage is sent to the PV inverter for further delivery into the grid as shown in Fig. 2. In case of two stages operation the maximum power point tracking is achieved by the DC/DC converter stage and DC/AC inverter stage delivers real power into the utility grid.

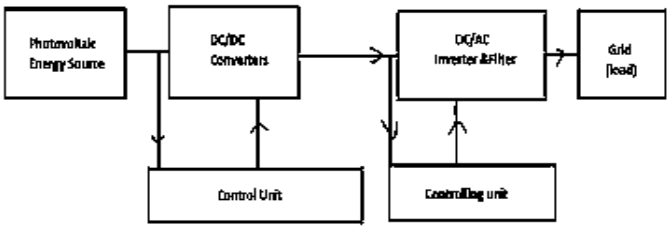

Fig. 2 Two stages grid connected PV system

C. Modeling of boost converter

The boost converter is a power processing and conditioning device used to increase the voltage level to the amount required at the input of inverter. The voltage generated by the PV panel is low and is step up by DC/DC boost converter, so that inverter does not involve any transformer to supply power into the utility grid. The operation and controlling of DC/DC boost converter is achieved with the help of pulse width modulation (PWM) technique in order to obtain highest amount of power from PV generator. Switching device is used for ON/OFF purpose, inductor for maintaining constant current, capacitor for charging purpose and diode to avoid flow of current in the reverse direction. Some components employed in the boost converter with the aim to increase the voltage level as shown in Fig. 3.

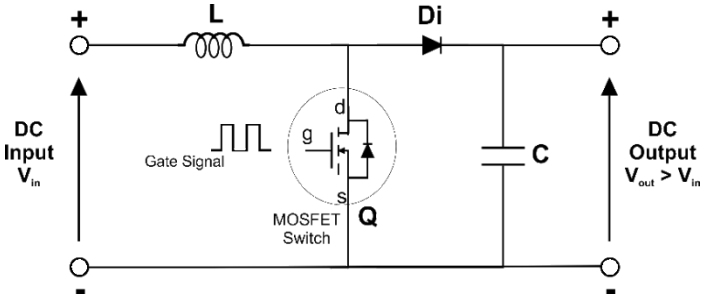

Fig. 3 Control of DC/DC boost converter

D. Modeling of L filter

The PV inverter is connected into the utility grid through passive filter in order to reduce harmonic distortion. In order to enhance the quality of output the passive filter used in this research work is L filter. The proposed filter is the first order filter due to which L filter is simple to design and implement.

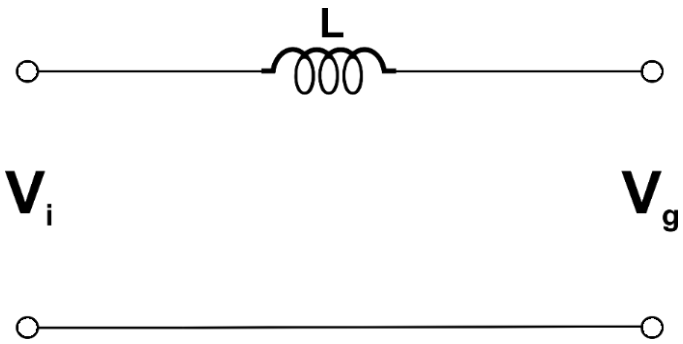

Fig. 4 Schematic of L filter

The current harmonics is due to switches in inverter is operating at high switching frequencies which ultimately results in high switching losses. In case of L filter switches generate an input (voltage) for the inductor and the output of inducor will be current. Then the output of the L filter which is actually the current to be feed into the grid, serve as the input to the utility grid and the output of the utility grid will be in the form constant AC voltage suitable for utilization. The schematic of the proposed filter is shown in Fig. 4.

III. Mathematical Modelling and Controller Designing

To achieve the purpose and objective this research work nonlinear control mechanism is proposed based on accurate mathematical modeling of Photovoltaic generator interfaced with weak grid system in terms of state space equation by using Backstepping technique and Lyapunov stability tool. Photovoltaic generating unit connected to weak grid system is designed and modeled in MATLAB/Simulink environment. For model designing and mathematical modeling it is necessary to make some assumptions. First is that consider all switches are ideal and their resistance can be easily ignored. Second assumption is that consider resistance of all inductors and capacitors are very low and can also be neglected. The entire system architecture consists of PV panels arranged in a series fashion, DC/DC boost converter for increasing voltage magnitude, H-Bridge inverter for production of AC output voltage and L filter for reduction of harmonics is connected to weak utility grid as shown in Fig. 5.

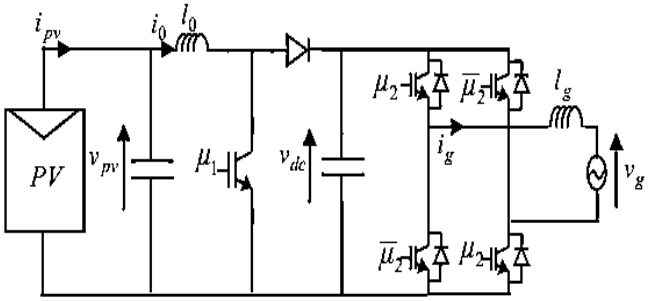

Fig. 5 Grid connected PV system

Basic circuit laws are applied to figure 5 in order to obtain differential equations. By applying KCL at PV side,

$$I_{PV} = I_0 + I_{CPV}$$

$$I_{CPV} = I_{PV} - I_0$$

As $I_C = C\, dV_c/dt$

$$C_{PV}\, dV_{PV}/dt = I_{PV} - I_0 \ldots. (i)$$

By applying KCL at Grid side,

$$I_0 = I_0 u_1 + I_C + I_g u_2$$

$$I_C = I_0 - I_0 u_1 - I_g u_2$$

$$C_{dc}\, dV_{dc}/dt = I_0 (1- u_1) - I_g u_2 \ldots. (ii)$$

Applying KVL on PV side,

$$V_{L0} + V_{dc} = V_{pv} + V_{dc} u_1$$

$$L_0 dI_0/dt = V_{pv} – V_{dc} (1- u_1) \ldots. (iii)$$

Applying KVL on Grid side,

$$V_g + V_{Lg} = V_{dc} u_2$$

$$L_g\, dI_g/dt = V_{dc} u_2 – V_g \ldots. (iv)$$

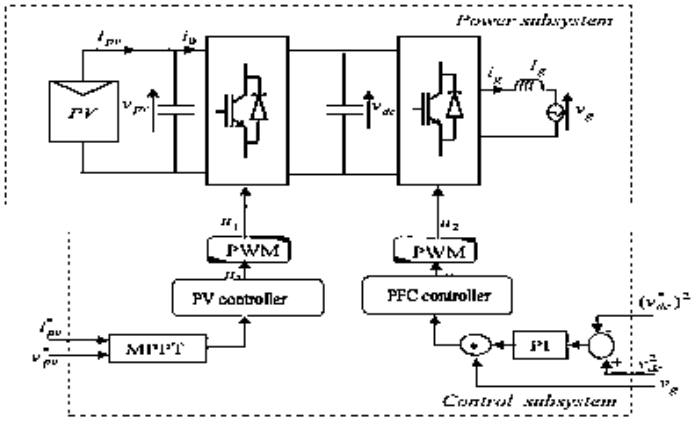

Fig. 6 Control circuit of grid connected PV system

The control circuit schematic of grid connected PV system is shown in Fig. 6 help us in designing and implementation of various controllers. The block diagram shown is to be simulated and implemented in Simulink/Matlab.

The differential equations obtained from instantaneous model cannot be used directly for controller design as it involves the binary inputs and in this research work control input needs to be of switched nature. For this purpose averaging model is used in the form of state space equations.

The above differential equations (i-iv) of grid connected Photovoltaic system can be expressed in the form of state space equation as,

$$C_{pv}\,\dot{g}_1 = I_{pv} - g_2 \quad (1)$$

$$L_0\,\dot{g}_2 = g_1 - (1-u_1)\,g_3 \quad (2)$$

$$C_{dc}\,\dot{g}_3 = (1-u_1)\,g_2 - u_2\,g_4 \quad (3)$$

$$L_g\,\dot{g}_4 = u_2\,g_3 - V_g \quad (4)$$

The g_1, g_2, g_3 and g_4 used in the above equations are the state variables. Whereas g_1 represent voltage produced by PV array (V_{pv}). While g_2, g_3 and g_4 represents input current to the boost converter (i_o), input voltage into the inverter (V_{dc}) and output current of the inverter (i_{grid}) respectively. Whereas u_1 and u_2 represents are the switching functions for converters.

A. PV Generator Voltage Controller Designing

The objective of designing this controller is to enable and enforce the voltage produced by the photovoltaic generator to follow the reference voltage (g_1, ref) generated by the P&O MPPT technique. To achieve this objective an error signal is generated between the reference value and the actual value. Backstepping controller will enable the photovoltaic generator voltage to track the reference voltage provided by the P&O MPPT algorithm and vanish the error variable. The stability of the system is validated by Lyapunov Stability method.

Let us introduce an error, e_1 between PV output voltage and the reference voltage.

$$e_1 = C_{pv}\,(g_1 - g_1, \text{ref})$$

The derivative of e_1 w.r.t time is,

$$\dot{e}_1 = C_{pv}\,\dot{g}_1 - C_{pv}\,\dot{g}_{1,\,ref}$$

Putting the value of Eq. (1) in above Equation,

$$\dot{e}_1 = i_{pv} - g_2 - C_{pv}\,\dot{g}_{1,\,ref} \quad (5)$$

The stability of Eq. (5) is validated by using Lyapunov stability technique. Consider Lyapunov function candidate,

$$X_1 = \tfrac{1}{2}\,e_1^2$$

Taking derivatives of X_1 w.r.t is,

$$\dot{X}_1 = e_1\dot{e}_1$$

Putting $\dot{e}_1 = -c1\ e_1$

$$\dot{X}_1 = -c_1\,e_1^2 \quad (6)$$

As the Eq. (6) is a negative definite, where c1 is a positive design parameter and by putting any positive value in the above equation will get $\dot{X}1$ less than or equal to zero, which shows the system is stable.

$$\dot{X}_1 \leq 0$$

As g_2 is viewed as input and proceeds to the design of actual control input, u_1, so we take it as a reference. From Eq. (5),

$$\dot{e}_1 = i_{pv} - g_{2,\,ref} - C_{pv}\,\dot{g}_{1,\,ref}$$

$$-c1\ e_1 = i_{pv} - g_{2,\,ref} - C_{pv}\,\dot{g}_{1,\,ref}$$

$$g_{2,\,ref} = c1\ e_1 + i_{pv} - C_{pv}\,\dot{g}_{1,\,ref}$$

$$C_{pv}\,\dot{g}_{1,\,ref} = i_{pv} + c1\ e_1 - g_{2,\,ref} \quad (7)$$

Putting Eq. (7) in Eq. (5),

$$\dot{e}_1 = i_{pv} - g_2 - (i_{pv} + c1\ e_1 - g_{2,\,ref})$$

$$\dot{e}_1 = -\,c1\ e_1 - (g_2 - g_{2,\,ref}) \quad (8)$$

As $g_{2,\,ref}$ is just a variable and not an actual controller. It is a reference for boost converter current, g_2.

Let us introduce new error, e_2 between the reference value and the desired value.

$$e_2 = L_0\,(g_2 - g_{2,\,ref}) \quad (9)$$

$$e_2 / L_0 = (g_2 - g_{2,\,ref}) \quad (10)$$

Putting Eq. (10) in Eq. (8) we get,

$$\dot{e}_1 = -\,c1\ e_1 - e_2 / L_0 \quad (11)$$

Take derivative of Eq. (9) w.r.t,

$$\dot{e}_2 = L_0\,\dot{g}_2 - L_0\,\dot{g}_{2,\,ref} \quad (12)$$

Putting values of $L_0\,\dot{g}_2$ from Eq. (2) in Eq. (12)

$$\dot{e}_2 = g_1 - (1-u_1)\,g_3 - L_0\,\dot{g}_{2,\,ref} \quad (13)$$

To check the stability of the system while defining second error variable using Lyapunov stability technique, we use both variables. Consider Lyapunov function candidate,

$$X_2 = X_1 + ½\ e_2^2$$

Take derivative of X_2 w.r.t is,

$$\dot{X}_2 = \dot{X}_1 + e_2\dot{e}_2 \quad (14)$$

$$\dot{X}_2 = -c_1\ e_1^2 + e_2\ (-c_2\ e_2)$$

$$\dot{X}_2 = -c_1\ e_1^2 - c_2\ e_2^2 \quad (15)$$

The Eq. (15) is a negative definite, where c_1 and c_2 are positive design parameters. By putting any positive value of c_1 or c_2 will results in $\dot{X}_2$ less than or equal to zero, showing the stability of the system.

$$\dot{X}_2 \leq 0$$

From the above conclusions controller for PV generator is deigned in the following manner by considering Eq. (13).

$$\dot{e}_2 = g_1 - g_3\ (1-u_1) - L_0\ \dot{g}_{2,\ ref}$$

Suppose $-c2\ e_2 = \dot{e}_2 - e_1 / L_0$

$$\dot{e}_2 = -c2\ e_2 + e_1 / L_0$$

Putting values of $\dot{e}_2$ in Eq. (13)

$$-c2\ e_2 + e_1 / L_0 = g_1 - g_3\ (1-u_1) - L_0\ \dot{g}_{2,\ ref}$$

$$g_3\ (1-u_1) = g_1 - L_0\ \dot{g}_{2,\ ref} + c2\ e_2 - e_1 / L_0$$

$$1-u_1 = 1/\ g_3\ (g_1 - L_0\ \dot{g}_{2,\ ref} + c2\ e_2 - e_1 / L_0)$$

$$u_1 = 1 - 1/\ g_3\ (g_1 - L_0\ \dot{g}_{2,\ ref} + c2\ e_2 - e_1 / L_0) \quad (16)$$

Eq. (16) is a designed control law for boost converter operation.

B. DC Link Voltage Controller Designing

The objective of designing this controller is to maintain constant voltage at the input of the inverter. The voltage available at the input of the inverter serves as the source for the grid and any changes in this input voltage vary the current to the inverter and hence changes power flow to the utility grid system. To achieve the purpose proportional integral (PI) controller is used to generate specific value of β and tune that value of β to such a degree as to forces the voltage at the input of the inverter, g_3 to track a given reference value, $g_{3,\ ref}$. Actually PI controller will regulate the square of output voltage to track a demanded reference value.

PI controller is tuned in such a way,

$$\beta = (k_p + k_i/s)\ (g_3 - g_{3,\ ref}) \quad (17)$$

In case of single stage operation the maximum voltage produced by the PV array will be the reference voltage, whereas in case of two stage operation reference voltage is taken as 400 V.

C. Power Factor Controller Designing

The main objective of this controller is to deliver power from PV array into the utility grid at unity power factor. The controller will generate reference value. The reference value is the multiplication of grid voltage and the output of the PI controller i.e. $g_{4,\ ref} = \beta\ V_g$. Backstepping controller enable the current, g_4 at the output of inverter to track the reference value. When current at output of inverter succeeds in achieving the reference value, then at this point current at the output of inverter and grid voltage will be synchronized and in phase with each other.

From Eq. (4) and using Backstepping approach,

$$L_g\ \dot{g}_4 = u_2\ g_3 - V_g$$

Let us introduce current, e_4 between grid current and reference value,

$$e_4 = L_g\ (g_4 - g_{4,\ ref})$$

Take derivatives of e_4 w.r.t is,

$$\dot{e}_4 = L_g\ \dot{g}_4 - L_g\ \dot{g}_{4,\ ref} \quad (18)$$

Putting the values of Eq. (4) in Eq. (18)

$$\dot{e}_4 = g_3\ u_2 - V_g - L_g\ \dot{g}_{4,\ ref} \quad (19)$$

Consider Lyapunov function candidate, in order to check the stability of the system.

$$X_4 = ½\ e_4^2$$

Take derivative w.r.t,

$$\dot{X}_4 = e_4\ \dot{e}_4$$

$$\dot{X}_4 = -c_4\ e_4^2 \quad (20)$$

As Eq. (20) is a negative definite and c_4 is a positive design parameter. Putting any positive value of c_4 in the above equation results in $\dot{X}_4$ less than or equal to zero, showing the system is stable.

$$\dot{X}_4 \leq 0$$

Putting $\dot{e}_4 = -\ c_4\ e_4$, in Eq. (19)

$$-\ c_4\ e_4 = g_3\ u_2 - V_g - L_g\ \dot{g}_{4,\ ref}$$

$$u_2 = 1/g_3\ (-\ c_4\ e_4 + V_g + L_g\ \dot{g}_{4,\ ref}) \quad (21)$$

Eq. (21) is the control law for power factor correction.

The stability of the controller is validated using Lyapunov stability technique. Consider Lyapunov function candidate,

$$X_4 = ½ e_4^2$$

Take derivative w.r.t,

$$\dot{X}_4 = e_4 \dot{e}_4 \quad (22)$$

Putting Eq. (19) in Eq. (22)

$$\dot{X}_4 = e_4 (g_3 u_2 - V_g - L_g \dot{g}_{4, ref}) \quad (23)$$

Putting Eq. (21) in Eq. (23)

$$\dot{X}_4 = e_4 [g_3\{1/g_3 (- c_4 e_4 + V_g + L_g \dot{g}_{4, ref})\} - V_g - L_g \dot{g}_{4, ref}]$$

$$\dot{X}_4 = e_4 (-c_4 e_4)$$

$$\dot{X}_4 = - c_4 e_4^2 \quad (24)$$

The Eq. (24) is a negative definite and putting any positive value of c_4 will result in $\dot{X}_4$ less than or equal to zero, showing the system is stable.

$$\dot{X}_4 \leq 0$$

IV. Results and Simulation

Both single stage and two stages photovoltaic inverter connected to weak grid system are simulated in MATLAB/Simulink environment and then compare the results by evaluating the overall performance. The operation and control of grid connected photovoltaic system shown in fig. 3 is designed and simulated in MATLAB/Simulink environment. The simulation and comparison results are shown in Fig. 7-17.

The Fig. 7 and Fig. 8 shows comparison of PV voltage provided by the PV array and tracking of reference voltage provided by the P&O MPPT algorithm. On comparison PV voltage in case of two stage operation shows fast and better response in tracking the reference voltage.

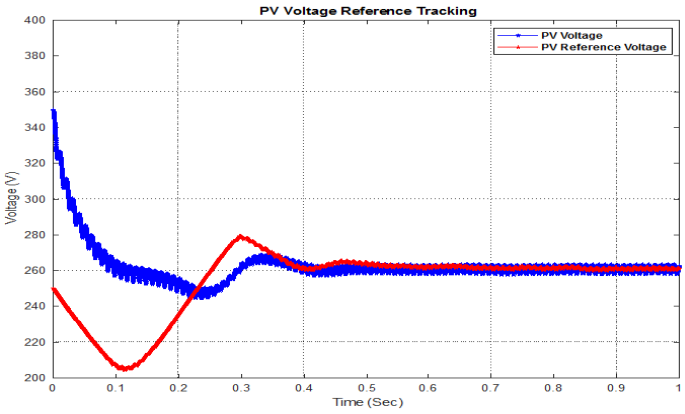

Fig. 7 PV voltage reference tracking (single stage)

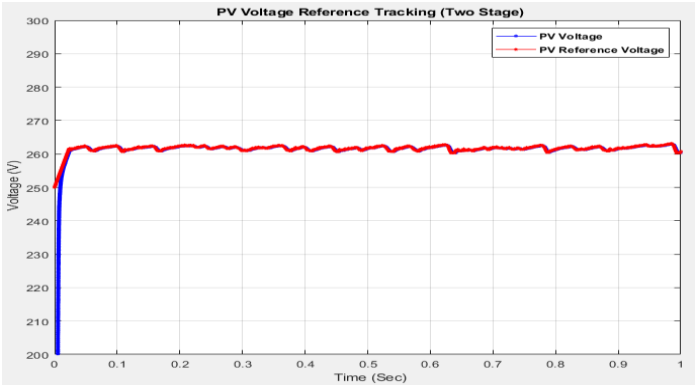

Fig. 8 PV voltage reference tracking (double stage)

The Fig. 9 and Fig. 10 shows regulation of voltage at input of the inverter to the desired voltage value. The two stage operation has fast and better response in tracking the desired voltage value.

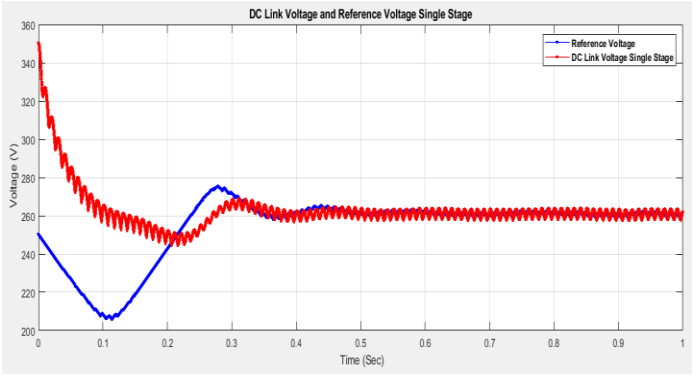

Fig. 9 DC link voltage regulation (single stage)

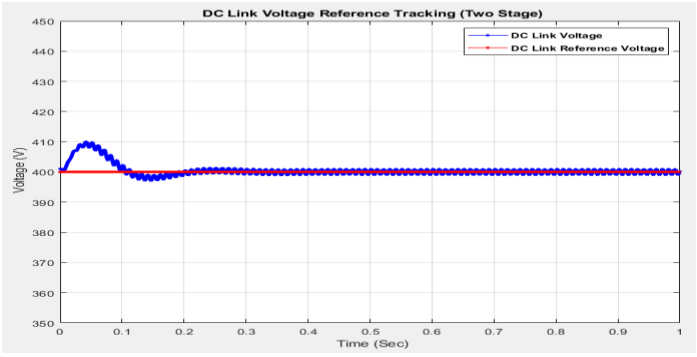

Fig. 10 DC link voltage regulation (double stage)

The Fig. 11 shows maximum amount of power generation by PV array that is approximately 1916 Watts in case of two stage operation. The Fig. 12 shows the amount of real power delivery to the weak grid system. In case of two stages operation inverter deliver maximum real power to the grid with minimum of distortions.

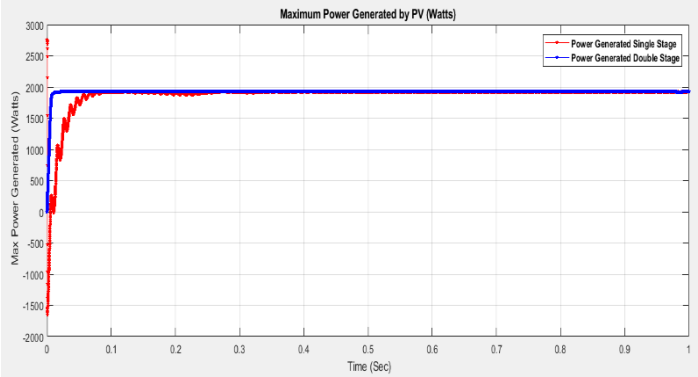

Fig. 11 Maximum power generation

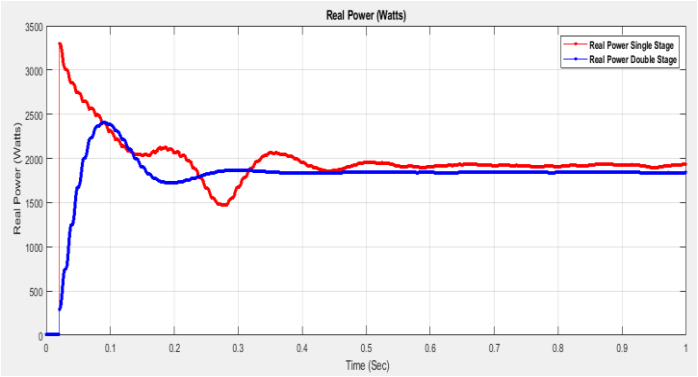

Fig. 12 Real power

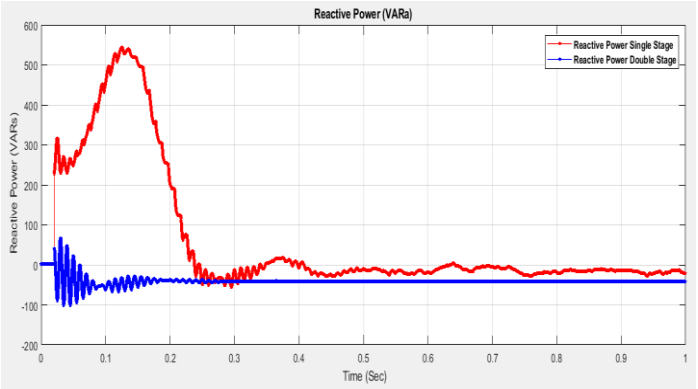

Fig. 13 Reactive power

The Fig. 14 and Fig. 15 shows comparison of synchronization of inverter output current and grid voltage in case of single stage and two stage operation. The inverter output current and grid voltage are synchronized and in phase with each other in both cases. The current is more sinusoidal in case of two stage operation and has better and distortion less response which leads to delivery of real power to the grid at unity power factor.

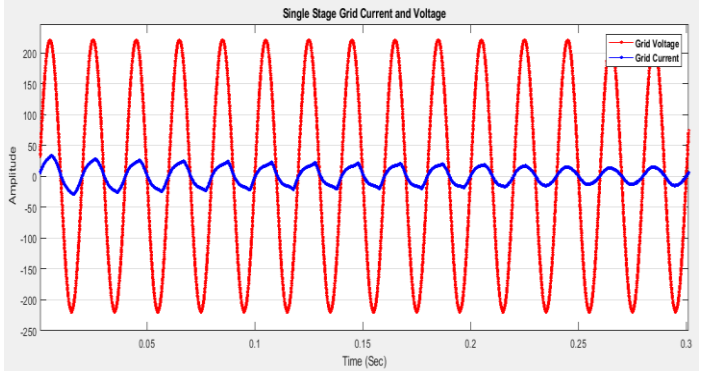

Fig. 14 Output current and grid voltage (single stage)

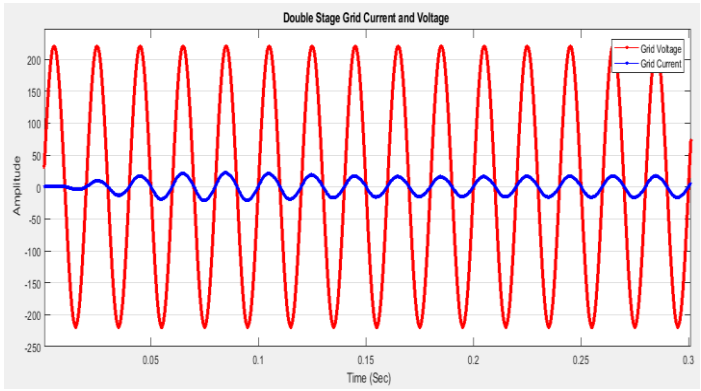

Fig. 15 Output current and grid voltage (two stage)

The Fig. 16 shows comparison of power factor in case of single stage and two stage operation. In both cases the inverter output current and grid voltage are in phase with each other. The two stage operation has smooth and better power factor response that is power factor is approximately near to unity.

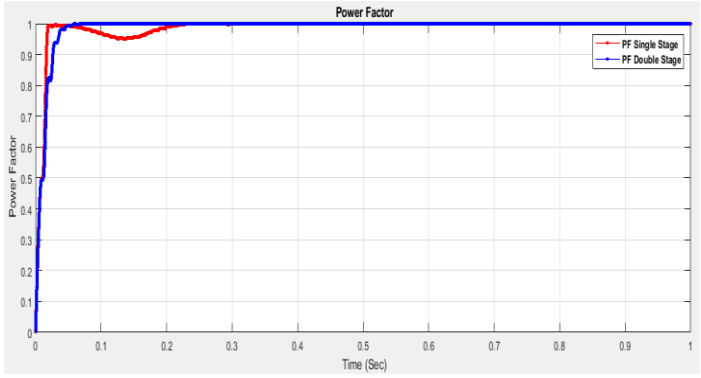

Fig. 16 Power factor

The Fig. 17 shows the overall efficiency comparison of single stage and two stages operation. The two stage operation has proved to have better and higher efficiency.

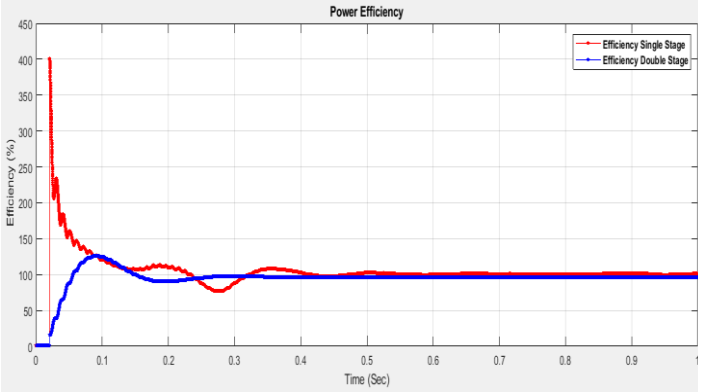

Fig. 17 Power efficiency

CONCLUSION

From the simulation results it can be easily concluded that two stages grid connected PV inverter has better and stable response as compared to the single stage grid connected PV inverter. Two stages operation has proved to have high efficiency, almost unity power factor and higher accuracy of tracking reference voltage. However two stages grid connected PV system has very complex structure and will have requires high investment in the beginning as compared to single stage grid connected PV system.

REFERENCES

[1] D. Poponi, "Analysis of diffusion paths for photovoltaic technology based on experience curves," *Sol. Energy*, vol. 74, no. 4, pp. 331–340, Apr. 2003, doi: 10.1016/S0038-092X(03)00151-8.

[2] Fangrui Liu, Yong Kang, Yu Zhang, and Shanxu Duan, "Comparison of P&O and hill climbing MPPT methods for grid-connected PV converter," in *2008 3rd IEEE Conference on Industrial Electronics and Applications*, Singapore, Jun. 2008, pp. 804–807, doi: 10.1109/ICIEA.2008.4582626.

[3] N. Femia, G. Petrone, G. Spagnuolo, and M. Vitelli, "Optimization of Perturb and Observe Maximum Power Point Tracking Method," *IEEE Trans. Power Electron.*, vol. 20, no. 4, pp. 963–973, Jul. 2005, doi: 10.1109/TPEL.2005.850975.

[4] B. M. T. Ho and H. S.-H. Chung, "An Integrated Inverter With Maximum Power Tracking for Grid-Connected PV Systems," *IEEE Trans. Power Electron.*, vol. 20, no. 4, pp. 953–962, Jul. 2005, doi: 10.1109/TPEL.2005.850906.

[5] Bo Yang, Wuhua Li, Yi Zhao, and Xiangning He, "Design and Analysis of a Grid-Connected Photovoltaic Power System," *IEEE Trans. Power Electron.*, vol. 25, no. 4, pp. 992–1000, Apr. 2010, doi: 10.1109/TPEL.2009.2036432.

[6] Yeong-Chau Kuo, Tsorng-Juu Liang, and Jiann-Fuh Chen, "Novel maximum-power-point-tracking controller for photovoltaic energy conversion system," *IEEE Trans. Ind. Electron.*, vol. 48, no. 3, pp. 594–601, Jun. 2001, doi: 10.1109/41.925586.

[7] A. Koran, K. Sano, and R.-Y. Kim, "Design of a Photovoltaic Simulator with a Novel Reference Signal Generator and Two-Stage LC Output Filter," p. 8.

[8] D. Casadei, G. Grandi, and C. Rossi, "Single-Phase Single-Stage Photovoltaic Generation System Based on a Ripple Correlation Control Maximum Power Point Tracking," *IEEE Trans. Energy Convers.*, vol. 21, no. 2, pp. 562–568, Jun. 2006, doi: 10.1109/TEC.2005.853784.

[9] Y. Huang, M. Shen, F. Z. Peng, and J. Wang, "Z-Source Inverter for Residential Photovoltaic Systems," *IEEE Trans. Power Electron.*, vol. 21, no. 6, pp. 1776–1782, Nov. 2006, doi: 10.1109/TPEL.2006.882913.

[10] S. B. Kjaer, J. K. Pedersen, and F. Blaabjerg, "A Review of Single-Phase Grid-Connected Inverters for Photovoltaic Modules," *IEEE Trans. Ind. Appl.*, vol. 41, no. 5, pp. 1292–1306, Sep. 2005, doi: 10.1109/TIA.2005.853371.

[11] V. Ravindran, S. K. Ronnberg, T. Busatto, and M. H. J. Bollen, "Inspection of interharmonic emissions from a grid-tied PV inverter in North Sweden," in *2018 18th International Conference on Harmonics and Quality of Power (ICHQP)*, Ljubljana, May 2018, pp. 1–6, doi: 10.1109/ICHQP.2018.8378887.

[12] B. N. Alajmi, K. H. Ahmed, G. P. Adam, and B. W. Williams, "Single-Phase Single-Stage Transformer less Grid-Connected PV System," *IEEE Trans. Power Electron.*, vol. 28, no. 6, pp. 2664–2676, Jun. 2013, doi: 10.1109/TPEL.2012.2228280.

[13] L. Chen, A. Amirahmadi, Q. Zhang, N. Kutkut, and I. Batarseh, "Design and Implementation of Three-Phase Two-Stage Grid-Connected Module Integrated Converter," *IEEE Trans. Power Electron.*, vol. 29, no. 8, pp. 3881–3892, Aug. 2014, doi: 10.1109/TPEL.2013.2294933.

[14] H. Hu, S. Harb, N. H. Kutkut, Z. J. Shen, and I. Batarseh, "A Single-Stage Microinverter Without Using Eletrolytic Capacitors," *IEEE Trans. Power Electron.*, vol. 28, no. 6, pp. 2677–2687, Jun. 2013, doi: 10.1109/TPEL.2012.2224886.

[15] N. Sukesh, M. Pahlevaninezhad, and P. K. Jain, "Analysis and Implementation of a Single-Stage Flyback PV Microinverter With Soft Switching," *IEEE Trans. Ind. Electron.*, vol. 61, no. 4, pp. 1819–1833, Apr. 2014, doi: 10.1109/TIE.2013.2263778.

[16] Y.-H. Kim, Y.-H. Ji, J.-G. Kim, Y.-C. Jung, and C.-Y. Won, "A New Control Strategy for Improving Weighted Efficiency in Photovoltaic AC Module-Type Interleaved Flyback Inverters," *IEEE Trans. Power Electron.*, vol. 28, no. 6, pp. 2688–2699, Jun. 2013, doi: 10.1109/TPEL.2012.2226753.

[17] C. Meza, D. Biel, D. Jeltsema, and J. M. A. Scherpen, "Lyapunov-Based Control Scheme for Single-Phase Grid-Connected PV Central Inverters," *IEEE Trans. Control Syst. Technol.*, vol. 20, no. 2, pp. 520–529, Mar. 2012, doi: 10.1109/TCST.2011.2114348.

[18] F. Blaabjerg, R. Teodorescu, M. Liserre, and A. V. Timbus, "Overview of Control and Grid Synchronization for Distributed Power Generation Systems," *IEEE Trans. Ind. Electron.*, vol. 53, no. 5, pp. 1398–1409, Oct. 2006, doi: 10.1109/TIE.2006.881997.

[19] J. He and Y. W. Li, "Generalized Closed-Loop Control Schemes with Embedded Virtual Impedances for Voltage Source Converters with LC or LCL Filters," *IEEE Trans. Power Electron.*, vol. 27, no. 4, pp. 1850–1861, Apr. 2012, doi: 10.1109/TPEL.2011.2168427.

How to cite this article:

Naveed Malik, Sami Ullah, Amir Khan and Farhan Ullah, Designing and Analysis of Single Stage and Two Stage PV Inverter Connected to Weak Grid System, International Journal of Engineering Works, Vol. 7, Issue 10, PP. 361-369, October 2020, https://doi.org/10.34259/ijew.20.710361368.

International Journal of Engineering Works
ISSN-p: 2521-2419
ISSN-e: 2409-2770
Vol. 7, Issue 10, PP. 369-374, October 2020
https://www.ijew.io/
https://doi.org/10.34259/ijew.20.710369374

Enhancing Service Life of Power Transformer through Inhibiting the Degradation of Insulating Oil by New Approach

Yasir Khan[1], Muhammad Iftikhar Khan[2],
[1,2]Department of Electrical Engineering, University of Engineering and Technology, Peshawar, Pakistan
engryasirkh@gmail.com[1], miftikhar74@gmail.com[2]
Received: 01 October, Revised: 11 October, Accepted: 16 October

***Abstract*—** Oil reclamation is a transformer insulation reconditioning technique, which may use as on-line or off-line. However, there is a need of evidence showing the effect of this process on conditions of the paper insulation, which indeed affects the life span of a transformer. This research work focuses on oil reclamation experiment on an old retired distribution transformer. Electrical testing and post-mortem analysis of the transformer were conducted, aimed at investigating the design aspects and collecting information on the insulation conditions prior to the oil reclamation. Temperature and moisture sensors were installed to monitor the conditions within the transformer during the oil reclamation [2]. The experimental process of transformer Oil reclamation was performed into two phases, with regular oil sampling to analyze the changes in key oil parameters, namely acidity number (AN), moisture and breakdown voltage (BV). This was accompanied by paper sampling at the end of each reclamation cycle to study the effects of oil reclamation on properties, particularly moisture, LMA and degree of polymerization.

The transformer which was used for the entire experimental process was about 45 years old, 200kVA, 1100 / 415-240V distribution transformer. In order to study the long-term effect of oil reclamation, oil samples were collected from an on-site reclamation exercise performed in a laboratory-accelerated thermal ageing experiment. Oil samples collected before and after the reclamation were aged alongside new oils for comparison [4]. Through the regular monitoring and measurement of oil parameters (AN, moisture and BD strength) over 144 hours and paper parameters (LMA, moisture and DP) at specific stages of phase 1, it was observed that the transformer oil-paper insulation system was significantly improved.

The entire research work was performed into two phases (phase 1 and phase 2). The "phase 1" was aimed to improve and restore the oil parameters comparable to the parameters of new oil as specified in "IEC-60296" and its effect on the paper insulation. "Phase 2" was aimed to compare the life span of reclaimed oil filled transformer with the transformer in which aged oil has been replaced by new oil[6].

Effective study of oil reclamation was analyzed through laboratory accelerated aging experiment and real time application on a 45 years old transformer. Through the regular monitoring and measurement of oil parameters (AN, moisture and BD strength) over 144 hours and paper parameters (LMA, moisture and DP) at specific stages of phase1, it was observed that the transformer oil-paper insulation system was significantly improved [15]

***Keywords*—** ageing, oil parameters, oil degradation, oil reclamation, paper insulation

I. INTRODUCTION

Transformers are the most essential integrating component of electrical network system. With the world moving towards a more resilient power network, the reliability of each network component becomes of utmost importance in ensuring uninterrupted power supply to the consumers. The study of aging problem of transformers has a great and serious interest, which increase their importance in the power system. These studies help gain valuable insights which could aid in prolonging the life of these assets and maintaining their reliability [1]. Ageing studies are gaining further prominence recently due to the large population of ageing assets in operation.

Market deregulation and an increased competition have urged utility operators to look into optimizing the utilization of their equipment in terms of operating efficiency and cost-effectiveness [2]. In response to this requirement, utility operators and service providers have adopted asset management techniques, targeted at enhancing the usage of the residual life time of the asset, with particular attention to ensuring reliability of service, and distribution of maintenance and re-investment costs. Due to the high value and large population [3], transformers are one of the main assets in the focus of asset management entities.

Now a day the majority of the power transformers, in electrical network are oil immersed, with cellulose as the solid insulation. The oil, apart from functioning as a coolant, also serves as an electrical insulation [8]. The ageing of transformers is generally due to deterioration of the paper and oil insulation

system. A utility can exercise various restoration techniques to improve the oil and paper condition by the removal unwanted products. Of these techniques, oil reclamation has recently become more effective to increase the life of power transformers [1, 2].

II. Experimental Setup and Procedure for Oil Reclamation

The oil reclamation process can be split into three distinct processes – drying and degassing, filtering, and fuller's earth reclamation [11]. The labeled diagram of the oil reclamation process is given in Fig. 1. The entire unit is operated through a central control panel, with built-in safety elements and controllers, apart from being provided with a range of alarms and interlocks.

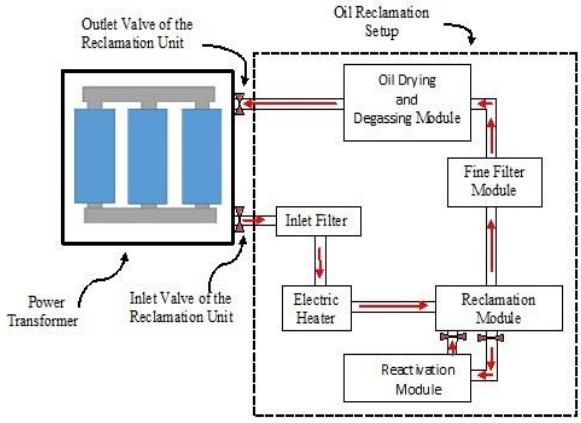

Figure 1. Labeled diagarm of oil reclamtion setup

A. Inlet Filter

At the inlet of the reclamation equipment, a coarse filter is used t remove the particles of about 80 µm or larger. Most of the sludge is filtered at this initial stage. The Inlet filter is replaced immediately after saturation.

B. Electric heater

The oil filtered through inlet filter is passed though a low watt heater of about 1.8 watt/cm$^{2.}$ The electric heater is used to increase the efficiency of the process by aiding easier spreading of the hot oil through coalesces and filters. The heater is designed to heat the incoming oil up to a temperature of 90 °C. The heating element also plays a key role in the removal of chemical ageing by-products, which is executed by the fuller's earth module [14]. The oil passes through a coarse inlet filter before entering the heater, designed to remove suspended particles of size larger than 80µm.

C. Reclamation Module

Reclamation module is the central main part of the oil reclamation process. This module mainly consists of a single column of fuller's earth. This column acts as adsorbent medium for the chemical ageing by-product removal process. The heated oil from the heater module is forced to pass through the fuller's earth columns, where the constituents causing acidity are gradually removed. These columns are reusable after saturation, through a process called reactivation.

D. Reactivation module

The adsorption module of the reclamation setup is the fuller's earth reactivation module. Reactivation of the adsorption medium needs to be initiated manually, at the discretion of the operator. The process consists of burning down the fuller's earth, along with all the adsorbed impurities. The oil present on the surface of the fuller's earth serves as fuel and hence the burning is started by a coil present at the top of the column [12]. The fuller's earth itself has an extremely high thermal capacity and does not get destroyed, regardless of temperatures within the columns reaching up to 700 °C. The exhaust gases produced are passed through an activated carbon column, before being released outside into the atmosphere.

E. Fine filter module

The CJC fine filter is used as primary filter. This filter can remove particles from the oil up to 0.3 µm with high dirt folding capacity. These filters can be replaced easily when get saturated.

F. Drying and degassing module

The drying and degassing of oil is performed by a specially designed welded tank. It consists of equally spaced sheets for equal distribution of oil. The oil is passed through these sheets under a vacuum of 5m bar. Water and other vapors are evacuated by the vacuum pump and then exhausted. This step was aimed to bring the water contents of oil to a level less than 5ppm.

G. Connecting the oil reclamation system to the transformer

The setup for the oil reclamation experiment is shown in Fig. 2. The outlet tap of the transformer is connected to the inlet of the oil processor module through a hose. The first step of oil flow is through the heater module, where the oil temperature is raised to required value [16]. The oil which has been heated is then sent to the fuller's earth column through a rerouting valve installed on the processor module. When oil is passed through the fuller's earth column, it is then sent back to the fine filter module for removing unwanted particles. Once the particle contaminant has been removed, the oil passes to the drying and degassing module. After the complete process, oil is then pumped back into the transformer tank through the outlet hose, which ejects the oil near the top of the transformer tank [13].

In the event, the fuller's earth column get saturated, the rerouting valve on the processor can be switched so that the oil flowing to the fuller's earth module is by-passed, allowing the reactivation process to get start. The oil processor unit operates continuously, while the adsorption module operates between cycles of processing and reactivation.

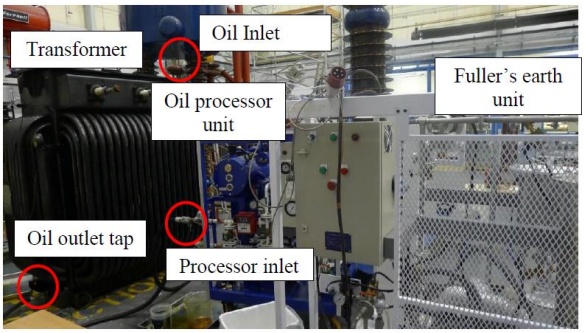

Figure 2. The experimental setup of oil reclamation process

Normally the reclamation process is repeated in many cycles to get the oil parameters as comparative to that of new oil. Commonly, in various researches it is aimed to improve the oil parameters. But we have to extent our research work by adding the effect of oil reclamation on entire insulation system coil and paper) land to compare the life span of transformer filled with reclaimed oil to the transformer in which the aged oil has been replaced with new oil. Thus our entire research work was carried out in two phase.

a) PHASE 1

The "phase-1" was aimed to improve the transformer insulation system as specified in "IEC-60296". The research work was focused to restore the oil parameters by reclamation process and its effect on the paper insulation.

b) PHASE 2

The main aim of "phase-2" is to compare the life span of transformed with reclaimed oil to that filled with new oil after aging.

III. Results and Discussions

The total capacity of liquid insulation (oil) in the tank of transformer was measured to be 300L approximately. The volume flow-rate of oil was adjusted to 150 L/h, thus it would take about 2 hours for the entire volume of oil to pass through reclamation unit. The experiment was carried out for 144 hours, so 72 cycles of oil though reclamation unit were carried out to complete the oil reclamation process (Table I).The temperature of oil was measured and monitored through the temperature sensors installed inside the transformer during sampling stage. It was recommended to operate the reclamation experiment at 70°C. The limit and profile of oil temperature was strictly monitored and controlled though out the entire process.

TABLE I. Experimental profile of Oil Reclamation process

Total volume of oil in transformer tank	300L
Flow rate of oil through reclamation unit	150L/h
Time required for entire volume of oil to pass through reclamation unit	300L / 150L/h= 2h
Number of working hours of reclamation unit	144h
Number of cycles of oil during 144 hours	144h/2h= 72 Cycles

IV. Oil parameters

A. Acidity Number (AN)

Acidity number (AN) is the amount of potassium hydroxide (KOH) in milligrams (mg) which is required to neutralize the acidity of 1 gram of oil. The AN of new oil is about 0.02mg KOH/g, which increases with the aging of oil. From the pre-experiment inspection, the AN of oil samples was measured to be 0.22 mg KOH/g. It was suggested to reduce the AN of aged oil as comparative to the new oil. It took about 144 hours (72 passes) to reduce the AN of aged oil up to 0.005 mg KOH/g, this value is much less than the AN of new oil. Small fluctuations in the graph (Fig. 3) are due to the mixing of acidity from paper into the oil.

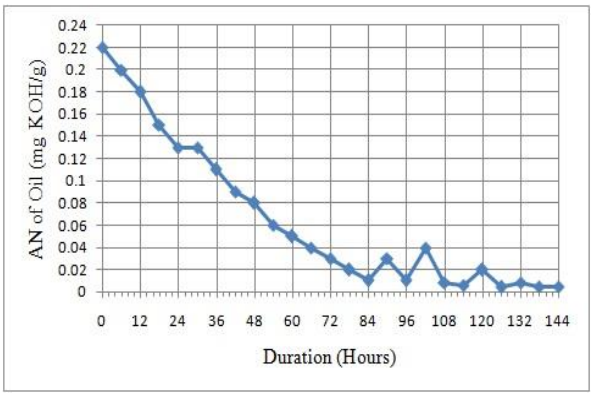

Figure 3. AN of oil duing reclamtion process

B. Moisture in oil

The presence of moisture decreases the dielectric strength of the insulating oil. The value of moisture in new oil is almost less than 10ppm, while the reclamation experiment decreases the moisture in the aged oil of transformer from 50ppm to 7 ppm, which shows the better quality of oil.

The profile of moisture during the reclamation process is given in Fig. 4. The variation in the level of moisture is due to the variation in temperature of oil in transformer tank and due to absorption of water content from the paper insulation.

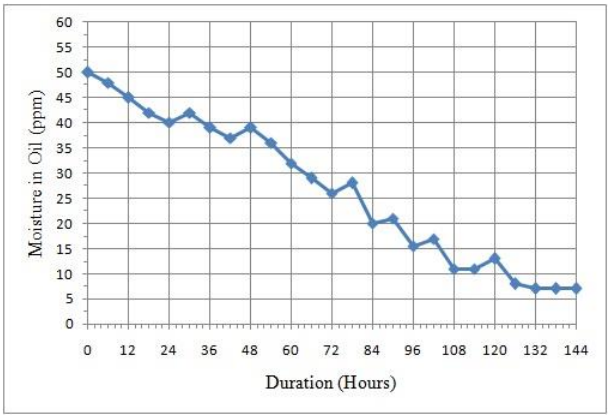

Figure 4. Moisture in oil duing reclamtion process

C. *Breakdown strength of oil*

The breakdown strength of oil is the amount of voltage in kV at which the insulating oil electrically breakdown. The breakdown voltage of new standard oil is about 60kv or greater. It was observed from the pre-experiment measurement that the breakdown voltage of degraded oil is approximately 13 kV which is much less than the cautionary value (25 kV for 11 kV transformers). The profile of improving process of breakdown voltage of degraded oil is given in Fig. 5.

After the 144 hours (72 passes) the breakdown voltage was achieved to be 72 kV which is much better than the breakdown voltage of new fresh oil.

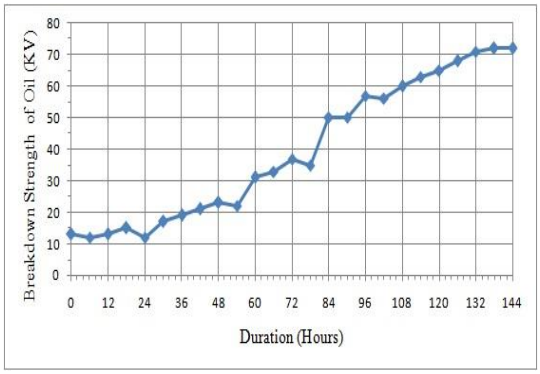

Figure 5. Breakdown Strength of oil duing reclamtion process

V. EFFECTS OF OIL RECLAMATION ON PAPER INSULATION

A. *Low Molecular Weight Acidity (LMA)*

The low molecular weight acidity (LMA) of paper insulation is directly affected by AN of oil. Prior to the reclamation experiment the LMA of paper samples was measured and found to be 12 mg KOH/g on the average. After the complete 72 passes of reclamation process, the LMA of paper insulation was measured and found to be approximately 4 mg KOH/g. thus about 67% decrease in LMA of paper insulation was achieved.

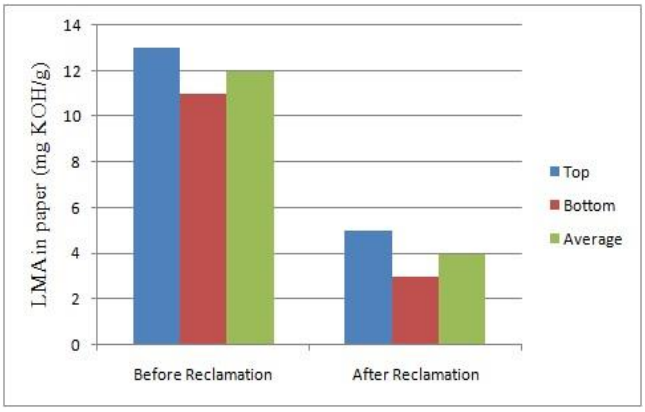

Figure 6. LMA in paper before and after the oil reclamation experiment

B. *Moisture in paper*

The moisture in paper insulation of transformer is about 99% as compared to moisture level of oil. This is the main bulk of moisture stored in paper insulation which mainly causes the failure of transformer. By inspecting the paper samples collected from the bottom and top of transformer oil, the value of moisture was obtained to be nearly 3.5 % on the average. After the complete reclamation experiment (72 passes), the paper samples from top and bottom of windings are collected again for measurement which give value of about 1.2% on the average. Thus a decrease of about 65.7% in the moisture was recorded.

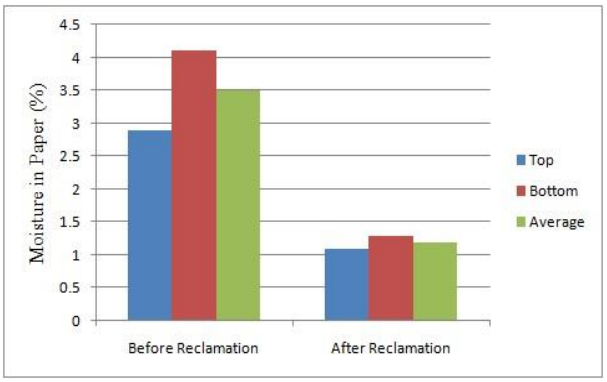

Figure 7. Moisture in paper before and after the oil reclamation experiment

C. *Degree of polymerization of paper (DP)*

The DP of paper insulation was measured for paper samples collected from different positions before and after the reclamation process. It is clear from the Fig. 8 that the increased temperature of oil for regeneration process has no noticeable effect on paper insulation.

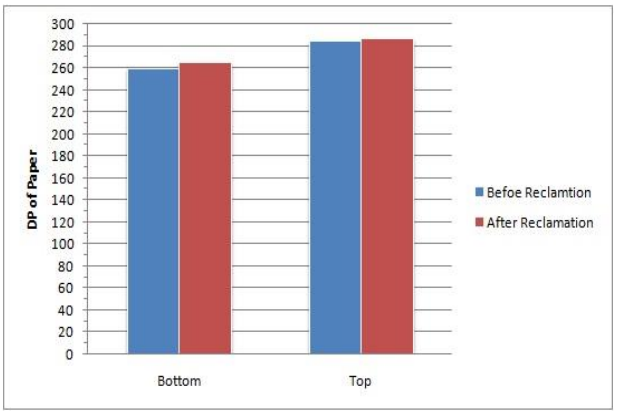

Figure 8. DP of paper before and after the oil reclamation experiment

CONCLUSIONS

This thesis is mainly aimed to improve and extend the service life of transformer by inhibiting the oil degradation through oil reclamation process. The experimented work was carried out on a 45years old, 200 KVA, 11 KV/415V-240V distribution transformers.

The entire research work was performed into two phases (phase 1 and phase 2). The “phase 1” was aimed to improve and restore the oil parameter as that of new oil and its effect on the paper insulation. “Phase 2” was aimed to compare the life span of the reclaimed oil filled transformer with the transformer in which aged oil has been replaced by new oil.

Effective study of oil reclamation was analyzed through laboratory accelerated aging experiment and real time application on a 45years old transformer. Through the regular monitoring and measurement of oil parameters (AN, moisture and BD strength) over 144 hours and paper parameters (LMA, moisture and DP) at specific stages of phase-1, it was observed that the transformer oil-paper insulation system was significantly improved as given in Table II and Table III.

TABLE II. IMPROVEMENT OF OIL PARAMETERS THROUGH RECLAMATION PROCESS

Oil Parameters	Before Reclamation	After Reclamation	Improvement
AN (mgKOH/g)	0.22	0.005	97.7%
Moisture (ppm)	50	7	86.0%
BD Strength (kV)	13	72	81.9%

TABLE III. IMPROVEMENT OF PAPER PARAMETERS THROUGH RECLAMATION PROCESS

Paper Parameters	Before Reclamation (Average value)	After Reclamation (Average value)	Improvement
LMA (mg KOH/g)	12	4	66.6%
Moisture (ppm, %)	3.5	1.2	65.7%

"Phase 2" of the research work is aimed to compare the efficiency of new oil replaced in the aged transformer. "IEC 60422; 2013- minerals insulating oils in electrical equipment supervision and maintenance guidance" give guidance on oil condition, is given in Table IV.

TABLE IV. GUIDANCE OF OIL PARAMETERS ACCORDING TO IEC 60422; 2013

Oil Parameters	New Oil	Cautionary
Breakdown strength (kV)	60	<30
Acidity number (mg KOH/g)	0.02	0.1 to 0.2
Moisture (ppm)	<10ppm	15 to 20

The "Supervision and maintenance guidance" recognizes the research which has been carried out over years. The aging profile of replaced oil was compared to the aging of reclaimed oil though laboratory accelerated aging experiment. It was observed that the aging profile of reclaimed oil is more efficient than replaced new oil in the aged transformer [7]. It is because of the stored residuals and depleting compounds in the paper and assembly of the transformer which start acting soon as transformer start operation with the replaced new oil. Such acidity; sludge and other depleting aging by product compounds are cleaned during the reclamation process, thus formation of these compounds get delayed to enhance the service life of transformer by several years (Fig. 9)

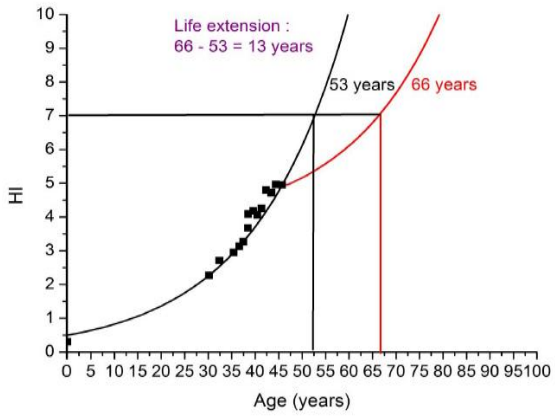

Figure 9. Estimate for improving life span of transformer

CONCLUSION/FUTURE WORK AND RECOMMENDATIONS

The investigation in this work employed equipment designed especially for indoor laboratory use, and therefore came with its own restrictions like the low speed of reclamation. Thus, there is a need to verify these findings with comprehensive industrial scale testing in order to find out the optimal oil reclamation procedure in terms of flow velocity, oil temperature and processing duration [12]. Furthermore, all the findings in this work were based on laboratory experimental work. There is a need for a model to evaluate the effect of life extension of the transformer achieved through oil reclamation. .

The ageing experiments conducted in this study utilized systems consisting of only new paper to study the performance of oil after reclamation. While these ageing experiments confirm the better performance of oil after being subject to oil reclamation procedure, they can be further extended utilizing systems of oil and service-aged paper. This would enable more comprehensive comparison of the long-term performance of paper when the transformer is subject to oil reclamation process, and aid in a more accurate estimation of life extension achieved through the procedure.

With substantial proof of the positive outcome of oil reclamation on improving the oil and paper insulation, the essential step would be to test the long-term performance of this intervention technique on an in-service transformer. Regular monitoring of the oil parameters for a period of time post-oil reclamation can confirm the long term effects of oil reclamation on the ageing rate of the transformer. These studies can also be carried out alongside similar transformers which have not been subject to oil reclamation and those which have undergone oil replacement, in order to enable comparison.

Ageing models proposed in the past rely upon the paper condition to guess the remnant life span of the transformer. However, these models solely incorporate the level of moisture and DP of paper as the indication of the ageing state. Recently, the effect of LMA on the ageing of paper insulation system was

proposed. Thus, there is a need to quantify the impact of LMA on paper ageing and incorporate it in the aging model.

REFERENCES

[1] A. J. Kachler and I. Hohlein, "Aging of cellulose at transformer service temperatures. Part 1: Influence of type of oil and air on the degree of polymerization of pressboard, dissolved gases, and furanic compounds in oil," *IEEE Electrical Insulation Magazine*, vol. 21, pp. 15-21, 2005.

[2] J. Schneider, A. J. Gaul, C. Neumann, J. Hogräfer, W. Wellßow, M. Schwan, and A. Schnettler, "Asset management techniques," International Journal of Electrical Power & Energy Systems, vol. 28, pp. 643-654, 2006.

[3] A. Jahromi, R. Piercy, S. Cress, J. Service, and W. Fan, "An approach to power transformer asset management using health index," *IEEE Electrical Insulation Magazine*, vol. 25, pp. 20-34, 2009.

[4] D. F. García, B. Garcia, and J. C. Burgos, "Modeling power transformer field drying processes," *Drying Technology*, vol. 29, pp. 896-909, 2011.

[5] J. Almendros-Ibaez, J. C. Burgos, and B. Garcia, "Transformer field drying procedures: a theoretical analysis," *IEEE Transactions on Power Delivery*, vol. 24, pp. 1978-1986, 2009.

[6] Q. L. N. Azis, Z.D. Wang, D. Jones, B. Wells ,G.M. Wallwork, "Experience of Oil Re-generation on a 132 kV Distribution Transformer," presented at the International Conference on Condition Monitoring and Diagnosis (CMD), 2014.

[7] W. G. A.-. (Declerq), "“Thermal performance of Transformers”, Technical brochure No 393," CIGRE, 2010.

[8] P. Jarman, Z. Wang, Q. Zhong, and T. Ishak, "End-of-life modelling for power transformers in aged power system networks," in *CIGRE 6th Southern Africa regional conference*, 2009.

[9] B. Pahlavanpour, R. Linaker, and E. Povazan, "Extension of life span of power transformer by on-site improvement of insulating oils," in *6th International Conference on Dielectric Materials, Measurements and Applications*, 1992, pp. 260-263.

[10] T. Rouse, "Mineral insulating oil in transformers," *IEEE Electrical Insulation Magazine*, vol. 14, pp. 6-16, 1998.

[11] P. Hodges, *Hydraulic fluids*: Butterworth-Heinemann, 1996.

[12] M. Heathcote, *J & P transformer book*: Newnes, 2011.

[13] A. Emsley and G. Stevens, "Review of chemical indicators of degradation of cellulosic electrical paper insulation in oil-filled transformers," *IEE Proceedings - Science, Measurement and Technology*, vol. 141, pp. 324-334, 1994.

[14] L. E. Lundgaard, W. Hansen, D. Linhjell, and T. J. Painter, "Aging of oil-impregnated paper in power transformers," *IEEE Transactions on Power Delivery*, vol. 19, pp. 230-239, 2004.

[15] E. Brancato, "Insulation aging a historical and critical review," *IEEE Transactions on Electrical Insulation*, pp. 308-317, 1978.

[16] A. White, "The desired properties and their effect on the life history of insulating papers used in a fluid-filled power transformer," in *IEE Colloquium on Assessment of Degradation Within Transformer Insulation Systems*, 1991, pp. 4/1-4/4.

How to cite this article:

Yasir Khan and Muhammad Iftikhar Khan, Enhancing Service Life of Power Transformer through Inhibiting the Degradation of Insulating oil by New Approach, International Journal of Engineering Works, https://doi.org/10.34259/ijew.20.710369374.

International Journal of Engineering Works
ISSN-p: 2521-2419
ISSN-e: 2409-2770
Vol. 7, Issue 10, PP. 375-378, October 2020
https://www.ijew.io/
https://doi.org/10.34259/ijew.20.710375378

Improving Efficiency and Stability of Organic Solar Cell

Muhammad Zeeshan
Department of Electrical Engineering, University of Engineering and Technology Peshawar
Received: 05 October, Revised: 15 October, Accepted: 17 October

***Abstract*—** Efficiency and stability are the main challenges of organic solar cells. In this research novel structure is investigated for organic solar cell which has improved efficiency and improved stability. Blend of PTB7 and PCBM elements was used for the active layer of cell. Thickness of this layer was varied from 80nm to 200nm and selected the optimized thickness of 90nm. On which the cell has maximum efficiency of 12.24 %. The influence of window layer material such as Zinc oxide (ZnO) and titanium dioxide (TiO_2) with various electrode materials including Indium tin oxide (ITO), Fluorine tin oxide (FTO), aluminum (Al) Silver (Ag) and Gold (Au) with different combinations have been investigated with the objective to enhance the absorption and PCE of the cell. Also varied the thicknesses of these different layers and selected the optimized thickness on which the cell had maximum efficiency. The structure of the proposed scheme was observed with ITO/Al as top and bottom electrode with thicknesses of 125nm and 100nm respectively and found that this holds the highest performance parameters including J_{sc}=0.*130*(mA/m^2), V_{oc}= *1* (V), *FF=94.1*% and η*=12.24*% respectively as compared to different electrode combination and window layers with the same photoactive absorber material PTB7: PCBM. This indicates that the proposed structure can be a good choice for replacing less efficient in-organic cell.

***Keywords*—** Organic solar cells, Bulk Heterojunction, PIF8BT: PDI, Buffer layer, Power Conversion Efficiency.

I. INTRODUCTION

It is well known that in today's life energy is the need of every person. Because everything around us is running on energy and specially the use of electrical energy is very large [1]. With no doubt Solar energy is a huge and endless amount of energy. Researchers are working from 19th century to make energy (in the form of electrical energy) from sun light which we are receiving at earth surface. The process in which electricity is made from sun light is called photo electric effect. The device with the help of which we convert this light into energy (Electrical Energy) is called solar cell (photo voltaic cell). These cells are divided into many types; among them the two are main types which are 1) organic solar cells, and 2) inorganic solar cells. But the demand of organic solar cells in the market is increasing day by day from the last 20 or 30 years. Because these cells (organic solar cells) have greater efficiency as compared to other type (inorganic solar cells) [2].The very first attempt to make inorganic solar cell was first done by bell labs in year 1954. He made cell from silicon material with 6% efficiency [3]. Then many scientists and researchers worked to improve the cell efficiency and they achieved a greater efficiency of 24% up till now [4]. The main difficulties with these cells are their high cost of production, their heavy weight and their complex fabrication process [2]. Contrary to this cell made from organic material (organic solar cells) have much lower production cost, also have less weight in comparison with inorganic cells. Size of cells which are made from organic materials is also thin in comparison with inorganic cells, so their production cost and weight is low. Organic cells are made of organic materials and their blends which can be synthesizes easily. The other thing with OSCs is their flexibility. These cells are made of many layers and parts, but the main part is the active part or layer, which is made from organic material and their mixture. Organic cells have also greater absorption capacity of light due to their structure and other properties. In early days scientists were using chlorophyll because of its good properties of light absorbing [5].But later researchers developed new materials which had good properties of light absorbing and useful use of this light [6, 7]. In 1980 the first organic solar cell was made with very low PCE of 0.1% [8].Then in 1995 Alan Heegar introduced idea of bulk hetero junction (BHJ) [9]. Bulk hetero junction is a structure in which there are two different materials (mixture of p and n type) in active layer. These materials are separated from each other by very small distance of Nano scale separation. The power conversion efficiency of these materials depends upon the structure and morphology of these [10, 11]. Scientists tried different type of morphologies to develop a good cell but are still working to find the best active layer material for the cell and to find a good morphology [12].

OSCs which are normally available in the market are made from P3HT poly (3-Hexylethiopanes) and fullerene derivatives particularly PCBM phenyl (C-61 Buteric acid methyle ester). P3HT is electron giving(donor)element and Pcbm is electrons acceptor element [13]. P3ht has the property to conduct free charges, and this is because it has single and double bond alternatively. PCBM is derived from fullerene. The placement of electrons in this element is responsible for good charge transfer. Researcher consider these very good for OSCs. Up till now Researchers have obtained about 5% PCE from these materials [14].The demand and market competition of OSCs

depends upon the production cost, PCE and stability of these structures. So, we need more focus and work on their efficiency and their stability to participate in market competition and show some outstanding performance which is not shown by inorganic cells. Now a days P3HT and PCBM material have attained the stability of up to 5000 hours [15]. But these are very less stable in the air when they are exposed to air .So we should investigate new material which has greater efficiency [16].

II. Device Modeling

The proposed investigated OSC structure is presented in Figure 1. Which consist of mainly five layers. Indium Tin Oxide (ITO) is used as top layer. Which works as electrode. Below ITO Buffer layer is placed which is made of PEDOT: PSS. This is also known as Hole transport layer (HTL) or Electron Blocking Layer (EBL), which helps in the transportation of holes and blocks the movement of electrons. PEDOT: PSS has good stability, high mechanical flexibility and is highly conductive [17-19]. Below the (BL) layer, have placed photo active layer which is made from the blends of different materials such as PIF8: PDI, P3HT: PCBM, PTB7: PCBM and PDTS-DTFBT: PCBM. Thickness of this layer was varied from 80nm to 150nm. Different window layers were used including zinc oxide (ZnO) and titanium dioxide (TiO2) as these window layers have high transparency, larger excitons binding energy and can enhance transmittance [20, 21].

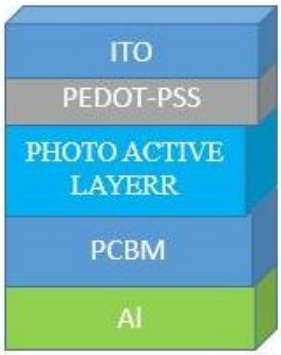

Figure:1 Proposed structure of cell

For simulations GPVDM software was used. This software was used because it is very good software as compared to other softwares because it can give us both optical and electrical properties of the cell very accurately [22, 23]. In proposed structure both electrical and optical properties were investegated. Different equations were used such as poison equation, Drift diffusion model, and continuity equations for electron-hole. Whereas, for recombination of carrier Shockley-Read-Hall (SRH) is used in 1D- and time domain [24-26].

III. Results and Discussions

For getting the highest efficiency and stability different photoactive materials and their different parameters were investigated and checked. First of all thickness of the photo active layer was varied, and observed the influence of thickness on the Voc, Jsc, FF and η for all materials .The reason for varying the absorber layer thickness is that this layer plays a key role in the overall cell performance of the cell [27, 28]. Different window layers were used and compared their results with each other. After analysis PEDOT: PSS was selected for window layer because its result was good as compared to other window layers [29]. The variation of efficiency and Jsc was observed. It was found that when the thickness of the absorber layer increases Jsc also increases. This rise in Jsc is due to the fact when the absorber layer thickness is increased the absorption of the photons is increased due to which Jsc is increased [30].It was also found that when thickness increases, efficiency also increases. This is because larger amount of photons are absorbed in this which results in greater number of excitons and hence efficiency increases [31]. Many structures which were made from different active materials were checked and observed among them one is discused below.

A. Proposed Structure

PTB7: PCBM material has been used for active layer shown in fig.2. Different perameters which include Voc, Jsc, efficiency etc of the cell were observed.

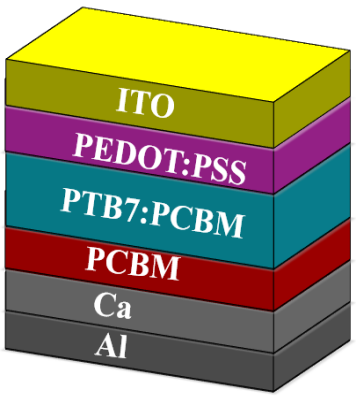

Figure 2: Structure which is made from PTB7: PCBM

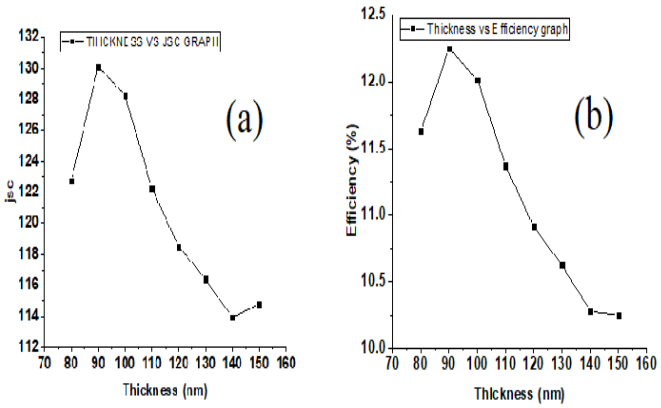

[1] Figure 3: Variation of (a) Jsc (b) η with thickness

When thickness was increased Jsc also increases a little bit which is represented in figure 3a. When thickness was increased from 80nm to 90nm the Jsc increases from 122 to 130 m A/m^2 as shown in figure 3(a).Upto 90nm Jsc is increases and then it decreases, when thickness reachs to 140nm it again starts

increasing.But 90nm was selected because as for OSCs the width of active layer material should not be greater than 120nm. Also it is shown in figure 3(b) that efficiency also increases with increase in thickness of the active material. When thickness of the proposed material was increased from 80nm to 90nm efficiency increases and when thickness was further increased efficiency decreases upto 140nm.But again 90nm uptimized thickness was selected for organic solar cell because further increase for the thickness of active layer is not good. The highest efficiency achieved for this structure was 12.248 at uptimized thickness of 90nm.

Performance of the proposed structure was also checked for different values of temperature and is shown in figure 4. Temperature increase in interval of 25 degree was started from 200k and reached upto 450k.It was noticed that as temperature increases from 200k to 250k the efficiency of the cell increases and when further increase the temperature then efficiency starts on decreasing as shown in figure 4(a). Highest achieved efficiency was 12.24% at the uptimized temperature of 250k.,The effect of temperature on Voc of the cell was also checked which is shown in figure 4(b) .Voc first increases with the increase in temperature upto 350k and then decrease with further increase in temperature as shown in the figure. The effect of temperature on other perameters such that fill factor was also checked and it was resulted that with the increase in temperature the performance of the cell is decreasing [37, 38].

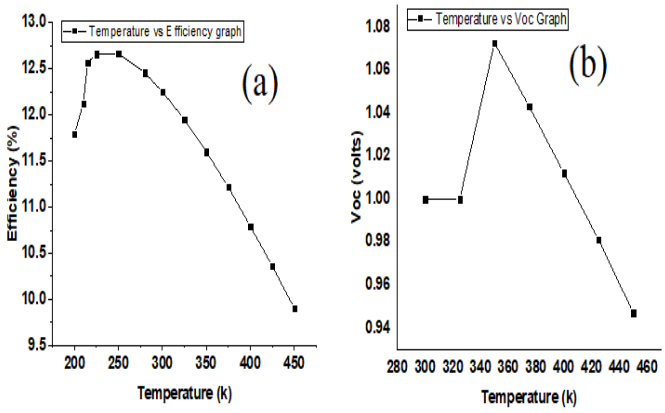

Figure 4: Effect of Temperature on (a) Efficiency (b) Voc

CONCUSLION

The central objective of this research was to obtain a high power converssion efficiency and good stability for OSCs using different substances and different morphologies. Different methods were tried to achieve high efficiency for example architecting and preparing novel electron donor and electron acceptor substances with high protons immersion ability and high mobility, designing and arranging the structure of the photo active layer materials, utilizing different layers such as buffer layers between the active layer and electrodes, designing and making new structures for devices. Different necessary layers made of different materials for cell were used. These layers are made of PEDOT: PSS, MoO3, TiO2, V2O5 etc. The results for different combinations of active layers with different electron holes transport layers were checked. Different materials for active layer were checked and finally selected the layer of PTB7: PCBM which absorbs large number of photons and give us good power conversion efficiency. Width of active layer was also checked as well as the width of anode and cathode. Thickness of all layers were varied one by one and at the last selected thicknesses for the layers which gave good power conversion efficiency and good stability. Optimized thickness for active layer was selected which is 90nm on which it has a highest efficiency of η=12.24%. Absorption of photons in each layer was also observed. The Recombination of electrons were observed such material was selected which allowed less number of recombination of electrons and holes. All the properties such as short circuit voltage (Voc), fill factor (FF), short circuit current density (Jsc) was observed whose values are V_{oc}= *1* (V), *FF=94.1*%, J_{sc}=0.*130* (mA/m^2) respectively.

REFERENCES

[1] Goetzberger, A., J. Luther, and G. Willeke, Solar cells: past, present, future. Solar energy materials and solar cells, 2002. 74(1-4): p. 1-11.

[2] Bagher, A.M., Comparison of organic solar cells and inorganic solar cells. International Journal of Renewable and Sustainable Energy, 2014. 3(3): p. 53-58.

[3] Goetzberger, A., J. Knobloch, and B. Voss, Crystalline silicon solar cells. New York, 1998: p. 114-118.

[4] Green, M.A., Corrigendum to 'Solar cell efficiency tables (version 46)'[Prog. Photovolt: Res. Appl. 2015; 23: 805–812]. Progress in Photovoltaics: Research and Applications, 2015. 23(9): p. 1202-1202.

[5] Sahare, S.A., Enhancing the Photovoltaic Efficiency of a Bulk Heterojunction Organic Solar Cell. 2016.

[6] Winder, C., et al., Sensitization of low bandgap polymer bulk heterojunction solar cells. Thin Solid Films, 2002. 403: p. 373-379.

[7] Zhang, F., et al., High photovoltage achieved in low band gap polymer solar cells by adjusting energy levels of a polymer with the LUMOs of fullerene derivatives. Journal of Materials Chemistry, 2008. 18(45): p. 5468-5474.

[8] Tang, C.W., Two - layer organic photovoltaic cell. Applied physics letters, 1986. 48(2): p. 183-185.

[9] 松本真哉, et al., 真空蒸着膜におけるビスアゾメチン色素の J 会合体. 色材協会誌, 2006. 79(11): p. 503-510.

[10] Peet, J., et al., Efficiency enhancement in low-bandgap polymer solar cells by processing with alkane dithiols. Nature materials, 2007. 6(7): p. 497-500.

[11] Schlenker, C.W. and M.E. Thompson, The molecular nature of photovoltage losses in organic solar cells. Chemical Communications, 2011. 47(13): p. 3702-3716.

[12] Chen, C.-C., et al., Visibly transparent polymer solar cells produced by solution processing. ACS nano, 2012. 6(8): p. 7185-7190.

[13] Li, J. and N. Wu, Semiconductor-based photocatalysts and photoelectrochemical cells for solar fuel generation: a review. Catalysis Science & Technology, 2015. 5(3): p. 1360-1384.

[14] Verploegen, E., et al., Manipulating the morphology of P3HT–PCBM bulk heterojunction blends with solvent vapor annealing. Chemistry of Materials, 2012. 24(20): p. 3923-3931.

[15] Jørgensen, M., et al., Stability of polymer solar cells. Advanced materials, 2012. 24(5): p. 580-612.

[16] Zhao, J., et al., Phase diagram of P3HT/PCBM blends and its implication for the stability of morphology. The Journal of Physical Chemistry B, 2009. 113(6): p. 1587-1591.

[17] Ouyang, J., Solution-processed PEDOT: PSS films with conductivities as indium tin oxide through a treatment with mild and weak organic acids. ACS applied materials & interfaces, 2013. 5(24): p. 13082-13088.

[18] Lipomi, D.J., et al., Electronic properties of transparent conductive films of PEDOT: PSS on stretchable substrates. Chemistry of Materials, 2012. 24(2): p. 373-382.

[19] Lang, U., N. Naujoks, and J. Dual, Mechanical characterization of PEDOT: PSS thin films. Synthetic Metals, 2009. 159(5-6): p. 473-479.

[20] Burgelman, M., et al., Modeling thin - film PV devices. Progress in Photovoltaics: Research and Applications, 2004. 12(2 - 3): p. 143-153.

[21] Farooq, W., et al., Enhancing the absorption and power conversion efficiency of organic solar cells. International journal of engineering works, 2019. 6: p. 94-97.

[22] MacKenzie, R.C., et al., Modeling nongeminate recombination in P3HT: PCBM solar cells. The Journal of Physical Chemistry C, 2011. 115(19): p. 9806-9813.

[23] Hanfland, R., et al., The physical meaning of charge extraction by linearly increasing voltage transients from organic solar cells. Applied Physics Letters, 2013. 103(6): p. 063904.

[24] Deschler, F., et al., Increasing organic solar cell efficiency with polymer interlayers. Physical Chemistry Chemical Physics, 2013. 15(3): p. 764-769.

[25] MacKenzie, R.C., et al., Extracting microscopic device parameters from transient photocurrent measurements of P3HT: PCBM solar cells. Advanced Energy Materials, 2012. 2(6): p. 662-669.

[26] Koster, L.J.A., et al. Performance enhancement of poly (3-hexylthiophene): methanofullerene bulk-heterojunction solar cells. in Organic Photovoltaics VII. 2006. International Society for Optics and Photonics.

[27] Koster, L., V. Mihailetchi, and P. Blom, Ultimate efficiency of polymer/fullerene bulk heterojunction solar cells. Applied Physics Letters, 2006. 88(9): p. 093511.

[28] Apaydın, D.H., et al., Optimizing the organic solar cell efficiency: role of the active layer thickness. Solar energy materials and solar cells, 2013. 113: p. 100-105.

[29] Hanna, M. and A. Nozik, Solar conversion efficiency of photovoltaic and photoelectrolysis cells with carrier multiplication absorbers. Journal of Applied Physics, 2006. 100(7): p. 074510.

[30] Fabiano, S., et al., Role of photoactive layer morphology in high fill factor all-polymer bulk heterojunction solar cells. Journal of Materials Chemistry, 2011. 21(16): p. 5891-5896.

[31] Vandewal, K., et al., The relation between open - circuit voltage and the onset of photocurrent generation by charge - transfer absorption in polymer: fullerene bulk heterojunction solar cells. Advanced Functional Materials, 2008. 18(14): p. 2064-2070.

How to cite this article:

Muhammad Zeeshan, Improving Efficiency and Stability of Organic Solar Cell, International Journal of Engineering Works, Vol. 7, Issue 10, PP. 375-378, October 2020, https://doi.org/10.34259/ijew.20.710375378.

IJEW 国际工程期刊 International Journal of Engineering Works انجینئرنگ کاموں کا بین الاقوامی جرنل

International Journal of Engineering Works
ISSN-p: 2521-2419
ISSN-e: 2409-2770
Vol. 7, Issue 10, PP. 379-383, October 2020
https://www.ijew.io/
https://doi.org/10.34259/ijew.20.710379383

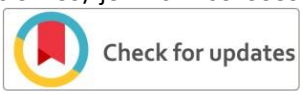

Response of Maize Yield Parameters to Different Inter Row Spacings and Sowing Methods

Shakir Ali[1], Zia Ul Haq[2], Abdul Malik[3]
[1,2,3]Department of Agricultural Engineering, University of Engineering & Technology Peshawar, Pakistan.
shakirali0661@gmail.com[1], chairagri@uetpeshawar.edu.pk[2], abdulmalik@uetpeshawar.edu.pk[3]
Received: 14 October, Revised: 20 October, Accepted: 24 October

***Abstract*—** A field work was conducted to evaluate the response maize yield parameters to different inter row spacing and sowing methods in district Mardan of Khyber Pakhtunkhwa, Pakistan, in 2019. A Randomized Complete Block Design (RCBD) was used for setting the experiment. All the treatments were replicated three times in the experiment. Five treatments i.e. S1 (Flat sowing with inter row spacing 0.60 m), S2 (Ridge-Furrow sowing with inter row spacing 0.60 m), S3 (Ridge-Furrow sowing with inter row spacing 0.75 m), S4 (Bed sowing with inter row spacing 0.60 m, in two row sowing, bed width 0.60 m) and S5 (Bed sowing with row spacing 0.75 m, in two row sowing, bed width 0.60 m) were evaluated. After performing the statistical analysis of the recorded data, it was noted that flat treatment S1 produced statically significant ($P<0.05$) higher kernel number (4.74 × 107 ha-1). While S5 produced minimum (3.52 × 107 ha-1) kernel number. Statistically no difference was observed in kernel number for S2, S3 and S4. Similarly, no significant difference was examined for number of rows per ear, number of kernels per row and number of kernels per ear among the different sowing methods. Therefore, it was concluded that to maximize maize kernel number (yield) it is suggested to use the flat method of sowing keeping the inter row spacing 0.60 m.

Keywords— Maize, Sowing methods, inter row spacing. Yield parameters.

I. Introduction

Transformers Agriculture is confronting a big challenge in completing the demand for agricultural products due to increasing population. Increasing population is a serious threat to food security. To reduce this food insecurity, the per hectare yield of major crops (like maize, wheat, rice etc.) should be increase [1]. According to a researcher, by 2050 the projected population will twice the present food requirements. To fulfill this demand the grain production need to be increased by 40 % [2].

In some (western) parts of the world, the term corn is interchangeably used for maize. This is because under early American and British trade all grains were called as corn. At that time Maize was the most commonly used grain for commerce so, the name also retained for it. It is believed that maize have originated from Mexico about 7000 years ago [3]. In the world almost 1050 million metric tons of maize produced in 2017 [4]. He added that FAO has forecasted that by 2050, 1200 million metric tons of maize will be harvested from only 200 million hectares of area.

In Pakistan about 60 percent maize production is used as a source of food for poultry purposes, 25 percent in different industries and the rest is used as a staple source of food by the human and animals [5]. Punjab and Khyber Pakhtunkhwa (KPK) is contributing 39% and 56% of the total area under maize respectively, similarly Punjab contributes 30% of the total production, KPK 63%, while Sindh and Baluchistan 5 % and 3 % [6]. Maize is mainly used for two purposes; primarily its grain is used as a source of food by humans and poultries also in various industries for extracting oil. Secondly, for farm animals it is used for forage purpose [7]. It has been predicted that by end of 2020 world population may reach over eight (8) billion [8]. Another prediction is that by the end of this century at least ten million people will remain hungry due to unavailability of food products [8].

Different planting techniques are used for raising the maize crop. The purpose of this study is to investigate the combine effect of both the sowing methods and inter row spacing on maize yield parameters in semi-arid region.

II. Materials and Method

Experiment was performed on summer maize in July 2019, in District Mardan. It is located (34º23′27″N, 71º55′33″E, 393 m Altitude) in Khyber Pakhtunkhwa, North of Pakistan. The site is semi-arid with mean annual precipitation of 557 mm occurs. Most rainfall occurs in the month of August. June is the hottest (41ºC) and January is the coldest (11ºC) month. The climate data was collected from the Sugar Crops Research Institute, Mardan, KPK, Pakistan. The Figure 1 represents the data concerning the temperature and precipitation of the experimental site.

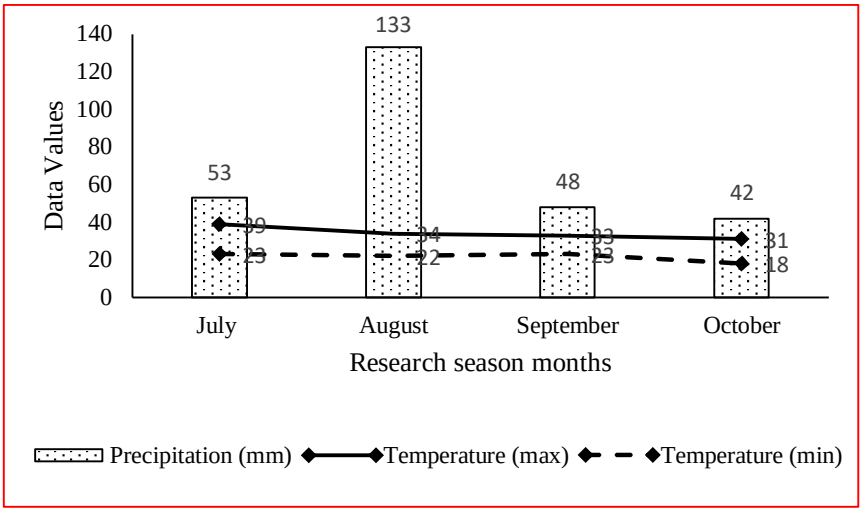

Figure 1: Precipitation and Temperatures at the experimental site

Before going towards the process of sowing the site was well irrigated. After attaining a proper soil moisture, the field was tilled properly two times to make the field fine for sowing. Fifteen plots of equal sizes (length 700 cm and width 610 cm) but of different patterns were made. Flat sowing method S1 row spacing 0.60 m, ridge method (S2) row spacing 0.60 m and ridge method (S3) row spacing 0.75 m, bed method (S4) row spacing 0.60cm and bed method (S5) row spacing 0.75 m were made in the field. A maize planter was used for sowing purpose to keep constant plant to plant distance. The plots were plotted according to a randomized complete block design. After one week, the area having no seedling emergence were refilled to maintain proper plant density. The fertilizer NPK was given to the fields i.e. ratio of 160:80:60 kg ha-1 as recommended by the Pakistan Agriculture Research Council (PARC). All the plots were well protected during the study period. Sketch of the five randomly assigned plots is given below:

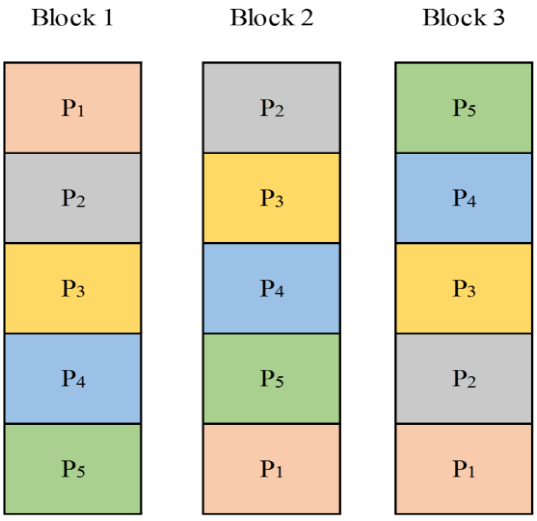

Figure 2: Sketch of randomly assign five sowing methods replicated three times

Data regarding the yield parameters is:

A. Number of Kernel Rows (ear-1)

Three average ears from each plot were selected. The number of rows in each ear was counted. The average number of rows per ear was calculated for each pattern.

B. Number of Kernels (row-1)

The ears taken for counting number of rows per ear, were used for counting the number of kernels per row. The number of kernels in each row was counted and averaged to calculate the number of kernels per row for each pattern.

C. Number of Kernels (ear-1)

After counting the number of rows and kernels in each row, the number of kernels per ear was calculated. The number of rows per ear were multiplied with the number of kernels per ear to get the number of kernels per ear. The average number of kernels ear-1 were taken for analysis purpose.

D. Kernels Number (ha-1)

At maturity stage (100 days after sowing) five representative ears from the center rows of the patterns were selected. The number of kernels per ear was counted. From the average number of kernels per ear, the number of kernels per treatment was calculated. The calculated number of kernels per treatment were converted to kernels per hectare.

According to completely randomized block design (CRBD) the data was analyzed [9] using MS-Excel and Statistix 8.1 software. Analysis of variance (ANOVA) and a pair wise multiple comparison of the five treatment mean values were calculated by the least significant difference test (LSD) at five percent level of probability.

III. Results and Discussions

A. Number of Kernel Rows (ear-1)

After statistical analysis of the recorded data (Table 1) it was observed that sowing method and row spacing combination

has no significant (P<0.05) effect on the number of kernel rows per ear. However, maximum kernel rows (14) were found in S1, S2 and S5. S3 and S4 produced 13.3 rows per ear (Figure 3). [10] have observed 15.44 kernel rows per ear using 60000 planting density as in our case in S5.

TABLE I. EFFECT OF PLANTING PATTERN AND ROW SPACING ON MAIZE YIELD PARAMETERS

Treatments	Number of kernel rows (ear^{-1})	Number of kernels (row-1)	Number of kernels (ear^{-1})	Kernels number $\times 10^7$ (ha^{-1})
S_1	14.00[a]	40.00[a]	556.00[a]	4.74[a]
S_2	14.00[a]	37.67[a]	527.33[a]	4.44[ab]
S_3	13.33[a]	41.33[a]	550.67[a]	3.41[ab]
S_4	13.33[a]	40.00[a]	532.67[a]	4.12[ab]
S_5	14.00[a]	39.33[a]	568.00[a]	3.52[b]
CV (%)	13.82	7.19	15.27	14.48

Means sharing the same letter (s) do not differ significantly at 0.05 level of probability.

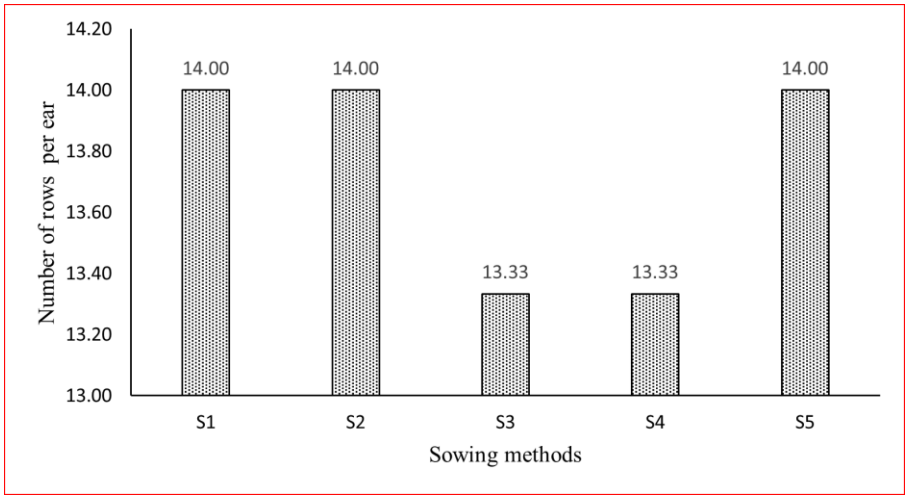

Figure 2: number of rows per ear in different sowing methods

B. Number of Kernels (row-1)

Data regarding the number of kernels per row was subjected to the statistical software Statistix. 8.1. From the results it was concluded that sowing method and row spacing combination has no significant (P<0.05) effect on the number of kernels per row. Maximum kernel per row (41.33) were observed in S3, while minimum (37.67) were found in S2 patten (Figure 4). [11] has observed the same effect that high plant density reduces the number of kernels per row as compared to low density.

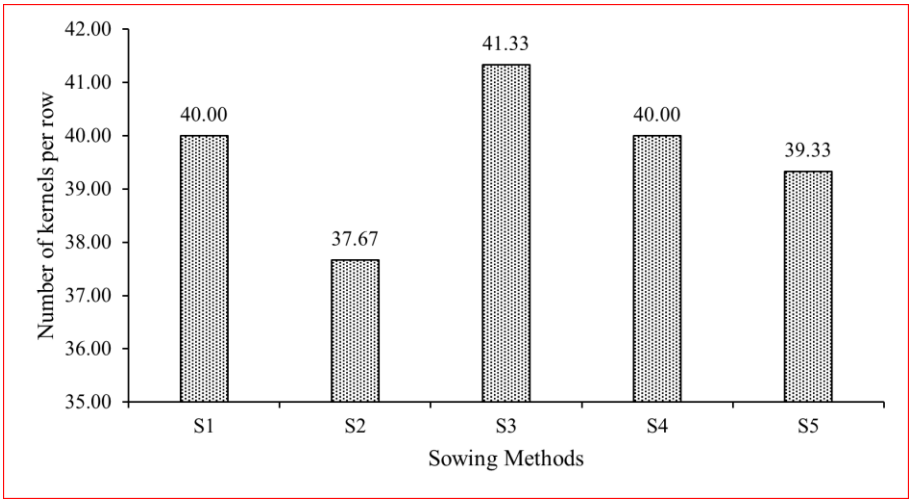

Figure. 3: Number of kernels per row in different sowing methods

C. Number of Kernels (ear-1)

Number of kernels per ear were analyzed to test the effect of different sowing methods and row spacings on the number of kernels per ear. it was observed that sowing method has not significantly (P<0.05) effected the kernels number per ear. However, maximum kernels per ear (568) were found in S5, followed by S1 (556) and S3 (550.67). S2 produced minimum (527.33) kernels per ear (Figure 5). [11] has concluded the same effect, that increased plant density reduces the kernel number per ear. [12] have observed maximum number of kernels (439.8) in ridge planting method followed by flat (412.8) as in our case.

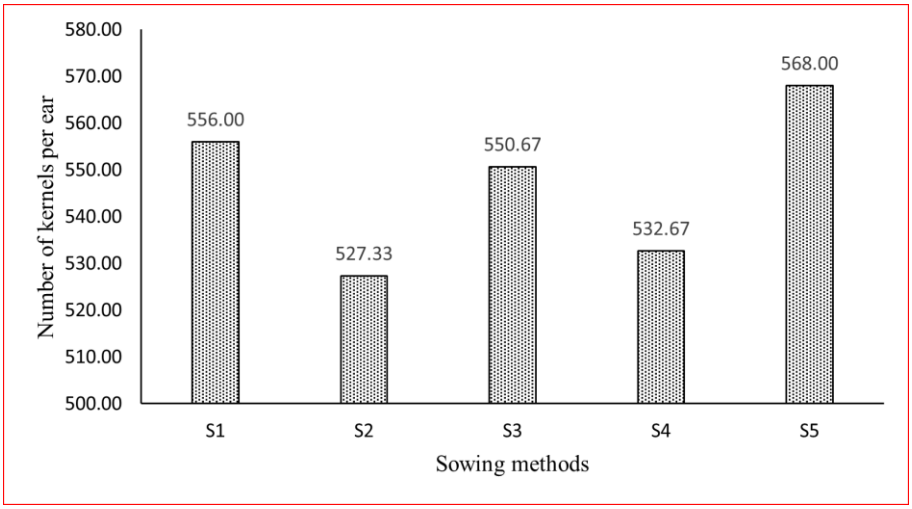

Figure. 4: Number of kernels per ear in different sowing methods.

D. Kernels Number (ha-1)

The data concerning to kernel number of maize plants as affected by different row spacings is presented in Figure 6. The statistical analysis of the data given in Table 1, revealed that planting pattern has a significant (P<0.05) effect on kernel number. Maximum (4.74×107 kernel ha-1) kernel number was observed in pattern S1 followed by S2 (4.44×107 kernel ha-1) while the minimum (3.41×107 kernel ha-1) were observed in pattern S3. Pattern P1 had statistically higher KN as compared to pattern S3 and S5. However, S2 and S4 have statistically no difference in their kernel numbers. [13] observed the similar fact. They conducted a field experiment to study the effect of row width and planting density upon the grain yield. They observed maximum grain yield at 90000 plants/ha. They observed 2% and 4% more grain yield as the row widths were narrowed i.e. from 0.76 m to 0.56 and 0.38 m. High plant density increases the kernel number as a result grain yield increas

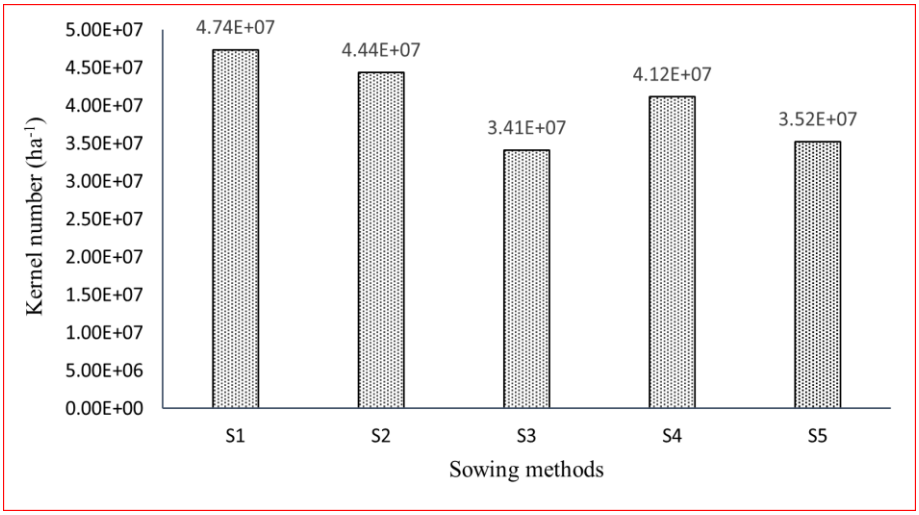

Figure. 5: Number of kernels number in different sowing methods

CONCLUSION

From the study it was concluded that sowing methods and row spacing does not affect the yield parameters. However, maximum kernel could be produced by using the flat method of sowing keeping 0.60 m row spacing.

ACKNOWLEDGMENT

The authors greatly acknowledge the analytical support from Dr. Kifayat Ullah.

REFERENCES

[1] M. Zamir, G. Yasin, H. Javeed, A. Ahmad, A. Tanveer, and M. Yaseen, "Effect of different sowing techniques and mulches on the growth and yield behavior of spring planted maize (Zea mays L.)," Cercetari agronomice in Moldova, vol. 46, pp. 77-82, 2013.

[2] Y. Niu, L. Zhang, H. Zhang, W. Han, and X. Peng, "Estimating Above-Ground Biomass of Maize Using Features Derived from UAV-Based RGB Imagery," Remote Sensing, vol. 11, p. 1261, 2019.

[3] P. Ranum, J. P. Peña - Rosas, and M. N. Garcia - Casal, "Global maize production, utilization, and consumption," Annals of the New York Academy of Sciences, vol. 1312, pp. 105-112, 2014.

[4] Á. Kovács, "Modelling of maize plant by the discrete element method," 2019.

[5] S. A. Raza, Y. Ali, and F. Mehboob, "Role of agriculture in economic growth of Pakistan," International Research Journal of Finance and Economics, 2012.

[6] K. Jabran, A. Zahid, and M. Faroo, "Maize: cereal with a variety of uses," DAWN–Business. Available on the: http://wwwdawn. com/2007/03/12/ebr5. htm, 2007.

[7] M. Ayub, R. Ahmad, A. Tanveer, and I. Ahmad, "Fodder yield and quality of four cultivars of maize (Zea mays L.) under different methods of sowing," Pakistan Journal of Biological Sciences, vol. 1, pp. 232-234, 1998.

[8] A. Saberi, "Effects of Plant Density and Planting Patterns on Yield and Yield Components of Corn (Zea mays L.) HSC 704 Cultivar," Int J Clin Med Info, vol. 2, pp. 18-23, 2019.

[9] K. A. Gomez and A. A. Gomez, Statistical procedures for agricultural research. Philippines: John Wiley & Sons, 1984.

[10] M. Abuzar, G. Sadozai, M. Baloch, A. Baloch, I. Shah, T. Javaid, et al., "Effect of plant population densities on yield of maize," The Journal of Animal & Plant Sciences, vol. 21, pp. 692-695, 2011.

[11] A. Hashemi - Dezfouli and S. Herbert, "Intensifying plant density response of corn with artificial shade," Agronomy Journal, vol. 84, pp. 547-551, 1992.

[12] J. Bakht, M. F. Siddique, M. Shafi, H. Akbar, M. Tariq, N. Khan, et al., "Effect of planting methods and nitrogen levels on the yield and yield components of maize," Sarhad Journal of Agriculture, vol. 23, p. 553, 2007.

[13] W. D. Widdicombe and K. D. Thelen, "Row width and plant density effects on corn grain production in the northern Corn Belt," Agronomy Journal, vol. 94, pp. 1020-1023, 2002.

How to cite this article:

Shakir Ali1, Zia Ul Haq, Abdul Malik, Response of Maize Yield Parameters to Different Inter Row Spacings and Sowing Methods, International Journal of Engineering Works, Vol. 7, Issue 10, PP. 379-383, October 2020, https://doi.org/10.34259/ijew.20.710379383.

IJEW 国际工程期刊 International Journal of Engineering Works انجینئرنگ کاموں کا بین الاقوامی جرنل

International Journal of Engineering Works
ISSN-p: 2521-2419
ISSN-e: 2409-2770
Vol. 7, Issue 10, PP. 384-389, October 2020
https://www.ijew.io/
https://doi.org/10.34259/ijew.20.710384389

The Reliability Analysis of PV Panels Installed in KP Region

Jawad Ahmad
MSc. Student USPCAS-E,EESE department, UET Peshawar
engr.jwd89@gmail.com
Received: 13 October, Revised: 19 October, Accepted: 24 October

***Abstract*--** Reliability and long term performance of photovoltaic (PV) system is of vital importance in switching from conventional sources to sustainable one. Design, study and analysis of key components in a photovoltaic power system starting from generation of power to withstands number of climatic stresses and uninterrupted power supply plays a key role. One of the key elements in photovoltaic system is photovoltaic module. Also power generated in photovoltaic system is dependent on a source of energy that changes in every instant and with the passage of time during its operation .Hence it is paramount to build a long lasting photovoltaic module and analyze characteristics of the PV module under various conditions. This paper presents an efficient PV module based on PV equivalent circuit model using MATLAB/Simulink, and compared the simulated model results with manufacturer's specifications like peak current, peak voltage, open circuit voltage and short circuit current .Also the performance of the module under variation of series resistance, irradiation, and temperature are analyzed. Data from five different areas across KP are noted and the results were Simulated and compared with the rated data.

Keywords: Matlab/Simulink, Irradiation, PV Module, Temperature.

Nomenclature used:
AM--- Air mass
A ---- Current in Amperes
W/m^2 --- Watts per meter square
KW ---Kilowatts
V --- Voltage
I --- Current
I_{sc}--- Short Circuit Current

V_{oc} --- Voltage Open Circuit
MWh ---- Mega Watt Hour
FF --- Fill Factor
STC --- Standard Test Conditions (25 °C, 1000 W/m^2)
G --- Irradiance
I_m --- Maximum current from PV
V_m --- Maximum voltage from PV
In^2 --- Inches square
KPK --- Khyber Pakhtunkhwa.

I. Introduction

Since 2008 Pakistan has experienced immense energy crisis, which resulted in 18 hours' power fall in remote area and around 12 hours in urban areas. Pakistan is blessed with a high potential of solar energy resources and is estimated that the annual sunshine in the country is about 3000-3300 hours [1], with daily effective sun-shine hours in most of its places are 7 to 8 hours [4]. Harvesting that potential the country has been flooded with different standards of PV panels, inverters, and batteries to fulfill the consumer energy demand. Initially due to lack of regulatory authorities mostly quality and installation guidelines were compromised.

The aim of this paper is to design a PV model, study the effect of different parameters on the system and collect data from different sites across KP, Pakistan for possible degradation and their performance variation from rated values during its course of operation, plot P-V and I-V graphs against their rated values. As for the large scale success of PV systems the long lasting performance, effective cost and ability to provide the desired results even in the severe conditions is paramount [3].

The end result concluded that raw material used in PV panels, system installing methodology, Vandalism, Array configuration and different climatic conditions have significantly affected the overall system performance and reliability.

II. PV Array's Equivalent circuit in MATLAB Simulink

The electrical equivalent circuit of photo Voltaic cell is shown in figure 1 (a). Here current in the cell are represented by Ip. Series and parallel resistances are represented by Rs and Rsh, these are the intrinsic resistances of the cell. In normal operating conditions the value of Rs are very low as compared to Rsh. That's why most the generated current passes through Rs. For the simplification purpose Rs is ignored [4]. In actual practices, PV cells are arranged in large groups which is called PV modules and their configuration is either series or parallel to form PV arrays, which produces electricity in PV generating plants. PV arrays equivalent circuit is shown in the figure 1.

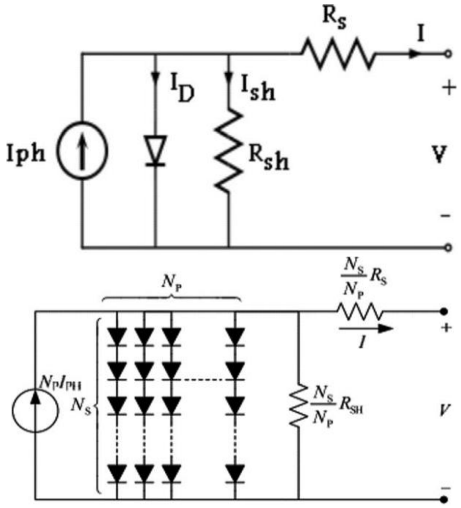

Figure 1: a) Solar Cell equivalent circuit (b) Solar Array equivalent circuit

The characteristics equation of voltage-current is provided as [5]

$$I_p = [I_{sc} + K_i(T - 298)] \times G/1000$$

Where,

I_p --- photo current (A)

I_{sh} --- Short circuit current (A)

K_i--- Short circuit current of cell at 25 ˚C and 1000 W/m^2

T --- Operating temperature (K)

G --- Solar irradiation (W/m^2)

Also the module reverses saturation current I_{rs}:

$$I_{rs} = I_{sc} / [\exp(q\, V_{oc}/N_s k n\, T) - 1]$$

As the cell temperature changes the module saturation current varies accordingly, the module saturated current expression is given as:

$$I_0 = \frac{I_{sc} + K_i(T - 298.15)}{\exp\left(\frac{q(V_{oc} + K_v(T - 298.15))}{aKTN_s}\right) - 1}$$

Where,

T --- Nominal temperature = 298.15 K

V_{oc} --- Open circuit voltage (V)

PV module output current is,

$$I = N_p \times I_p - N_p \times I_o \times \left[\exp\left(\frac{\frac{V}{N_S} + I \times \frac{R_S}{N_P}}{n \times V_t}\right) - 1\right] - I_{sh}$$

Where,

q --- Electron charge, = 1.6 × 10^{-19} C

N_s --- Number of cells connected in series

n --- The ideality factor of the diode

k --- Boltzmann's constant, = 1.3805 ^{23} J/K

III. Reference Model

Solar power module of 100 W is taken as reference module, based on the above mathematical equations the Simulink model developed is shown the figure 2 and 3.

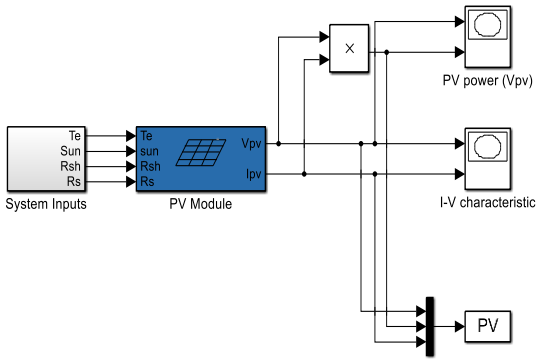

Figure 1: Block diagram of PV System

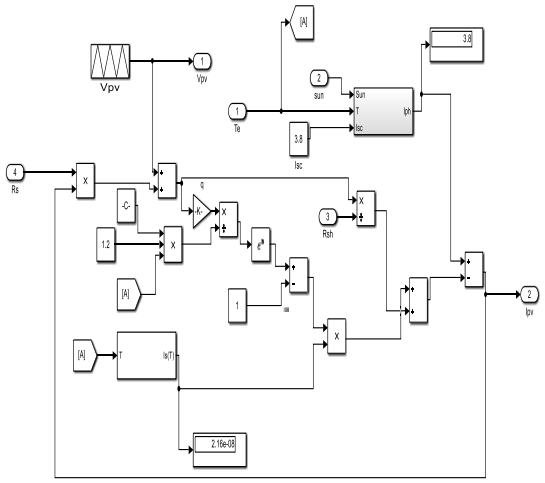

Figure 2: Mathematical model for PV module

The figure 3, shows the block diagram of PV system. The input parameters that change the entire system output are Temperature, Solar irradiance, Parallel resistance and series resistance of the circuit. The second figure 3.4, shows the PV

array mathematical model including the fundamental components of current source, shunt resistance and parallel resistor and diode in Simulink environment with tags. The value of constants as previously enlisted are feed in Simulink model.

IV. AND PV CURVES OF DIFFERENT SITES ACROSS KP

The ratings of the system and their respective I-V and P-V curves of different panels at different sites are as below;

A. Peshawar

Peshawar Pakistan (latitude 34.0151° N, longitude 71.5249° E), This system was installed in the mid of 2014 by local technicians and was placed on the roof top of the house, it has an installed capacity of 5.2 kW with 16 poly crystalline solar panels each of 325 W rating, 2 panels were connected in series to form a string and the strings were then connected in parallel. 84 V DC input were given to the inverter, the inverter had a rating of 5KW and had a battery bank, comprises of 8 batteries, each of 150 Ah. Data collected is shown in the given table 1.

TABLE 1: MODELING PARAMETERS FOR PESHAWAR SITE

S.No	1	2	3
Module temperature	45 ℃	45 ℃	45 ℃
Ns	60	60	60
Np	1	1	1
G W/m^2	835	830	840
Im (Rated)	8.66 A	8.66 A	8.66 A
Vm (Rated)	36.5 V	36.5 V	36.5 V
Pm (Rated)	325 W	325 W	325 W
Im (Noted)	7.01 A	6.98 A	7.03 A
Vm (Noted)	35.1 V	35 V	35.1 V

The readings were taken from various panels during my visit to the site. I-V and P-V curves were plotted for the rated and actual readings. As the actual measured readings were almost identical, so here in this section, one I-V and P-V curve has been plotted for the analysis as shown in figure 4.

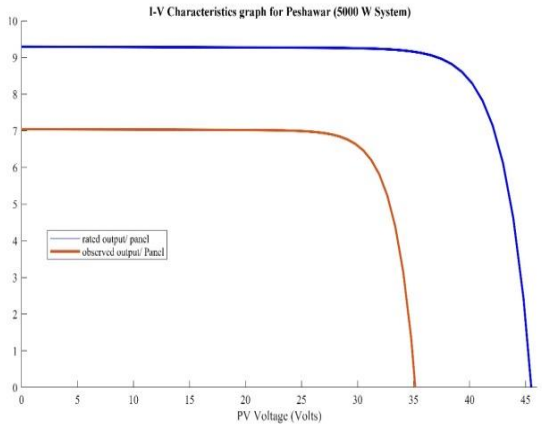

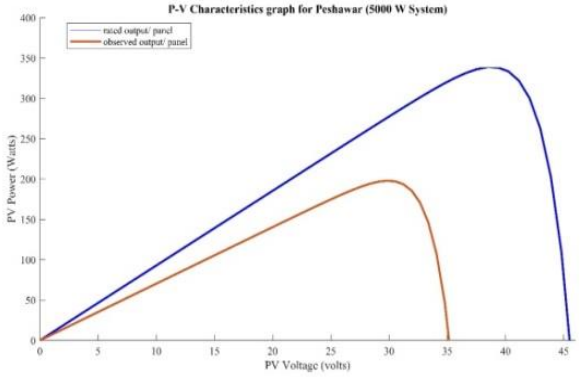

Figure IV: I-V and P-V Curve of PV for Peshawar site

As from the above curves in figure 4.5, it has been shown that the performance of all the panels on ground has varied by a reasonable margin from its rated values. From this analysis we can forecast the performance degradation of PV modules in coming years.

B. Swat

Swat Pakistan (latitude 35.2227° N, longitude 72.4258° E). The system was installed in the start of 2013 by local technicians according to the owner and was placed on the roof top of the house, it has an installed capacity of 3 kW with 12 poly crystalline solar panels each of 250 W rating, 2 panels were connected in series to form a string and the strings were then connected in parallel. 72 V DC input were given to the inverter, the inverter had a rating of 4 KW and had a battery bank, comprises of 4 batteries, each of 110 Ah. The collected data has been shown in the below table 2.

TABLE 2: MODELING PARAMETERS FOR SWAT SITE

S.No	**1**	**2**	**3**
Module temperature	38 ℃	38 ℃	38 ℃
Ns	72	72	72
Np	1	1	1
G W/m2	980	965	972
Im (Rated)	6.38 A	6.38 A	6.38 A
Vm (Rated)	36 V	36 V	36 V
Pm (Rated)	250 W	250 W	250 W
Im (Noted)	5.98 A	6.01 A	5.96 A
Vm (Noted)	34.5 V	34.48 V	34.49 V

The readings were taken from various panels during my visit to the site. I-V and P-V curves were plotted for the rated and actual readings. As the actual measured readings were almost identical, so here in this section, one I-V and P-V curve has been plotted for the analysis as shown in figure 5.

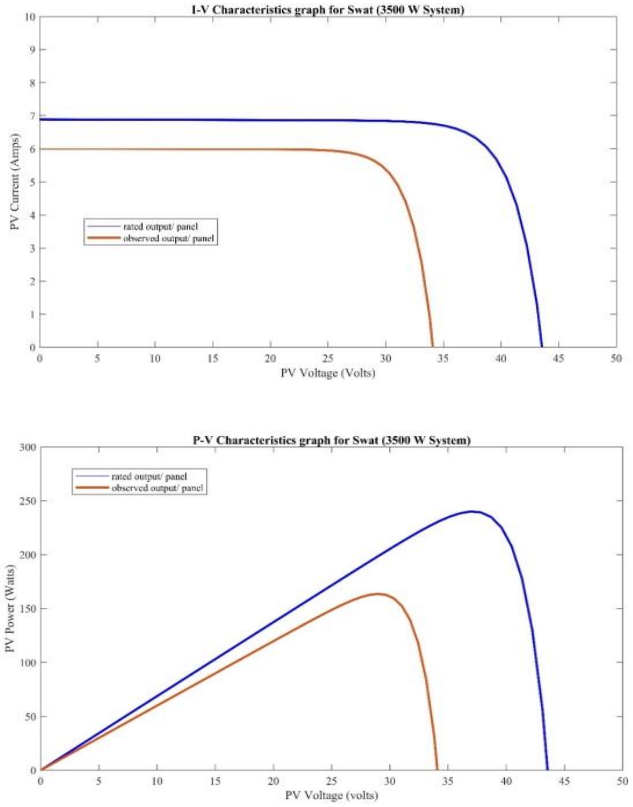

Figure 5: I-V and P-V Curve of PV for Swat site

As from the above curves in figure 4.5, it has been shown that the performance of all the panels on ground has varied by a reasonable margin from its rated values

C. Mardan

Mardan Pakistan (latitude 34.1989° N, longitude 72.0231° E). The system was installed in December,2013 by local technicians and was placed on the roof top of the house, it has an installed capacity of 4.32 kW with 16 poly crystalline solar panels each of 275 W rating, 2 panels were connected in series to form a string and the strings were then connected in parallel. 60.4 V DC input were given to the inverter, the inverter had a rating of 4 KW and had a battery bank comprises of 4 batteries, each of 110 Ah. Data collected is shown in the given table 3.

TABLE 3: MODELING PARAMETERS FOR MARDAN SITE

S.No	**1**	**2**	**3**
Module temperature	44 °C	44 °C	44 °C
Ns	72	72	72
Np	1	1	1
G W/m^2	884	859	875
Im (Rated)	8.72 A	8.72 A	8.72 A
Vm (Rated)	30.8 V	30.8 V	30.8 V
Pm (Rated)	270 W	270 W	270 W
Im (Noted)	6.15 A	6.2 A	6.17 A
Vm (Noted)	28.5 V	28.43 V	28.47 V

The readings were taken from various panels during visit to the site. I-V and P-V curves were plotted for the rated and actual readings. As the actual measured readings were almost identical, so here in this section, one I-V and P-V curve has been plotted for the analysis as shown in figure 6.

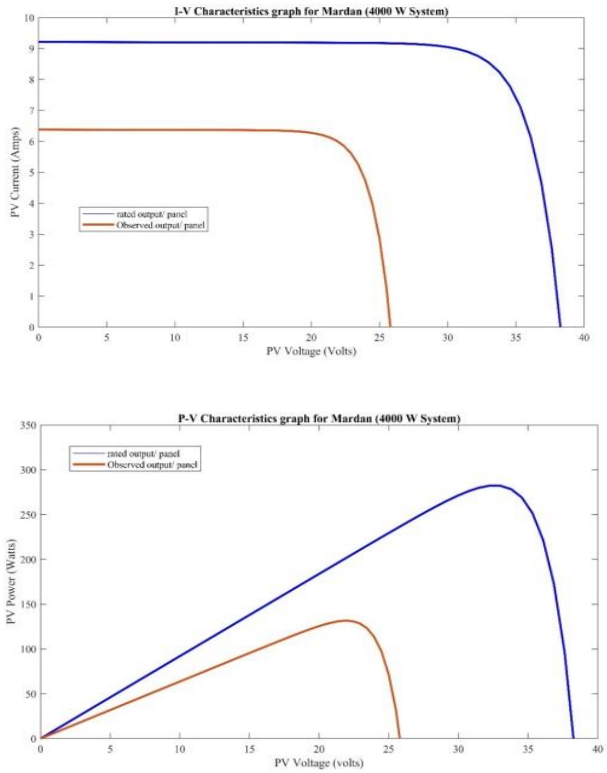

Figure 6: I-V and P-V Curve of Mardan site

As from the above curves in figure 4.7, it has been shown that the performance of all the panels on ground has varied by a reasonable margin from its rated values.

D. Swabi

Swabi (latitude34.1241° N, longitude 72.4613° E). The system was installed in March,2014 by local technicians and was placed on the roof top of the house, it has an installed capacity of 2.4 kW with 8 mono crystalline solar panels each of 300 W rating, 2 panels were connected in series to form a string and the strings were then connected in parallel. 78 V DC input were given to the inverter, the inverter had a rating of 2.4 KW and had a 2 batteries backup, each of 110 Ah in table 4.

TABLE 4: MODELING PARAMETERS FOR SWABI SITE

S.No	**1**	**2**	**3**
Module temperature	43 °C	43 °C	43 °C
Ns	60	60	60
Np	1	1	1
G W/m^2	903	898	890
Im (Rated)	8.3 A	8.3 A	8.3 A
Vm (Rated)	36.1 V	36.1 V	36.1 V
Pm (Rated)	300 W	300 W	300 W

Im (Noted)	7.03 A	6.99 A	7.01 A
Vm (Noted)	31.9 V	31.9 V	31.88 V

The readings were taken from various panels during my visit to the site. I-V and P-V curves were plotted for the rated and actual readings. As the actual measured readings were almost identical, so here in this section, one I-V and P-V curve has been plotted for the analysis as shown in figure 7.

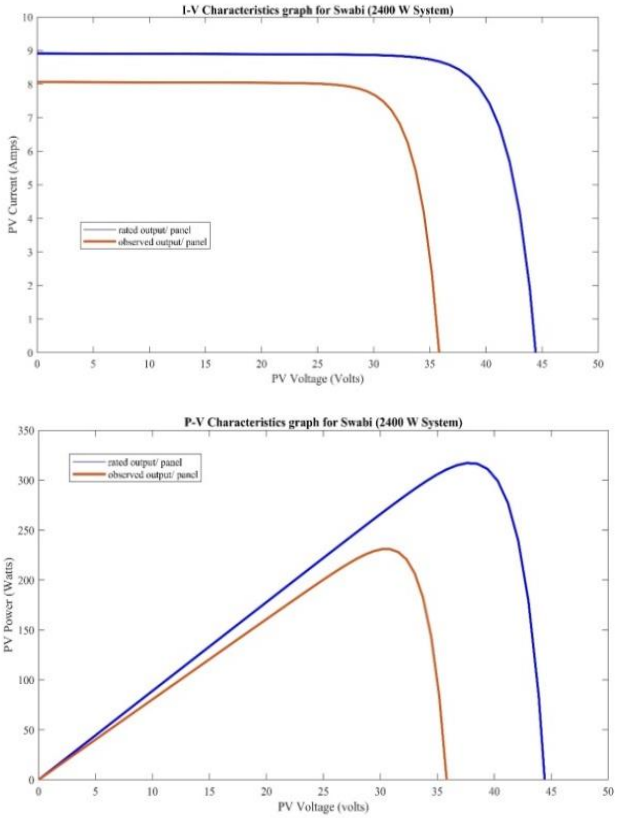

Figure 7: I-V and P-V Curve of PV from Swabi site

As from the above curves in figure 4.8, it has been shown that the performance of all the panels on ground has varied by a reasonable margin from its rated values.

4.4. Lower Dir

Lower Dir Malakand division Pakistan (latitude 34.9161° N, longitude 71.8097° E). This system was installed in April,2013 by local technicians and was placed on the roof top of the house, it has an installed capacity of 4160 kW with 16 poly crystalline solar panels each of 260 W rating, 2 panels were connected in series to form a string and the strings were then connected in parallel. 62 V DC input were given to the inverter, the inverter had a rating of 5 KW and had a 4-battery backup, each of 150 Ah.

TABLE 5: MODELING PARAMETERS FOR LOWER DIR SITE

S.No	**1**	**2**	**3**
Module temperature	37 °C	37 °C	37 °C
Ns	60	60	60
Np	1	1	1
G W/m^2	954	961	949
Im (Rated)	8.3 A	8.3 A	8.3 A
Vm (Rated)	31.1 V	31.1 V	31.1 V
Pm (Rated)	260 W	260 W	260 W
Im (Noted)	7.05 A	7.01 A	6.99 A
Vm (Noted)	28.03 V	28.05 V	28.00 V

The readings were taken from various panels during my visit to the site. I-V and P-V curves were plotted for the rated and actual readings. As the actual measured readings were almost identical, so here in this section, one I-V and P-V curve has been plotted for the analysis as shown in figure 8.

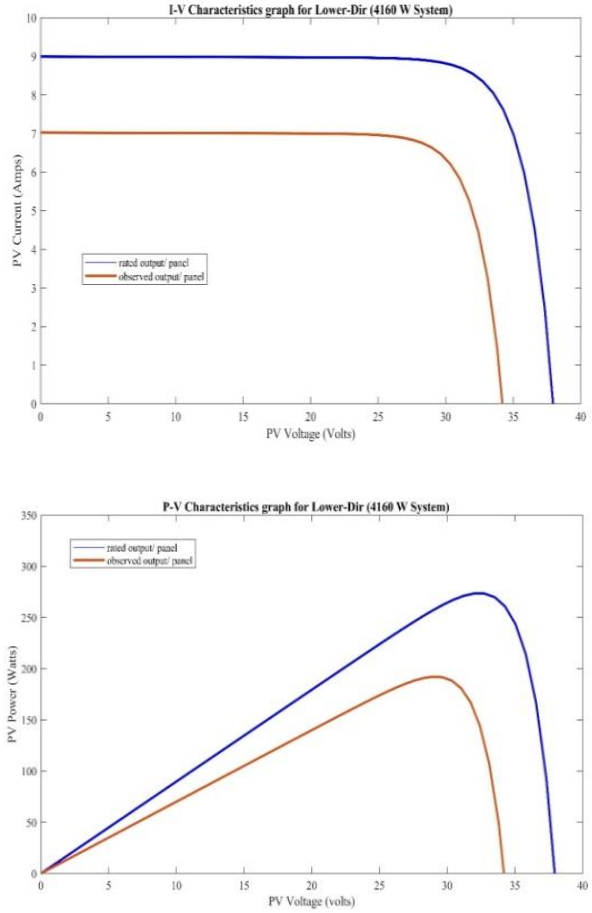

Figure 8: I-V and P-V Curve of PV from Lower Dir site

As from the above curves in figure 4.9, it has been shown that the performance of all the panels on the ground has varied by relatively fewer margins from its rated values.

CONCLUSION

To illustrate the long term performance and variation from the rated data over a course of time during operation, I selected five different sites across KPK, visited the all the sites and noted its system capacities, installation Methods and checked for all possible visual degradation since from their installation till date. I put all the acquired data into my

MATLAB model with the temperature, Series and Parallel combination noted from each site and acquired the I-V and P-V curves of the noted data and compared with the rated capacities of each panel mention on its nameplate. It reveals the decrease in power capacities over a course of time as some cells perform poorly after ye.ars of operation.

REFERENCES

[1] I. Ulfat, F. Javed, F. A. Abbasi et al., "Estimation of solar energy potential for Islamabad, Pakistan," Energy Procedia, vol. 18, pp.1496–1500, 2013.

[2] M. Ashraf Chaudhry, R. Raza, and S. A. Hayat, "Renewable energy technologies in Pakistan: prospects and challenges," Renewable and Sustainable Energy Reviews, vol. 13, no. 6-7, pp. 1657–1662, 2009.

[3] Wohlgemuth, J. H., Cunningham, D. W., Nguyen, A. M., Miller, J., "Long Term Reliability of PV Modules," Proceedings of the 20th European Photovoltaic Solar Energy Conference, Barcelona, Spain, 2005

[4] Pandiarajan N, Muthu R (2011) Mathematical modeling of photovoltaic module with Simulink. International Conference on Electrical Energy Systems (ICEES 2011), p 6

[5] Salmi T, Bouzguenda M, Gastli A, Masmoudi A (2012) Matlab/simulink based modelling of solar photovoltaic cell. Int J Renew Energy Res 2(2):6

How to cite this article:

Jawad Ahmad, The Reliability Analysis of PV Panels Installed in KP Region, International Journal of Engineering Works, Vol. 7, Issue 10, PP. 384-389, October 2020, https://doi.org/10.34259/ijew.20.710384389.

IJEW 国际工程期刊 International Journal of Engineering Works انجینئرنگ کاموں کا بین الاقوامی جرنل

International Journal of Engineering Works
ISSN-p: 2521-2419
ISSN-e: 2409-2770
Vol. 7, Issue 11, PP. 390-393, November 2020
https://www.ijew.io/
https://doi.org/10.34259/ijew.20.711390393

Optimization of Shape, Size and Material of Plasmonic Nano Particles in Thin Film Solar Cell

Asadullah[1], Fazal E Hilal[2]
[1,2] University of Engineering and Technology Peshawar, Pakistan, U.S Pakistan Center for Advanced Studies in Energy (USPCAS-E)
asadullah8080@gmail.com[1]
Received: 19 October, Revised: 27 October, Accepted: 04 November

***Abstract*—** In this study we present optimized shape, size and material of plasmonic nanoparticles in thin film solar cell. For this purpose, we chose silicon active layer solar cell, on the top of active layer another layer of silicon dioxide was used as antireflection coating. Thickness of ARC layer was kept 71nm. On the top of ARC layer metallic nanoparticles were placed. Parameters of NP's such as shape, size and material were varied. Respective variations in the absorption of light in the active silicon layer were observed respectively. Absorption patterns were plotted against wavelength range of 400nm to 1400nm of incident light radiation using Finite Element Method (FEM).

Results revealed the most optimized size and shape of nanoparticles that can contribute to the absorption of light in the active layer of the solar cell. Results also distinguished the best material for nanoparticle.

***Keywords*—** Nanoparticles, Array, Absorption, Wavelength Renewable Energy.

I. INTRODUCTION

On the basis of advancement in technology solar cells can be divided into three generations namely first generation, second generation and third generation. First generation solar cells are known for their high-cost and high efficiency [8]. But production of first generation solar cells is a laboured task which is one of the major factor that are responsible for its high cost. second generation solar cells also called thin film solar cells emerged in 1990's as a mean to reduce the material costs. But because of thin active layer they cannot absorb sufficient amount of light and most of the light transmit through the cell. An alternative way to enhance capability of photo-catalyst or photo-electrode to absorb more light is the use of photosensitizer for e.g. certain inorganic quantum dots and organic dyes. Unluckily organic dyes can absorb only a narrow band of visible spectrum, and are less stable when exposed to solar radiation. The transfer rate of electron to the active semiconductor layer from quantum dots is slower and relatively inefficient. Moreover, most of the inorganic quantum dots produce toxic effects under sunlight and are highly unstable [21]. Plasmonic metal nanoparticles on the other hand have ability to absorb broad light absorption band and provide larger absorption cross-section, which results excellent photosensitization in semiconductor material.

Furthermore, plasmonic metal nanoparticles can also be used for scattering and trapping of radiation [22].

Recently, verity of nanostructures has been used in thin film solar cells to improve the absorption efficiency, such as Park experementally presented the performance enhancement of organic photovoltaic by using plasmonic gold nanoparticle clusters [29], Cheng Sun reported on silver nanoparticles based structural design of thin film solar cell, in which they used silicon as absorbing layer [17], P.H.Wang used hydrogenated amorphous silicon as an active absorbing layer, silver nanoparticles of random size and with different fixed periodic inter–particle placement, a silver mirror as back reflector [30], ZhixiaoWang et al reported a study of front surface modification of silicon solar cell [32], Knight et al used metallic nano antennas to enhance light absorption. Among these all surface plasmons resonances structure of metals have drawn much attention due to enhanced solar radiation absorption in thin active layer. The simultaneous excitation of the free electrons in nanoparticles and the energy incident light, through the excitation of surface plasmon resonances (SPR), strong near field enhancement and high scattering cross-sections of light absorption can be attained. Till date many studies exist regarding surface plasmon enhances light absorption using metals mostly silver and gold NP's.

In this study, Optical simulations were used to examine and compare the effect of three different kinds of nanoparticles namely gold, aluminum and silver.

II. METHODOLOGY

The Different techniques and tools are used word wide for the purpose of simulation, these techniques include Finite Difference Time Domain (FDTD), Integral Equation (IE), and Finite Element Method (FEM). Various tools are used that can carry out results by using any of the above mentioned techniques, among these tools, COMSOL is one the frequently used and detailed to study the nature and behavior of the nanoparticles.

Therefore, for the current study we preferred COMSOL over all other tools. This tool is based upon the Finite Element Method (FEM), which is one the most efficient techniques for solving electromagnetic problems and produce results that are nearest to the real ones.

We used COMSOL to study the absorption of radiation in the thin film solar cell. nanoparticles sprinkled over the active silicon layer were subjected to light radiation. Transmission T(ω) through solar cell and Reflection R(ω) from the top surface of the assembly were calculated directly during the simulation. The parameter of interest i.e. Absorption A(ω) was calculated from the following equation.

$$A(\omega) = 1 - R(\omega) - T(\omega)$$

Where 'I' is the total incident light falling on the surface of solar cell. All three parameters Transmission, Reflection, Absorption are treated as a function of frequency of light. The structure is composed of mainly three layers, top layer is composed of nanoparticles, in this case we used three different types of metals i.e. gold, silver and aluminum, second layer is antireflection layer, in which Silicon dioxide (SiO2) is used as an anti-reflecting material. The bottom layer is active silicon layer. All parameters and dimension of the model and the cuboidal box are studied on nanoscale. The data obtained from COMSOL multiphysics and was furthered analyzed in MATLAB.

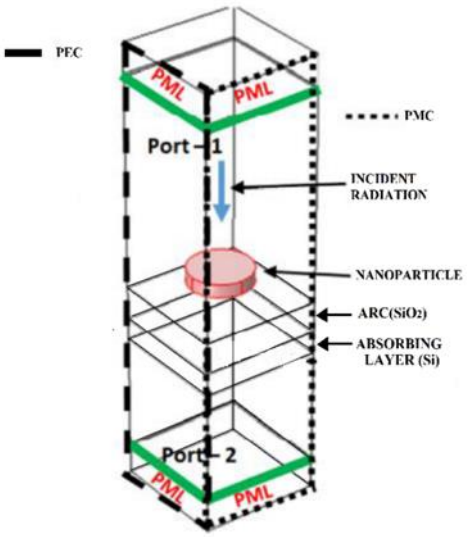

Figure 1 Model of Three layered thin film solar cell

III. Results and Discussion

A. Impact of Material of Nanoparticle on Absorption

Material of nanoparticles plays an important role in the enhancement of photocurrent density in thin-film solar cells. In this work we used nanoparticles made of three different kinds of material i.e. gold (Au), silver(Ag) and aluminum(Al) these three material were selected on the basis of their good conducting properties [1, 2]. Both optical and electrical properties were observed for all three materials under identical circumstances, and were compared at the end. The comparison is shown in figure 2. Results revealed that all material exhibit almost similar impact on absorption of light, except a few distinguished peak by each material [3]. Beside this other physical parameter were also considered such as cost effectiveness, availability, stability etc. By further investigation we explore that as compare to Aluminum; Gold and Silver have more conduction losses, moreover, these materials are costlier than Aluminum [4]. On the other way around Aluminum is one of the most available element on the earth crest and is less costly as compare to gold and silver. Further Aluminum is stable to outer environment.

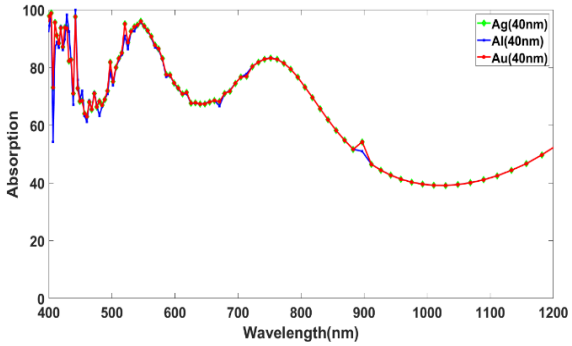

Figure 2 Comparison Among Three Different Types Of Materials

B. Impact of Shape of Nanoparticle

Shape is another crucial parameter that plays an important role in the absorption of light. Keeping in view previous works, process of fabrication and impact on light absorption, we selected five different shapes for nanoparticles i.e. circular disc, sphere, pyramid, rectangle, and square. Nanoparticles were placed in XY plane on the top surface of thin film solar cell [5]. The light beam was directed on the NP's from above in the negative Z-direction. Nanoparticles of all shapes were subjected radiation under similar conditions. The absorption pattern of radiation was obtained and was plotted for all shapes against wavelength ranging from 400nm to 1200nm. All the results obtained were compared and plotted in one graph shown in figure 3.

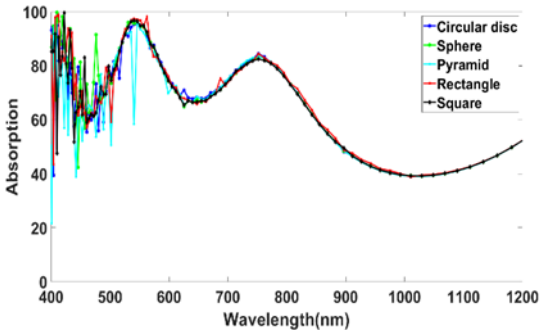

Figure 3. Absorption of light with respect to wavelengths of incident light by using different nanoparticles shapes: circular discs, sphere, pyramid, rectangular and Square

C. Impact of Size of Nanoparticle on Absorption

After optimizing the shape, size of nanoparticle is an important parameter that cannot be ignored. Size of nanoparticles contribute a vital role in the absorption of light radiation and in turn the photocurrent density in the active layer of solar cell. For the purpose of optimization of size, the size of

nanoparticle was governed by varying it under unchanged circumstances [6]. Five sizes (radii) were tested on the top surface of solar cell i.e. 20nm, 40nm, 60nm, 80nm and 100nm. Sizes of nanoparticles were varied under similar condition [7]. Results of each size was plotted against wavelength at the end all absorption patterns were analyzed, compared and were plotted in single graph as shown in figure 4.

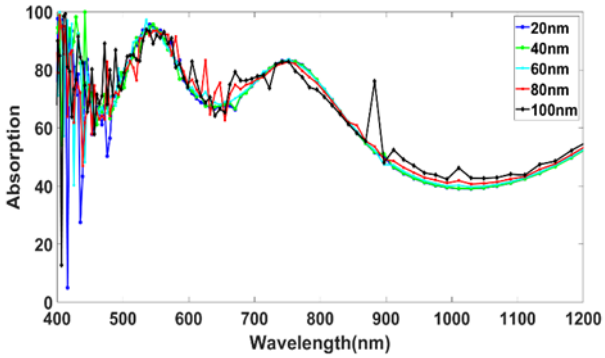

Figure 4. Optimization of size of nanoparticles: Absorption curves for 20nm, 40nm, 60nm, 80nm and 100nm

CONCLUSION

Considering both optical and electrical properties of nanoparticles, three types of nanoparticles were used in current work i.e. Aluminum, Gold, and Silver. Nanoparticles of all three were deposited on the top surface of solar cell, and subjected to light radiation under identical condition.

Almost all three types of nanoparticles showed similar results, except with some of the exceptional peaks by each type. Considering the impact of types of nanoparticles along with other parameters such as stability, radial availability of raw material, and cost effectiveness, we found that gold and silver exhibit electrical losses as compare to Aluminum. Further gold and silver possess more cost than aluminum. On the other hand, aluminum is available radially, and is more stable in open environment. We concluded from the above discussion and simulation results that, Aluminum is the best choice among all three types of nanoparticles.

To study the impact of shape of nanoparticles on the current density in the active layer of solar cells, we established a rational relationship between light absorption and shape of the nanoparticles. Five different types of nanoparticles were used for this purpose namely, circular disc, sphere, square, and rectangular. Among all experimented shape, we observed that sphere shape is the most optimized size of nanoparticle as shown in the figure. Beside the impact on absorption of light, sphere nanoparticles are capable of producing high, surface plasmons, polaritron, strong near field enhancement and larger scattering angle [8, 9]. These are the most important parameters for enhanced current density.

Optimization of size of nanoparticles was governed by varying the size of sphere nanoparticles as 20nm, 40nm, 60nm, 80nm and 100nm. All size nanoparticles were exposed to light under similar condition. Results for each size were plotted against the range of wavelengths. As the size of nanoparticles went on increasing, the current density/absorption increased accordingly. Selecting the optimized size of nanoparticles was a crucial step then.

We found that nanoparticle of 40nm showed dominant curve in the range of lower visible wavelength i.e. 400 to 450nm. In wavelength 450 to 550nm, nanoparticles of all radii produce almost similar curves, except 100nm showing dominancy towards the end. Nanoparticles of 80nm showed dominant curve in the wavelength range of 550 to 680nm. From 680 to 850nm all nanoparticles showed better and almost similar behavior except 100nm nanoparticles. Nanoparticles of 100nm dominated in the wavelength range 850 and onward.

Analysis of simulations revealed that nanoparticles of 80nm and 100nm have more peaks as compare to other radii. Considering other parameters, process of fabrication and specially cost effectiveness we realized that nanoparticles of radius 40nm can overcome the lower current density by its lower cost. The efficiency to cost ratio of 40nm is far more than others sizes.

REFERENCES

[1] A. D. Khan and G. Miano, "Higher order tunable Fano resonances in multilayer nanocones," Plasmonics, vol. 8, pp. 1023-1034, 2013.

[2] A. D. Khan and G. Miano, "Investigation of plasmonic resonances in mismatched gold nanocone dimers," Plasmonics, vol. 9, pp. 35-45, 2014.

[3] A. D. Khan and M. Amin, "Tunable salisbury screen absorber using square lattice of plasmonic nanodisk," Plasmonics, vol. 12, pp. 257-262, 2017.

[4] A. D. Khan, A. D. Khan, S. D. Khan, and M. Noman, "Light absorption enhancement in tri-layered composite metasurface absorber for solar cell applications," Optical Materials, vol. 84, pp. 195-198, 2018.

[5] W. Farooq, A. D. Khan, M. Khan, and J. Iqbal, "Enhancing the absorption and power conversion efficiency of organic solar cells," International journal of engineering works, vol. 6, pp. 94-97, 2019.

[6] S. Jamal, A. D. Khan, and A. D. Khan, "High performance perovskite solar cell based on efficient materials for electron and hole transport layers," Optik, p. 164787, 2020.

[7] W. Farooq, A. D. Khan, A. D. Khan, A. Rauf, S. D. Khan, H. Ali, et al., "Thin-Film Tandem Organic Solar Cells With Improved Efficiency," IEEE Access, vol. 8, pp. 74093-74100, 2020.

[8] F. E. Subhan, A. D. Khan, F. E. Hilal, A. D. Khan, S. D. Khan, R. Ullah, et al., "Efficient broadband light absorption in thin-film a-Si solar cell based on double sided hybrid bi-metallic nanogratings," RSC Advances, vol. 10, pp. 11836-11842, 2020.

[9] F. E. Subhan, A. D. Khan, A. D. Khan, N. Ullah, M. Imran, and M. Noman, "Optical optimization of double-side-textured monolithic perovskite–silicon tandem solar cells for improved light management," RSC Advances, vol. 10, pp. 26631-26638, 2020

Asad Ullah received B.Sc. degree in Electrical Engineering from the University of Engineering and Technology (UET), Lahore, Pakistan, in 2016. He has completed his Master degree in Renewable Energy Engineering from U.S Pakistan Center for Advanced Studies in Energy, UET, Peshawar, Pakistan.

His research interests include optoelectronic modeling of photovoltaic devices, photonics nano-technology for light management in third generation solar cell, renewable energy materials & technology modeling, smart grid and power electronics.

How to cite this article:

Asadullah, Fazal E Hilal, Optimization of Shape, Size and Material of Plasmonic Nano Particles in Thin Film Solar Cell, International Journal of Engineering Works, Vol. 7, Issue 11, PP. 390-393, November 2020, https://doi.org/10.34259/ijew.20.711390393.

International Journal of Engineering Works
ISSN-p: 2521-2419
ISSN-e: 2409-2770
Vol. 7, Issue 11, PP. 394-400, November 2020
https://www.ijew.io/
https://doi.org/10.34259/ijew.20.711394400

Comparative Analysis of PV System Performance in Different Environmental Conditions

Muhammad Azaz[1], Sajad Ullah[2], Jawad Ul Islam[3]
[1,2,3]Department of Electrical Energy System Engineering, US-Pakistan Center for Advanced Studies in Energy (US-PCASE), UET Peshawar
azazkhan8511@gmailcom[1], sajad.ullah@yahoo.com[2], jawad_ulislam@ yahoo.com[3]
Received: 10 November, Revised: 15 November, Accepted: 23 November

***Abstract*—** Apart from many other factors the overall performance of PV depends on temperature and solar irradiance because as the day progresses the energy received by PV panels from the sun changes and temperature also changes throughout the day. In this paper effects of temperature and solar irradiance variation were studied on a 240V PV panel's maximum power, efficiency, and fill factor. The model is designed in Simulink/Matlab software which has two variable inputs in the form solar irradiance and temperature and three output parameters i.e. efficiency, fill factor and maximum power. First the performance parameters are observed under STC conditions and then one of the input is changed from STC whereas the other one is kept constant. At the end the second input is varied whereas the first one is held at STC. Simulations were performed and results obtained in terms of maximum power, efficiency and fill factor shows percent variation from its reference value for every one degree centigrade change in temperature and for every 20W/m2 change in the solar irradiance.

***Keywords*—** Temperature, Irradiance, Efficiency, Fill Factor, Maximum power, Matlab/Simulink.

I. INTRODUCTION

Because of increased energy demand and current energy crises traditional energy sources are declining and are unable to meet the energy demands of the world. Furthermore the conventional energy sources has a negative impact on our environment and causes many problems like air pollution, acid rain and greenhouse effect etc [1]. Therefore renewable energy (RE) is becoming a global source of clean and environmental friendly energy for the earth. The most common and world widely used source of renewable energy is sun. Energy from sun can be obtained by many ways like solar thermal, solar PV and solar heat. But using photovoltaic effect which is the most sustainable and essential source of renewable energy has shown a great success [2]. In Photovoltaic system electricity is generated by solar cells. A semiconductor device which directly converts solar energy to electrical energy using the PV effect is called a photovoltaic or solar cell. Photovoltaic cells are mostly made of silicon which may be non-crystalline, polycrystalline or crystalline depending upon the efficiency of cell and cost of material used [3]. A PV panel is formed as a result of several combinations of solar cells, which are installed on the rooftop of our homes and is used at basic level. The combinations of solar panels forms PV arrays, these arrays consists of thousands of identical cells which works as a local power station, and can be used at residential, commercial and industrial level [4]. According to a report published by international agency of energy the photovoltaic (PV) is going to produce 11% of the electricity produced by the whole world, which is going to reduce the emission of carbon dioxide (CO2) by an amount of 2.3 Giga tons per annum[5]. Several environmental factors effects the performance of a PV panel like temperature, wind, humidity, solar intensity, dust and rain etc. But the two fundamental factors which changes the efficiency, fill factor and maximum power of a solar panel to a great extent are solar irradiance and operating temperature [6]. Although PV panel performance decreases with increase in temperature (T), but the temperature at standard test conditions also has a significant impact on the performance parameters of a PV panel as it has linear relation with the performance of a PV Panel [7]. In addition to temperature solar irradiance (G) also greatly impact performance parameters of a solar panel. With an increase in solar irradiance both open circuit voltage (Voc) and short circuit current (Isc) changes because of which the maximum power (Pmax) varies with it [8]. As these two factors have a great non-linear behavior and changes continuously at any interval of time, however temperature is directly responsible for a change in voltage of a solar panel. With an increase in temperature of the panel its voltage decreases and vice versa. Similarly current of the panel varies greatly with a change in solar irradiance of the panel [9]. Now with variation in either current or voltage or both will eventually affect the performance of a PV. The three performance parameters of a PV panel are functions of PV module current and voltage. So with variation in current and voltage, which is caused by temperature and irradiance variation, will eventually causes a disparity in performance parameters of the PV system [10].

II. METHADOLOGY

The system for 240V PV panel is designed in Simulink/Matlab which is very useful tool for modeling, simulation and modulation analysis of dynamic systems. The inputs to the panel are irradiance and temperature, while its output includes currents and voltages namely voltage at maximum power point (Vmax), current at maximum power point (Imax), open circuit voltage (Voc) and short circuit current (Isc). These four parameters are very useful and are first studied under STC then at varying temperature (21oC to 29oC) and at the end at varying irradiance (0.92KW/m2 to 1.08KW/m2). The performance parameters are then measured with the help of these basic parameters.

A. Open circuit voltage

It is the maximum available voltage at the output of the PV panel at no load. The net current at Voc inside PV is zero. The Voc is dependent on temperature and irradiance and is given by the following equation.

$$Voc = Voc0 + D.Vt.log(G/Go) + Kv.(T - To) \quad (1)$$

Here Voc0 is STC conditions open circuit voltage, D is diode ideality factor, T and G are the respective temperature and irradiance values at which Voc is measured, Kv (-0.369%/oC) represents the temperature coefficient of voltage and Vt is the terminal voltage which is given by

$$Vt = (Ns.Kb.T)/q \quad (2)$$

Here Ns (60) is the number of cells per module and Kb is the Boltzmann constant (1.3806*10^-23Kg.m2.K-1.s-2) and q represents electronic charge (1.602*10^-23C).

B. Short circuit current

It is the output current at zero voltage i.e. when the panel is short circuited. It is the highest value of y-axis at I-V curve when then the x-axis value is zero. It is also dependable on temperature and irradiance. The equation of Isc is given by

$$Isc = (G/Go).(Isc0 + Ki(T - To)) \quad (3)$$

Where Isc0 is STC condition short circuit current and Ki represents the temperature coefficient of current (0.087% /oC). The above equation clearly indicates that the effect of solar irradiance will be more as compare to that of the temperature, which is exactly converse of its effects on Voc.

C. Voltage at maximum power point

It is also known as peak power voltage and it is the actual maximum voltage available at the output when the system is under loaded condition. Like the open circuit voltage Vmax also depends on temperature and solar irradiance except that it has no diode ideality factor and its equation is written as

$$Vmax = Vmax0 + Vt.log(G/Go) + Kv.(T - To) \quad (4)$$

D. Current at maximum power point

The current at which a PV panel generates maximum power is known as its maximum current (Imax). Its value is also depends upon the behavior of temperature and irradiance. The relationship between Imax and the two input variables is given by the equation.

$$Imax = (G/Go).(Imax0 + Ki(T - To)) \quad (5)$$

III. PERFORMANCE PARAMETERS

A. Maximum power produced by the panel

The maximum output power of a panel which is represented by the knee of a V-I curve is known as maximum power (Pmax) of that PV panel. The maximum power of a panel is mainly affected by open circuit voltage (Voc) and short circuit current (Isc), and both these terms are directly varied by temperature and solar irradiance. So this means that Pmax is dependent on temperature and solar irradiance. it is first observed on STC conditions then temperature is varied from STC (To=25oC) and irradiance is kept constant and then solar irradiance is varied from its STC (Go=1000 W/m2) and temperature is kept constant.

B. Efficiency of the panel

The measure of sunlight energy which is directly convertible to electrical energy through photovoltaic effect is known as Efficiency (η) of a solar panel. Mathematically it is the output to input power ratio of a PV panel.

$$\eta = Pout/Pin \quad (6)$$

Where Pout is the electrical power output and can be represented as the product of Imax and Vmax

$$Pout = Imax.Vmax \quad (7)$$

Pin represents power input from sun which represents the amount of sunlight energy (G) in W/m2 which strikes surface area (A) of PV panel and is given as

$$Pin = A.G \quad (8)$$

So PV panel efficiency will be written as

$$\eta = Vmax.Imax/A.G \quad (9)$$

From the above equation it is clear that efficiency of PV is dependent upon the surface area A, solar irradiance G and temperature T because Imax and Vmax both depends on temperature.

C. Fill factor of the panel

The quality measure of a PV is known as its Fill factor (FF), which compares maximum power produced by a PV to theoretical power of that PV. The maximum power can be written as a product of its maximum power point voltage and current while theoretical power represents product of Voc and Isc.

$$FF = Imax.Vmax / Isc.Voc \quad (10)$$

In the above equation all four parameters that makes up the fill factor are dependent on irradiance and temperature, which indicates that fill factor is an indirect function of both these variable parameters.

Table 1. Panel parameters

Parameter	Rating
1soltech 1STH-240-WH	240V
Maximum power (Pmax)	239.679V
Voc	37.1V
Isc	8.58A
Vmax	29.7V
Imax	8.07A
Numbers of cells per module (Ns)	60
Temperature coefficient of Voc (Kv)	-0.369%/^{o}C
Temperature coefficient of Isc (Ki)	0.087%/^{o}C
Diode ideality factor (D)	1.0133
Area of module (A)	1.63m^2
Efficiency of module (ɳ)	14.7%
Fill factor (FF)	0.753
STC temperature (To)	25^{o}C
STC irradiance (Go)	1000W/m^2

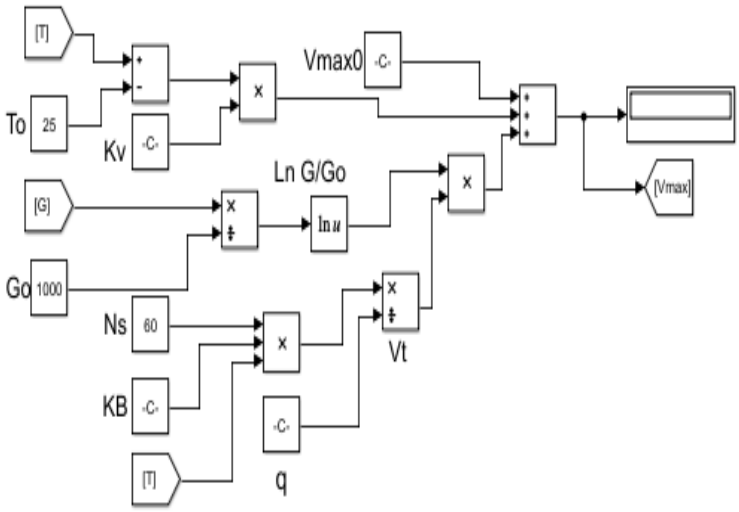

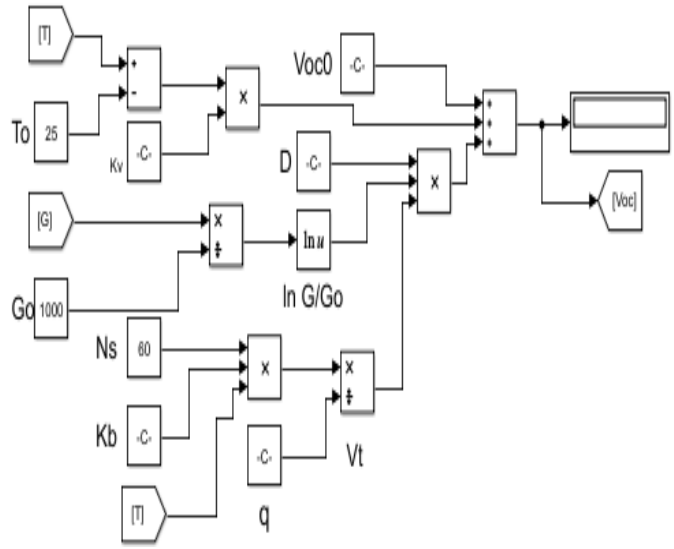

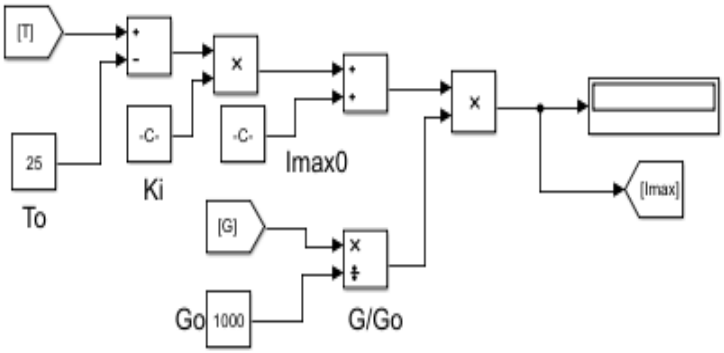

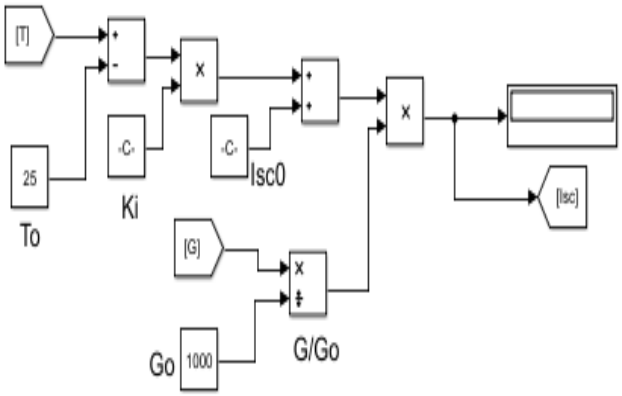

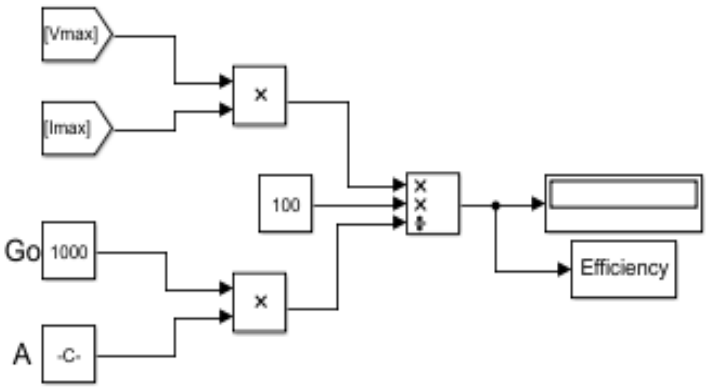

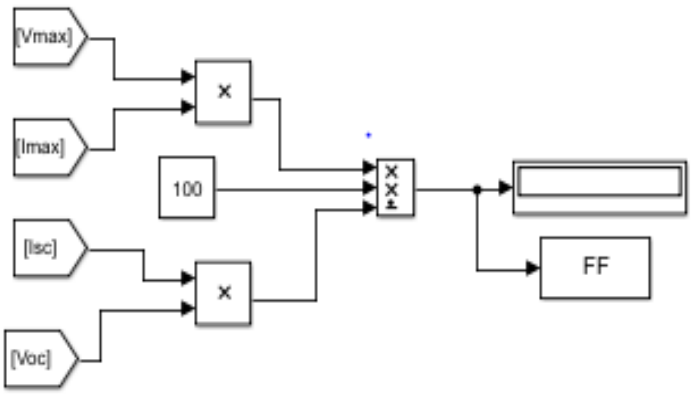

IV. RESULTS

The results of maximum power, efficiency and fill factor were observed under varying temperature and solar irradiance. The results of maximum power are obtained from the I-V curve at various different irradiance and temperature while that of efficiency and fill factor are noted from model designed in Simulink.

A. Results of maximum power

The maximum power results are noted under two different scenarios. In first scenario temperature is varied below and above of its STC values ranging from 21oC to 29oC at costant irradiance. In this case by increasing temperature maximum output power decreases and vice versa. But overall change in power is very small, it is because when the temperature is increased then there is a decreases in open circuit voltage and a slight increases short circuit current but the decrease in Voc is large as compare to the increase in Isc and as a result Pmax decreases and vice versa. In second scenario variation of irradiance from 920W/m2 to 1080W/m2 with an interval of 20W/m2 indicates that by increasing solar irradiance there is an increase in short circuit current whereas open circuit voltage remains nearly constant and as a result maximum output power of the PV panel increases.

B. Results of efficiency

The efficiency (η) of 240V panel under variable temperature indicates that if there is an increase in PV panel temperature, then efficiency of panel decreases and vice versa. This is due to the fact that efficiency is dependent on Imax and Vmax and by increasing temperature these two variable also varies. With temperature increase, Imax increases slightly and there is a significant decrease in Vmax due to which there is a slight decrease in the efficiency of the panel. The efficiency under variable irradiance shows that if solar irradiance of the panel is increased then the efficiency of the panel also increases and vice versa. The reason for this is that by increasing solar irradiance there is an increase in maximum current while maximum voltage decreases but the increase in the Imax is more significant than the decrease in the Vmax, so the efficiency of the panel increases significantly.

C. Results of fill factor

The fill factor of 240V panel under temperature variations shows that if temperature is increased at constant solar irradiance then there is a decrease in fill factor and vice versa. As fill factor represents the ratio of maximum power point current and voltage to the short circuit current and open circuit voltage. So if temperature is increased then both the voltages decreases and both the currents increases and the product of respective current and voltage changes. The voltages decreases in a proportional manner but the increase in Isc is more compare to increase in maximum current due to which the FF of panel decreases. Fill factor under varying irradiance indicates that by increasing solar irradiance the FF also increases and vice versa. This is because that by increasing solar irradiance both the voltages increases slightly and both the currents decreases significantly but the overall change in the FF is very small at this very little change in the solar irradiance.

CONCLUSION

Along with many more advantages there are several challenges to the PV system. One of the significant challenge is its too much dependency on whether conditions and installed location. In this paper a 240V PV panel performance is studied in variable temperature and solar irradiance conditions using Simulink environment. The performance parameters were first studied under STC conditions. Now the variation in either temperature or irradiance or in both will eventually cause a variation in maximum power point current and/or maximum power point voltage and/or open circuit voltage and/or short circuit current, which eventually causes variations in maximum power, efficiency and fill factor. If irradiance is held at constant and temperature is increased from its STC value then its maximum power, efficiency and fill factor decreases and vice versa. Similarly if temperature is kept constant and there is an increase in irradiance then all these three parameters also increases and vice versa. For every one degree change in the temperature of 240V PV panel there is an average change of 0.38% in the maximum power, 0.12% in the efficiency and 0.18% in the fill factor. Similarly for every 20W/m2 variation in solar irradiance of 240V PV panel there is an average change of 1.91% in the maximum power, 2.0% in the efficiency and 0.0017% in fill factor. From the above statistics it is clear that the effect of variation in temperature mostly effects the maximum power and that in solar irradiance effects efficiency of PV panel.

In future the proposed model can be used for any different ratings PV panel or for any other PV system. Furthermore it can also be used with variation in both temperature and irradiance at the same time.

REFERENCES

[1] Darwish, Z.A., et al., Impact of some environmental variables with dust on solar photovoltaic (PV) performance: review and research status. International J of Energy and Environment, 2013. 7(4): p. 152-159.

[2] Singh, G.K., Solar power generation by PV (photovoltaic) technology: A review. Energy, 2013. 53: p. 1-13.

[3] Pandiarajan, N. and R. Muthu. Mathematical modeling of photovoltaic module with Simulink. in 2011 1st International Conference on Electrical Energy Systems. 2011. IEEE.

[4] Touati, F., et al., Investigation of solar PV performance under Doha weather using a customized measurement and monitoring system. Renewable Energy, 2016. 89: p. 564-577.

[5] Aksakal, A. and S. Rehman, Global solar radiation in northeastern Saudi Arabia. Renewable Energy, 1999. 17(4): p. 461-472.

[6] Kim, I.-S., Robust maximum power point tracker using sliding mode controller for the three-phase grid-connected photovoltaic system. Solar Energy, 2007. 81(3): p. 405-414.

[7] Van Dyk, E., et al., Temperature dependence of performance of crystalline silicon photovoltaic modules. South African Journal of Science, 2000. 96(4).

[8] Kawajiri, K., T. Oozeki, and Y. Genchi, Effect of temperature on PV potential in the world. Environmental Science & Technology, 2011. 45(20): p. 9030-9035.

[9] Dubey, S., J.N. Sarvaiya, and B. Seshadri, Temperature dependent photovoltaic (PV) efficiency and its effect on PV production in the world–a review. Energy Procedia, 2013. 33: p. 311-321.

[10] Kane, A.N. and V. Verma, Performance enhancement of building integrated photovoltaic module using thermoelectric cooling. International Journal of Renewable Energy Research (IJRER), 2013. 3(2): p. 320-324.

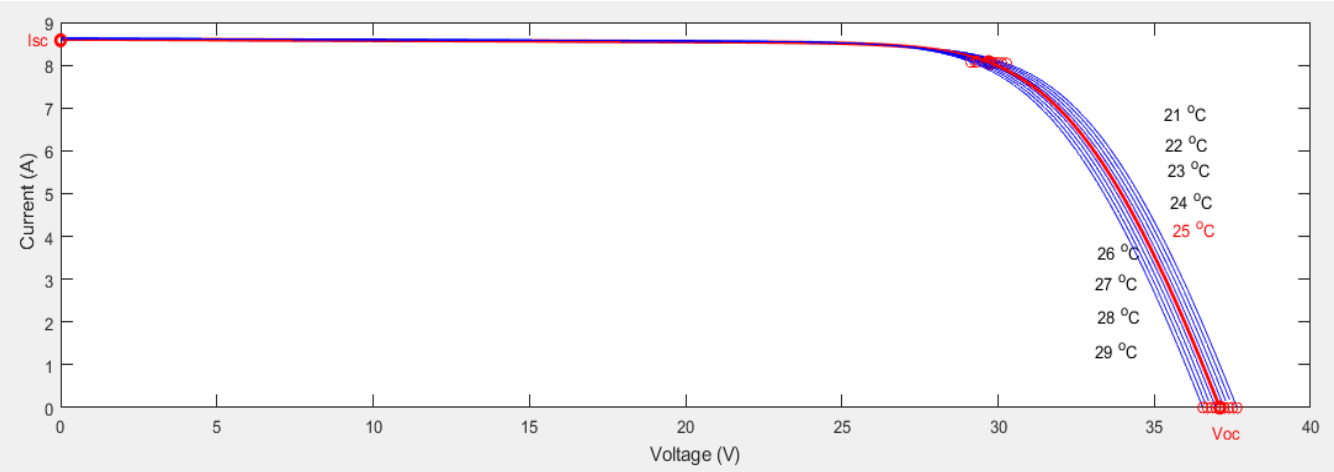

Figure 1. V-I curve at various temperatures from which Pmax is found

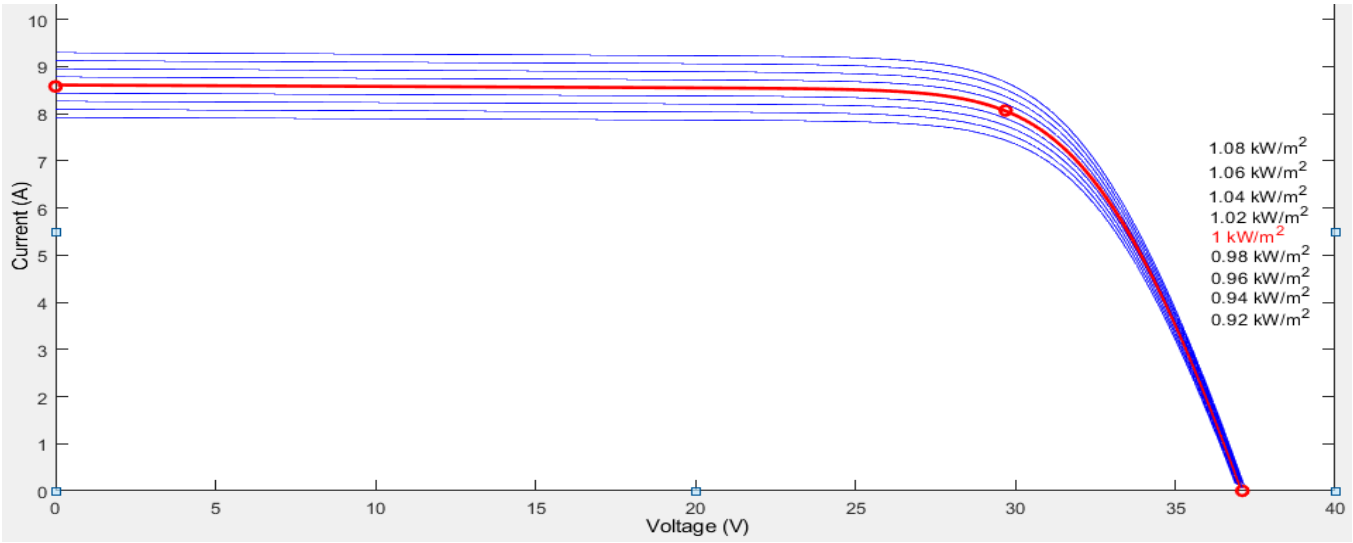

Figure 2. V-I curve at various irradiances from which Pmax is found

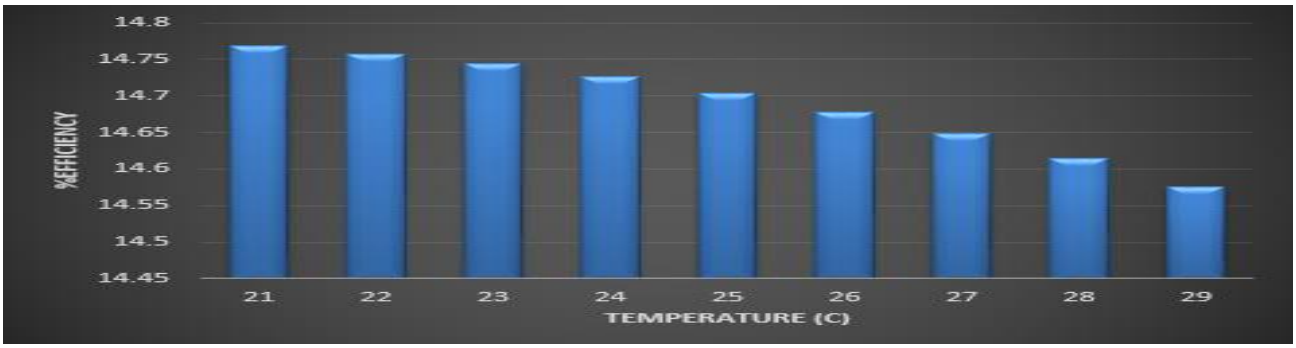

Figure 3. Efficiency at different temperatures

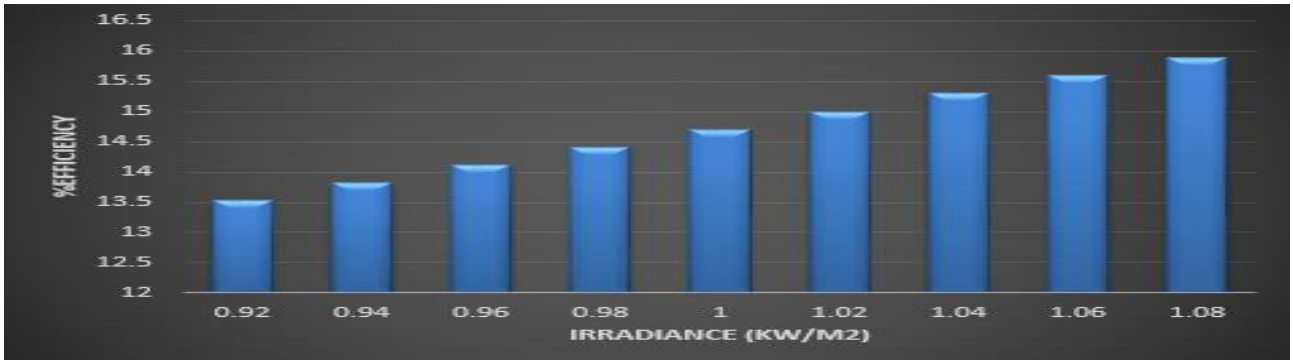

Figure 4. Efficiency at various irradiances

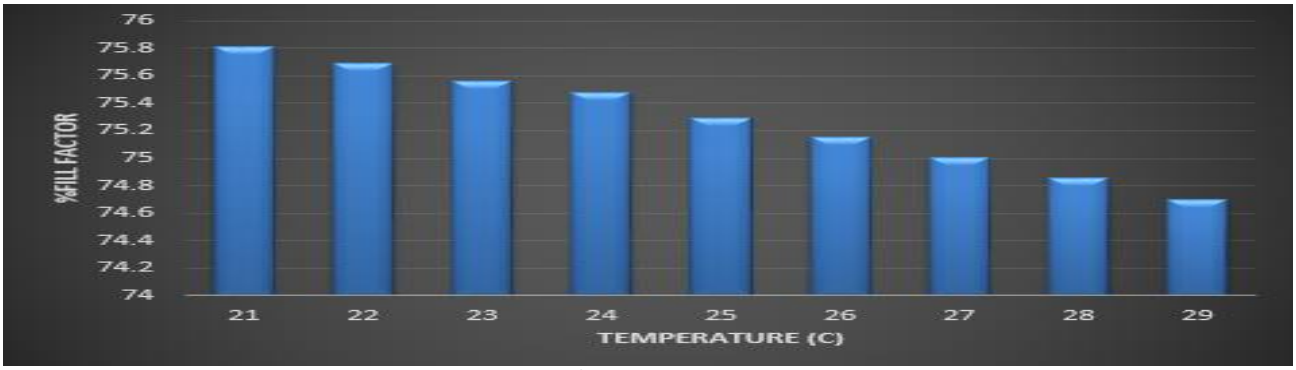

Figure 5. Fill factor at various temperatures

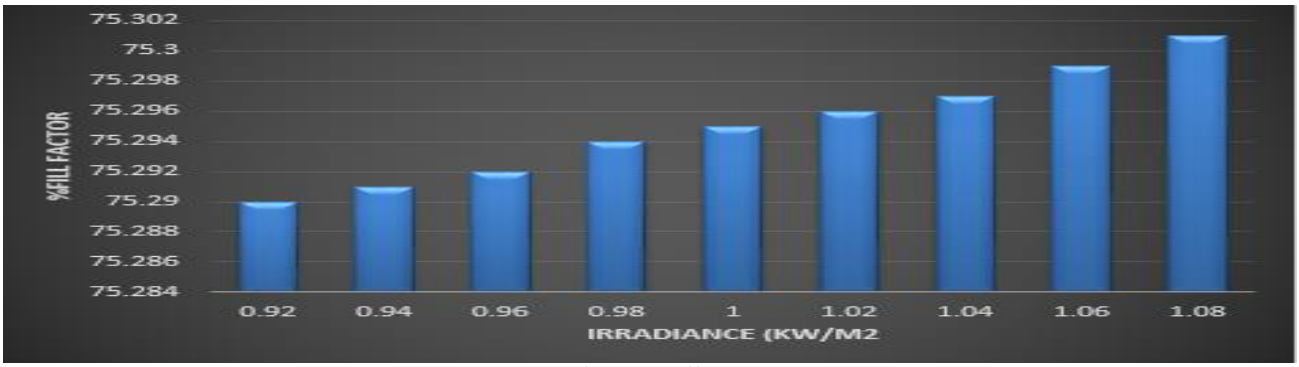

Figure 6. Fill factor at different irradiances

Table 2. Parameters against temperature

T(°C)	21	22	23	24	25	26	27	28	29
Vm	31.176	30.807	30.438	30.069	29.700	29.331	28.962	28.593	28.224
Im	7.721	7.808	7.895	7.962	8.070	8.157	8.244	8.331	8.418

Voc	38.576	38.207	37.836	37.469	37.100	36.731	36.362	35.993	35.624
Isc	8.231	8.318	8.405	8.492	8.580	8.667	8.754	8.841	8.928
Pm	243.40	242.40	241.41	240.30	239.70	238.20	237.30	236.21	235.20
% η	14.769	14.758	14.744	14.726	14.704	14.678	14.648	14.614	14.576
FF	75.810	75.688	75.562	75.481	75.295	75.154	75.008	74.857	74.701

Table 3. parameters against irradiance

G(W/m²)	920	940	960	980	1000	1020	1040	1060	1080
Vm	29.689	29.692	29.694	29.697	29.70	20.702	29.705	29.707	29.709
Im	7.424	7.585	7.747	7.908	8.070	8.231	8.392	8.554	8.715
Voc	37.089	37.091	37.094	37.097	37.100	37.102	37.105	37.107	37.110
Isc	7.893	8.065	8.236	8.408	8.580	8.751	8.923	9.094	9.266
Pm	220.80	225.50	230.10	234.70	239.70	243.90	248.40	253.00	257.50
% η	13.522	13.813	14.113	14.408	14.704	14.999	15.295	15.590	15.885
FF	75.290	75.291	75.292	75.294	75.295	75.296	75.297	75.299	75.300

How to cite this article:

Muhammad Azaz, Sajad Ullah, Jawad Ul Islam, "Comparative Analysis of PV System Performance in Different Environmental Conditions", International Journal of Engineering Works, Vol. 7, Issue 11, PP. 394-3400, November 2020, https://doi.org/10.34259/ijew.20.711394400.

International Journal of Engineering Works
ISSN-p: 2521-2419
ISSN-e: 2409-2770
Vol. 7, Issue 12, PP. 401-405, December 2020
https://www.ijew.io/
https://doi.org/10.34259/ijew.20.712401405

Effect of Variation in Temperature, Band gap and thickness of Active Layer on Efficiency of Organic Solar Cell

Wahid Amin[1], Zulfiqar Ali[2], Muhammad Babar Iqbal[3], Muhammad Arsalan Wahid[4]
Renewable Energy Engineering USPCAS-E UET, Peshawar, Pakistan
wahidamin70@gmail.com[1], zulfiqar32862@gmail.com[2], mbighost@gmail.com[3], arsh.shani@gmail.com[4]
Received: 20 November, Revised: 30 November, Accepted: 11 December

***Abstract*—**The virtual simulation of organic solar cell is carried in General purpose Photovoltaic Device Model (GPVDM) software. In this work performance of Organic solar cell is investigated. Organic solar cell is composed of 3-hexyl thiophene (P3HT:PCBM) a polymer as an active layer. The poly (3, 4-ethylenedioxy thiophene) poly (styrenesulfonate) (PEDOT:PSS) is added as an electron blocking layer and Indium Tin Oxide (ITO) film is used as top layer because of its high conductivity and very low resistance to transmission of light in visible range. GPVDM is used for light harvesting device simulations. It works on basis of Poisson's Equations to equate the device internal parameters that may be electrical or optical. Shockley-Read-Hall (SRH) formulations are used to calculate recombination and carrier trapping or mobility. In this study the temperature, band gap and active layer thickness is studied, how they affect the performance of organic solar cell. Variation in temperature inversely affects the efficiency. With increase in Band Gap efficiency also increase till band gap reaches 1.6eV, moreover increase in band gap increases efficiency but open circuit voltage value gets negative. The optimum value of active layer we got is 20nm which gives high efficiency.

***Keywords*—** GPVDM, organic solar cell, P3HT:PCBM, PEDOT:PSS efficiency of solar cell, temperature effect, band gap effect, thickness of active layer.

I. INTRODUCTION

The photovoltaic energy is clean source of energy and the type organic photovoltaic material which is a type of photovoltaic material gets much attention in recent studies because they are much environmental friendly and a very low cost solution. On the other hand the inorganic materials which are composed of a complex in process of production as well as in equipment's usage and the conversion efficiency almost reached to its most extreme peak points and the research area in inorganic photovoltaic materials are very limited in recent studies. The organic photovoltaic devices are the most consideration devices in the most recent decade due to its applications. The organic photovoltaic materials have shown the most flexible, renewable non-preservationist energy resources [1-2]. The organic solar cell are knows as the most favorable solar cell. The organic solar cells are considered the alternative solar cell to the inorganic solar cell [3-4]. Following benefits of organic solar cell material that include, it consist of lightweight, having mechanical flexibility and very easy to fabricate at normal temperature as well as the fabrication cost is low. The organic solar cells performances are affected by following factors which are savior that includes the low charging mobility of these materials. Due to this factor it faces very bad conductivity which directly affects its efficiency. The bulk-hetero junction achieves the highest power conversion of organic photo cell.

Many solar cell technologies have been introduced but among them the organic solar cell technology is the advanced technology that exists. A great exploration has been carried out since the exploration of organic materials for photovoltaic application a very efficient method is being made the transfer of charge between organic donors and acceptors. The bulk hetero junction (BHJ) of conjugate polymers P3HT (poly 3-hexylthiophene) and PCBM (phynyl-C70 butyric acid methyl ester) solar cells are recorded the highest performing material and the most advanced, vast and have been considered as largest research studies and investigating material [5-6]. In the organic blends the combination of the P3HT and PCBM are approaching are resent study carried out which is 6% energy- conversion efficiency [7] and 6.1% efficiency was achieved using PCDTBT and PC70BM blends. The BHJ, Bulk Hetero junction Organic Solar Cell are considered as the most generated excitations reach a nearby donor - acceptor interface, where they associate into free charge carriers (electron and hole). Harvesting efficiently excitations in BHJ solar cell will result a huge and highest possible power conversion which will result in a good efficiency output. The general impact of electronic transport component is perceived to have great impact, when thick dynamic layer films are utilized to expand light harvesting [8]. The thinner films can display nearly transformation of assimilated photon into collected carriers [9].

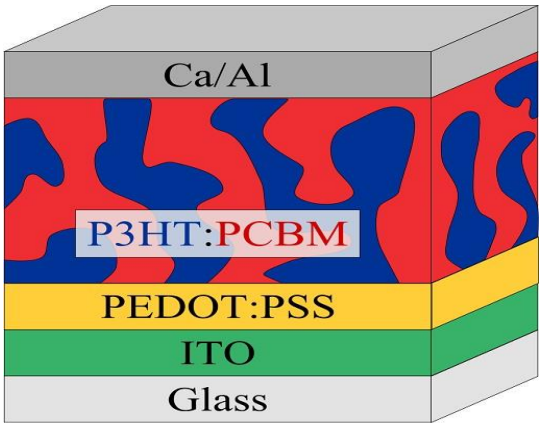

Figure1. Organic Solar Cell

II. DEVICE STRUCTURE

An electron donor polymer (P3HT) with a conjugate polymer an electron acceptor polymer (PCBM) is forming a bulk hetero-junction mixture which permits the light absorption, excitons generation and excitons splitting at the interface of donor and acceptor that is followed by systematic transport of electrons toward positive electrode and holes toward negative electrode. Two conjugate polymers are mostly mixed together to form a bulk hetero-junction. The two conjugate polymers will self-assembled into an interpenetrating system connecting the two electrodes [10]. The Bulk hetero-junction structure is of a great advantage in a way that large number of excitons reaches to nearby interface of donor and acceptor where the excitons are separated into opposite pair of charges (free charge carriers). P3HT chemical formula name 3-hexyl thiophene a polymer in hetero junction solar cell being a good material as electrons donor is a good transporter of positive charges and PCBM chemically known as [6, 6]-phenyl C71- butyric acid methyl ester is a material that can accept electrons at its best. The electrons from a molecule to another molecule are transported effectively in this way. A transparent electrode which is made of Indium Tin Oxide (ITO) film is used because of its high conductivity and very low resistance to transmission of light in visible range. For improvement of ITO work function a layer of PEDOT: PSS or poly (3, 4- ethylenedioxy thiophene) poly (styrenesulfonate) is added. The materials PEDOT: PSS layer of work function 5.2eV is used as an electron blocking layer and hole transporting layer. To block or avoid the wrong direction flow of electrons and holes this layer can be applied between active layer and electrode as a buffer layer. Following figure 2 is showing the bulky hetero junction organic solar cell structure.

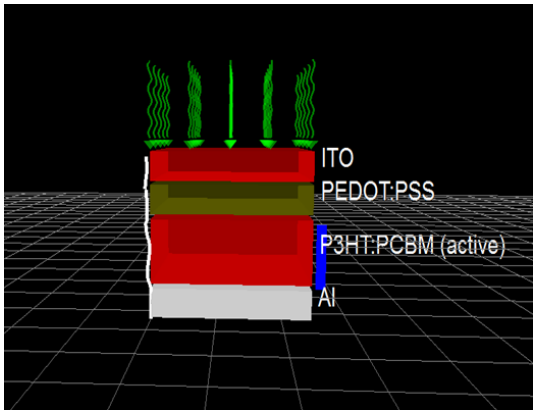

Figure2. Bulk Hetero junction solar cell

III. METHADOLOGY

In this research work, the bulk hetero junction solar cell is designed by the GPVDM software to study the I-V characteristics at active layer thickness and temperature. The simulation parameters are shown in table 1.

TABLE 1. PARAMETERS FOR SIMULATIONS

Sr.No	Parameters	Values	Units
1	Electron trap density	3.8×2610	-3-1**m** eV
2	Hole trap density	$1.45x10^{25}$	-3-1 **m** eV
3	Electron mobility	$2.48x10^{-7}$	m2 V-1S-1
4	Hole mobility	$2.48x10^{-7}$	m2 V-1S-1
5	Trapped electron to free electron	$2.5x10^{-20}$	m-2
6	Trapped hole to free electron	$4.67x10^{-26}$	m-2
7	Free electron to trapped electron	$2.5x10^{-20}$	m-2
8	Free hole to trapped hole	$4.86x10^{-22}$	m-2
9	Temperature	300	K
10	Shunt resistance	$1.9x10^{5}$	Ω
11	Device breadth	0.003464	M
12	Device width	0.003464	M
13	ITO (electrode) thickness	1 x10-7	M
14	PEDOT:PSS layer thickness	1 x10-7	M
15	P3HT:PCBM layer thickness	2 x10-7	M
16	Aluminum (electrode) thickness	1 x10-7	M

A. Effect of Active Layer Thickness on Efficiency

In this work, the simulation was run twice; the first for different P3HT: PCBM set layer thickness and the second for different set of temperature. During the first simulation process, the thickness layer of organic solar cell (P3HT: PCBM) was optimized varying it from 50nm to 400nm in a step of 50nm, i.e. the thickness that gives the highest efficiency of 4.59% is 200nm.

TABLE 2. SOLAR CELL PARAMETERS FOR DIFFERENT ACTIVE LAYER THICKNESS

Thickness (nm)	Voc	FF	MPP	Conversion efficiency %
50	0.621	0.78	31.6	3.16
100	0.611	0.76	37.3	3.73
150	0.602	0.72	36.2	3.62
200	0.604	0.68	45.9	4.59
250	0.598	0.65	41.7	4.17
300	0.592	0.62	38.3	3.83
400	0.585	0.57	36.9	3.69

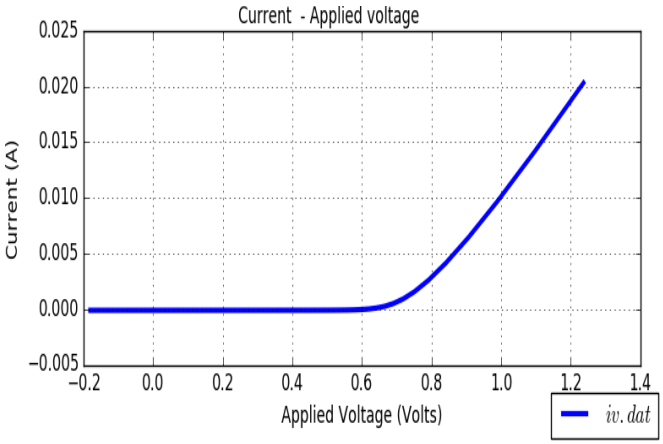

(A)

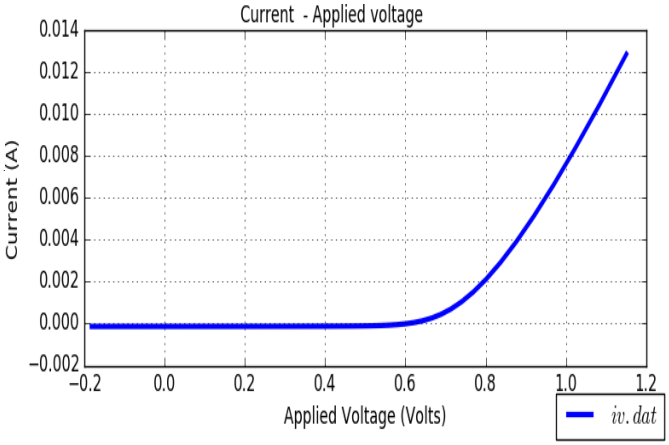

(B)

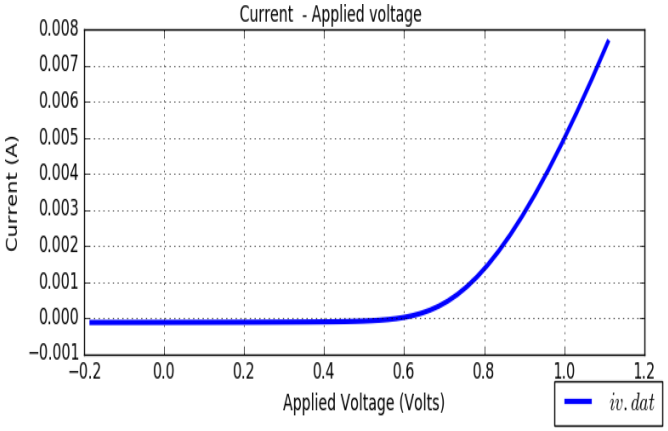

(C)

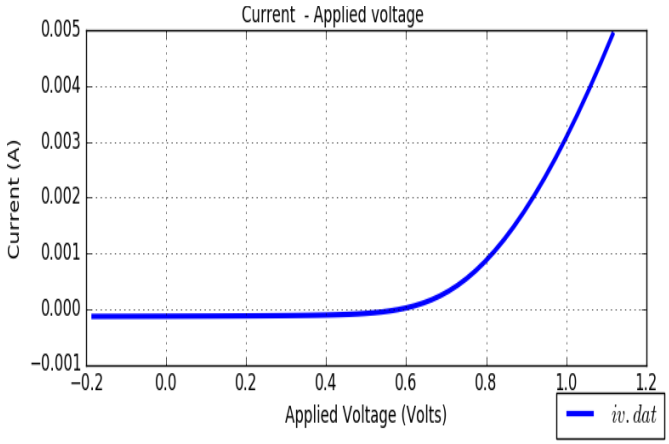

(D)

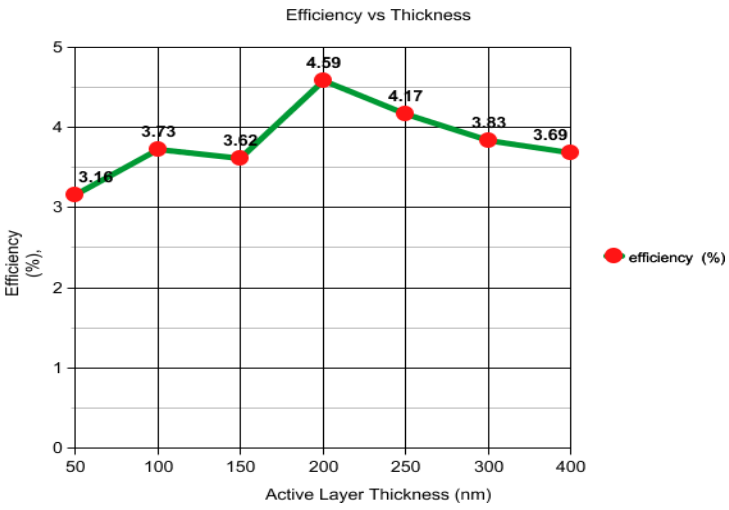

(E)

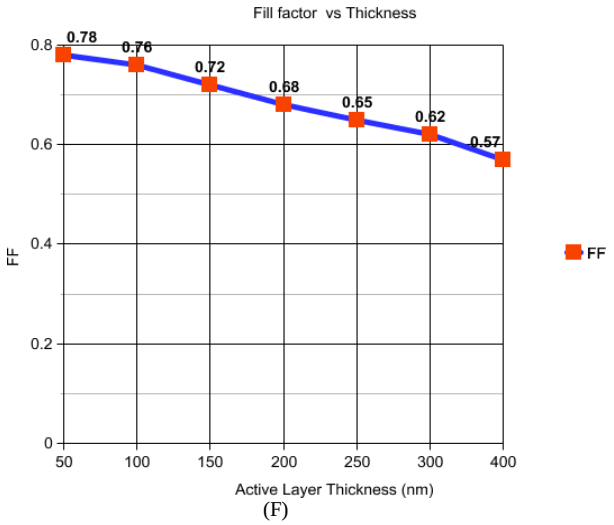

(F)

Figure 3. Current-Voltage (I-V) curves with different active layer thickness: (A) 1 x10^{-7} m (B) 2 x10^{-7} m (C) 3 x10^{-7} m (D) 4 x10^{-7} m (E)Active layer thickness Vs efficiency (F) Active layer thickness Vs fill factor

B. *Effect of Temperature on Efficiency*

The optimal thickness obtained in the first simulation was used in the second simulation. Here the temperature was varied from 300K to 350K in a step of 10 K.

TABLE 3. SOLAR CELL PARAMETERS FOR DIFFERENT TEMPERATURE VALUES

Temp (K)	Voc	FF	MPP	Conversion efficiency %
300	0.604	0.681	45.92	4.59
310	0.593	0.687	45.54	4.55
320	0.582	0.688	44.87	4.48
330	0.570	0.691	44.25	4.42
340	0.560	0.690	43.43	4.34
350	0.548	0.692	42.62	4.26

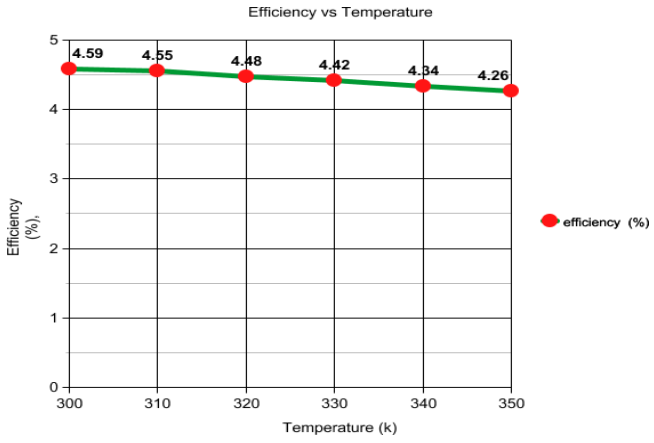

Figure 4. Effect of temperature variation on efficiency

C. *Effect of Band gap on Efficiency*

The P3HT: PCBM based organic solar cell simulated with GPVDM and performance of varying active layer band gap vs The allowed band gap (Eg) of P3HT: PCBM is around 1.9 eV, but limit the absorbance to below a wavelength of about 650 nm. From the simulation we identified that varying P3HT: PCBM band gap, short circuit current density (J_{sc}) remains constant and not effected by Eg. Also other parameters studied such as open circuit voltage (V_{oc}) fill factor (FF) and efficiency. V_{oc} increases linearly as the band gap increases. The band gap of active layer is varied from 1.1ev to 1.5ev as shown in figure and a great improvement in efficiency has been achieved. When Eg passes from 1eV to 1.5ev the fill factor reaches a maximum value of 0.74.

TABLE 4. SOLAR CELL PARAMETERS FOR DIFFERENT BAND GAP VALUES

Band gap (Eg)	Voc	FF	Efficiency %
1.1	0.60	0.67	4.5
1.2	0.70	0.69	5.4
1.3	0.80	0.71	6.4
1.4	0.90	0.73	7.4
1.5	1.02	0.74	8.4

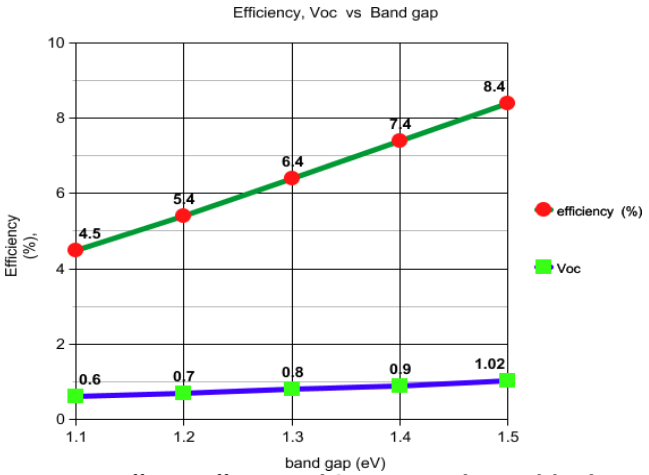

Figure 5. Effect on Efficiency and Open circuit voltage with band gap variation

CONCLUSION

In this work, the P3HT: PCBM based organic solar cell has been studied in ITO/PEDOT: PSS/P3HT: PCBM/Al structure. The simulation was carried out by GPVDM software. The output characteristic I-V curve of organic photovoltaic cell was simulated. The efficiency of device increases as the active layer thickness increases. The optimum thickness layer is 2×10-7m at which efficiency is 4.59%.while the fill factor FF decreases with increase in active layer thickness. Highest fill factor (FF) at active layer thickness of 1 x 10-7 m.

The influence of device temperature also deliberate and the optimal working temperature was found to be 300 K, where power conversion efficiency and FF are 4.59 % and 0.68 respectively. As the temperature of device increases, efficiency and open circuit voltage (Voc) slightly fall down. We noticed a considerable improvement in efficiency with band gap energy increase, at which the efficiency reaches a value of about 8.4%. So as a result it is better to use that material in which energy gap is higher so high efficiency of organic solar cell is achieved.

REFERENCES

[1] N.S. Sariciftci, L. Smilowitz, A. J. Heeger, and F. Wudl., Photo induced electron transfer from a conducting polymer to bulkminsterfullerene. Science 258, 1474 (1992).

[2] G. Yu, J. Gao, J. C. Hummelen, F. Wudl, and A. J. Heeger. Optimization of conjugate-polymer based bulk hetero junction. Science 270, 1789 (1995).

[3] N. Rastogi, N. Singh, and M. Saxena, A brief review on current need of organic solar cells. International Journal of Innovative Research in Science, Engineering and Technology, 2, 12, (2013).

[4] S. C. Jain, M. Willander, and V. Kumar, Conducting organic material and devices (Academic, San Diego, (2007).

[5] W. J. Belcher, K. I. Wagner, and P. C. Dastoor, The effect of porphyrin inclusion on the spectral response of ternaryP3HT: PCBM bulk hetero junction solar cells, Sol. Energy Mater. Sol. Cells 91 447- 452 (2007).

[6] Y. Kim, S. Cook, S. M. Tuladhar, S. A. Choulis, J. Nelson, J. R. Durrant, D. D. C. Bradley, M. Giles, I. McCulloch, C. S. Ha,

[7] and M. Ree, A strong regioregularity effect in self-organizing conjugated polymer films and high-efficiency polythiophene fullerene solar cells, Nat. Mater. 5 197-203 (2006).

[8] S. H. Park, A. Roy, S. Beaupre, S. Cho, N. Coates, J.S. Moon, D. Moses, M. Leclerc, K. Lee, and A. J. Heeger, Bulk hetero junction solar cells with internal quantum efficiency approaching 100%, Nature Photonics 3, 297–302 (2009).

[9] F. C. Krebs, et al., A round robin study of flexible large-area roll- to-roll processed polymer solar cell modules, Solar Energy Material and Solar Cells 93, 1968–1977 (2009)

[10] W. Ma, C. Yang, X. Gong, K. S. Lee, A. J. Heeger, Thermally stable, efficient polymer solar cells with nanoscale control of the interpenetrating network morphology, Advanced Functional Materials 15 ,1617–1622 (2005).

[11] P.P. Boix, A. Guerrero, L.F. Marchesi. G.J. Garcia-Belmonte, Bisquert, Current–voltage characteristics of bulk hetero junction organic solar cells: connection between light and dark curves, Adv. Energy Mater 1, 1073–1078 (2011).

How to cite this article:

Wahid Amin, Zulfiqar Ali, Muhammad Babar Iqbal, Muhammad Arsalan Wahid, "Effect of variation in Temperature, Band gap and Thickness of Active Layer on Efficiency of Organic Solar Cell", International Journal of Engineering Works, Vol. 7, Issue 12, PP. 401-405, December 2020, https://doi.org/10.34259/ijew.20.712401405.

IJEW 国际工程期刊 International Journal of Engineering Works انجینئرنگ کاموں کا بین الاقوامی جرنل

International Journal of Engineering Works
ISSN-p: 2521-2419
ISSN-e: 2409-2770
Vol. 7, Issue 12, PP. 406-413, December 2020
https://www.ijew.io/
https://doi.org/10.34259/ijew.20.712406413

Social and Environmental Analysis of Decentralized Energy System and Its Future Prospects

Majid Ullah[1], Sayed Kamal[2], Malik Amad Khalil[3], Sheraz Khan[4]
[1,2,3,4] US:-Pakistan Centre for Advanced Studies in Energy, University of Engineering & Technology, Peshawar, Pakistan
mullah2@asu.edu[1]

Received: 20 November, Revised: 01 December, Accepted: 15 December

***Abstract*—**Energy is the key driver and frequently assume their role play as a catalyst for the sustainable development. Universally the per capita consumption of energy is frequently utilized as a guage for the economic and sustainable development of any country. Sustainable Energy plays a critical part being an imperative segment for the social values, energy poverty eradication and economic development, The huge inadequacy of power because of substantial dependence on imported fuels has turned into a noteworthy obstacle to economic and sustainable growth of any developing country in general and to particular in Pakistan. This situation makes an expansion in nearby fuel costs and cutoff points possibilities in the foundation of new industries. The ongoing gap between the demand and supply of power in Pakistan is around 7000-8000 MW with a consistent increment of 6-8% per annum. Consequently, hence to overcome this situation, sustainable power sources are intensely required to conquer the current issue Pakistan is blessed with enormous sustainable power source assets, for example, wind, sunlight based, hydro, and bio-mass. These resources have the tendency to be major contributors of future energy creation framework, climate change minimization, energy decarboniztion, energy independency, sustainable growth and development of the country. This research narrates the alternative energy resources like renewables, to inrease energy efficiencies and related possibilities for full-scale advancement which can be viable for sustainable development.

***Keywords*—** Climate change, Energy Poverty, Social Values, Energy Decarbonization.

I. INTRODUCTION

Energy is viewed as a preliminary operator in the generation of wealth and furthermore a signicant factor in the socail, economic and sustainable development [1]. The significance of energy in economic development has been perceived all around, the historical data authentify a solid connection between the accessibility of energy and financial actions [2].meanwhile the past two decades the risk and reality of ecological deterioration have sort out to be more clear. increasing trends of environmental issues is just because of a blend of a little elements since then the innate effect of human activities has developed extremely in view of the sheer addition of total populace, usage, mechanical action, and so on. Accomplishing answers for ecological issues that we are facing today posses hard work potential activities for practical improvement. In such way, sustainable power sources seem, by all accounts, to be the a standout amongst to be the most efcient and compelling allignments. That is the reason there is a cozy association between sustainable power source and supportable advancement [3]. Pakistan is a standout amongst the most populated nations in the southern Asia area, contributing approximately2.56% of the aggregate worldwide populace [4]. The nation is normal to fill in as a universal exchange and energy hall in the not so distant future because of its energy area [5], [6]. Thus, among other social, economical, and political variables,Pakistan needs to guarantee its energy supplies meet the immediate and roundabout requests of the nation not just for keeping up economics development yet in addition for supporting local and worldwide financial activities. The immense shortage amongst demand and supply of power recorded in 2009-2010 was 26.82%: This figure has expanded up to 50% during the late spring of 2012 [5]. A normal issue is that power supply can't be kept up during peak hours, bringing about continuous power shutdown (load shedding) of 1314 hours in urban zones, and 1619 hours in country territories. Therefore, numerous business visionaries and industrialists have contributed and moved their organizations to neighboring nations [6]. Subsequently, short-and longterm measures are needed to comprehend the current energy issues. The current situation with Pakistan's energy assets is abridged (Fig. 1).

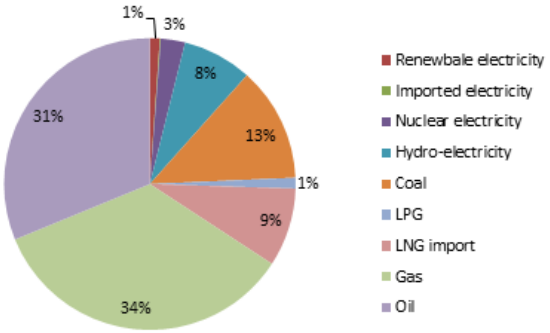

Figure 1. Energy Supply Mix of Pakistan [5]

It can be seen that indigenous energy sources essentially comprise of oil (34 %), renewable (1%) hydro (8%), gaseous petrol (27%), and coal (3%) [5]. Economical supply of energy to match the present and future household and large scale demand in Pakistan will depend on potendemand in Pakistan tail energy production from the distinctive energy sources with a specific end goal to make noteworthy commitments to the production network. current energy generation has an enormous economics related potentials on the nation's economy due to the imports of oil to help existing energy mix, and the circumstance is uplifted by the quick depreciation of household gas resources. As per the Board of Investment Pakistan, the introduced control limit is 22,797MW: Nonetheless, current age remains in the vicinity of 12,000 and 13,000 everyday, against top a request of 17,000 to 21,000MW. Figure 2 shows Energy is the principal link between human and planetary human being [6]. The real elective energy assets bottomless all through the pakistan are solar based, wind energy, wood and biomass, and biogas generation. In making energy nutilization practical and adequate to other financial parameters of improvement, the accompanying factor must be followed into consideration [7]:

- Sustainability of the biological system through suitable and appropriate asset administration;
- Economic and money related manageability through framework and administration headway that keeps reasonableness altogether to the front in view of the impeded rustic populaces;
- Social supportability through affirming that the poor advantage, and that ladies' salaries and concerns, legitimate rights for all, and youngsters' rights are altogether valued and upheld;
- Administrative supportability through guaranteeing that there is managerial limit with respect to program usage, and that this will be kept up or expanded after some time.
- Energy is the principal link between human and planetary wellbeing. In this regard, micro-hydropower is clean and environmentally sounds technology. Setting this framework, and debating the social value of energy services Pakistan is one of the countries who is also meeting with the issue of extreme energy crises.

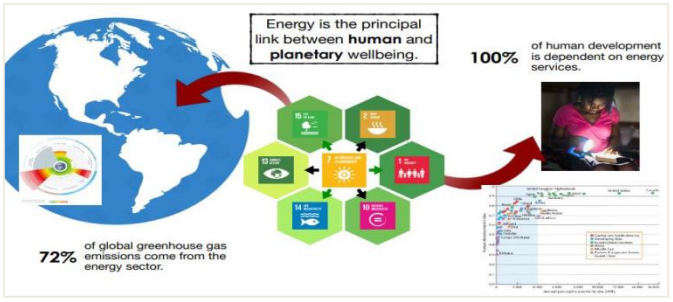

Figure 2. Energy is the principal link between human and planetary human being [6]

A. *Domestic Fuel used in Pakistan*

Current measurement, proficient, social, and creative slanting way act enormous challenges to the whole deal viability of the overall imperativeness system [6]. In case lawmaking bodies don't diagram approaches past those starting at now existed and masterminded among now and 2030, it is evaluated that [7]: imperativeness use will increment by completed half (53%); the energy mix will remain truly enduring and powers (80%share); vitality related CO2 releases will augment by completed half (55%); huge peoples of the world's poor will regardless continue having nonattendance of accessto control (around 1.5 billion) and present day cooking and warming organizations (around 2.5 billion). In this circumstance, vitality use increases from 12,467 million tons of oil proportionate (Mtoe) in 2008 to 14,765 Mtoe in 2020 [4]. Over 70% of this advancement is required to start from making nations, which overpower OECD countries as vitality customers sooner or later around 2014. About segment of the improvement in world fundamental vitality use goes to conveying force and onefifth of the expansion to tending to transportation needs [8] [9] [7]. Improvement in vitality usage and GHG releases is depended upon to be especially engaged in a couple of zones. The sectoral quick supporters of improvement in vitality utilize are required to be control age (35%), industry (15%), transport (12%) and structures (6%) in making countries, trailed by control age (11%) and transport (6%) in OECD countries [8]. proficienting profitability and declining carbondioxide (CO2) drains should percieve early thought in these high improvement areas, in light of the way that these goals are caught and down to earth to accomplish at the period of new advancement than at later retrofit stages. It is foreseen that the world Energy mix will remain really unfaltering and instructed by oil based goods to 2030 in view of the edge and latency of the vitality structure and the inability to modify it hastly. In such case, no fuel's offer of the mix alter by more than two or three rate centers in current situation. Oil subordinates remain the greatest and humble vitality source speaking to about 80%of overall demand in 2008 and 78% in 2030 [10]. The usage of each non-sustainable power source creates at different eras and rates, so their offers of the total move springily oil tumbles from 34% of the total in 2008 to 32% in 2030; coal rises from 25% to 26%; and gas climbs from 21% to 23%. Stresses over continued with high usage of oil and gas.

II. SOCIAL VALUE OF ENERGY SERVICE

A. Energy Demand and Poverty Alleviation

Energy adds to an upright cycle of human, monetary and social changes that are major to sensible change in making countries alluding. Sufficient supplies of clean energy are the explanation behind raising lifestyles, upgrading the quality besides, measure of human capital, enhancing the business and customary condition, and extending the capability of government courses of action [11], [12]. In any case, energy dejection remains a vital issue for human prosperity, money related headway and environmental reasonability in various parts of the world. Around 1.6 billion people generally in the natural districts of Sub-Saharan Africa, South and East Asia, and Latin America require access to control, and 2.5 billion people rely upon ordinary biomass for cooking and warming [10] [12]. Around 1.3 million people generally women and children kick the pail imprudently consistently because of introduction to indoor air defilement from cooking and warming with coventional, inefficient biomass stoves (see Fig. 3). Enthusiasm for energy is growing exponentially in making countries in view of fast people improvement (especially in Africa) and snappy financial advancement (especially in China and India). This is foreseen to provoke a nearby duplicating in basic energy use, a considerable amount of it unsustainable, by making countries in the accompanying two decades. As a result of this advancement, making countries will speak to 50% of basic energy use and 52% of energy related CO2 releases constantly 2030 [13], [14], [15]. China will experience the best addition in energy request, speaking to 43% of all making country improvement and 30% of signify world advancement. India, other Asia, the Middle East and Africa will show medium advancement in energy usage [12]. Concerning energy sources, coal will be the greatest creating energy source took after by oil. Gas will continue being used extensively in the Middle East and Latin America, while the use of biomass and waste will increase in Africa [13], [12]. Massive endeavors are required in additional and substitution restrain concerning making, evolving over, transporting and dispersing energy in making countries to address future issues. Most of this wander is required in the power fragment, particularly in China, India and other Asian countries . Diverse locale require financing furthermore for oil and gas change and use [13]. Then again, hypothesis at these strange states addresses a twofold test. Governments need to set game plans that draw in sufficient private theory and change help. Making country governments, together with theorists and advocates, need to find more capable and more moderate techniques for passing on energy benefits so the money related save assets might be placed assets into other sensible progression needs. They should in like manner ensure sensible cases of age and usage of energy supplies and organizations [16]. capable and more moderate techniques for passing on energy benefits so the money related hold assets might be placed assets into other achievable progression needs. They should similarly ensure sensible cases of creation and use of energy supplies and organizations [14].

B. Sustainable and Viable Energy Sources

Lack of access to moderate power and substantial dependence on the wasteful and unsustainable utilization of conventional biomass energizes (i.e.,fuelwood, charcoal, agrriculture waste and animal dung) are the two appearances and reasons for neediness. Power and other present day energy sources assume a basic part in economic and social improvement. Only they can't mitigate destitution however they are key to supportable improvement [17]. Present day energy administrations upgrade the life of the poor in incalculable ways. Electric light broadens the day, giving additional hours to perusing and work. Present day cook-stoves spare ladies and kids from every day introduction to poisonous cooking vapor. Refrigeration broadens nourishment freshness and dodges wastage. Centers with power can disinfect instruments and securely store prescriptions through refrigeration. Assembling and administration ventures with current energy can be more profitable and can expand the quality and scope of their items along these lines making employments and higher wages [9],. In numerous nations, neediness is drawn out especially by the unsustainable accumulation of biomass and its utilization in customary, wasteful stoves [18].This makes indoor smoke contamination prompting genuine wellbeing harm, for example, respiratory illnesses, obstetrical issues, visual impairment and coronary illness. It requires extensive sums of time for fuel gathering diminishing the time accessible for other profitable exercises, for example, cultivating and training . It causes biological harm (e.g. deforestation and soil disintegration) and nearby shortage of wood in a few regions. What's more, it draws horticultural deposits also, manure far from their utilization as compost, in this way decreasing agrarian profitability [18]. It is assessed that to accomplish the Millennium Development goals (MDGs), the quantity of individuals lacking power would require to decline to beneath 1 billion and those depending on customary biomass would need to tumble to 1:2 billion by 2015. Deliberate government activity with help from the industrialized nations is expected to accomplish these objectives, together with expanded subsidizing from both open and private sources [17]. Then again, arrangements need to deliver obstructions to access, reasonableness and supply of power and elective energizes, which are as of now accessible at sensible cost, e.g. gas-let go stoves and barrels. Access to practical energy sources should shape a focal part of more extensive advancement methodologies [19], [20], [21].

III. ENERGY RELATED CLIMATE CHANGE POLICIES

A. Transformation of economic instruements

Economics or "market based" instruments can be a successful and economically proficient methods for accomplishing feasible and sustainable policy objectives much of the time. These incorporate taxes, outflow exchanging, appropriation change, and special duties. Then again, economically viable instruments offer the potential for both static effectiveness and dynamic proficiency. They give expanded adaptability to governments and industry through

expanding on the activity of the market and the value framework. They can give government income that can be utilized for an assortment of purposes [2, 20]. Ecologically related assessmentspresent value flags so makers and buyers consider the expenses of contamination and asset utilize related with their exercises. Thusly, carbon assessments would disguise the cost of ozone depleting substance emanations and raise the cost of specific energizes, procedures and items. These financial motivating forces would decrease interest for hurtful items and increment interest for elective powers, for example, renewables whose costs turn out to be more focused. Ecologically related expenses additionally increment motivating forces for the private division to embrace R&D on supportable advancements and further advances. Worry about diminishing the aggressiveness of energy escalated parts is a noteworthy snag to the full execution of carbon charges. energy escalated enterprises regularly get aggregate or fractional exclusions from such expenses despite the fact that huge worldwide decreases in carbon emanations could be accomplished. In collecting carbon imposes, the compete based effects can be diminished by:

- Enlarging and extending and make the group of countries that put similar,affordable and parallel policies in place,
- requiring outskirt charge modifications on items from nations having Less stringent expenses,
- Recycling a bit of the duty incomes back to the influenced firms Numerous nations are currently considering such methodologies for utilizing carbon charges to advance more sustainable and viable energy framework

B. Clean Development Mechanism (CDM)

Under the Clean Development Mechanism (CDM), industrialized nations can accomplish some part of their required ozone-depleting substance duties under the Kyoto Protocol from ”credits” produced through lower-cost outflow diminishments in ventures past their own fringes. Governments, financial specialists and privately owned businesses in industrialized nations can get credits for lessening ventures they do in ”have/merchant” nations. Each CDM venture must [21] [8] [22]:

- diminish GHG discharges well beyond ”nothing new”;
- represent GHG discharges that happen outside the undertaking limit that are inferable from the task;
- hold fast to strict physical limits inside which GHG discharges will be decreased;
- not include atomic innovation nor surpass universally concurred restricts on ranger service credits and exercises;
- be deliberate and have the host nation’s endorsement;
- meet the manageable improvement objectives characterized by the host nation;
- incorporate the support of influenced networks, gatherings or people;
- not add to ecological decay;
- happen in a creating nation that is Party to the Kyoto

There has been a fast development in action under the CDM, which is as of now anticipated that would prompt discharge alleviation of in excess of 1.8 billion tons from more than 1700 individual undertakings by 2012 [23]. Be that as it may, in spite of the fact that there is a colossal potential for sustainable power source and energy proficiency ventures, quite a bit of it stays ”undiscovered”, with these undertaking composes representing about a fifth of aggregate expected credits from the CDM. There are a few explanations behind this at the national, universal and undertaking levels, including constrained institutional limit, challenges in getting adequate venture back in nations with a high sovereign hazard, and the generally little size of numerous sustainable power source and energy proficiency projects [6]. The sectorial crediting system (SCM) would center around financial areas, as opposed to ventures, in creating nations.E mission execution baselines for a predetermined period would be set up for chosen divisions (e.g. iron and steel and concrete) in partaking creating nations. These nations would then get tradable discharge decrease credits, which they could use as they wish appropriating them to singular organizations in the area or offering them for general income [24, 25]. Sectorial attributing components are a promising intends to support interest in atmosphere well-disposed energy frameworks. By the by, building up a compelling framework that is achievable to arrange and set up presents certain difficulties because of wide varieties in ozone-harming substance forces among nations and offices, and the requirement for specialized aptitudes for assessing, checking and confirming sectorial crediting proposition. The interest for credits must be moderately sure to try advantageous, and the ecological adequacy of the instrument must be anchored.

The main reason of the dismantled plants was maintenance. The plants constructed with government subsidy were dismantled. It was observed during the visit that there were only two types of the plants installed in KPK. In which 60% of the plants were fixed dome plants. While 40% of the plants were floating type. It is worth noting that the plants installed by PCRET with the government subsidies were floating type.

IV. METHODOLOGY

A. Descriptive Analysis

The collected data from the households were entered into the Statistical Package for Social Scientists (SPSS). For this, we have taken two samples, the first one for 100 households connected to the central grid and the other 100 sample of household’s connected to MHP. Then study the result of each sample independently through the statistical package. The data of family unit size and limit, a source of money and area of agricultural and ripe land, and so all were passed into SPSS. Different factors like the primary source of lighting, accessibility of power in 6 hours, month to month bill and association costs, and so all were examined. The fulfillment and Gratification level of family units with respect to the MHP power and WAPDA power was additionally broke down and assumed about. In this study, the expansive fuel for cooking and

heating was similarly analyzed. Other sources of energy for lighting purposes such as generators, LPG, UPS, Kerosene oil, and DC chargeable lights were added for the analysis. All the analysis was done for the two entities on the basis of electrical energy they are using. Besides, the additional use and costs made by WAPDA clients are likewise anticipated. the relative cost of unit capital cost (Rs. /kWh) and unit electricity cost (Rs. /kWh) of micro-hydro power is calculated. We also consider unit electricity value per kilowatt-hour of WAPDA. The capital cost is resolved depends on the underlying capital expense of the plant and its absolute introduced limit kilowatt. The electricity cost is determined by separating the fixed every month bill on the absolute units expended every month in kilowatt-hour.

B. Economic Analysis

The economic analysis includes looking at the doings and cash flows of a commercial or business firm, public organization or assembly of the association. The aims of economic-related analysis are to update the partners required, to regulate the economic system perfectly, and to illuminate contributors and open organizations. The yields of this investigation are the income of elements, return on investment, and working expenditure plans of people and measures of distant promises required. Financial investigation of the task relates the advantages and expenses to the industry. It considers the market costs and expenditures to decide the parity of assumption and the manageability of the undertaking Economic Analysis and furthermore assesses the surges of assets among gatherings of different groups and their impact on society all in all. Cost-effective investigation evaluates projects from the assessment of the community completely (the host country economy). It compares the expenses and profits of the total economy of the country. The economic study depends on the opportunity cost of the benefit. It also depends on market value and the demand for customers available in the market. The opening price replicates charge of using limited assets of the community. On the other hand financial study practices commercial amount that is changed from marketplace bill by discounting tax, return and grant, etc. This inspection is projected on excel spreadsheets. Facts and figures that were used for this investigation is preliminary investment charge of Micro hydropower plants, operational and repairs cost and total charge. These statistics were achieved over the initial investigation after the owners of the electrical power plants. The paybacks of the project and the prices gathered from the families and owners of industries and facilitate workshops which use the electrical power by Micro hydropower projects. The data of profits in regulatory rapports were passed in into the excel sheet.

C. Environmental Analysis of Distributed Energy

As solar and hydro generate clean energy and produce no greenhouse gas emissions. Therefore the installation of these projects will also contribute to the protection of environment and the renewables will replace the use of fossil fuels which produce GHG emissions.

D. Energy baseline and its improvement

Energy baseline is the source of energy, which is used in the rural areas in the absence of project activity. The emission baseline is analyzed by using the aggregate of annual kilowatt-hour output of all the micro-hydropower plants times the CO_2 emission factor for the fuel displaced.

Electricity generation per annum kwh/year = plant capacity factor kW

Annual CO_2 emissions tones of CO_2eq = power generation kwh/year * emission factor tones of CO_2/ kWh.

To find the total emission reductions, calculating the total annual energy generation by summing the installed capacity of each micro-hydropower plant in hours, then multiplies this with the emission factor of the displaced fuel which is diesel. After that convert it to tones of CO_2eq and the formula is given below,

Kw* hours* 1.83 kg CO_2eq /kWh = tone of CO_2

An emission factor of 1.83 kg CO_2eq /kWh is used for this analysis.

E. Research Design

This analysis is established in a descriptive investigation scheme. The research is focusing on the socio-economic aspect of micro-hydro projects in remote areas. This research shows how benefit takes benefit from the project and use energy for economic activities. The study is focusing on the social and environmental impacts of distributed energy before and after the installation of micro hydropower projects. Energy is not only part of our society but nowadays it is considered as a multitrillion-dollar business hub.

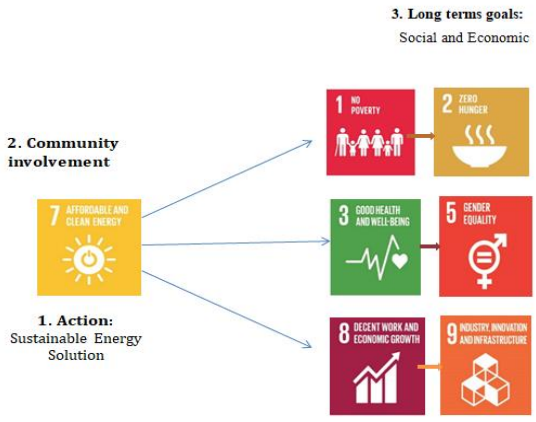

Figure 3. The Social Value of Energy Services [Research design framework]

In rural areas, there is no productive use of energy mostly people use electrical energy for lighting and cooking purpose. The projects installed by the PEDO and SRSP are less effective and has no sustainability. The community involvement is the basic issue and also the financial and social structure is not defined. Linking the community involvement (affordable and clean energy) with the social and economic analysis (SDGs 1, 2, 3, 5, 8, and 9) is the basic framework and the baseline for the

social value of energy services. By bringing full time solar energy and environmentally friendly storage to villages the project offers affordable and clean energy (SDGs 7 and 13). Using local renewable energy sources keeps money in the community that w ould otherwise be spent on the purchase of power and fuels elsewhere. Harvesting local energy will reduce poverty in the community (SDG 1). The revenues generated and the availability of power will allow for economic growth and work in appropriate, well-lit and heated or cooled, depending on the season, circumstances (SDG 8) while training young people to help multiply the concept. Being able to work in decent circumstances will help maintain health and well-being, while the electrification of the local health centers for people as well as animals will help to improve general health in the community (SDG 3). Electrification of the local schools will allow for quality education, while the training programs necessary to build, operate and maintain new microgrids increase education leading to good jobs (SDG 4). Better chances for education improve the chances of girls and women to participate in social life and employment (SDG 5). Decreasing the dependency of power and fuels imported to the community reduces the risk of conflicts and increases the chances of peace (SDG 16). The availability of power will likely reduce the risk of food perishing, reducing the risk of hunger (SDG 2). The introduction of solar based microgrids combines with storage provides the necessary energy infrastructure for rural communities to thrive (SDG 9). Thriving create space for support to the marginalized and disadvantaged (SDG 10). The availability of power might create an opening for two-, three- or more wheeled electric mobility, allowing the community to leapfrog the use of combustion engine vehicles (SDG 11) and the noise, heat and exhaust fume pollution related to them (SDG 15).

V. EXPLANTORY ANALYSSI

A. social and economic results of distributrd energy system

This portion of the research presents the outcomes and experiential results that were found through SPSS. In this portion first analyzed the social and economic results of the sample and after that additional analysis is carried out.

TBALE. 1 ECONOMIC ACTIVITIES CONNETED WITH MHP HOUSEHOLDS AND GRID-CONNECTED HOUSEHOLDS

		LABOR	AGRICULTURE	GOV. SERVICE	BUSINESS
MHP (HOUSEHOLDS)	PERCENTAGE				
GRID-CONNECTED (HOUSEHOLD)	PRECENTAGE	30	18	19	16

In this analysis, the percentage of households in government service or labor is greater or less equal. Actually, the MHP homes are situated relatively in the far-flung and mountainous area; as a result of the people over, there are not reachable to the commercial and colonial work. On the other hand, the grid-connected households are reasonably thriving in terms of productive use of energy like job opportunities, business, and overseas employment. If we talk about the ownership arrangement with respect to agriculture lands here both micro-hydro users and grid-connected households are changed. Households connected to the MHP are agriculture than grid-connected households.

B. People perception and satisfaction

In this analysis, we deal with the perception and the degree of satisfaction of rural areas about the provision of electricity by solar and micro hydro power plant (MHPP) and WAPDA.

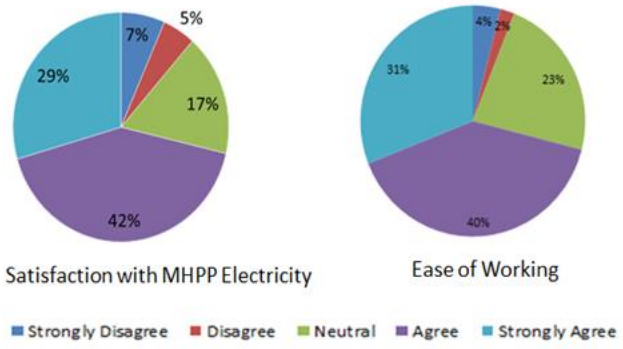

Figure 4. levels of satisfaction (Percentage of household)

Foreign employment, self-oriented business, agriculture service are the key livelihood/earnings sources of the inspection households. Supplementary profession contains fishing, hunting, daily wage, etc. The number and the ratio of survey families have shown in the table below. Greater number of families is depending on the overseas occupation. Though on the view of 45 households are connected to agriculture but then again some homes are totally hung on cultivation because agriculture is there main income sources.

The figure shows that people 23% are dependent on foreign employment. The households 40% are totally dependent on agriculture. 12% are involved in the services sector. 7% of people are engaged in their own business and 2 % are in others such as daily wages.

C. Environmental Analysis

Micro hydropower is a clean source of energy that produces no greenhouse gas emissions. The production of clean energy from micro-hydro will replace the fuelwood and kerosene oil in the targeted area and therefore will lead to the CO_2 emission reduction.

The total number of MHPs visited is shown in fig 4-8, were two major MHPs are operating and generating electricity in Kalamm valley. These plants are operating by the SRSP. MHPs plants have different capacities. Jungle inn MHPP has two turbines 200 kW each have a total capacity of 400 kW while the Ashuran MHPP has capacity of 1.2 MW. These MHPPs are of

proper design and the turbines are from a Chinese manufacturer.

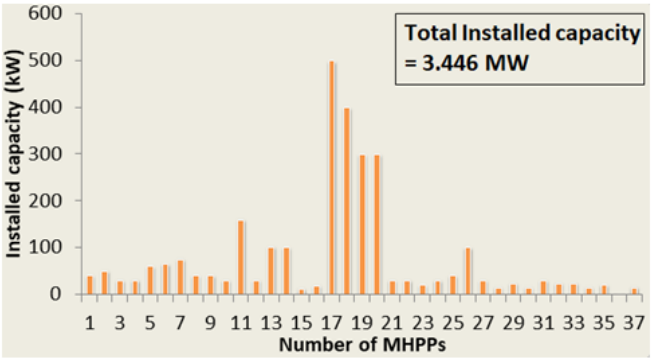

Figure 5. Installed capacity of each MHP

D. Green house gas emission reductions

This part shows the reduction of greenhouse gas emissions in the surveys area. As there is no access to the grid electricity due to the geographical location and remoteness of the area, so there is more probability of using fuelwood and kerosene oil by the local community. This will not lead only to the cutting of local forests but will also cause GHG emissions. Moreover, due to the increase in population and more demand for electrical energy, there are more chances that there will be more diesel generators in the community near in future. Therefore, the existing MHPs and expected new power plants will reduce GHG emissions. The total installed capacity of Ashuran and Jungle Inn MHPs are 1600 kW which is equal to 1.6 MW. From the survey report, it was found that each MHP power plant operates for 20-22 hours. Therefore, the average operating time per day is 21 hours. So this will give electrical energy generation in kWh per day.

Total installed capacity of the MHPs = 1600 kW

Operational time per day = 1600 kW * 10 hours = 16000 kwh/day

Month: 16000 kWh * 30 = 160000 kWh

Annual: 160000 kWh * 10 = 1600000 kWh

Therefore on annual basis the total electricity generation by the plants will be 1600000 kWh per annum.

Now multiplying this with the emission factor of 1.38 kg of CO_2eq/kwh, this gives total baseline emissions.

1,600,000 kWh * 1.38 kg CO_2eq/kwh = 2,208,000 tones CO_2eq/annum.

Now for the total 37 micro hydro sites,

Now the Total installed capacity of 37 MHPs = 3,446 kW

Operational time per day = 3,446 kW * 10 hours = 34,460 kwh/day

Month: 34,460 kWh * 30 = 1,033,800 kWh

Annual: 1,033,800 kWh * 10 = 10,338,000 kWh

Now multiplying this with the emission factor 1.38 kg of CO_2eq/kwh

10,338,000 kWh * 1.38 kg of CO_2eq/kwh= 14,266,440 tones CO_2eq/annum

VI. CONCLUSION

In remote areas of Pakistan people has no access to grid electricity mostly they spend their time in a dark situation. But the potential of natural resources like hydro, solar energy and biomass is tremendous. So by installing micr hydro or solar grid in a rural area is the ultimate solution of their poverty and social standard. The conclusion of this research is pointed: they have enriched the social and economic status of the communities. It has created new business opportunities and job for the local people. Kerosene oil was in expansive option for the people but now due to the availability of micro hydro power plants, it has reduced their expenditures. Those households which are not connected to the MHP are less developed and still use the traditional sources of energy for their light and cooking purpose. Consumption of electrical energy is highly related to high development and human welfare factor. The study hours of students have improved quite nicely and they give more time to the study because of the availability of light. Now the people are qualified and they have opened tuition academies for the children's. the use of traditional energy sources such as kerosene oil, firewood, and biogas have reduced. Energy from the hydro is the cheapest source of energy and people can eradicate poverty and improve their life standard through energy innovation in this in this field.

REFRENCES

[1] K. Kaygusuz, "Energy and environmental issues relating to greenhouse gas emissions for sustainable development in turkey," Renewable and Sustainable Energy Reviews, vol. 13, no. 1, pp. 253–270, 2009.

[2] I. Dincer, "Renewable energy and sustainable development:a crucial review," Renewable and sustainable energy reviews, vol. 4, no. 2, pp. 157–175, 2000.

[3] S. Z. Farooqui, "Prospects of renewables penetration in the energy mix of pakistan," Renewable and Sustainable Energy Reviews, vol. 29, pp. 693–700, 2014.

[4] M. H. Sahir and A. H. Qureshi, "Assessment of new andrenewable energy resources potential and identification of barriers to their significant utilization in pakistan," Renewable and Sustainable Energy Reviews, vol. 12, no. 1, pp. 290–298, 2008.

[5] J. Soussan, Primary resources and energy in the third world.Taylor & Francis, 1988.

[6] R. H. Jones, "Energy poverty: How to make modern energy access universal," Special early excerpt of the World Energy Outlook, 2010.

[7] I. E. A. O. of Energy Technology, R. . D., and G. of Eight (Organization), Energy technology perspectives. InternationalEnergy Agency, 2008.

[8] A. Ie, "Energy technology perspectives scenarios and strategies to 2050: in support of the g8 plan of action," 2006.

[9] B. K. Hodge, Alternative energy systems and applications. John Wiley & Sons, 2017.

[10] N. A. Owen, O. R. Inderwildi, and D. A. King, "The status of conventional world oil reserveshype or cause for concern?" Energy policy, vol. 38, no. 8, pp. 4743–4749, 2010.

[11] R. Woodward, The organisation for economic co-operation and development (OECD). Routledge, 2009.

[12] S. Teske, J. Muth, S. Sawyer, T. Pregger, S. Simon, T. Naegler, M. O'Sullivan, S. Schmid, J. Pagenkopf, B. Frieskeet al., Energy [r] evolution-a sustainable world energy outlook. Greenpeace International, EREC and GWEC, 2012.

[13] C. Venkataraman, A. Sagar, G. Habib, N. Lam, and K. Smith, "The indian national initiative for advanced biomass cookstoves: the benefits of clean

combustion," Energy for Sustainable Development, vol. 14, no. 2, pp. 63–72, 2010.

[14] T. Dietz, G. T. Gardner, J. Gilligan, P. C. Stern, and M. P. Vandenbergh, "Household actions can provide a behavioral wedge to rapidly reduce us carbon emissions," Proceedings of the National Academy of Sciences, vol. 106, no. 44, pp. 18 452–18 456, 2009.

[15] M. Asaduzzaman, D. F. Barnes, and S. Khandker, Restoring balance: Bangladesh's rural energy realities. The World Bank, 2010.

[16] S. Ohshita, "Exercising power: Chinas transition to efficient, renewable energy," in Germany's Energy Transition. Springer, 2016, pp. 133–163.

[17] S. Tracey and B. Anne, OECD insights sustainable development linking economy, society, environment: Linking economy,society, environment. OECD Publishing, 2008.

[18] K. Kaygusuz, "Energy services and energy poverty for sustainable rural development," Renewable and Sustainable Energy Reviews, vol. 15, no. 2, pp. 936–947, 2011.

[19] M. G¨uney and K. Kaygusuz, "Hydrokinetic energy conversion systems: A technology status review," Renewable and Sustainable Energy Reviews, vol. 14, no. 9, pp. 2996 3004, 2010.

[20] K. Kaygusuz, "Wind energy status in renewable electrical energy production in turkey," Renewable and Sustainable Energy Reviews, vol. 14, no. 7, pp. 2104–2112, 2010.

[21] K. Kaygusuz, "Wind energy status in renewable electrical energy production in turkey," Renewable and Sustainable Energy Reviews, vol. 14, no. 7, pp. 2104–2112, 2010.

[22] "Prospect of concentrating solar power in turkey: the sustainable future," Renewable and Sustainable Energy Reviews, vol. 15, no. 1, pp. 808–814, 2011.

[23] S. O. Oyedepo, "Energy and sustainable development in nigeria: the way forward," Energy, Sustainability and Society, vol. 2, no. 1, p. 15, 2012.

[24] M. A. Rosen, "Energy sustainability: A pragmatic approach and illustrations," Sustainability, vol. 1, no. 1, pp. 55–80, 2009.

[25] S. Adeyemo and A. Odukwe, "Energy conservation as a viable pathway towards energy stability," 200

How to cite this article:

Majid Ullah, Sayed Kamal, Malik Amad Khalil, Sheraz Khan, "Social and Environmental Analysis of Decentralized Energy System and Its Future Prospects", International Journal of Engineering Works, Vol. 7, Issue 12, PP. 406-413, December 2020, https://doi.org/10.34259/ijew.20.712406413.

International Journal of Engineering Works
ISSN-p: 2521-2419
ISSN-e: 2409-2770
Vol. 7, Issue 12, PP. 422-428, December 2020
https://www.ijew.io/
https://doi.org/10.34259/ijew.20.712422428

Life Cycle Assessment of Monocrystalline Versus Polycrystalline Imported Photovoltaic Panels in Context of Energy

Malik Amad Khalil[1], Majid Ullah[2], Wisal Muhammad Khalil[3]
[1, 2]US:-Pakistan Centre for Advanced Studies in Energy, University of Engineering & Technology, Peshawar, Pakistan, [3]Electrical Department, University of Engineering & Technology, Peshawar, Pakistan
mkhali10@asu.edu[1], mullah2@asu.edu[2], wisalmalik038@gmail.com[3]
Received: 20 November, Revised: 01 December, Accepted: 25 December

***Abstract*—** Solar energy is one of the most promising and sustainable energy suppliers among other energies. Geologically Pakistan is residing in the territory of highest solar radiation fall in the world. The average radiation falls is range from 4.656 - 4.864 kWh/m^2/day daily on Pakistan. It shows the high potential solar energy exists in Pakistan, but still Pakistan is unsuccessful to trap solar energy in abundant manner due to many reason. Pakistan is facing energy crisis for many years and still many of the regions are not electrified due to accessibility and other issues. So the local people are using the standalone solar system for fulfilling the basic need but the survey found very bad quality solar panels selling in the market which are imported from china and other countries. However, it discourages indirectly the local people by using such panels by getting the low output. So this research is carried to conduct the life cycle assessment (LCA) of solar module. It is a technique that quantifies the product impact on the environment and identifies other important factors which ensure the quality and market development. In this research the LCA found the processes and operation used in manufacturing the solar module, which contribute larger part in the emission and energy consumption. The transformation of metallurgical grade silicon to solar grade silicon and panels assembly is the two main processes which consumed more than 70% of energy and take part in higher emission. The results showed 1416 MJ/panel and about 79 kg of equivalent CO2/panel generated. So it is proposed that Pakistan should start their manufacturing.

***Keywords*—** Energy Payback period (EPBT), Global warming potential (GWP).

I. INTRODUCTION

In last decade the energy demand in Pakistan is significantly increases. Pakistan has energy crisis and most of the rural areas are still not electrified. The Demand and supply gap is increasing every year. Due to such energy crisis the rural area has load shedding of about 16-18 hours and urban area faces 10-12 hours of shortfall during hot summer [1]. Geologically Pakistan territory reside in very high solar radiation [2]. On domestic level, people use solar panels to fulfil their basic need of energy; they used the imported solar panels of different companies.

Life cycle assessment (LCA) is a tool and technique used for the assessment of the product related with improvement and finding its impact and their potential throughout a product life [3]. Globally the non-renewable resources contribute the larger part in polluting the environment and create abundantly energy crisis [4]. Due to such worst resultant of non-renewable resources, the world start shifting toward the renewable energies, which pollute environment less than non-renewable resources or have high potential to save carbon emission in abundant manner [3,4]. Solar power is well known for having the high potential in free energy and capacity to decrease pollution, energy consuming reduction and end production of energy [3].

Since commencement of new century, the remarkable growth has been recorded in the solar PV manufacturing and market application [2,3]. The Chinese market in PV manufacturing results a rapid growth, advancement and act like the leader in the globe [4]. In current situation, the shipment of PV module reached to 27.4 GWp in 2013, which is about 50% of the whole shipment in the world. Moreover, the efficiency of the solar cell increase annually, it got increase from 12% to 18%, the mitigation in consumption of energy on production of solar grade silicon has also been experienced [6]. Additionally, the system cost and module cost are decreased as well [7]. Some of the researcher raised point against the energy yield of solar energy that it could not fulfil the atonement of consumed energy in manufacturing. Some other points also rose that it is not a clean energy because of hazard materials emitted during manufacturing of solar module especially when the molten grade silicon is converted into solar grade silicon [8]. It is difficult task to show the solid results or proof by considering only energy and material flows. There are different materials emission and energy consumed on different stages which have their own impacts on environment. Overall the Solar system is considered the clean system for energy production and also maintenance free. However, the pollution and the consumption of energy should account when considering the whole life cycle

of solar system [8]. The solar system produced certain amount of energy which provides the exceeded atonement of consumed energy during manufacturing [9]. Therefore, it is need to assess the life cycle of solar system to identify whether it is environmental friendly or not.The recent research has been done by California University and MIT, Stanford University on the energy and atmosphere program. Their studies found the atmospheric result of 139 countries which shows the solar radiation falls and potential of hydropower. The report reveals that Pakistan is one of the blessed countries in the world which has highest potential in solar energy, which can fulfil about 92% of energy requirement [4]. Figure-I-1 shows the map of solar radiation that falls daily on Pakistan territory which unveils the solar energy potential in Pakistan.

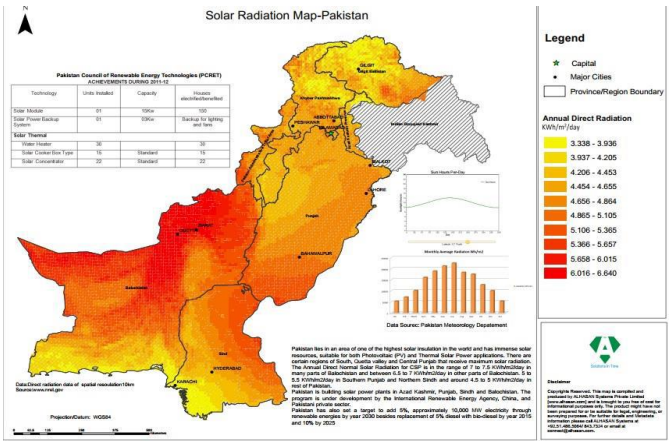

Figure –I-1 Solar Radiation Map of Pakistan [4]

Pakistan has currently few of their solar projects that are operational since last few years. The country need to be more relying on solar energy. To avail such potential of solar, Pakistan has to boost solar installation. Pakistan has only one solar grid in Bahawalpur Punjab that produces 100 MW of electricity [2]. In KPK the different companies of solar panels are available that have numbers of varieties and output. However, no standard company's panels found yet. There are three type of panels found, monocrystalline, polycrystalline and thin film, having different watts' output and Cost. But the survey found polycrystalline is the most selling panels. To find the more efficient and quality PV panels, it need to conduct the life cycle assessment (LCA) of solar Panels that are imported from china. LCA include the very first stage goal and product scope, the take analysis of inventories, after that assessment conduct of impacts and then finally interpretation [5]. The goal and scope of the LCA identify the objectives of the study, the functional unit and boundaries. The inventory analysis describes the different flows, resources and materials. These flows and hazards material which create the different environmental problems are aggregated and then assessments are taken for final conclusion in the interpretation stage [5]. It is the method for comparing the different products or products with different level for further improvement and environmental protection. After many decades' researcher realized that the human life and environmental protection is more important than technology development, so LCA is used as tool to find the potential for improvement in product. The LCA mainly used to account the sustainability of the product, greenhouse gas emission (GHGs) and energy payback time (EPBT) [10].

II. METHODOLOGY

LCA is one of the hard projects to undertake, I have used GaBi software for LCA. All the materials that are used for inflow and outflow like energies, emissions and recourses taking from very first like cradle to grave, are accounted for environmental impact assessment. The LCA methodology includes the goal and scope. The goal and scope define the boundaries of the systems or product, quality of data and many numerous materials. The LCA processes have different results for every process. According to ISO-14014 the standardized LCA can be perform by specified principles and frameworks, which leads to the correct LCA performing. There are four main phases in LCA, which are Goal and Scope, inventory Analysis, impact assessment and interpretation, which are shown in the below figure II-1 [5]. All other methods and process have taking under these phases and methods.

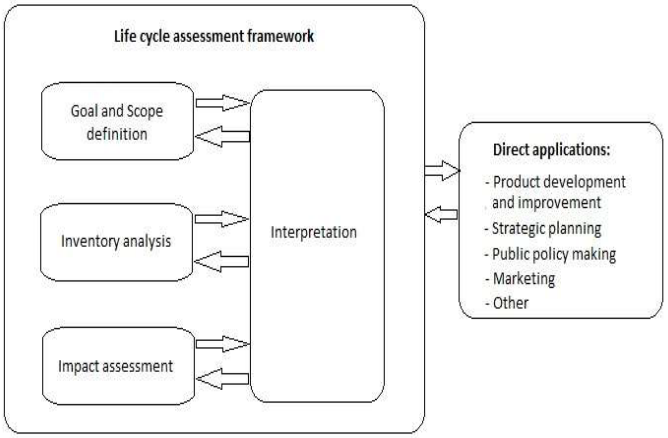

Figure II-1: charts shows LCA different stages

A. *Goal and Scope*

The Goal and Scope define the typical aspects that are commonly found in LCA. Some of the question that should be consider in goal and scope of LCA. The goal should define:

- Reason of this study carrying out
- The result will be used for
- Which product is using

There are many reasons for conducting LCA of Solar panels but researcher main focus will be the identification of sustainability domain of the monocrystalline versus polycrystalline imported solar panels for Pakistan territory, which are used locally in abundant manner[2]. Other reasons include the development of the product, providing best product to the customers and products comparison. The importance of goal also affects the scope side of LCA because of having interrelation with each other; the goal of your study may define the scope of your product study. It will settle the boundaries and circle of study [11]. Scope defines the boundaries of the product and it will fulfill goals. The scope includes the following steps and method. Selection of different function enables comparison between two products. It gives the quantified measurement of the services and performance. To quantify and measure the product, both FU should include all the inflow process and methods. In LCA the FU has very important role because of the comparison of the two products [12]. For example, if we take the solar panels of two different models of different companies, both have function to give the solar energy; it will give the comparison opportunity according to the territory suitability. The system will include those processes that are important for the LCA [13]. It is impossible to carry out all the process because sometime it includes most of the irrelevant process which later lead to the time consumption in LCA. So that is why the boundaries are described to conduct the relevant data [13].

- Natural systems defined boundaries
- Geographical systems defined boundaries
- Boundaries of time
- Other product Boundaries

A. Life cycle inventory (LCI)

The input or inflow resources and materials like water, energy, fuels and many other materials should be consider for the system studies during life cycle [14]. The materials that are emitted from the system like acidified liquid to the ground, hazardous gases to the air, other by-products and products should be identified. These in and out flow of the system at every stage and process should be quantified. The collected data should then present for assessment stage. To conduct the data, every input and output of the system should be monitored or measured [15]. There are some databases also available through which online data can be extracted. After collection of the specified data, it should be then categorizing, which would be arranged in categories as per impact on environment. The collected data is then calculated per function unit.

B. Impact Assessment

The impact assessment for pulling out the result in easy way [16]. The classification of the raw data limited the inventory analysis up to 15 categories for clear and easy consequences of the results. There is no specified categories for impact assessment because of absence of harmony on categories, that which categories should avoided and which should take, to solve such uncertainties general categories should be taking like effect on human health, recourses consumption and effects on ecology [17]. These main categories include the further sub categories which will identify data more effectively. The subcategories are shown in figure II-2. There are some of the compounds which are included in more than in one category; it should be mentioned. For example, the output of NO (nitrogen oxide) would be included in category of ozone depletion, GWP and acidification [18]. After collecting the data of elementary flow, the data should be categories in different category. It would be then translated into one single element that will represent the rest of compound potential called characterization [19]

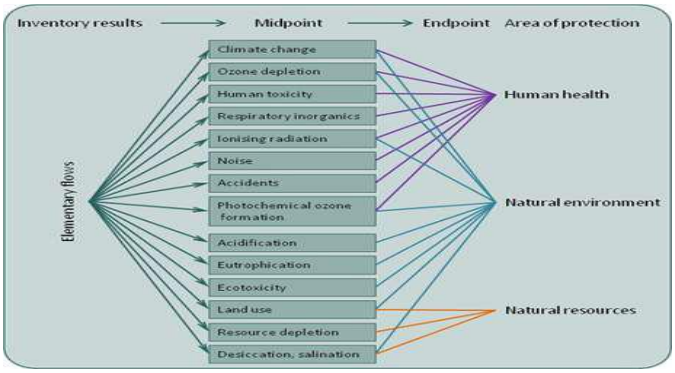

Figure II-2: charts shows LCA different stages

III. PROCESSES AND YIELDS

The results from this research include the three different phases of LCA for solar panels. These phases define the whole life cycle of this product and concluded the impacts on the Pakistan territory. These phases include the upstream, midstream and then the downstream. Upstream processes include quartz mining, solid grade silicon (sog-Si) purification, silicon ingot growth and wafer slicing and finally the production of modules. Midstream processes involve the installation, operation and then the outputs from their energy and CO2 emission. Lastly, downstream processes include PV system operation and retirement of PV stations, the decomposition of the solar panels and the reuse of the secondary input as primary input. Figure III-1 shows model of LCA.

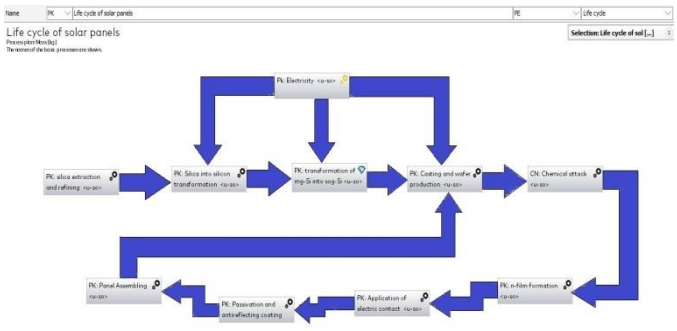

Figure III-1: Modeling LCA of solar panel

A. Upstream process

The simulation result shows the different process contribution in the output of the different materials and their percentage in Global Warming Potential (GWP). There are three processes which show the larger contribution in the GWP and energy consumption. One is the transformation of metallurgic

grade silicon to solar grade silicon, the second one is panel assembling and the other one is casting and wafers production. The first one contributes about 48% in the emission and consumes about 1180 MJ/panels. The casting and wafer production contribute 15% while the panels assembling create about 18% of material and consume 12 MJ/panel and 224.14 MJ/panels of energy. The rest processes have very less outflow. Some of them are very negligible output and energy consumption. Here is the proportionality method is suited in better manners. The processes which consume more energy are the main emitter of materials and have larger impact on environment. Some of the statistics are shown in the figure III-2.

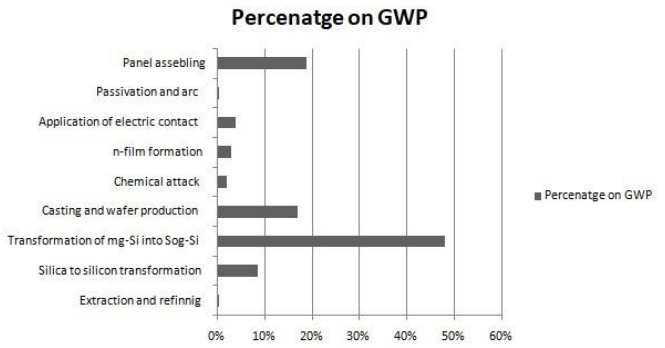

Figure III-2: Percentage on Global warming potential

Here are some other aspects that are account for the greater emissions and energy consumption. That is the use of methods, techniques and technology for the manufacturing of photovoltaic panels. The most advanced technology is nowadays used for the production of very efficient panels which have greater efficiency and have very low consumption and output, but they are not commercialize yet. Here is some of the research shows the contribution of each process in GWP, the emission of 314 kg-CO2 eq/m2. This emission is occurring for the production of multicrystalline panels of efficiency 16%.

i. Emission by solar wafer manufacturing

The emission due to solar wafer manufacturing includes the emission carbon dioxide, solvent, hazardous water, silicon dioxide, silicon dust, argon gas and many other materials as shown in the figure 4.3. A 6 % deficiency in silver paste usage can result the reduction in Impact on human life, marine ecosystems, and metal resources respectively which would be 4.43%, 5.13%, and 2.47%. All of these materials are taken according to the carbon dioxide equivalent. The impact potentials are comparing with carbon dioxide and simply multiply when it found more or less than carbon dioxide potential. The mineral oil is emitted in larger magnitude from the wafer manufacturing which is about the 15 g per wafer shown in the figure III-3. The second number is silicon carbide which is about 14 g per wafer. It can cause the lung cancer in animal, cause the eye irritation in human and resultant the respiratory difficulties in human and animals. The other high emission includes the KOH and argon gas. The KOH causes the damage of respiratory track, lung damages and other skin problems. It is very destructive to all body tissue and causes serious problem to human body. The argon gas causes Inhalation problem, the excessive inhalation causes the dizziness, vomiting, nausea, consciousness losing and finally death. So to avoid such serious impacts the manufacturing should be far from urban areas

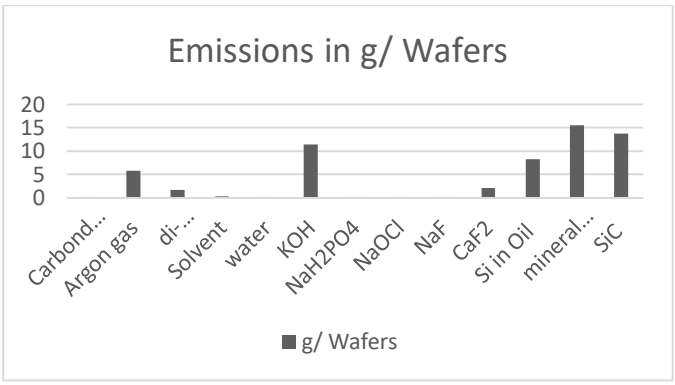

Figure III-3: Emission from wafer production

ii. Emission Due to molten grade silicon

Figure III-4 shows the emission of different material which are emitted due to the conversion of molten grade silicon (mg-Si) to solar grade silicon (Sog-Si). The high magnitude of emission includes the 4.7 kg of carbon dioxide (CO2) shown in figure 4.4, this emission is taken as equivalent of other chemical substances. The carbon dioxide is the hazardous substance for the environment. The main problem it causes is the respiratory system damages. Along with carbon dioxide and other outputs are accounted toxic for the marine life and human life. These emissions are related to the energy consumption. If the consumption of electricity reduced to 98 kWh/kWp, nearly 23.09%, 2.15%, 0.60%, and 25.80% of the total impact on environment in the specified matter production, toxicity of marine ecosystem, metal resources depletion, and fossil energy depletion will be curtailing respectively. The interpretation of these results describes the emission of certain materials are negligible. It cannot cause the serious impacts on the environment if some protective acts would apply.

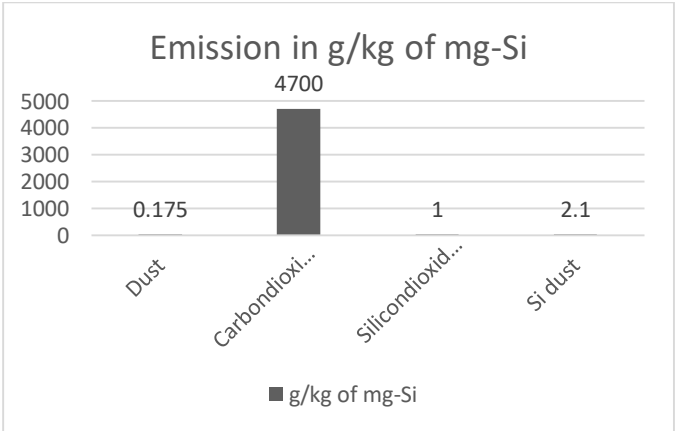

Figure III-4: Emission from molten grade silicon

iii. Emission due to solar grade silicon

The different materials are emitted from the production of solar grade silicon. These emissions include silicon dioxide, calcium fluoride and silicon dust shown in figure III-5. The high magnitudes of emission possess the calcium fluoride, which has greater contribution in climate change, marine toxicity and resources depletion. The critical impacts which contribute the dominant role in environmental burdens are human toxicity, threat to marine life and resources depletion. The other impacts which are resulted from non-renewable resources depletion, formation of matters and acidification of land have insignificant impact. Some other emissions are recorded from this operation but they are negligible

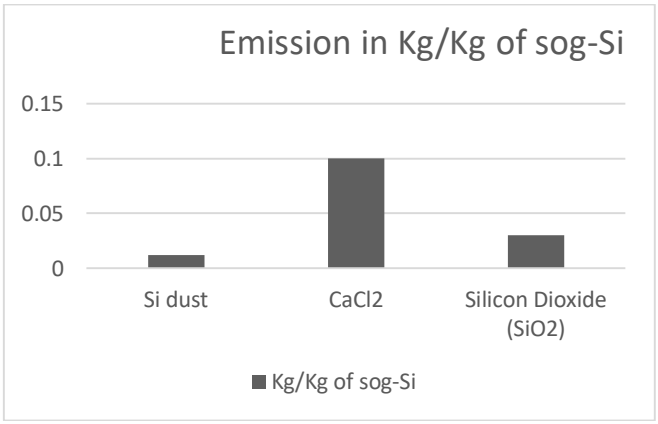

Figure III-5: Emission due to solar grade silicon

iv. Emissions Due to panel assembly

The panel assembly wastes include the EVA output, silicon adhesive and aluminium in abundant manner shown in figure 4.6. These materials contribute in soil contaminations, water, biotic and Abiotic impacts occur due to these wastes. The results show that the usage of wasted aluminium as primary aluminium, it can give the greater benefits to the environment and energy consumption. If this step will follow by the industries, it is approximately 1.60 kg CO2 equivalent and 0.52 kg fuel equivalent of environmental benefits and energy resources benefits can avail. The other important material like tellurium, semiconductor and glass output if used as primary product the huge burden can be diminish by industries. Therefore, the usage of secondary material as primary material is high recommended for promoting the achievement by using the less resources and low energy.

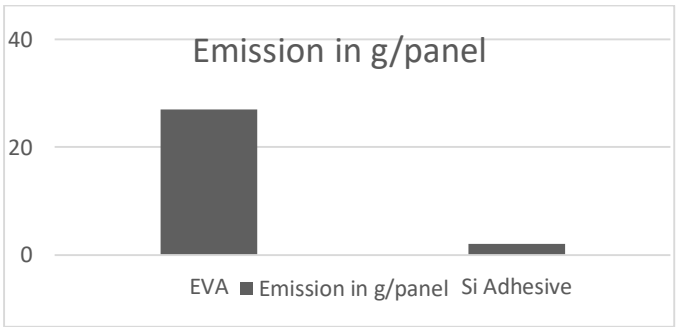

Figure III-6: Emission due to Panel assembly

B. Midstream Process

The midstream process includes the installation of the solar grid, their operation and then retirement. All these process are accounted in term of the energy consumption, emission and the payback period. The resulted data are taken under consideration of different factor like the energy consumed by solar panel during the installation, their transportation, transmission and other components involving. These results are taken from the 67 kW of solar station installed in English biscuit company in Haripur. They had installed two arrays of module. One includes the 560 panels of polycrystalline while the other has 650 panels. The total panels were 1210 in number. Each panel has 250 watts of capacity. The real time data are used in GaBi software and result the different data. The figure III-7 shows the energy consumption by installation monocrystalline and polycrystalline photovoltaic panels of 250 watts of each panel. Which shows the monocrystalline consumed more energy than polycrystalline. The monocrystalline consumed 2810.4 GJ of energy per 67 kW of solar system while the polycrystalline consumed 2215.49 GJ.

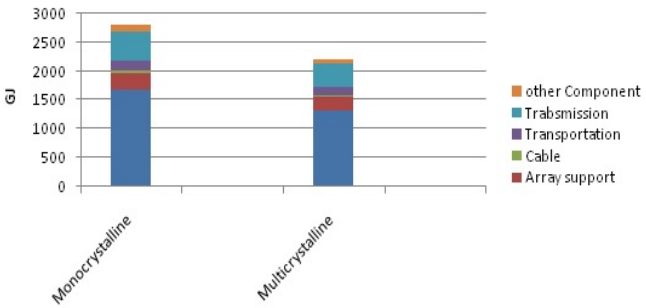

Figure III-7: Energy requirements for small scale PV system (GJ / kW)

The figure III-8 shows the CO2 emission of mono versus polycrystalline of solar panels which again show the monocrystalline have emission then polycrystalline. The high emission includes the 153.64 ton of CO2 eq from the 67 kW of solar system, while the polycrystalline have 128.8 ton of CO2 eq.

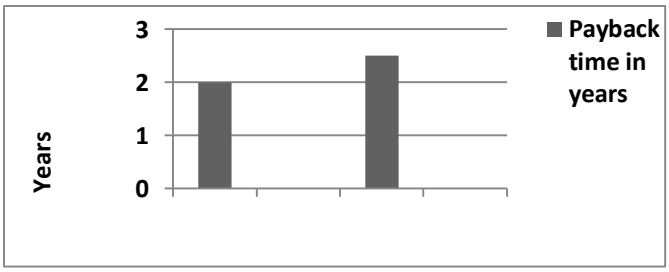

Figure III-8: C02 emission of PV system (t-CO2 / kW)

The figure III-9 shows the payback period of monocrystalline has 2 years while the polycrystalline have 2.5 years. Here it shows the monocrystalline has lower pay back period than polycrystalline. It because of mono has higher efficiency than polycrystalline solar panels. The monocrystalline exists in 17 to 18% efficiency in market but the polycrystalline have 16 to 17%.

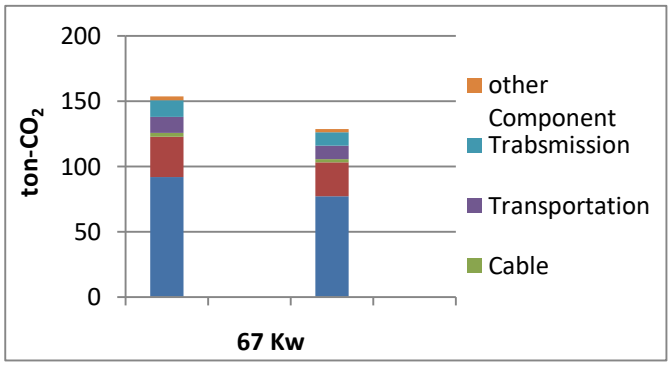

Figure III-9: Payback period of Solar PV system (Years)

C. Downstream Process

The downstream process includes the retirement and decommissioning of the solar modules.There are some of the investigation and results found on the recycling and decommissioning of the solar system. One of the major problem faced by solar industry is the separation of stratify module, because of the polymers linked cross sectional. The industries yet found the solution to dismantle the solar module and reused some part of it in the solar module production. One of the solar companies found the liberation method of wafers and reused them. This method includes the dipping of module in NHO3 for 25 hours. The wafers extracted from this method are then passed with special process and prepare it for moderate performance. But this method is costly than the normal wafer production. The solar cells produced by such method described above are efficient or not, it is not cleared yet or silicon wafer need to re-melt by casting and sawing method. In such cases the energy required to reproduced and separate the silicon by casting and sawing method which tend to increase in the cost per module. But from the results it has found that the aluminum frame can be reuse in the module production.

D. Impact Assessment

The figure III-10 shows below the most significant impacts and results from output of toxic material and their contribution to human toxicity, marine system damaging, and metal resources depletion. The most momentous materials which contribute in human body damaging are Pb (lead), As (arsenic), and Hg (mercury) to air, it causes the bladder and lung cancer by respiratory system in human and animals. The other reports also showed that the skin changes due to Ag (silver) paste, producing glass and electricity. Similarly, the marine ecosystem damages due to copper and nickel to water and air, these substances are mainly produce from Ag pastes and glass. The metal resources depletion is caused by the Ag paste producing method. It gives the dominant contribution in metal depletions. The reduction in cultivated land is the main impact of the larger solar system installation. The average land required for 1 MW solar system is 5-6 acre of land. The results show the output substances contribute about 80% of the ozone layer depletion; these substances will be taken equivalent to the CFCs. The recent researches showed the 2,25x108 kg CFC-11 eq/ kWh.

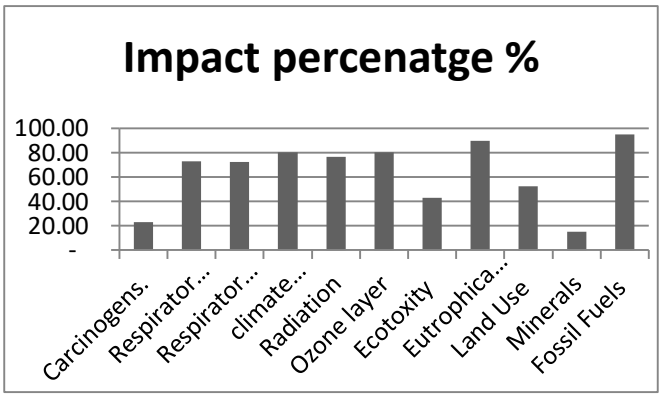

Figure III-10: impact percentage on the environment

CONCLUSION

During the manufacturing of solar panels, the major emissions are occurring due to the energy get from fossil fuels, for manufacturing different components and taking the different operation. these emissions depend on the country, because each country have different energy mix, so the different country have different emission. Briefly the analysis and assumption resulted that the total gross energy requirement (GER) for one solar panel is 1416 MJ /panel and about 79 kg of equivalent CO2/panel generated. And Pakistan can sustain such amount of emission because according to the national GHG inventory of Pakistan for the total GHG emissions annually is 369 MtCO2e with 45.9% part of energy, 44.8% agriculture and livestock sector and the rest contribute the other parts while china who is the largest contributor in global warming produce 7.3 Gton of CO2 annually just from coal. By comparing these two countries we can conclude, Pakistan should start their own manufacturing of solar module. For calculating the energy payback period, it is assumed Pakistan produces 200 panels of 350 watts per day. So it will consume 283 GJ/panels on average. So the EPBT will be about 2-3 years. The most censorious phase in the solar manufacturing is transformation of mg-silicon into sg-silicon and the assembling of panels. Moreover, its estimated that energy payback time would be shorter than the panel life spans. According to researcher survey it had been found that the multicrystalline solar panels are best-selling solar panels in Pakistan. Multi-Si PV system has slightly low efficiency then Mono-Si system, but their energy consumption is less than mono-crystalline. Pakistan has abundant of solar raw material resources, it need to be utilize and take advantage because of energy crises and CO2 emission caused by electricity generation in Pakistan by other non-renewable sources. Therefore, multicrystalline should take in account for manufacturing in Pakistan. Moreover, there are millions of solar panels installed in Pakistan in residential area and non-residential area. There number of these panels are not yet clarified but after 20 and 30 years. These panels will be considering as burden over in pace

of wastes product. These wasted panels can be reuse as secondary product.

REFRENCES

[1] Farooq M, Shakoor A. Severe energy crises and solar thermal energy as a viable option for Pakistan. J Renew Sustain Energy Rev 2013;5:013104
[2] Water and Power Development Authority. ⟨http://www.wapda.gov.pk/⟩.
[3] Mirza Umar K, Mercedes Maroto-Valer M, Ahmad Nasir. Status and outlook of solar energy use in Pakistan. Renew Sustain Energy Rev 2003;7.6:501–14
[4] Ahmad Firoz, Intikhab Ulfat. Empirical models for the correlation of monthly average daily global solar radiation with hours of sunshine on a horizontal surface at Karachi, Pakistan. Turkish J of Phys2004;28.5:301–7
[5] ISO 14040. Environmental management – life cycle assessment – principles and framework; 1997
[6] Wang Yu, Zhou Sheng, Huo Hong. Cost and CO2 reductions of solar photovoltaic power generation in China: perspectives for 2020. Renew Sustain Energy Rev 2014;39:370–80.
[7] Stephen Connors, Katherine Martin, Michael Adams, Edward Kern, Baafour Asiamah- Adjei. Emissions reductions from solar photovoltaic (PV) systems, LFEE Report No.: 2004– 003
[8] Bakhiyi Bouchra, Labrèche France, Zayed Joseph. The photovoltaic industry on the path to a sustainable future–environmental and occupational health issues. Environ. Int. 2014;73:224–34.
[9] Hosenuzzaman M, Rahim NA, Selvaraj J, Hasanuzzaman M, Malek ABMA, Nahar A. Global prospects, progress, policies, and environmental impact of solar photovoltaic power generation. Renew Sustain Energy Rev 2015;41:284–97
[10] Sun Honghang, Zhi Qiang, Wang Yibo, Yao Qiang, Su Jun. China's solar photovoltaic industry development: the status quo, problems and approaches. Appl Energy 2014;118:221– 30
[11] Yuwen Zhao. Current development status and future trend of China PV industry. In: 13th China photovoltaic conference: Beijing; September 5–7, 2013
[12] Li Junfeng, Wang Sicheng, Wang Bohua, et al. Annual review and outlook for China PV industry 2013, By the Chinese renewable energy industries association and the China Photovoltaic Industries Association.
[13] Liu Dawei, Shiroyama Hideaki. Development of photovoltaic power in China: a transition perspective. Renew Sustain Energy Rev 2013;25:782–92
[14] Baharwani Vishakha, Meena Neetu, Dubey Alka, Brighu Urmila, Mathur Jyotirmay. Life cycle analysis of solar PV system: a review. Int J Environ Res Dev 2014;4(2):183–90
[15] Stamford L, Azapagic A. Life cycle environmental impacts of UK shale gas. Appl Energy 2014;134:506–18
[16] Different Solar Potential Co-Ordinates of Pakistan by Fazal Muhammad*, Muhammad Waleed Raza, Surat Khan and Faizullah Khan Electrical Engineering Department BUITEMS, Pakistan
[17] ISO 14041. Environmental management – life cycle assessment – goal and scope definition and inventory analysis; 1998.
[18] Pakistan Council of Renewable Energy Technologies (PCRET)
[19] Hunt LP. Total energy use in the production of silicon solar cells from raw materials to finished product. In: 12th IEEE PV Specialists Conference. New York; November 15–18, 1976. p. 347–52

How to cite this article:

Malik Amad Khalil, Majid Ullah, Wisal Muhammad Khalil, "Life Cycle Assessment of Monocrystalline Versus Polycrystalline Imported Photovoltaic Panels in Context of Energy", International Journal of Engineering Works, Vol. 7, Issue 12, PP. 422-428, December 2020, https://doi.org/10.34259/ijew.20.712422428.

IJEW 国际工程期刊 International Journal of Engineering Works انجینئرنگ کاموں کا بین الاقوامی جرنل

International Journal of Engineering Works
ISSN-p: 2521-2419
ISSN-e: 2409-2770
Vol. 7, Issue 12, PP. 414-421, December 2020
https://www.ijew.io/
https://doi.org/10.34259/ijew.20.712414421

Optimal Design and Analysis of Integrating Solar Energy in Off-Grid Telecommunication Sites

Farhan ullah, Naveed Malik, Dawood Shah, Amir Khan

[1,2,3,4] Department of Electrical Energy System Engineering, US-Pakistan Center for Advanced Studies in Energy (USPCAS-E), UET Peshawar
farhan.ullah58@gmail.com[1], engrmalikuet@gmail.com[2], dawoodshah396@gmail.com[3], amirkaahn@gmail.com[4]

Received: 03 December, Revised: 15 December, Accepted: 29 December

***Abstract*—** In the last decade, the number of mobile subscription all over the world growing at a magnificent pace and providing connectivity to everyone around the globe is indispensable, which led to an increasing number of mobile base stations (BSs). In urban community mobile operator has easy access to grid electricity and they can easily installed BTS in these locations in a cost-effective way. But the rural areas face huge problem of electricity and grid electricity is not spread out in all the region, so, mobile operator face a huge problem while deploying BTS. Most of the rural region of Pakistan facing the problem of load shedding, power failure and no grid electricity access, so, mobile operator usually employed diesel generator to cater these issues, but due to escalating price of diesel oil and global warming it's very costly in term of energy production and is environmentally unfriendly too. So, mobile operator needs some alternative ways of energy production in these locations. To power up BTS in remote areas, renewable energy sources are the best solution and incorporation with diesel generator make the system further efficient and reliable. This study furnishes the design and simulation of stand-alone HRES along with their feasibility report and economic analysis using HOMER. Another aim of this work is the comparison of the existing system and the proposed hybrid system for the telecommunication site. A sensitivity analysis is also carried out to observe and analyze the effect of variation in different parameter on the COE and NPC. It is evident from the optimization results that the integration of solar energy along with battery bank is the most optimum. Furthermore, due to the integration of renewable energy emission of greenhouses gases get abated.

***Keywords*—** Base Transceiver Station (BTS), Net Present Cost (NPC), Cost of Energy (COE), HRES

I. INTRODUCTION

All over the world energy is the most influential pre-requisite, which play a major role in countries economic development, industrialization and improving quality of life. In developing countries sustainability of energy is very important for sustainable economic growth, so continuous supply of electricity appeared as a backbone and play a paramount role in economic development and quality of life. According to[1] in developing countries, electrified regions are more developed than the non-electrified regions in spite of having great electric power growth. Despite having appreciable development in the technical field, the world couldn't even solve the global warming issue, but it is increasing very rapidly due to increasing energy demand around the globe. Most of the energy around the globe is generated from the fossil fuels and in late 1960 almost 94% of the global power was generated from the fossil fuels and in 2014 it is reduced to 80%. Nevertheless, the energy generated by fossil fuels has still a great share and also heating up the globe[2].

According to[3] Pakistan has limited conventional resources and is laboriously relying on the import of fossil fuels and every year greater than 20% earnings gain through the foreign exchange is used upon oil imports. Pakistan is confronting huge energy crises right now, and the energy gap between supply and demand is shooting up. The domestic and commercial consumer confronting too many problems, so policymakers and energy planners must take a step for several auxiliary sources of energy which are economically viable and practically feasible. Folks living in the rural areas of five provinces in Pakistan are about 63.623% of the total population of Pakistan in compliance with Pakistan economic survey 2017-2018. Global Energy Systems (GESs) is too much relying on conventional energy sources but now there is a global shift towards the clean energy. The total global investment was $62 billion in 2004 and raised to $333.5 billion in 2017[4].

Nowadays, a great percentage of world energy consumption met through conventional energy sources. However, these sources cannot overcome the demand of future electricity requirement due to their economic and environmental problem. Also for electrification of remote and scattered populated areas, more reliable, robust and less maintenance system is need to design because in these areas consistent maintenance and replacement is not practicable due their geographical locations.

So, renewable energy sources in these remote and scattered populated areas are the best way to overcome the energy demand but there are several problems associated with these sources when they are used to supply the local community load discretely, such as high capital cost and little security of supply due to their intermittent and undetermined nature[2]. Also, a single renewable source cannot provide a reliable system so, a new notion, namely Hybrid Renewable Energy Systems (HRESs) has unfolded which can solve the above mention problems[5]. HRES is an integration of renewable sources with each other and with other conventional sources e.g. fossil fuels which can supply a local load either in grid annexed mode or in a stand-alone fashion. HRES divide the energy demand among these resources and provide a reliable, economical and secure system. The world is moving with a great pace towards a hybrid renewable energy system due to several advantages and because of the great innovation in power electronics devices and renewable energy technologies[6]. A lot of improvement and innovation in technology have made it possible to control several generating units at the same time to meet the demand of consumers in a more economical, secure and reliable way.

Solar energy percentage around the globe is in excessive amount that other renewable sources but all the energy resources are exploited in a balanced and appropriate ways for the stability of natural resources[7]. Each renewable energy source has a crucial role in power sector in regards to cost, output and nature dependency. In[8] author witnessed that load demand of 24 hours cannot be satisfied by the existence of mammoth amount of solar/wind energy when these resources are used in standalone mode so that there should be hybrid system composed renewable energy sources with DG or battery storage systems. Additionally, in[9] authors discussed Wind/PV/ DG hybrid system and witness that by using this combination power system is more reliable.

Intermittent nature of solar radiation and wind speed resulting in variable and uncertain output that cannot be able to meet the load demand, consequently, a battery storage technology is presented for stable output and to mitigate the intermittent nature of the renewable sources. Maintenance of hybrid system is also possible with the addition of batteries[10]. The solar, and diesel hybrid power system is best for decreasing consumption of diesel as well as eliminating power outages. Additionally, Economic and environmental aspects are in favors of using renewable sources but cost of the renewable energy system are too high. Nowadays, cost of renewable energy sources is minimized by exploiting latest techniques. In[11] authors defined the reputation of photovoltaic (PV) technology around the globe thousands of PV based stand-alone and hybrid power systems are installed and many of them are under working process.

Solar photovoltaic (PV) has enormous potential around the globe and solar irradiance in different locations of Pakistan are available lavishly which makes solar energy the most probable and likely among all the renewable energy sources[12]. Additionally, nearly all base transceiver stations (BTS) are mounted and operated in open and high places that are visible to direct sunlight and make it easier for energy production in telecom sites from solar energy. In[13] the author suggested a model comprising of solar photovoltaic (PV) and fuel cell (FC) hybrid power system for the operation of telecom network operators. Furthermore, in[14] the author discoursed about hybrid system and came across numerous techniques for optimization such as wind turbine size can be minimized by integrating of other renewable resources such as the addition of solar energy along with batteries backup[15].

Reliable and economically feasible diversification of the telecommunication system in rural and remote areas has initiated a very tough and challenging issue. Grid extension in these areas are either not practically possible or their extension can be tremendously costly. As most of the rural areas of Pakistan facing the issue of load shedding, power failure and even no grid-electricity approach, so these issues create a huge problem for telecommunication companies, they do not work properly under these circumstances because for the proper functioning of BTS they need a continuous supply of electricity. Mostly, Diesel Generators (DGs) are employed for the proper functioning of these BTS, although the initial cost of DG is less but the running cost of DG is high. Escalating fuel prices and delivery cost of fuels to these remote locations and also global warming associated with the use of DG drive the mobile operator to implement some other ways for the production energy. So, Renewable Energy Sources (RESs) are the best alternative for energy production in these telecommunication sites, and the system could be either on-grid or off-grid depending on the location of BTS. In this research, we are only considering off-grid locations, and a renewable energy source such as solar PV is used for energy production in these locations to power up BTS. If solar PV is integrated with diesel generator than the system becomes more reliable, robust and economical with less Net Present Cost (NPC) value and COE.

In all the above work the authors has employed HOMER for simulation of the hybrid model after inserting all the required data. The optimization results of the HOMER can be easily interpreted and the optimized system among different system can be obtained. In this paper same software is employed for designing and optimization of off-grid hybrid power system comprising of solar PV, Diesel generator and battery backup. This study contrast the above mentioned related studies in terms of approach, application, load demand, climatic data, and location of the area. In this paper, we shall see technical, economic and financial grounds for SCO to use alternative energy resources instead of fossil energy sources. After that, we consider a typical case of BTS in Skardu, one of the districts of Gilgit Baltistan (GB), Pakistan performing an economic evaluation of its Installation and operations, and calculating the NPC of the project over an operating period of twenty five years along with sensitivity analysis by taking fuel price as the sensitivity variable.

II. RESEARCH METHODOLOGY

The methodology of this research work comprised of several most important steps for the design of optimal and economically viable hybrid stand-alone system for the selected off-grid telecom site. The steps carried out for the completion of this research work are the following

i. Collection of load data site description

ii. Meteorological data collection i.e. solar/ Resource assessment or estimation

iii. Component assessment

iv. Hybrid energy system design

v. System optimization through HOMER

vi. Optimization results

The most influential requirement for this analysis is load data and we need peak and average load demand for the selected site for the whole year which can be obtained by visiting the selected site, it's a pre-design preparation. After getting load data the next step is the assessment of resources available at the selected site, as this research is about the hybrid system of PV-diesel so the solar resource assessment is important. Solar irradiance changes with the location and is dependent on weather condition so for every specific site solar irradiance will change which in turn change the component requirement. The information about the solar irradiation is acquired from the National Aeronautics and Space Administration (NASA) website. After getting this information put this information in HOMER software and design a model, the HOMER simulates the design model and shows the optimized model and compare it with other models.

III. SITE ELUCIDATION AND LOAD ESTIMATION

A. *Site Elucidation*

The selected site is located in Skardu one of the districts of Gilgit Baltistan, Pakistan. The network operator working there is the Special Communication Organization (SCO). The selected areas have both on-grid and off-grid communication sites but this research focuses on the prototype of a hybrid stand-alone system for the off-grid site. The geographical location of Skardu GB is 35oN 74oE with time zone (UTC + 05:00) Islamabad, Karachi.

B. *Load Estimation*

The most significant element of the research is electrical load estimation for simulation and optimization of the system. In fact, load estimation is a paramount task in other power generation units too in all around the world. Figure 4.3 portrays the daily electrical load profile for the selected site. The load data of each site is congregated from the nearest SCO exchange. The load data portray that average load at the selected site is about 3.5 kW with 4.06 kW peak load. Almost 84kWh is the average energy utilization on a daily basis. As the average load is 3.5 kW and by adding random variability to the load the peak of the load is changed. Real load data have some variability so HOMER offers the functionality of adding the random variability which will make the load data more realistic. So by the inclusion of random variability to the average load of 3.5 kW, the peak load goes to 4.06 kW with a load factor of 0.86. Figure 1 manifest average load of each month for the whole year.

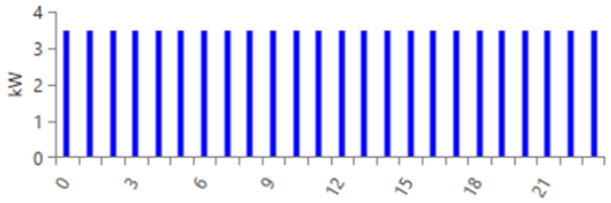

Figure 1. Daily Average Load

Manual calculation of the total energy load (EloadTotal) is

$$E_{\text{Load Total}} = \frac{E_{\text{load}}}{\eta_{\text{BOS}}} \quad (1)$$

E_{load} narrate daily load for the selected site and η_{BOS} narrate balance of system efficiency and its approximated value is about 70%. Now the power needed to accommodate the energy demand of fewer peak hours is calculated using the relation below

$$P_{PV} = \frac{E_{\text{load Total}}}{PSH.\eta_{\text{nonStc}}} \quad (2)$$

IV. SOLAR RESOURCE POTENTIAL

Solar irradiance statistics are obtainable on the NASA Surface Meteorology and Solar Energy website. They provide information about the solar irradiance at a specific location over a 22-year period (July1983-June2005). So at the selected site solar irradiance statistics are collected from the NASA website. Solar irradiance can be downloaded from National Renewable Energy Lab (NREL) too. Figure 2 shows the monthly average Global Horizontal Irradiance (GHI) and clearness index data for the selected site. Solar irradiance is maximum in summer and in winter it is less. The maximum solar irradiance occurs in the month of June.

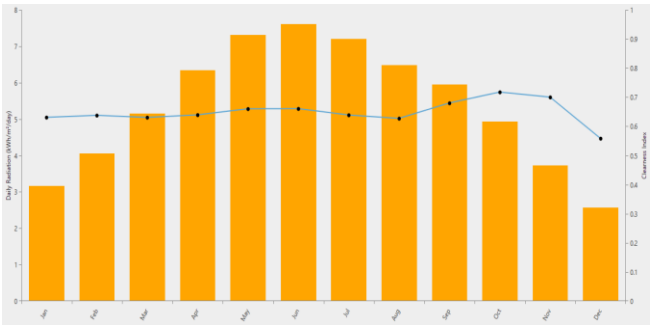

Figure 2. Monthly Average Global Horizontal Irradiance and Clearness Index Data

Table I shows the average monthly GHI of Skardu, GB. Annual average solar irradiation is 5.38 kWh/m2/day. HOMER calculate clearness index using the below formula

$$k_T = \frac{H_{ave}}{H_{o,ave}} \quad (3)$$

H_{ave} represents the average radiation on monthly basis falling on the earth surface horizontally in kWh/m2/day.

$H_{o.ave}$ narrate radiation on the straight surface at the summit of the earth atmosphere in kWh/m2/day, it's also called extraterrestrial horizontal radiation. For calculating the intensity

of solar radiation HOMER use equation 4, it gives the intensity at the top of the Earth's atmosphere.

$$G_{on} = G_{sc}(1 + 0.033.cos\frac{360n}{365} \quad (4)$$

G_{sc} in the above formula represents the solar constant, which have a value of 1.367 kW/m2 and n narrate 1 to 365 days for the whole year. For calculation of extraterrestrial radiation from the sun's rays which are normal to the horizontal facet, HOMER uses the subsequent equation.

$$G_o = G_{on}cos\theta_z \quad (5)$$

Where 〖 θ 〗_z represents zenith angle in degrees. The table below shows the average monthly global horizontal irradiance (GHI) at Skardu, Gilgit Baltistan.

TABLE I. AVERAGE MONTHLY GHI OF SKARDU, GB

Month	Clearness Index	Daily Radiation (kWh/m²/day)
January	0.630	3.170
February	0.637	4.052
March	0.630	5.154
April	0.638	6.344
May	0.659	7.315
June	0.660	7.614
July	0.638	7.204
August	0.626	6.474
September	0.679	5.950
October	0.717	4.936
November	0.699	3.719
December	0.588	2.575

V. COMPONENT SIZING AND COST ESTIMATION

The main components for the design and implementation of the described hybrid system are PV array, Diesel generator, Battery and converter. The subsequent section briefly explains different characteristics of each component as well as the cost of each component such as Capital, replacement and O&M cost. These all are necessary for the optimization process and finding the best-optimized system.

A. Solar Photovoltaic Panels

Solar energy is transformed into electrical energy with the aid of solar PV cells and the effect is known as the photovoltaic effect. For generation and load demand to be balanced it is necessary to install enough solar panels for the generation of electricity. The output of the PV array is DC in nature and is directly proportional to the solar irradiance. In this research work Canadian Solar Dymond 285watt, 60 cell and double glass PV array having the efficiency of 17.3% are used. It can tolerate snow load up to 6000 Pascal (pa), and wind load up to 4000 Pascal. Solar panels output decreases with several factors with the passage of time such as temperature, dust, tilting and shading so here we consider derating factor of 80% for each solar panel. Table II demonstrate different parameters and properties of the solar PV panels.

TABLE II. SPECIFICATION OF SOLAR PV PANEL

Monocrystalline Silicon PV Module	
Capital Cost (Rs), 1kW	60,000
Replacement Cost (Rs)	0
O&M Cost/Year (Rs)	16,000
Derating Factor (%)	80
Lifetime Span (Year)	25
Efficiency	17.33
Rated Capacity	285 W
Operating Temperature (°C)	45
Tracking System	No Tracking System

B. Battery Storage

Battery is exploited for storing electrical energy and it is necessary for the reliable operation of the grid. Batteries provide backup power during night hours and when diesel generator power is not available due to maintenance. The battery exploited in the proposed model is the lead acid battery (Surrette S-500EX). Capital cost, replacement cost and physical properties of the selected battery is mentioned in the below table III.

TABLE III. COST AND PROPERTIES OF BATTERY

Physical Specification of Lead Acid Battery	
Model	Surrette S-500EX
Capital Cost (Rs) of 1 battery	104,000
Replacement Cost (Rs)	104,000
O&M Cost/Year (Rs)	10,000
Nominal Voltage (V)	6
Lifetime Span (Year)	12
Roundtrip Efficiency (%)	80
Maximum Capacity (Ah)	517
Throughput (kWh)	3693.50
Maximum Charge Current (A)	121
Maximum Discharge Current (A)	121

The battery storage for the electrical load is calculated by the mathematical relation given below

$$E_{Battery} = \frac{E_{load}.n}{DOD.\eta_{BBOS}} \quad (6)$$

DOD in the above formula flaunt the depth of discharge, E_{load} appeared as a day-to-day load profile, the number of self-sufficiency/autonomy days is depicted through n and η_{BBOS} is the efficiency balance of system to compensate the inverter losses.

C. Converter

Converter is very important in the design of PV-Diesel hybrid system. Converter is a device exploited to convert Alternating (AC) into Direct Current (DC) and DC into AC according to the demand. It turns DC, which we acquire from the solar PV into AC to meet the load demand, it also converts AC into DC to power the telecom equipment's. In the proposed model the converter is used between AC and DC bus. Table 4.4

shows the cost and other parameters of the converter used in this research work.

TABLE IV. COST AND PROPERTIES OF CONVERTER

Specification of Converter	
Capital Cost (Rs) of 8 kW	150,000
Replacement Cost (Rs)	150,000
O&M Cost/Year (Rs)	0
Lifetime Span (Year)	15
Efficiency (%)	95
Relative Capacity (%)	100

D. Diesel Generator

DG is employed to dispense electrical energy to the load in night hours and during daytime when no PV power is available due to extreme weather conditions. It is also used for charging the batteries when PV supply is not enough. Generic 10kW fixed capacity generator is used for the selected site. Capital cost, maintenance cost and other peculiarities of the selected DG are shown in the table below.

TABLE V. COST AND OTHER PROPERTIES OF DG

Specification of 10kW DG	
Capital Cost (Rs)	500,000
Replacement Cost (Rs)	300,000
O&M Cost/Year (Rs/hr.)	20
Capacity (kW)	10
Lifetime Span (Hours)	30,000
Minimum Load Ratio (%)	25
Fuel Consumption (L/hr.)	0.480
CO Emission (g/L)	19.76

VI. EXISTING AND PROPOSED HYBRID SYSTEM

In this section simulation model of the existing power system and proposed system for the off-grid sites are presented. HOMER analyze these model and provides a better, genuine and cost-effective way of powering the BTS and remote areas.

A. Existing Power System

The existing system at the BTS for the selected site consists of diesel generator and battery backup shown in figure 3. The DG provides the necessary power to BTS all the time but due to some maintenance work of DG battery backup provide the necessary power to the BTS for the continuous and reliable operation.

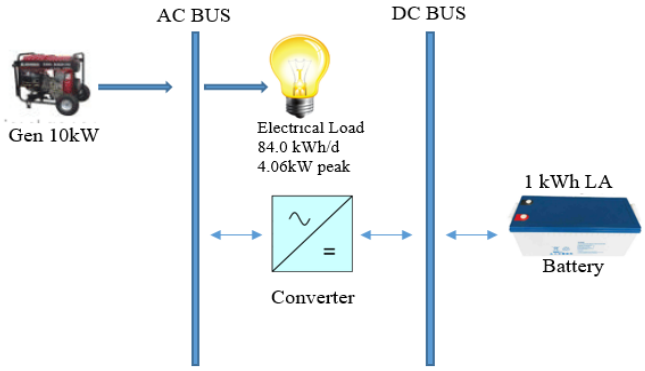

Figure 3. Model of Existing Power System for Off-Grid Site

B. Proposed Hybrid Power System

The suggested or recommended hybrid system for the off-grid sites comprise of diesel generator, PV and battery backup. In the proposed system HOMER perform analysis on different configuration such as PV/DG/Battery/Converter, PV/DG/Converter and DG/Battery/Converter and gives their NPC and COE, on the basis of these parameters the best-optimized system can be selected for the proposed site. Figure 4 shows the hybrid system for the off-grid telecommunication site.

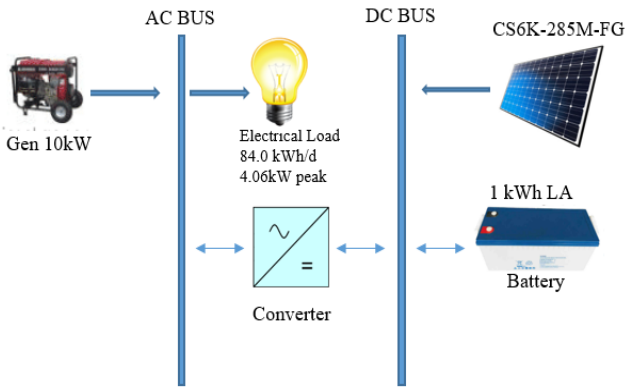

Figure 4. Model of Proposed Hybrid Power System for Off-Grid Site

The specific objective of proposed power systems are as follows:

• To minimize the cost of existing systems by integration of solar energy.

• Load shedding and power outages issues are resolved.

• Reduction in DG running time minimizes net present cost (NPC) and cost of energy (COE) of the system and environmental pollution can be mitigated.

VII. RESULTS AND DISCUSSION

This section presents the optimized result of the existing power system and proposed hybrid power system along with their techno-economic analysis. Optimized results of both system e.g. current power system having DG/Converter and battery backup and proposed hybrid system having

PV/DG/Converter and battery backup are compared. After that sensitivity analysis is performed using different fuel prices. HOMER needs different input parameter for the system designing and optimization process. The diagram below shows the general structure of HOMER modelling.

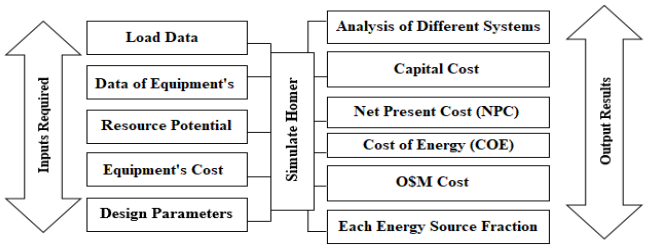

Figure 5. HOMER Modeling with Several Input Parameters

A. Optimized Results (considering fuel price 120Rs/L)

HRES consist of different components, search space provides a way where we can define the size of these components such as inverter size, PV size etc. HOMER simulates all the feasible combinations and find out the most reliable and cost-effective combination. In this section, we simulate our proposed system with pre-defined values and get the results on the basis of which we can select the most efficient configuration. From the figure, it can be seen that component sizing for HRES is 8kW PV, converter size is 8kW, 21 batteries and 10kW diesel generator which is installed to satisfy energy requirement during emergency and cloudy weather situations, for the recommended hybrid power system, but for the existing system generator size is 10kw along with the 8 batteries for backup and 8kW converter. Here the fuel price is considered 120Rs/L.

Architecture					Cost				System	
CS6K-285M-FG (kW)	Gen10 (kW)	Sun5-500EX	Converter (kW)	Dispatch	NPC (Rs)	COE (Rs)	Operating cost (Rs/yr)	Initial capital (Rs)	Ren Frac (%)	Total Fuel (L/yr)
8.00	10.0	6	8.00	CC	Rs18.0M	Rs45.43	Rs1.26M	Rs1.75M	35.1	8,294
8.00	10.0		8.00	CC	Rs23.0M	Rs58.06	Rs1.69M	Rs1.13M	12.9	11,846
	10.0	1	8.00	LF	Rs24.4M	Rs61.47	Rs1.83M	Rs754,000	0.00515	12,973

Figure 6. Simulation Results for Off-Grid Site

The simulation results depict that, the NPC and COE of the proposed hybrid system are less than the existing system and other configuration. For the proposed hybrid system NPC is 18M and COE is 45.43/kWh which is less compared with the existing system with NPC 23M and COE 58.06, so, COE and NPC are much higher than the proposed system. Although the initial capital cost of the proposed system is higher than other configurations but operating cost, NPC and COE is very less compared to other, so, it is the most efficient and optimized system for the selected site. Greenhouse gases emission get reduced by the addition of 35.1% renewable fraction.

TABLE VI. ELECTRICITY PRODUCTION AND CONSUMPTION SUMMARY

Production	kWh/yr	%	Consumption	kWh/yr	%
Canadian Solar Dymond (CS6K-285M-FG)	15,179	43.3	AC Primary Load	30,660	100
Generic 10kW Genset	19,909	56.7	DC Primary Load	0	0
Total	35,088	100	Total	30,660	100

The above table explicitly summarize the energy production and consumption phenomenon, as total energy generated together from PV and generator is 35,088 kWh/yr, nearly 42.7% of the total energy is generated for solar panels which is 15,179kWh/yr, on the other hand, DG generate 29,909 kWh/yr which is nearly 56.7 % of the total energy generated. Energy generation is higher than consumption and almost 3,288 kWh/yr energy is in excess amount, which is almost 9.37% of the total energy production, which can be fed to the grid in case of the grid-connected system. Figure 7 portray average energy production scenario on a monthly basis.

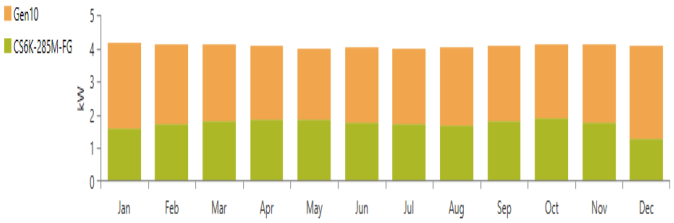

Figure 7. Monthly Average Electric Production

Above figure explicitly portray power production from solar PV and DG during different months for the whole year. It can also comprehend that from the diagram, solar PV share is highest during summer and in the winter it declines drastically. In the month of December production from solar PV is very less compared to other months. As mentioned in the previous section it's a hybrid system some of the energy portion is generated from solar PV during day time, which is directly fed to the load after conversion and some energy is used for charging of batteries, during night time and cloudy weather condition if battery backup is not available DG come into play in that case.

B. Optimized Results (considering fuel price 106Rs/L)

Analysis of the proposed hybrid system is carried out for the fuel price of 106Rs/L to get optimized results. Fuel price is a variable quantity so its value varies over the passage of time, so it is a sensitivity variable here. Figure 8 below shows that HOMER optimization result for several configurations.

Architecture					Cost				System	
CS6K-285I (kW)	Gen10 (kW)	Sun5-5	Converter (kW)	Dispatch	NPC (Rs)	COE (Rs)	Operating cost (Rs/yr)	Initial capital (Rs)	Ren Frac (%)	Total Fuel (L/yr)
8.00	10.0	6	8.00	CC	Rs16.5M	Rs41.57	Rs1.14M	Rs1.75M	35.2	8,299
8.00	10.0		8.00	CC	Rs20.9M	Rs52.66	Rs1.53M	Rs1.13M	12.9	11,846
	10.0	1	8.00	CC	Rs22.0M	Rs55.55	Rs1.64M	Rs754,000	0	12,974

Figure 8. Simulation Results for Off-Grid Site

The results show different configuration such as PV/DG/Battery/Converter, PV/Battery/Converter, DG/Battery/Converter, only DG and PV/DG/Converter. These are the different feasible architecture for the proposed site. In the figure above the first combination of PV/DG/Battery/Converter consist of 8kW PV, 21 batteries with 11.2 autonomy hours, 10 kW diesel generator and converter size 8 kW. This combination is the most optimal one as HOMER determine the best-optimized system on the basis of less NPC and less COE. The NPC of the first combination is 16.5M and COE is 41.57/kWh, which is less as compared to other combinations. But the initial capital cost of the system is high due to 8 kW PV system and 21 batteries but COE and NPC are less compared to other combinations. Renewable fraction in this combination is 35.2% so, which in turn reduces greenhouses gases emission. Comparison with the existing system shows that NPC of the existing system which comprises of DG/Battery/Inverter, is 22.0M and COE is 55.5/kWh which is too much high, although the initial capital cost is low. In this case, the renewable fraction is zero.

From the above debate, it is concluded that the first layout which is comprised of PV/DG/Converter/Battery is the most economical system for the off-grid site. The cost of energy is less as compared with the existing power system composed of DG/Battery/Converter.

C. Sensitivity Analysis

In this research work, a sensitivity analysis is carried out by entering different values for a certain variable which alters the result. HOMER carry out the optimization process for different values of the sensitivity variable and the results obtained tell us about how different values affect the results. Here fuel cost is considered a sensitivity variable. One value for fuel cost is 120/L and other value is 106/L. HOMER perform optimization process on these two values and tells us how fuel cost effects the system cost as this variable only affects NPC, COE and operating cost etc. Below detail of every scenario is presented.

TABLE VII. EFFECT OF SENSITIVITY VARIABLE ON DIFFERENT PARAMETERS

Parameters	Fuel price 120Rs/L	Fuel price 106Rs/L
NPC (Rs)	18.0M	16.5M
COE (Rs)	45.3	41.57
Operating Cost (Rs)	1.26M	1.14M

The above table represents the effect of varying fuel price on the different parameter for the proposed hybrid system only. It can be easily seen from the above table that with the change of fuel price it also affects different parameters such as NPC, COE and operating cost.

D. Gases Emission

This section compares the emission of greenhouses gases for both systems i.e. existing system and the proposed hybrid system for the off-grid site. Table VIII depicts the ejection of greenhouse gases for the proposed hybrid system.

TABLE VIII. POLLUTANT EMISSION OF PROPOSED HYBRID SYSTEM

Quantity	Value	Units
Carbon Dioxide	21,681	Kg/yr
Carbon Monoxide	164	Kg/yr
Unburned Hydrocarbons	5.98	Kg/yr
Particulate Matter	9.94	Kg/yr
Sulfur Dioxide	53.2	Kg/yr
Nitrogen Oxides	186	Kg/yr

The table depicts emission of several gases from the hybrid system in term of their weights for the period of one year. Table IX depicts the case of an existing system composed of DG/Converter/Battery storage.

TABLE IX. POLLUTANT EMISSION OF EXISTING HYBRID SYSTEM

Quantity	Value	Units
Carbon Dioxide	33,893	Kg/yr
Carbon Monoxide	256	Kg/yr
Unburned Hydrocarbons	9.34	Kg/yr
Particulate Matter	15.5	Kg/yr
Sulfur Dioxide	83.2	Kg/yr
Nitrogen Oxides	291	Kg/yr

From the tables above it can be concluded that the emission of carbon dioxide is 18,924 kg/yr and carbon monoxide is 143 kg/yr. For the existing system as shown in the above figure CO2 emission is 32,915kg/yr and carbon monoxide is 249 kg/yr. When these results are compared with each other than it is clear from the results that emission of greenhouses gases reduced with the incorporation of solar PV in the existing system. The inclusion of the solar PV in the current system has reduced the emission of CO2 to a great extent.

CONCLUSION

Mobile operator in rural areas facing the problem of power outage and load shedding due to unreliable grid power supply. Most of the mobile BTS are operating in a standalone diesel generator and battery backup hybrid power system due to no access to grid electricity. The considered area for this research work is Skardu, Gilgit Baltistan, Pakistan. The layout of the stand-alone hybrid system along with the economic analysis is presented in this chapter for the off-grid SCO telecommunication site. The suggested hybrid system comprises of solar PV, diesel generator, converter and battery backup where the current power system consists of DG, converter and battery backup.

HOMER software is employed for economic analysis and design purpose of the stand-alone hybrid renewable energy system. For the complete economic analysis HOMER need s several inputs for analysis purpose, the inputs are load data, data of equipment's, resources potential at the selected site such is solar PV, equipment's costs and other design parameters. HOMER perform an economic analysis of the designed system on the basis of these inputs and most optimized system with less NPC and COE are obtained among different configurations. The evaluation standards for this research work are capital cost, operating cost, net present cost, and cost of energy. These are the main factors on the basis of which HOMER declared the most optimized system among several configurations.

In the above section, HOMER performs optimization through HOMER search space. For the first scenario the fuel price of 120Rs/L and 106Rs/L for the second scenario is selected, different values of fuel are taken for sensitivity analysis to be performed. The results depict that the most optimized system is DG/PV/Converter/battery having less NPC and COE. But the existing system has very large COE, NPC and operating cost although the initial capital cost of the system is less compared to the proposed system.

Greenhouse gases emission is an important factor for the selection of power system among different configurations shown by HOMER. Greenhouses gases emission get reduced to a huge extent with the penetration of solar energy, this is a very important factor for environmental stability because these harmful gases emission causes global warming which is very dangerous for the whole world. So our proposed system is best, efficient and most economic for the BTS sites in rural areas and also discharge less CO2.

REFERENCES

[1] M. Usman, A. M. Malik, A. Mahmood, A. Kousar, and K. Sabeel, "HOMER Analysis for Integrating Solar Energy in Off-Grid and On-Grid SCO Telecommunication Sites," 2019 1st Glob. Power, Energy Commun. Conf., pp. 270–275, 2019.

[2] R. Sen and S. C. Bhattacharyya, "Off-grid electricity generation with renewable energy technologies inIndia: An application of HOMER," Renew. Energy, vol. 62, pp. 388–398, 2014.

[3] A. Helal, R. El-Mohr, and H. Eldosouki, "Optimal design of hybrid renewable energy system for electrification of a remote village in Egypt," 2nd Int. Conf. Commun. Comput. Control Appl. CCCA 2012, pp. 1–6, 2012.

[4] P. Bajpai, N. P. Prakshan, and N. K. Kishore, "Renewable hybrid stand-alone telecom power system modeling and analysis," IEEE Reg. 10 Annu. Int. Conf. Proceedings/TENCON, pp. 0–5, 2009.

[5] M. Nurunnabi and N. K. Roy, "Grid connected hybrid power system design using HOMER," Proc. 2015 3rd Int. Conf. Adv. Electr. Eng. ICAEE 2015, pp. 18–21, 2016.

[6] D. K. Yadav, S. P. Girimaji, and T. S. Bhatti, "Optimal hybrid power system design using HOMER," India Int. Conf. Power Electron. IICPE, no. 1, pp. 1–6, 2012.

[7] M. Jarahnejad and A. Zaidi, "Exploring the Potential of Renewable Energy in Telecommunications Industry," 2018.

[8] M. A. Ghaffar, "The energy supply situation in the rural sector of Pakistan and the potential of renewable energy technologies," Renew. Energy, vol. 6, no. 8, pp. 941–976, 1995.

[9] M. Muthuramalingam and P. S. Manoharan, "Energy comparative analysis of MPPT techniques for PV system using interleaved soft-switching boost converter," World J. Model. Simul., vol. 11, no. 2, pp. 83–93, 2015.

[10] M. Y. Raza, M. Wasim, and M. S. Sarwar, "Development of Renewable Energy Technologies in rural areas of Pakistan," Energy Sources, Part A Recover. Util. Environ. Eff., vol. 0, no. 00, pp. 1–21, 2019.

[11] S. A. Chowdhury, V. Roy, and S. Aziz, "Renewable energy usage in the telecommunication sector of Bangladesh: Prospect and progress," Proc. 1st Int. Conf. Dev. Renew. Energy Technol. ICDRET 2009, pp. 234–238, 2009.

[12] S. Bahramara, M. P. Moghaddam, and M. R. Haghifam, "Optimal planning of hybrid renewable energy systems using HOMER: A review," Renew. Sustain. Energy Rev., vol. 62, pp. 609–620, 2016.

[13] P. Bajpai and V. Dash, "Hybrid renewable energy systems for power generation in stand-alone applications : A review," Renew. Sustain. Energy Rev., vol. 16, no. 5, pp. 2926–2939, 2012.

[14] A. Helal, R. El-Mohr, and H. Eldosouki, Optimal design of hybrid renewable energy system for electrification of a remote village in Egypt. 2012.

[15] R. Ramakumar, I. Abouzahr, and K. Ashenayi, "A knowledge-based approach to the design of integrated renewable energy systems," IEEE Trans. Energy Convers., vol. 7, no. 4, pp. 648–659, 1992.

How to cite this article:

Farhan ullah, Naveed Malik, Dawood Shah, Amir Khan, "Optimal Design and Analysis of Integrating Solar Energy in Off-Grid Telecommunication Sites", International Journal of Engineering Works, Vol. 7, Issue 12, PP. 414-421, December 2020, https://doi.org/10.34259/ijew.20.712414421.